Universiteit Leiden
The Netherlands

Exploitation of host chemokine signalling by pathogenic mycobacteria

Torraca, V.

Citation

Torraca, V. (2016, November 17). *Exploitation of host chemokine signalling by pathogenic mycobacteria*. Retrieved from https://hdl.handle.net/1887/44243

Version:	Not Applicable (or Unknown)
License:	Licence agreement concerning inclusion of doctoral thesis in the Institutional Repository of the University of Leiden
Downloaded from:	https://hdl.handle.net/1887/44243

Note: To cite this publication please use the final published version (if applicable).

Cover Page

Universiteit Leiden

Leiden University Repository

The handle http://hdl.handle.net/1887/44243 holds various files of this Leiden University dissertation.

Author: Torraca, V.
Title: Exploitation of host chemokine signalling by pathogenic mycobacteria
Issue Date: 2016-11-17

Exploitation of host chemokine signalling by pathogenic mycobacteria

Vincenzo Torraca

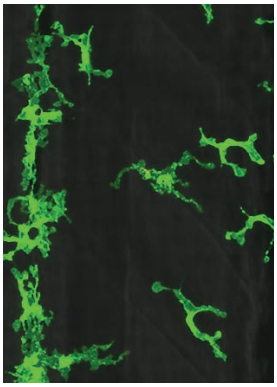

Cover: Macrophages (green) in the trunk of a 2-day-old zebrafish embryo. One (centre) has phagocytosed a *Mycobacterium marinum* cell (yellow) which was injected 1 hour before the image was taken.

ISBN: 978-94-6328-090-7

Printed by: Wöhrmann Print Service, Zutphen, The Netherlands

Exploitation of host chemokine signalling by pathogenic mycobacteria

Proefschrift

ter verkrijging van
de graad van Doctor aan de Universiteit Leiden,
op gezag van Rector Magnificus prof. mr. C.J.J.M Stolker,
volgens besluit van het College voor Promoties
te verdedigen op donderdag 17 november 2016
klokke 16:15 uur

door

Vincenzo Torraca

Geboren te Salerno, Italië
op 6 september 1987

Promotiecommissie

Promotores:	Prof. dr. Annemarie H. Meijer Prof. dr. Herman P. Spaink
Promotiecommisie:	Prof. dr. Ariane Briegel Prof. dr. Johannes M. F. G. Aerts Prof. dr. Annemieke Geluk Dr. Serge Mostowy (Imperial College London)

"Humans are not the pinnacle of evolutionary progress but only an aberrant side branch of fish evolution"

Peter B. Moyle,
Distinguished Professor Emeritus,
University of California, Davis

Table of contents

Chapter 1 Introduction and thesis outline.....1

Chapter 2 Macrophage-pathogen interactions in infectious diseases: new therapeutic insights from the zebrafish host model..... 27

Chapter 3 The CXCR3-CXCL11 signalling axis mediates macrophage recruitment and dissemination of mycobacterial infection.....57

Chapter 4 Disruption of chemotactic signalling primes the lysosomal function of macrophages to counteract mycobacterial parasitism.....97

Chapter 5 CRISPR/Cas9 mutagenesis of zebrafish Cxcr3.3 suggests opposing functions of atypical and canonical Cxcr3 paralogues on mycobacterial infection control..... 121

Chapter 6 The chemokine receptor CXCR4 promotes granuloma formation by sustaining a mycobacteria-induced angiogenesis programme..... 155

Chapter 7 The inflammatory chemokine Cxcl18b exerts neutrophil specific chemotaxis via the promiscuous chemokine receptor Cxcr2 in zebrafish.....173

Chapter 8 General discussion and final conclusions..... 193

Summary.....221

Dutch summary / Samenvatting.....225

List of abbreviations.....230

Nomenclature of zebrafish chemokine ligands.....232

Nomenclature of zebrafish chemokine receptors.....235

Curriculum vitae..... 237

List of publications.....238

Chapter 1

Introduction and thesis outline

Chapter 1

Introduction and thesis outline

Bacterial infections remain a major cause of morbidity and mortality for mankind. In particular, the WHO Global Tuberculosis report (2015) estimated that one third of the world population is infected with *Mycobacterium tuberculosis* and that 9.6 million people have contracted tuberculosis (TB) in 2014 alone. An emergent problem is the prominence of multidrug and extensively drug-resistant strains. The evolution of antibiotic resistance is inevitable and requires continuous development of alternative therapeutic strategies. Therefore, a deeper understanding of the host-pathogen interface is needed. If the molecular mechanisms underlying host-pathogen interactions will be better understood, it may become possible to treat intracellular infections by targeting host cell functions that support bacterial growth, rather than targeting the pathogen itself. An important advantage of this approach is that it is more difficult for the pathogen to develop resistance to a host-targeted therapy. In this thesis, we investigated the host-pathogen dynamics during mycobacterial infection and we focused on the mechanisms by which mycobacteria can hijack chemokine signalling. Chemokines are small secreted signalling proteins that play multiple functions in a vast range of diseases. Chemokine receptors are highly expressed by immune cells and chemokine ligands are largely induced by inflammatory processes, including mycobacterial infections. However, since chemokine ligands and receptors are largely redundant in function and expression patterns, it has been difficult to address the relevance of different chemokine signalling axes for the onset and the progression of inflammatory diseases. Research on chemokine functions in TB has been particularly complicated in the most widely studied murine model. In this thesis, we alternatively applied the zebrafish (*Danio rerio)-Mycobacterium marinum* model to dissect how chemokines orchestrate the response of immune cells to mycobacterial infection. Several chemokine axes are conserved from fish to mammals and the similarities between human-*M. tuberculosis* and zebrafish-*M. marinum* pathology are remarkable. In this introduction, we briefly describe these aspects, which, together with the suitability of the zebrafish for microscopic analysis and genetic manipulations, have made us choose this model to investigate chemokine function in mycobacterial disease.

GRAPHICAL ABSTRACT

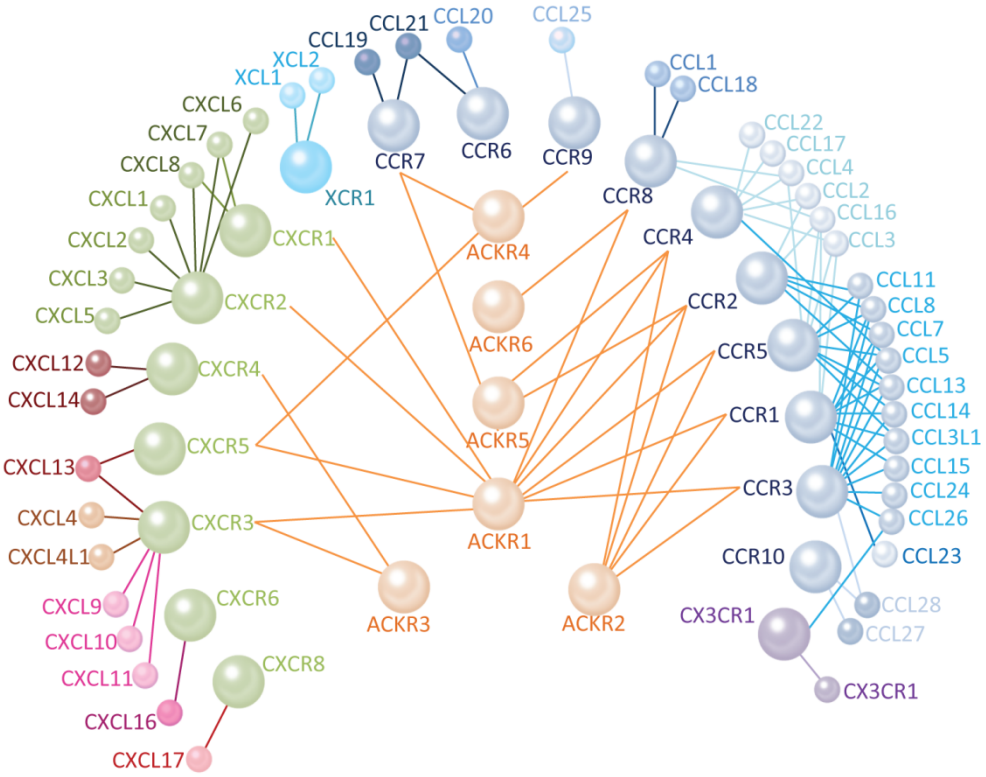

The human chemokine network as currently known consists of 25 receptors and 45 ligands. Ligand-receptor connecting lines indicate binding specificity. The AKCR family comprises atypical receptors that lack the motif for signalling through G-proteins and can antagonise the activities of other chemokine receptors (connected with orange lines) by binding one or more of their ligands. The chemokine receptor families include CXCR (green), XCR (cyan), CCR (blue), CX3CR (violet), ACKR (orange). Chemokine ligand families include CXCL (ELR+ chemokines in shades of green, homoeostatic chemokines in shades of red, platelet chemokines in shades of orange, dual function chemokines in shades of pink), XCL (cyan), CCL (shades of blue) and CX3CL (violet).

The zebrafish model system for biomedical research

Zebrafish initially emerged as a powerful vertebrate model organism to study embryonic development and morphogenesis[1,2,3,4,5] and this model species is now used to study the mechanisms of a wide variety of human diseases[5]. Due to their optical accessibility, the early embryonic and larval stages are ideally suited for non-invasive intravital imaging and longitudinal *in vivo* studies[1]. The short generation time (3-4 months) together with the external fertilisation and the possibility to daily obtain a large number of fertilised eggs from a zebrafish adult colony has permitted the efficient application of genetic tools, thereby providing the zebrafish field with transgenic lines that fluorescently label distinct tissues, organs, cell types, but also the cellular ultrastructural components, such as the nucleus, autophagosomes and the cytoskeleton[6].

The genome of zebrafish has been sequenced and forward genetics approaches have been successfully applied to mutate a vast array of genes[3,4]. Additionally, reverse genetic approaches, including morpholino knockdown and mRNA injection-based overexpression, are widely used in zebrafish embryos and have permitted rapid screening of gene functions. The zebrafish model also keeps up with state-of-the-art technologies, such as novel genome editing techniques (e.g. TALENS and CRISPR/Cas9)[7,8,9] and the application of cell/tissue-specific RNA-sequencing analysis[10], which are contributing to exponentially increase the availability of tools and data for this model system.

Due to their continuous exchanges with the surrounding water, embryos and larvae are easily penetrated by a variety of drugs and vital dyes and are therefore chemically and pharmacologically tractable. With the increase of tools and successes in using zebrafish, we have gained a grounded knowledge on how to exploit this model to study diverse biological processes. Therefore, not surprisingly, the zebrafish field has promptly expanded from the initial niche in developmental research to other scientific branches, spanning from eco/toxicology to neuronal physiology, behavioural studies and immunology. The potential of zebrafish research and its translational value to develop new treatments for human diseases is also underscored by new therapeutics that emerged from initial studies in zebrafish. In particular, a milestone for the zebrafish translational research was achieved when the first drug developed through the use of zebrafish has passed phase 1 trial and advanced to phase 2 clinical studies[11,12].

Despite the many advantages of using the zebrafish as a model for human diseases, there are also several limitations that should be taken into account when extrapolating conclusions from experiments in this animal model. The first important aspect to consider is the evolutionary divergence. There are about 445 millions of years of evolutionary divergence between the zebrafish and the human species, which is approximately 5-fold higher than the rodents-human divergence (93 millions of years). While key aspects of the immune signalling architecture are maintained between human and zebrafish, some significant differences exist between fish and mammalian immunology. An example is the fact that the Toll-like receptor Tlr4, differently than in mammals, is not involved in bacterial lipopolysaccharide sensing in zebrafish and many other fish species, which explains also the high tolerance of fish to this compound[13]. Another difficulty when working with zebrafish, resides in the fact that the teleost genome has undergone genome duplication, which means that a variety of genes are present in two copies in these species. Some gene families have also experienced species-specific expansions in zebrafish *per se*

(e.g. the chemokine ligand families[14]). Adding to this, the different gene copies have sometimes undergone functional specialisation and have diverged to assume slightly different roles[15].

Oftentimes regarded as an advantage, the small size of the zebrafish can be, in some circumstances, a limiting factor. In fact, the reduced dimension of zebrafish makes it difficult (in juveniles and adults) or nearly impossible (in embryos and larvae) to collect body fluids or organs, and therefore to precisely quantify bioactive molecules and chemicals in the blood or specific tissues. This has been a relevant limit, especially for the application of zebrafish larvae for high-throughput screening of drugs via bath exposure, including anti-tubercular therapeuticals[16,17]. In fact, not all the drugs can infiltrate through the skin and the impossibility of blood and tissue sampling made it impossible to distinguish inactive compounds from non-permeable false negatives. However, protocols for sampling the yolk sac have been described and it has been shown that dosage of compounds from these specimens can be used as an indication for the compound uptake, enabling therefore, to discriminate ineffective compounds from those that could not cross the skin barrier[18].

The zebrafish community additionally suffers from the poor availability of immunological reagents, and from the inefficiency of site-directed genome manipulation strategies, which effectively apply to the murine model. However, the lack of antibodies is well compensated by the expanding availability of transgenic reporter lines and the possibility to apply whole mount RNA *in situ* hybridisation. Additionally, the recent advances in genome editing technology (e.g. CRISPR/Cas9 editing) has enabled precise gene disruptions and generation of conditional knockout, at par of those available in mice[19,20].

Finally, another limit of the zebrafish model consists in the fact that, differently from rodents, strict breeding and husbandry protocols are not widely applied in the zebrafish community and true inbred zebrafish lines are not adopted in the majority of studies. However, generation of clonal zebrafish lines is possible, either by conventional repeated sibling incrosses or even directly via gynogenesis[21]. Therefore, it is expected that the zebrafish community will increasingly adopt these lines and more standardised culturing protocols for future research.

Taken together, despite some drawbacks, the zebrafish model holds great promise for translational biomedical research as it concentrates in a single vertebrate system several useful features, including remarkable homology to mammals in biological processes, optical transparency, availability of genetic tools, chemical tractability, adaptability to high-throughput research methods and finally, suitability to address research questions at multiple levels, from the molecular level to the whole organism level.

Tuberculosis and mycobacterial infection in the zebrafish-*M. marinum* surrogate model

Mycobacterium tuberculosis (*Mtb*) is a respiratory pathogen responsible for tuberculosis (TB). The main pathologic feature of mycobacterial infection is the formation of granulomas, which are inflammatory collections of immune cells that contain the infection and that are often chronically maintained[22]. TB is a life threatening and global disease, with high prevalence in all human populations[23]. Although many organs and tissues can be

infected with *M. tuberculosis*, the disease most often affects the lungs, with 75-80% of TB cases where the infection is exclusively pulmonary[24]. Approximately 1.5 million people die of tuberculosis each year, and there are over nine million new cases annually[23]. Although drug treatments are available, the therapeutic regimen is long and requires a combination of several pharmaceuticals. In addition, drug-resistant strains have evolved that do not respond to the currently available treatments. One third of the world population is estimated to be infected with *Mtb*. Only about 10% of infected individuals will manifest active TB disease while, in the vast majority of cases, the pathology is contained although not eliminated (latent TB). In case of latency, people are generally not contagious, and may never develop active TB. However, the infection can reactivate even many years later, especially in immune-suppressed/compromised patients, for example people subjected to chemotherapies or carrying HIV infection.

The granuloma, the histopathological hallmark of TB disease, is composed mostly of infected and non-infected immune cells that have migrated to the infectious focus. The signals responsible for granuloma formation and maintenance are only partly elucidated and it is clear that both host and pathogen signals integrate together to initiate the cellular and molecular programme that leads to granuloma formation[22]. As further elaborated on in **Chapter 2**, *M. marinum* (*Mm*) is a closely related species to *Mtb* that is a natural pathogen of zebrafish and other ectothermic animals. *Mm* causes necrotic granulomatous lesion formation in host tissues and these lesions are histologically very similar to those generated by *Mtb* in TB patients[25,26,27]. Additionally, the *Mm*-zebrafish surrogate model has been proven to recapitulate key aspects of TB, including bacterial dormancy/reactivation, the coordination of host and pathogen components in the formation of granulomas, the dynamicity of these structures and the key role of the inflammatory status in controlling the infection[28,29,30,31]. The striking conservation of molecular mechanisms, cellular dynamics and histopathological features between human and fish tuberculosis, together with the unique accessibility of the early stages of granuloma formation in zebrafish larvae, made the zebrafish-*Mm* host-pathogen pair a valuable platform to unravel the core pathogenic processes of mycobacterial infections. However, it must be taken into account that experimental fish embryo infections are generally performed using non-natural infection routes. Most commonly, the bacteria are delivered directly into the blood and generate a systemic infection that anatomically poorly represents the lung disease that is evoked in *M. tuberculosis*-infected patients. While use of a fish model makes it obviously impossible to model the organ-specific effects of TB pathology, a variety of alternative routes can be used to mimic and study specific aspects of the disease. For example, the importance of the epithelium for the initial steps of macrophage recruitment and granuloma formation has been addressed by delivering the bacteria into the hindbrain cavity[32], which is delimited by an epithelial barrier that resembles the alveolar lumen. Similarly, the relevance of the vasculature response could be addressed by delivering the pathogens in the poorly vascularised trunk tissue, where progression of the infection substantially depends on the induction of local angiogenesis[33].

Human infections with *Mm* are rare and generally limited to granulomatous nodules in the tissues of the skin, owing to the optimal growth of this pathogen at lower temperatures than that of the human body. Hence, *Mm* does not represent a serious risk for health, when compared to *Mtb*. The limited safety concern and the possibility to handle *Mm* under biosafety level 2 instead of level 3 conditions greatly expands the research opportunities that can be explored using the zebrafish-*Mm* surrogate model.

Chemokines and chemokine receptors, the portrait of an "extended" family

Chemokines are chordate-specific signalling molecules. Their primary function is to control cell movements by activating specific heterotrimeric G-protein coupled receptors (GPCRs), a class of 7 transmembrane (7TM) receptors (**Figure 1**, **Table 1**). Chemokines and chemokine receptors play critical roles in a wide context of biological processes, both in physiological and pathological conditions, which include development[34], ontogenesis and homing of immune cells[35], angiogenesis[36], organogenesis[37], autoimmune reactions[38], infectious diseases[39] and cancer[40,41]. These activities are not exclusively related to chemokine function in chemotaxis and cell migration, since multiple signal transduction pathways can be activated by GPCRs, including cell proliferation and differentiation[42].

GPCRs are the largest and most diverse group of membrane receptors in eukaryotes[43] and their pleiotropic functions, despite similar protein and signalling architecture, have greatly influenced modern medical research. In fact, GPCRs mainly signal via well-described pathways, which has facilitated drug discovery and testing. Additionally, they are involved in a variety of biological processes and therefore therapeutic targeting of GPCRs is relevant for many diseases. It has been recently estimated that between 1/3 and 1/2 of all the drugs available on the market target GPCRs[44,45].

At the intracellular side of the plasma membrane, inactive GPCR/chemokine receptors constitutively interact with a three subunit G-protein complex, also known as heterotrimeric G-proteins. G-proteins are able to bind and exchange guanosine triphosphate (GTP) with guanosine diphosphate (GDP). Specifically, it is the Gα subunit of the heterotrimer that exchanges GDP/GTP in response to conformational changes of the receptor[46]. Receptor conformational switches are evoked by binding of cognate chemokine ligands to their receptors. In the inactive form, Gα is bound to GDP. Activation of the receptor evokes physical replacement of GDP with GTP. This affects the conformation of the Gα subunit, which in turn dissociates from both the receptor and the Gβ-γ heterodimer. Both Gα-GTP and Gβ-γ possess lipid anchors and therefore diffuse laterally on the plasma membrane, where they interact with their downstream signalling partners[46]. This phenomenon is transient and, as soon as Gα-GTP decays to Gα-GDP, it re-associates to the GPCR receptor and to Gβγ. Despite this highly conserved signalling mechanism, vertebrate genomes encode multiple variants of G-proteins, which therefore can transduce diverse downstream signalling[47]. Some chemokine receptors have also shown selectivity for coupling with G-protein complexes containing specific G isoforms[47].

The cascade initiated by GPCR/chemokines receptors commonly includes the activation of phosphoinositide 3-kinase (PI3K), which leads to changes in intracellular phosphatidylinositol-3,4,5-triphosphate, and mediates the recruitment of pleckstrin homology (PH) domain–containing proteins to the cell membrane[48]. Several components of the Rho family of small GTPases, as well as their GTP/GDP exchange factors (GEFs) and kinases, also contain PH domains. Activation of the small GTPases (e.g. RAC1, CDC42, RHOA) is critical to link chemoattractant receptors to cytoskeletal changes and the formation/maintenance of cell polarity[49].

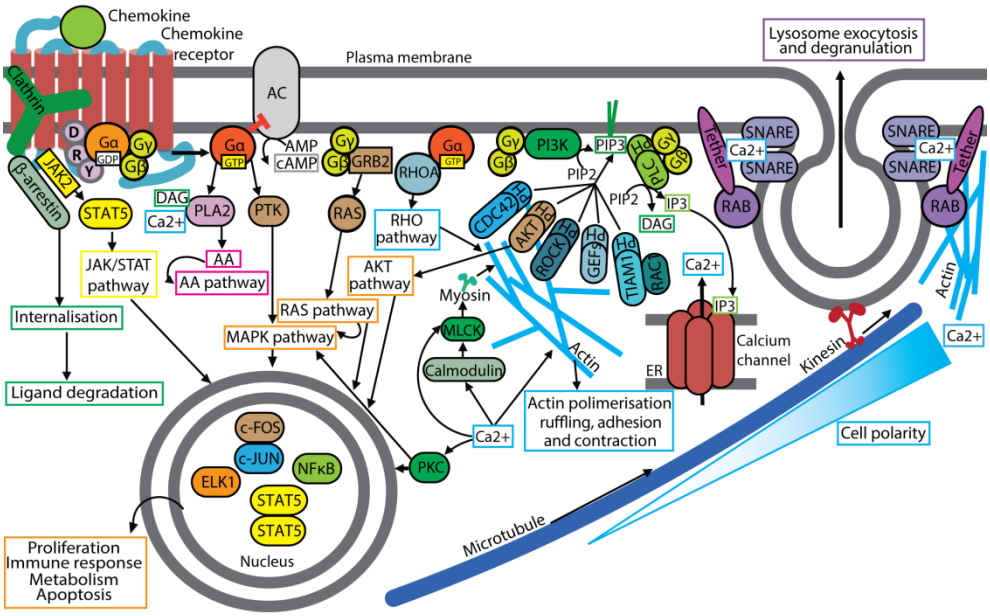

Figure 1. Downstream pathways activated by chemokine signalling. Most of the downstream signals evoked by chemokine ligand/receptor binding depend on receptor dissociation from heterotrimeric G-proteins (Gα-β-γ) and on the GDP-GTP (guanosine diphosphate and triphosphate) exchange in the Gα subunit. Different families of Gα-proteins exist (Gs, Gi, and Gq), which can activate RHOA (RAS homologue A), PLC or PLA2 (phospholipase C or A2) and PTK (protein tyrosine kinase). Gi (shown in figure) can additionally inhibit AC (adenylyl cyclase), while Gs can stimulate this enzyme and production of cAMP (cyclic adenosine monophosphate). PLA2 controls AA (arachidonic acid) release and affects the synthesis of pro/anti-inflammatory derivatives. PTK activates the MAPK (mitogen-activated protein kinases), while RHOA evokes actin polymerisation and sustains cell migration. Gβ-γ modulates GRB2 (growth factor receptor-bound protein 2), which via activation of RAS proteins, leads to downstream effects synergistic with the MAPK. Gβ-γ also activates PI3K (phosphoinositide 3-kinase) and production of PIP3 (phosphatidylinositol-3,4,5-triphosphate). PIP3 is key to maintain cell asymmetry by mediating cortical recruitment and activation of PH (pleckstrin homology) domain-containing proteins, including small GTPases and their regulators (e.g. TIAM1/RAC1, GEFs, ROCK, CDC42). PIP3 also activates AKT and PLC. AKT controls a phosphorylation cascade while PLC leads to IP3 (inositol-1, 4, 5-triphosphate) and DAG (diacylglycerol) production. IP3 mobilises Ca^{2+} from the ER (endoplasmic reticulum) and evokes profound changes in the cell, as Ca^{2+} controls cytoskeleton dynamics and modulates a variety of targets, such as PLA2 and PKC (protein kinase C). Calmodulin and MLCK (myosin light chain kinase) control contractility of actin fibres in a Ca^{2+}-dependent manner. Additionally, microtubule elongation depends on Ca^{2+} gradients. As a consequence, lysosomes and secretion granules that are trafficked on microtubule tracks via the motor protein kinesin accumulate towards the cell periphery. Ca^{2+} also controls the activity of RABs and synaptotagmins, which are involved in the formation of the SNARE (Soluble NSF attachment protein receptor) complexes, evoking membrane fusion and exocytosis. G-protein signalling terminates with the modulation of gene expression via an array of transcription factors, including NFκB (nuclear factor kappa B) and others (e.g. c-FOS/c-JUN, ELK1). The effects are pleiotropic and span from proliferation/apoptosis to immune defence and metabolism. Chemokines can also induce G-protein independent signalling, for example via direct activation of JAK2/STAT5 (Janus kinase 2/signal transducer and activator of transcription 5) or via β-arrestin. The latter is also involved in clathrin-dependent internalisation of chemokine ligand/receptor complex, which ultimately leads to ligand degradation and recycling of the receptor to the plasma membrane.

Chemokine sensing also activates phospholipase C (PLC)[47], which hydrolyses phosphatidylinositol-(4,5)-bisphosphate to produce inositol-1,4,5-triphosphate (IP3) and diacylglycerol (DAG). IP3 induces the mobilisation of intracellular calcium stores, which in turn has effects on calmodulin and myosin light-chain kinase (MLCK). Increased intracellular calcium is a hallmark of chemoattractant stimulation as this mediates, for example, cytoskeleton redistribution and relocation of focal adhesions[50]. Ca^{2+} also controls microtubule stability and their directional elongation in the direction of the cell movement. Secretion granules and lysosomes, which are trafficked in the cells via kinesin (a microtubule-associated motor protein), follow microtubule tracks and tend to accumulate at the cortex of the leading edge. Here the coordinated activity of Ca^{2+}, RABs and synaptotagmins – the main components of the SNARE (Soluble NSF attachment protein receptor) complex – will mediate fusion and exocytosis[51]. This process will, in turn, deliver phospholipids to the plasma membrane to sustain emission of protrusions and will determine secretion of enzymes and signalling mediators into the extracellular space, to facilitate locomotion and to transmit signals to neighbouring cells.

Another target of G-proteins is adenylyl cyclase (AC), which catalyses synthesis of cyclic adenosine monophosphate (cAMP). Some versions of Gα can activate this signalling while others (called inhibitory Gα or Gi) can instead negatively control this enzyme. Most chemokine receptors seem to associate with Gi complexes and therefore tend to antagonise this signalling pathway[52]. The activated G-proteins can also have a variety of other effects. These include activation of RAS/mitogen-activated protein kinase (MAPK) pathways[53,54] and modulation of phospholipase A2 (PLA2)[55], with downstream effects as diverse as apoptosis and cell proliferation[54], immune responses[56,57], arachidonic acid (AA) signalling[55] and metabolic control[58] (**Figure 1**).

Chemokine receptors were originally thought to act entirely through G-protein-mediated processes. However, we now know that some chemokine receptors can also initiate alternative signalling pathways, that do not require G-protein-coupling. For example, some chemokines can directly activate the JAK-STAT (Janus kinase-signal transducer and activator of transcription) signalling[59] or β-arrestin signalling[60,61], with the latter being associated with clathrin-mediated ligand/receptor complex internalisation and desensitisation. There is also a class of these receptors that are completely incapable of transmitting any G-signalling, known as atypical chemokine receptors which are further discussed below. Notably, their ligand-mediated internalisation/recycling remains intact (or even enhanced), since this requires only direct β-arrestin coupling. This aberrant signalling mechanism is responsible for the role of these receptors as ligand scavengers, as the internalisation of the ligand/receptor complex mediates degradation of the cargo and recycling of the empty receptor to the plasma membrane, where new cycles of scavenging can take place[62,63].

Chemokine ligands are classified into the CXC, CC, XC (or C) and CX3C subfamilies, according to the arrangement of four conserved cysteine residues, which are important for maintenance of their tridimensional structure[64,65]. In mammals as in teleost fish, the CXC and the CC families are the two largest subfamilies, whereas the CX3C and C families only contain few members (**Table 1**). In zebrafish, another fish-specific chemokine subfamily was also identified, namely CX chemokines. These CX chemokines lack one of the two conserved cysteine residues in the N-terminus but retain the third and the

fourth. This distinguishes them from the XC subfamily chemokines, which only retain the second and fourth of the signature cysteine residues[14].

CCR	CCL	Function	Specificity	Significance of the axis in TB
CCR1	CCL3-3L1-5-6*-7-8-9*-13-14-15-16-23	Inflammatory	M(Φ) , DC, B, T, mast cells, basophils, eosinophils	-
CCR2	CCL2-7-8-11-12*-13-16	Inflammatory	M(Φ), DC, T , NK	Controversial. Recruitment of M(ϕ) and DCs via CCR2 permitted better containment of high *Mtb* doses when injected intravenously. However, *CCR2* KO mice were indistinguishable from wt when exposed to lower doses, most likely due to compensations.
CCR3	CCL3L1-5-7-8-11-13-14-15-24-26-28	Inflammatory	T, eosinophils	-
CCR4	CCL2-4-3-5-17-22	Dual	M(Φ), DC, T, NK, NKT, basophils	Controversial. Differential recruitment/priming of T cells and iNKT evoked increased susceptibility of *CCR4* KO mice to *M. bovis*-BCG. However, no impairment was found in *CCR4* KO animals when exposed to low *Mtb* doses.
CCR5	CCL3-3L1-4-5-8-11-13-14-16	Inflammatory	M(Φ), microglia, DC, eosinophils,	Controversial. Pathology of *CCR5* KO mice was indistinguishable from that of wt, most likely due to compensation by CCR1. However, studies performed with *CCL5* KO animals suggest a beneficial effect of this axis early after exposure with low infection dose.
CCR6	CCL20-21	Dual	DC, B, T, NKT	Impaired recruitment of iNKT and T cells in *CCR6* KO mice increased susceptibility to *M. bovis*-BCG. Follow-up experiments with *Mtb* still necessary.
CCR7	CCL19-21	Homoeostatic	DC, B, T	Beneficial. Reverse migration of DCs to the draining lymph nodes is delayed in *CCR7* KO animals, which delays activation of T cell-mediated response against *Mtb*.
CCR8	CCL1-4-16-18	Dual	DC, B, T, NK	-
CCR9	CCL25	Homoeostatic	T	-
CCR10	CCL27-28	Homoeostatic	B, T, eosinophils	-

Table 1. Mammalian chemokine axes, and their roles in tuberculosis as emerging from murine knockout (KO) studies *(continued on the next page)*. B: B-lymphocytes; T: T-lymphocytes; M(Φ): monocyte/macrophages; NΦ: neutrophils; DC: dendritic cells, NK: natural killers; NKT: natural killer T cells. Underlined names indicate the existence of zebrafish orthologues, based on synteny and sequence alignment. * CCL6-9-12 and CXCL15 are absent in humans but present in rodents.

CXCR	CXCL	Function	Specificity	Significance of the axis in TB
CXCR1	CXCL6-7-8	Inflammatory	NΦ,	-
CXCR2	CXCL1-2-3-5-6-7-8	Inflammatory	NΦ, NK	Detrimental. *CXCR2* KO animals presented reduced lung pathology, due to contained Nϕ infiltration, which limited inflammation.
CXCR3	CXCL4-4L1-9-10-11-13	Dual	M(Φ), microglia, T, NK	Detrimental. *CXCR3* KO mice displayed attenuated lung pathology, attributed to differential T cell priming.
CXCR4	CXCL12-14	Homoeostatic	M(Φ), B, T	KO not available, since embryonic lethal.
CXCR5	CXCL13	Homoeostatic	B, T	Beneficial. Aberrant recruitment of lymphocytes limited *Mtb* control in *CXCR5* KO mice.
CXCR6	CXCL16	Dual	B, NKT	-
-	CXCL15*	Inflammatory	NΦ	-
CXCR8 (GPR35)	CXCL17	Homoeostatic	M(Φ), DC	-

CX3CR/XCR	CX3CL/XCL	Function	Specificity	Significance of the axis in TB
CX3CR1	CX3CL1, CCL26	Inflammatory	M(Φ), microglia, DC, T	Dispensable. Following low-dose aerosol challenge with *Mtb*, *CX3CR1* KO mice were indistinguishable from wt in terms of survival and infection burden.
XCR1	XCL1-2	Dual	T	-

ACKR	ACKRL	Function	Specificity	Significance of the axis in TB
DARC (ACKR1)	CCL1-2-5-7-8-11-13-14-16-17-18, CXCL1-2-3-5-6-7-8-9-10-11-13	Atypical	ligand scavenger	-
D6 (ACKR2)	CCL2-3-3L1-4-4L1-5-7-8-11-12-13-14-17-22-23-24-26	Atypical	ligand scavenger	Beneficial. *D6* KO mice are highly susceptible to low doses of *Mtb*. The phenotype is linked to an increased number of M(Φ)s, DCs and T cells infiltrating the infected tissues.
CXCR7 (ACKR3)	CXCL11-12	Atypical	ligand scavenger/ gradient control	KO not available, since lethal *in utero*.
CCRL1 (ACKR4)	CCL19-21-25, CXCL13	Atypical	ligand scavenger	-
CCRL2 (ACKR5)	CCL2-19	Atypical	ligand scavenger	-
PITPNM3 (ACKR6)	CCL18	Atypical	ligand scavenger	-

Table 1. Mammalian chemokine axes and their implication in tuberculosis as emerging from murine knockout (KO) studies *(continued from the previous page)***.**

In mammals, CXC chemokines can be further divided into ELR and non-ELR chemokines, based on the presence of the ELR (Glu-Leu-Arg) motif upstream of their CXC motif[64]. In these species, the presence of the ELR motif distinguishes neutrophil-competent chemokines (ELR-positive) from non-neutrophil-competent chemokines (ELR-negative), which attract other myeloid and lymphoid cells (monocyte/macrophages, lymphocytes, dendritic cells and natural killer cells)[66,67] (**Table 1**). Mammalian ELR+ chemokines are CXCL1-2-3-5-6-7-8-15. These act mostly through receptors CXCR1-2. ELR− chemokines include CXCL4-9-10-11-12-13-14-16-17 and interact with receptors CXCR3-4-5-6-8. In fish, the ELR motif is not conserved and is not essential for the attraction of neutrophils by fish neutrophil-chemotactic chemokines[68].

The chemokine receptors are also classified in subgroups, namely CXCR, CCR, XCR or CX3CR, depending on the ligands that they can bind (**Table 1**)[64,65]. A CXR family (which should bind the zebrafish-specific CX chemokines) has not been identified and the interacting partners of CXL ligands remain unknown[14]. In addition to classical chemokine receptors, a new group of receptors (or more precisely, interceptors) has been introduced to include non-classical chemokine receptors. This group phylogenetically belongs to the same protein family, but differs functionally, due to the inability to mediate classical GPCR signal transduction by coupling with G-proteins. This heterogeneous group of "decoy" receptors mostly act as broad spectrum ligand scavengers and are designated as atypical chemokine receptors or ACKR[69]. Most atypical receptors lack or display an altered E/DRY (Glu/Asp-Arg-Tyr) motif, which is key to couple 7TM receptors with G-proteins and mediate classical signalling (**Figure 1**).

Chemokines can be functionally classified as homoeostatic (or constitutive) or inflammatory according to the regulation and pattern of their expression[65]. The homoeostatic chemokines are generally expressed by a variety of tissues in physiological situations, while the expression of inflammatory chemokines requires inflammation/exposure to pathogens. However, this classification is not strict and many chemokines (e.g. CXCL9-10-11) exert a dual function, by controlling both physiological and pathological responses (**Table 1**).

The number of chemokines identified and characterised has expanded rapidly in the past decades, both for human and animal models[65]. In humans, 25 chemokine receptors (including ACKRs, **Table 1**) and 45 chemokine ligands have been identified, while in zebrafish at least 36 putative chemokine receptors and 75 putative chemokine ligands have been mapped[65]. Studies have revealed high levels of redundancy in the function and expression patterns of both chemokines and chemokine receptors[41]. Several receptors bind multiple chemokines and several chemokines can also bind to more than one receptor (**Table 1**). During infection/inflammation and development, a variety of chemokine ligands can be expressed at a specific site and multiple chemokine receptors can be expressed by the chemoattracted cells. Taken together, chemokine ligands and receptors can be highly synergistic, complementary or, in some cases, even antagonistic[41,42]. Due to this complexity, it is very difficult to accurately assess to what extent the chemokine axes are really redundant. Current understanding of the roles and dynamics of each chemokine in the complexity of an *in vivo* system is also incomplete. Therefore, the evolutionary, functional and regulative forces, that permitted expansion and radiation of diverse chemokine ligand and receptor lineages, remain largely unknown[65].

Homologies between the chemokine signalling axes of human and zebrafish

While most of the ligand-receptor interacting partners have been identified in human and mammalian models, functional roles in zebrafish are only beginning to be examined[70]. At transcriptional level, several zebrafish chemokines have been found to be expressed in discrete areas/organs and tissues (homoeostatic) and others were found to be highly responsive to inflammation (inflammatory), like in humans[14,71,72,73,74]. In a recent review on the translational value of zebrafish and other teleosts to study chemokine functions[70], it was reported that only one CCL chemokine axis has been currently shown to have clear *in vivo* functional homologies with the human and mammalian system. In this study, the zebrafish Ccl25a gene was found essential for normal T cell lymphotaxis to the thymus[73].

While the CCL ligand family is more divergent between mammals and teleosts, the CXCL family is much better conserved. For example, 11 canonical CXCRs and 20 CXCLs can be currently identified in zebrafish, versus 7 CXCRs and 17 CXCLs described in humans[14]. Several true homologies between zebrafish and mammals (corroborated by sequence alignments, synteny studies and functional analyses) have been demonstrated for CXC axes. As described in this thesis (**Chapter 3**), the CXCR3/CXCL9-10-11 axis exists in zebrafish. On the ligand side, a cluster of seven CXCL11-like tandem-duplicated genes have been identified. Some of these genes are infection-inducible, similar to their mammalian counterpart, and we showed that two of the CXCL11-like chemokines encoded by these infection-inducible genes signal via an orthologue of CXCR3, the zebrafish receptor Cxcr3.2 (**Chapter 3-4**). The *CXCR3* gene is also duplicated in zebrafish and two paralogues of *cxcr3.2* exist, namely *cxcr3.1* and *cxcr3.3*. In zebrafish embryos and larvae the *cxcr3.2* and *cxcr3.3* genes are expressed by macrophages and neutrophils (**Chapter 3**), while the expression of *cxcr3.1* is very low in these cells. Preliminary data suggest that *cxcr3.1* is detectable at higher levels than the other two orthologues in *lck*$^{+}$ cells (immature T cells)[75]. Therefore, it is possible that the three isoforms regulate chemotaxis of different cell types and represent sub-functionalisation of the mammalian CXCR3 that is expressed by both myeloid and lymphoid leukocytes (T cells, natural killer cells, dendritic cells, macrophages and microglial cells). However, this remains speculative, since the expression patterns remain to be further examined in adult zebrafish. The function of Cxcr3.3 has not been yet elucidated. However, as described in **Chapter 5**, *cxcr3.3* genes exist exclusively in fish and in most cases they present peculiar sequence adaptations, including disruption of the E/DRY-motif consensus, that suggest atypical functions.

Two clear orthologous CXCL12/CXCR4 axes have also been reported in zebrafish and extensive functional studies have been performed for both systems[72,76,77,78,79] (**Chapter 6**). Both CXCL12 and CXCR4 are in fact duplicated in fish (Cxcl12a/b and Cxcr4a/b). Cxcr4a and Cxcr4b are mostly expressed in separate tissues and cell types, which corroborates the hypothesis that after gene duplication the two receptors have divided functions between the two copies[80]. It appears that Cxcr4a evokes more potent responses via Cxcl12b while Cxcr4b predominantly signals via Cxcl12a, however, cross-reactivity has also been described[81]. Importantly, it has been demonstrated that cross-communication between the zebrafish and human ligands and receptors takes place, supporting the translational value of the zebrafish model[40]. The mammalian CXCL12 and either one or both of the zebrafish counterparts, Cxcl12a/b, are chemotactic for endothelial cells, haematopoietic progenitor cells, lymphocytes and several

other types of leukocytes. In agreement with their more homoeostatic function, these axes were implicated in the development of morphogenetic/organogenetic programs, such as the formation of blood and lymphatic vessels, the migration of germ cells and of the lateral line primordium, the organisation and patterning of the nervous system and the homing of haematopoietic stem cells[72,76,79,82,83]. The axis (mostly the Cxcr4b/Cxcl12a paralogue axis) has also been shown to play a crucial function during inflammatory responses, for example, promoting the metastatic behaviour of CXCR4-positive cancer human-xenotransplants[40]. Notably in both mammalian models and in zebrafish, this axis is regulated by the activity of the atypical chemokine receptor CXCR7/ACKR3, which acts as a Cxcl12 ligand scavenger to maintain an efficient formation of ligand gradient and facilitate cell migration[76].

At least 2 *cxcl8* genes were identified and characterised in zebrafish, which are both induced by inflammation, wounding and infection. Similar to the human CXCL8 (IL8), the zebrafish paralogues are potent neutrophil chemoattracts via the Cxcr2 receptor, although in contrast to humans, expression of Cxcr1 alone does not seem to permit any significant Cxcl8-dependent recruitment[84,85,86,87]. In mammals, CXCR2 is highly promiscuous and can respond to a range of CXC-chemokines (**Table 1**). Therefore, it is likely that multiple ligands also exist for this receptor in zebrafish. As indicated in this thesis (**Chapter 7**), the zebrafish-specific chemokine Cxcl18b also partly requires signalling via Cxcr2, and not Cxcr1, to evoke optimal recruitment of neutrophils.

Chemokine function in mycobacterial diseases

Since chemokines and chemokine receptors direct cells to specific sites within the tissues, these molecules may be highly relevant for the progression of TB and granuloma formation, for example by directly controlling the cellular trafficking at the granuloma. There have been a variety of studies aimed at characterising expression of chemokines in response to *Mtb in vitro* and *in vivo*. *Mtb* is a strong inducer of chemokine expression. Following *Mtb* infection of human or mice macrophages *in vitro,* these cells exhibit rapid expression of many chemokines, detectable as early as 2 hours post-infection[88,89]. Mammalian macrophages can produce the chemokines CCL2-3-4-5-7-12, CXCL2-9-10-11, and CX3CL1 with a response that, in many cases, depends on the pathogen virulence[90,91,92,93,94,95,96,97]. The cell wall components of mycobacteria are considered crucial for chemokine induction, as the production of several chemokines is significantly reduced following exposure to wall-deficient mycobacteria[97]. Macrophages are not the only cells inducing expression of chemokines upon *Mtb* infection. Chemokine expression is also induced in cells intrinsic to tissue surrounding the infection and other attracted leukocytes[88,98]. Expression of CCL2 and CXCL5-8-9-10-11 was detected in human or murine epithelial cells in response to virulent strains of *M. tuberculosis*[98,99,100,101]. Circulating granulocytes from TB patients produced high levels of CCL2-3 and CXCL1-8[102,103], bronchoalveolar lavage of patients displayed elevated levels of CCL2-5-7-12, CXCL8-10[90,104,105] and plasma/serum level of CCL4-11-24-26 and CXCL10 were also found increased[106,107,108]. Two other studies that profiled gene expression of *Mtb*-infected murine and non-human-primate lungs described overall upregulation of CXCL1-2-3-5-9-10-11-13 and CCL2-3-4-5-7-8-12-19-20[98,109,110]. Recent studies also revealed that, in TB of the central nervous system (TB meningitis), microglia (specialised macrophages residing in the brain) can also produce several chemokines, including CCL2-5 and CXCL10[111]. These studies indicate that a variety of cells participate in generating chemotactic/chemokinetic

cues in response to mycobacteria (**Figure 2**). Regarding the specificity of recruited cells, the chemokines reported are known to induce mobilisation of diverse types of cells (monocyte/macrophages, neutrophils, eosinophils, T cells, natural killer cells, dendritic cells, and others) according to the expression pattern of their receptor counterparts on target cells (**Table 1**, **Figure 2**)[41,42,65].

Regulation of the expression of signals inducing chemokine ligands still requires complete characterisation, as much in TB as in other physiological and pathological contexts. Chemokines are regulated by many cytokines and infection-related products. There is evidence for example that IFNγ, TNFα and *Mtb*-components can induce expression of chemokines (**Figure 2**). Expression of chemokines by macrophages appears to be highly influenced by TNFα production, which controls CCL2-5 and CXCL9-10-11[112.] TNFα is produced by macrophages themselves in response to *Mtb* infection and blockade of TNFα signalling can attenuate chemokine production. Notably, CXCL9-10-11, which are generally regarded as IFNγ inducible chemokines, were also found to be induced by TNFα during mycobacterial infection[112,113]. However, IFNγ itself is also found increased in TB patients and TNFα/IFNγ may synergise to induce these and other chemokines.

While expression of chemokines is increased by *Mtb* infection, the expression of chemokine receptors remains much more stable. However, transcriptional profiling of the murine lung revealed a general upregulation of CXCR3-6 and of CCR1-5-9[98,110]. Clinically relevant might be also the fact that monocytes increase expression of CCR5 and CXCR4 (HIV co-receptors) in response to intracellular *Mtb*, which may result in increased infectivity of HIV in cases of *Mtb*/HIV co-infections[114,115]. In another study, dendritic cells having taken up *Mtb* were found to upregulate CCR7, which induces their reverse migration from the infection focus to the draining lymph nodes (expressing its ligands CCL19-21) and permits a faster priming of the T cell-mediated adaptive immunity[116,117]. Similarly, upon recruitment to the lung, T cells upregulate CXCR3 and CCR5 receptors. However, this upregulation maintains them at the infected locus, since high levels of CXCR3 and CCR5 ligands are produced at the lesion[118].

Leprosy represents another relevant mycobacterial disease, caused by the species *Mycobacterium leprae*. The disease, which essentially affects the skin and the peripheral nervous system, is still endemic in several developing countries, where it represents a relevant cause of permanent disability[119]. Leprosy manifests itself in two main polarised forms, namely lepromatous leprosy and tuberculoid leprosy. Lepromatous leprosy is characterised by exuberant bacillary replication and failure of T-helper 1 activation (which is essential to counteract the pathogen). Conversely, tuberculoid leprosy, is characterised by reduced count of bacilli, expression of T-helper 1 cytokines and is generally restricted to delimited skin lesions. Compared to TB, leprosy still remains poorly understood, for several limitations, which include the scarce cultivability in axenic conditions[120,121,122] and the limited availability of animal models[123,124]. However, several studies have demonstrated that expression levels of different chemokines, including CXCL8-9-10 and CCL2-3-7, are sensitive to leprosy infection[125,126,127,128,129]. Notably, recent studies have also demonstrated that the expression of several chemokine ligands and receptors can be specifically correlated with the different manifestations of leprosy.

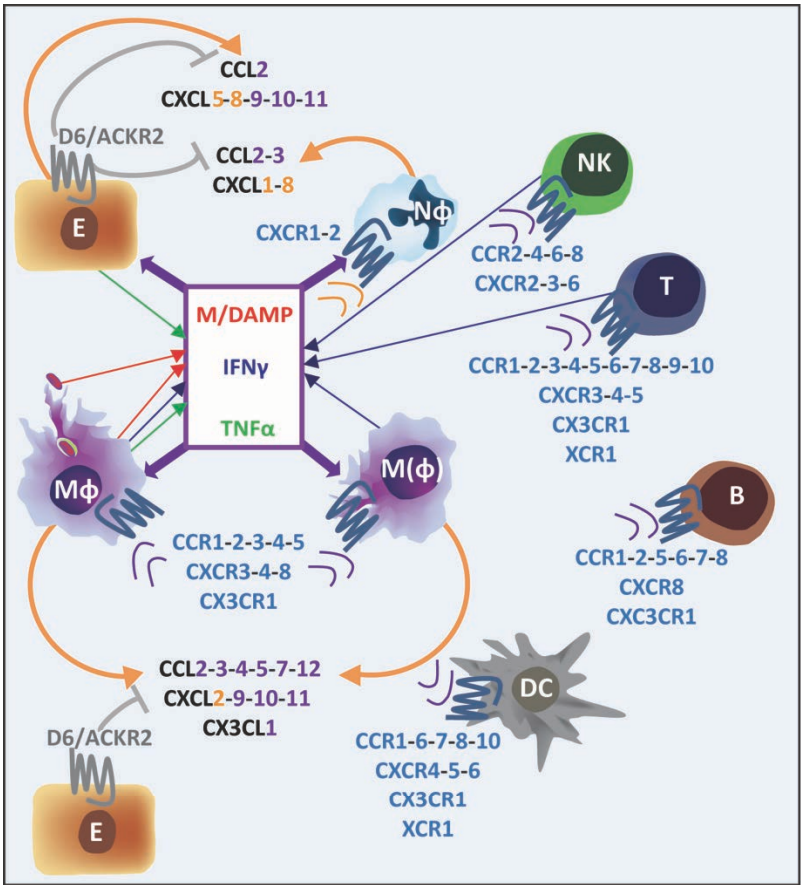

Figure 2. Schematic representation of main chemokine ligands and receptors implicated in the response to mycobacterial infection. Infected macrophages (MΦ) and epithelial/endothelial cells (E) respond to microbe/damage-associated molecular patterns (M/DAMPs and red arrows) by producing cytokines and several chemokines, including interferon γ (IFNγ and blue arrows), tumour necrosis factor α (TNFα and green arrows), CCL2-3-4-5-7-12, CXCL1-2-5-8-9-10-11 and CX3CL1 (orange arrows). TNFα and IFNγ can act on other cells in the surrounding microenvironment (initially, mainly monocyte/macrophages, epithelial, endothelial, stromal cells and neutrophils) and stimulate the production of more chemokines. Different types of leukocytes express different kinds of chemokine receptors (blue names) and, depending on their ligand specificity, these receptors mediate chemotaxis of leukocytes to the initial infection focus. CXCL1-2-5-8 (orange names) are mostly chemotactic towards neutrophils (NΦ), while other chemokines, such as CCL2-3-4-5-7-11, CXCL9-10-11 and CX3CL1 (violet names) are chemotactic towards monocyte/macrophages (M(Φ)), dendritic cells (DCs), T, B and/or natural killer (T, B, NK) cells. Antigen presenting activity by M(Φ) and DCs, will support activation of adaptive B and T cell-mediated immune responses. Additionally activated NK and T cells will produce high levels of inflammatory cytokines (especially IFNγ), which will sustain further stimulation of the innate immune cells and additional release of inflammatory chemokines, which in turn will support supplementary infiltration of leukocytes. The atypical chemokine receptor D6/ACKR2 (grey) is also upregulated in the cells surrounding the infection site and exerts a scavenging activity against a wide spectrum of CC-cytokines, contributing to tight control of chemokine levels. Ultimately these forces permit aggregation of immune cells at the infection focus and contribute to the formation of tubercular granulomas.

In particular, it was identified that expression of CCL17 or CCL18 are either correlated to the lepromatous (CCL18) or to the tuberculoid (CCL17) form[130], and that the expression levels of both CXCR3 and its ligand CXCL10 can be used as indicator of leprosy type 1 reaction, a severe complication of leprosy, characterised by acute activation of the cell-mediated immune response with consequent inflammation and nerve damage[131].

In vivo analysis of chemokine axes in murine TB models

While large amounts of data are available from *in vitro* studies, the expression and relevance of chemokines have only been characterised to a limited degree *in vivo* and the real meaning of these molecules for the pathology of TB remains elusive and speculative in several cases (**Table 1**). Using knockout murine models it was shown that CCR2 and its ligand CCL2 are essential for migration of macrophages and dendritic cells to the lungs and to control infection[92,94]. However, the susceptibility of these mice was found to be dose-dependent, since these animals were highly susceptible to a moderate or high dose of *Mtb* administered intravenously, but did not have increased bacterial loads compared to wildtypes (wt) when exposed to low dose aerosol or intravenous infection[132,133]. Another controversial finding came from the study of a *CCR4* knockout (KO). In a model of acute *M. bovis*-BCG pulmonary infection, these animals exhibited higher susceptibility and increased bacterial burden. However, a follow-up study showed that *CCR4*$^{-/-}$ mice were not more susceptible to low dose of *Mtb* infection[110,134]. *CCR6* mutants also displayed increased susceptibility to *M. bovis*[135], but studies with *Mtb* are still necessary. The function of CCR5 signalling is also controversial; an initial study in *CCR5*$^{-/-}$ mice reported no difference in the bacterial burden evoked by *Mtb*[136] and suggested that another receptor, such as CCR1 (which can bind the same ligands of CCR5, including CCL3-5), could compensate for CCR5 loss. Another study performed with *CCL5* mutant mice with low dose aerosol infection, revealed instead an increased bacterial burden early after infection. In this study, recruitment of immune cells via CCL5 was predominantly evoked by CCR5, suggesting that compensation may occur at later time points but that CCR5 and CCR1 are not entirely redundant early after infection[137]. Furthermore, in the *CCR2*$^{-/-}$ mice studies described above, it was reported that while the number of macrophages migrating to the infection is initially lower, new cohorts of monocyte/macrophages can still be recruited at later time points. It was hypothesised that the initial increased burden in these animals evokes a higher upregulation of other chemokines in a second phase, which still sustains infiltration of immune cells and formation of granulomas[92,94]. These examples illustrate well the difficulties that can be experienced when addressing chemokine function *in vivo*.

A murine model was also employed to study the function of CXCR3 and its ligands CXCL9-10-11 during *Mtb* infection. A beneficial effect of *CXCR3* mutation was observed, with associated decrease in number, size and density of granulomas[110,138]. Unexpectedly, the recruitment of T cells was increased, rather than diminished in *CXCR3* mutants, and the improved resistance of *CXCR3*-deficient mice was attributed to the function of CXCR3 in T-cell priming, rather than T-cell recruitment[138,139]. Mice deficient for either *CXCR2* or its ligand *CXCL5* had reduced lung pathology in comparison to their wt counterparts, and this phenotype was linked to a reduced accumulation of neutrophils in the mutants and to decreased detrimental neutrophil-dependent inflammation[101]. CXCL8, one of the most potent chemoattractants for neutrophils in humans, which is abundantly expressed upon *Mtb* infection, is however absent in mice[140], which makes it difficult to exactly address the role of CXCR2-signalling using this model. Finally, a study of *Mtb* infection in a

CX3CR1$^{-/-}$ mouse model, showed that this mutation, while affecting infiltration of different leukocyte subsets, did not lead to protection or increased susceptibility to the pathogen, indicating that this receptor is dispensable[141].

In few cases, specific chemokine axes have been shown to play unique, non-redundant, functions *in vivo*. For example, both receptor and ligand mutants of the *CXCR5*/*CXCL13* pair were shown to display decreased control of *Mtb*, linked to aberrant recruitment of a specific set of CXCR5^{+} lymphocytes[114,115,142]. Similarly, the function of CCR7 in dendritic cell reverse migration to the draining lymph nodes to prime the adaptive immune response was also found to be unique[116,117].

Regarding the relevance of atypical chemokine receptors for the response to mycobacterial infection, a recent study on *D6*/*ACKR2* KO mice showed that these animals are highly susceptible to low dose aerosol exposure to *Mtb*, owing to the increased number of monocyte/macrophages, dendritic cells and T cells infiltrated in the lesioned tissues. Blockade of a wide spectrum of chemokines with a cocktail of antibodies could rescue the phenotype of *D6* deficiency, which suggests that the activity of *D6*/*ACKR2* as a chemokine scavenger receptor is fundamental to maintain a balanced activation of leukocyte recruitment via chemokine signalling[143].

Despite the seemingly large redundancy in function exerted by chemokines in TB suggested by *in vitro* and *in vivo* models, human studies have still shown associations between mutations of multiple chemokine ligands (CCL2-5, CXCL8-10) and TB, indicating that besides the apparent redundancy, several chemokines may have defined roles to play in the pathogenesis of TB which we still do not entirely comprehend[144,145,146,147,148,149,150,151].

Taken together, it has been difficult to dissect the function of chemokine signalling in TB using the mice as an *in vivo* model. This situation may reflect, at least partly, the fact that mice do not represent an ideal model for TB, since *Mtb* is not a natural murine pathogen and infection in mice does not recapitulate the primate pathology. Additionally, the use of the murine-*Mtb* infection model leads to restrictions in terms of research opportunities. *In vivo* imaging and longitudinal studies in rodents require invasive and technically challenging procedures. Furthermore, work with the mouse model imposes severe ethical restrictions, since adult animals must be sacrificed for the experiments or for intra-uterine collection of embryos/foetuses. Moreover, research prospects are severely limited by the use of the *Mtb* pathogen, which represents a serious health risk for the researchers. To circumvent all these difficulties, in this thesis we have exploited the zebrafish-*Mm* natural infection model to evaluate the role of chemokines in mycobacterial infection. Using this surrogate system, we took advantage of its attractive optical and genetic tools to obtain a more dynamic representation of how the chemokine axes calibrate the immune response to mycobacteria.

Contribution of this thesis: a brief outline

In this thesis, we applied the zebrafish (*Danio rerio)-Mycobacterium marinum* natural infection model to obtain novel insights into the dynamic processes underlying host-pathogen interactions and, in particular, to dissect how chemokines, a class of small chemotactic proteins, orchestrate the response of immune cell types to mycobacterial

infection. Several chemokine axes are conserved from fish to mammals and the similarities between human-*M. tuberculosis* and zebrafish-*M. marinum* pathology are remarkable. These two aspects, together with the excellent possibilities for intravital imaging provided by zebrafish transparency, have enabled us to study more dynamically chemokine-dependent processes in an *in vivo* context and allowed us to dissect how these axes are implicated in defined spatio-temporal windows of mycobacterial disease.

The work presented in this thesis has helped to elucidate the function of several chemokine axes in mycobacterial disease, and contributed to interpret the translational impact of the zebrafish model for biomedical research. This chapter (**Chapter 1**) introduces the chemokine signalling system and the current knowledge of its role in tuberculosis from *in vitro* and murine studies. **Chapter 2** elaborates on the translational value of the zebrafish model and reviews how the application of this model has advanced our understanding of host-pathogen interactions for different infectious diseases. **Chapter 3** and **Chapter 4** dissect the function of the chemokine receptor Cxcr3.2 and of its ligands Cxcl11aa and Cxcl11af during the response to mycobacterial infection, expanding on the effects of this signalling system for both direct chemotaxis of macrophages and control of their intrinsic microbicidal competence against mycobacteria. **Chapter 5** describes the generation and initial characterisation of a *cxcr3.3* mutant zebrafish line and explores the possibility of atypical receptor crosstalk at play between Cxcr3.3 and Cxcr3.2. **Chapter 6** presents the importance of the homoeostatic chemokine receptor Cxcr4b in order to sustain a pro-granuloma angiogenetic programme. In **Chapter 7** we characterised the function of the chemokine ligand Cxc18b, a fish-specific inflammatory chemokine that, similarly to Cxcl8, exerts a neutrophil-specific chemotactic activity, at least partly via Cxcr2. Finally, **Chapter 8** summarises and contextualises the findings of this thesis in relation to the current scientific literature.

Due to the high redundancy of chemokines and to the practical limitations when attempting to study tuberculosis in a murine system, the use of a zebrafish platform to address chemokine signalling during mycobacterial pathogenesis promises to greatly contribute to our understanding of the actual *in vivo* significance of these multifaceted signalling systems.

REFERENCES

1 Grunwald DJ, Eisen JS. Headwaters of the zebrafish -- emergence of a new model vertebrate. Nat Rev Genet. 2002 Sep;3(9):717-24.
2 Streisinger G, Walker C, Dower N, Knauber D, Singer F. Production of clones of homozygous diploid zebra fish (Brachydanio rerio). Nature. 1981 May 28;291(5813):293-6.
3 Amsterdam A. Insertional mutagenesis in zebrafish. Dev Dyn. 2003 Nov;228(3):523-34.
4 Busch-Nentwich E, Kettleborough R, Dooley CM, Scahill C, Sealy I, White R, Herd C, Mehroke S, Wali N, Carruthers S, Hall A, Collins J, Gibbons R, Pusztai Z, Clark R, Stemple DL. Sanger Institute Zebrafish Mutation Project mutant data submission. ZFIN Direct Data Submission. 2013.
5 Meeker ND, Trede NS. Immunology and zebrafish: spawning new models of human disease. Dev Comp Immunol. 2008;32(7):745-57.
6 Torraca V, Cui C, Boland R, Bebelman JP, van der Sar AM, Smit MJ, Siderius M, Spaink HP, Meijer AH. The CXCR3-CXCL11 signaling axis mediates macrophage recruitment and dissemination of mycobacterial infection. Dis Model Mech. 2015 Mar;8(3):253-69.
7 Jao LE, Wente SR, Chen W. Efficient multiplex biallelic zebrafish genome editing using a CRISPR nuclease system. Proc Natl Acad Sci U S A. 2013 Aug 20;110(34):13904-9.

8 Hwang WY, Fu Y, Reyon D, Maeder ML, Tsai SQ, Sander JD, Peterson RT, Yeh JR,Joung JK. Efficient genome editing in zebrafish using a CRISPR-Cas system. Nat Biotechnol. 2013 Mar;31(3):227-9.
9 Auer TO, Del Bene F. CRISPR/Cas9 and TALEN-mediated knock-in approaches in zebrafish. Methods. 2014 Sep;69(2):142-50.
10 Rougeot J, Zakrzewska A, Kanwal Z, Jansen HJ, Spaink HP, Meijer AH. RNA sequencing of FACS-sorted immune cell populations from zebrafish infection models to identify cell specific responses to intracellular pathogens. Methods Mol Biol. 2014;1197:261-74.
11 North TE, Goessling W, Walkley CR, Lengerke C, Kopani KR, Lord AM, Weber GJ, Bowman TV, Jang IH, Grosser T, Fitzgerald GA, Daley GQ, Orkin SH, Zon LI. Prostaglandin E2 regulates vertebrate haematopoietic stem cell homeostasis. Nature. 2007 Jun 21;447(7147):1007-11.
12 Cutler C, Multani P, Robbins D, Kim HT, Le T, Hoggatt J, Pelus LM, Desponts C, Chen YB, Rezner B, Armand P, Koreth J, Glotzbecker B, Ho VT, Alyea E, Isom M, Kao G, Armant M, Silberstein L, Hu P, Soiffer RJ, Scadden DT, Ritz J, Goessling W, North TE, Mendlein J, Ballen K, Zon LI, Antin JH, Shoemaker DD. Prostaglandin-modulated umbilical cord blood hematopoietic stem cell transplantation. Blood. 2013 Oct 24;122(17):3074-81.
13 Kanwal Z, Wiegertjes GF, Veneman WJ, Meijer AH, Spaink HP. Comparative studies of Toll-like receptor signalling using zebrafish. Dev Comp Immunol. 2014 Sep;46(1):35-52.
14 Nomiyama H, Hieshima K, Osada N, Kato-Unoki Y, Otsuka-Ono K, Takegawa S, Izawa T, Yoshizawa A, Kikuchi Y, Tanase S, Miura R, Kusuda J, Nakao M, Yoshie O. Extensive expansion and diversification of the chemokine gene family in zebrafish: identification of a novel chemokine subfamily CX. BMC Genomics. 2008 May 15;9:222
15 Rytkönen KT, Akbarzadeh A, Miandare HK, Kamei H, Duan C, Leder EH, Williams TA, Nikinmaa M. Subfunctionalization of cyprinid hypoxia-inducible factors for roles in development and oxygen sensing. Evolution. 2013 Mar;67(3):873-82.
16 Carvalho R, de Sonneville J, Stockhammer OW, Savage ND, Veneman WJ, Ottenhoff TH, Dirks RP, Meijer AH, Spaink HP. A high-throughput screen for tuberculosis progression. PLoS One. 2011 Feb 16;6(2):e16779.
17 Takaki K, Cosma CL, Troll MA, Ramakrishnan L. An in vivo platform for rapid high-throughput antitubercular drug discovery. Cell Rep. 2012 Jul 26;2(1):175-84.
18 Ordas A, Raterink RJ, Cunningham F, Jansen HJ, Wiweger MI, Jong-Raadsen S, Bos S, Bates RH, Barros D, Meijer AH, Vreeken RJ, Ballell-Pages L, Dirks RP, Hankemeier T, Spaink HP. Testing tuberculosis drug efficacy in a zebrafish high-throughput translational medicine screen. Antimicrob Agents Chemother. 2015 Feb;59(2):753-62.
19 Hisano Y, Sakuma T, Nakade S, Ohga R, Ota S, Okamoto H, Yamamoto T, Kawahara A. Precise in-frame integration of exogenous DNA mediated by CRISPR/Cas9 system in zebrafish. Sci Rep. 2015 Mar 5;5:8841.
20 Ablain J, Zon LI. Tissue-specific gene targeting using CRISPR/Cas9. Methods Cell Biol. 2016;135:189-202.
21 Mizgirev I, Revskoy S. Generation of clonal zebrafish lines and transplantable hepatic tumors. Nat Protoc. 2010 Mar;5(3):383-94.
22 Ramakrishnan L. Revisiting the role of the granuloma in tuberculosis. Nat Rev Immunol. 2012 Apr 20;12(5):352-66.
23 Global tuberculosis report 2015, World Health Organisation (WHO).
24 Kulchavenya E. Extrapulmonary tuberculosis: are statistical reports accurate? Ther Adv Infect Dis. 2014 Apr;2(2):61-70.
25 Prouty MG**,** Correa NE, Barker LP, Jagadeeswaran P, Klose KE. Zebrafish-Mycobacterium marinum model for mycobacterial pathogenesis. FEMS Microbiol Lett. 2003 Aug 29;225(2):177-82.
26 Swaim LE, Connolly LE, Volkman HE, Humbert O, Born DE, Ramakrishnan L. Mycobacterium marinum infection of adult zebrafish causes caseating granulomatous tuberculosis and is moderated by adaptive immunity. Infect Immun. 2006 Nov;74(11):6108-17. Erratum in: Infect Immun. 2007 Mar;75(3):1540.
27 Parikka M, Hammarén MM, Harjula SK, Halfpenny NJ, Oksanen KE, Lahtinen MJ, Pajula ET, Iivanainen A, Pesu M, Rämet M. Mycobacterium marinum causes a latent infection that can be reactivated by gamma irradiation in adult zebrafish. PLoS Pathog. 2012 Sep;8(9):e1002944.
28 Ramakrishnan L. The zebrafish guide to tuberculosis immunity and treatment.Cold Spring Harb Symp Quant Biol. 2013;78:179-92.
29 Cronan MR, Tobin DM. Fit for consumption: zebrafish as a model for tuberculosis. Dis Model Mech. 2014 Jul;7(7):777-84.
30 van Leeuwen LM, van der Sar AM, Bitter W. Animal models of tuberculosis: zebrafish. Cold Spring Harb Perspect Med. 2014 Nov 20;5(3):a018580.
31 Meijer AH. Protection and pathology in TB: learning from the zebrafish model. Semin Immunopathol. 2016 Mar;38(2):261-73.

32 Cambier CJ, Takaki KK, Larson RP, Hernandez RE, Tobin DM, Urdahl KB, Cosma CL, Ramakrishnan L. Mycobacteria manipulate macrophage recruitment through coordinated use of membrane lipids. Nature. 2014 Jan 9;505(7482):218-22.
33 Oehlers SH, Cronan MR, Scott NR, Thomas MI, Okuda KS, Walton EM, Beerman RW, Crosier PS, Tobin DM. Interception of host angiogenic signalling limits mycobacterial growth. Nature. 2015 Jan 29;517(7536):612-5.
34 Gordon RJ, McGregor AL, Connor B. Chemokines direct neural progenitor cell migration following striatal cell loss. Mol Cell Neurosci. 2009 Jun;41(2):219-32.
35 Cyster JG, Ngo VN, Ekland EH, Gunn MD, Sedgwick JD, Ansel KM. Chemokines and B-cell homing to follicles. Curr Top Microbiol Immunol. 1999;246:87-92; discussion 93.
36 Mehrad B, Keane MP, Strieter RM. Chemokines as mediators of angiogenesis. Thromb Haemost. 2007 May;97(5):755-62.
37 Perlin JR, Talbot WS. Signals on the move: chemokine receptors and organogenesis in zebrafish. Sci STKE. 2007 Aug 21;2007(400):pe45.
38 Bondar C, Araya RE, Guzman L, Rua EC, Chopita N, Chirdo FG. Role of CXCR3/CXCL10 axis in immune cell recruitment into the small intestine in celiac disease. PLoS One. 2014 Feb 20;9(2):e89068.
39 Monin L, Khader SA. Chemokines in tuberculosis: the good, the bad and the ugly. Semin Immunol. 2014 Dec;26(6):552-8.
40 Tulotta C, Stefanescu C, Beletkaia E, Bussmann J, Tarbashevich K, Schmidt T, Snaar-Jagalska BE. Inhibition of signaling between human CXCR4 and zebrafish ligands by the small molecule IT1t impairs the formation of triple-negative breast cancer early metastases in a zebrafish xenograft model. Dis Model Mech. 2016 Feb 1;9(2):141-53.
41 Lira SA, Furtado GC. The biology of chemokines and their receptors. Immunol Res. 2012 Dec;54(1-3):111-20.
42 Kunkel SL, Strieter RM, Lindley IJ, Westwick J. Chemokines: new ligands, receptors and activities. Immunol Today. 1995 Dec;16(12):559-61.
43 Kolakowski LF Jr. GCRDb: a G-protein-coupled receptor database. Receptors Channels. 1994;2(1):1-7.
44Lappano R, Maggiolini M. G protein-coupled receptors: novel targets for drug discovery in cancer. Nat Rev Drug Discov. 2011 Jan;10(1):47-60.
45 Jacobson KA. New paradigms in GPCR drug discovery. Biochem Pharmacol. 2015 Dec 15;98(4):541-55.
46 Li J, Ning Y, Hedley W, Saunders B, Chen Y, Tindill N, Hannay T, Subramaniam S. The Molecule Pages database. Nature. 2002 Dec 12;420(6916):716-7.
47 Kuang Y, Wu Y, Jiang H, Wu D. Selective G protein coupling by C-C chemokine receptors. J Biol Chem. 1996 Feb 23;271(8):3975-8.
48 Curnock AP, Logan MK, Ward SG. Chemokine signalling: pivoting around multiple phosphoinositide 3-kinases. Immunology. 2002 Feb;105(2):125-36.
49 Jones GE, Allen WE, Ridley AJ. The Rho GTPases in macrophage motility and chemotaxis. Cell Adhes Commun. 1998;6(2-3):237-45.
50 Pettit EJ, Fay FS. Cytosolic free calcium and the cytoskeleton in the control of leukocyte chemotaxis. Physiol Rev. 1998 Oct;78(4):949-67.
51 Colvin RA, Means TK, Diefenbach TJ, Moita LF, Friday RP, Sever S, Campanella GS, Abrazinski T, Manice LA, Moita C, Andrews NW, Wu D, Hacohen N, Luster AD. Synaptotagmin-mediated vesicle fusion regulates cell migration. Nat Immunol. 2010 Jun;11(6):495-502.
52 Hall DA, Beresford IJ, Browning C, Giles H. Signalling by CXC-chemokine receptors 1 and 2 expressed in CHO cells: a comparison of calcium mobilization, inhibition of adenylyl cyclase and stimulation of GTPgammaS binding induced by IL-8 and GROalpha. Br J Pharmacol. 1999 Feb;126(3):810-8.
53 Hu XM, Liu YN, Zhang HL, Cao SB, Zhang T, Chen LP, Shen W. CXCL12/CXCR4 chemokine signaling in spinal glia induces pain hypersensitivity through MAPKs-mediated neuroinflammation in bone cancer rats. J Neurochem. 2015 Feb;132(4):452-63.
54 Vlahakis SR, Villasis-Keever A, Gomez T, Vanegas M, Vlahakis N, Paya CV. G protein-coupled chemokine receptors induce both survival and apoptotic signaling pathways. J Immunol. 2002 Nov 15;169(10):5546-54.
55 Locati M, Lamorte G, Luini W, Introna M, Bernasconi S, Mantovani A, Sozzani S. Inhibition of monocyte chemotaxis to C-C chemokines by antisense oligonucleotide for cytosolic phospholipase A2. J Biol Chem. 1996 Mar 15;271(11):6010-6.
56 Sallusto F, Mackay CR, Lanzavecchia A. The role of chemokine receptors in primary, effector, and memory immune responses. Annu Rev Immunol. 2000;18:593-620.
57 Ye RD. Regulation of nuclear factor kappaB activation by G-protein-coupled receptors. J Leukoc Biol. 2001 Dec;70(6):839-48.
58 Liu B, Hassan Z, Amisten S, King AJ, Bowe JE, Huang GC, Jones PM, Persaud SJ. The novel chemokine receptor, G-protein-coupled receptor 75, is expressed by islets and is coupled to stimulation of insulin secretion and improved glucose homeostasis. Diabetologia. 2013 Nov;56(11):2467-76.

59 Mellado M, Rodríguez-Frade JM, Aragay A, del Real G, Martín AM, Vila-Coro AJ, Serrano A, Mayor F Jr, Martínez-A C. The chemokine monocyte chemotactic protein 1 triggers Janus kinase 2 activation and tyrosine phosphorylation of the CCR2B receptor. J Immunol. 1998 Jul 15;161(2):805-13.
60 Steen A, Larsen O, Thiele S, Rosenkilde MM. Biased and G-protein-independent signaling of chemokine receptors. Front Immunol. 2014 Jun 23;5:277.
61 Signoret N, Hewlett L, Wavre S, Pelchen-Matthews A, Oppermann M, Marsh M. Agonist-induced endocytosis of CC chemokine receptor 5 is clathrin dependent. Mol Biol Cell. 2005 Feb;16(2):902-17.
62 Rajagopal S, Kim J, Ahn S, Craig S, Lam CM, Gerard NP, Gerard C, Lefkowitz RJ. Beta-arrestin- but not G protein-mediated signaling by the "decoy" receptor CXCR7. Proc Natl Acad Sci U S A. 2010 Jan 12;107(2):628-32.
63 Borroni EM, Cancellieri C, Vacchini A, Benureau Y, Lagane B, Bachelerie F, Arenzana-Seisdedos F, Mizuno K, Mantovani A, Bonecchi R, Locati M. β-arrestin-dependent activation of the cofilin pathway is required for the scavenging activity of the atypical chemokine receptor D6. Sci Signal. 2013 Apr 30;6(273):ra30.1-11, S1-3.
64 Bacon K, Baggiolini M, Broxmeyer H, Horuk R, Lindley I, Mantovani A, Maysushima K, Murphy P, Nomiyama H, Oppenheim J, Rot A, Schall T, Tsang M, Thorpe R, Van Damme J, Wadhwa M, Yoshie O, Zlotnik A, Zoon K; IUIS/WHO Subcommittee on Chemokine Nomenclature. Chemokine/chemokine receptor nomenclature. J Interferon Cytokine Res. 2002 Oct;22(10):1067-8.
65 Nomiyama H, Osada N, Yoshie O. Systematic classification of vertebrate chemokines based on conserved synteny and evolutionary history. Genes Cells. 2013 Jan;18(1):1-16.
66 Clark-Lewis I, Schumacher C, Baggiolini M, Moser B. Structure-activity relationships of interleukin-8 determined using chemically synthesized analogs. Critical role of NH2-terminal residues and evidence for uncoupling of neutrophil chemotaxis, exocytosis, and receptor binding activities. J Biol Chem. 1991 Dec 5;266(34):23128-34.
67 Clark-Lewis I, Dewald B, Geiser T, Moser B, Baggiolini M. Platelet factor 4 binds to interleukin 8 receptors and activates neutrophils when its N terminus is modified with Glu-Leu-Arg. Proc Natl Acad Sci U S A. 1993 Apr 15;90(8):3574-7.
68 Cai Z, Gao C, Zhang Y, Xing K. Functional characterization of the ELR motif in piscine ELR+ CXC-like chemokine. Mar Biotechnol (NY). 2009 Jul-Aug;11(4):505-12.
69 Graham GJ, Locati M, Mantovani A, Rot A, Thelen M. The biochemistry and biology of the atypical chemokine receptors. Immunol Lett. 2012 Jul 30;145(1-2):30-8.
70 Bird S, Tafalla C. Teleost Chemokines and Their Receptors. Biology (Basel). 2015 Nov 11;4(4):756-84.
71 Rotman J, van Gils W, Butler D, Spaink HP, Meijer AH. Rapid screening of innate immune gene expression in zebrafish using reverse transcription - multiplex ligation-dependent probe amplification. BMC Res Notes. 2011 Jun 15;4:196.
72 Tamplin OJ, Durand EM, Carr LA, Childs SJ, Hagedorn EJ, Li P, Yzaguirre AD, Speck NA, Zon LI. Hematopoietic stem cell arrival triggers dynamic remodeling of the perivascular niche. Cell. 2015 Jan 15;160(1-2):241-52.
73 Hess I, Boehm T. Intravital imaging of thymopoiesis reveals dynamic lympho-epithelial interactions. Immunity. 2012 Feb 24;36(2):298-309.
74 Chen LC, Chen JY, Hour AL, Shiau CY, Hui CF, Wu JL. Molecular cloning and functional analysis of zebrafish (Danio rerio) chemokine genes. Comp Biochem Physiol B Biochem Mol Biol. 2008 Dec;151(4):400-9.
75 Cui C. Chemokine signaling in innate immunity of zebrafish embryos. Doctoral Thesis, Leiden University. 2012 Dec 20.
76 Donà E, Barry JD, Valentin G, Quirin C, Khmelinskii A, Kunze A, Durdu S, Newton LR, Fernandez-Minan A, Huber W, Knop M, Gilmour D. Directional tissue migration through a self-generated chemokine gradient. Nature. 2013 Nov 14;503(7475):285-9.
77 Harrison MR, Bussmann J, Huang Y, Zhao L, Osorio A, Burns CG, Burns CE, Sucov HM, Siekmann AF, Lien CL. Chemokine-guided angiogenesis directs coronary vasculature formation in zebrafish. Dev Cell. 2015 May 26;33(4):442-54.
78 Haas P, Gilmour D. Chemokine signaling mediates self-organizing tissue migration in the zebrafish lateral line. Dev Cell. 2006 May;10(5):673-80.
79 Diotel N, Vaillant C, Gueguen MM, Mironov S, Anglade I, Servili A, Pellegrini E, Kah O. Cxcr4 and Cxcl12 expression in radial glial cells of the brain of adult zebrafish. J Comp Neurol. 2010 Dec 15;518(24):4855-76.
80 Chong SW, Emelyanov A, Gong Z, Korzh V. Expression pattern of two zebrafish genes, cxcr4a and cxcr4b. Mech Dev. 2001 Dec;109(2):347-54.
81 Chong SW, Nguyet LM, Jiang YJ, Korzh V. The chemokine Sdf-1 and its receptor Cxcr4 are required for formation of muscle in zebrafish. BMC Dev Biol. 2007 May 22;7:54.
82 Bussmann J, Wolfe SA, Siekmann AF. Arterial-venous network formation during brain vascularization involves hemodynamic regulation of chemokine signaling. Development. 2011 May;138(9):1717-26.

83 Knaut H, Werz C, Geisler R, Nüsslein-Volhard C; Tübingen 2000 Screen Consortium. A zebrafish homologue of the chemokine receptor Cxcr4 is a germ-cell guidance receptor. Nature. 2003 Jan 16;421(6920):279-82.
84 Deng Q, Sarris M, Bennin DA, Green JM, Herbomel P, Huttenlocher A. Localized bacterial infection induces systemic activation of neutrophils through Cxcr2 signaling in zebrafish. J Leukoc Biol. 2013 May;93(5):761-9.
85 Sarris M, Masson JB, Maurin D, Van der Aa LM, Boudinot P, Lortat-Jacob H, Herbomel P. Inflammatory chemokines direct and restrict leukocyte migration within live tissues as glycan-bound gradients. Curr Biol. 2012 Dec 18;22(24):2375-82.
86 de Oliveira S, Reyes-Aldasoro CC, Candel S, Renshaw SA, Mulero V, Calado A. Cxcl8 (IL-8) mediates neutrophil recruitment and behavior in the zebrafish inflammatory response. J Immunol. 2013 Apr 15;190(8):4349-59.
87 de Oliveira S, Lopez-Muñoz A, Martínez-Navarro FJ, Galindo-Villegas J, Mulero V, Calado Â. Cxcl8-l1 and Cxcl8-l2 are required in the zebrafish defense against Salmonella Typhimurium. Dev Comp Immunol. 2015 Mar;49(1):44-8.
88 Rhoades ER, Cooper AM, Orme IM. Chemokine response in mice infected with Mycobacterium tuberculosis. Infect Immun. 1995 Oct;63(10):3871-7.
89 Thuong NT, Dunstan SJ, Chau TT, Thorsson V, Simmons CP, Quyen NT, Thwaites GE, Thi Ngoc Lan N, Hibberd M, Teo YY, Seielstad M, Aderem A, Farrar JJ, Hawn TR. Identification of tuberculosis susceptibility genes with human macrophage gene expression profiles. PLoS Pathog. 2008 Dec;4(12):e1000229.
90 Sadek MI, Sada E, Toossi Z, Schwander SK, Rich EA. Chemokines induced by infection of mononuclear phagocytes with mycobacteria and present in lung alveoli during active pulmonary tuberculosis. Am J Respir Cell Mol Biol. 1998 Sep;19(3):513-21.
91 Saukkonen JJ, Bazydlo B, Thomas M, Strieter RM, Keane J, Kornfeld H. Beta-chemokines are induced by Mycobacterium tuberculosis and inhibit its growth. Infect Immun. 2002 Apr;70(4):1684-93.
92 Peters W, Scott HM, Chambers HF, Flynn JL, Charo IF, Ernst JD. Chemokine receptor 2 serves an early and essential role in resistance to Mycobacterium tuberculosis. Proc Natl Acad Sci U S A. 2001 Jul 3;98(14):7958-63.
93 Lin Y, Gong J, Zhang M, Xue W, Barnes PF. Production of monocyte chemoattractant protein 1 in tuberculosis patients. Infect Immun. 1998 May;66(5):2319-22.
94 Scott HM, Flynn JL. Mycobacterium tuberculosis in chemokine receptor 2-deficient mice: influence of dose on disease progression. Infect Immun. 2002 Nov;70(11):5946-54.
95 Hingley-Wilson SM, Connell D, Pollock K, Hsu T, Tchilian E, Sykes A, Grass L, Potiphar L, Bremang S, Kon OM, Jacobs WR Jr, Lalvani A. ESX1-dependent fractalkine mediates chemotaxis and Mycobacterium tuberculosis infection in humans. Tuberculosis (Edinb). 2014 May;94(3):262-70.
96 Guirado E, Schlesinger LS, Kaplan G. Macrophages in tuberculosis: friend or foe. Semin Immunopathol. 2013 Sep;35(5):563-83.
97 Indrigo J, Hunter RL Jr, Actor JK. Influence of trehalose 6,6'-dimycolate (TDM) during mycobacterial infection of bone marrow macrophages. Microbiology. 2002 Jul;148(Pt 7):1991-8.
98 Kang DD, Lin Y, Moreno JR, Randall TD, Khader SA. Profiling early lung immune responses in the mouse model of tuberculosis. PLoS One. 2011 Jan 13;6(1):e16161.
99 Sauty A, Dziejman M, Taha RA, Iarossi AS, Neote K, Garcia-Zepeda EA, Hamid Q, Luster AD. The T cell-specific CXC chemokines IP-10, Mig, and I-TAC are expressed by activated human bronchial epithelial cells. J Immunol. 1999 Mar 15;162(6):3549-58.
100 Wickremasinghe MI, Thomas LH, Friedland JS. Pulmonary epithelial cells are a source of IL-8 in the response to Mycobacterium tuberculosis: essential role of IL-1 from infected monocytes in a NF-kappa B-dependent network. J Immunol. 1999 Oct 1;163(7):3936-47.
101 Nouailles G, Dorhoi A, Koch M, Zerrahn J, Weiner J 3rd, Faé KC, Arrey F, Kuhlmann S, Bandermann S, Loewe D, Mollenkopf HJ, Vogelzang A, Meyer-Schwesinger C, Mittrücker HW, McEwen G, Kaufmann SH. CXCL5-secreting pulmonary epithelial cells drive destructive neutrophilic inflammation in tuberculosis. J Clin Invest. 2014 Mar;124(3):1268-82.
102 Hilda JN, Narasimhan M, Das SD. Neutrophils from pulmonary tuberculosis patients show augmented levels of chemokines MIP-1α, IL-8 and MCP-1 which further increase upon in vitro infection with mycobacterial strains. Hum Immunol. 2014 Aug;75(8):914-22.
103 Riedel DD, Kaufmann SH. Chemokine secretion by human polymorphonuclear granulocytes after stimulation with Mycobacterium tuberculosis and lipoarabinomannan. Infect Immun. 1997 Nov;65(11):4620-3.
104 Miotto D, Christodoulopoulos P, Olivenstein R, Taha R, Cameron L, Tsicopoulos A, Tonnel AB, Fahy O, Lafitte JJ, Luster AD, Wallaert B, Mapp CE, Hamid Q. Expression of IFN-gamma-inducible protein; monocyte chemotactic proteins 1, 3, and 4; and eotaxin in TH1- and TH2-mediated lung diseases. J Allergy Clin Immunol. 2001 Apr;107(4):664-70.
105 Kurashima K, Mukaida N, Fujimura M, Yasui M, Nakazumi Y, Matsuda T, Matsushima K. Elevated chemokine levels in bronchoalveolar lavage fluid of tuberculosis patients. Am J Respir Crit Care Med. 1997 Apr;155(4):1474-7.

106 Xiong W, Dong H, Wang J, Zou X, Wen Q, Luo W, Liu S, He J, Cai S, Ma L. Analysis of Plasma Cytokine and Chemokine Profiles in Patients with and without Tuberculosis by Liquid Array-Based Multiplexed Immunoassays. PLoS One. 2016 Feb 16;11(2):e0148885.
107 Sharifabadi AR, Hassanshahi G, Ghalebi SR, Arababadi MK, Khorramdelazad H, Zainodini N, Shabani Z. All eotaxins CCL11, CCL24 and CCL26 are increased but to various extents in pulmonary tuberculosis patients. Clin Lab. 2014;60(1):93-7.
108 Juffermans NP, Verbon A, van Deventer SJ, van Deutekom H, Belisle JT, Ellis ME, Speelman P, van der Poll T. Elevated chemokine concentrations in sera of human immunodeficiency virus (HIV)-seropositive and HIV-seronegative patients with tuberculosis: a possible role for mycobacterial lipoarabinomannan. Infect Immun. 1999 Aug;67(8):4295-7.
109 Mehra S, Pahar B, Dutta NK, Conerly CN, Philippi-Falkenstein K, Alvarez X, Kaushal D. Transcriptional reprogramming in nonhuman primate (rhesus macaque) tuberculosis granulomas. PLoS One. 2010 Aug 31;5(8):e12266.
110 Slight SR, Khader SA. Chemokines shape the immune responses to tuberculosis. Cytokine Growth Factor Rev. 2013 Apr;24(2):105-13.
111 Rock RB, Hu S, Gekker G, Sheng WS, May B, Kapur V, Peterson PK. Mycobacterium tuberculosis-induced cytokine and chemokine expression by human microglia and astrocytes: effects of dexamethasone. J Infect Dis. 2005 Dec 15;192(12):2054-8.
112 Algood HM, Lin PL, Flynn JL. Tumor necrosis factor and chemokine interactions in the formation and maintenance of granulomas in tuberculosis. Clin Infect Dis. 2005 Aug 1;41 Suppl 3:S189-93.
113 Groom JR, Luster AD. CXCR3 ligands: redundant, collaborative and antagonistic functions. Immunol Cell Biol. 2011 Feb;89(2):207-15.
114 Mayanja-Kizza H, Wajja A, Wu M, Peters P, Nalugwa G, Mubiru F, Aung H, Vanham G, Hirsch C, Whalen C, Ellner J, Toossi Z. Activation of beta-chemokines and CCR5 in persons infected with human immunodeficiency virus type 1 and tuberculosis. J Infect Dis. 2001 Jun 15;183(12):1801-4.
115 Juffermans NP, Paxton WA, Dekkers PE, Verbon A, de Jonge E, Speelman P, van Deventer SJ, van der Poll T. Up-regulation of HIV coreceptors CXCR4 and CCR5 on CD4(+) T cells during human endotoxemia and after stimulation with (myco)bacterial antigens: the role of cytokines. Blood. 2000 Oct 15;96(8):2649-54.
116 Bhatt K, Hickman SP, Salgame P. Cutting edge: a new approach to modeling early lung immunity in murine tuberculosis. J Immunol. 2004 Mar 1;172(5):2748-51.
117 Olmos S, Stukes S, Ernst JD. Ectopic activation of Mycobacterium tuberculosis-specific CD4+ T cells in lungs of CCR7-/- mice. J Immunol. 2010 Jan 15;184(2):895-901.
118 Campbell JD, HayGlass KT. T cell chemokine receptor expression in human Th1- and Th2-associated diseases. Arch Immunol Ther Exp (Warsz). 2000;48(6):451-6.
119 Chaptini C, Marshman G. Leprosy: a review on elimination, reducing the disease burden, and future research. Lepr Rev. 2015 Dec;86(4):307-15.
120 Biswas SK. Cultivation of Mycobacterium leprae in artificial culture medium. Indian J Med Sci. 1989 Jan;43(1):5-10.
121 Levy L, Ji B. The mouse foot-pad technique for cultivation of Mycobacterium leprae. Lepr Rev. 2006 Mar;77(1):5-24. Review. Erratum in: Lepr Rev. 2006 Jun;77(2):170
122 Singh S, Eldin C, Kowalczewska M, Raoult D. Axenic culture of fastidious and intracellular bacteria. Trends Microbiol. 2013 Feb;21(2):92-9.
123 Balamayooran G, Pena M, Sharma R, Truman RW. The armadillo as an animal model and reservoir host for Mycobacterium leprae. Clin Dermatol. 2015 Jan-Feb;33(1):108-15.
124 Adams LB, Pena MT, Sharma R, Hagge DA, Schurr E, Truman RW. Insights from animal models on the immunogenetics of leprosy: a review. Mem Inst Oswaldo Cruz. 2012 Dec;107 Suppl 1:197-208.
125 Bobosha K, Tjon Kon Fat EM, van den Eeden SJ, Bekele Y, van der Ploeg-van Schip JJ, de Dood CJ, Dijkman K, Franken KL, Wilson L, Aseffa A, Spencer JS, Ottenhoff TH, Corstjens PL, Geluk A. Field-evaluation of a new lateral flow assay for detection of cellular and humoral immunity against Mycobacterium leprae. PLoS Negl Trop Dis. 2014 May 8;8(5):e2845.
126 Geluk A, van Meijgaarden KE, Wilson L, Bobosha K, van der Ploeg-van Schip JJ, van den Eeden SJ, Quinten E, Dijkman K, Franken KL, Haisma EM, Haks MC, van Hees CL, Ottenhoff TH. Longitudinal immune responses and gene expression profiles in type 1 leprosy reactions. J Clin Immunol. 2014 Feb;34(2):245-55.
127 Geluk A, van der Ploeg-van Schip JJ, van Meijgaarden KE, Commandeur S, Drijfhout JW, Benckhuijsen WE, Franken KL, Naafs B, Ottenhoff TH. Enhancing sensitivity of detection of immune responses to Mycobacterium leprae peptides in whole-blood assays. Clin Vaccine Immunol. 2010 Jun;17(6):993-1004.
128 Medeiros MF, Rodrigues MM, Vital RT, da Costa Nery JA, Sales AM, de Andrea Hacker M, Ferreira H, Chimelli L, Sarno EN, Antunes SL. CXCL10, MCP-1, and other immunologic markers involved in neural leprosy. Appl Immunohistochem Mol Morphol. 2015 Mar;23(3):220-9.
129 Guerreiro LT, Robottom-Ferreira AB, Ribeiro-Alves M, Toledo-Pinto TG, Rosa Brito T, Rosa PS, Sandoval

FG, Jardim MR, Antunes SG, Shannon EJ, Sarno EN, Pessolani MC, Williams DL, Moraes MO. Gene expression profiling specifies chemokine, mitochondrial and lipid metabolism signatures in leprosy. PLoS One. 2013 Jun 14;8(6):e64748.
130 Berrington WR, Kunwar CB, Neupane K, van den Eeden SJ, Vary JC Jr, Peterson GJ, Wells RD, Geluk A, Hagge DA, Hawn TR. Differential dermal expression of CCL17 and CCL18 in tuberculoid and lepromatous leprosy. PLoS Negl Trop Dis. 2014 Nov 20;8(11):e3263.
131 Sharma I, Singh A, Mishra AK, Singh LC, Ramesh V, Saxena S. Is CXCL10/CXCR3 axis overexpression a better indicator of leprosy type 1 reaction than inducible nitric oxide synthase? Indian J Med Res. 2015 Dec;142(6):681-9.
132 Lu B, Rutledge BJ, Gu L, Fiorillo J, Lukacs NW, Kunkel SL, North R, Gerard C, Rollins BJ. Abnormalities in monocyte recruitment and cytokine expression in monocyte chemoattractant protein 1-deficient mice. J Exp Med. 1998 Feb 16;187(4):601-8.
133 Kipnis A, Basaraba RJ, Orme IM, Cooper AM. Role of chemokine ligand 2 in the protective response to early murine pulmonary tuberculosis. Immunology. 2003 Aug;109(4):547-51.
134 Stolberg VR, Chiu BC, Schmidt BM, Kunkel SL, Sandor M, Chensue SW. CC chemokine receptor 4 contributes to innate NK and chronic stage T helper cell recall responses during Mycobacterium bovis infection. Am J Pathol. 2011 Jan;178(1):233-44.
135 Stolberg VR, Chiu BC, Martin BE, Shah SA, Sandor M, Chensue SW. Cysteine-cysteinyl chemokine receptor 6 mediates invariant natural killer T cell airway recruitment and innate stage resistance during mycobacterial infection. J Innate Immun. 2011;3(1):99-108.
136 Algood HM, Chan J, Flynn JL. Chemokines and tuberculosis. Cytokine Growth Factor Rev. 2003 Dec;14(6):467-77.
137 Vesosky B, Rottinghaus EK, Stromberg P, Turner J, Beamer G. CCL5 participates in early protection against Mycobacterium tuberculosis. J Leukoc Biol. 2010 Jun;87(6):1153-65.
138 Seiler P, Aichele P, Bandermann S, Hauser AE, Lu B, Gerard NP, Gerard C, Ehlers S, Mollenkopf HJ, Kaufmann SH. Early granuloma formation after aerosol Mycobacterium tuberculosis infection is regulated by neutrophils via CXCR3-signaling chemokines. Eur J Immunol. 2003 Oct;33(10):2676-86.
139 Chakravarty SD, Xu J, Lu B, Gerard C, Flynn J, Chan J. The chemokine receptor CXCR3 attenuates the control of chronic Mycobacterium tuberculosis infection in BALB/c mice. J Immunol. 2007 Feb 1;178(3):1723-35.
140 Zlotnik A, Yoshie O, Nomiyama H. The chemokine and chemokine receptor superfamilies and their molecular evolution. Genome Biol. 2006;7(12):243.
141 Hall JD, Kurtz SL, Rigel NW, Gunn BM, Taft-Benz S, Morrison JP, Fong AM, Patel DD, Braunstein M, Kawula TH. The impact of chemokine receptor CX3CR1 deficiency during respiratory infections with Mycobacterium tuberculosis or Francisella tularensis. Clin Exp Immunol. 2009 May;156(2):278-84.
142 Slight SR, Rangel-Moreno J, Gopal R, Lin Y, Fallert Junecko BA, Mehra S, Selman M, Becerril-Villanueva E, Baquera-Heredia J, Pavon L, Kaushal D, Reinhart TA, Randall TD, Khader SA. $CXCR5^{+}$ T helper cells mediate protective immunity against tuberculosis. J Clin Invest. 2013 Feb;123(2):712-26.
143 Di Liberto D, Locati M, Caccamo N, Vecchi A, Meraviglia S, Salerno A, Sireci G, Nebuloni M, Caceres N, Cardona PJ, Dieli F, Mantovani A. Role of the chemokine decoy receptor D6 in balancing inflammation, immune activation, and antimicrobial resistance in Mycobacterium tuberculosis infection. J Exp Med. 2008 Sep 1;205(9):2075-84.
144 Gao Q, Du Q, Zhang H, Guo C, Lu S, Deng A, Tang M, Liu S, Wang Y, Huang J, Guo Q. Monocyte chemotactic protein-1 -2518 gene polymorphism and susceptibility to spinal tuberculosis. Arch Med Res. 2014 Feb;45(2):183-7.
145 Feng WX, Flores-Villanueva PO, Mokrousov I, Wu XR, Xiao J, Jiao WW, Sun L, Miao Q, Shen C, Shen D, Liu F, Jia ZW, Shen A. CCL2−2518 (A/G) polymorphisms and tuberculosis susceptibility: a meta-analysis. Int J Tuberc Lung Dis. 2012 Feb;16(2):150-6.
146 Chu SF, Tam CM, Wong HS, Kam KM, Lau YL, Chiang AK. Association between RANTES functional polymorphisms and tuberculosis in Hong Kong Chinese. Genes Immun. 2007 Sep;8(6):475-9.
147 Sánchez-Castañón M, Baquero IC, Sánchez-Velasco P, Fariñas MC, Ausín F, Leyva-Cobián F, Ocejo-Vinyals JG. Polymorphisms in CCL5 promoter are associated with pulmonary tuberculosis in northern Spain. Int J Tuberc Lung Dis. 2009 Apr;13(4):480-5.
148 Flores-Villanueva PO, Ruiz-Morales JA, Song CH, Flores LM, Jo EK, Montaño M,Barnes PF, Selman M, Granados J. A functional promoter polymorphism in monocyte chemoattractant protein-1 is associated with increased susceptibility to pulmonary tuberculosis. J Exp Med. 2005 Dec 19;202(12):1649-58.
149 Tang NL, Fan HP, Chang KC, Ching JK, Kong KP, Yew WW, Kam KM, Leung CC, Tam CM, Blackwell J, Chan CY. Genetic association between a chemokine gene CXCL-10 (IP-10, interferon gamma inducible protein 10) and susceptibility to tuberculosis. Clin Chim Acta. 2009 Aug;406(1-2):98-102.

150Lindenau JD, Guimarães LS, Friedrich DC, Hurtado AM, Hill KR, Salzano FM, Hutz MH. Cytokine gene polymorphisms are associated with susceptibility to tuberculosis in an Amerindian population. Int J Tuberc Lung Dis. 2014 Aug;18(8):952-7.
151 Ma X, Reich RA, Wright JA, Tooker HR, Teeter LD, Musser JM, Graviss EA. Association between interleukin-8 gene alleles and human susceptibility to tuberculosis disease. J Infect Dis. 2003 Aug 1;188(3):349-55.

Chapter 2

Macrophage-pathogen interactions in infectious diseases: new therapeutic insights from the zebrafish host model

Vincenzo Torraca, Samrah Masud, Herman P. Spaink and Annemarie H. Meijer

Institute of Biology, Leiden University, The Netherlands

Disease Models and Mechanisms, 2014 Jul;7(7):785-97

Chapter 2

Macrophage-pathogen interactions in infectious diseases: new therapeutic insights from the zebrafish host model

Vincenzo Torraca, Samrah Masud, Herman P. Spaink and Annemarie H. Meijer

Institute of Biology, Leiden University, The Netherlands

Studying macrophage biology in the context of a whole living organism provides unique possibilities to understand the contribution of this extremely dynamic cell subset in the reaction to infections, and has revealed the relevance of cellular and molecular processes that are fundamental to the cell-mediated innate immune response. In particular, various recently established zebrafish infectious disease models are contributing substantially to our understanding of the mechanisms by which different pathogens interact with macrophages and evade host innate immunity. Transgenic zebrafish lines with fluorescently labelled macrophages and other leukocyte populations enable non-invasive imaging at the optically transparent early life stages. Furthermore, there is a continuously expanding availability of vital reporters for subcellular compartments and for probing activation of immune defence mechanisms. These are powerful tools to visualise the activity of phagocytic cells in real time and shed light on the intriguing paradoxical roles of these cells in both limiting infection and supporting the dissemination of intracellular pathogens. This Review will discuss how several bacterial and fungal infection models in zebrafish embryos have led to new insights into the dynamic molecular and cellular mechanisms at play when pathogens encounter host macrophages. We also describe how these insights are inspiring novel therapeutic strategies for infectious disease treatment.

GRAPHICAL ABSTRACT

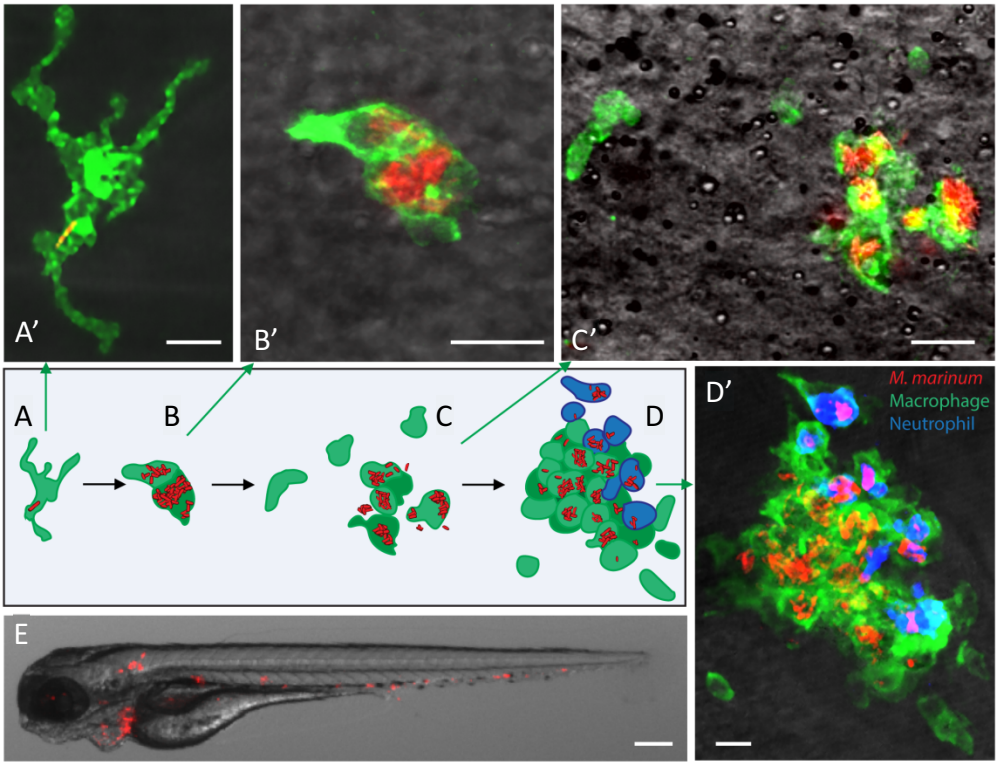

The zebrafish-*M. marinum* model has become widely used to study human tuberculosis since the initial stages of granuloma formation recapitulate closely those initiated by *M. tuberculosis* in human lungs. The first step for granuloma formation is the establishment of an intra-macrophage infection niche (A-A'). Pathogenic mycobacteria (shown in red) resist in the host macrophage (shown in green) and replicate intracellularly until the host cell is unable to counteract the infection and activates mechanisms of programmed cell death (B-B'). Cell fragments and extracellular bacteria released by dying macrophages readily recruit new macrophages, which phagocytose the debris and take up the pathogen (C-C'). Repeated cycles of phagocytosis/bacterial expansion/macrophage death will determine the formation of the granuloma, an inflammatory lesion, predominantly consisting of macrophages that confine the infection. Neutrophils (shown in blue) associate poorly to the very initial stages of granuloma formation but become an important part of the lesion at later stages and can also contribute to bacterial clearance (D-D'). Lymphocytes are not essential to initiate granulomas but associate with these structures (both in adult zebrafish and in humans) in their more advanced stages. Lacking fully-developed adaptive immune cells, the embryonic and larval stages of the zebrafish infected with *M. marinum* (E) can serve as a platform to study the initiation of granulomas and the function of the innate immune cells in a context that anticipates the development of acquired immunity. Scale bars A-D: 10 µm. F: 200 µm.

INTRODUCTION

The immune system has evolved through the constant interplay between microbes and their multicellular hosts. Selective forces acting on both sides have driven the evolution of a wide variety of virulence mechanisms in pathogens and alternative control mechanisms in their hosts. *In vivo* modelling of infectious disease is essential for understanding this complexity and translating it into novel therapeutic interventions. The immune system, innate and adaptive, is well conserved among vertebrates. The zebrafish (*Danio rerio*) offers an optically and genetically accessible vertebrate model to study host-pathogen interactions[1,2,3]. At the embryonic and early larval stages, zebrafish provide the opportunity of studying the relevance of innate immunity in a context where no adaptive response has yet been developed, given that early lymphocytes make their first appearance in 4-day-old larvae and a full adaptive immunity requires several weeks to be mounted[4,5].

Macrophages and neutrophils are the main phagocytic cell types of the innate immune system. Zebrafish models provide unique tools for studying the function of phagocytic cells, and these studies can effectively complement studies in other infectious disease models. Other recent reviews highlighted the use of zebrafish for understanding neutrophil biology[6,7]. Here, we will discuss six zebrafish models for important human pathogens (*Mycobacterium*, *Salmonella*, *Burkholderia*, *Staphylococcus*, *Shigella* and *Candida*), emphasising the novel insights that these models have recently provided into macrophage biology and highlighting how this could lead to the finding of new host-derived therapeutic strategies.

ZEBRAFISH MACROPHAGE BIOLOGY AND TOOLS FOR INVESTIGATING MACROPHAGE FUNCTION

Ontogeny and properties of early macrophages in zebrafish

The first macrophage precursors appear in the zebrafish embryo as early as 20 hours post fertilisation (hpf) from the anterior lateral plate mesoderm[8]. Following migration to the yolk sac, they differentiate and either invade the head mesenchyme, where they will later differentiate into microglial cells (the resident macrophages of the brain) or enter the blood circulation[8,9]. These cells, named primitive macrophages, retain proliferative capability and have been reported to exist in mammals too[8,10]. They can remove apoptotic cells, are able to sense and respond to invading microbes and can eradicate non-pathogenic infections. Primitive macrophages readily phagocytose microbes from the blood circulation or when present in tissues. In contrast, neutrophils (which develop slightly later) are less efficient in phagocytosing microbes in the blood but are potent scavengers of surface-associated bacteria[11].

Primitive macrophages are gradually replaced by different lineages of macrophages deriving from definitive haematopoiesis, the process that will produce specialised pluripotent cells with the ability to differentiate into all types of mature blood cells. The first wave of definitive haematopoiesis starts at 24 hpf in the posterior blood island or caudal haematopoietic tissue (CHT) with the differentiation of erythromyeloid progenitors[12]. By 48 hpf, these pluripotent progenitors are replaced with another subset of haematopoietic stem and progenitor cells (HSPCs), now able to also differentiate into the lymphoid lineage. These cells originate from the AGM (aorta, gonads and mesonephros), derived from the lateral posterior mesoderm. After leaving the AGM, they migrate to and

nest in the CHT and will provide the second wave of definitive haematopoiesis[12,13]. Development of HSPCs and their emergence from aortic endothelium is remarkably conserved between zebrafish and mammals[14,15,16].

Following the second wave of haematopoiesis, macrophage precursors are released into the circulation and will extravasate to seed tissues throughout the whole body, where they differentiate into tissue macrophages. Starting from 4 days post fertilisation (dpf), the kidney marrow, which is the main haematopoietic tissue of the adult fish, develops and will progressively replace the embryonic haematopoietic system. Another component of the mononuclear phagocyte system is represented by the dendritic cell (DC) population, which is also present in zebrafish larvae and can be detected from 8–12 dpf [17,18].

The infection studies discussed below, using zebrafish embryo and larval models, do not distinguish macrophages from circulating monocytes. Furthermore, possible functional differences between macrophages from primitive or definitive haematopoietic origins are generally not addressed. For more detailed and comparative descriptions of the processes of haematopoiesis in zebrafish and mammals we refer to other reviews[19,20].

Macrophage defence mechanisms and subversion by intracellular pathogens

Macrophages sense the presence of infection through microbial-specific molecules and host-derived inflammatory mediators. Their chemoattraction to the site of infection depends largely on the function of G-protein-coupled receptors[21,22]. Scavenger and complement receptors play a major role in phagocytosis[23] and Toll-like receptors (TLRs), in cooperation with other pattern-recognition receptors (PRRs), initiate the innate immune response[24]. TLRs, found on the cell surface and membranes of vesicular compartments, recognise pathogen- and damage-associated molecular patterns (PAMPs and DAMPs, respectively). Another main class of PRRs, the NOD-like receptors (NLRs), performs the same function in the cytosol[25,26]. Some NLRs participate in the assembly of the inflammasome, a multiprotein complex able to activate the caspase-1 cascade, which triggers processing of pro-inflammatory cytokines, such as IL1β (interleukin 1 beta) and full activation of the innate immune response[27].

When engulfed by macrophages, microorganisms are exposed to a number of defence mechanisms within the resulting phagosome and through its subsequent fusion with lysosomes. These include the production of reactive oxygen and nitrogen species (ROS and RNS, respectively)[28,29], exposure to antimicrobials, the activity of proteases and acidification[30,31,32]. Escape from the phagosome triggers septin caging and antibacterial autophagy as additional defence mechanisms[33,34].

Intracellular pathogens have evolved many strategies to counteract these defences. These counter-strategies are mediated by virulence factors, which are often secreted directly into the host cell via specialised secretion systems such as the T3SS (type III secretion system) of Gram-negative pathogens and the T7SS (type VII secretion system) of pathogenic mycobacteria[35,36]. Pathogens can also induce significant reprogramming of their host cells through manipulation of signalling pathways and chromatin remodelling; however, these mechanisms are still poorly understood[37,38]. Intracellular pathogens often block phagosome maturation and fusion with lysosomes or manipulate the vesicular system such that the phagosome is modified to resemble the endoplasmic reticulum or a Golgi-like

compartment[39]. Furthermore, several pathogens inject virulence factors that promote actin polymerisation to actively stimulate their uptake by both non-phagocytic and phagocytic cells[40]. Pathogens that are able to escape from the phagosome have mechanisms to evade autophagy and can spread from the initially infected cell to other cells by acquiring actin-based motility[40,41]. Other virulence mechanisms can induce inflammation and different cell-death programs to facilitate the dissemination of infection[42]. These different virulence strategies are schematically depicted in **Figure 1**.

Macrophage markers and transgenic lines

The development of transgenic zebrafish lines with fluorescently labelled leukocytes (**Supplementary Table 1**) has been key to the successful application of zebrafish for immunological studies. However, until recently, the lack of a specific reporter for the macrophage lineage limited the study of this myeloid subset. This has now been remedied with the development of the *csf1ra* and *mpeg1* reporter lines[43,44]. These genes are robust markers for macrophages at embryonic and larval stages, because they are co-expressed with the pan-leukocytic marker *lcp1* but not with the neutrophil markers *mpx* and *lyz*[45,46]. Despite the fact that *csf1ra* is macrophage-specific within the immune cell types, it is also expressed in neural crest cells and derivatives, such as the xanthophores. Nevertheless, the highly motile macrophages can be distinguished easily from the immobile xanthophores in time-course experiments[43]. Reporter lines using the *mpeg1* promoter label macrophages but not xanthophores (**Figure 2A**, **Supplementary Movie 1**) and, combined with a neutrophil marker, can show the different kinetics of macrophage and neutrophil responses to infection and wounding, as well as the dynamic interactions between the two cell types[44]. The *mpeg1* reporter also labels microglia and it has been suggested to label other antigen-presenting cells, such as the Langerhans dendritic cells, but these could not be detected before 8–9 dpf[18].

Expression of the Gal4 transcription factor under the control of macrophage or neutrophil promoters in combination with a UAS:nitroreductase-mCherry line allows for the specific ablation of one of the two phagocyte populations. This approach can be used to investigate their individual contributions to the immune response and infectious disease pathogenesis[43,47]. Alternatively, *spi1/pu.1* antisense morpholino knockdown can be used to block the development of either macrophages exclusively or of both macrophages and neutrophils, depending on the concentration used[48]. Similarly, *irf8* tools have also been used to deplete specific myeloid cell populations and to skew the development of their progenitors towards macrophages or neutrophils. Morpholino knockdown of *irf8* can completely deplete macrophage differentiation while stimulating an increased output of neutrophils and *irf8* overexpression can direct myeloid development towards macrophage differentiation[49].

Many other transgenic lines that label either the entire myeloid population, the early myeloid subset, microglia or all antigen-presenting cells are also very useful for the study of macrophage biology (**Supplementary Table 1**).

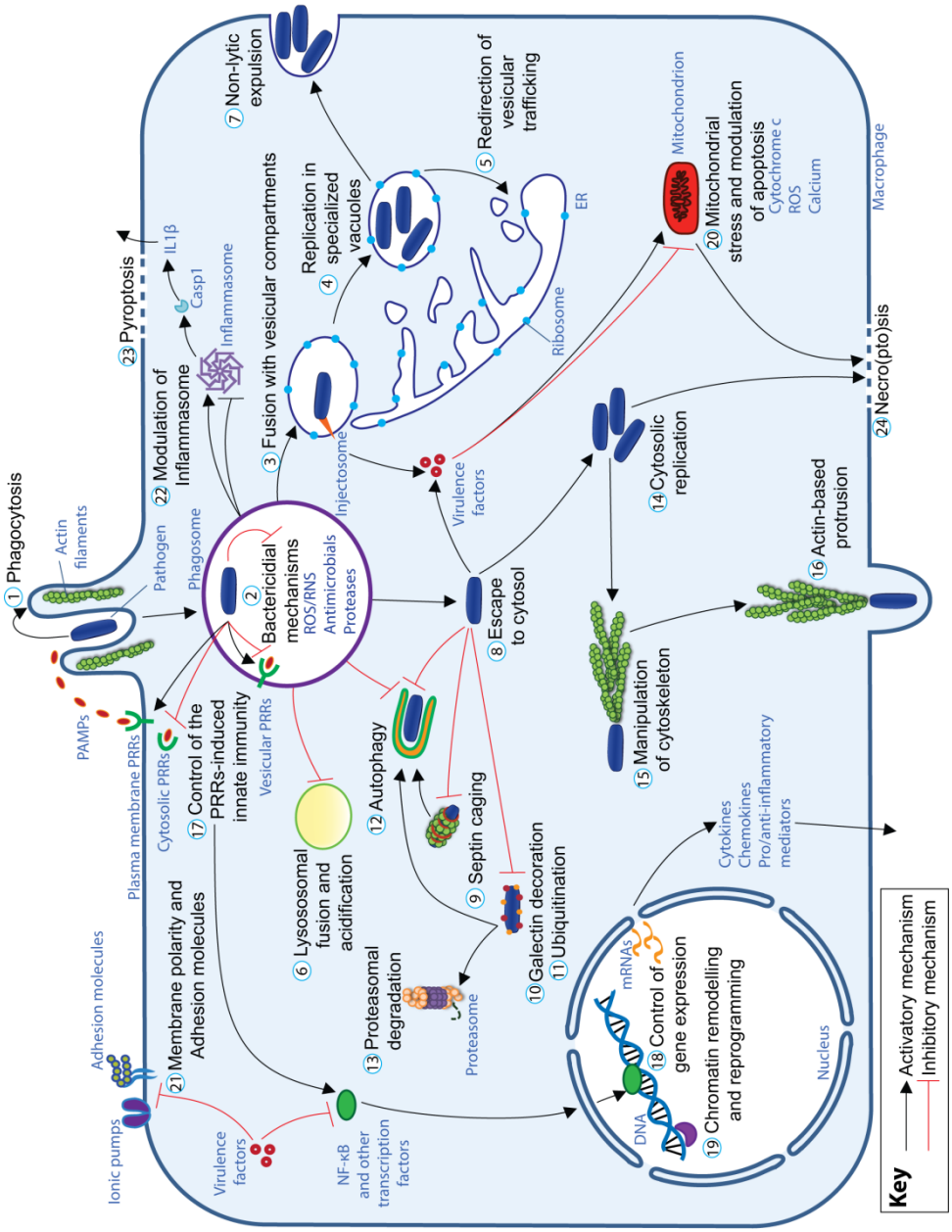

Figure 1. Evasion of macrophage defence mechanisms by intracellular pathogens *(Legend on the next page)*.

Figure 1. Evasion of macrophage defence mechanisms by intracellular pathogens *(Figure on the previous page)*. Upon phagocytosis (1), the pathogens generally reside within phagosomal compartments where a plethora of microbicidal components cooperate in a multidirectional assault to the microbes (2). By transferring virulence factors, often via secretion systems (injectosomes), some pathogens can avoid the classical maturation steps of these compartments, creating a favourable niche for their intracellular growth (3, 4, 5). Fusion of the phagosome with endosomes and/or lysosomes can be blocked (6) and fusion with Golgi- and reticulum-like vesicles can be promoted (3), resulting in the formation of specialised replicative vacuoles (4, 5), in some cases also directed to non-lytic expulsion (7). Several intracellular pathogens are able to escape directly into the cytosol (8). Here, septin cages (9), galectin decoration (10), ubiquitylation (11) and specific routes of antimicrobial autophagy (12) are activated to capture the escapers and redirect them to lytic compartments. Additionally, ubiquitylation of microbial proteins (11) labels these for proteasomal degradation (13). Several intracellular pathogens can efficiently counteract this second line of intracellular defence and replicate freely within the cytosol (14), frequently also manipulating the cell cytoskeleton (15) to sustain their extrusion and dissemination to other host cells (16). Intracellular infections have profound influences also on a wide spectrum of host functions. Cell signalling pathways can be manipulated to modulate the host inflammatory response (17) and control gene expression (18). Some pathogens are also known to induce epigenetic modification of their host cells, leading to reprogramming (19). Some virulence factors directly impact the homoeostatic mechanisms by interfering with normal mitochondrial functionality (20), membrane polarity and communication with the extracellular milieu (21). The ultimate possibility for the host to eradicate the infection is to initiate cell (pyroptotic, apoptotic or necroptotic) suicide programs (20, 22, 23, 24). However, the death mechanisms can also be modulated by pathogens, which can benefit from them by the induction of host damage, pathogen dissemination and the initiation of new replicative cycles.

In vivo visualisation of macrophage function

Visualisation of live macrophage behaviour in zebrafish embryos can be achieved with great structural detail using digitally enhanced differential interference contrast (DIC) microscopy[8,50,51,52]. More recently, there has been tremendous progress in the use of transgenic marker lines (**Supplementary Table 1**) and labelled pathogens that facilitate live imaging in spatial and temporal dimensions (**Figure 2, Supplementary Movies 2-3**).

Photoconvertable fluorescent proteins such as Kaede and Dendra2 have been exploited to show that cells from the CHT can be recruited distally to infection foci and wounds[53] and that *Mycobacterium*-infected macrophages egress from primary granulomas to initiate secondary infection foci[52]. For imaging of phagocyte migration, pathogens or specific chemoattractants can be injected subcutaneously or into body cavities such as the otic vesicle and hindbrain ventricle, which can be reached without generating extensive tissue damage, thereby preventing wound-induced leukocyte mobilisation[11,54,55,56,57,58]. To visualise phagocytosis and the intracellular fate of bacteria, the pHrodo dye can be conjugated to bioparticles or to live or heat-killed bacteria (**Figure 2D**), providing constitutive fluorescence in one channel and additional fluorescence in another channel following exposure to an acidic environment[59]. Furthermore, the nature of the compartments where the pathogens reside can be investigated with combinations of different vital stains, most of which are permeable into zebrafish embryos when added to the water. Several pH-sensitive dyes (LysoSensor and LysoTracker) do not distinguish between lysosome-dependent or -independent phagosome acidification mechanisms, but they can be used simultaneously with methods for detection of the activity of lysosomal proteases (MagicRed-Cathepsin and DQ-BSA)[60].

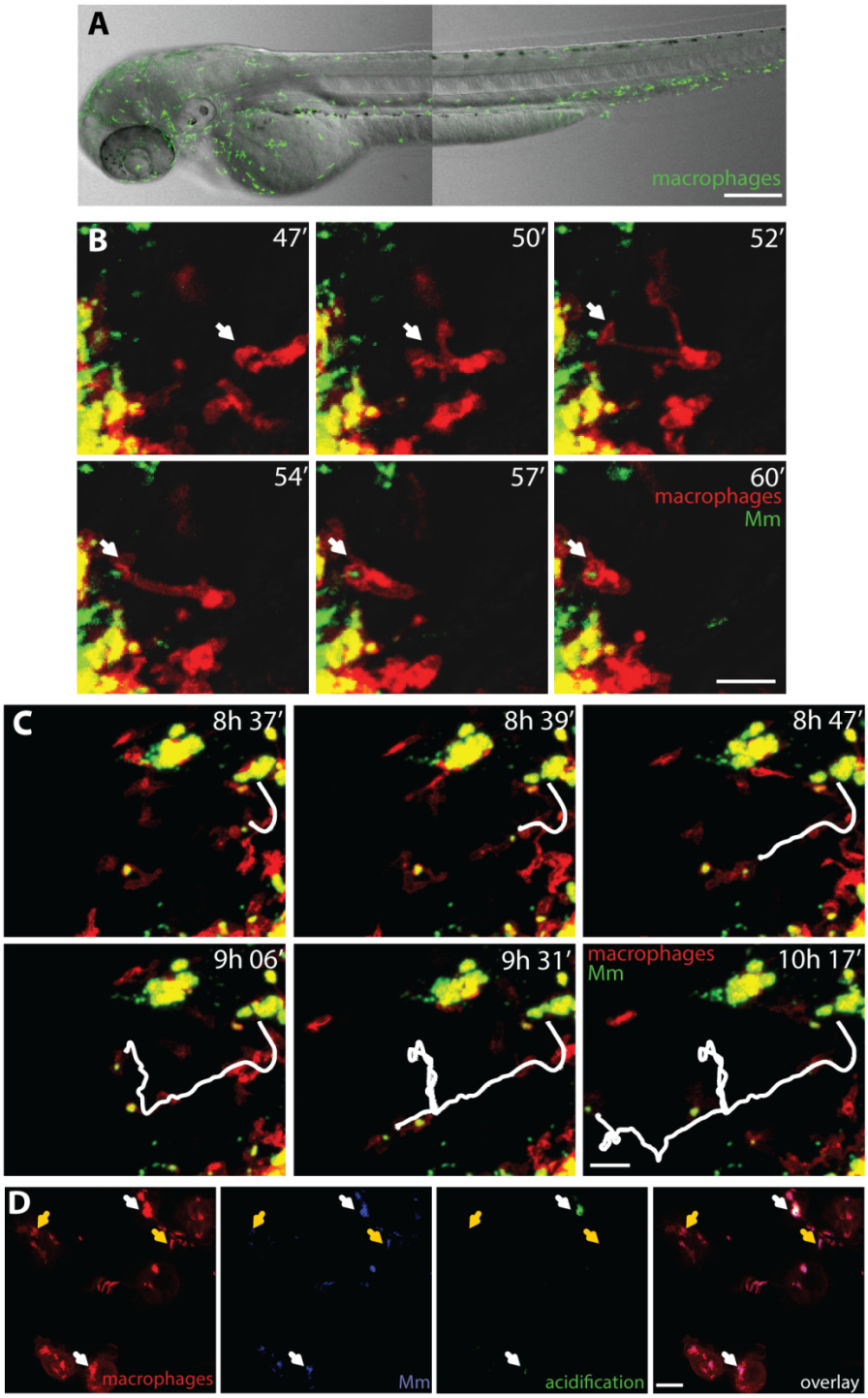

Figure 2. ***In vivo*** **imaging of macrophage responses to infection** *(Legend on the next page)*.

Figure 2. ***In vivo* imaging of macrophage responses to infection** *(Figure on the previous page)*. **A.** A 3-dpf *Tg(mpeg1:Gal4-VP16/UAS-E1b:Kaede)* zebrafish embryo showing the distribution pattern of macrophages (green). Random patrolling of macrophages is shown in Supplementary Movie 1. **B.** Phagocytosis of *M. marinum* (*Mm*; green) injected into the subcutaneous area overlying a somite in a 2-dpf *Tg(mpeg1:mCherry-F)* embryo. The arrow points at a macrophage (red) in the process of phagocytosis between 47 and 60 minutes post infection. The images are particulars and stills from **Supplementary Movie 2** (10 to 60 minutes post infection). **C.** Macrophage-mediated dissemination of *M. marinum* infection. The white track represents the path of an infected macrophage migrating away from the infection focus. The images are stills and particulars from **Supplementary Movie 3**, which was taken from the same embryo as in B at a more advanced stage of infection (~8 to ~10 hours post infection). **D.** Partial acidification of phagocytosed *M. marinum*. Bacteria double-labelled with constitutive mCrimson and pH-sensitive green pHrodo are contained within subcellular compartments of macrophages, which are intensely labelled by the membrane-bound mCherry of the *Tg(mpeg1:mCherry-F)* line. White arrows point at bacteria in acidified compartments, where the pHrodo dye is activated. Yellow arrows point at bacteria in non-acidified compartments. Note that most of the intracellular mycobacteria are not acidified, consistent with the ability of this pathogen to counteract phagosome maturation. Macrophages were imaged in the yolk sac circulation valley 5 hours after injection of bacteria into the caudal vein at 2 dpf. Images in A–C were acquired with the Zeiss Observer 6.5.32 laser-scanning confocal, with 10× (A) or 20× (B-C) objectives. Images in D were acquired with Leica TCS SPE confocal with a 20× objective. Figures and movies were processed with ImageJ. The zebrafish transgenic lines *Tg(mpeg1:Gal4-VP16/UAS-E1b:Kaede)* and *Tg(mpeg1:mCherry-F)* were previously described in other reports[44,61]. Scale bars: (A) 200 µm; (B-C) 25 µm; (D) 10 µm.

Different methods allow *in situ* detection of ROS and RNS responses during infection in zebrafish embryos[62,63,64,65]. Also, tools for visualising ATP, calcium effluxes and apoptosis have been efficiently used in zebrafish[60,66,67]. Furthermore, an increasing number of transgenic marker lines for vesicular compartments are becoming available that will help in elucidating the subcellular locations where pathogens reside *in vivo* (**Supplementary Table 2**).

NEW INSIGHTS INTO MACROPHAGE-PATHOGEN INTERACTIONS

Mycobacterium marinum

M. marinum is a natural pathogen of zebrafish that causes granulomatous necrotic lesion formation in host tissues. These lesions are histologically very similar to those generated by *Mycobacterium tuberculosis*, the aetiological agent of human tuberculosis[68,69]. In adult zebrafish, *M. marinum* can cause a latent infection and the bacteria can be reactivated from dormancy by immunosuppressive treatment, as is the case for *M. tuberculosis*, which is estimated to have infected one-third of the world population[70,71]. Tuberculosis therapy is limited by a number of problems, including the poor response of dormant mycobacteria to antibiotics, the increasing prevalence of multidrug-resistant strains and the lack of an effective vaccine against latent or reactivated tuberculosis[72]. The lack of a mouse model for tuberculosis that fully recapitulates the disease and the risk of working with the human pathogen owing to its airborne transmission emphasise the need for alternative models. The unique accessibility of the early stages of granuloma formation in zebrafish larvae has made the zebrafish-*M. marinum* host-pathogen pair one of the most productive models used to unravel the core pathogenic processes of mycobacterial infections[3,50,73] (**Figure 3A**). Notably, the use of this model has already provided several direct translational applications for human disease treatments (**Table 1**).

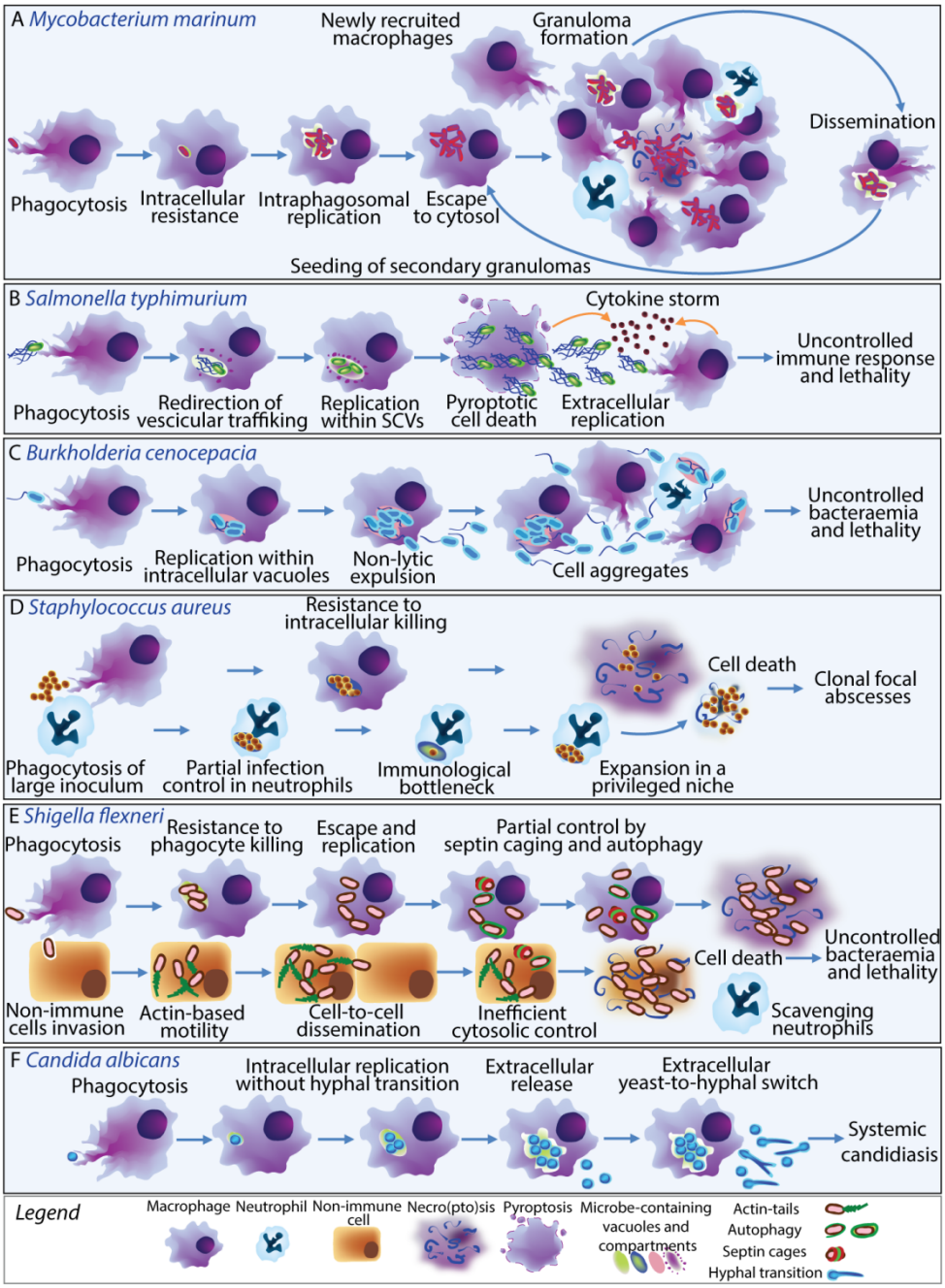

Figure 3. Models of intracellular infections in zebrafish *(Legend on the next page)*.

Figure 3. Models of intracellular infections in zebrafish *(Legend on the previous page)*. Schematic comparison of the infection phenotypes caused by different pathogens following intravenous injection in zebrafish embryos. **A.** *M. marinum* can replicate within phagosomes and also escape into the cytosol. Eventually, the host macrophages succumb to the infection and the pathogen spreads to new macrophages that have been recruited through bacterial virulence mechanisms. This leads to the formation of granulomatous lesions. Occasionally, infected macrophages can egress from the primary granuloma and seed secondary granulomas. **B.** *S. typhimurium* avoids the phagosomal defences by inducing the formation of non-lytic compartments [*Salmonella*-containing vacuoles (SCVs)]. Upon replication, the pathogen induces pyroptotic cell death. Extracellular *Salmonella* continues to replicate. Damage- and pathogen-associated signals contribute to uncontrolled inflammation ('cytokine storm'), which is rapidly fatal for the host. **C.** *B. cenocepacia* can also replicate within intracellular compartments. Additionally, it can be non-lytically expelled from the host macrophages. Within the extracellular environment, the pathogen stimulates leukocyte aggregation and continues replication. The resulting uncontrolled bacteraemia is the major cause of the fatal complications. **D.** *S. aureus* is largely resistant to intracellular killing when phagocytosed by macrophages and leads to their necrotic death. By contrast, when phagocytosed by neutrophils, most of the pathogen can be efficiently neutralised. However, resistant clones occasionally emerge and expand within these cells. This "intraphagocyte niche" is the reason of the monoclonality of focal staphylococcal abscesses. **E.** *S. flexneri* can invade non-immune cells. Within these cells, the pathogen escapes immediately into the cytosol and gains actin-based motility, by which it disseminates from cell to cell. Within macrophages, the pathogen can also escape from the phagosome, but here a more efficient cytosolic control partially combats the invader, delaying (although not avoiding) macrophage cell death. Neutrophils represent efficient scavengers for extracellular *Shigella* released from dying epithelial cells and macrophages but the infection is still rapidly lethal. **F.** Phagocytosis of *C. albicans* by macrophages leads to a standoff phase, where the host does not degrade the pathogen, but its virulence is contained as it remains locked into a yeast form. The fungus can still slowly replicate and eventually is released. Extracellularly, the yeast can germinate and the resulting fast-replicating hyphae will invade the whole organism, leading to systemic infection.

Infection of zebrafish embryos with *M. marinum* has demonstrated that macrophages are sufficient to initiate granuloma formation in the absence of adaptive immunity[50]. Subsequently, this model changed the widespread view of granulomas, historically regarded solely as host-protective structures, by showing that early granulomas promote mycobacterial dissemination (**Figure 3A**) and that their formation is driven by virulence determinants of the RD1 locus, encoding ESX-1, a secretion system conserved in all pathogenic mycobacteria[3,35,52,74]. Furthermore, the ESX-1-secreted protein ESAT-6 (Early secreted antigenic target 6) was found to induce matrix metalloproteinase Mmp9 production by epithelial cells surrounding the infection focus, which in turn facilitates macrophage infiltration. As a result, the application of Mmp9 antagonists has been suggested as a host-directed anti-tuberculosis therapy[75] (**Table 1**). The notion that granulomas are dynamic structures, even during latent infection, is supported by a study of *M. tuberculosis* infection in the macaque model[76].

Mycobacteria are well known for developing drug tolerance. The zebrafish embryo model has demonstrated that their intramacrophage localisation correlates with development of resistance and that granulomas promote dissemination of this resistant population. Upregulation of bacterial efflux pumps, which are required for intracellular growth, can mediate drug tolerance both in *M. marinum*-infected zebrafish and in *M. tuberculosis*-infected human macrophages. Efflux-pump inhibitors, already available on the market, can reduce this tolerance and their addition to standard anti-tuberculosis therapy might, therefore, shorten treatment duration[77,78] (**Table 1**).

Target	Susceptible pathogens	Desired drug effect	Drugs tested	Ref.
MMP9 Matrix metalloproteinase 9	Mycobacteria	Reduction of ESAT6/Mmp9-dependent macrophage infiltration to mycobacterial infection	Not tested	75
Efflux pumps Multiple bacterial genes	Wide spectrum of bacteria	Prevention of drug tolerance development mediated by a macrophage-induced efflux mechanism	Verapamil* Reserpine*	77,78
GR Glucocorticoid receptor	Mycobacteria	Suppress detrimental inflammation in mycobacterial infection in patients with proinflammatory genotypes	Glucocorticoids*	84
COXs Cyclooxygenases	Mycobacteria	Suppress detrimental inflammation in mycobacterial infection in patients with proinflammatory genotypes	Acetylsalicylic acid (Aspirin)*	84
BLT1 LTB4 receptor	Mycobacteria	Suppress detrimental inflammation in mycobacterial infection in patients with proinflammatory genotypes	U-75302***	84
CYPD Cyclophilin D	Mycobacteria	Prevention of mitochondrial permeability transition, limiting ROS-dependent necroptosis	Alisporivir**	83
ASMase Acid sphingomyelinase	Wide spectrum of intracellular pathogens	Prevention of ceramide production, limiting ROS-dependent necroptosis	Desipramine*	83
ROS Reactive oxygen species	Wide spectrum of intracellular pathogens	Scavenging of ROS	N-acetylcysteine* Amifostine* Tempol*	83
HIF-1α/HIF-2α pathway Hypoxia-induced factor 1 and 2 α	Wide spectrum of pathogens	Stimulation of protective Hif- and iNOS-mediated RNS production in neutrophils	Not tested	65
iNOS Inducible nitric oxide synthase	Wide spectrum of pathogens	Stimulation of protective RNS production and beneficial emergency haematopoiesis	Not tested	62,65
IRG1 pathway Immunoresponsive gene 1	Wide spectrum of pathogens	Modulation of fatty acids catabolism and of mitochondrial ROS production	Not tested	63
SQSTM1/p62 Sequestosome 1	Wide spectrum of intracellular pathogens	Enhancement of infection control by selective autophagy mechanisms	Not tested	86

Table 1. Therapeutic strategies inspired by the zebrafish model to counteract intracellular infections *(Legend on the next page)*.

Table 1. Therapeutic strategies inspired by the zebrafish model to counteract intracellular infections *(Table on the previous page)***.** The zebrafish host model has contributed extensively to the investigation of novel therapeutic strategies, oriented on modulating host-derived responses. Metalloproteinase inhibitors can reduce the tissue inflammatory response guiding phagocytes towards mycobacterial infections, thus attenuating the expansion of primary granulomas and the seeding of secondary infectious foci. Efflux pumps, although not representing a host target, impact directly on the capability of the pathogens to adapt to the intracellular growth and their blockade can reduce drug tolerance. Several classes of established anti-inflammatory drugs are beneficial for subsets of tuberculosis and leprosy patients, dependent on their genotypically-determined inflammatory status (suppression of excessive inflammatory response). Levels of ROS and RNS work as a double-edged sword and their tight control can stimulate a positive outcome of the infectious process. Drugs scavenging, suppressing, or boosting ROS/RNS production are thereby valuable therapeutic tweezers to fine tune their balance. Finally, the possibility of stimulating pathogen-selective autophagy is a promising therapeutic approach. Specific drugs tested in the zebrafish model and supporting these approaches are listed: *Accepted drug; **Drug accepted for clinical trial; ***Not accepted for clinical trial.

Another important insight into tuberculosis pathogenesis concerns the relevance of the inflammatory status. A zebrafish mutagenesis screen revealed Lta4h (Leukotriene A4 hydrolase) as a host factor that strongly correlates with *M. marinum* susceptibility[79]. This enzyme is required for producing LTB4 (Leukotriene B4), a powerful proinflammatory chemoattractant. Lta4h deficiency correlates with a less inflamed status, due to redirection of its substrates to anti-inflammatory lipoxins, resulting in reduced levels of proinflammatory cytokines such as tumour necrosis factor (TNF). The crucial role of TNF in controlling mycobacterial infection is exemplified by the increased risk of tuberculosis in patients with chronic inflammatory disorders treated with TNF antagonists[80]. However, excessive production of TNF is also associated with higher susceptibility to tuberculosis. This has been shown in zebrafish and other animal models as well as in tuberculosis meningitis patients, where a polymorphism at the *LTA4H* locus that causes increased TNF production has been linked with more progressive disease symptoms[79,81]. Hyper-inflamed and hypo-inflamed statuses have both been associated with necrotic death of infected macrophages and consequent extracellular release of the pathogen[82,83]. In conditions of low inflammation, macrophages passively undergo necrotic death because they are unable to control intracellular bacterial growth, whereas, in conditions of high inflammation, macrophages actively initiate two ROS-mediated necroptotic pathways, dependent on the activation of the mitochondrial permeability transition pore complex (mPTPC) and of the lysosomal acid sphingomyelinase (aSMase). Drugs targeting these pathways prevent activation of the necroptotic program in the zebrafish model[82]. The crucial role of the inflammatory status emphasises the importance of designing personalised patient therapies: patients with the proinflammatory *LTA4H* genotype might benefit from classical anti-inflammatory drugs [such as corticosteroids or non-steroidal anti-inflammatory drugs (NSAIDs)]; however, these drugs should be avoided in patients with the opposite genotype[79,84]. Drugs that directly block the ROS-linked necroptotic pathways will benefit the proinflammatory genotypes without generating detrimental effects on the other genotypes, because the necroptotic pathways are exclusively triggered in hyper-inflamed conditions[83] (**Table 1**).

The inflammatory response is initiated by TLR recognition of PAMPs. Myd88, a central adaptor in TLR signalling, was recently shown to be required for control of systemic *M. marinum* infection in zebrafish embryos[85]. In contrast, the initial recruitment of macrophages to a localised *M. marinum* infection in the hindbrain was found to be largely

Myd88 independent[58]. This effect was linked to the presence of PDIM (phthiocerol dimycocerosate) lipid on the surface of pathogenic mycobacteria, which masks the underlying PAMPs. Non-pathogenic mycobacteria, which lack PDIM, induce a robust immune response and are efficiently contained. Mutation of the PDIM transporter (*ΔmmpL7*) and of a factor involved in PDIM synthesis (*Δmas*) can restore Myd88-dependent macrophage recruitment and allow an efficient intracellular RNS response against invading bacteria. Interestingly, in the absence of a TLR response, macrophages can still be recruited. This Myd88-independent recruitment was found to be mediated by cell-surface phenolic glycolipids (PGLs), which induce macrophage recruitment through a pathway that is analogous to the mammalian CCL2-CCR2 (CC-motif chemokine ligand–receptor 2) axis. The macrophages recruited in this situation are suggested to be more permissive to intracellular bacterial growth, because they do not drive the strong intracellular RNS response. These observations might also explain why *M. tuberculosis* establishes infection in the lower rather than in the higher respiratory tracts, because the latter is exposed to resident and environmental microbes that can make macrophages more competent for intracellular killing via a continuous transduction of TLR-dependent immune signalling[58].

Although macrophages are the main cell type infected by *M. marinum* following intravenous injection, neutrophils are also important for early infection control in zebrafish. In the early granuloma, the protective role of neutrophils was found to depend on ROS production[56]. Prior to granuloma formation, neutrophils, both infected and non-infected, also produce RNS[65]. This RNS production is dependent on inducible nitric oxide synthase (iNOS) and can be modulated by genetic or pharmacological modulation of Hif-α (Hypoxia-inducible factor alpha) transcription factors. Increasing Hif-1α signalling or decreasing Hif-2α signalling primes neutrophils with higher levels of RNS prior to infection, thereby limiting susceptibility to mycobacterial infection. Increasing host RNS output by therapeutic targeting of the Hif-α pathway might shift the balance in favour of the host and can thereby be explored as a strategy to complement antibiotic interventions (**Table 1**).

In addition to the classical microbicidal mechanisms of macrophages, antibacterial autophagy has emerged as an important supplementary control mechanism in mycobacterial infections[34]. Using the zebrafish model, colocalisation of mycobacteria with the autophagic marker Lc3 has been demonstrated *in vivo*[2]. Moreover, actin tail formation and recruitment of septin cages have been visualised, the latter also being associated with Lc3 and autophagy[86]. The induction of dram1 (DNA damage-regulated autophagy modulator 1) during infection suggests an immunological function of this autophagy modulator and the zebrafish model could be further exploited to investigate therapeutic targeting of selective autophagy pathways[86,87].

Very recently, a zebrafish larval model has also been established to study a rapidly growing *Mycobacterium*, *M. abscessus*, an emerging pathogen that causes severe pulmonary infections in individuals with cystic fibrosis[61]. The study showed that the virulent rough morphotype of *M. abscessus* is transported to the central nervous system by macrophages, where bacteria released from dying cells form massive amounts of serpentine cords that grow too large to be phagocytosed, leading to acute and lethal infection. Furthermore, *M. tuberculosis* can also be disseminated by zebrafish larval macrophages and is sensitive to antibiotic treatment in this model[88]. It will be of interest to investigate novel therapeutic

strategies emerging from the study of *M. marinum* (**Table 1**) also in the zebrafish models for these human pathogens.

Salmonella enterica serovar Typhimurium (*S. typhimurium*)

Like many other Gram-negative enterobacteria, *Salmonella* can infect a diverse range of hosts and cause zoonotic diseases[89]. The *S. enterica* serovar Typhimurium, often referred to as *S. typhimurium*, represents a common agent of enteric fever, gastroenteritis and bacteraemia, often linked to food poisoning. Although the bacterium is not a natural fish pathogen, zebrafish embryos are strongly susceptible to *S. typhimurium* in experimental settings. Pathogenesis in fish involves some of the acute symptoms seen in humans, including bacteraemia and a strong proinflammatory host response ('cytokine storm'), which are associated with early lethality of the zebrafish embryos[90,91]. The life cycle of *S. typhimurium* has been well characterised in infected cell cultures and in mammalian systems: the pathogen is able to alternate phases of intracellular replication within phagocytes and extracellular growth within the damaged tissue[92,93]. Similar observations have been made in the zebrafish embryo model. *S. typhimurium*, like *M. marinum*, can survive intracellularly in macrophages of zebrafish embryos (**Figure 3B**), but infected cells do not disseminate into tissues. Instead, following intravenous injection, the infection remains restricted to the vasculature, with bacteria multiplying both in macrophages and extracellularly at the epithelium of blood vessels[90]. Although infection with wildtype bacteria causes early lethality, bacteria with mutations in lipopolysaccharide (LPS) are attenuated in macrophages and are more sensitive to extracellular lysis, likely due to complement factors[90].

In sharp contrast with *M. marinum* infection, S. *typhimurium* infection leads to a cytokine storm within hours after intravenous injection[2,91,94]. At the transcriptional level, this response is similar to that observed in infection with the natural fish pathogen *Edwardsiella tarda*[85]. This proinflammatory transcriptional response provides a useful readout for characterising the consequences of mutation or knockdown of host genes involved in the immune response. Deficiencies in the TLR signalling components Myd88 and Traf6 strongly reduce expression of transcriptional regulators, signalling components and effectors of the immune response[85,95]. Conversely, these gene groups are hyper-induced following knockdown of the protein tyrosine phosphatase Shp1 (also known as Ptpn6)[96]. These observations are consistent with the function of these genes in mammalian animal models and human patients, where MYD88 and TRAF6 mutations are associated with immunodeficiencies and SHP1 mutations cause inflammatory phenotypes and autoimmune defects. Control of *S. typhimurium* and other infections in zebrafish is impaired both under conditions of a reduced or hyper-induced immune response, indicating the importance of highly balanced regulatory mechanisms[85,96]. Micro-RNAs (miRNAs), including members of the miR-146 family, have been implicated in fine-tuning of the mammalian innate immune response and, in zebrafish embryos, miR-146 is induced by *S. typhimurium* in a Myd88-Traf6-dependent manner. Although no major effects on known targets of the Myd88-Traf6 pathway were observed, apolipoprotein-mediated lipid transport emerged as a newly identified infection-inducible pathway under control of this miRNA family[97].

The signals involved in recruitment of phagocytes to local infection remain to be elucidated. Chemokines, such as Cxcl8 (Il8) and the orphan ligand Cxcl-c1c/Cxcl18b, are highly induced rapidly upon *S. typhimurium* infection[91]. Using other bacterial infection

models, the function of the CXCL8-CXCR2 signalling axis in neutrophil recruitment has been shown to be conserved in zebrafish[55,57]. Local *S. typhimurium* infection has also been shown to induce the recruitment of macrophages via the chemokine receptor Cxcr3.2, one of the zebrafish orthologues of human CXCR3[46]. The ligand association of Cxcr3.2 remains to be established.

In addition to phagocyte recruitment, localised infection also triggers emergency-driven haematopoiesis[62]. Early neutropaenia is a frequent outcome of *S. typhimurium* hindbrain infection in zebrafish embryos and this is compensated for by increased granulopoiesis. The activity of iNOS (and thus the production of the pleiotropic mediator nitric oxide), was found to be necessary to stimulate the expansion and proliferation of HSPCs in response to infection-dependent neutropaenia. The induction of iNOS is dependent on expression of the transcription factor C/ebpβ (CCAAT enhancer-binding protein β) in HSPCs. This is suggested to be an effect of elevated circulating levels of Gcsf (Granulocyte colony stimulating factor), produced by activated macrophages at the infection site[62].

The *S. typhimurium* infection model has recently led to new insight into the connection between infection control and host cell metabolic modulation[63]. Profound adaptations in glucose and lipid metabolism occur within infected immune cells. For example, in response to stimulation by *Salmonella* pathogenic factors, macrophages increase their uptake of lipids to fuel ROS production[63]. In line with this, *S. typhimurium* infection induces the expression of the mitochondria-associated enzyme Irg1 (Immunoresponsive gene 1) within infected zebrafish macrophages. This protein directs the catabolism of fatty acids to sustain mitochondrial oxidative phosphorylation and in turn leads to the production of mitochondrial ROS, contributing to intracellular degradation of phagocytosed bacteria. Irg1 holds promise as a new therapeutic target at the interface of inflammation and metabolism[62] (**Table 1**).

Burkholderia cenocepacia

The *B. cepacia* complex (*Bcc*) is represented by several closely related Gram-negative species that are able to survive freely in the environment or replicate within different hosts, including amoebae, invertebrates, vertebrates and plants[98]. In humans, opportunistic infection by *Bcc* frequently occurs in cystic fibrosis or immunocompromised individuals and represents a recurrent cause of fatal complications[99]. The capability to survive and infect a wide range of hosts suggests that *Bcc* species are highly adaptable to different niches and produce multiple virulence factors; however, the complex mechanisms of host-pathogen interactions underlying infections with *B. cenocepacia* and other *Bcc* strains remain largely unknown. In particular, it has been difficult to establish conclusively whether *B. cenocepacia* can survive intracellularly. Visualising infection in zebrafish embryos helped to answer this key question, by demonstrating the ability of this pathogen to survive within macrophages (**Figure 3C**). Following the creation of an intramacrophage replication niche, the bacterial infection disseminates by non-lytic expulsion from infected cells, induces immune cell aggregations and ultimately causes fatal systemic bacteraemia[100].

The zebrafish model system has also provided a valuable contribution to the investigation of the *in vivo* relevance of several *B. cenocepacia* virulence factors. A quorum-sensing-deficient cepR strain was shown to be strongly attenuated, indicated by a reduced ability to

replicate intracellularly and to disseminate efficiently from infected macrophages. Furthermore, differences in virulence were observed between strains from a panel of clinical isolates[100]. Loss of the third replicon, pC3 (a non-essential megaplasmid associated with several virulence determinants), results in highly attenuated infection in multiple hosts, including zebrafish embryos[101,102]. Mutants in pC3 are not able to grow significantly *in vivo* but are not eradicated, suggesting that the pC3-linked virulence factors are dispensable for intramacrophage survival[101]. A function in adaptation to a wide range of environments, rather than a direct role in modulating intracellular growth, might explain the prevalence of the pC3 replicon among *Bcc* isolates[102].

Together, these studies demonstrate the usefulness of the zebrafish model for analysis of *B. cenocepacia* mechanisms of intracellular survival and virulence.

Staphylococcus aureus

S. aureus is the causative agent of a wide range of infectious pathologies such as sty, pneumonia, endocarditis, osteomyelitis and septicaemia[103], which remain important causes of morbidity and of complications in hospitalised patients. Although not a natural pathogen of zebrafish, both embryos[104] and adults[105] exhibit clear acute symptoms when infected with this Gram-positive pathogen, providing a useful model for bacteraemia (**Figure 3D**).

S. aureus has long been considered an extracellular pathogen, but there is accumulating evidence that it can also survive and replicate in phagocytes[106]. The zebrafish embryo model has contributed significantly to our understanding of the nature and relevance of the intracellular phase in the life cycle of this pathogen[47,104]. Live imaging showed that, upon intravenous infection, *S. aureus* is completely phagocytosed by macrophages and neutrophils[104,107]. Although some embryos clear the infection in a phagocyte-dependent manner, other embryos develop overwhelming infection, indicating that the bacteria can subvert the phagocyte-killing mechanisms[47].

When larvae are co-infected with two isogenic, but differently labelled, *S. aureus* clones, the infection evolves by forming focal lesions that are predominantly monoclonal and, during the course of overwhelming infection, the ratio between the original strains is often skewed towards one predominating strain[47]. This phenomenon is fully dependent on phagocyte activity. These data suggest that most of the phagocytes are able to clear the infection but a population of phagocytes provides an intracellular protective niche in which some bacteria gain the ability to replicate and resist, to ultimately be released and disseminate. Consistent with this, co-infection in a murine sepsis model resulted in kidney abscesses that contained predominantly one strain of *S. aureus* and thus were likely founded by single bacteria[108]. The relevance of this work for clinical treatments is underscored by a recent study showing that the use of sub-curative antibiotic doses can support the preferential expansion of antibiotic-resistant bacteria during a mixed infection[109]. Selective ablation of macrophages or neutrophils in the zebrafish model has revealed that neutrophils are most likely to form the privileged niche responsible for disseminated infection of *S. aureus*[104]. Interesting remaining questions include elucidation of the mechanisms by which some bacteria from the initial inoculum are able to avoid being killed by neutrophils and determination of whether *S. aureus* can also resist macrophages *in vivo*, as suggested by human cell culture studies[110].

Shigella flexneri

S. flexneri, a human-adapted *Escherichia coli* species, is a causative agent of diarrhoea and dysentery in humans, generally deriving from orofaecal contaminations. Like other enterobacteria, it mostly affects the digestive tract; however, in advanced infectious stages, it can lead to bacteraemia and systemic sepsis. In the early phase of infection, the pathogen can interact with membranes of host cells, inject virulence determinants and induce ruffling and internalisation[40]. In this actively induced ingestion mechanism resides its capability to establish intracellular infection in non-phagocytic cells, such as epithelial cells associated with the digestive tract. Once it is internalised, it can escape from phagosomes and survive freely in the cytosol. Subsequently, the pathogen can spread through intestinal epithelial cells by actin-based motility (**Figure 3E**). Microfold cells allow *Shigella* to transverse the intestinal epithelium, where they encounter macrophages. Death of infected macrophages and subsequent destabilisation of the epithelium due to inflammation allows more *Shigella* to infiltrate the tissue and invade epithelial cells through the basal membrane. Survival and replication in macrophages, eventually followed by macrophage pyroptosis, is fundamental to allowing dissemination and extensive colonisation of the intestinal epithelium[111].

Recently, a zebrafish model for *S. flexneri* was established and this has been used to show that intravenously administrated bacteria can survive and replicate both in macrophages and in non-immune cells[86]. The pathogenicity of *Shigella* is highly dependent on the presence of T3SS virulence factors and avirulent strains can be successfully combated by the zebrafish innate immune system and are not able to induce phagocytosis in non-phagocytic cells. Live imaging shows that replication of *S. flexneri* in macrophages ultimately induces cell death, whereas bacteria are more efficiently contained and degraded within neutrophils. Neutrophils also act as scavengers, eliminating infected dead cells. Macrophages are not able to retain the infection within vacuoles and bacteria spread into the cytosol, where they can colocalise with actin and septin cages (**Figure 3E**).

In mammalian cultured cells, cytosolic *S. flexneri* can be targeted for autophagy via both ubiquitin-dependent and -independent pathways, and, as a counteractive mechanism, the bacteria can secrete virulence factors to escape autophagy[41,112]. Colocalisation with the autophagy marker Lc3 followed by electron microscopic analysis in the zebrafish model confirmed that autophagy targeting is associated with entrapment of *S. flexneri* in septin cage-like structures[33,86]. Reduction of autophagy, via knockdown of the autophagy-related receptor p62, increases the infection burden of zebrafish larvae and this effect is specific only for the T3SS-positive strain that is able to escape into the cytosol[86]. These data support the hypothesis that antibacterial protection provided by efficient autophagic machinery is essential to properly counteract *S. flexneri* infection. The ability to monitor *S. flexneri* infection in a transparent zebrafish host provides new possibilities to assess the relevance of autophagy *in vivo* in immune and non-immune cells, and to develop new strategies for anti-bacterial therapies targeting this process (**Table 1**).

Candida albicans

C. albicans is an opportunistic dimorphic fungus that grows in yeast and hyphal forms[113]. Most of the human population carries *C. albicans* as a harmless constituent of the epidermal, mucosal and intestinal flora. However, uncontrolled systemic candidiasis and fungal growth on the mucosal surfaces can cause severe and life-threatening infectious complications, particularly in immunocompromised individuals. In zebrafish embryos, as

in humans, *C. albicans* can be phagocytosed by both neutrophils and macrophages[114,115]. Live observations reveal that, in a non-compromised zebrafish host, this intracellular localisation leads to a transitory standoff phase in which the yeast form survives and replicates, but does not germinate or lyse the host cell (**Figure 3F**). Subsequently, the fungi switch to the more virulent hyphal form and proliferate exuberantly in individuals that fail to contain the infection, whereas they revert to the yeast form in most surviving embryos[115]. Intracellular yeast forms are unable to undergo the yeast-to-hyphal transition, even under conditions of impaired oxidative-stress response, in contrast with previous *in vitro* data in which filamentous growth was observed within cultured macrophages[116]. Therefore, macrophages apparently have an enhanced ability to control infection in the *in vivo* environment.

Although germination was shown to be independent of the phagocyte-specific NADPH oxidase (PHOX), this enzyme was found to be essential to produce an efficient oxidative-stress response against *C. albicans* and to control filamentous growth[115,116]. Previously, the limitation of fungal growth was ascribed mainly to direct fungal destruction by ROS; however, imaging in zebrafish revealed a non-canonical role for PHOX and for the epithelial dual NADPH oxidase (DUOX) in recruitment of phagocytes to *C. albicans* infection sites. Therefore, impaired phagocyte recruitment to invading *Candida* under conditions of NADPH oxidase deficiency seems to be the cause of the overall reduction in containment of the infection and, consequently, of massive extracellular hyphal growth. Although localised infection with wildtype *C. albicans* is unable to induce chemoattraction under conditions of NADPH oxidase deficiency, infection with a yeast-locked mutant strain (*edt1Δ/Δ*) can be efficiently counteracted by phagocyte recruitment and internalisation, even in pan-NADPH-oxidase-depleted conditions. This suggests that the hyphal transition (or another edt1-associated program) is also able to attenuate ROS-independent phagocyte recruitment, thus explaining the relevance of host ROS-driven chemoattraction mechanisms to counteract *C. albicans* infection[116].

CONCLUDING REMARKS

The study of intracellular pathogens in zebrafish macrophages has led to new mechanistic insights that are inspiring novel host-directed therapeutic strategies (**Table 1**). The real-time imaging possibilities in zebrafish will also be very useful for elucidating the mechanisms underlying macrophage migration processes, as has already been demonstrated by the study of neutrophils in the larval system[6,7,55]. A question that is very relevant both for infectious diseases and for cancer biology concerns the presence of different pro- and anti-inflammatory macrophage subtypes in zebrafish. Classically activated (M1) and alternatively activated (M2) macrophages, resembling the phenotypes of mammalian macrophages, have been identified in different fish species[117]. That different macrophage subtypes might already be present in early zebrafish larvae has been suggested, but this remains to be further investigated[118]. The early larval stages, which are optimally suited for imaging and for genetic and pharmacological interventions, can give much information on the intracellular survival mechanisms of pathogens, as demonstrated by the studies discussed herein. The early larval stages are also very useful for studying the response of microglia to brain injuries or infection, contributing to a deeper understanding of the role of these specialised macrophages in neurodegenerative diseases[67,119]. Studying the antigen-presentation function of macrophages and DCs at later developmental stages is becoming increasingly feasible owing to advances in technologies for generating stable

mutant lines[120,121,122]. Dynamic interactions between macrophages and neutrophils that are emerging from recent studies in zebrafish are of considerable interest for further study[44,56,65]. The use of the zebrafish model has already provided insights into the *in vivo* relevance of intracellular defence mechanisms such as ROS and RNS production and autophagy. We expect that further use of this powerful model will continue to make important contributions towards the understanding of innate immunity and of the virulence strategies that pathogens use to subvert innate host defences.

ACKNOWLEDGMENTS

The authors thank Georges Lutfalla (University of Montpellier II) and Graham J. Lieschke (Monash University) for the kind gift of the *Tg(mpeg1:mCherry-F)* and *Tg(mpeg1:Gal4-VP16/UAS-E1b:Kaede)* lines, respectively. These lines were used to make **Figure 2** and **Supplementary Movies 1-2**.

V.T. is a Marie Curie fellow in the Initial Training Network FishForPharma (PITN-GA-2011-289209) funded by the 7th Framework Programme of the European Commission. S.M. is supported by a fellowship from the Higher Education Commission of Pakistan. Work that led to this Review was additionally supported by the European 7th framework project ZF-Health (FP7-Health-2009-242048), by the Smart Mix Program (NWOA_6QY9BM) of The Netherlands Ministry of Economic Affairs and The Netherlands Ministry of Education, Culture and Science, and by the Leiden University Fund (LUF).

FOOTNOTES

This article is part of a Special Issue, Spotlight on Zebrafish: Translational Impact.

The format and spelling of the contents in this chapter have been adapted from the published article to conform it to the thesis outline.

Marker	Transgenic line	Specificity	Promoter sequence	Ref.
apoeb apolipoprotein Eb	*Tg(apoeb:lyn-eGFP)*	Microglial cells	Obtained from a BAC clone containing the *apoeb* locus, by BAC recombineering at the translation start	60
coro1a coronin, actin binding protein, 1A	*Tg(coro1a:eGFP)*	Macrophages, neutrophils and thymocytes[(a)]	-7.03 kb of *coro1a* upstream the translation start	123
csf1ra/fms colony stimulating factor 1 receptor, a	*TgBAC(csf1ra:Gal4-VP16 / UAS-E1b:Eco.NfsB-mCherry)*	Macrophages (highly motile), and xantophore cells (immobile)	Obtained from a BAC clone containing the *csf1ra* locus, by BAC recombineering at the translation start	43
fli1a friend leukaemia integration 1a	*Tg(fli1a:eGFP)*	Primitive macrophages (dull), endothelial cells (bright) and subsets of erythrocytes (dull)	5'UTR of *fli* was obtained from a PAC library	124
lyz/lysC lysozyme	*Tg(lyz:eGFP)*	Neutrophils[(b)]	-11 kb of *lyz* upstream the translation start	125
	Tg(lyz:DsRed2)	Neutrophils[(b)]	-6.35 kb of *lyz* upstream the translation start	125
	Tg(-4.1lyz:eGFP)	Neutrophils[(b)]	-4.1 kb of *lyz* upstream the translation start	126
	Tg(-2.4lyz:eGFP)	Neutrophils and primitive macrophages[(c)]	-2.4 kb of *lyz* upstream the translation start	127
	Tg(lyz:Gal4-VP16)	Neutrophils[(b)]	-11 kb of *lyz* construct as in ref.[125]	128
mhc2dab major histocompatibility complex class II DAB gene	*Tg(mhc2dab:eGFP)* *Tg(mhc2dab:mCherry)*	Antigen presenting cells (APCs)[(d)]	-3.8 kb of *mhc2dab* upstream the transcription start	17
mpeg1 macrophage expressed 1	*Tg(mpeg1:eGFP)* *Tg(mpeg1:mCherry)* *Tg(mpeg1:Gal4-VP16)*	Macrophages[(e)]	-1.86 kb of *mpeg1* upstream the translation start	44
	Tg(mpeg1:mCherry-F)	Macrophages	-1.86 kb of *mpeg1* upstream the translation start	61
	Tg(mpeg1:Dendra2)	Macrophages[(e)]	As in ref.[44]	129
	Tg(mpeg1:YFP)	Macrophages[(e)]	As in ref.[44]	83
mpx/mpo myeloid-specific peroxidase	*TgBAC(mpx:eGFP)*	Neutrophils[(f)]	Obtained from a BAC clone containing the *mpx* locus, by BAC recombineering at the translation start	130
	Tg(mpx:GFP)	Neutrophils (bright) and a subset of macrophages (dull)	-8 kb of *mpx* upstream the translation start	131
	Tg(-8mpx:mCherry) *Tg(-8mpx:DsRed-F)* *Tg(-8 mpx:eGFP-F)*	Neutrophils (bright) and a subset of macrophages (dull)	As in ref.[131]	132
	Tg(-8mpx:Dendra2)	Neutrophils (bright) and a subset of macrophages (dull)	As in ref.[131]	133

Supplementary Table 1. Zebrafish fluorescent reporter lines for immune cells *(continued on the next page)***.**

myd88 myeloid differentiation primary response gene (88)	*Tg(myd88:eGFP)* *Tg(myd88:DsRed2)*	Subsets of myeloid leukocytes, distal pronephric ducts and cloaca	-3.7 kb of *myd88* upstream the translation start	59
ptprc/cd45 protein tyrosine phosphatase, receptor type, C	*Tg(ptprc:DsRed)*	Macrophages, granulocytes and T lymphocytes	-7.6 kb of *ptprc* upstream the transcription start	14
spi1b/pu.1 spleen focus forming virus (SFFV) proviral integration oncogene spi1b	*Tg(-5.3spi1b:eGFP)*	Early myeloid cells[(g)]	-5.3 kb of *spi1b* upstream the translation start	134
	Tg(-9.0spi1b:eGFP)	Early myeloid cells (bright) and muscles (dull)[(g)]	-9 kb of *spi1b* upstream the translation start	135
	Tg(-4spi1b:Gal4 / UAS:eGFP)	Early myeloid cells[(g)]	-4 kb of *spi1b* upstream the translation start	60
	Tg(-4spi1b:lyn-eGFP)	Early myeloid cells[(g)]	As in ref.[60]	46

Supplementary Table 1. Zebrafish fluorescent reporter lines for immune cells *(continued from the previous page)*. Notes: [(a)] Expression in macrophages, neutrophils and thymocytes was shown for embryonic and young larval stages. Expression in myelomonocyte progenitors in head-kidneys of adults was also documented; [(b)] Discrepancies about expression of the construct in primitive macrophages reported; [(c)] Observations limited to embryonic and early larval stage. Labelling of primitive macrophages was determined based on the presence of fluorescent cells over the yolk at 26 hpf. Expression in macrophages from the second wave of primitive haematopoiesis and definitive haematopoiesis not demonstrated. [(d)] APCs are here indicated as macrophages, dendritic cells, B lymphocytes and eosinophils. Fluorescence visible from 5dpf and abundantly labelling APCs only from 12dpf; expression in keratinocytes reported in adults and juveniles; [(e)] Loss of expression after 6 dpf and in the adults reported; labelling of Langerhans dendritic cells in larvae suggested; [(f)] Existence of a set of GFP^{low} macrophage-like cells distinguishable by confocal microscopy reported by some laboratories; [(g)] Expression documented from 12 to 30 hpf; Expression in early lymphoid cells reported for adult *Tg(-9.0spi1b:eGFP).*

Marker	Reporter construct	Specificity	Notes	Ref.
rab5c RAB5c, member RAS oncogene family	*Tg(h2afx:eGFP-rab5c)*[(a)]	Early endosomes	-	136
	Tg(UAS:mCherry-rab5c_S36N)[(b)]	Early endosomes	S36N substitution, dominant negative	136
	Tg(UAS:mCherry-rab5c_Q81L)[(b)]	Early endosomes	Q81L substitution, constitutively active	136
rab7a RAB7, member RAS oncogene family a	*Tg(h2afx:eGFP-rab7)*[(a)]	Late endosomes	-	136
	Tg(UAS:mCherry-rab7_T22N)[(b)]	Late endosomes	T22N substitution, dominant negative	136
	Tg(UAS:mCherry-rab7_Q67L)[(b)]	Late endosomes	Q67L substitution, constitutively active	136
rab7b RAB7, member RAS oncogene family b	*Plasmid(UAS:GFP-rab7b_T22N)*[(b)]	Late endosomes	T22N substitution, dominant negative; the reporter consists of a UAS-expression plasmid	137
rab11a RAB11a, member RAS oncogene family	*Tg(h2afx:eGFP-rab11a)*[(a)]	Recycling endosomes	-	136
	Tg(UAS:mCherry-rab11a_S25N)[(b)]	Recycling endosomes	S25N substitution, dominant negative	136
	Tg(UAS:mCherry-rab11a_Q70L)[(b)]	Recycling endosomes	Q70L substitution, constitutively active	136
lamp1 lysosomal-associated membrane protein 1	*Tg(hsp70l:lamp1-RFP)*[(c)]	Lysosomes	-	137
lamp2 lysosomal membrane glycoprotein 2	*Tg(hsp70l:lamp2-eGFP)*[(c)]	Lysosomes	-	137
cd63/lamp3 Cd63 antigen	*Plasmid(CMV/SP6:GFP-cd63)*[(d)]	Lysosomes	The reporter consists of an expression plasmid for CMV-expression or mRNA preparation	60
map1lc3b microtubule-associated protein 1 light chain 3 beta	*Tg(CMV:eGFP-map1lc3b)*[(d)]	Autophagosomes	-	138
	Tg(hsp70l:RFP-Rno.Map1lc3b)[(c)]	Autophagosomes	Contains the Map1lc3b sequence from the rat (*Rattus norvegicus*)	137
gabarapa GABA(A) receptor-associated protein a	*Tg(CMV:eGFP-gabarapa)*[(d)]	Autophagosomes	-	138
rab32a RAB32a, member RAS oncogene family	*Tg(4xUAS:eGFP-rab32a,myl7:eGFP)*[(b)]	Vesicular trafficking	-	137
	Plasmid(UAS:GFP-rab32a_T27N)[(b)]	Vesicular trafficking	T27N substitution, dominant negative; the reporter consists of a UAS-expression plasmid	137
rab38b	*Tg(UAS:GFP-rab38b-T23N, cmlc2:GFP)*[(b)]	Vesicular trafficking	T23N substitution, dominant negative	137

Supplementary Table 2. Zebrafish reporters of subcellular compartments. Notes: [(a)] *h2afx*: H2A histone family, member X constitutive promoter; [(b)] *UAS*: Upstream Activating Sequence for Gal4-dependent expression; [(c)] *hsp70l*: heat shock cognate 70-kd protein, like inducible promoter; [(d)] *CMV*: Cytomegalovirus constitutive promoter.

HYPERLINK TO SUPPLEMENTARY MOVIES

Supplementary Movies are available online at the following URL:
https://drive.google.com/open?id=0B_188Sfgn4xoUkRVNjNKdlNhSEE

REFERENCES

1 Renshaw SA, Trede NS. A model 450 million years in the making: zebrafish and vertebrate immunity. Dis Model Mech. 2012 Jan;5(1):38-47.
2 van der Vaart M, Spaink HP, Meijer AH. Pathogen recognition and activation of the innate immune response in zebrafish. Adv Hematol. 2012;2012:159807.
3 Ramakrishnan L. Looking within the zebrafish to understand the tuberculous granuloma. Adv Exp Med Biol. 2013;783:251-66.
4 Lam SH, Chua HL, Gong Z, Lam TJ, Sin YM. Development and maturation of the immune system in zebrafish, Danio rerio: a gene expression profiling, in situ hybridization and immunological study. Dev Comp Immunol. 2004 Jan;28(1):9-28.
5 Page DM, Wittamer V, Bertrand JY, Lewis KL, Pratt DN, Delgado N, Schale SE, McGue C, Jacobsen BH, Doty A, Pao Y, Yang H, Chi NC, Magor BG, Traver D. An evolutionarily conserved program of B-cell development and activation in zebrafish. Blood. 2013 Aug 22;122(8):e1-11.
6 Henry KM, Loynes CA, Whyte MK, Renshaw SA. Zebrafish as a model for the study of neutrophil biology. J Leukoc Biol. 2013 Oct;94(4):633-42.
7 Shelef MA, Tauzin S, Huttenlocher A. Neutrophil migration: moving from zebrafish models to human autoimmunity. Immunol Rev. 2013 Nov;256(1):269-81.
8 Herbomel P, Thisse B, Thisse C. Ontogeny and behaviour of early macrophages in the zebrafish embryo. Development. 1999 Sep;126(17):3735-45.
9 Herbomel P, Thisse B, Thisse C. Zebrafish early macrophages colonize cephalic mesenchyme and developing brain, retina, and epidermis through a M-CSF receptor-dependent invasive process. Dev Biol. 2001 Oct 15;238(2):274-88.
10 Takahashi K, Naito M, Takeya M. Development and heterogeneity of macrophages and their related cells through their differentiation pathways. Pathol Int. 1996 Jul;46(7):473-85.
11 Colucci-Guyon E, Tinevez JY, Renshaw SA, Herbomel P. Strategies of professional phagocytes in vivo: unlike macrophages, neutrophils engulf only surface-associated microbes. J Cell Sci. 2011 Sep 15;124(Pt 18):3053-9.
12 Bertrand JY, Kim AD, Violette EP, Stachura DL, Cisson JL, Traver D. Definitive hematopoiesis initiates through a committed erythromyeloid progenitor in the zebrafish embryo. Development. 2007 Dec;134(23):4147-56.
13 Murayama E, Kissa K, Zapata A, Mordelet E, Briolat V, Lin HF, Handin RI,Herbomel P. Tracing hematopoietic precursor migration to successive hematopoietic organs during zebrafish development. Immunity. 2006 Dec;25(6):963-75.
14 Bertrand JY, Chi NC, Santoso B, Teng S, Stainier DY, Traver D. Haematopoietic stem cells derive directly from aortic endothelium during development. Nature. 2010 Mar 4;464(7285):108-11.
15 Kissa K, Herbomel P. Blood stem cells emerge from aortic endothelium by a novel type of cell transition. Nature. 2010 Mar 4;464(7285):112-5.
16 Boisset JC, van Cappellen W, Andrieu-Soler C, Galjart N, Dzierzak E, Robin C. In vivo imaging of haematopoietic cells emerging from the mouse aortic endothelium. Nature. 2010 Mar 4;464(7285):116-20.
17 Wittamer V, Bertrand JY, Gutschow PW, Traver D. Characterization of the mononuclear phagocyte system in zebrafish. Blood. 2011 Jun 30;117(26):7126-35.
18 Svahn AJ, Graeber MB, Ellett F, Lieschke GJ, Rinkwitz S, Bennett MR, Becker TS. Development of ramified microglia from early macrophages in the zebrafish optic tectum. Dev Neurobiol. 2013 Jan;73(1):60-71.
19 Stachura DL, Traver D. Cellular dissection of zebrafish hematopoiesis. Methods Cell Biol. 2011;101:75-110.
20 Jagannathan-Bogdan M, Zon LI. Hematopoiesis. Development. 2013 Jun;140(12):2463-7.
21 Xu LL, Warren MK, Rose WL, Gong W, Wang JM. Human recombinant monocyte chemotactic protein and other C-C chemokines bind and induce directional migration of dendritic cells in vitro. J Leukoc Biol. 1996 Sep;60(3):365-71.
22 Cotton M, Claing A. G protein-coupled receptors stimulation and the control of cell migration. Cell Signal. 2009 Jul;21(7):1045-53.
23 Elomaa O, Kangas M, Sahlberg C, Tuukkanen J, Sormunen R, Liakka A, Thesleff I, Kraal G, Tryggvason K. Cloning of a novel bacteria-binding receptor structurally related to scavenger receptors and expressed in a subset of macrophages. Cell. 1995 Feb 24;80(4):603-9.

24 O'Neill LA, Golenbock D, Bowie AG. The history of Toll-like receptors - redefining innate immunity. Nat Rev Immunol. 2013 Jun;13(6):453-60.
25 Bertin J, Nir WJ, Fischer CM, Tayber OV, Errada PR, Grant JR, Keilty JJ, Gosselin ML, Robison KE, Wong GH, Glucksmann MA, DiStefano PS. Human CARD4 protein is a novel CED-4/Apaf-1 cell death family member that activates NF-kappaB. J Biol Chem. 1999 May 7;274(19):12955-8.
26 Inohara N, Koseki T, del Peso L, Hu Y, Yee C, Chen S, Carrio R, Merino J, Liu D, Ni J, Núñez G. Nod1, an Apaf-1-like activator of caspase-9 and nuclear factor-kappaB. J Biol Chem. 1999 May 21;274(21):14560-7.
27 Martinon F, Burns K, Tschopp J. The inflammasome: a molecular platform triggering activation of inflammatory caspases and processing of proIL-beta. Mol Cell. 2002 Aug;10(2):417-26.
28 Minakami R, Sumimotoa H. Phagocytosis-coupled activation of the superoxide-producing phagocyte oxidase, a member of the NADPH oxidase (nox) family. Int J Hematol. 2006 Oct;84(3):193-8.
29 El-Gayar S, Thüring-Nahler H, Pfeilschifter J, Röllinghoff M, Bogdan C. Translational control of inducible nitric oxide synthase by IL-13 and arginine availability in inflammatory macrophages. J Immunol. 2003 Nov 1;171(9):4561-8.
30 Schmidtchen A, Frick IM, Andersson E, Tapper H, Björck L. Proteinases of common pathogenic bacteria degrade and inactivate the antibacterial peptide LL-37. Mol Microbiol. 2002 Oct;46(1):157-68.
31 Park YK, Bearson B, Bang SH, Bang IS, Foster JW. Internal pH crisis, lysine decarboxylase and the acid tolerance response of Salmonella typhimurium. Mol Microbiol. 1996 May;20(3):605-11.
32 Vandal OH, Pierini LM, Schnappinger D, Nathan CF, Ehrt S. A membrane protein preserves intrabacterial pH in intraphagosomal Mycobacterium tuberculosis. Nat Med. 2008 Aug;14(8):849-54.
33 Mostowy S, Bonazzi M, Hamon MA, Tham TN, Mallet A, Lelek M, Gouin E, Demangel C, Brosch R, Zimmer C, Sartori A, Kinoshita M, Lecuit M, Cossart P. Entrapment of intracytosolic bacteria by septin cage-like structures. Cell Host Microbe. 2010 Nov 18;8(5):433-44.
34 Deretic V, Saitoh T, Akira S. Autophagy in infection, inflammation and immunity. Nat Rev Immunol. 2013 Oct;13(10):722-37.
35 Abdallah AM, Gey van Pittius NC, Champion PA, Cox J, Luirink J, Vandenbroucke-Grauls CM, Appelmelk BJ, Bitter W. Type VII secretion—mycobacteria show the way. Nat Rev Microbiol. 2007 Nov;5(11):883-91.
36 Baxt LA, Garza-Mayers AC, Goldberg MB. Bacterial subversion of host innate immune pathways. Science. 2013 May 10;340(6133):697-701.
37 Masaki T, Qu J, Cholewa-Waclaw J, Burr K, Raaum R, Rambukkana A. Reprogramming adult Schwann cells to stem cell-like cells by leprosy bacilli promotes dissemination of infection. Cell. 2013 Jan 17;152(1-2):51-67.
38 Wang Y, Curry HM, Zwilling BS, Lafuse WP. Mycobacteria inhibition of IFN-gamma induced HLA-DR gene expression by up-regulating histone deacetylation at the promoter region in human THP-1 monocytic cells. J Immunol. 2005 May 1;174(9):5687-94.
39 Duclos S, Desjardins M. Subversion of a young phagosome: the survival strategies of intracellular pathogens. Cell Microbiol. 2000 Oct;2(5):365-77.
40 Ogawa M, Handa Y, Ashida H, Suzuki M, Sasakawa C. The versatility of Shigella effectors. Nat Rev Microbiol. 2008 Jan;6(1):11-6.
41 Ogawa M, Yoshimori T, Suzuki T, Sagara H, Mizushima N, Sasakawa C. Escape of intracellular Shigella from autophagy. Science. 2005 Feb 4;307(5710):727-31.
42 Hilbi H, Moss JE, Hersh D, Chen Y, Arondel J, Banerjee S, Flavell RA, Yuan J, Sansonetti PJ, Zychlinsky A. Shigella-induced apoptosis is dependent on caspase-1 which binds to IpaB. J Biol Chem. 1998 Dec 4;273(49):32895-900.
43 Gray C, Loynes CA, Whyte MK, Crossman DC, Renshaw SA, Chico TJ. Simultaneous intravital imaging of macrophage and neutrophil behaviour during inflammation using a novel transgenic zebrafish. Thromb Haemost. 2011 May;105(5):811-9.
44 Ellett F, Pase L, Hayman JW, Andrianopoulos A, Lieschke GJ. mpeg1 promoter transgenes direct macrophage-lineage expression in zebrafish. Blood. 2011 Jan 27;117(4):e49-56.
45 Meijer AH, van der Sar AM, Cunha C, Lamers GE, Laplante MA, Kikuta H, Bitter W, Becker TS, Spaink HP. Identification and real-time imaging of a myc-expressing neutrophil population involved in inflammation and mycobacterial granuloma formation in zebrafish. Dev Comp Immunol. 2008;32(1):36-49.
46 Zakrzewska A, Cui C, Stockhammer OW, Benard EL, Spaink HP, Meijer AH. Macrophage-specific gene functions in Spi1-directed innate immunity. Blood. 2010 Jul 22;116(3):e1-11.
47 Prajsnar TK, Hamilton R, Garcia-Lara J, McVicker G, Williams A, Boots M, Foster SJ, Renshaw SA. A privileged intraphagocyte niche is responsible for disseminated infection of Staphylococcus aureus in a zebrafish model. Cell Microbiol. 2012 Oct;14(10):1600-19.
48 Su F, Juarez MA, Cooke CL, Lapointe L, Shavit JA, Yamaoka JS, Lyons SE. Differential regulation of primitive myelopoiesis in the zebrafish by Spi-1/Pu.1 and C/ebp1. Zebrafish. 2007 Fall;4(3):187-99.
49 Li L, Jin H, Xu J, Shi Y, Wen Z. Irf8 regulates macrophage versus neutrophil fate during zebrafish primitive myelopoiesis. Blood. 2011 Jan 27;117(4):1359-69.

50 Davis JM, Clay H, Lewis JL, Ghori N, Herbomel P, Ramakrishnan L. Real-time visualization of mycobacterium-macrophage interactions leading to initiation of granuloma formation in zebrafish embryos. Immunity. 2002 Dec;17(6):693-702.
51 Herbomel P, Levraud JP. Imaging early macrophage differentiation, migration, and behaviors in live zebrafish embryos. Methods Mol Med. 2005;105:199-214.
52 Davis JM, Ramakrishnan L. The role of the granuloma in expansion and dissemination of early tuberculous infection. Cell. 2009 Jan 9;136(1):37-49.
53 Yoo SK, Starnes TW, Deng Q, Huttenlocher A. Lyn is a redox sensor that mediates leukocyte wound attraction in vivo. Nature. 2011 Nov 20;480(7375):109-12.
54 Benard EL, van der Sar AM, Ellett F, Lieschke GJ, Spaink HP, Meijer AH. Infection of zebrafish embryos with intracellular bacterial pathogens. J Vis Exp. 2012 Mar 15;(61). pii: 3781.
55 Sarris M, Masson JB, Maurin D, Van der Aa LM, Boudinot P, Lortat-Jacob H, Herbomel P. Inflammatory chemokines direct and restrict leukocyte migration within live tissues as glycan-bound gradients. Curr Biol. 2012 Dec 18;22(24):2375-82.
56 Yang CT, Cambier CJ, Davis JM, Hall CJ, Crosier PS, Ramakrishnan L. Neutrophils exert protection in the early tuberculous granuloma by oxidative killing of mycobacteria phagocytosed from infected macrophages. Cell Host Microbe. 2012 Sep 13;12(3):301-12.
57 Deng Q, Sarris M, Bennin DA, Green JM, Herbomel P, Huttenlocher A. Localized bacterial infection induces systemic activation of neutrophils through Cxcr2 signaling in zebrafish. J Leukoc Biol. 2013 May;93(5):761-9.
58 Cambier CJ, Takaki KK, Larson RP, Hernandez RE, Tobin DM, Urdahl KB, Cosma CL, Ramakrishnan L. Mycobacteria manipulate macrophage recruitment through coordinated use of membrane lipids. Nature. 2014 Jan 9;505(7482):218-22.
59 Hall C, Flores MV, Chien A, Davidson A, Crosier K, Crosier P. Transgenic zebrafish reporter lines reveal conserved Toll-like receptor signaling potential in embryonic myeloid leukocytes and adult immune cell lineages. J Leukoc Biol. 2009 May;85(5):751-65.
60 Peri F, Nüsslein-Volhard C. Live imaging of neuronal degradation by microglia reveals a role for v0-ATPase a1 in phagosomal fusion in vivo. Cell. 2008 May 30;133(5):916-27.
61 Bernut A, Herrmann JL, Kissa K, Dubremetz JF, Gaillard JL, Lutfalla G, Kremer L. Mycobacterium abscessus cording prevents phagocytosis and promotes abscess formation. Proc Natl Acad Sci U S A. 2014 Mar 11;111(10):E943-52.
62 Hall CJ, Flores MV, Oehlers SH, Sanderson LE, Lam EY, Crosier KE, Crosier PS. Infection-responsive expansion of the hematopoietic stem and progenitor cell compartment in zebrafish is dependent upon inducible nitric oxide. Cell Stem Cell. 2012 Feb 3;10(2):198-209.
63 Hall CJ, Boyle RH, Astin JW, Flores MV, Oehlers SH, Sanderson LE, Ellett F, Lieschke GJ, Crosier KE, Crosier PS. Immunoresponsive gene 1 augments bactericidal activity of macrophage-lineage cells by regulating β-oxidation-dependent mitochondrial ROS production. Cell Metab. 2013 Aug 6;18(2):265-78.
64 Bilan DS, Pase L, Joosen L, Gorokhovatsky AY, Ermakova YG, Gadella TW, Grabher C, Schultz C, Lukyanov S, Belousov VV. HyPer-3: a genetically encoded H(2)O(2) probe with improved performance for ratiometric and fluorescence lifetime imaging. ACS Chem Biol. 2013 Mar 15;8(3):535-42.
65 Elks PM, Brizee S, van der Vaart M, Walmsley SR, van Eeden FJ, Renshaw SA, Meijer AH. Hypoxia inducible factor signaling modulates susceptibility to mycobacterial infection via a nitric oxide dependent mechanism. PLoS Pathog. 2013;9(12):e1003789.
66 Cheung CY, Webb SE, Love DR, Miller AL. Visualization, characterization and modulation of calcium signaling during the development of slow muscle cells in intact zebrafish embryos. Int J Dev Biol. 2011;55(2):153-74.
67 Sieger D, Moritz C, Ziegenhals T, Prykhozhij S, Peri F. Long-range Ca2+ waves transmit brain-damage signals to microglia. Dev Cell. 2012 Jun 12;22(6):1138-48.
68 Prouty MG, Correa NE, Barker LP, Jagadeeswaran P, Klose KE. Zebrafish-Mycobacterium marinum model for mycobacterial pathogenesis. FEMS Microbiol Lett. 2003 Aug 29;225(2):177-82.
69 Swaim LE, Connolly LE, Volkman HE, Humbert O, Born DE, Ramakrishnan L. Mycobacterium marinum infection of adult zebrafish causes caseating granulomatous tuberculosis and is moderated by adaptive immunity. Infect Immun. 2006 Nov;74(11):6108-17.
70 Parikka M, Hammarén MM, Harjula SK, Halfpenny NJ, Oksanen KE, Lahtinen MJ, Pajula ET, Iivanainen A, Pesu M, Rämet M. Mycobacterium marinum causes a latent infection that can be reactivated by gamma irradiation in adult zebrafish. PLoS Pathog. 2012 Sep;8(9):e1002944.
71 Gengenbacher M, Kaufmann SH. Mycobacterium tuberculosis: success through dormancy. FEMS Microbiol Rev. 2012 May;36(3):514-32.
72 Ottenhoff TH, Kaufmann SH. Vaccines against tuberculosis: where are we and where do we need to go? PLoS Pathog. 2012;8(5):e1002607.

73 Cronan MR, Tobin DM. Fit for consumption: zebrafish as a model for tuberculosis. Dis Model Mech. 2014 Jul;7(7):777-84.
74 Volkman HE, Clay H, Beery D, Chang JC, Sherman DR, Ramakrishnan L. Tuberculous granuloma formation is enhanced by a mycobacterium virulence determinant. PLoS Biol. 2004 Nov;2(11):e367.
75 Volkman HE, Pozos TC, Zheng J, Davis JM, Rawls JF, Ramakrishnan L. Tuberculous granuloma induction via interaction of a bacterial secreted protein with host epithelium. Science. 2010 Jan 22;327(5964):466-9.
76 Lin PL, Rodgers M, Smith L, Bigbee M, Myers A, Bigbee C, Chiosea I, Capuano SV, Fuhrman C, Klein E, Flynn JL. Quantitative comparison of active and latent tuberculosis in the cynomolgus macaque model. Infect Immun. 2009 Oct;77(10):4631-42.
77 Adams KN, Takaki K, Connolly LE, Wiedenhoft H, Winglee K, Humbert O, Edelstein PH, Cosma CL, Ramakrishnan L. Drug tolerance in replicating mycobacteria mediated by a macrophage-induced efflux mechanism. Cell. 2011 Apr 1;145(1):39-53.
78 Adams KN, Szumowski JD, Ramakrishnan L. Verapamil, and its metabolite norverapamil, inhibit macrophage-induced, bacterial efflux pump-mediated tolerance to multiple anti-tubercular drugs. J Infect Dis. 2014 Aug 1;210(3):456-66.
79 Tobin DM, Vary JC Jr, Ray JP, Walsh GS, Dunstan SJ, Bang ND, Hagge DA, Khadge S, King MC, Hawn TR, Moens CB, Ramakrishnan L. The lta4h locus modulates susceptibility to mycobacterial infection in zebrafish and humans. Cell. 2010 Mar 5;140(5):717-30.
80 Wallis RS. Tumour necrosis factor antagonists: structure, function, and tuberculosis risks. Lancet Infect Dis. 2008 Oct;8(10):601-11.
81 Tsenova L, Bergtold A, Freedman VH, Young RA, Kaplan G. Tumor necrosis factor alpha is a determinant of pathogenesis and disease progression in mycobacterial infection in the central nervous system. Proc Natl Acad Sci U S A. 1999 May 11;96(10):5657-62.
82 Clay H, Volkman HE, Ramakrishnan L. Tumor necrosis factor signaling mediates resistance to mycobacteria by inhibiting bacterial growth and macrophage death. Immunity. 2008 Aug 15;29(2):283-94.
83 Roca FJ, Ramakrishnan L. TNF dually mediates resistance and susceptibility to mycobacteria via mitochondrial reactive oxygen species. Cell. 2013 Apr 25;153(3):521-34.
84 Tobin DM, Roca FJ, Oh SF, McFarland R, Vickery TW, Ray JP, Ko DC, Zou Y, Bang ND, Chau TT, Vary JC, Hawn TR, Dunstan SJ, Farrar JJ, Thwaites GE, King MC, Serhan CN, Ramakrishnan L. Host genotype-specific therapies can optimize the inflammatory response to mycobacterial infections. Cell. 2012 Feb 3;148(3):434-46.
85 van der Vaart M, van Soest JJ, Spaink HP, Meijer AH. Functional analysis of a zebrafish myd88 mutant identifies key transcriptional components of the innate immune system. Dis Model Mech. 2013 May;6(3):841-54.
86 Mostowy S, Boucontet L, Mazon Moya MJ, Sirianni A, Boudinot P, Hollinshead M, Cossart P, Herbomel P, Levraud JP, Colucci-Guyon E. The zebrafish as a new model for the in vivo study of Shigella flexneri interaction with phagocytes and bacterial autophagy. PLoS Pathog. 2013;9(9):e1003588.
87 Meijer AH, van der Vaart M, Spaink HP. Real-time imaging and genetic dissection of host-microbe interactions in zebrafish. Cell Microbiol. 2014 Jan;16(1):39-49.
88 Carvalho R, de Sonneville J, Stockhammer OW, Savage ND, Veneman WJ, Ottenhoff TH, Dirks RP, Meijer AH, Spaink HP. A high-throughput screen for tuberculosis progression. PLoS One. 2011 Feb 16;6(2):e16779.
89 Fàbrega A, Vila J. Salmonella enterica serovar Typhimurium skills to succeed in the host: virulence and regulation. Clin Microbiol Rev. 2013 Apr;26(2):308-41.
90 van der Sar AM, Musters RJ, van Eeden FJ, Appelmelk BJ, Vandenbroucke-Grauls CM, Bitter W. Zebrafish embryos as a model host for the real time analysis of Salmonella typhimurium infections. Cell Microbiol. 2003 Sep;5(9):601-11.
91 Stockhammer OW, Zakrzewska A, Hegedûs Z, Spaink HP, Meijer AH. Transcriptome profiling and functional analyses of the zebrafish embryonic innate immune response to Salmonella infection. J Immunol. 2009 May 1;182(9):5641-53.
92 Dunlap NE, Benjamin WH Jr, Berry AK, Eldridge JH, Briles DE. A 'safe-site' for Salmonella typhimurium is within splenic polymorphonuclear cells. Microb Pathog. 1992 Sep;13(3):181-90.
93 Salcedo SP, Noursadeghi M, Cohen J, Holden DW. Intracellular replication of Salmonella typhimurium strains in specific subsets of splenic macrophages in vivo. Cell Microbiol. 2001 Sep;3(9):587-97.
94 Ordas A, Hegedus Z, Henkel CV, Stockhammer OW, Butler D, Jansen HJ, Racz P, Mink M, Spaink HP, Meijer AH. Deep sequencing of the innate immune transcriptomic response of zebrafish embryos to Salmonella infection. Fish Shellfish Immunol. 2011 Nov;31(5):716-24.
95 Stockhammer OW, Rauwerda H, Wittink FR, Breit TM, Meijer AH, Spaink HP. Transcriptome analysis of Traf6 function in the innate immune response of zebrafish embryos. Mol Immunol. 2010 Nov-Dec;48(1-3):179-90.
96 Kanwal Z, Zakrzewska A, den Hertog J, Spaink HP, Schaaf MJ, Meijer AH. Deficiency in hematopoietic phosphatase ptpn6/Shp1 hyperactivates the innate immune system and impairs control of bacterial infections in zebrafish embryos. J Immunol. 2013 Feb 15;190(4):1631-45.

97 Ordas A, Kanwal Z, Lindenberg V, Rougeot J, Mink M, Spaink HP, Meijer AH. MicroRNA-146 function in the innate immune transcriptome response of zebrafish embryos to Salmonella typhimurium infection. BMC Genomics. 2013 Oct 10;14:696.
98 Mahenthiralingam E, Baldwin A, Dowson CG. Burkholderia cepacia complex bacteria: opportunistic pathogens with important natural biology. J Appl Microbiol. 2008 Jun;104(6):1539-51.
99 Saiman L, Siegel J. Infection control in cystic fibrosis. Clin Microbiol Rev. 2004 Jan;17(1):57-71.
100 Vergunst AC, Meijer AH, Renshaw SA, O'Callaghan D. Burkholderia cenocepacia creates an intramacrophage replication niche in zebrafish embryos, followed by bacterial dissemination and establishment of systemic infection. Infect Immun. 2010 Apr;78(4):1495-508.
101 Agnoli K, Schwager S, Uehlinger S, Vergunst A, Viteri DF, Nguyen DT, Sokol PA, Carlier A, Eberl L. Exposing the third chromosome of Burkholderia cepacia complex strains as a virulence plasmid. Mol Microbiol. 2012 Jan;83(2):362-78.
102 Agnoli K, Frauenknecht C, Freitag R, Schwager S, Jenul C, Vergunst A, Carlier A, Eberl L. The third replicon of members of the Burkholderia cepacia Complex, plasmid pC3, plays a role in stress tolerance. Appl Environ Microbiol. 2014 Feb;80(4):1340-8.
103 Lowy FD. Staphylococcus aureus infections. N Engl J Med. 1998 Aug 20;339(8):520-32.
104 Prajsnar TK, Cunliffe VT, Foster SJ, Renshaw SA. A novel vertebrate model of Staphylococcus aureus infection reveals phagocyte-dependent resistance of zebrafish to non-host specialized pathogens. Cell Microbiol. 2008 Nov;10(11):2312-25.
105 Lin B, Chen S, Cao Z, Lin Y, Mo D, Zhang H, Gu J, Dong M, Liu Z, Xu A. Acute phase response in zebrafish upon Aeromonas salmonicida and Staphylococcus aureus infection: striking similarities and obvious differences with mammals. Mol Immunol. 2007 Jan;44(4):295-301.
106 Rigby KM, DeLeo FR. Neutrophils in innate host defense against Staphylococcus aureus infections. Semin Immunopathol. 2012 Mar;34(2):237-59.
107 Li YJ, Hu B. Establishment of multi-site infection model in zebrafish larvae for studying Staphylococcus aureus infectious disease. J Genet Genomics. 2012 Sep 20;39(9):521-34.
108 Holtfreter S, Radcliff FJ, Grumann D, Read H, Johnson S, Monecke S, Ritchie S, Clow F, Goerke C, Bröker BM, Fraser JD, Wiles S. Characterization of a mouse-adapted Staphylococcus aureus strain. PLoS One. 2013 Sep 2;8(9):e71142.
109 McVicker G, Prajsnar TK, Williams A, Wagner NL, Boots M, Renshaw SA, Foster SJ. Clonal expansion during Staphylococcus aureus infection dynamics reveals the effect of antibiotic intervention. PLoS Pathog. 2014 Feb 27;10(2):e1003959.
110 Kubica M, Guzik K, Koziel J, Zarebski M, Richter W, Gajkowska B, Golda A, Maciag-Gudowska A, Brix K, Shaw L, Foster T, Potempa J. A potential new pathway for Staphylococcus aureus dissemination: the silent survival of S. aureus phagocytosed by human monocyte-derived macrophages. PLoS One. 2008 Jan 9;3(1):e1409.
111 Ashida H, Ogawa M, Kim M, Suzuki S, Sanada T, Punginelli C, Mimuro H, Sasakawa C. Shigella deploy multiple countermeasures against host innate immune responses. Curr Opin Microbiol. 2011 Feb;14(1):16-23.
112 Mostowy S, Sancho-Shimizu V, Hamon MA, Simeone R, Brosch R, Johansen T, Cossart P. p62 and NDP52 proteins target intracytosolic Shigella and Listeria to different autophagy pathways. J Biol Chem. 2011 Jul 29;286(30):26987-95.
113 Gow NA, van de Veerdonk FL, Brown AJ, Netea MG. Candida albicans morphogenesis and host defence: discriminating invasion from colonization. Nat Rev Microbiol. 2011 Dec 12;10(2):112-22.
114 Chao CC, Hsu PC, Jen CF, Chen IH, Wang CH, Chan HC, Tsai PW, Tung KC, Wang CH, Lan CY, Chuang YJ. Zebrafish as a model host for Candida albicans infection. Infect Immun. 2010 Jun;78(6):2512-21.
115 Brothers KM, Newman ZR, Wheeler RT. Live imaging of disseminated candidiasis in zebrafish reveals role of phagocyte oxidase in limiting filamentous growth. Eukaryot Cell. 2011 Jul;10(7):932-44.
116 Brothers KM, Gratacap RL, Barker SE, Newman ZR, Norum A, Wheeler RT. NADPH oxidase-driven phagocyte recruitment controls Candida albicans filamentous growth and prevents mortality. PLoS Pathog. 2013;9(10):e1003634.
117 Forlenza M, Fink IR, Raes G, Wiegertjes GF. Heterogeneity of macrophage activation in fish. Dev Comp Immunol. 2011 Dec;35(12):1246-55.
118 Feng Y, Santoriello C, Mione M, Hurlstone A, Martin P. Live imaging of innate immune cell sensing of transformed cells in zebrafish larvae: parallels between tumor initiation and wound inflammation. PLoS Biol. 2010 Dec 14;8(12):e1000562.
119 Sieger D, Peri F. Animal models for studying microglia: the first, the popular, and the new. Glia. 2013 Jan;61(1):3-9.
120 Clark KJ, Voytas DF, Ekker SC. A TALE of two nucleases: gene targeting for the masses? Zebrafish. 2011 Sep;8(3):147-9.
121 Blackburn PR, Campbell JM, Clark KJ, Ekker SC. The CRISPR system—keeping zebrafish gene targeting fresh. Zebrafish. 2013 Mar;10(1):116-8.

122 Kettleborough RN, Busch-Nentwich EM, Harvey SA, Dooley CM, de Bruijn E, van Eeden F, Sealy I, White RJ, Herd C, Nijman IJ, Fényes F, Mehroke S, Scahill C, Gibbons R, Wali N, Carruthers S, Hall A, Yen J, Cuppen E, Stemple DL. A systematic genome-wide analysis of zebrafish protein-coding gene function. Nature. 2013 Apr 25;496(7446):494-7.
123 Li L, Yan B, Shi YQ, Zhang WQ, Wen ZL. Live imaging reveals differing roles of macrophages and neutrophils during zebrafish tail fin regeneration. J Biol Chem. 2012 Jul 20;287(30):25353-60.
124 Lawson ND, Weinstein BM. In vivo imaging of embryonic vascular development using transgenic zebrafish. Dev Biol. 2002 Aug 15;248(2):307-18.
125 Hall C, Flores MV, Storm T, Crosier K, Crosier P. The zebrafish lysozyme C promoter drives myeloid-specific expression in transgenic fish. BMC Dev Biol. 2007 May 4;7:42.
126 Zhang Y, Bai XT, Zhu KY, Jin Y, Deng M, Le HY, Fu YF, Chen Y, Zhu J, Look AT, Kanki J, Chen Z, Chen SJ, Liu TX. In vivo interstitial migration of primitive macrophages mediated by JNK-matrix metalloproteinase 13 signaling in response to acute injury. J Immunol. 2008 Aug 1;181(3):2155-64.
127 Kitaguchi T, Kawakami K, Kawahara A. Transcriptional regulation of a myeloid-lineage specific gene lysozyme C during zebrafish myelopoiesis. Mech Dev. 2009 May-Jun;126(5-6):314-23.
128 Elks PM, van Eeden FJ, Dixon G, Wang X, Reyes-Aldasoro CC, Ingham PW, Whyte MK, Walmsley SR, Renshaw SA. Activation of hypoxia-inducible factor-1α (Hif-1α) delays inflammation resolution by reducing neutrophil apoptosis and reverse migration in a zebrafish inflammation model. Blood. 2011 Jul 21;118(3):712-22.
129 Harvie EA, Green JM, Neely MN, Huttenlocher A. Innate immune response to Streptococcus iniae infection in zebrafish larvae. Infect Immun. 2013 Jan;81(1):110-21.
130 Renshaw SA, Loynes CA, Trushell DM, Elworthy S, Ingham PW, Whyte MK. A transgenic zebrafish model of neutrophilic inflammation. Blood. 2006 Dec 15;108(13):3976-8.
131 Mathias JR, Perrin BJ, Liu TX, Kanki J, Look AT, Huttenlocher A. Resolution of inflammation by retrograde chemotaxis of neutrophils in transgenic zebrafish. J Leukoc Biol. 2006 Dec;80(6):1281-8.
132 Yoo SK, Deng Q, Cavnar PJ, Wu YI, Hahn KM, Huttenlocher A. Differential regulation of protrusion and polarity by PI3K during neutrophil motility in live zebrafish. Dev Cell. 2010 Feb 16;18(2):226-36.
133 Yoo SK, Huttenlocher A. Spatiotemporal photolabeling of neutrophil trafficking during inflammation in live zebrafish. J Leukoc Biol. 2011 May;89(5):661-7.
134 Ward AC, McPhee DO, Condron MM, Varma S, Cody SH, Onnebo SM, Paw BH, Zon LI, Lieschke GJ. The zebrafish spi1 promoter drives myeloid-specific expression in stable transgenic fish. Blood. 2003 Nov 1;102(9):3238-40.
135 Hsu K, Traver D, Kutok JL, Hagen A, Liu TX, Paw BH, Rhodes J, Berman JN, Zon LI, Kanki JP, Look AT. The pu.1 promoter drives myeloid gene expression in zebrafish. Blood. 2004 Sep 1;104(5):1291-7.
136 Clark BS, Winter M, Cohen AR, Link BA. Generation of Rab-based transgenic lines for in vivo studies of endosome biology in zebrafish. Dev Dyn. 2011 Nov;240(11):2452-65.
137 Ellis K, Bagwell J, Bagnat M. Notochord vacuoles are lysosome-related organelles that function in axis and spine morphogenesis. J Cell Biol. 2013 Mar 4;200(5):667-79.
138 He C, Bartholomew CR, Zhou W, Klionsky DJ. Assaying autophagic activity in transgenic GFP-Lc3 and GFP-Gabarap zebrafish embryos. Autophagy. 2009 May;5(4):520-6.

Chapter 3

The CXCR3-CXCL11 signalling axis mediates macrophage recruitment and dissemination of mycobacterial infection

Vincenzo Torraca[1], Chao Cui[1], Ralf Boland[1], Jan-Paul Bebelman[2], Astrid M. van der Sar[3], Martine J. Smit[2], Marco Siderius[2], Herman P. Spaink[1] and Annemarie H. Meijer[1]

[1]Institute of Biology, Leiden University, The Netherlands; [2]Amsterdam Institute for Molecules, Medicines and Systems, VU University, The Netherlands; [3]Department of Medical Microbiology and Infection Control, VU University Medical Center, The Netherlands.

Disease Models and Mechanisms, 2015 Mar;8(3):253-69

Chapter 3

The CXCR3-CXCL11 signalling axis mediates macrophage recruitment and dissemination of mycobacterial infection

Vincenzo Torraca[1], Chao Cui[1], Ralf Boland[1], Jan-Paul Bebelman[2], Astrid M. van der Sar[3], Martine J. Smit[2], Marco Siderius[2], Herman P. Spaink[1] and Annemarie H. Meijer[1]

[1]Institute of Biology, Leiden University, The Netherlands; [2]Amsterdam Institute for Molecules, Medicines and Systems, VU University, The Netherlands; [3]Department of Medical Microbiology and Infection Control, VU University Medical Center, The Netherlands.

The recruitment of leukocytes to infectious foci depends strongly on the local release of chemoattractant mediators. The human CXC chemokine receptor 3 (CXCR3) is an important node in the chemokine signalling network and is expressed by multiple leukocyte lineages, including T cells and macrophages. The ligands of this receptor originate from an ancestral CXCL11 gene in early vertebrates. Here, we used the optically accessible zebrafish embryo model to explore the function of the CXCR3-CXCL11 axis in macrophage recruitment and show that disruption of this axis increases the resistance to mycobacterial infection. In a mutant of the zebrafish orthologue of *CXCR3* (*cxcr3.2*), macrophage chemotaxis to bacterial infections was attenuated, although migration to infection-independent stimuli was unaffected. Additionally, attenuation of macrophage recruitment to infection could be mimicked by treatment with NBI74330, a high-affinity antagonist of CXCR3. We identified two infection-inducible CXCL11-like chemokines as the functional ligands of Cxcr3.2, showing that the recombinant proteins exerted a Cxcr3.2-dependent chemoattraction when locally administrated *in vivo*. During infection of zebrafish embryos with *Mycobacterium marinum*, a well-established model for tuberculosis, we found that Cxcr3.2 deficiency limited the macrophage-mediated dissemination of mycobacteria. Furthermore, the loss of Cxcr3.2 function attenuated the formation of granulomatous lesions, the typical histopathological features of tuberculosis, and led to a reduction in the total bacterial burden. Prevention of mycobacterial dissemination by targeting the CXCR3 pathway, therefore, might represent a host-directed therapeutic strategy for treatment of tuberculosis. The demonstration of a conserved CXCR3-CXCL11 signalling axis in zebrafish extends the translational applicability of this model for studying diseases involving the innate immune system.

GRAPHICAL ABSTRACT

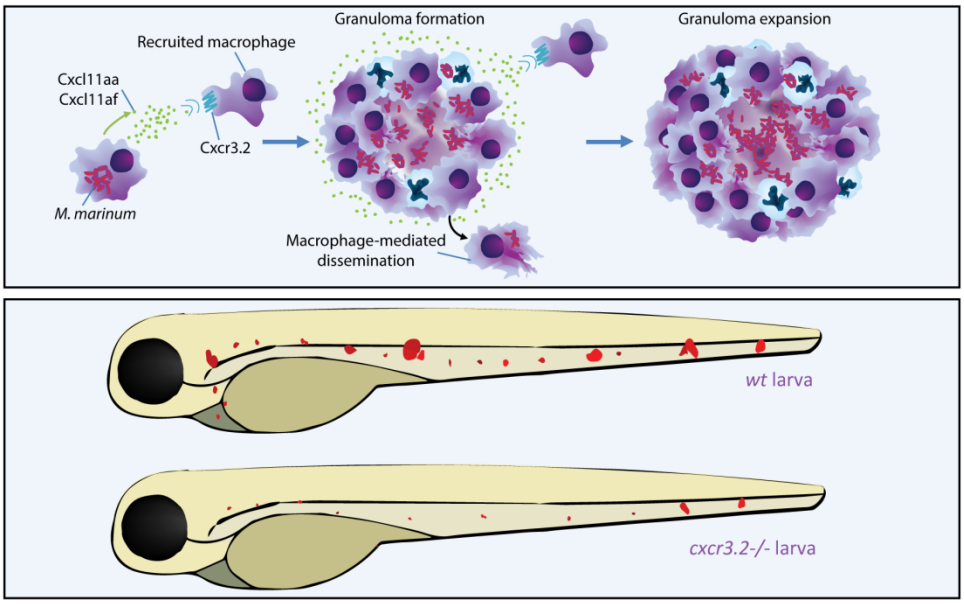

In zebrafish, the chemokine receptor Cxcr3.2 is important to guide macrophage recruitment to mycobacterial infection foci, via infection-dependent induction of its ligands Cxcl11aa and Cxcl11af. Cxcr3.2 mutants display reduced trafficking of macrophages to the nascent granuloma lesions, which both limits granuloma expansion and the dissemination of the pathogen via macrophage carriers. As a consequence, *cxcr3.2* mutation is beneficial for the host and reduces susceptibility to the mycobacterial disease.

TRANSLATIONAL IMPACT

Clinical issue - Mycobacteria are the causative agents of chronic, life-long debilitating infectious diseases such as tuberculosis and leprosy. In order to replicate and spread within their host, mycobacteria highjack one of the primary immune defence cells: the macrophage. Recruitment of macrophages relies heavily on the production of chemokines by the infected host. However, the role of chemokine signalling in mycobacterial disease remains poorly explored. CXC chemokine receptor 3 (CXCR3) is an important node in the chemokine signalling network and has been extensively studied in T cells. Emerging evidence suggests that CXCR3 also has important functions in macrophages that might be linked with immune-related diseases.

Results - In this study, the authors used a zebrafish model of tuberculosis to investigate the role of CXCR3 in macrophages during the early stages of mycobacterial infection. They found that mutation of a zebrafish CXCR3 homologue attenuates the infection-dependent recruitment of macrophages and limits the dissemination of the pathogen via macrophage carriers. This results in a reduced formation of granulomatous lesions, typical of mycobacterial disease. Similar attenuation of macrophage attraction to local infections could be achieved by treatment with NBI74330, a high-affinity antagonist of CXCR3. The authors also purified the zebrafish counterparts of the human chemokine (C-X-C motif) ligand 11 (CXCL11) family and demonstrated that two of these are inducible by infection and specifically recruit macrophages via the CXCR3 receptor in the zebrafish model.

Implications and future directions - This study is the first to implicate the CXCR3-CXCL11 signalling axis in macrophage responses that drive the initiation and expansion of mycobacterial granulomas, the pathological hallmark of tuberculosis disease. The beneficial effect of CXCR3 mutation on the control of mycobacterial infection in the zebrafish host should drive further research into the CXCR3-CXCL11 axis as a potential target for host-directed therapy against tuberculosis. Research into such novel therapeutic approaches is important in view of the increasing prevalence of antibiotic-resistant mycobacterial strains. Defects in CXCR3 signalling have also been associated with other immune-related diseases, including cancer and inflammatory disorders. Therefore, the finding that the CXCR3-CXCL11 axis and its sensitivity to pharmacological inhibition are conserved between human and zebrafish has broad implications for the translational value of this model.

INTRODUCTION

Macrophages are extremely dynamic phagocytic cells, able to integrate and respond to a wide spectrum of signals from infected tissues. A variety of receptors on their cell membrane can sense pathogen-associated molecular patterns (PAMPs), which induce the innate immune response[1]. Some of these PAMPs, such as N-formylated bacterial peptides, have direct chemoattractant activity on phagocytes[2]. Moreover, a crucial contribution to efficient phagocyte recruitment is provided by lipidic and peptidic chemoattractant factors, produced or activated directly by the host locally at the infection site[3,4,5]. In this group of compounds, the inflammatory chemokines play a major role. This subclass of small chemotactic proteins is induced upon infection and is able to exert target-specific activities towards subsets of leukocytes, both myeloid and lymphoid[6]. In humans, CXCL9 [also known as MIG (monokine-induced by IFN-γ)], CXCL10 [IP-10 (IFN-γ-inducible protein 10)] and CXCL11 [I-TAC (IFN-inducible T cell α chemoattractant)] are IFN-inducible chemokines and mediate recruitment of T cells, natural killer (NK) cells and monocytes/macrophages at the infection site, predominantly through their cognate G-protein coupled receptor, CXCR3[7,8]. This signalling axis has been implicated in several physiological activities, including maturation of T cells and vasculogenesis[9,10]. Additionally, CXCR3 and its ligands have been linked to inflammatory and immune-related diseases, of autoimmune[9,11,12,13], infectious[14,15,16,17] or malignant[18,19,20,21] nature.

Most of the literature on mammalian systems focuses on the role of this receptor in maturation, priming, activation and migration of T cells[9,11,22]. However, recent studies have demonstrated that CXCR3 also plays an important role in directing macrophage activities, both under physiological and under pathological conditions[10,20,23,24].

The zebrafish embryo model provides a useful platform to study chemokine-dependent cell migration, combining excellent possibilities for intravital imaging with the availability of a vast array of genetic tools[25]. Homologous relationships between mammalian and zebrafish CXCR4-CXCL12 and CXCR2-CXCL8 receptor-ligand pairs have been well established and studies in zebrafish have contributed significantly to the understanding of the role of these signalling axes in developmental processes, neutrophil motility, long-range neutrophil mobilisation and infection-induced chemotaxis[26,27,28,29,30]. Based on phylogeny reconstructions, the CXCR3-CXCL11 axis emerged for the first time in a common ancestor of zebrafish and mammals[31]. In placental mammals, amphibians and reptiles, a single copy per haplotype of *CXCR3* is generally present, whereas *CXCR3* was lost in the divergence of avian and marsupial mammalian clades. Several teleost fish show an expansion of the CXCR3 family[31,32,33], including zebrafish, where three copies, namely *cxcr3.1* (ENSDARG00000007358), *cxcr3.2* (ENSDARG00000041041) and *cxcr3.3* (ENSDARG00000070669), are located in tandem on chromosome 16[34]. The *CXCL9-CXCL10-CXCL11* triplet of CXCR3 ligands in mammals is likely to have originated from a relatively recent common ancestor[35]. The situation in fish is variegated and, in some cases, specific expansions have taken place. In zebrafish, a cluster of seven putative *cxcl11* genes, which are grouped together in a single locus on chromosome 5, share both homology and synteny with human *CXCL11*[34]. However, an association between the different isoforms of Cxcl11 ligands and Cxcr3 receptors has not been described, and the *in vivo* relevance of this signalling axis in the zebrafish model has not been addressed.

In previous work we have shown that one of the three *CXCR3* paralogues, *cxcr3.2*, is expressed in macrophages of 1-day-old zebrafish embryos[36]. In the present study, we used a *cxcr3.2* mutant to investigate the role of Cxcr3 signalling in macrophage mobilisation and function. In agreement with previous morpholino knockdown results, the receptor loss-of-function resulted in the attenuation of macrophage recruitment to local infection with *Salmonella typhimurium*. Moreover, we identified two infection-inducible CXCL11-like chemokines, which act as functional ligands of Cxcr3.2 with chemoattractant activity on macrophages. Finally, we demonstrate here that *cxcr3.2* is required for efficient recruitment of macrophages to *Mycobacterium marinum* infection and for the dissemination of this pathogen into host tissues, which is driven by macrophages. The zebrafish-*M. marinum* host-pathogen pair is widely used to model human tuberculosis and has provided important insights into the interaction of mycobacteria with host macrophages[37,38,39,40,41,42]. *M. marinum* is closely related to the human pathogen *Mycobacterium tuberculosis*, and the zebrafish model replicates the formation of granulomas, the typical histopathological hallmark of human tuberculosis[43,44]. The results presented here demonstrate a novel function for the CXCR3-CXCL11 signalling axis in macrophage responses that drive the initiation and expansion of these granulomatous lesions that are crucial for the dissemination of mycobacterial infection.

RESULTS

cxcr3.2 is expressed in phagocyte populations during zebrafish embryonic and larval development

We previously reported that *cxcr3.2* expression could be detected by fluorescent *in situ* hybridisation at 1 day post fertilisation (dpf) in phagocytes expressing the macrophage marker *csf1r* (*colony stimulating factor 1 receptor*) and not in cells positive for the neutrophil marker *mpx* (*myeloperoxidase*)[36]. However, we were unable to detect its expression with the same method at later stages. To determine whether *cxcr3.2* continues to be expressed in macrophages during the embryonic and larval development, we analysed RNA expression levels from FACS-sorted *mpeg1:mCherry-F*$^{+}$ and *mpx:eGFP*$^{+}$ cells from the double-transgenic line *Tg(mpeg1:mCherry-F/mpx:eGFP)*. These data show that macrophages (*mpeg1:mCherry-F*$^{+}$ population) maintain *cxcr3.2* expression at 2 and at 6 dpf (**Figure 1A–C** and **Supplementary Figure 1**). Expression of *cxcr3.2* could also be detected in neutrophils (*mpx:eGFP*$^{+}$ population). In addition, *cxcr3.3* could be detected in both phagocyte types, whereas *cxcr3.1* was not specifically enriched in the sorted cell populations (**Figure 1C** and **Supplementary Figure 1**).

The cxcr3.2^{hu6044} line carries a nonsense mutation in *cxcr3.2*

Sequencing of an ENU (N-ethyl-N-nitrosourea)-mutagenised zebrafish library resulted in the identification of a *cxcr3.2* mutant allele, *cxcr3.2*^{hu6044}, which carries a T-to-G (deoxythymidine to deoxyguanosine) substitution, creating a premature stop codon. This mutation leads to the interruption of the protein translation after 15 amino acids, before the region that encodes all the transmembrane domains that are essential for the function of the receptor (**Figure 1D** and **Supplementary Figure 2**). The nonsense *cxcr3.2*^{hu6044} mutation is not likely to lead to a functional truncated protein by using a downstream AUG codon as a signal for translation initiation. The second AUG in frame is located 354 nucleotides (118 amino acid residues) downstream from the canonical start codon and use of this codon as a translation start would lead to a truncated product lacking both the most N-terminal extracellular domain and the first two transmembrane domains. Furthermore, because the mutation occurs downstream of all the splicing sites, the possibility of alternative splicing and/or altered pre-RNA maturations seems unlikely and this was excluded by sequencing of the cDNA of *cxcr3.2* in mutants and wildtypes (wt). The *cxcr3.2* locus is closely linked to the loci of *cxcr3.1* and *cxcr3.3* owing to their chromosome proximity. To evaluate the presence of additional alterations in these genes as a consequence of the ENU mutagenesis, we sequenced their genetic loci in the AB/TL wt strain in our facility (used to outcross the mutant) and in two families of *cxcr3.2*$^{+/+}$ and *cxcr3.2*$^{-/-}$ fish. We did not identify additional nonsense mutations, although we could detect several non-synonymous single-nucleotide polymorphisms (nsSNPs), which are described in **Supplementary Table 1**. However, all the nsSNPs that were found in the *cxcr3.2*$^{-/-}$ line were also present in the AB/TL fish line, indicating that these changes are likely to be natural wt polymorphisms and not an effect of the ENU mutagenesis. To address the possible relevance of these nsSNPs with respect to the protein function, we used the PROVEAN software tool (Protein Variation Effect Analyser; http://provean.jcvi.org)[45,46]. None of the nsSNPs was predicted to impact on the protein functionality (**Supplementary Table 1**). Therefore, it is unlikely that single amino acid replacements in the protein sequences of Cxcr3.1 or Cxcr3.3 would affect the phenotype of fish carrying the *cxcr3.2*^{hu6044} nonsense allele.

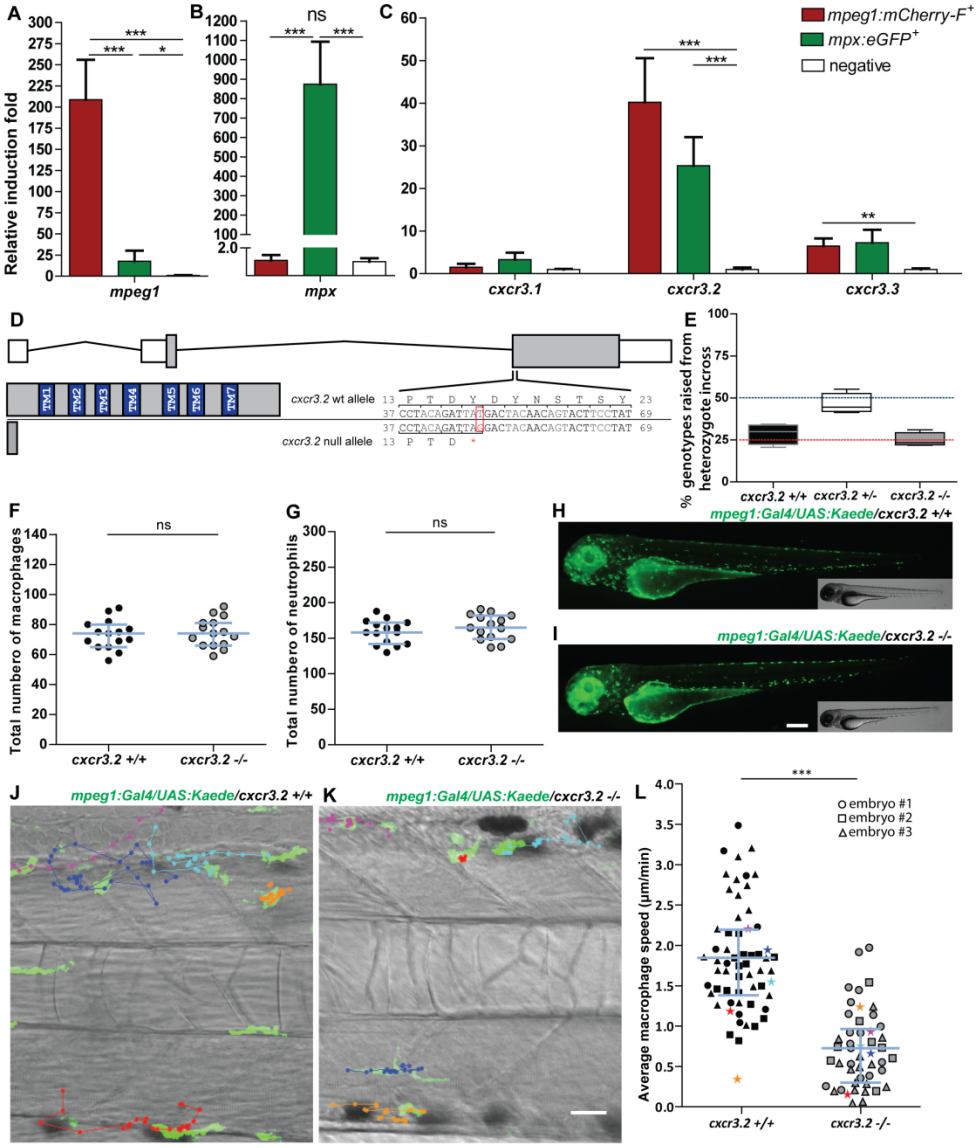

Figure 1. Characterisation of *cxcr3.2*$^{-/-}$ embryos in unchallenged conditions *(Legend on the next page)*.

Figure 1. Characterisation of *cxcr3.2*$^{-/-}$ embryos in unchallenged conditions *(Figure on the previous page)***. A–C**. Expression of *cxcr3.2* and its paralogues *cxcr3.1* and *cxcr3.3* in FACS-sorted phagocytes. Graphs represent the relative induction fold of the macrophage marker *mpeg1* (A), the neutrophil marker *mpx* (B), and of the *cxcr3* paralogues (C) in FACS-sorted macrophages and neutrophils from the combined transgenic line *Tg(mpeg1:mCherry-F/mpx:eGFP)* at 2 dpf. Expression of *cxcr3.2* and *cxcr3.3* could be detected in both macrophages and neutrophils, whereas *cxcr3.1* was not significantly enriched in the FACS-sorted populations when compared with the non-labelled cell fraction. Sample size (*n*): five replicates. Errors bars: mean±s.e.m. Reference gene: *eif4a1b*. **D.** Effect of the *cxcr3.2* point mutation. Top: gene structure of *cxcr3.2*. Boxes represent exons, of which the grey parts correspond to the coding sequence. Bottom right: *cxcr3.2* wildtype (wt) and mutant allele. A single T-to-G mutation at nucleotide 48 generates an early stop codon. Bottom left: consequence of *cxcr3.2* mutation at the protein level. In *cxcr3.2* mutant zebrafish, only a peptide of 15 amino acids can be translated, which lacks all the conserved transmembrane domains (TM1-7). Nucleotide and amino acid positions are enumerated from the translation start codon. **E.** Normal viability of *cxcr3.2*$^{-/-}$ mutants. Percentage of genotypes deriving from *cxcr3.2*$^{+/-}$ incross. No significant deviation from the Mendelian 1:2:1 ratio was observed. The genotypes were evaluated on 122 adult fish from four independent breedings. The boxplots represent the area of the distributions between the first and the third quartiles. Whiskers represent the minimum and maximum end points of the distributions. **F-G**. Quantification of macrophages and neutrophils. Combined Leukocyte-plastin (Lp) immunostaining and Myeloperoxidase (Mpx) staining were performed on *cxcr3.2*$^{+/+}$ and *cxcr3.2*$^{-/-}$ embryos at 3 dpf and the numbers of stained cells residing in the caudal haematopoietic tissue were counted. Exclusively Lp-stained cells were considered as macrophages (F) and Lp/Mpx double-positive cells as neutrophils (G). No significant differences were detected. Total number of larvae (*n*) per group in both F and G: 15. Error bars: median and interquartile range. **H-I.** Spatial distribution of macrophages. A macrophage-specific transgenic reporter driven by the *mpeg1* promoter [*Tg(mpeg1:Gal4/UAS:Kaede)*[66]] was crossed into the *cxcr3.2* mutant background. Representative images of the resulting *Tg(mpeg1:Gal4/UAS:Kaede) cxcr3.2*$^{+/+}$ (H) and *cxcr3.2*$^{-/-}$ (I) larvae at 3 dpf show no major differences in the macrophage distribution pattern. Scale bar: 200 µm. **J-K.** Macrophage basal migratory capability. Paths of five representative macrophages in the trunk of *Tg(mpeg1:Gal4/UAS:Kaede) cxcr3.2*$^{+/+}$ (J) and *cxcr3.2*$^{-/-}$ (K) larvae at 3 dpf. Mutant and wt larvae were mounted in agarose on the same dish and behaviour of mutant and wt macrophages were simultaneously followed for 3 hours. Time-lapse images were taken every 6 minutes. The paths were followed and analysed using ImageJ ManualTrack plugin. See also **Supplementary Movies 1-2**. Scale bar: 20 µm. (L) Quantification of basal migration difference. The average speed of individual macrophages was calculated by tracking 15–21 macrophages from three different *Tg(mpeg1:Gal4/UAS:Kaede) cxcr3.2*$^{+/+}$ and *cxcr3.2*$^{-/-}$ larvae (each larva is indicated with a different symbol) and was significantly reduced in *cxcr3.2*$^{-/-}$ macrophages. Total number of tracks (*n*): 61, 48. Error bars: mean and interquartile range. ns, non-significant; **P*<0.05; ****P*<0.001.

cxcr3.2 mutation does not affect macrophage development but alters their basal motility

Crossing of heterozygous *cxcr3.2*^{hu6044} carriers generated homozygous embryos in Mendelian proportions with their heterozygous and wt siblings. Screening of the adult offspring from a heterozygous incross showed that, in laboratory conditions, *cxcr3.2*$^{-/-}$ fish do not exhibit differences in survival and development compared with their wt siblings (**Figure 1E**) and could only be distinguished by genotyping.

Based on combined immunostaining for the pan-leukocyte marker Leukocyte-plastin (Lp) and Mpx activity staining[47], *cxcr3.2*$^{-/-}$ embryos showed similar numbers of macrophages and neutrophils as their wt siblings (**Figure 1F-G**). With the aim of investigating the relevance of *cxcr3.2* expression in macrophage behaviour, we crossed the *cxcr3.2* mutation into the *Tg(mpeg1:Gal4/UAS:Kaede)* background. Labelled macrophages showed similar numbers and spatial distribution in mutant and wt (**Figure 1H-I**). However, a basal macrophage migratory deficiency was observed in the mutants (**Figure 1J–L** and

Supplementary Movies 1-2). The aberrant motility might be explained by the presence of constitutive quantities of Cxcr3.2 ligands in the macrophage microenvironment, which could contribute to a higher basal activity of *cxcr3.2*$^{+/+}$ macrophages.

Mutation of *cxcr3.2* does not affect chemoattraction of macrophages by*Cxcr3.2*-independent factors

To test whether the basal motility defect of *cxcr3.2*$^{-/-}$ macrophages affected the stimulus-directed chemoattraction to *cxcr3.2*-independent factors, we locally injected the chemoattractant factors leukotriene B4 (LTB_4) and N-formyl-methionyl-leucyl-phenylalanine peptide (fMLP) into the hindbrain ventricle of embryos at 30 hpf (hours post fertilisation). At this developmental stage, the neutrophil population is not fully differentiated[48,49] and the population of phagocytes infiltrating the hindbrain upon chemotactic stimulation consists predominantly of macrophages (**Supplementary Figure 3**); therefore, we could use Lp immunostaining to identify recruited macrophages. No significant difference was observed in the numbers of *cxcr3.2*$^{+/+}$ and *cxcr3.2*$^{-/-}$ macrophages accumulated to either stimuli in 3 hours (**Figure 2A–H**). In addition, we also employed a previously described chemically induced inflammation (ChIn) assay[50], using copper sulphate treatment of embryos at 3 dpf to induce acute inflammation of lateral line neuromast hair cells. At this stage, macrophages were counted as Lp-positive and Mpx-negative cells using the combined Lp/Mpx staining. Also in this assay, no significant difference in the numbers of macrophages recruited to the inflamed neuromasts was observed between *cxcr3.2*$^{+/+}$ and *cxcr3.2*$^{-/-}$ larvae (**Figure 2I**). Therefore, we concluded that *cxcr3.2* mutation does not affect the capability of macrophages to respond to stimulatory sources independent of Cxcr3.2 signalling and that the basal motility defect does not influence the experimentally induced macrophage recruitment.

Early migration of macrophages to localised infection is affected by mutation of *cxcr3.2* or treatment with a CXCR3 antagonist

To determine whether Cxcr3.2 signalling contributes significantly to the recruitment of macrophages to different types of bacterial infections, we injected either *M. marinum* or *S. typhimurium* into the hindbrain ventricle of embryos at 30 hpf. In both infection models, a significant reduction of the number of macrophages accumulating at the infected site was detected in *cxcr3.2*$^{-/-}$ embryos at 3 hpi (hours post injection) (Figure 3A). A similar reduction of macrophage recruitment was also observed when *M. marinum* was locally injected into the otic vesicle at 3 dpf (**Figure 3B**). To visualise the dynamics of the macrophage migration *in vivo*, we used the combined mutant-transgenic line *Tg(mpeg1:Gal4/UAS:Kaede)/cxcr3.2*$^{-/-}$ and followed the early response of *mpeg1*-positive cells to *M. marinum* infection in the otic vesicle of 4 dpf larvae by confocal time-lapse imaging. In agreement with the previous results, a difference in the trend of macrophage recruitment was observed between the mutant and the wt over a time course of 5 hours (**Figure 3C-H**, **Supplementary Movies 3-4**). Furthermore, at locations distal from the infection site, macrophages in wt larvae showed more frequently an activated morphology with formation of branched protrusions (**Figure 3E**) when compared with the mutant line (**Figure 3H**). To quantify this phenomenon, we classified the distal macrophages of locally infected larvae according to their circularity index (CI), which estimates by an index between 0 and 1 the level of divergence of the cell shape projection from a perfect circle (CI=1).

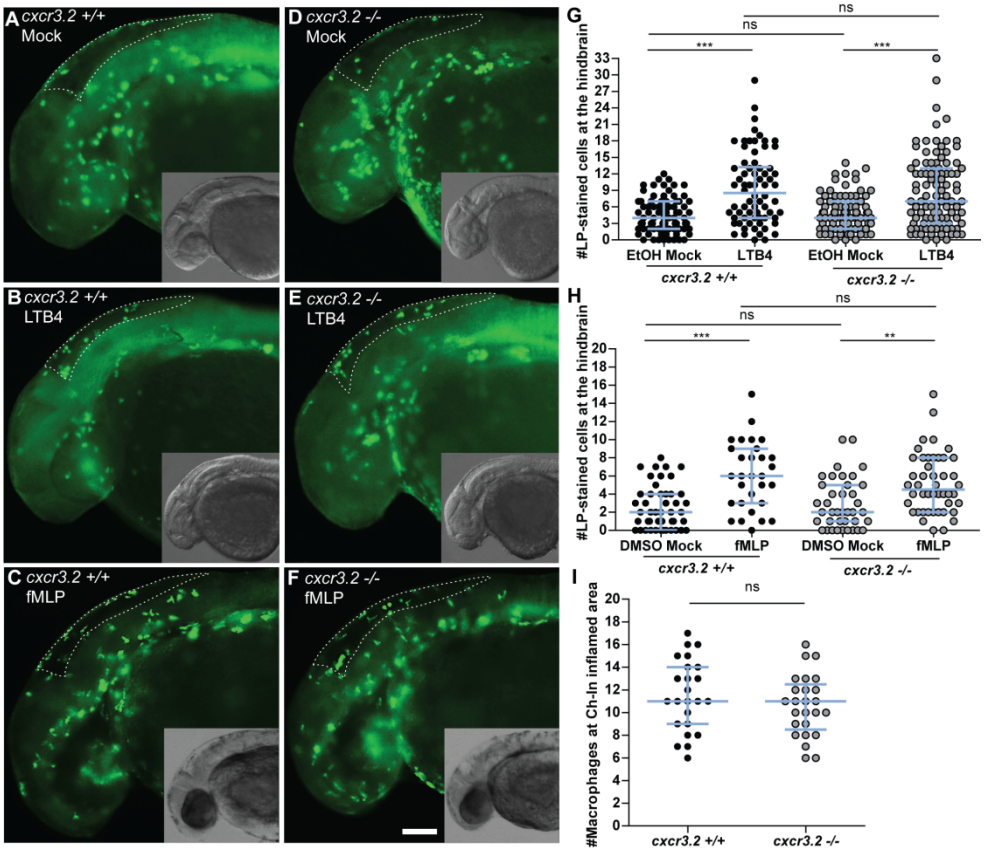

Figure 2. Macrophage chemoattraction by Cxcr3.2-independent factors. A–H. Chemoattraction of macrophages by LTB_4 and fMLP. *cxcr3.2*$^{+/+}$ (A–C) and *cxcr3.2*$^{-/-}$ (D–F) embryos at 30 hpf were locally injected into the hindbrain cavity with 10.1 ng/ml (30 nM) LTB_4 (representative images B and E) or with 0.2 mg/ml (0.5 mM) of fMLP (representative images C and F). Mock control injections with the solvents were 0.02% EtOH in PBS for the LTB_4 treatment and 5% DMSO in PBS for the fMLP treatment (representative images A and D). Lp-stained cells accumulated in 3 hours within the hindbrain limits (dotted line) were counted as macrophages, as neutrophils do not significantly contribute to the total number of leukocytes recruited to the hindbrain at this developmental stage (**Supplementary Figure 3**). LTB_4 and fMLP stimulation resulted in significantly increased macrophage recruitment, compared with the mock injection, and this was independent of *cxcr3.2* mutation (G-H). Scale bar in A–F: 100 µm. Data were accumulated from three independent experiments. Sample size (*n*) in G: 82, 70, 86, 100; Sample size (*n*) in H: 47, 30, 39, 46. Error bars: median and interquartile range. **I.** Local macrophage recruitment to $CuSO_4$ chemically-induced inflammation. Copper sulphate treatment was performed on 3 dpf embryos and macrophages accumulated in 3 hours at the damaged neuromasts of the lateral line were counted as Lp-stained cells minus Lp/Mpx double-positive cells, representing neutrophils. Similar numbers of macrophages were recruited to inflamed areas in both *cxcr3.2*$^{+/+}$ and *cxcr3.2*$^{-/-}$ embryos. Sample size (*n*): 24, 25. Error bars: median and interquartile range. ns, non-significant; $^{**}P<0.01$; $^{***}P<0.001$.

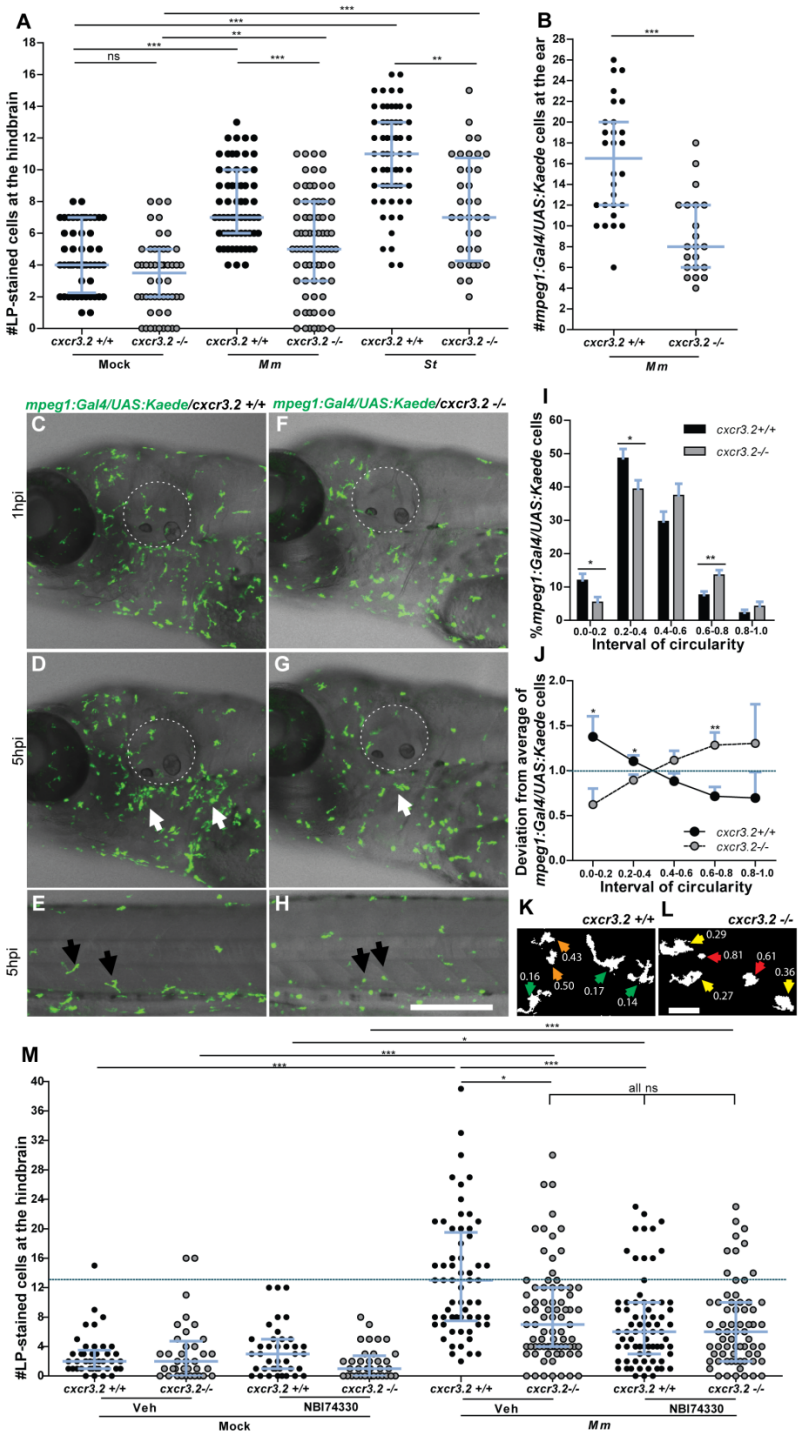

Figure 3. Cxcr3.2-dependent macrophage recruitment to localised bacterial infections *(Legend on the next page)*.

Figure 3. Cxcr3.2-dependent macrophage recruitment to localised bacterial infections *(Figure on the previous page)***. A.** *M. marinum* and *S. typhimurium* infection in the hindbrain ventricle. *cxcr3.2*$^{+/+}$ and *cxcr3.2*$^{-/-}$ embryos were injected at 30 hpf with 200 CFU of *M. marinum* (*Mm*) or *S. typhimurium* (*St*), or mock injected with 2% polyvinylpyrrolidone-40 in PBS. Lp-stained cells accumulated in 3 hours within the hindbrain limits were counted as macrophages, because neutrophils do not significantly contribute to the total number of leukocytes recruited to the hindbrain at this developmental stage (**Supplementary Figure 3**). Significant reduction of macrophage chemotaxis to infection is determined by *cxcr3.2* mutation. Data were accumulated from two (*St*) or three (*Mm*) independent experiments. Sample size (*n*): 52, 52, 63, 75, 60, 36. Error bars: median and interquartile range. **B–H.** Macrophage recruitment and systemic activation following *M. marinum* infection in the otic vesicle. *Tg(mpeg1:Gal4/UAS:Kaede) cxcr3.2*$^{+/+}$ and *Tg(mpeg1:Gal4/UAS:Kaede) cxcr3.2*$^{-/-}$ larvae were injected with 200 CFU of *M. marinum* into the otic vesicle (dotted line) at 3 (B) or 4 (C–H) dpf. At 4 hpi of 3 dpf larvae, the accumulation of *mpeg1:Gal4/UAS:Kaede*-positive cells within the perimeter of the otic vesicle was reduced in *cxcr3.2*$^{-/-}$ larvae (B). Following injection at 4 dpf, macrophages are less able to penetrate the otic vesicle, but accumulate in the surrounding area (white arrows in D and G), as shown in representative time course movies (**Supplementary Movies 3-4**) and stills from these movies at 1 hpi (C,F) and 5 hpi (D,G). A reduced accumulation was observed in the *cxcr3.2* mutant. At a distal location in the trunk (E,H), macrophages seemed to show more frequently a branched morphology in *cxcr3.2*$^{+/+}$ and a round morphology in *cxcr3.2*$^{-/-}$ (black arrows in E and H). Sample size (*n*) in B: 28, 21. Error bars: median and interquartile range. Scale bar in C–H: 250 µm. **I–L.** Quantification of distal macrophage activation following local *M. marinum* infection. In order to quantify the distal activation of macrophages upon *M. marinum* infection, 200 CFU of bacteria were injected in the otic vesicle of 3 dpf *mpeg1:Gal4/UAS:Kaede* larvae. Images of the macrophages were acquired from the trunk of the infected larvae at 4 hpi and the circularity index (CI) of the distal macrophages was calculated. The graph in I represents the percentage of macrophages residing in the different intervals of CI, whereas the graph in J represents the divergence in distribution of the *cxcr3.2*$^{+/+}$ and *cxcr3.2*$^{-/-}$ macrophages in the different classes of CI, calculated as the ratio between the percentage of *cxcr3.2*$^{+/+}$ or *cxcr3.2*$^{-/-}$ macrophages in a certain CI interval and the overall mean percentage [(mutant + wt)/2] of macrophages in that interval (see Materials and Methods). Macrophages of *cxcr3.2*$^{+/+}$and *cxcr3.2*$^{-/-}$ larvae were distributed in a different fashion along the different classes, with the classes of high circularity more populated in the mutants and the classes of reduced circularity more populated in the wildtype (wt). K and L show representative macrophages analysed in I and J and their corresponding CI. Green arrows: 0.0≤CI<0.2; yellow arrows: 0.2≤CI<0.4; orange arrows: 0.4≤CI<0.6; red arrows: 0.6≤CI≤1.0. Sample size (*n*) in I–L: 390 *cxcr3.2*$^{+/+}$ and 293 *cxcr3.2*$^{-/-}$ cells from 14 and 16 embryos, respectively. Error bars: mean±s.e.m. Scale bar in K-L: 40 µm. **M.** Attenuation of macrophage recruitment to *M. marinum* via treatment with the CXCR3 antagonist NBI74330. *cxcr3.2*$^{+/+}$ and *cxcr3.2*$^{-/-}$ embryos were bath-exposed to 50 µM NBI74330 or to vehicle only (Veh; 0.5% DMSO in medium) for 3 hours and then injected in the hindbrain ventricle at 30 hpf with mock or 200 CFU of *Mm.* Embryos were kept in NBI74330 or vehicle medium for an additional 3 hours and then collected for Lp immunostaining. Treatment with NBI74330 reduced the macrophage chemotaxis to infection in *cxcr3.2*$^{+/+}$ embryos to similar levels as the vehicle-treated *cxcr3.2*$^{-/-}$ embryos, and no significant additive effect of *cxcr3.2* mutation and NBI74330 treatment was observed. Data were accumulated from two independent experiments. Sample size (*n*): 41, 36, 39, 36, 61, 79, 73, 67. Error bars: median and interquartile range. ns, non-significant; **P*<0.05; ***P*<0.01; ****P*<0.001.

The different intervals of circularity were differently populated in wt and mutant larvae, with the classes of reduced circularity (0 to 0.4) being more populated in *cxcr3.2*$^{+/+}$ larvae and the classes of higher circularity (0.6–0.8) being more populated in *cxcr3*.2$^{-/-}$ larvae (**Figure 3I–L**). These results provide evidence that the Cxcr3.2-dependent signalling pathway mediates a significant component of the macrophage recruitment to pathogens in the early phase of the infection. To determine whether the infection-dependent macrophage recruitment can also be modulated pharmacologically, we tested a chemical inhibitor of human CXCR3, NBI74330[51], which binds with high affinity to a pocket formed by the transmembrane domains of CXCR3. Key amino acid residues in this pocket are conserved

between the human and the zebrafish receptors (**Supplementary Figure 4**). Treatment with this CXCR3 antagonist attenuated the macrophage recruitment to local *M. marinum* infection in *cxcr3.2*$^{+/+}$ embryos to a similar level as that of the vehicle-treated *cxcr3.2*$^{-/-}$ embryos and did not show a cooperative effect with the *cxcr3.2* mutation (**Figure 3M**). These results support the conservation of CXCR3 signalling between fish and mammals.

A group of CXCL11-like chemokines are inducible upon local and systemic infection in zebrafish

Although our analysis of the *cxcr3.2* mutant supports the role of Cxcr3.2 in macrophage chemotaxis to infections, the chemokine ligands that signal via this receptor are unknown. The assignment of ligand-receptor pairs is complicated by the relatively poor conservation of chemokine sequences among vertebrates and the species-specific expansions of the chemokine gene clusters[34]. However, systematic study of the orthologous relationships between vertebrate chemokines indicated that seven *CXCL11*-like chemokine genes, located in tandem on chromosome 5 (*cxcl11aa*, *cxcl11ac*, *cxcl11ad*, *cxcl11ae*, *cxcl11af*, *cxcl11ag*, *cxcl11ah*), have evolved in zebrafish as a counterpart to the mammalian *CXCL9*, *CXCL10* and *CXCL11* genes[34]. The amino acid similarity between the CXCL11-like chemokines in zebrafish and human CXCL11 exceeds the similarity that human CXCL9, CXCL10 and CXCL11 show among each other (**Supplementary Figure 5**; **Supplementary Table 2**). We, therefore, considered the zebrafish CXCL11-like chemokines as putative ligands for the Cxcr3.2 receptor. Because Cxcr3.2 was clearly involved in the early phase of the infection response, we reasoned that the ligands that induce Cxcr3.2-mediated chemotaxis should be promptly upregulated upon local infection. For this reason, we collected RNA samples from whole embryos infected in the hindbrain with 200 colony-forming units (CFU) of either *S. typhimurium* or *M. marinum* at 1 and 3 hpi and designed gene-specific primers for the members of the *cxcl11* gene cluster. Because of the high level of sequence conservation between *cxcl11af* and *cxcl11ag* (only 2 bp difference on the cDNA leading to a single semiconservative residue change of an aspartic acid with a glutamic acid), a promiscuous primer pair was used that can amplify both gene transcripts (*cxcl11af/ag*). Analysis by qRT-PCR revealed that, at 1 hpi, *cxcl11af/ag* showed twofold upregulation with *M. marinum* infection and fourfold upregulation with *S. typhimurium* infection, although no statistical significance was observed compared with the mock-injected controls (**Figure 4A**). At 3 hpi the expression of *cxcl11aa*, *cxcl11ae* and *cxcl11af/ag* was significantly upregulated to levels of two- to 4.5-fold (**Figure 4B**). In particular, *cxcl11aa* displayed the highest levels of induced transcription (~4.5-fold induction) with both the pathogens tested, suggesting this chemokine as an effective signalling ligand of Cxcr3.2 involved in the response to infection. We verified that the genes induced by local infection were also responsive to systemic infection with *M. marinum*. Upregulation of *cxcl11aa* and *cxcl11ae* was detected both at 4 hpi and at 4 dpi (days post injection) during *M. marinum* systemic infection, whereas *cxcl11af/ag* was significantly induced to levels of ~fourfold only at the later stage of infection (**Figure 4C-D**). Additionally, at this time point, *cxcl11ac* and *cxcl11ad* were also significantly upregulated to levels of 1.5- to two-fold (**Figure 4D**).

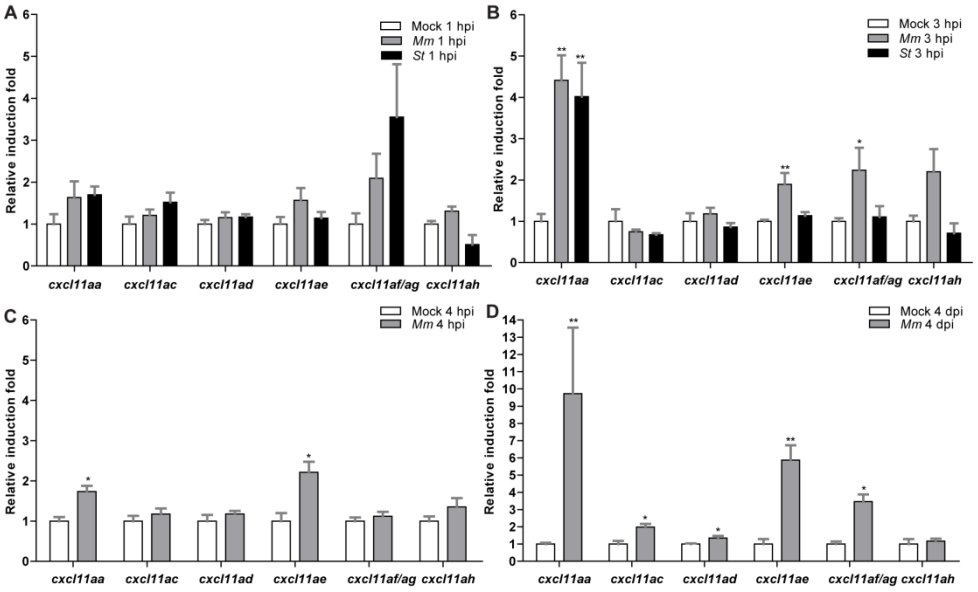

Figure 4. Inducibility of a subset of *cxcl11-like* genes upon bacterial infection. A-B. Quadruplicate pools of 18–20 embryos infected in the hindbrain with 200 CFU of *M. marinum* (*Mm*) or *S. typhimurium* (*St*) at 30 hpf or mock-injected with PBS were collected at 1 hpi (A) and 3 hpi (B). A subset of *CXCL11*-like chemokine genes shows upregulation by qPCR in the infected groups, which becomes significant at 3 hpi. Error bars: mean±s.e.m. **C-D.** Triplicate pools of 18–20 embryos systemically infected with *M. marinum* (*Mm*) at 1 dpf or mock-injected with PBS were collected at 4 hpi (C) and 4 dpi (D). Expression of *cxcl11aa* and *cxcl11ae* was significantly induced at both time points, whereas *cxcl11ac*, *cxcl11ad* and *cxcl11af/ag* were significantly induced only at 4 dpi. Error bars: mean±s.e.m. *P<0.05; **P<0.01.

Recombinant Cxcl11aa and Cxcl11af exert macrophage chemoattraction *in vivo* in a Cxcr3.2-dependent manner

To assess the chemoattractant properties of the infection-inducible chemokines Cxcl11aa, Cxcl11af and Cxcl11ae, we used *Pichia pastoris* strain *X-33* to express recombinant proteins. As a control, we also expressed zebrafish Cxcl8a (Il8), known to be a potent and neutrophil-specific chemoattractant[27,29]. All three purified CXCL11-like chemokines showed chemoattractant capabilities towards macrophages when locally injected *in vivo* into the hindbrain at 30 hpf (**Figure 5**), whereas no significant macrophage recruitment was exerted by Cxcl8a (**Supplementary Figure 6**). Similar levels of these chemokines were injected in the otic vesicle at 54 hpf to evaluate their chemoattractant capabilities towards neutrophils (**Supplementary Figure 6B-C**). Cxcl11aa and Cxcl11af did not show chemoattraction of neutrophils under these conditions, whereas Cxcl11ae and Cxcl8a exerted significant neutrophil chemoattraction. To determine whether the macrophage chemoattraction is dependent on *cxcr3.2*, hindbrain injections of the recombinant proteins were performed in both wt and *cxcr3.2* mutants. Both Cxcl11aa and Cxcl11af did not stimulate recruitment upon local injection in *cxcr3.2* mutants when compared with their mock controls (**Figure 5A**,**C**). In contrast, the chemoattraction of phagocytes mediated by Cxcl11ae was independent of *cxcr3.2* mutation (**Figure 5B**, **Supplementary Figure 6C**). Taken together, these results support a direct ligand-receptor interaction between Cxcr3.2 and the chemokines Cxcl11aa and Cxcl11af that mediates the chemoattraction of

macrophages. Differently, Cxcl11ae, which exerted a Cxcr3.2-independent phagocyte chemoattraction, is likely to signal via a yet-unidentified receptor.

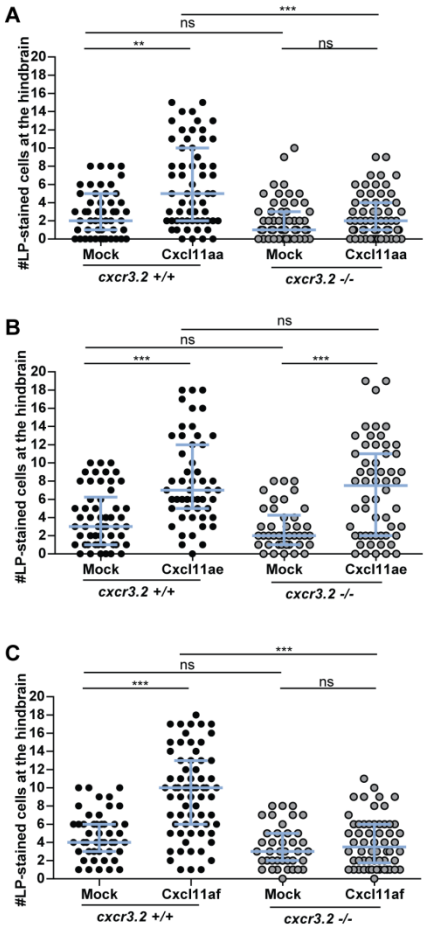

Figure 5. Macrophage chemoattraction by locally injected recombinant chemokines in *cxcr3.2* mutant and wildtype siblings. Recombinant proteins or buffer (mock) were injected into the hindbrain ventricle at 30 hpf and macrophages accumulating in 3 hours within the hindbrain limits were counted as Lp-stained cells. Data were accumulated from three independent experiments. **A.** Cxcl11aa (1.2 mg/ml). Sample size (*n*): 51, 60, 55, 60. **B.** Cxcl11ae (0.5 mg/ml). Sample size (*n*): 54, 51, 42, 56. **C.** Cxcl11af (0.5 mg/ml). Sample size (*n*): 47, 68, 39, 58. Error bars: median and interquartile range. Note that macrophage chemoattraction mediated by Cxcl11aa and Cxcl11af is abolished by *cxcr3.2* mutation, whereas the chemoattraction mediated by Cxcl11ae is independent of *cxcr3.2*. ns, non-significant; ***P*<0.01; ****P*<0.001.

Mutation of *cxcr3.2* affects mycobacterial infection dissemination and granuloma formation

Pathogenic mycobacteria have the ability to resist intracellular macrophage digestion and they can use the macrophages as a vector for distal dissemination of the infection[38]. We hypothesised that *cxcr3.2* depletion, preventing a high level of macrophage accumulation to the local infection site, might also prevent extensive dissemination and help to locally restrict the infection. To test this hypothesis we followed *M. marinum* hindbrain infection for 24 hours and evaluated the frequency of infection dissemination in *cxcr3.2*$^{+/+}$ and *cxcr3.2*$^{-/-}$ zebrafish embryos. At 24 hpi, almost 50% of the wt embryos displayed dissemination of the infection from the head to the trunk and tail, whereas, in more than 80% of the mutants, the infection remained locally confined (**Figure 6A–F**).

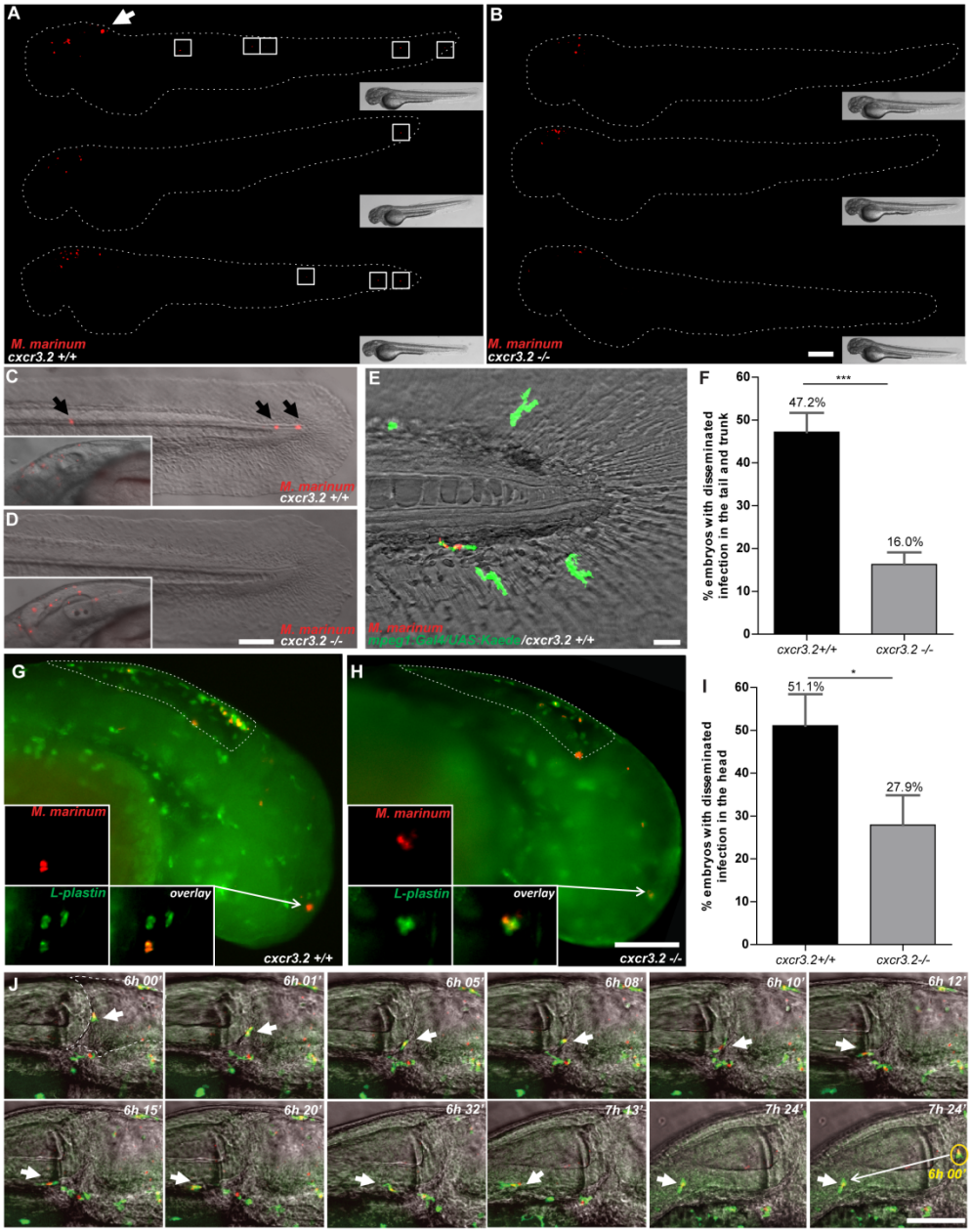

Figure 6. Effect of *cxcr3.2* mutation on dissemination of local mycobacterial infection within 24 hpi *(Legend on the next page)*.

Figure 6. Effect of *cxcr3.2* mutation on dissemination of local mycobacterial infection within 24 hpi *(Figure on the previous page)*. **A-B.** Representative images of *cxcr3.2*$^{+/+}$ and *cxcr3.2*$^{-/-}$ embryos with local and disseminated mycobacterial infection. Embryos were infected at 30 hpf by injecting 200 CFU of *M. marinum* into the hindbrain and images were taken at 24 hpi (54 hpf). In *cxcr3.2*$^{+/+}$ embryos, single infected cells are visible distally from the infection (white boxes). Scale bar: 200 µm. **C–E.** Details of distal infection emerging from hindbrain infection. The black arrows (C) point at single *M. marinum*-infected cells, present in the tail of a *cxcr3.2*$^{+/+}$fish at 24 hpi but notably absent in the example of a *cxcr3.2*$^{-/-}$ fish (D). Particulars of the infected hindbrains of the same embryos are shown in the boxed inserts on the left, indicating similar levels of local infection. Use of the *Tg(mpeg1:Gal4/UAS:Kaede)* line (E) shows that the infection disseminated from the hindbrain resides in macrophages in *cxcr3.2*$^{+/+}$. Scale bars in C and D: 100 µm; scale bar in E: 20 µm. **F.** Quantification of *M. marinum* infection dissemination in the trunk and tail in *cxcr3.2*$^{+/+}$ and *cxcr3.2*$^{-/-}$ embryos. Embryos were scored positive for dissemination if one or more infected macrophages were observed in the trunk or tail region. The graph demonstrates a significant difference in the total percentage of embryos showing infection dissemination at 24 hpi. Data were accumulated from three independent experiments. Sample size (*n*): 125, 172. Error bars: mean±s.e.m. **G–I.** Quantification of *M. marinum* infection dissemination in the head in *cxcr3.2*$^{+/+}$ and *cxcr3.2*$^{-/-}$ embryos. Representative figures of *cxcr3.2* wildtype (wt; G) and mutant (H) embryos and quantification (I) of dissemination in the head at 6 hours post *M. marinum* infection in the hindbrain. Embryos were scored positive for dissemination if one or more infected macrophages were observed outside the hindbrain limits (dotted line). Insets in G and H show details of infected macrophages outside the hindbrain. The graph in I demonstrates a significant difference in the total percentage of embryos showing infection dissemination at this time point. Arrows in the figures point at the particular of a disseminated infection. Sample size (*n*): 47, 43. Error bars: mean±s.e.m. Scale bar: 200 µm. **J.** Time course of a *M. marinum*-infected macrophage egressing from the hindbrain. The image sequence (taken from a *cxcr3.2*$^{+/+}$ embryo) represents over a time course of ~1.5 hours that macrophages (green) can facilitate the dissemination of *M. marinum* (red) that is locally delivered in the hindbrain ventricle. The dashed line in the first image represents the hindbrain limits and arrow points at an infected macrophages adhering to the hindbrain boundary. In the subsequent images the arrow points at the infected macrophage egressing from the hindbrain. The yellow circle in the last image of the sequence contains an inset of the infected macrophage from the first image to represent its initial position (6 hpi) compared with its position at the end of the image sequence (~7.5 hpi). Scale bar: 100 µm. **P*<0.05; ****P*<0.001.

Dissemination to other areas of the head could be seen already as early as 6 hpi and also this phenotype was attenuated in *cxcr3.2*$^{-/-}$ embryos (**Figure 6G–I**). Disseminated bacteria outside the hindbrain and/or midbrain were residing in phagocytes and, in time course experiments, we could visualise that egression of mycobacteria from the ventricles is facilitated by macrophages (**Figure 6J**), in agreement with previously published results[38]. When dissemination to the tail and trunk occurred, one to five dissemination foci could be detected in the *cxcr3.2*$^{+/+}$ embryos, whereas *cxcr3.2*$^{-/-}$ embryos never showed more than one or two bacterial clusters distally from the original injection point. At 5 dpi, the bacterial burden in the hindbrain was similar between wt and mutant larvae, but mutants still showed lower levels of dissemination of the infection towards distal areas (**Figure 7A-B**). The infection foci generated distally developed into typical granuloma-like aggregates, as previously described for the zebrafish-*M. marinum* model[26]. The size of these granulomatous lesions was significantly reduced in the *cxcr3.2*$^{-/-}$ mutant larvae (**Figure 7C-F**). Therefore, we concluded that *cxcr3.2*-mediated signalling strongly influences the dynamics of the infection progression and of granuloma formation. To further investigate the relevance of *cxcr3.2* signalling in the formation of granulomas, we injected 200 CFU of *M. marinum* systemically in 1 dpf embryos via the caudal vein, which, in the wt leads to many granulomatous lesions[38]. Images of single granulomas at 5 dpi, stained for both macrophages and neutrophils, revealed that granuloma-like aggregates could still be formed in *cxcr3.2* mutants. Similar structures and phagocyte compositions were observed

when lesions of similar sizes in wt and mutant were compared (**Figure 8A-B**). However, it must be noted that a large variation in granuloma structure and composition already exists when comparing different granulomas within the same larva or between different wildtypes, and this makes it very difficult to assess the effect of a mutation on the general architecture of the granulomas.

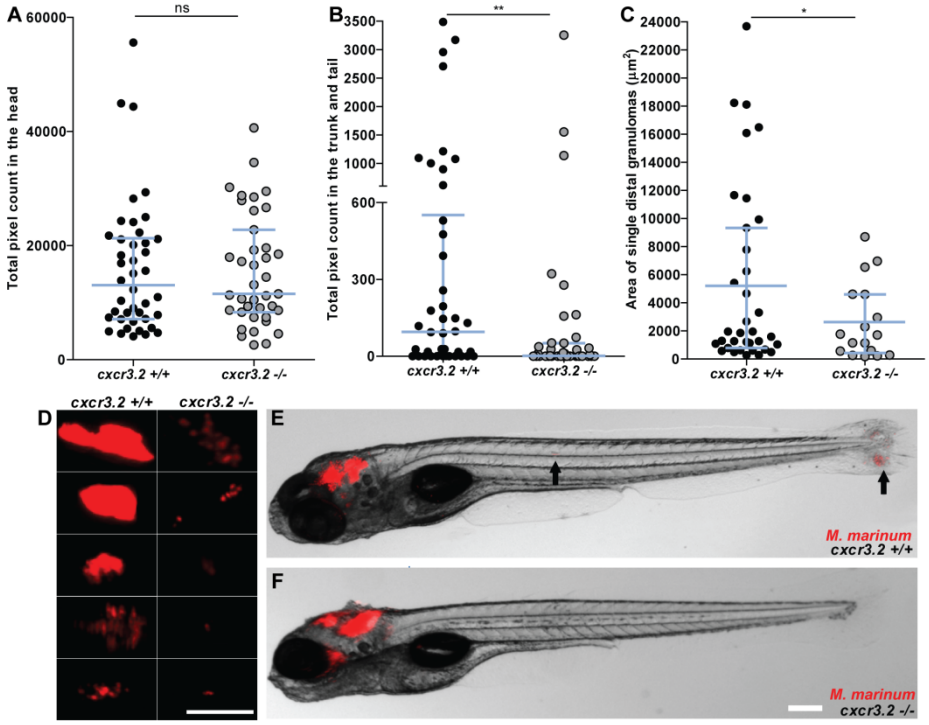

Figure 7. Effect of *cxcr3.2* mutation on dissemination of local mycobacterial infection at 5 dpi. A-B. Quantification of total levels of infection burden in the head and in the trunk and tail of 6 dpf zebrafish larvae. Embryos were injected at 30 hpf in the hindbrain ventricle with 200 CFU of *M. marinum*. Comparable levels of infection are reached locally in the head (A), but disseminated infection burden in the trunk and tail was significantly reduced in *cxcr3.2*$^{-/-}$ larvae (B). Data were accumulated from two independent experiments. Sample size (*n*): 42, 39. Error bars: median and interquartile range. **C-D.** Size and morphology of distal granulomas in *cxcr3.2*$^{+/+}$ and *cxcr3.2*$^{-/-}$ larvae. Distal bacterial clusters that originated occasionally in *cxcr3.2*$^{-/-}$ embryos appeared generally smaller than the ones more frequently formed in the *cxcr3.2*$^{+/+}$ siblings. Size was determined by fluorescent bacterial quantification of single distant granulomas in *cxcr3.2*$^{+/+}$ and *cxcr3.2*$^{-/-}$ (C) and five representative images of each are shown (D). Data were accumulated from two independent experiments. Sample size (*n*): 35 and 17 distal granulomas from 42 and 39 observed *cxcr3.2*$^{+/+}$ and *cxcr3.2*$^{-/-}$ embryos, respectively. Scale bar: 200 µm. Error bars: median (A,B) or mean (C) and interquartile range. **E-F.** Late effects of distal infection emerging from hindbrain infection. Representative images of *cxcr3.2*$^{+/+}$ (E) and *cxcr3.2*$^{-/-}$ (F) embryos at 5 dpi. Black arrows point at distal dissemination foci in the *cxcr3.2*$^{+/+}$ larva. Scale bar: 200 µm. ns, non-significant; **P*<0.05; ***P*<0.01.

Despite this, we observed that Cxcr3.2 deficiency provided partial protection against mycobacterial infection. Not only did mutants exhibit reduced levels of infection burden (**Figure 8C-E**), but also a reduced number of bacterial clusters (**Figure 8F**) and smaller average bacterial cluster size (**Figure 8G**). Taken together with the results of hindbrain infection, these data demonstrate the important role of Cxcr3.2-dependent signalling in guiding macrophage-mycobacteria interactions, and show how this signalling leads to direct effects on the infection progression.

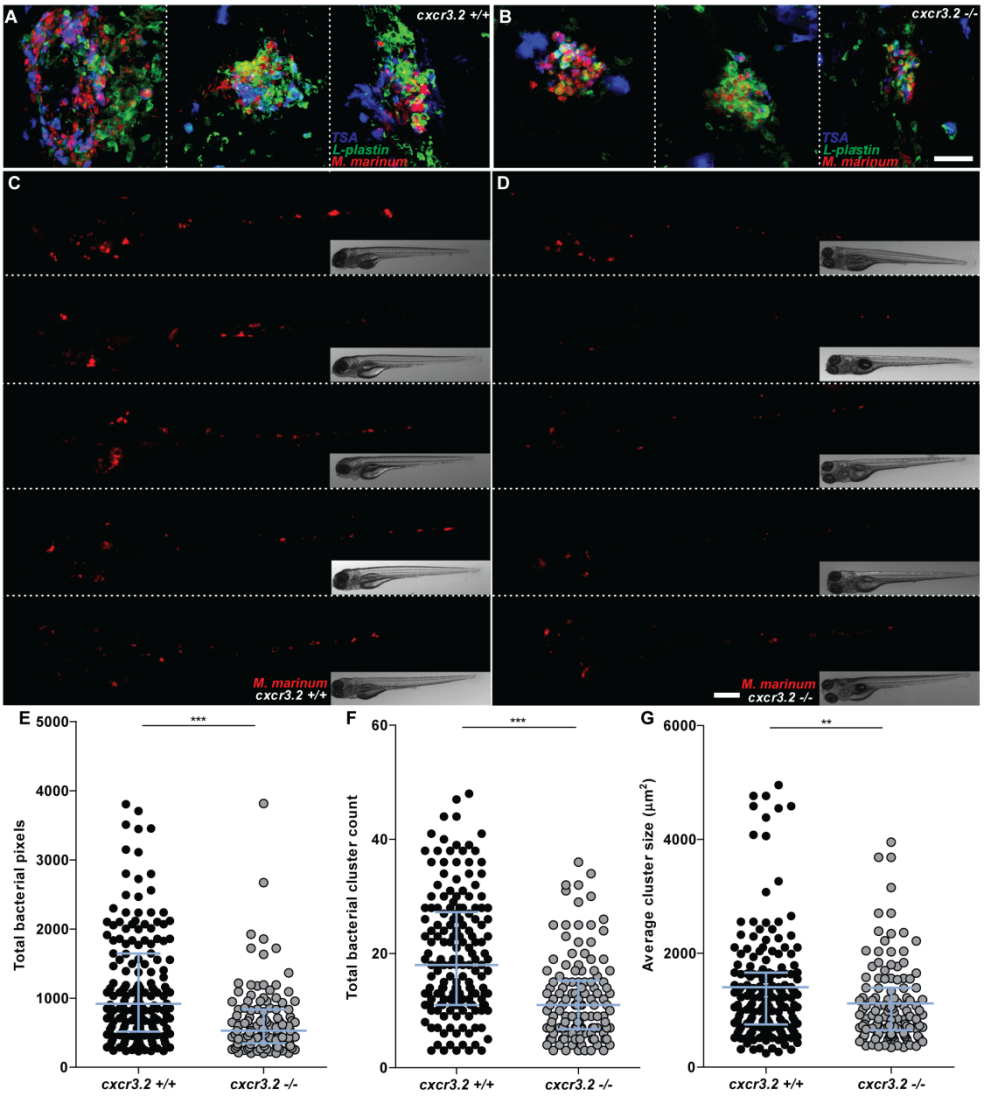

Figure 8. Effect of *cxcr3.2* mutation on granuloma formation following systemic mycobacterial infection *(Legend on the next page)***.**

Figure 8. Effect of *cxcr3.2* mutation on granuloma formation following systemic mycobacterial infection *(Figure on the previous page)*. **A–D.** Representative images of granulomas in systemically infected *cxcr3.2*$^{+/+}$ and *cxcr3.2*$^{-/-}$ larvae. Embryos were systemically infected at 1 dpf, injecting 200 CFU of *M. marinum* into the caudal vein. Images of three representative granuloma-like structures of wildtype (wt; A) or mutant (B) larvae were taken on samples fixed at 6 dpf and simultaneously stained for Lp and Mpx (TSA stain) to distinguish macrophages (Lp-positive, TSA-negative) from neutrophils (TSA-positive). Images of representative *cxcr3.2*$^{+/+}$ (C) or *cxcr3.2*$^{-/-}$ (D) larvae were acquired live at 6 dpf. Scale bar in A-B: 40 µm. Scale bar in C-D: 200 µm. **E–G.** Quantification of the impact of *cxcr3.2* mutation on mycobacterial granuloma formation. Total infection burden (total infection fluorescent pixels; E), total number of bacterial clusters (F) and average area of bacterial clusters (G) are significantly reduced under *cxcr3.2*-deficient conditions. Data were accumulated from three independent experiments. Sample size (*n*): 170, 122. Error bars: median (E-F) or mean (G) and interquartile range. $^{**}P<0.01$; $^{***}P<0.001$.

DISCUSSION

The chemokine receptor CXCR3 and its ligands play important roles in the pathogenesis of infectious diseases, autoimmune disorders and cancer[11,14,15,16,17,19,20,21,22,23,24]. In this study, we report on the function of CXCR3 signalling in macrophage recruitment to infection foci and in the early establishment of mycobacterial granulomas. We found that the Cxcr3.2 receptor, one of the three zebrafish homologues of human CXCR3, interacts with infection-inducible zebrafish homologues of the CXCL11 ligand family and is required for the mobilisation of macrophages to different pathogens, such as locally delivered *M. marinum* or *S. typhimurium*. Furthermore, mutation of *cxcr3.2* reduced the macrophage-mediated dissemination of *M. marinum*, leading to attenuation of the formation and expansion of granulomatous lesions in both local and systemic models of mycobacterial infection.

CXCR3 is best known as a canonical marker for Th1 cells, but several recent studies have raised interest in the expression of this receptor by macrophages. These studies have implicated CXCR3 signalling in processes as diverse as the recruitment of macrophages to allografts[24], the macrophage-mediated remodelling of blood vessels[10] and the polarisation of macrophages towards an M2 phenotype that promotes tumour progression[20]. Furthermore, CXCR3 signalling has been shown to play a crucial role in the murine neonatal response to sepsis[23]. Like murine neonates, zebrafish embryos and early larvae rely heavily on their innate immune system for defence against infection. During zebrafish embryogenesis, macrophages are the first leukocyte cell type to develop and they express *cxcr3.2* from day 1[36]. In mutants of *cxcr3.2*, or in wt embryos treated with a human CXCR3 antagonist (NBI74330), we observed a significant reduction in the recruitment of macrophages to local bacterial infection in the hindbrain. In contrast, Cxcr3.2-deficient macrophages were able to normally migrate in response to chemically induced wounding or towards Cxcr3.2-independent chemoattractants, such as LTB_4 and fMLP. These data suggest that Cxcr3.2 signalling is specifically activated by pathogen-induced chemokine signals. We considered a cluster of CXCL11-like chemokines as the putative ligands of Cxcr3.2 and confirmed that two of these, Cxcl11aa and Cxcl11af, exerted chemoattractant activity on macrophages following hindbrain injection of the recombinant proteins. Most likely, Cxcl11ag, which is near-identical to Cxcl11af, also signals through Cxcr3.2. It is currently unknown whether the *cxcl11* genes in zebrafish are IFN-γ-inducible like their mammalian counterparts, but IFN-γ responsive elements are present in the promoters of these genes[52]. In addition, because we were unable to detect expression of the zebrafish *cxcl11* genes *in situ*, the cell types producing these chemokines remain to be established. However, qRT-PCR showed rapid upregulation of *cxcl11aa* and *cxcl11af/ag* gene

expression following infection, supporting their function as the ligands mediating the infection-dependent recruitment of Cxcr3.2-positive macrophages.

Expression analysis on FACS-sorted phagocyte populations showed that also *cxcr3.3* is expressed in macrophages, but macrophage motility and recruitment defects in the *cxcr3.2* mutant line indicates that expression of *cxcr3.3* cannot compensate for the loss of function of *cxcr3.2*. In addition, the expression analysis revealed that also neutrophils express *cxcr3.2* at 2 and 6 dpf. Injection of Cxcl11aa or Cxcl11af into the otic vesicle at 2 dpf did not chemoattract a higher number of neutrophils within 3 hours than mock injections, whereas comparable concentrations of these chemokines were able to recruit macrophages into the hindbrain, and comparable concentrations of Cxcl8a and Cxcl11ae mobilised neutrophils when delivered in the otic vesicle. Different explanations can be given for this effect. Firstly, it is possible that different concentrations of chemokines are required to efficiently chemoattract different cell types. Secondly, the requirement of co- stimulatory signals or cell-specific co-receptors might be different between the phagocyte populations. Thirdly, although macrophages and neutrophils at 2 dpf seem to express comparable levels of *cxcr3.2* mRNA, it remains unknown whether similar protein levels of Cxcr3.2 are exposed on their membranes. It should be noted that macrophages and their progenitors are marked by *cxcr3.2* expression already at 1 dpf, whereas its expression could not be detected at this time point on neutrophil progenitors[36]. In line with this consideration, it is possible that this different timing in messenger expression impacts the protein levels at 2 dpf.

Macrophages are essential for the dissemination of pathogenic mycobacteria and mediate the formation of both primary and secondary granulomas in the zebrafish host following infection with *M. marinum*[38,39]. When *M. marinum* was locally injected into the hindbrain ventricle of 1-day-old embryos, almost half of the embryos exhibited dissemination within 24 hours, where single infected macrophages migrated out of the ventricle and localised distally. In *cxcr3.2* mutants, this dissemination of the infection was significantly reduced, which might be a consequence of the diminished macrophage attraction to the primary infection source or a direct effect on the retromigration ability of *cxcr3.2* mutant macrophages. When the bacteria were injected intravenously, *cxcr3.2* mutation reduced the formation and the expansion of granulomas, thereby attenuating the dissemination of bacteria and the overall burden of systemic infection. This phenotype might be explained by the reduced motility of macrophages in *cxcr3.2* mutants because it has been shown that early granulomas in zebrafish larvae expand by spreading of the infection to newly recruited macrophages[53]. In agreement, the phenotype of *cxcr3.2* mutant larvae resembles those caused by deficiency in other host (*mmp9*) or bacterial (ESAT-6) factors that also impair macrophage recruitment[53,54].

The zebrafish larval tuberculosis model is limited to the study of the initial stages of granuloma formation by macrophages in a context where the adaptive immune system is not yet functional. A beneficial effect of *CXCR3* mutation has also been observed during chronic infection of BALB/c mice with *Mycobacterium tuberculosis*[14]. In this model, the resistance of CXCR3-deficient mice was attributed to the function of *CXCR3* in T-cell priming. Another study using C57BL/6 mice showed that *CXCR3* mutation affected early granuloma formation after aerosol *M. tuberculosis* infection and correlated this with the invasion of polymorphonuclear neutrophils that produce chemokine signalling via CXCR3[17]. Together, the studies in mice and zebrafish models support further investigation

of the CXCR3 signalling axis as a host therapeutic target for tuberculosis. Our study is the first to implicate this signalling axis in macrophage responses that drive the initiation and expansion of mycobacterial granulomas. In future work it will, therefore, be of great interest to investigate how macrophage and T-cell responses determined by CXCR3 signalling cooperate in the control of mycobacterial infections, using adult zebrafish or mammalian models of tuberculosis.

Recently, another chemokine receptor, Ccr2, has also been shown to mediate macrophage recruitment following hindbrain infection of *M. marinum* in zebrafish embryos[37]. This Ccr2-mediated pathway is dependent on the presence of phenolic glycolipids on the mycobacterial cell surface and it recruits a population of macrophages that are permissive for mycobacterial growth, because activation of the host immune response is largely avoided owing to the presence of other cell surface lipids in virulent mycobacteria (phthiocerol dimycocerosate lipids), which physically mask the underlying PAMPs. *M. marinum* bacteria lacking phenolic glycolipids were still able to recruit macrophages, and morpholino knockdown of either Ccr2 or its ligand Ccl2 attenuated recruitment but did not fully abolish it. These observations indicate that redundant and/or synergistic mechanisms are cooperating in macrophage mobilisation. Combined experiments will be necessary to reveal whether the Ccr2-Ccl2 axis is (partially) redundant or synergistic with the Cxcr3-Cxcl11-mediated macrophage recruitment shown here.

Interestingly, we found that Cxcr3.2 is also involved in the basal motility of macrophages under physiological conditions. We hypothesise that the lower basal motility of macrophages in *cxcr3.2* mutants could be due to the inability to sense small amounts of Cxcr3.2 ligands secreted in the macrophage microenvironment. Possibly, the macrophages themselves could be involved in an autocrine or paracrine secretion of these ligands. Similar mechanisms acting via CXCR3 signalling have already been described in the literature. Keratinocytes have been shown to express CXCL10 and CXCR3 to guide their own migration for re-epithelialisation in a wound-healing response[55]. Similarly, synovial fibroblasts use this ligand-receptor pair to regulate their invasion of joints in rheumatoid arthritis[56]. Furthermore, myeloid cells and haematopoietic progenitors secrete many different chemokines, including CXCR3 ligands, to regulate haematopoiesis in an autocrine or paracrine manner[57]. The autocrine or paracrine production of Cxcr3.2 ligands could potentially work as a local macrophage stimulator, which might significantly contribute to the surveillance activities that macrophages exert in tissues. During mycobacterial disease, similar mechanisms might be stimulated within the core of the granulomatous lesions, and could be involved in the in-and-out trafficking properties of macrophages, characteristic of these dynamic structures[58,59]. In various animal models of tuberculosis, including the most clinically relevant macaque model, abundant expression of CXCR3 ligands is detected in the core and in the direct neighbourhood of the granulomatous lesions[59,60,61]. Our study suggests that this is relevant not only for the recruitment of T cells, but also for regulating macrophage activities in the immunopathology of the granulomatous lesion. A number of studies with selective agonists or antagonists of CXCR3 have already shown beneficial effects on inflammation-associated diseases[62,63] and the zebrafish model might be a suitable model to test their effectiveness on mycobacterial infections.

Concluding, here we propose a dual biological role of Cxcr3.2-Cxcl11aa/af ligand-receptor signalling. First, our results implicate Cxcr3.2 and its ligands in surveillance against

pathogens by promoting the random patrolling of inactive macrophages. Second, we show that this pathway is involved in the mobilisation of macrophages during infection. Depending on the specific interactions of different pathogens with their hosts, a Cxcr3.2-dependent response could be beneficial for the resolution of infection or have an unfavourable effect because, on the one hand, it can sustain the recruitment of macrophages to the infection site, but, on the other hand, it can promote the dissemination of bacteria, as in the case of mycobacterial infection.

MATERIALS AND METHODS

Zebrafish lines and maintenance – Zebrafish lines were handled in compliance with the local animal welfare regulations and maintained according to standard protocols (zfin.org). The breeding of adult fish was approved by the local animal welfare committee (DEC) of the University of Leiden (license number: 10612) and adhered to the international guidelines specified by the EU Animal Protection Directive 2010/63/EU. Adult zebrafish were not sacrificed for this study. All experiments in this study were performed on embryos/larvae before the free-feeding stage and did not fall under animal experimentation law according to the EU Animal Protection Directive 2010/63/EU.

Fish lines used in this work were the following: wildtype (wt) strain AB/TL, double-transgenic line *Tg(mpeg1:mCherry-F/mpx:eGFP)*[64,65] homozygous mutant (*cxcr3.2*$^{-/-}$) and wt siblings (*cxcr3.2*$^{+/+}$) of *cxcr3.2*^{hu6044}, *Tg(mpeg1:Gal4-VP16/UAS-E1b:Kaede)*, in short referred to as *Tg(mpeg1:Gal4/UAS:Kaede)*[66], and the combination of *Tg(mpeg1:Gal4/UAS:Kaede)* with the *cxcr3.2* mutant strain. The *cxcr3.2*^{hu6044} allele was identified by sequencing of an ENU (N-ethyl-N-nitrosourea)-mutagenised zebrafish library and was obtained from the Hubrecht Laboratory and the Sanger Institute Zebrafish Mutation Resource. Heterozygous F2 carriers were outcrossed twice against wt and were subsequently incrossed. Resulting *cxcr3.2*$^{-/-}$ and *cxcr3.2*$^{+/+}$ siblings were raised and used to obtain embryos for all the experiments. The combined mutant-transgenic line *Tg(mpeg1:Gal4/UAS:Kaede/cxcr3.2*$^{-/-}$ or *cxcr3.2*$^{+/+}$*)* were obtained by crossing heterozygous carriers with the original transgenic line and subsequently incrossing the heterozygous offspring. For genotyping, genomic DNA was amplified using forward primer 5′-GGCATCTTTTTTGTTACAGCCTACAGCTTA-3′ and reverse primer 5′-TGGCGATATCGGCGGATAACA-3′, amplifying a 201 base pair (bp) product containing the mutation. The forward primer introduces an additional base change, which only in combination with the mutant allele generates the consensus for *Dde*I restriction enzyme. Therefore, the mutant allele was distinguished from the wt by specific digestion into a 174 fragment that can be separated from the undigested wt amplicon on a 2.5% agarose gel. Alternatively, genotyping was performed by KASP assay using the primers 5′-CATCATAGGAAGTACTGTTGTAGTCA-3′, 5′-CATCATAGGAAGTACTGTTGTAGTCC-3′ and 5′-GGCATCTTTTTTGTTACAGCCTACAGATT-3′. Robustness of both methods was verified several times by sequencing of the amplicons.

Embryos were grown at 28.5°C in egg water (60 µg/ml sea salt, Sera Marin, Heinsberg, Germany). For live-imaging or injection assays, larvae were anaesthetised in egg water medium containing 0.02% buffered Tricaine (3-aminobenzoic acid ethyl ester; Sigma-Aldrich, St Louis, MO, USA). To prevent melanisation, larvae were generally maintained in egg water supplemented with 0.003% PTU (1-phenyl-2-thiourea; Sigma-Aldrich).

Sequencing – Sequencing of the full coding sequence of *cxcr3.1*, *cxcr3.2* and *cxcr3.3* was obtained by amplification with primers described in **Supplementary Table 3**. For *cxcr3.2* and *cxcr3.3*, both genomic and cDNA templates extracted from pools of 15–20 embryos were used. Amplification was performed with Phusion high-fidelity DNA polymerase (Thermo-Scientific, Pittsburgh, PA, USA). DNA amplicons were then gel-extracted on 1.5% agarose and column-purified with PureLink quick gel extraction and PCR purification kit (Invitrogen, Life Technologies, Carlsbad, CA, USA). Sequencing with M13Fw, M13Rv universal primers (incorporated in the amplification primers) or with custom-made primers was outsourced to Baseclear (Leiden, The Netherlands). For *cxcr3.1*, sequencing results derive exclusively from genomic DNA amplifications. Amplification of cDNA templates for *cxcr3.2* resulted in a band of identical size in mutant, wt and AB/TL, thereby excluding altered exon/intron arrangements attributable to the ENU-mutagenesis per se or to the *cxcr3.2*^{hu6044} allele.

Bacterial cultures and infection delivery – Approximately 200 CFU (1 nl) of *M. marinum* strain Mma20 expressing mCherry[67], or *Salmonella enterica* serovar Typhimurium (*S. typhimurium*) strain SL1027 expressing DsRed[68], were grown and harvested as described previously[47,69]. Embryos were staged at 30 hpf and bacteria or mock control [phosphate buffer saline (PBS) supplemented with 0.1% phenol red (Sigma-Aldrich) and 2% polyvinylpyrrolidone-40 (Sigma-Aldrich)] were locally injected in the hindbrain cavity as described previously[47,69]. Injections of bacteria in the otic vesicle, as shown in **Figure 3**, were performed either at 3 dpf (**Figure 3B**,**I-L**) or at 4 dpf (**Figure 3C-H**). When infection was delivered systemically, the same dose was instead injected in the caudal vein as in reference[69]. As a control, the same dose was spotted onto plates, incubated and counted. Embryos were kept into fresh PTU egg water, incubated at 28.5°C, and collected for qRT-PCR or used for imaging at 1–6 dpf. In **Figure 8A**,**B**, embryos were fixed at 6 dpf in 4% paraformaldehyde in PBSTx (1× PBS supplemented with 0.8% Triton X-100; Sigma-Aldrich) and prepared for Myeloperoxidase (Mpx) activity stain with TSA staining kit (PerkinElmer Inc., Waltham, MA, USA), followed by immunostaining against the pan-leukocyte marker Leukocyte-plastin (Lp) as described previously[47,69].

FACS-sorting, RNA isolation and qRT-PCR – *Mpeg1:mCherry-F*-positive, *mpx:eGFP*-positive and unlabelled cells were sorted from *Tg(mpeg1:mCherry-F/mpx:eGFP)* at 2 and 6 dpf. FACS-protocol and RNA isolation were performed according to reference[70]. To evaluate the induction of the *cxcl11* genes upon infections, pools of 18–20 embryos were collected for RNA isolation, snap-frozen in liquid nitrogen and subsequently stored at −80°C. RNA was extracted using Qiazol reagent (Qiagen, Valencia, CA, USA) according to the manufacturer's guidelines. Residual genomic DNA was removed by DNA-free kit (Ambion, Life Technologies). The cDNA was prepared using the iScript cDNA-synthesis kit (Invitrogen, Life Technologies) and was used as a template for qRT-PCR reaction with iQ SYBR Green Supermix according to the manufacturer's instructions (Bio-Rad Laboratories, Munich, Germany). Specificity of the amplification reaction was analysed using dissociation curves. Each qRT-PCR was performed in technical duplicate and on biological replicates as indicated in the figure legends. Reference genes were *eif4a1b* or *eif5* (eukaryotic translation initiation factor 4a isoform 1b or 5*)* for FACS-sorted cells and *ppiab* (*peptidylprolyl isomerase ab/cyclophilin a*) for infection experiments. Fold changes were determined using the ΔΔ comparative threshold method. Primers are reported in **Supplementary Table 3**.

Production of recombinant chemokines and local injections – Synthetic coding sequences for Cxcl11aa, Cxcl11af, Cxcl11ae and Cxcl8a (included as negative control) were generated (Baseclear) according to database accessions (**Supplementary Table 2**). To enable secretion in yeast, the sequences were codon optimised and the predicted zebrafish signal peptide was replaced with yeast alpha-factor secretion signal, as a result from cloning into pPICZα expression vector (Invitrogen, Life Technologies). Additionally, a HA (human influenza haemagglutinin)-tag was added at the C-terminus to facilitate the purification process and identification. The recombinant chemokines were produced by *Pichia pastoris* strain *X-33* transformed with the chemokine vectors as described previously[71]. Proteins were purified via Fast Protein Liquid Chromatography in NaCl salt gradient and finally desalted and concentrated by membrane filtrations on Amicon Ultra Centrifugal filter devices with a nominal molecular weight limit of 3 kilodaltons (Amicon, Merck KGaA, Ireland), using 50 mM sodium phosphate buffer pH 6.5 as a washing and suspension vehicle. Purity and identity of the proteins were confirmed by trypsinisation and electrospray mass-spectrometry. The recombinant chemokines (0.5–1.2 mg/ml), LTB_4 (leukotriene B4; Santa Cruz Biotechnology, Santa Cruz, CA, USA; 10.1 ng/ml), fMLP (N-formyl-methionyl-leucyl-phenylalanine; Sigma-Aldrich; 0.2 mg/ml) or mocks [sodium phosphate buffer pH 6.5 for the chemokines, 5% DMSO (Sigma-Aldrich) in PBS for fMLP and 0.02% ethanol (Sigma-Aldrich) in PBS for LTB_4] were supplemented with 0.1% phenol red and injected at 30 hpf in the hindbrain ventricle (1 nl) or at 52 hpf in the otic vesicle (0.5 nl) as described previously[47,69]. In both cases, embryos were fixed at 3 hpi in 4% paraformaldehyde in PBSTx and prepared for Lp immunostaining as in reference[47]. At 30 hpf, the population of fully differentiated leukocytes is represented almost exclusively by macrophages[48,49]; thereby, we could assume that nearly all the Lp-stained cells able to migrate and infiltrate in the ventricle represented macrophages at this developmental stage. As is shown in **Supplementary Figure 3**, only one to two *mpx*-positive cells [*mpx*-whole mount *in situ* hybridisation as in reference[47]] could be counted within the perimeter of the hindbrain in this experimental setting at 3 hours post local bacterial infection, which is less than 10% of the cells positive for the macrophage marker *mfap4*. At later developmental stages, in order to discern between neutrophils and macrophages, samples were processed also with a neutrophil-specific Mpx activity staining as described previously[47]), by using the leukocyte peroxidase (Myeloperoxidase) staining kit (Sigma-Aldrich) for the histochemical detection of the enzymatic activity of Mpx. Leukocytes accumulated at the injected cavity (macrophages: Lp-positive and Mpx-negative; neutrophils: Mpx-positive) were counted using a Leica MZ16FA fluorescence stereomicroscope (Leica Microsystems, Rijswijk, The Netherlands).

Chemically induced (ChIn) inflammation assay – 3-dpf larvae were exposed to 10 μM copper sulphate ($CuSO_4$; Sigma-Aldrich) for 2 hours as described previously[50]. Treated larvae were then fixed and used for combined Mpx activity staining and Lp immunostaining as described above.

Pharmacological treatment with NBI74330 – Bath-treatment with the CXCR3 high-affinity antagonist NBI74330 or vehicle treatment (0.5% DMSO) was started at 27 hpf by exposing dechorionated embryos to 50 μM of the drug in medium. Embryos were incubated for 3 hours at 28.5°C and then injected in the hindbrain with mock or *M. marinum* as described above. Injected embryos were maintained for an additional 3 hours in 50 μM NBI74330 or vehicle alone and then fixed in 4% paraformaldehyde/PBSTx and prepared for Lp immunostaining as described previously[47].

Imaging and image quantification – Fixed or live embryos and larvae were imaged using a Leica MZ16FA fluorescence stereomicroscope. For time-lapse experiments, samples were mounted in 2% low-melting-point agarose (SphaeroQ, Burgos, Spain) and images were acquired with a laser-scanning confocal microscope (Leica TCS SPE, Leica Microsystems or Zeiss Observer 6.5.32, Carl Zeiss, Sliedrecht, The Netherlands). To assess the average speed of macrophages (**Figure 1J-K**), a time-lapse experiment was performed and quantification was obtained on overlaid z-stacks by Fiji/ImageJ software (NIH, Bethesda, MD, USA) using the ManualTrack plug-in as described elsewhere[72]. The average speed was calculated as the average of all the speeds assumed by every single macrophage at each time point. Analysis was performed by cumulating three experiments in which 15–21 macrophages per embryo were followed. To quantify the morphological differences between macrophages in *cxcr3.2* mutants and wt, bacteria were injected into the otic vesicle of *Tg(mpeg1:Gal4/UAS:Kaede/cxcr3.2*$^{+/+}$ or *cxcr3.2*$^{-/-}$*)* larvae at 3 dpf and fixed at 4 hpi. Images of macrophages were acquired in the trunk. Perimeter and area of the cells were obtained by Fiji/ImageJ using the Analyse Particles plug-in. The circularity index (CI) corresponding to each cell was obtained by the formula: $CI=4\pi$ (area/perimeter^2), resulting in an index that ranges from 0 (infinitely branched structure) to 1 (perfect circle). Macrophages were classified in five different intervals of circularity based on their CI (0.0 to 0.19, 0.2 to 0.39, 0.4 to 0.59, 0.6 to 0.79, 0.8 to 1.0) and the average percentages of macrophages in each interval were estimated for *cxcr3.2*$^{+/+}$ or*cxcr3.2*$^{-/-}$ (**Figure 3I**). To estimate the divergence of distribution of *cxcr3.2*$^{+/+}$and *cxcr3.2*$^{-/-}$ macrophages from the overall mean, the percentages in each interval were divided by the average percentage of mutants and wt assumed in that interval, using the formulas: $\text{Deviation}_{(cxcr3.2+/+)}= \%cxcr3.2^{+/+}/[(\%cxcr3.2^{+/+} + \%cxcr3.2^{-/-})/2]$ and $\text{Deviation}_{(cxcr3.2-/-)}= \%cxcr3.2^{-/-}/[(\%cxcr3.2^{+/+} + \%cxcr3.2^{-/-})/2]$ (**Figure 3J**). To quantify the dissemination of bacterial infection (**Figure 6F**,**I**), the presence or absence of infection distally from the infected site was evaluated, giving a score of 1 in case of dissemination and a score of 0 in case of absent dissemination. Quantification of total bacterial pixels (**Figure 7A-B** and **Figure 8E**) was obtained using dedicated bacterial pixel count program as in reference[73]. Total bacterial cluster count (**Figure 8F**) was performed manually from images. Quantification of the area of single distal clusters (**Figure 7C**) and average area of disseminated granulomas (**Figure 8G**) were performed using ImageJ quantification tools as in reference[74]).

Statistical analysis – In the survival test (**Figure 1E**), non-significant deviation from Mendelian rate was evaluated by χ^2 test on four independent replicates. For qRT-PCR, statistical significance was estimated on five (**Figure 1A-C**), four (**Figure 4A-B**) or three (**Figure 4C-D**) biological replicates by two-tailed *t*-tests on ln(n)-transformed relative induction folds. All the other experiments were statistically analysed using GraphPad Prism 4 or 5 (GraphPad Software, La Jolla, CA, USA). Where correction for non-parametric distribution was required (**Figure 1F**,**G**, **Figure 2**, **Figure 3A**,**B**, **Figure 3M**, **Figure 5**, **Figure 6**, **Figure 7A**,**B**, **Figure 8E**,**F**), comparisons between two groups were performed with two-tailed Mann-Whitney test and comparisons among more than two groups were performed with Kruskal-Wallis test, followed by Dunn's multiple comparison test. When a parametric distribution was assumed (**Figure 1A-C**, **Figure 1L**, **Figure 3I-J**, **Figure 4**, **Figure 8G**), comparisons between two groups were performed with a two-tailed *t*-test. In **Figure 7C**, significance was estimated with an unpaired *t*-test with Welch's

correction, suitable to compare parametric data having different variances. Significance (*P*-value) is indicated with: ns, non-significant; **P*<0.05; ***P*<0.01; ****P*<0.001.

ACKNOWLEDGMENTS

We thank B. Ewa Snaar-Jagalska and Claudia Tulotta for valuable discussions. We are grateful to Fons Verbeek and Alex Nezhinsky (Leiden Institute of Advanced Computer Science) for making their pixel quantification software available prior to publication and to Erica Benard for RNA samples of *M. marinum* systemically infected embryos. For providing the zebrafish knockout allele *cxcr3.2*^{hu6044} we thank the Hubrecht Laboratory and the Sanger Institute Zebrafish Mutation Resource.

This work was supported by the Smart Mix Program of the Netherlands Ministry of Economic Affairs and the Ministry of Education, Culture and Science, the European Commission 7th framework project ZF-HEALTH (contract number HEALTH-F4-2010-242048), and the European Marie-Curie Initial Training Network FishForPharma (contract number PITN-GA-2011-289209). The funders had no role in study design, data collection and analysis, decision to publish or preparation of the manuscript.

FOOTNOTES

The format and spelling of the contents in this chapter have been adapted from the published article to conform it to the thesis outline.

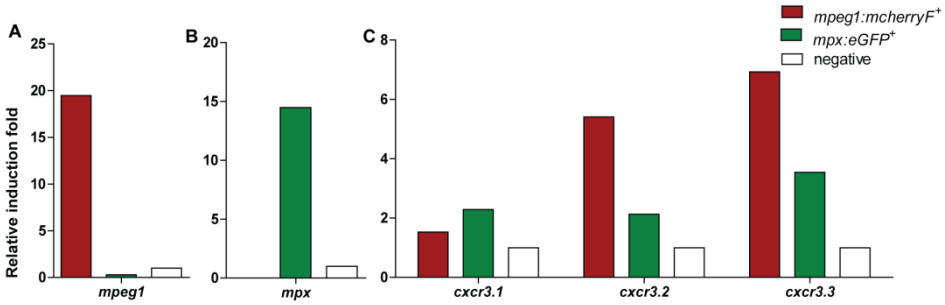

Supplementary Figure 1. Expression of *cxcr3.2* and its paralogues *cxcr3.1* and *cxcr3.3* in FACS-sorted phagocytes at 6 dpf. Graphs represent the relative induction fold of the macrophage marker *mpeg1* (A), the neutrophil marker *mpx* (B), and of the *cxcr3* paralogues (C) in FACS-sorted macrophages and neutrophils from the combined transgenic line *Tg(mpeg1:mCherry-F/mpx:eGFP)* at 6 dpf. Expression of *cxcr3.2* and *cxcr3.3* could be detected in both macrophages and neutrophils, while *cxcr3.1* was not significantly enriched in the FACS-sorted populations when compared to the non-labelled cell fraction. Reference gene: *eif5*.

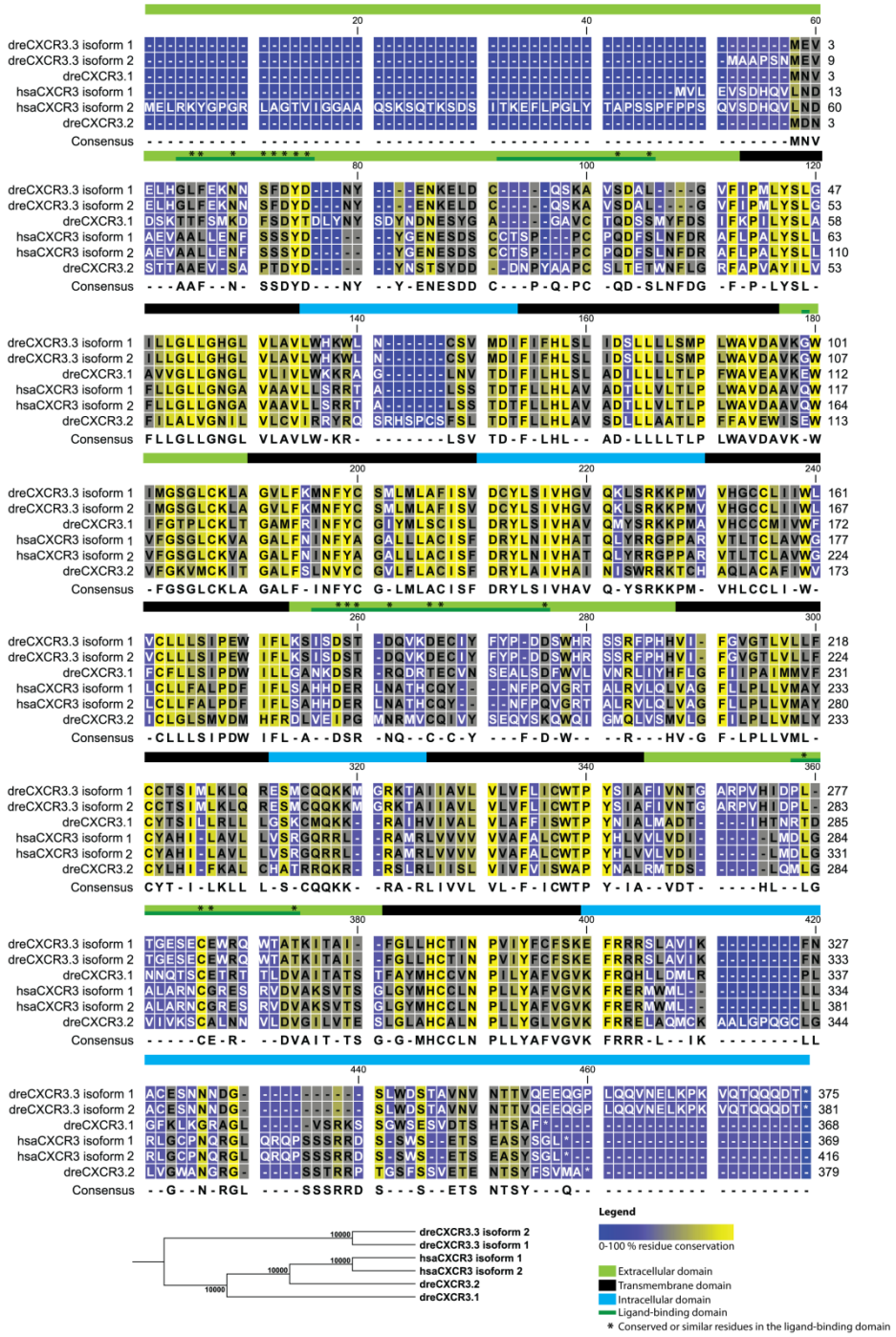

Supplementary Figure 2. Protein sequence multiple alignment of human and zebrafish CXCR3 chemokine receptors *(Legend on the next page)*.

Supplementary Figure 2. Protein sequence multiple alignment of human and zebrafish CXCR3 chemokine receptors *(Figure on the previous page)***.** Residue colour from blue to yellow indicates increasing degree of amino acid conservation. The alignment and the tree were obtained using CLC main workbench 6.8.4 by Neighbour-Joining Algorithm. Gap costs were given with a penalty score of 10 for each gap open, and an additional score of 1 per each extension; no cost was associated to end gaps. Extracellular (light green bars), Transmembrane (black bars), and Intracellular (light blue bars) domains were predicted with CLC main workbench 6.8.4. Ligand binding domains (dark green bars) and conserved residues or similar residues within the binding domains (black asterisks) were predicted according to reference[75]. The numbers at the tree nodes denote the bootstrap for 10000 replicates. Single alignment of the predicted zebrafish chemokine receptor proteins to the canonical isoform of CXCR3 (hsaCXCR3 isoform 1) were performed with clustalO algorithm (http://www. uniprot.org/align) and provided the following % of identity: dreCXCR3.1 (ENSDARG00000007358): 39.1%, dreCXCR3.2 (ENSDARG00000041041): 35.7%, dreCXCR3.3 (ENSDARG00000070669) isoform 1: 29.8% and dreCXCR3.3 isoform 2: 29.6%.

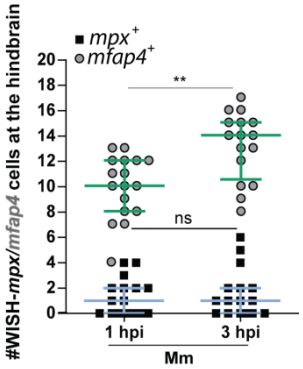

Supplementary Figure 3. Macrophages are the predominant phagocyte cell type recruited to local hindbrain infection in 31-33 hpf embryos. Embryos were locally injected into the hindbrain cavity at 30 hpf with 100 CFU of *M. marinum* and fixed at 1 and 3 hpi. Double fluorescent *in situ* hybridisation was performed with *mfap4* as a macrophage marker and *mpx* as a neutrophil marker[36]. The average number of *mfap4*-positive macrophages in the hindbrain at 1 or 3 hpi exceeds the average number of *mpx*-positive neutrophils approximately 10-fold and a significant difference between the time points was observed only for macrophages. Sample size (n): 17, 16. Error bars: median and interquartile range. ns, non-significant; **P<0.01.

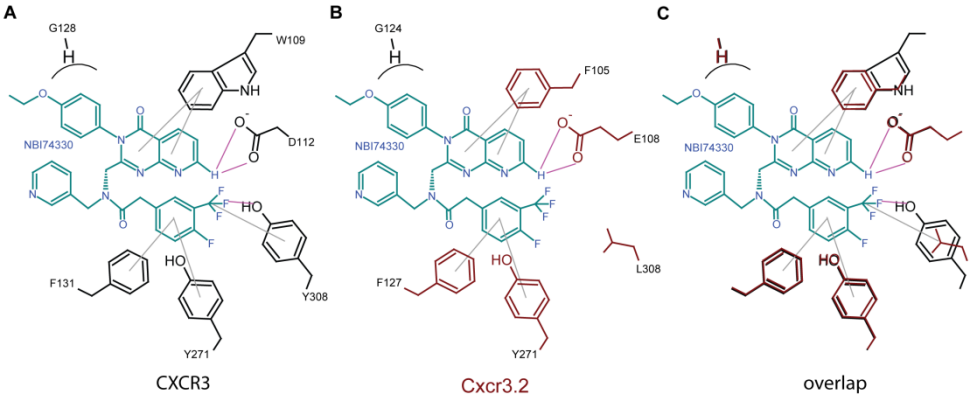

Supplementary Figure 4. Predicted molecular docking of NBI74330 into the transmembrane minor pocket of Cxcr3.2 The figure represents the high conservation of the transmembrane minor pocket of zebrafish Cxcr3.2 with human CXCR3. **A-B.** Side chains of proposed interacting residues are shown in black for CXCR3 (A) and in red for Cxcr3.2 (B). The ligand NBI74330 is shown in cyan. Suggested receptor/ ligand interactions are depicted as coloured lines. Polar and hydrogen bonding interactions are shown as pink lines, whereas aromatic interactions are shown as grey lines. **C.** Overlay of the CXCR3 and Cxcr3.2 binding pocket. Prediction of ligand binding for CXCR3 is according to reference[51]. Predictions of ligand binding for Cxcr3.2 is according to sequence alignment and amino acid similarity in the corresponding positions between CXCR3 and Cxcr3.2.

Supplementary Figure 4. Predicted molecular docking of NBI74330 into the transmembrane minor pocket of Cxcr3.2

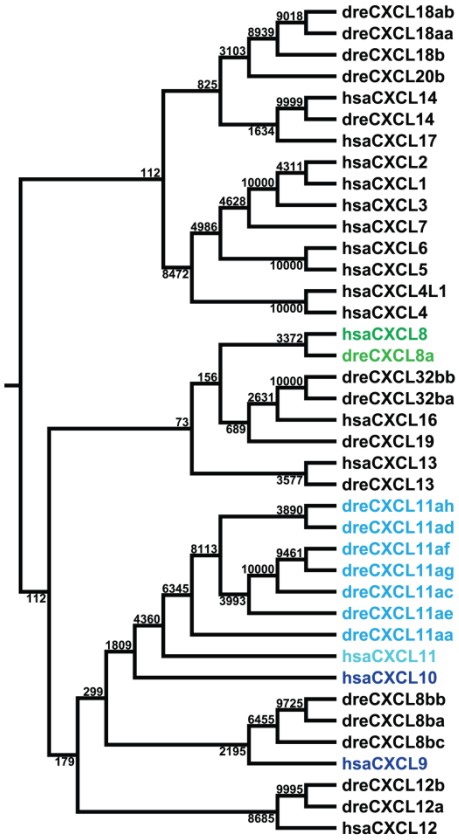

Supplementary Figure 5. Phylogenetic tree of human and zebrafish chemokine protein sequences. The alignment and the tree were obtained using CLC main workbench 6.8.4 by Neighbour-Joining Algorithm. Gap costs were given with a penalty score of 10 for each gap open, and an additional score of 1 per each extension; no cost was associated to end gaps. Additionally, the CXC motif of the chemokine was set as fixed alignment point. The numbers at the tree nodes denote the bootstrap for 10000 replicates. Light blue: Cxcl11-like cluster, containing human CXCL11 and seven zebrafish Cxcl11-like chemokines. Dark blue: human CXCL9 and CXCL10. Green: Cxcl8-like cluster, containing human CXCL8 (IL8) and zebrafish Cxcl8a (Il8). Nomenclature according to reference[34].

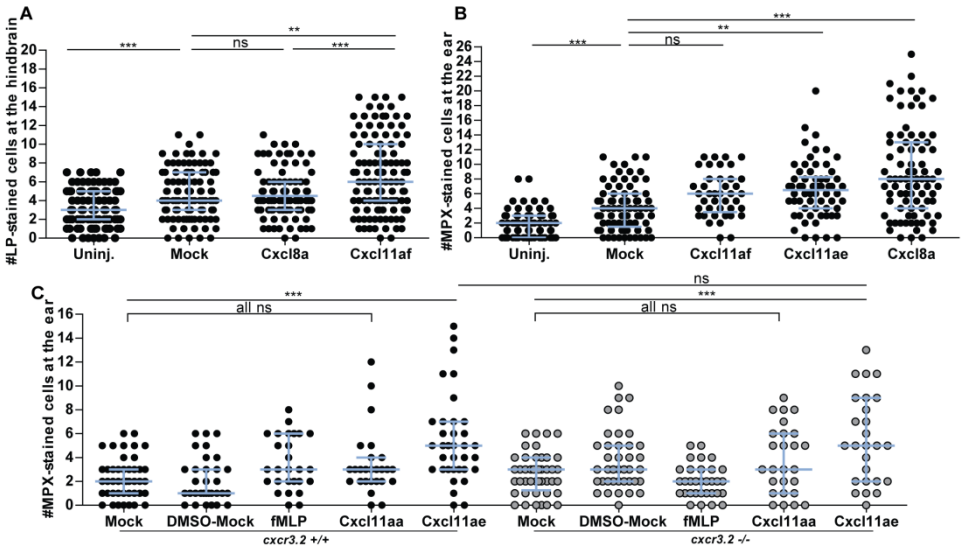

Supplementary Figure 6. Chemoattractive effects of recombinant chemokines on different phagocytes. A. Chemoattraction of macrophages to the hindbrain ventricle. Recombinant proteins or buffer (mock) were injected into the hindbrain ventricle of wildtype (AB/TL) embryos at 30 hpf and Lp-stained cells accumulating in 3 hours within the hindbrain limits were counted as macrophages. Cxcl11af but not Cxcl8a significantly attracted macrophages. Sample size (n): 106, 100, 94, 112. Error bars: median and interquartile range. **B-C.** Chemoattraction of neutrophils to the otic vesicle. Recombinant proteins or mock were injected into the otic vesicle of wildtype (AB/TL) embryos (B) or cxcr3.2$^{+/+}$ and cxcr3.2$^{-/-}$ siblings (C) at 54 hpf and neutrophils accumulating in 3 hours within the otic vesicle were counted after Mpx activity staining. Neutrophil attraction by recombinant Cxcl8a (Il8) (B) was in agreement with previous reports[27]. Note that Cxcl11ae significantly recruited neutrophils in all zebrafish lines, while Cxcl11af (B), Cxcl11aa (C), and fMLP (C) did not exert significant neutrophil attraction above mock injections. Sample size (n) in B: 75, 77, 41, 62, 83. Sample size (n) in C: 44, 32, 27, 26, 35, 44, 39, 32, 26, 26. Error bars: median and interquartile range. ns, non-significant; **P<0.001.

Protein	Amino acid position	Strain	Variant	PROVEAN score	Predicted effect
Cxcr3.1	203	*Reference**	E	0.000	Neutral
		AB/TL	E/K	-0,945	Neutral
		cxcr3.2$^{+/+}$	E/K	-0,945	Neutral
		cxcr3.2$^{-/-}$	E	0.000	Neutral
Cxcr3.1	292	*Reference*	E	0.000	Neutral
		AB/TL	E/K	-1.803	Neutral
		cxcr3.2$^{+/+}$	E	0.000	Neutral
		cxcr3.2$^{-/-}$	K	-1.803	Neutral
Cxcr3.1	351	*Reference*	K	0.000	Neutral
		AB/TL	R	0.645	Neutral
		cxcr3.2$^{+/+}$	R	0.645	Neutral
		cxcr3.2$^{-/-}$	R	0.645	Neutral
Cxcr3.2	16	*Reference*	Y	0.000	Neutral
		AB/TL	Y	0.000	Neutral
		cxcr3.2$^{+/+}$	Y	0.000	Neutral
		cxcr3.2$^{-/-}$	**STOP**	*cxcr3.2*^{hu6044}	Non-sense
Cxcr3.2	93	*Reference*	V	0.000	Neutral
		AB/TL	I	0.048	Neutral
		cxcr3.2$^{+/+}$	I	0.048	Neutral
		cxcr3.2$^{-/-}$	I	0.048	Neutral
Cxcr3.3	48	*Reference*	M	0.000	Neutral
		AB/TL	L	0.332	Neutral
		cxcr3.2$^{+/+}$	L	0.332	Neutral
		cxcr3.2$^{-/-}$	L	0.332	Neutral
Cxcr3.3	75	*Reference*	C	0.000	Neutral
		AB/TL	C/P	-0.547	Neutral
		cxcr3.2$^{+/+}$	C/P	-0.547	Neutral
		cxcr3.2$^{-/-}$	C	0.000	Neutral
Cxcr3.3	95	*Reference*	S	0.000	Neutral
		AB/TL	T	2.931	Neutral
		cxcr3.2$^{+/+}$	T	2.931	Neutral
		cxcr3.2$^{-/-}$	T	2.931	Neutral
Cxcr3.3	236	*Reference*	E	0.000	Neutral
		AB/TL	E/D	-0.328	Neutral
		cxcr3.2$^{+/+}$	E/D	-0.328	Neutral
		cxcr3.2$^{-/-}$	E	0.000	Neutral
Cxcr3.3	238	*Reference*	M	0.000	Neutral
		AB/TL	M/L	-0.611	Neutral
		cxcr3.2$^{+/+}$	M/L	-0.611	Neutral
		cxcr3.2$^{-/-}$	M	0.000	Neutral
Cxcr3.3	244	*Reference*	M	0.000	Neutral
		AB/TL	M/I	-0.473	Neutral
		cxcr3.2$^{+/+}$	M/I	-0.473	Neutral
		cxcr3.2$^{-/-}$	I	-0.473	Neutral
Cxcr3.3	297	*Reference*	T	0.000	Neutral
		AB/TL	S	-0.463	Neutral
		cxcr3.2$^{+/+}$	S	-0.463	Neutral
		cxcr3.2$^{-/-}$	S	-0.463	Neutral
Cxcr3.3	327	*Reference*	L	0.000	Neutral
		AB/TL	L/Q	-2.562	Neutral
		cxcr3.2$^{+/+}$	L/Q	-2.562	Neutral
		cxcr3.2$^{-/-}$	Q	-2.562	Neutral
Cxcr3.3	346	*Reference*	D	0.000	Neutral
		AB/TL	D/E	0.098	Neutral
		cxcr3.2$^{+/+}$	D/E	0.098	Neutral
		cxcr3.2$^{-/-}$	D	0.000	Neutral
Cxcr3.3	350	*Reference*	V	0.000	Neutral
		AB/TL	V/E/D	0.895/1.275	Neutral
		cxcr3.2$^{+/+}$	V/E/D	0.895/1.275	Neutral
		cxcr3.2$^{-/-}$	D	0.895	Neutral
Cxcr3.3	378	*Reference*	Q	0.000	Neutral
		AB/TL	Q/E	-0.077	Neutral
		cxcr3.2$^{+/+}$	Q/E	-0.077	

Supplementary Table 1. Non-synonymous single nucleotide polymorphisms in *cxcr3.1*, *cxcr3.2*, and *cxcr3.3* coding sequences *(Legend on the next page)***.**

Supplementary Table 1. Non-synonymous single nucleotide polymorphisms in *cxcr3.1*, *cxcr3.2*, and *cxcr3.3* coding sequences *(Legend on the next page)***.** Several non-synonymous single nucleotide polymorphisms (nsSNPs) are present in *cxcr3.1*, *cxcr3.2*, and *cxcr3.3* genes that are inherited in association with the ENU-mutagenised *cxcr3.2*^{hu6044} allele. Except for the Cxcr3.1 E292K variant, all the nsSNPs linked to the *cxcr3.2*$^{-/-}$ fish did not differ from the ones represented also in the *cxcr3.2*$^{+/+}$ fish. Furthermore, all nsSNPs, including the Cxcr3.1 E292K variant, were detected also in the AB/TL wt strain. Analysis using the PROVEAN software tool (Protein Variation Effect Analyser, http://provean.jcvi.org)[45,46], predicts that the nsSNPs are unlikely to have an impact on the protein functionality. The threshold to score the possibility of protein non functionality was set to -4.1[46]. Note: Amino acid notations for Cxcr3.3 are represented accordingly to their position in Cxcr3.3 splicing isoform 2. No additional amino acid replacements were specifically found in the splicing isoform 1. *Reference: according to ENSEMBL accessions.

Name	Gene Accession	Protein Sequence
hsaCXCL9	ENSG00000138755	mkksgvlfllgiillvligvqgTPVVRKGRCSCISTNQGTIHLQSLKDLKQFAPSPSCEKIEIIATLKNGVQTCLNPDSADVKELIKKWEKQVSQKKKQKNGKKHQKKKVLKVRKSQRSRQKKTT
hsaCXCL10	ENSG00000169245	mnqtailiccliflslgiqgVPLSRTVRCTCISISNQPVNPRSLEKLEIIPASQFCPRVEIIATMKKKGEKRCLNPESKAIKNLLKAVSKERSKRSP
hsaCXCL11	ENSG00000169248	msvkgmaialavilcatvvqgFPMFKRGRCLCIGPGVKAVKVADIEKASIMYPSNNCDKIEVIITLKENKGQRCLNPKSKQARLIIKKVERKNF
dreCxcl11aa	Gene ID: 798892	mktvtalllvslavvaiegQHMKSQRCVCLGAGLNMVKPVLIEKIEILPSSPSCGHMEVIATLKNGAGKRCLNPKSKFTKKIIDKIEKNNRNAR
dreCxcl11ac	Gene ID:100334604	mktlaaflltcliagkvngQDNTSRARCFCADKGINMVLLKNIEKVEIFPPSPSCNKNEIVVTLKNGAGQKCLNPDSKFTQNVVLKAIGKRMQQSVPHSTTTGTVKSSMTSSTSAPTAFK
dreCxcl11ad	Gene ID: 567656	mktlaavvllgyllvikvegQARAPRSRCLCADKGVNMVSPKLIEKVDIIPPTPSCGNLEIVVTLKNGAEPKCLSPDSKFTQKYLMKALEKRTLQK
dreCxcl11ae	ENSDARG00000092423	mktaaflvflaffifipgQKKFNRCSCVGKGLDRVALRNIEKFEIIHPSPSCGKQEIIVTMKSSEQKCLNPESKFTQELIRRALEK
dreCxcl11af	ENSDARG00000094706	mktlaafllllscliagevngQDRSSRARCFCVDKGLNMVLLKNLDKVEIFPPSPSCNKHEIVVTLKNGAGQKCLNPDSKFTKNVVLKAIGKRMQQSVPHSTTTGTVKSSMTSSTSAPTAFK
dreCxcl11ag	ENSDARG00000093779	mktlaafllllscliagevngQDRSSRARCFCVDKGLNMVLLKNLEKVEIFPPSPSCNKHEIVVTLKNGAGQKCLNPDSKFTKNVVLKAIGKRMQQSVPHSTTTGTVKSSMTSSTSAPTAFK
dreCxcl11ah	ENSDARG00000095747	mktaaafvalgcflmvevkgKIPDLKNRCLCADKGANNVNLKTIEKIQIIHPSPSCKRLEIVVTLMKGAGKKCLNPESNLGKNILKALRKKKLTAVRRMNPA
dreCxcl8a	Gene ID: 100002946	mtskiisvcvivflafltiiegMSLRGLAVDPRCRCIETESRRIGKHIKSVELFPPSPHCKDLEIIATLMTTGQEICLDPSAPWVKKIIDRIIVNRKP
hsaCXCR3 isoform 1	ENSG00000186810	MVLEVSDHQVLNDAEVAALLENFSSSYDYGENESDSCCTSPPCPQDFSLNFDRAFLPALYSLLFLLGLLGNGAVAAVLLSRRTALSSTDTFLLHLAVADTLLVLTLPLWAVDAAVQWVFGSGLCKVAGALFNINFYAGALLLACISFDRYLNIVHATQLYRRGPPARVTLTCLAVWGLCLLFALPDFIFLSAHHDERLNATHCQYNFPQVGRTALRVLQLVAGFLLPLLVMAYCYAHILAVLLVSRGQRRLRAMRLVVVVVVAFALCWTPYHLVVLVDILMDLGALARNCGRESRVDVAKSVTSGLGYMHCCLNPLLYAFVGVKFRERMWMLLLRLGCPNQRGLQRQPSSSRRDSSWSETSEASYSGL

Supplementary Table 2. List of chemokines and chemokine receptors used in this work with accession codes and protein sequences *(continued on the next page)***.** Red letters: amino acids at the splicing sites of the mRNA; blue letters: conserved CXC-chemokine motifs. Part in grey: active chemokine upon removal of the signal peptide.

Name	Gene Accession	Protein Sequence
hsaCXCR3 isoform 2	ENSG00000186810	MELRKYGPGRLAGTVIGGAAQSKSQTKSDSITKEFLPGLYTAPSSPFPPSQ VSDHQVLNDAEVAALLENFSSSYDYGENESDSCCTSPPCPQDFSLNFDRA FLPALYSLLFLLGLLGNGAVAAVLLSRRTALSSTDTFLLHLAVADTLLVLTLPL WAVDAAVQWVFGSGLCKVAGALFNINFYAGALLLACISFDRYLNIVHAT QLYRRGPPARVTLTCLAVWGLCLLFALPDFIFLSAHHDERLNATHCQYNF PQVGRTALRVLQLVAGFLLPLLVMAYCYAHILAVLLVSRGQRRLRAMRLV VVVVVAFALCWTPYHLVVLVDILMDLGALARNCGRESRVDVAKSVTSGL GYMHCCLNPLLYAFVGVKFRERMWMLLLRLGCPNQRGLQRQPSSSRRD SSWSETSEASYSGL
dreCxcr3.1	ENSDARG00000007358	MNVDSKTTFSMKDFSDYTDLYNYSDYNDNESYGAGAVCTQDSSMYFDSI FKPILYSLAAVVGLLGNGLVLIVLWKKRAGLNVTDIFILHLSLADILLLLTLPF WAVEAVKEWIFGTPLCKLTGAMFRINFYCGIYMLSCISLDRYLSIVHAVQ MYSRKKPMAVHCCCMIVWFFCFLLSIPDWILLGANKDSRRQDRTECVNS EALSDFWVLVNRLIYHFLGFIIPAIMMVFCYTSILLRLLLGSKCMQKKRAIH VIVALVLAFFISWTPYNIALMADTIHTNRTDNNQTSCETRTTLDVAITATST FAYMHCCVNPILYAFVGVKFRQHLLDMLRPLGFKLKGRAGLVSRKSSGW SESVDTSHTSAF
dreCxcr3.2	ENSDARG00000041041	MDNSTTAAEVSAPTDYDYNSTSYDDDNPYAAPCSLTETWNFLGRFAPVA YILVFILALVGNILVLCVIRRYRQSRHSPCSFSLTDTFLLHLAVSDLLLAATLPF FAVEWISEWVFGKVMCKITGALFSLNVYCGVLFLACISFDRYLAIVHAINIS WRRKTCHAQLACAFIWVICLGLSMVDMHFRDLVEIPGMNRMVCQIVYS EQYSKQWQIGMQLVSMVLGFILPLLVMLYCYLHIFKALCHATRRQKRRSL RLIISLVIVFVISWAPYNALRMTDSLQMLGVIVKSCALNNVLDVGILVTESL GLAHCALNPLLYGLVGVKFRRELAQMCKAALGPQGCLGLVGWANGRGS STRRPTGSFSSVETENTSYFSVMA
dreCxcr3.3 isoform 1	ENSDARG00000070669	MEVELHGLFEKNNSFDYDNYENKELDCQSKAVSDALGVFIPMLYSLGILL GLLGHGLVLAVLWHKWLNCSVMDIFIFHLSLIDSLLLLSMPLWAVDAVKG WIMGSGLCKLAGVLFKMNFYCSMLMLAFISVDCYLSIVHGVQKLSRKKP MVVHGCCLIIWLVCLLLSIPEWIFLKSISDSTDQVKDECIYFYPDDSWHRSS RFPHHVIFGVGTLVLLFCCTSIMLKLQRESMCQQKKMGRKTAIIAVLVLVF LICWTPYSIAFIVNTGARPVHIDPLTGESECEWRQWTATKITAIFGLLHCTI NPVIYFCFSKEFRRRSLAVIKFNACESNNNDGSLWDSTAVNVNTTVQEEQ GPLQQVNELKPKVQTQQQDT
dreCxcr3.3 isoform 2	ENSDARG00000070669	MAAPSNMEVELHGLFEKNNSFDYDNYENKELDCQSKAVSDALGVFIPML YSLGILLGLLGHGLVLAVLWHKWLNCSVMDIFIFHLSLIDSLLLLSMPLWA VDAVKGWIMGSGLCKLAGVLFKMNFYCSMLMLAFISVDCYLSIVHGVQK LSRKKPMVVHGCCLIIWLVCLLLSIPEWIFLKSISDSTDQVKDECIYFYPDDS WHRSSRFPHHVIFGVGTLVLLFCCTSIMLKLQRESMCQQKKMGRKTAIIA VLVLVFLICWTPYSIAFIVNTGARPVHIDPLTGESECEWRQWTATKITAIFG LLHCTINPVIYFCFSKEFRRRSLAVIKFNACESNNNDGSLWDSTAVNVNTT VQEEQGPLQQVNELKPKVQTQQQDT

Supplementary Table 2. List of chemokines and chemokine receptors used in this work with accession codes and protein sequences *(continued from the previous page)*.

Primers used in qRT-PCR reactions

Gene Name	Gene Accession	Sequence (5'-3')
cxcr3.1	ENSDARG00000007358	**Fw:** CTTTCCTGCATCAGTCTCGACC **Rv:** TGACGTCTGGAGTCCTTGTTGG
cxcr3.2	ENSDARG00000041041	**Fw:** CCTCTGTTGGTAATGCTGTATTGC **Rv:** ACACGATGACTAAGGAGATGATGAG
cxcr3.3	ENSDARG00000070669	**Fw:** GCTCTCAATGCCTCTCTGGG **Rv:** GACAGGTAGCAGTCCACACT
ppiab	ENSDARG00000042247	**Fw:** ACACTGAAACACGGAGGCAAAG **Rv:** CATCCACAACCTTCCCGAACAC
cxcl11aa	Gene ID: 798892	**Fw:** ACTCAACATGGTGAAGCCAGTGCT **Rv:** CTTCAGCGTGGCTATGACTTCCAT
cxcl11ac	Gene ID:100334604	**Fw:** TCTGACCTGCCTGATCGCTGGA **Rv:** TGCCTTTGTCAGCACAGAAGCACC
cxcl11ad	Gene ID: 567656	**Fw:** AGGCCAGGCGAGAGCTCCAA **Rv:** TCCACAAGAAGGGGTCGGTGGT
cxcl11ae	ENSDARG00000092423	**Fw:** AGGGTTGCACTGAGGAACATTGAGA **Rv:** AGCCCTCCTGATTAATTCCTGGGT
cxcl11af/ag	ENSDARG00000094706 ENSDARG00000093779	**Fw:** GCTGGAGAGGTCAACGGTCAGGA **Rv:** TGCAAGATGGACTCGGAGGGAAGA
cxcl11ah	ENSDARG00000095747	**Fw:** GAGGTGAAAGGCAAAATA **Rv:** TGCTCCTTTATCAGCACACAAACA

Primers used for amplification and sequencing of *cxc3.1*, *cxcr3.2* and *cxcr3.3*

- **Amplification of genomic DNA templates**

Gene Name		Sequence (5'-3')
cxcr3.1	Set 1	**Fw:** GTTGTAAAACGACGGCCAGTATGAATGTTGACTCAAAAACAAC **Rv:** CAGGAAACAGCTATGACCTATTATCCAAAAACATTCTTTTCCTCAC
cxcr3.1	Set 2	**Fw:** GTAAAACGACGGCCAGGGGAAACGGCTTGGTTCTGA **Rv:** CAGGAAACAGCTATGACTGTATGCATGAAACAGCAAAGAGAA
cxcr3.1	Set 3	**Fw:** GTAAAACGACGGCCAGGATTTGGAACAACCTTTTTCAGCA **Rv:** CAGGAAACAGCTATGACCTTGAAGCCCAGAGGTCGTA
cxcr3.1	Set 4	**Fw:** GTTGTAAAACGACGGCCAGTCTTCATTTGCATCTTTCTTCATCAG **Rv:** CAGGAAACAGCTATGACCTCAGAAAGCAGATGTGTGGG
cxcr3.2		**Fw:** GTAAAACGACGGCCAGGGCGCCTTATAATGCTCTGC **Rv:** CAGGAAACAGCTATGACCCATGGAAAGCTTCAGTTTTTAC
cxcr3.3	Set 1	**Fw:** GTAAAACGACGGCCAGTTCCCAGCAGATGCGTTACA **Rv:** CAGGAAACAGCTATGACGTGCGCAAGCAAACGTAAAC
cxcr3.3	Set 2	**Fw:** GTAAAACGACGGCCAGGTTCCGCCAACTGCTTTACTTT **Rv:** CAGGAAACAGCTATGACTAAACAGCGTCTTTACCAGATCCC
cxcr3.3	Set 3	**Fw:** GTAAAACGACGGCCAGGACTGCTACCTGTCCATCGTT **Rv:** CAGGAAACAGCTATGACGCTCATGTCTAAATACAGTTTGCTG

- **Amplification of cDNA templates**

Gene Name	Sequence (5'-3')
cxcr3.2	**Fw:** GTTGTAAAACGACGGCCAGTATGGACAACTCAACAACAGCCGCAG **Rv:** CAGGAAACAGCTATGACCTCAGGCCATGACAGAAAAGTACGAAGTG
cxcr3.3 isoform2 Fw	**Fw:** GTTGTAAAACGACGGCCAGTATGGCAGCACCTTCAAACATGG
cxcr3.3 isoform1 Fw	**Fw:** GTTGTAAAACGACGGCCAGTATGGAGGTAGAGCTTCACGG
cxcr3.3 common Rv	**Rv:** CAGGAAACAGCTATGACCTCATGTATCCTGCTGCTGGG

- **Primers used for sequencing**

Gene Name	Sequence (5'-3')
M13 universal Fw	**Fw:** GTAAAACGACGGCCAG
M13 universal Rv	**Rv:** CAGGAAACAGCTATGAC
Cxcr3.2 E1 cDNA Rv	Rv: CGCCAGGATAAACACCAG
Cxcr3.3 cDNA Rv	Rv: GGCAGTCCAGTTCTTTGTTC

Supplementary Table 3. List of qRT-PCR, amplification, and sequencing primers used in this work.

HYPERLINK TO SUPPLEMENTARY MOVIES

Supplementary Movies are available online at the following URL:
https://drive.google.com/open?id=0B_188Sfgn4xoUkRVNjNKdlNhSEE

REFERENCES

1 Medzhitov R, Janeway C Jr. Innate immune recognition: mechanisms and pathways. Immunol Rev. 2000 Feb;173:89-97.
2 Schiffmann E, Corcoran BA, Wahl SM. N-formylmethionyl peptides as chemoattractants for leucocytes. Proc Natl Acad Sci U S A. 1975 Mar;72(3):1059-62.
3 Ford-Hutchinson AW, Bray MA, Smith MJ. Lipoxygenase products and the polymorphonuclear leucocyte. Agents Actions. 1980 Dec;10(6):548-50.
4 Lira SA, Furtado GC. The biology of chemokines and their receptors. Immunol Res. 2012 Dec;54(1-3):111-20.
5 Sun L, Ye RD. Role of G protein-coupled receptors in inflammation. Acta Pharmacol Sin. 2012 Mar;33(3):342-50.
6 Groom JR, Luster AD. CXCR3 ligands: redundant, collaborative and antagonistic functions. Immunol Cell Biol. 2011 Feb;89(2):207-15.
7 Janatpour MJ, Hudak S, Sathe M, Sedgwick JD, McEvoy LM. Tumor necrosis factor-dependent segmental control of MIG expression by high endothelial venules in inflamed lymph nodes regulates monocyte recruitment. J Exp Med. 2001 Nov 5;194(9):1375-84.
8 Loetscher M, Gerber B, Loetscher P, Jones SA, Piali L, Clark-Lewis I, Baggiolini M, Moser B. Chemokine receptor specific for IP10 and mig: structure, function, and expression in activated T-lymphocytes. J Exp Med. 1996 Sep 1;184(3):963-9.
9 Liu L, Callahan MK, Huang D, Ransohoff RM. Chemokine receptor CXCR3: an unexpected enigma. Curr Top Dev Biol. 2005;68:149-81.
10 Zhou J, Tang PC, Qin L, Gayed PM, Li W, Skokos EA, Kyriakides TR, Pober JS, Tellides G. CXCR3-dependent accumulation and activation of perivascular macrophages is necessary for homeostatic arterial remodeling to hemodynamic stresses. J Exp Med. 2010 Aug 30;207(9):1951-66.
11 Bondar C, Araya RE, Guzman L, Rua EC, Chopita N, Chirdo FG. Role of CXCR3/CXCL10 axis in immune cell recruitment into the small intestine in celiac disease. PLoS One. 2014 Feb 20;9(2):e89068.
12 Lacotte S, Brun S, Muller S, Dumortier H. CXCR3, inflammation, and autoimmune diseases. Ann N Y Acad Sci. 2009 Sep;1173:310-7.
13 Müller M, Carter S, Hofer MJ, Campbell IL. Review: The chemokine receptor CXCR3 and its ligands CXCL9, CXCL10 and CXCL11 in neuroimmunity--a tale of conflict and conundrum. Neuropathol Appl Neurobiol. 2010 Aug;36(5):368-87.
14 Chakravarty SD, Xu J, Lu B, Gerard C, Flynn J, Chan J. The chemokine receptor CXCR3 attenuates the control of chronic Mycobacterium tuberculosis infection in BALB/c mice. J Immunol. 2007 Feb 1;178(3):1723-35.
15 Cohen SB, Maurer KJ, Egan CE, Oghumu S, Satoskar AR, Denkers EY. CXCR3-dependent $CD4^+$ T cells are required to activate inflammatory monocytes for defense against intestinal infection. PLoS Pathog. 2013;9(10):e1003706.
16 Rosas LE, Barbi J, Lu B, Fujiwara Y, Gerard C, Sanders VM, Satoskar AR. CXCR3-/- mice mount an efficient Th1 response but fail to control Leishmania major infection. Eur J Immunol. 2005 Feb;35(2):515-23.
17 Seiler P, Aichele P, Bandermann S, Hauser AE, Lu B, Gerard NP, Gerard C, Ehlers S, Mollenkopf HJ, Kaufmann SH. Early granuloma formation after aerosol Mycobacterium tuberculosis infection is regulated by neutrophils via CXCR3-signaling chemokines. Eur J Immunol. 2003 Oct;33(10):2676-86.
18 Fulton AM. The chemokine receptors CXCR4 and CXCR3 in cancer. Curr Oncol Rep. 2009 Mar;11(2):125-31.
19 Kawada K, Hosogi H, Sonoshita M, Sakashita H, Manabe T, Shimahara Y, Sakai Y, Takabayashi A, Oshima M, Taketo MM. Chemokine receptor CXCR3 promotes colon cancer metastasis to lymph nodes. Oncogene. 2007 Jul 12;26(32):4679-88.
20 Oghumu S, Varikuti S, Terrazas C, Kotov D, Nasser MW, Powell CA, Ganju RK, Satoskar AR. CXCR3 deficiency enhances tumor progression by promoting macrophage M2 polarization in a murine breast cancer model. Immunology. 2014 Sep;143(1):109-19.
21 Pan J, Burdick MD, Belperio JA, Xue YY, Gerard C, Sharma S, Dubinett SM, Strieter RM. CXCR3/CXCR3 ligand biological axis impairs RENCA tumor growth by a mechanism of immunoangiostasis. J Immunol. 2006 Feb 1;176(3):1456-64.

22 Slütter B, Pewe LL, Kaech SM, Harty JT. Lung airway-surveilling CXCR3(hi) memory CD8(+) T cells are critical for protection against influenza A virus. Immunity. 2013 Nov 14;39(5):939-48.
23 Cuenca AG, Wynn JL, Kelly-Scumpia KM, Scumpia PO, Vila L, Delano MJ, Mathews CE, Wallet SM, Reeves WH, Behrns KE, Nacionales DC, Efron PA, Kunkel SL, Moldawer LL. Critical role for CXC ligand 10/CXC receptor 3 signaling in the murine neonatal response to sepsis. Infect Immun. 2011 Jul;79(7):2746-54.
24 Kakuta Y, Okumi M, Miyagawa S, Tsutahara K, Abe T, Yazawa K, Matsunami K, Otsuka H, Takahara S, Nonomura N. Blocking of CCR5 and CXCR3 suppresses the infiltration of macrophages in acute renal allograft rejection. Transplantation. 2012 Jan 15;93(1):24-31.
25 Raz E, Mahabaleshwar H. Chemokine signaling in embryonic cell migration: a fisheye view. Development. 2009 Apr;136(8):1223-9.
26 David NB, Sapède D, Saint-Etienne L, Thisse C, Thisse B, Dambly-Chaudière C, Rosa FM, Ghysen A. Molecular basis of cell migration in the fish lateral line: role of the chemokine receptor CXCR4 and of its ligand, SDF1. Proc Natl Acad Sci U S A. 2002 Dec 10;99(25):16297-302.
27 Deng Q, Sarris M, Bennin DA, Green JM, Herbomel P, Huttenlocher A. Localized bacterial infection induces systemic activation of neutrophils through Cxcr2 signaling in zebrafish. J Leukoc Biol. 2013 May;93(5):761-9.
28 Doitsidou M, Reichman-Fried M, Stebler J, Köprunner M, Dörries J, Meyer D, Esguerra CV, Leung T, Raz E. Guidance of primordial germ cell migration by the chemokine SDF-1. Cell. 2002 Nov 27;111(5):647-59.
29 Sarris M, Masson JB, Maurin D, Van der Aa LM, Boudinot P, Lortat-Jacob H, Herbomel P. Inflammatory chemokines direct and restrict leukocyte migration within live tissues as glycan-bound gradients. Curr Biol. 2012 Dec 18;22(24):2375-82.
30 Walters KB, Green JM, Surfus JC, Yoo SK, Huttenlocher A. Live imaging of neutrophil motility in a zebrafish model of WHIM syndrome. Blood. 2010 Oct 14;116(15):2803-11.
31 Xu Q, Li R, Monte MM, Jiang Y, Nie P, Holland JW, Secombes CJ, Wang T. Sequence and expression analysis of rainbow trout CXCR2, CXCR3a and CXCR3b aids interpretation of lineage-specific conversion, loss and expansion of these receptors during vertebrate evolution. Dev Comp Immunol. 2014 Aug;45(2):201-13.
32 Aghaallaei N, Bajoghli B, Schwarz H, Schorpp M, Boehm T. Characterization of mononuclear phagocytic cells in medaka fish transgenic for a cxcr3a:gfp reporter. Proc Natl Acad Sci U S A. 2010 Oct 19;107(42):18079-84.
33 Chang MX, Sun BJ, Nie P. The first non-mammalian CXCR3 in a teleost fish: gene and expression in blood cells and central nervous system in the grass carp (Ctenopharyngodon idella). Mol Immunol. 2007 Feb;44(6):1123-34.
34 Nomiyama H, Osada N, Yoshie O. Systematic classification of vertebrate chemokines based on conserved synteny and evolutionary history. Genes Cells. 2013 Jan;18(1):1-16.
35 O'Donovan N, Galvin M, Morgan JG. Physical mapping of the CXC chemokine locus on human chromosome 4. Cytogenet Cell Genet. 1999;84(1-2):39-42.
36 Zakrzewska A, Cui C, Stockhammer OW, Benard EL, Spaink HP, Meijer AH. Macrophage-specific gene functions in Spi1-directed innate immunity. Blood. 2010 Jul 22;116(3):e1-11.
37 Cambier CJ, Takaki KK, Larson RP, Hernandez RE, Tobin DM, Urdahl KB, Cosma CL, Ramakrishnan L. Mycobacteria manipulate macrophage recruitment through coordinated use of membrane lipids. Nature. 2014 Jan 9;505(7482):218-22.
38 Clay H, Davis JM, Beery D, Huttenlocher A, Lyons SE, Ramakrishnan L. Dichotomous role of the macrophage in early Mycobacterium marinum infection of the zebrafish. Cell Host Microbe. 2007 Jul 12;2(1):29-39.
39 Davis JM, Clay H, Lewis JL, Ghori N, Herbomel P, Ramakrishnan L. Real-time visualization of mycobacterium-macrophage interactions leading to initiation of granuloma formation in zebrafish embryos. Immunity. 2002 Dec;17(6):693-702.
40 Roca FJ, Ramakrishnan L. TNF dually mediates resistance and susceptibility to mycobacteria via mitochondrial reactive oxygen species. Cell. 2013 Apr 25;153(3):521-34
41 Torraca V, Masud S, Spaink HP, Meijer AH. Macrophage-pathogen interactions in infectious diseases: new therapeutic insights from the zebrafish host model. Dis Model Mech. 2014 Jul;7(7):785-97
42 van der Vaart M, Korbee CJ, Lamers GE, Tengeler AC, Hosseini R, Haks MC, Ottenhoff TH, Spaink HP, Meijer AH. The DNA damage-regulated autophagy modulator DRAM1 links mycobacterial recognition via TLR-MYD88 to autophagic defense. Cell Host Microbe. 2014 Jun 11;15(6):753-67.
43 Cronan MR, Tobin DM. Fit for consumption: zebrafish as a model for tuberculosis. Dis Model Mech. 2014 Jul;7(7):777-84.
44 Ramakrishnan L. The zebrafish guide to tuberculosis immunity and treatment.Cold Spring Harb Symp Quant Biol. 2013;78:179-92
45 Kumar P, Henikoff S, Ng PC. Predicting the effects of coding non-synonymous variants on protein function using the SIFT algorithm. Nat Protoc. 2009;4(7):1073-81.

46 Choi Y, Sims GE, Murphy S, Miller JR, Chan AP. Predicting the functional effect of amino acid substitutions and indels. PLoS One. 2012;7(10):e46688.
47 Cui C, Benard EL, Kanwal Z, Stockhammer OW, van der Vaart M, Zakrzewska A, Spaink HP, Meijer AH. Infectious disease modeling and innate immune function in zebrafish embryos. Methods Cell Biol. 2011;105:273-308.
48 Henry KM, Loynes CA, Whyte MK, Renshaw SA. Zebrafish as a model for the study of neutrophil biology. J Leukoc Biol. 2013 Oct;94(4):633-42.
49 Lieschke GJ, Oates AC, Crowhurst MO, Ward AC, Layton JE. Morphologic and functional characterization of granulocytes and macrophages in embryonic and adult zebrafish. Blood. 2001 Nov 15;98(10):3087-96.
50 d'Alençon CA, Peña OA, Wittmann C, Gallardo VE, Jones RA, Loosli F, Liebel U, Grabher C, Allende ML. A high-throughput chemically induced inflammation assay in zebrafish. BMC Biol. 2010 Dec 22;8:151.
51 Scholten DJ, Roumen L, Wijtmans M, Verkade-Vreeker MC, Custers H, Lai M, de Hooge D, Canals M, de Esch IJ, Smit MJ, de Graaf C, Leurs R. Identification of overlapping but differential binding sites for the high-affinity CXCR3 antagonists NBI-74330 and VUF11211. Mol Pharmacol. 2014 Jan;85(1):116-26.
52 van der Aa LM, Chadzinska M, Derks W, Scheer M, Levraud JP, Boudinot P, Lidy Verburg-van Kemenade BM. Diversification of IFNγ-inducible CXCb chemokines in cyprinid fish. Dev Comp Immunol. 2012 Oct;38(2):243-53.
53 Davis JM, Ramakrishnan L. The role of the granuloma in expansion and dissemination of early tuberculous infection. Cell. 2009 Jan 9;136(1):37-49.
54 Volkman HE, Pozos TC, Zheng J, Davis JM, Rawls JF, Ramakrishnan L. Tuberculous granuloma induction via interaction of a bacterial secreted protein with host epithelium. Science. 2010 Jan 22;327(5964):466-9.
55 Kroeze KL, Boink MA, Sampat-Sardjoepersad SC, Waaijman T, Scheper RJ, Gibbs S. Autocrine regulation of re-epithelialization after wounding by chemokine receptors CCR1, CCR10, CXCR1, CXCR2, and CXCR3. J Invest Dermatol. 2012 Jan;132(1):216-25.
56 Laragione T, Brenner M, Sherry B, Gulko PS. CXCL10 and its receptor CXCR3 regulate synovial fibroblast invasion in rheumatoid arthritis. Arthritis Rheum. 2011 Nov;63(11):3274-83.
57 Majka M, Janowska-Wieczorek A, Ratajczak J, Ehrenman K, Pietrzkowski Z, Kowalska MA, Gewirtz AM, Emerson SG, Ratajczak MZ. Numerous growth factors, cytokines, and chemokines are secreted by human CD34(+) cells, myeloblasts, erythroblasts, and megakaryoblasts and regulate normal hematopoiesis in an autocrine/paracrine manner. Blood. 2001 May 15;97(10):3075-85.
58 Chensue SW. Chemokines in innate and adaptive granuloma formation. Front Immunol. 2013 Feb 25;4:43.
59 Fuller CL, Flynn JL, Reinhart TA. In situ study of abundant expression of proinflammatory chemokines and cytokines in pulmonary granulomas that develop in cynomolgus macaques experimentally infected with Mycobacterium tuberculosis. Infect Immun. 2003 Dec;71(12):7023-34.
60 Aly S, Laskay T, Mages J, Malzan A, Lang R, Ehlers S. Interferon-gamma-dependent mechanisms of mycobacteria-induced pulmonary immunopathology: the role of angiostasis and CXCR3-targeted chemokines for granuloma necrosis. J Pathol. 2007 Jul;212(3):295-305.
61 Khader SA, Rangel-Moreno J, Fountain JJ, Martino CA, Reiley WW, Pearl JE, Winslow GM, Woodland DL, Randall TD, Cooper AM. In a murine tuberculosis model, the absence of homeostatic chemokines delays granuloma formation and protective immunity. J Immunol. 2009 Dec 15;183(12):8004-14.
62 O'Boyle G, Fox CR, Walden HR, Willet JD, Mavin ER, Hine DW, Palmer JM, Barker CE, Lamb CA, Ali S, Kirby JA. Chemokine receptor CXCR3 agonist prevents human T-cell migration in a humanized model of arthritic inflammation. Proc Natl Acad Sci U S A. 2012 Mar 20;109(12):4598-603.
63 van Wanrooij EJ, de Jager SC, van Es T, de Vos P, Birch HL, Owen DA, Watson RJ, Biessen EA, Chapman GA, van Berkel TJ, Kuiper J. CXCR3 antagonist NBI-74330 attenuates atherosclerotic plaque formation in LDL receptor-deficient mice. Arterioscler Thromb Vasc Biol. 2008 Feb;28(2):251-7.
64 Bernut A, Herrmann JL, Kissa K, Dubremetz JF, Gaillard JL, Lutfalla G, Kremer L. Mycobacterium abscessus cording prevents phagocytosis and promotes abscess formation. Proc Natl Acad Sci U S A. 2014 Mar 11;111(10):E943-52.
65 Renshaw SA, Loynes CA, Trushell DM, Elworthy S, Ingham PW, Whyte MK. A transgenic zebrafish model of neutrophilic inflammation. Blood. 2006 Dec 15;108(13):3976-8.
66 Ellett F, Pase L, Hayman JW, Andrianopoulos A, Lieschke GJ. mpeg1 promoter transgenes direct macrophage-lineage expression in zebrafish. Blood. 2011 Jan 27;117(4):e49-56.
67 van der Sar AM, Abdallah AM, Sparrius M, Reinders E, Vandenbroucke-Grauls CM, Bitter W. Mycobacterium marinum strains can be divided into two distinct types based on genetic diversity and virulence. Infect Immun. 2004 Nov;72(11):6306-12.
68 van der Sar AM, Musters RJ, van Eeden FJ, Appelmelk BJ, Vandenbroucke-Grauls CM, Bitter W. Zebrafish embryos as a model host for the real time analysis of Salmonella typhimurium infections. Cell Microbiol. 2003 Sep;5(9):601-11.

69 Benard EL, van der Sar AM, Ellett F, Lieschke GJ, Spaink HP, Meijer AH. Infection of zebrafish embryos with intracellular bacterial pathogens. J Vis Exp. 2012 Mar 15;(61). pii: 3781.
70 Rougeot J, Zakrzewska A, Kanwal Z, Jansen HJ, Spaink HP, Meijer AH. RNA sequencing of FACS-sorted immune cell populations from zebrafish infection models to identify cell specific responses to intracellular pathogens. Methods Mol Biol. 2014;1197:261-74.
71 Wu S, Letchworth GJ. High efficiency transformation by electroporation of Pichia pastoris pretreated with lithium acetate and dithiothreitol. Biotechniques. 2004 Jan;36(1):152-4.
72 Meijering E, Dzyubachyk O, Smal I. Methods for cell and particle tracking. Methods Enzymol. 2012;504:183-200.
73 Stoop EJ, Schipper T, Rosendahl Huber SK, Nezhinsky AE, Verbeek FJ, Gurcha SS, Besra GS, Vandenbroucke-Grauls CM, Bitter W, van der Sar AM. Zebrafish embryo screen for mycobacterial genes involved in the initiation of granuloma formation reveals a newly identified ESX-1 component. Dis Model Mech. 2011 Jul;4(4):526-36.
74 Elks PM, Brizee S, van der Vaart M, Walmsley SR, van Eeden FJ, Renshaw SA, Meijer AH. Hypoxia inducible factor signaling modulates susceptibility to mycobacterial infection via a nitric oxide dependent mechanism. PLoS Pathog. 2013;9(12):e1003789.
75 Trotta T, Costantini S, Colonna G. Modelling of the membrane receptor CXCR3 and its complexes with CXCL9, CXCL10 and CXCL11 chemokines: putative target for new drug design. Mol Immunol. 2009 Dec;47(2-3):332-9.

Chapter 4

Disruption of chemotactic signalling primes the lysosomal function of macrophages to counteract mycobacterial parasitism

Vincenzo Torraca, Eveline in't Veld and Annemarie H. Meijer

Institute of Biology, Leiden University, The Netherlands

Manuscript in preparation

Chapter 4

Disruption of chemotactic signalling primes the lysosomal function of macrophages to counteract mycobacterial parasitism

Vincenzo Torraca, Eveline in't Veld and Annemarie H. Meijer

Institute of Biology, Leiden University, The Netherlands

Chemokine receptors and their cognate ligands are essential host factors that control leukocyte migration and inflammation. We previously described that disruption of the CXCR3-CXCL11 receptor-ligand signalling axis in zebrafish carrying a *cxcr3.2* null mutation attenuates macrophage motility and recruitment to infectious foci. Importantly, these defects in macrophage function are associated with increased resistance to *Mycobacterium marinum*, a zebrafish pathogen widely used to study tuberculosis pathogenesis and macrophage parasitism. Here we revealed by RNA deep sequencing that lysosomal genes are significantly upregulated in sorted macrophages from the *cxcr3.2* mutant. *In vivo* assays subsequently showed increased lysosomal content, augmented acidification of phagosomes containing bacteria, and increased microbicidal capacity in *cxcr3.2* mutants. Tracking of macrophage lysosomes *in vivo* revealed that these organelles mostly localise at the leading edge of motile cells. We show that maintenance of polarised lysosomes during cell migration requires a functional *cxcr3.2* gene, suggesting that Cxcr3.2-dependent signalling affects lysosomal content by sustaining lysosomal exocytosis. Strikingly, macrophages respond to *M. marinum* infection by upregulation of Cxcl11aa, the cognate ligand of Cxcr3.2, in a Myd88/Nfκb dependent manner. This suggests that mycobacteria take advantage of the Myd88-immune signalling to sustain *cxcl11aa* expression, manipulate the Cxcr3.2 pathway and ultimately control the lysosomal content of the parasitised cell. Taken together, these data reveal a molecular pathway that links macrophage chemotaxis to lysosomal function. In the absence of this pathway, macrophages are primed for antimicrobial defence by enhanced lysosomal gene expression and microbicidal capacity. In turn, exploitation of this circuit by intracellular parasites could lead to a more permissive replicative niche where the infection is initiated.

GRAPHICAL ABSTRACT

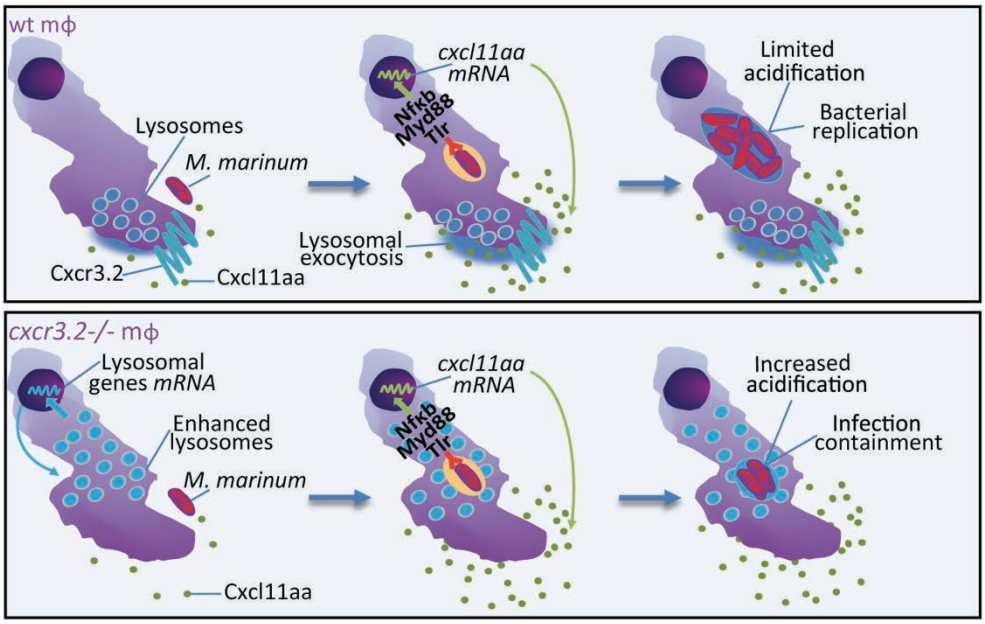

Chemokine signalling via Cxcr3.2-Cxcl11aa controls the distribution of lysosomes in macrophages and regulates coordinated transcription of lysosomal genes. Cxcr3.2 signalling maintains cell polarisation and localisation of lysosomes to the leading edge of the cell, where lysosome exocytosis is thought to facilitate cell migration. Deficiency of *cxcr3.2* reduces random migration as well as lysosome polarisation and results in upregulation of lysosomal genes. As a consequence, *cxcr3.2* mutants have a better capability to counteract bacterial replication, due to their enhanced lysosomal function. *Mycobacterium marinum* can induce high upregulation of *cxcl11aa* in infected macrophages via TLR/Myd88-mediated recognition. Exploitation of this autocrine system could benefit the pathogen as it triggers the chemokine/lysosome circuit which would further suppress lysosomal function and generate a more permissive environment for bacterial replication.

INTRODUCTION

Chemokines are a class of endogenous peptides with chemoattractive properties, produced at sites of infection and inflammation to induce the recruitment of leukocytes[1]. These motogenic mediators can control both random and directional motility, also known as chemokinesis and chemotaxis, respectively[2]. Activation of chemokine receptors transduces a complex cascade of signals that results in cell polarisation[3], characterised by an asymmetrical shape of the cell body and by an unequal distribution of the cytosolic contents, including organelles such as mitochondria and lysosomes[4,5]. To efficiently migrate into inflamed tissues, macrophages must acquire and maintain these spatial and functional asymmetries, and therefore expression of chemokine receptors on their plasma membrane is critical for their function.

In both mammalian and teleost species, macrophages express the CXC-motif chemokine receptor CXCR3[6,7], which, via its cognate ligands CXCL9-10-11, has been shown to exert remarkably pleiotropic functions on these cells. These activities not only include a direct control of macrophage trafficking to localised infectious/inflamed foci[8,9,10,11] but also their capability to activate differential functional programs in response to microenvironmental signals. This is well exemplified, for instance, by the impairment of macrophage-mediated vascular remodelling[12], the skewing of M1/M2 differentiation[13] and the increased clearance of pathological protein aggregates[14] or steatotic lipid inclusions[15] in CXCR3-deficient conditions.

Despite that much effort has been made to elucidate the sequence of events activated by the transduction of chemokine signals, we are only beginning to understand the transcriptional and subcellular effects of the chemokine-mediated cell polarisation and the implications of these effects on the immune function of leukocytes. Additionally, our current understanding of chemokine responses derives mostly from studies performed *in vitro*. Here we used the zebrafish model and RNA-sequencing analysis of sorted macrophages to elucidate the downstream targets affected by chemokine signalling *in vivo*. Using the mutant line of the chemokine receptor *cxcr3.2* (a functional homologue of the mammalian CXCR3), we show that the disruption of CXCR3-CXCL11 signalling results in transcriptional upregulation of lysosomal genes and primes the microbicidal function of macrophages. This transcriptional signature is linked with reduced macrophage motility in *cxcr3.2* mutants and attenuated susceptibility to the fish and macrophage pathogen *Mycobacterium marinum* (*Mm*)[10].

Our findings provide a novel addition to the current understanding of the leukocyte chemotactic process, since it was recently shown that lysosome delivery to the leading edge of motile cells and their local exocytosis is critical to permit chemotactic migration and to fuel lipid endomembranes to the lamellipodium. Strikingly, we found that mycobacterial immune recognition by Myd88-dependent signalling can induce large autocrine induction of Cxcl11aa, the cognate ligand of Cxcr3.2. Therefore, this immune recognition/chemokine/lysosome circuit might represent an unexpected macrophage-autonomous mechanism of pathogen virulence. Mycobacterial parasitism may exploit the chemokine signalling to dissipate lysosomal function and maintain a macrophage phenotype that is more permissive for the establishment of the infection.

RESULTS

Macrophage chemotactic signalling controls lysosomal function

To identify genes and pathways affected by chemoattractant-induced chemotaxis, we used a zebrafish *cxcr3.2* null model which displays attenuated macrophage motility and aberrant macrophage recruitment to infection foci (**Figure 1**)[10]. By deep-sequencing analysis of FACS-sorted *cxcr3.2* mutant and wildtype (wt) *mpeg1:mCherry-F*-positive macrophages, we found 699 significantly regulated genes. Using gene enrichment analysis tools we classified the regulated genes according to the affected pathways, cellular components, molecular functions and biological processes (**Table 1-2**). These functional analyses suggested alterations in lysosome biogenesis/maturation, Golgi-to-lysosome vesicular trafficking and lysosomal maintenance. Classification of gene products according to their cellular localisation also revealed that lysosome- and Golgi-related genes are mostly upregulated in the *cxcr3.2* mutants (**Figure 2**). Taken together, these data suggest that a coordinated induction of lysosomal genes takes place in *cxcr3.2* mutant macrophages and that Cxcr3.2 signalling exerts a negative transcriptional control on lysosomal biogenesis and function.

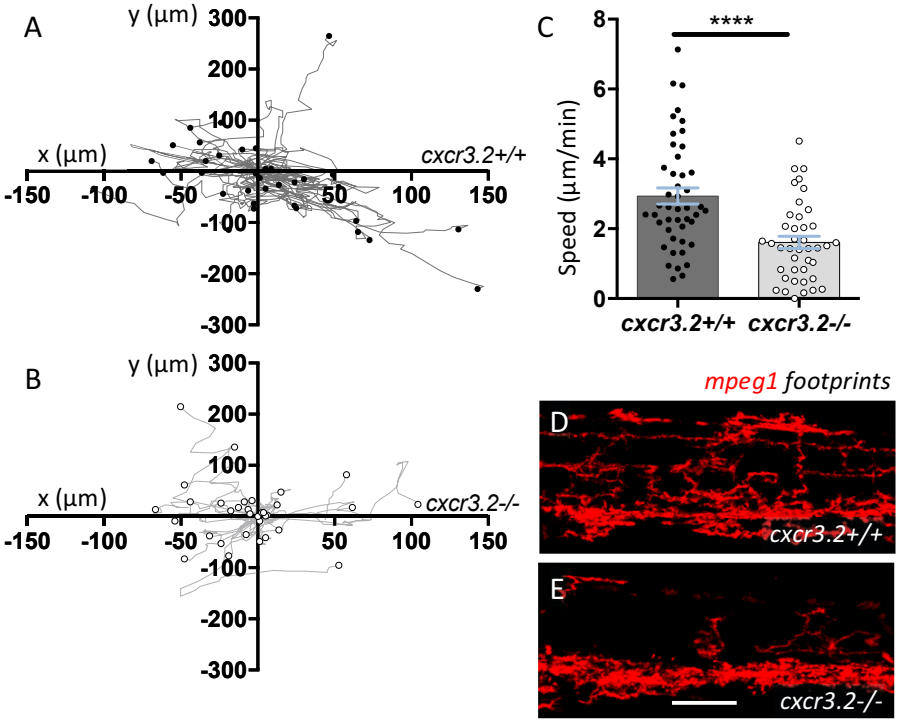

Figure 1. *cxcr3.2* mutation affects macrophage basal motility. A-B. XY plot of *cxcr3.2*$^{+/+}$ and *cxcr3.2*$^{-/-}$ macrophage tracks; **C.** Average speed of wt and mutant macrophage movement; **D-E.** Representative macrophage footprints in a wt and a mutant embryo during the time of observation Mutant and wt siblings expressing *Tg(mpeg1:mCherry-F)* were imaged at 2 dpf in the trunk area (1 h track, 1 frame/2 min, 63x objective). Scale bar: 100 µm. Data derive from 2 cumulated experiments, run with 3 mutants and 3 wt each.

KEGG-pathways

Term	Count	P-Value	Fisher Exact	Fold Enrichment
Endocytosis	17	4,5E-03	1,9E-03	2,2
Lysosome	13	3,6E-03	1,3E-03	2,6
Neurotrophin signalling pathway	13	5,8E-03	2,1E-03	2,5
Tight junction	12	2,6E-02	1,1E-02	2,1
PPAR signalling pathway	12	1,3E-04	2,6E-05	4,1
Leukocyte transendothelial migration	12	1,1E-02	4,0E-03	2,4
Antigen processing and presentation	10	7,9E-03	2,5E-03	2,8
Adipocytokine signalling pathway	10	1,8E-03	4,6E-04	3,5

GO:Cellular components

Term	Count	P-Value	Fisher Exact	Fold Enrichment
Cell				
Perinuclear region of cytoplasm	24	4,00E-04	1,60E-04	2,3
Vacuole	20	2,40E-03	1,00E-03	2,2
Lysosome	17	4,90E-03	2,00E-03	2,2
Pigment granule	13	9,40E-05	2,10E-05	4
Coated vesicle	12	3,20E-02	1,40E-02	2,1
Membrane				
Basolateral plasma membrane	17	3,30E-03	1,40E-03	2,3
Membrane raft	12	1,60E-02	6,50E-03	2,3
Organelle outer membrane	13	4,20E-04	1,10E-04	3,4
Cytoplasmic vesicle membrane	12	1,30E-02	5,20E-03	2,3

GO:Molecular functions

Term	Count	P-Value	Fisher Exact	Fold Enrichment
Transporter activity				
Inorganic cation TMT activity	15	1,6E-03	5,6E-04	2,6
Monovalent inorganic TMT activity	12	1,8E-03	5,2E-04	3,1
Hydrogen ion TMT activity	10	6,5E-03	2,0E-03	3
Anion TMT activity	13	9,3E-03	3,6E-03	2,4
Primary active TMT activity	10	4,0E-02	1,7E-02	2,2
P-P-bond-hydrolysis-driven TMT activity	10	4,0E-02	1,7E-02	2,2
Protein binding				
Protein complex binding	16	7,0E-03	3,0E-03	2,2
Unfolded protein binding	15	1,0E-04	2,6E-05	3,5
Heat shock protein binding	10	1,7E-03	4,3E-04	3,6
Transcription corepressor activity	12	2,1E-02	8,5E-03	2,2
Cysteine-type peptidase activity	11	4,0E-02	1,7E-02	2,1

Table 1. KEGG-pathways, cellular components and molecular functions affected in *cxcr3.2* mutants. Terms related to lysosomes are marked in grey. See Materials and Methods for more details. TMT: transmembrane transporter.

GO:Biological processes

Term	Count	P-Value	Fisher Exact	Fold Enrichment
Biological regulation				
Regulation of cell death	66	5,0E-09	2,2E-09	2,2
Response to organic substance	61	4,3E-09	1,8E-09	2,3
Negative regulation of molecular function	28	1,5E-04	6,2E-05	2,2
Small GTPase mediated signal transduction	25	5,1E-04	2,2E-04	2,2
Negative regulation of catalytic activity	23	7,6E-04	3,2E-04	2,2
Regulation of binding	18	6,0E-05	1,7E-05	3,1
Response to bacterium	18	9,6E-04	3,5E-04	2,5
Regulation of cell motion	16	6,1E-03	2,5E-03	2,2
Regulation of transcription factor activity	14	1,2E-04	3,0E-05	3,6
Regulation of I-kappaB kinase/NF-kappaB cascade	13	6,6E-04	1,8E-04	3,2
Response to oxidative stress	13	2,1E-02	8,9E-03	2,1
Negative regulation of protein modification process	12	5,1E-03	1,7E-03	2,7
Regulation of immune effector process	11	4,5E-03	1,4E-03	2,9
Negative regulation of response to stimulus	11	4,2E-03	1,3E-03	2,9
Innate immune response	11	3,5E-02	1,5E-02	2,1
Detection of stimulus	10	3,3E-02	1,3E-02	2,3
Cellular process				
Cell death	56	3,4E-07	1,5E-07	2,1
Membrane organisation	32	4,3E-05	1,8E-05	2,2
Mitochondrion organisation	14	2,0E-03	6,8E-04	2,7
Histone modification	10	4,0E-02	1,7E-02	2,2
Protein folding	19	1,2E-04	3,7E-05	2,9
Regulation of translation	11	3,3E-02	1,4E-02	2,1
Localisation				
Intracellular transport	51	1,4E-06	6,4E-07	2,1
Protein targeting	17	7,1E-03	3,1E-03	2,1
Golgi vesicle transport	14	1,3E-03	4,0E-04	2,8
Nucleocytoplasmic transport	14	5,8E-03	2,2E-03	2,4
Organic acid transport	12	2,3E-02	9,9E-03	2,2
Protein localisation in organelle	13	8,8E-03	3,4E-03	2,4
Protein import	12	1,0E-02	3,8E-03	2,4
Metabolic process				
Monosaccharide metabolic process	18	4,2E-03	1,8E-03	2,2
Carbohydrate catabolic process	14	2,2E-04	5,6E-05	3,4
Purine ribonucleotide metabolic process	11	3,5E-02	1,5E-02	2,1

Table 2. Biological processes affected in *cxcr3.2* mutants. Terms related to lysosomes are marked in grey. See Materials and Methods for more details.

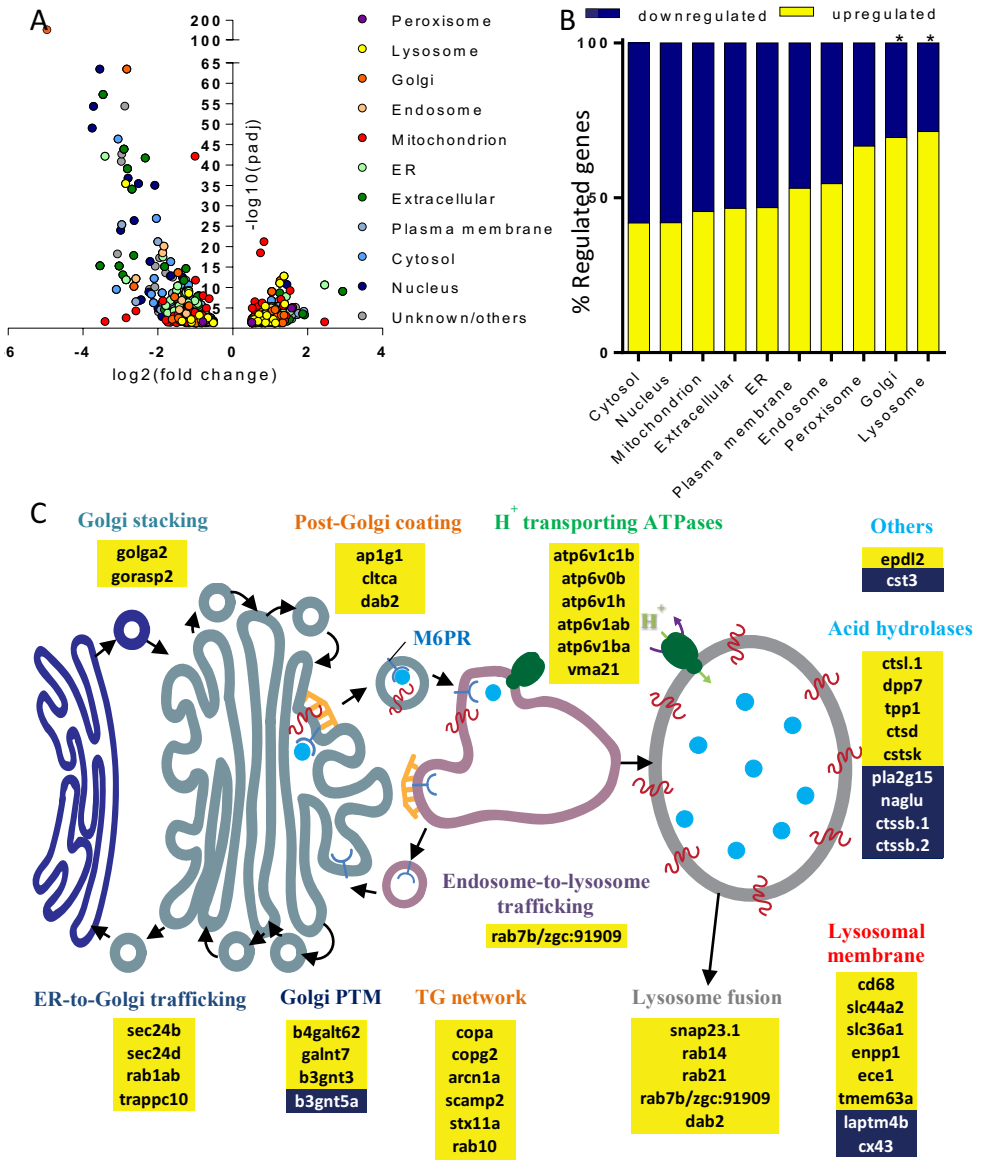

Figure 2. Graphical representation of enrichment analysis. **A.** Volcano plot representing the dispersion of the regulated genes. To note, while *cxcr3.2* mutation generally seems to affect target genes by downregulation (negative log2(fold change)), lysosomal genes are mostly affected towards upregulation (yellow). **B.** % upregulated (yellow) and downregulated (blue) genes classified by compartment. Chi-squared test analysis (with Bonferroni *post-hoc* correction for False Discovery Rate) shows that lysosome- and Golgi-related genes are significantly coordinated towards upregulation and diverge from the general trend of the other regulated genes. To note, not necessarily genes were univocally assigned to one single compartment. **C.** Functional classification of key Golgi- and lysosome-related genes affected by *cxcr3.2* deficiency. Gene names in yellow boxes indicate upregulated genes, while gene names in blue boxes indicate downregulated genes. ER: Endoplasmic reticulum; PTM: post translational modification; TG: trans-Golgi; M6PR: mannose-6-phosphate receptor.

Deficiency in *cxcr3.2* signalling affects intra-macrophage replication of mycobacteria

To quantify the lysosomal content of *cxcr3.2*$^{-/-}$ and *cxcr3.2*$^{+/+}$ macrophages, we stained lysosomes using LysoTracker, which is permeable in zebrafish larvae by bath exposure[16]. Notably, macrophages in *cxcr3.2* mutant embryos displayed an increased staining when compared to wt (**Figure 3A**). To determine whether the lysosomal function is dysregulated in *cxcr3.2* mutant macrophages, we injected pH-rodo labelled *E. coli* bioparticles and quantified phagosome acidification *in vivo*. In *cxcr3.2*-deficient embryos, the level of acidification at 30-45 minutes post injection (mpi) was significantly increased (~2 fold), indicating that lysosomes are still functional and that phagolysosome maturation is increased by *cxcr3.2* deficiency (**Figure 3B-D**). Therefore, both RNA-sequencing analysis and functional *in vivo* assays suggested an increased lysosomal function.

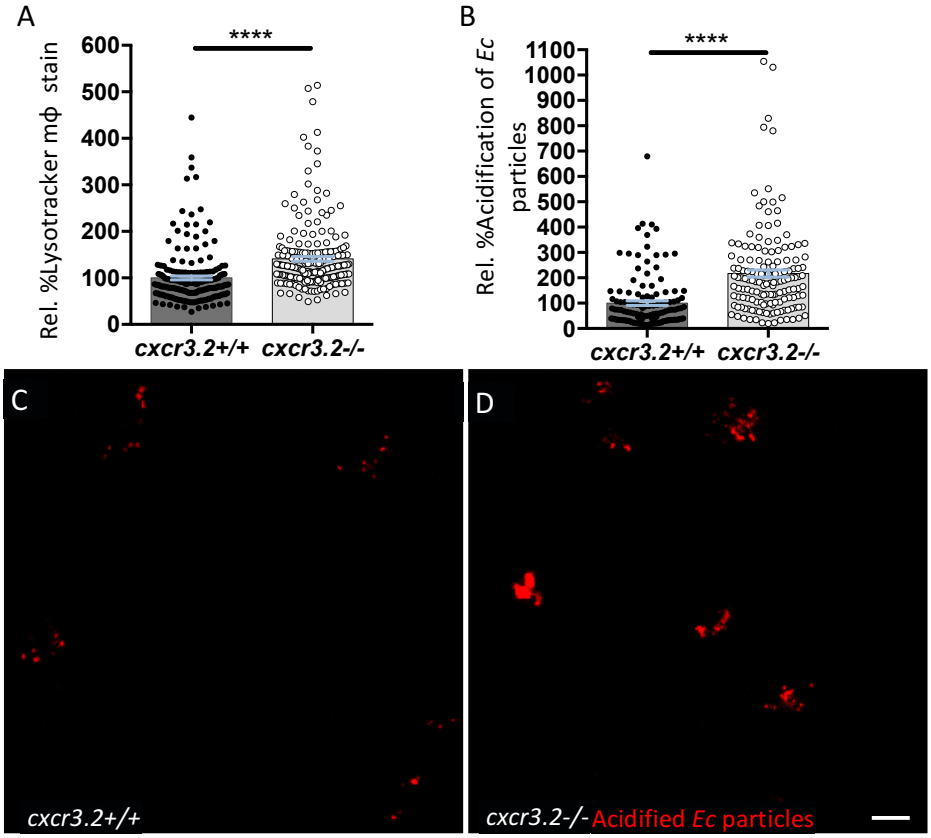

Figure 3. cxcr3.2 mutant macrophages display augmented lysosomal function and phagolysosome maturation. A. % (relative to wt) of LysoTracker intensity staining overlapping with the macrophage (mΦ)-specific *mpeg1:mCherry-F* transgene in 2 dpf mutant and wt siblings. Data derive from >12 individuals per group. Each data point represents a single *mpeg1:mCherry-F* cluster. 1 representative of 2 similar replicates. **B.** % (relative to wt) of pH-rodo intensity of *E. coli* bioparticle clusters at 30-45 mpi. Mean intensity was calculated per *E. coli* bioparticle cluster. Data derive from 12 individuals per group injected in experimental groups of 3-4 mutants and 3-4 wt. 1 representative of 2 similar replicates. **C-D.** Representative images of the yolk valley of a wt and mutant embryo at 30 minutes post *E. coli* bioparticle injection (63x objective). Scale bar: 10 µm.

To evaluate whether the enhanced lysosomal functionality results in better infection control, we investigated the capability of *cxcr3.2* mutant macrophages to counteract initial infection with the intra-macrophage bacterial parasite *M. marinum* strain M (*Mm*M), a wt isolate of the natural fish pathogen, which represents an established paradigm to study human mycobacterial diseases, such as tuberculosis and leprosy[17,18,19,20]. As expected, the acidification of *Mm*M (24-28 hours post infection, hpi) was increased in *cxcr3.2* mutants (**Figure 4A**). To assess the basal intracellular killing ability of macrophages in wt and *cxcr3.2* mutant embryos, we injected *MmΔerp* bacteria[21,22,23] and scored the capability of macrophage to contain the infection at 44 hpi. Consistent with previous acidification results, we found the intracellular killing of *MmΔerp* to be significantly increased in *cxcr3.2* mutants (**Figure 4B-C**).

We have previously shown that *cxcr3.2* mutants display deficient macrophage-dependent mycobacterial dissemination and a reduced expansion rate of granuloma-like structures, which was attributed to the reduced macrophage trafficking within the granulomatous lesions[10]. However, the assays used here are performed at an initial infection stage that precedes the granulomatous phase. Furthermore, *MmΔerp* stain fails to induce macrophage aggregation[21]. Additionally, since bacteria are systemically delivered, the direct implication of macrophage recruitment at this stage is unlikely, as all bacteria are readily available to circulating macrophages and are rapidly phagocytosed. Of note, the level of intracellular bacteria at 30 mpi (*Mm*M) and the number of established intra-macrophage infectious niches at 44 hpi (*MmΔerp*) were found similar in *cxcr3.2* mutants and wt (**Figure 4D-E**), suggesting no difference in the level of initial phagocytosis and mycobacteria multiplicity per macrophage but only in their intramacrophage replication/killing rate. Taken together, these data show that *cxcr3.2* mutation, by increasing the lysosomal functionality, exerts a bacteriostatic function and antagonises intra-macrophage bacterial replication.

Cxcr3.2 controls macrophage polarity and lysosome localisation to the leading edge

Previous *in vitro* studies linked CXCR3 signalling to lysosomal function. Stimulation of chemokine-dependent motility affected localisation of lysosomes into the cell and mediated their calcium-dependent fusion to the plasma membrane, a mechanism also known as lysosome exocytosis[5]. Despite that LysoTracker staining could not be trusted to quantify the occurrence of exocytosis in terms of signal decrease during cell migration (due to high frequency of image acquisition and high laser intensity, provoking bleaching) we could use this vital staining to determine whether macrophages displayed asymmetrical lysosome distribution during cell migration *in vivo*. Strikingly, we could establish that in wt macrophages, lysosomes are significantly localised to the leading edge of the moving cell, while their position remained central or non-correlated in non-moving macrophages (**Figure 5**, **Supplementary Movie 1-2**). In contrast, in *cxcr3.2*-deficient embryos, the lysosomal content of macrophages did not correlate with the movement of the cell. These observations strongly suggest that a *cxcr3.2*-dependent signalling is required to maintain lysosomal recruitment to the leading edge and anterior-posterior macrophage asymmetry.

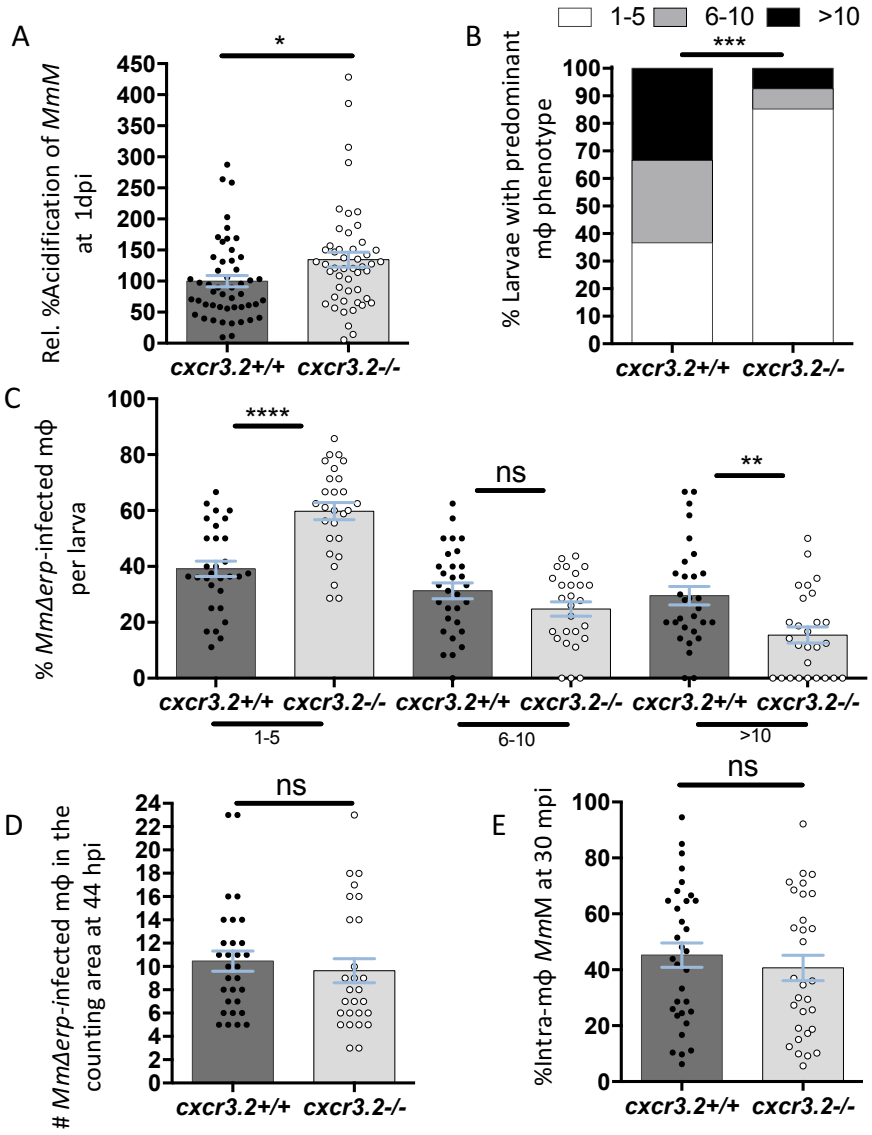

Figure 4. *cxcr3.2* mutant macrophages counteract more efficiently initial mycobacterial replication. A. % (relative to wt) of LysoTracker intensity staining of *Mm*M in mutant and wt at 1dpi. Data derive from >22 mutant or wt embryos per group per replicate. Each data point represents a single embryo. The graph is cumulative of 2 experiments. **B-D.** Intracellular replication of *MmΔerp.* At 44 hpi intra-macrophage sites of bacterial growth were classified into three categories according to the number of bacteria (1-5, 6-10 or >10). In B, larvae were classified according to the predominant macrophage phenotype. C represents the % of macrophages per larva in each class. D represents the number of intra-macrophage *MmΔerp* sites at 44hpi. B-D are cumulative of 2 experiments performed each with >10 individuals per group. **E.** Phagocytosis of *Mm*M at 30 mpi in mutant and wt.

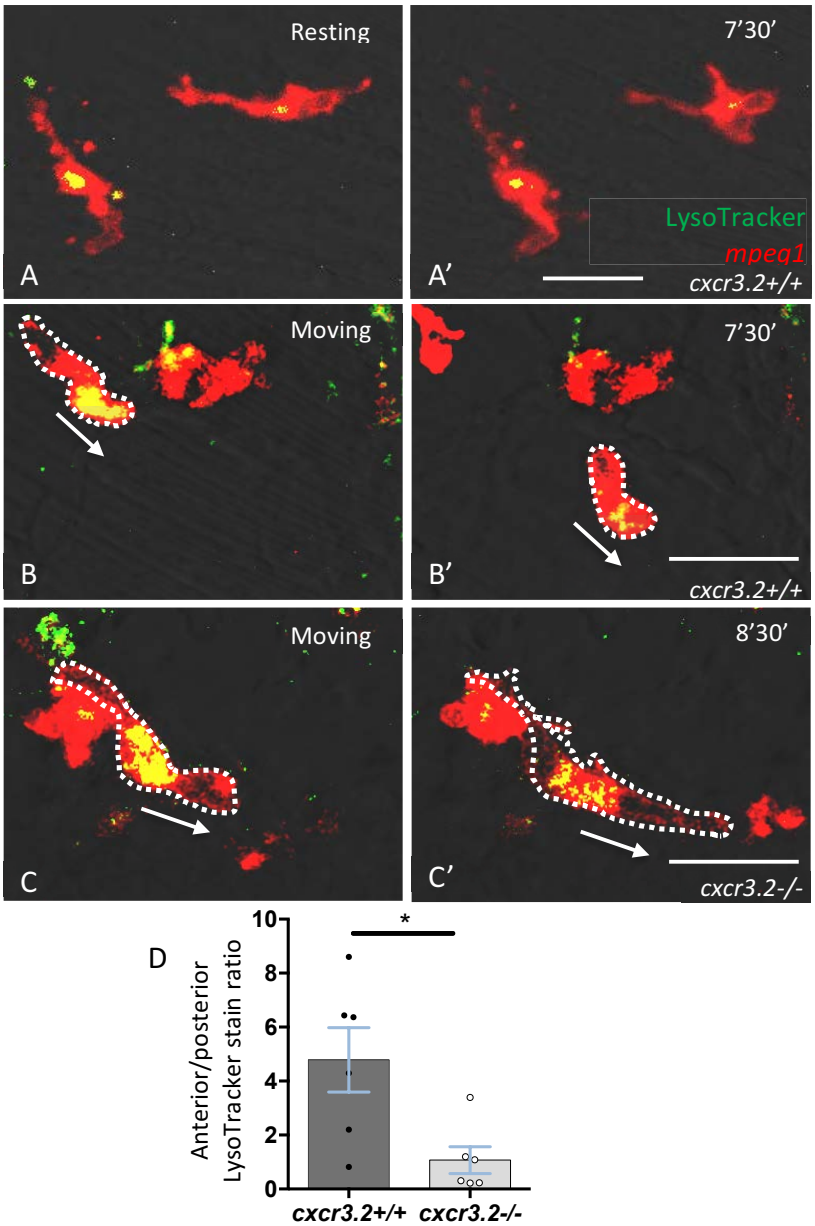

Figure 5. *cxcr3.2* controls localisation of lysosomes to the leading edge of moving macrophages. **A-A'.** Immotile wt macrophages with central LysoTracker staining. **B-B'.** Moving wt macrophage with LysoTracker staining highly committed to the lamellipodium. **C-C'.** Moving mutant macrophage with LysoTracker staining not associated with the leading edge. **D.** Ratio of LysoTracker staining between the anterior and posterior half of moving macrophages in wt and mutant Each data point indicates a single tracked cell from an independent embryo (N: 6 cells/group). Images were acquired at 2 dpf (40x objective rate < 1 photogram/30 sec) and the time interval between images from the same cell is indicated. See also **Supplementary Movie 1-2**. Scale bars: 20 µm.

Infected macrophages express Cxcl11aa via Myd88-dependent immune recognition

We previously demonstrated that *cxcl11aa* is highly upregulated during mycobacterial infection[10]. To determine the source of Cxcl11aa, we FACS-sorted *mpeg1:mCherry-F* positive macrophages from *Mm* infected and mock-injected larvae and quantified the level of *cxcl11aa* expression in the fluorescent (macrophages) and unlabelled (negative) cell fraction. In uninfected conditions, the expression of *cxcl11aa* was significantly enriched in the macrophage cell fraction (**Figure 6A**). This finding is in agreement with the function of Cxcr3.2 in the maintenance of the basal macrophage patrolling, which is most likely exerted via a chemokinetic autocrine/paracrine mechanism[10]. Additionally, during infection, macrophages significantly upregulated the expression levels of *cxcl11aa* (**Figure 6A**).

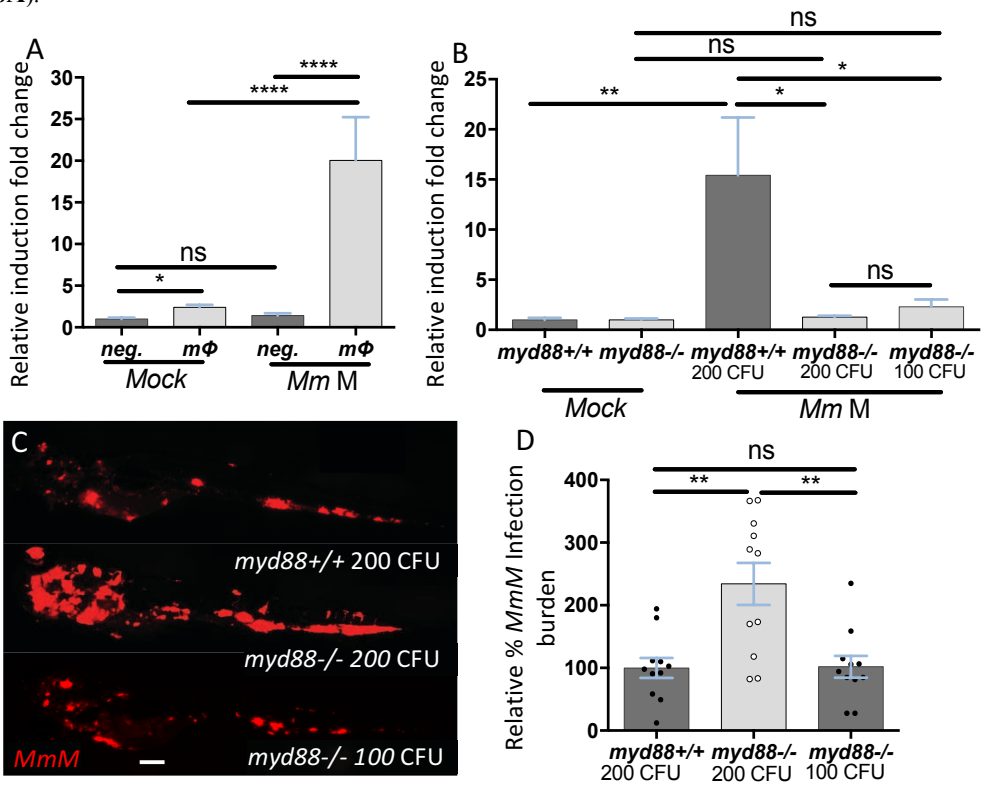

Figure 6. *cxcl11aa* expression is upregulated in macrophages upon infection and requires an active Myd88-immune signalling. A. Expression of *cxcl11aa* in *Tg(mpeg1:mCherry-F)* sorted cells and its infection-dependent induction (relative to negative/mock fraction). *Mm*M- (or mock-) injected larvae (>100 per replicate per condition) were dissociated at 5 dpi. Results are cumulative of two independent experiments each run by collecting 4 samples per condition. **B-D.** Dependency of *cxcl11aa* induction from *myd88*. qRT-PCR samples (B), representative burden pictures (C) and representative burden analysis (D) derive from larvae collected at 4 dpi. Results in B (folds relative to mock) are cumulative of two independent experiments each run by collecting 3 samples (pools of >10 individuals) per condition. Each point in D represents 1 infected larva from a representative pool. Scale bar: 200 µm.

Notably, this did not require the bacterial locus RD1 (Region of Difference 1), a pathogenicity locus encompassing the secretion system of ESAT-6 (Early Secreted Antigenic Target 6 kDa), which is associated with mycobacterial virulence and formation of tubercular granulomas[24] (**Supplementary Figure 1**).

Next, we asked whether *cxcl11aa* induction requires the central immune mediator Myd88, which links pathogen recognition by Toll-like receptors to activation of the transcription factor Nfκb[25]. Therefore, we quantified the expression levels of Cxcl11aa in *myd88* deficient larvae. Since *myd88* mutants display an increased infection level when infected with the same initial infection load as wt siblings[25], we compensated this with a reduced inoculum, to obtain a similar infection level at 4 days post infection (**Figure 6B-D**). Both with the reduced and the regular inoculums, *myd88* mutants displayed a marked incapability to upregulate *cxcl11aa*, indicating that transduction of an active Myd88/Nfκb signalling is key to upregulate macrophage production of Cxcl11aa (**Figure 6B)**. In agreement with this, we observed that Nfκb activation is also required to maintain the random patrolling of macrophages under uninfected conditions, suggesting that Myd88/Nfkb signalling is required for both induction and constitutive expression of *cxcl11aa* (**Supplementary Figure 2**).

Based on our results, we propose a novel mechanism by which mycobacteria recognition can trigger acquisition of a permissive (lysosome-low) macrophage phenotype. Intracellular infection leads to immune recognition via Myd88. This, in turn, leads to induction of *cxcl1aa* and autocrine activation of its cognate chemokine receptor Cxcr3.2. Since in the absence of the Cxcr3.2-mediated pathway transcription of lysosomal genes is enhanced, wt activation of Cxcr3.2 signalling might contribute to attenuate the lysosome function and facilitate their exocytosis by controlling their recruitment to the leading edge. These effects would dissipate the innate capability of macrophages to counteract infection via lysosomal acidification and, therefore, increase the chances of successful establishment of an intracellular replication niche.

DISCUSSION

Lysosomes have long been known as cellular organelles that are principally involved in degradation and recycling of senescent/damaged cellular parts and undesired cytosolic contents, such as unfolded proteins and invading microbes. However, much broader functions for lysosomes are recently emerging. Not only have lysosomes been shown to function as signalling centres that control cellular adaptation to environmental cues, but lysosomes have also been shown to play a critical role in cell migration. Here we report a novel link between chemotactic signalling and transcriptional regulation of lysosomal function. Our study of a zebrafish mutant in the orthologue of chemokine receptor CXCR3 demonstrates that upregulation of lysosomal gene expression due to suppressed CXCR3-dependent motility can prime macrophages to better control intracellular infection. Furthermore, we show that mycobacterial parasitism activates this chemokine signalling cell-autonomously in the host macrophages, which suggests that intracellular mycobacterial colonisation, by exploiting CXCL11-CXCR3 signalling, might attenuate the lysosomal function and facilitate the establishment of parasitosis.

CXCR3 is best known for its expression by T cells, but evidence that this receptor is crucial to control the function of monocyte/macrophage lineages (including tissue

macrophages[8,9], perivascular macrophages[12], tumour associated macrophages[13], microglial[14], Kupffer[15] and dendritic cells[26,27]) continue to emerge, with a range of implications spanning from chemotaxis to cell homoeostatic maintenance and regulation of gene expression. Notably, expression of CXCR3 orthologues by the myelomonocytic lineages (and its chemotactic properties towards CXCL9-10-11 cues) is conserved among vertebrates, from fish to mammals[6,7,8,9,10,12,28,29,30]. We previously described that macrophage motility and recruitment to infectious foci is attenuated in zebrafish carrying a null mutation in *cxcr3.2*, the orthologue of mammalian *CXCR3*. Furthermore, we found this mutation to be associated with increased resistance to tuberculosis caused by *Mm* infection. Here, by analysing the transcriptional signature dependent on Cxcr3.2, we found that the presence of this receptor on macrophages affects the transcriptional control of lysosomal genes. Failure to execute the Cxcr3.2-dependent pathway in null mutants led to a transcriptional reprogramming of macrophages, characterised by a predominant upregulation of genes involved in Golgi and lysosomal vesicle trafficking as well as various lysosomal genes, including proton-transporting ATPases and endopeptidases, for example cathepsin L. By functional *in vivo* assays we subsequently demonstrated that mutation of *cxcr3.2* also prevents lysosome polarisation during macrophage migration, and, as a consequence of the upregulation of lysosomal genes, *cxcr3.2*-deficient macrophages display an increased lysosomal content, an increased acidification rate of bacteria-containing compartments and enhanced *Mm* killing.

The link between lysosomal function and chemotaxis has only recently emerged. Chemotactic signals, by stimulating an increase in cytosolic calcium, enable migration of lysosomes to the leading edge of moving cells[5]. At the leading edge, high levels of cytosolic calcium mediate formation of SNARE complexes by modulating the activity of proteins of the synaptotagmin family, including SYT7 and SYTL5. Synaptotagmins, together with specific RABs, permit docking and fusion of lysosomes to the plasma membrane (lysosomal exocytosis). This process is thought to facilitate cell migration by providing a source of phospholipid bilayer and by promoting the release of the uropod (trailing edge). Lysosome exocytosis has also been reported to occur for plasma membrane repair and for various secretion processes, for example by cytotoxic T-cells and mast cells[31,32]. Notably, apart from chemotactic triggers, lysosomal exocytosis has been described during several intracellular infections, including of mycobacterial nature[33].

In agreement with the *in vitro* evidence for the role of lysosomes in sustaining chemotaxis, our *in vivo* results demonstrate that Cxcr3.2-dependent signalling controls localisation of lysosomes in the moving cell at the leading edge, the site where they eventually exocytose. Our study additionally revealed that reduced transduction of chemokine signals can affect lysosomal maintenance also at transcriptional level, since depletion of *cxcr3.2* led to upregulation of lysosomal gene expression. The existence of a concerted transcriptional basis that controls lysosomal homoeostasis is consistent with recent reports[34]. The master transcription factor EB (TFEB) was reported to control the Coordinated Lysosomal Expression and Regulation (CLEAR) gene network[35]. Under aberrant lysosomal storage conditions, or when lysosomes are under stress (for example during the response to infections), TFEB dissociates from the lysosome surface and translocates to the nucleus where it promotes direct transcription of lysosomal genes. We suspect that reduced trafficking of lysosomes, as a consequence of abolished basal motility in *cxcr3.2* mutants, may be sensed as a stressor and lead to activation of the CLEAR response, which in turn will increase intracellular lysosome content and thereby prime Cxcr3.2-deficient

macrophages to better withstand infection. In line with this hypothesis, it has been reported that TFEB and the CLEAR-network are activated to increase the pool of lysosomes in the proximity of the plasma membrane and to promote their exocytosis[36]. Interestingly, this mechanism is mediated by raising intracellular Ca^{2+} levels through the activation of lysosomal Ca^{2+} channels, differently from chemokine-based Ca^{2+} fluxes, which mostly derive from IP3-dependendent modulation of endoplasmic reticulum storage. This may suggest that the CLEAR response in the chemotactic-deficient conditions of *cxcr3.2* mutants attempts to restore normal lysosome trafficking by stimulating the alternative mobilisation of Ca^{2+} from lysosomal storage. Notably, the CLEAR network appears to be involved in the regulation of additional lysosome-associated processes, including autophagy, exo/endocytosis, melanogenesis, phagocytosis, and immune response, as well as in several non-lysosomal responses, such as expression of digestive enzymes, genes related to sugar metabolism, MAPK signalling, adipocytokine signalling pathway, chemokine signalling etc[37]. This might in part explain why several of these CLEAR-related pathways appear regulated also in our study (**Table 1-2**).

Multiple genetic diseases, including lysosomal storage disorders such as Gaucher's, Niemann-Pick's disease and Tay-Sachs syndrome, are associated with impaired lysosomal function and increased susceptibility to infections[38,39,40]. Knockdown of the zebrafish orthologues of three genes linked to lysosomal storage disorders in man (*glucocerebrosidase 1*, *hexosaminidase A*, and *arylsulfatase A*) was recently found to result in hypersusceptibility to tuberculosis[41]. Similarly, knockdown of the gene for cathepsin L and mutation of a transcriptional coregulator, Snapc1b, which regulates cathepsin L, caused tuberculosis hypersusceptibility in the zebrafish model[41]. All these genetic deficiencies are associated with an inability of macrophages to contain the mycobacterial infection due to a severe migration defect that results from the progressive accumulation of cellular debris in lysosomes[41]. A comparable defect is found in zebrafish mutants in components of Rag-regulator complex, which is part of the CLEAR network[42]. In these mutants, microglial cells (the resident macrophages of the brain) are unable to digest apoptotic neurons despite an expanded lysosomal compartment. Adding to these studies, our work reveals that lysosome function can be genetically enhanced by a transcriptional response that is directly linked with chemotactic signalling. Macrophages in *cxcr3.2* mutants are still able to migrate normally in response to Cxcr3.2-independent cues, but their basal motility and ability to disseminate mycobacterial infection are reduced[10]. We propose that these altered chemotactic responses together with the enhanced lysosomal function act synergistically to increase the resistance of *cxcr3.2* mutants to tuberculosis. In addition, we have shown that, by exploiting a Myd88-dependent signalling axis, mycobacteria can increase the expression of Cxcl11aa, the cognate ligand of Cxcr3.2. This implicates that immune recognition of the pathogen can lead to activation of the chemokine/lysosome circuit that will ultimately suppress the antimicrobial capability of the host cells.

The regulative function exerted by CXCR3 on lysosomal maintenance seems to be conserved between zebrafish and mammals. A previous study in CXCR3-knockout mice revealed that microglial cells can eliminate more efficiently amyloid deposits and prevent the onset of Alzheimer disease more efficiently in CXCR3-deficient conditions. This phenotype was, at least partly, due to an increased size of the lysosomal compartment and to a more efficient maturation of phagolysosomes occurring in these cells[14]. Furthermore, CXCR3 expression was linked to diet-induced steatohepatitis (liver inflammation with fat

accumulation) through induction of lipogenic genes and impairment of autophagolysosome maturation. In this model, pharmacological blockade of CXCR3 using receptor antagonists could reverse the disease and facilitated clearance of lipid inclusions[15].

Taken together, our work indicates that CXCR3-CXCL11 signalling exerts multiple functions on macrophages during the inflammatory processes, by controlling their initial recruitment to infection foci, their reverse migration facilitating tissue dissemination of mycobacteria, their motility during granuloma formation and, as shown in here, their intrinsic microbicidal/degradative capabilities. Mycobacteria seem to have evolved multiple mechanisms for manipulating this signalling axis to regulate macrophage trafficking to the infection focus, drive macrophage-dependent dissemination and ultimately suppress the basal bactericidal property of the host cell. Application of anti CXCR3-therapies may, therefore, represent a valuable strategy to combat mycobacterial diseases on multiple fronts, and possibly to counteract also other non-infectious diseases that arise from lysosomal dysfunctions.

MATERIALS AND METHODS

Zebrafish lines and maintenance – Zebrafish lines were handled in compliance with the local animal welfare regulations and maintained according to standard protocols (zfin.org). The breeding of fish lines was approved by the local animal welfare committee (DEC) of Leiden University (license number: 10612) and adhered to the international guidelines specified by the EU Animal Protection Directive 2010/63/EU. All experiments were performed on embryos/larvae that had not reached the stage of independent feeding. Fish lines used in this work were the following: the macrophage reporter line *Tg(mpeg1:mCherry-F^{ump2})*[43], *(cxcr3.2^{hu6044})*[10] homozygote mutant (*cxcr3.2$^{-/-}$*) and wildtype (*cxcr3.2$^{+/+}$*) siblings, the combination of (*cxcr3.2^{hu6044}*) allele with *Tg(mpeg1:mCherry-F^{ump2})*, and the (*myd88^{hu3568}*)[25] homozygote mutant (*myd88$^{-/-}$*) and wildtype (*myd88$^{+/+}$*) siblings. Embryos were generally maintained at 28.5°C in egg water (60 µg/ml sea salt, Sera Marin, Heinsberg, Germany). For pH sensitive experiments (pH-rodo acidification assay, LysoTracker staining), embryos were placed in E2 medium (15 mM NaCl; 0.5 mM KCl, 1.0 mM MgSO4, 150 µM KH_2PO_4, 50 µM Na_2HPO_4, 1mM $CaCl_2$; 0.7 mM $NaHCO_3$) at least 6 h before the experiment and maintained in E2 medium during the experimental work. Larvae destined to image acquisition were maintained in medium water supplemented with 0.003% PTU (1-phenyl-2-thiourea; Sigma-Aldrich, St Louis, MO, USA) from ~8 hpf to prevent pigmentation. Anaesthesia of embryos/larvae was achieved with 0.02% buffered Tricaine (3-aminobenzoic acid ethyl ester; Sigma-Aldrich) in egg water or E2 medium.

FACS-sorting, RNA isolation, cDNA preparation and RNA-sequencing analysis – *mpeg1:mCherry-F*-positive and unlabelled cells were sorted from *Tg(mpeg1:mCherry-F/cxcr3.2$^{-/-}$)* and wt siblings at 6 dpf. Dissociation of larvae and FACS was performed according to reference[44]. RNA was obtained using the miRNeasy mini kit (Qiagen), and residual genomic DNA was eliminated by DNase treatment (RNase-Free DNase Set, Qiagen). cDNA preparation was performed using the SMARTer® Universal Low Input RNA Kit for Sequencing (Clontech) according to the manufacturer's guidelines. Illumina RNA sequencing and the mapping and counting of reads was outsourced to ZF-screens (Leiden, the Netherlands) and performed as in reference[44]. Statistical analysis of the read count data was performed using the DESeq2 bioinformatic package

(https://bioconductor.org/packages/release/bioc/html/DESeq2.html)[45] and default settings for paired analysis test, using triplicate data sets of *mpeg1:mCherry-F* positive cells, derived from three pools of > 150 larvae/each, obtained from three independent group crosses of *cxcr3.2*$^{-/-}$ and *cxcr3.2*$^{+/+}$. Before processing, lowly expressed genes (sum of reads from three mutant and three wt replicates < 50 total reads), were removed. For gene ontology analysis, we selected significantly expressed genes using a p.adj < 0.05 and ⎸log2(fold change)⎸> 0.5 cut off. Significantly affected KEGG-pathways, GO:cellular components, GO:molecular functions or GO:biological processes (**Table 1-2**) were predicted by submission of the list of human orthologues of the significantly regulated zebrafish genes to DAVID bioinformatic tools (https://david.ncifcrf.gov)[46]. Zebrafish-human orthologous correspondences were derived from g:profiler (http://biit.cs.ut.ee/gprofiler)[47] and curated with manual annotations (zebrafish gene products that did not have an annotated human orthologue were assigned to the closest human orthologue based on the same gene name or high protein sequence identity when blasted to the Ensembl human protein database; genes that did not have any clear human orthologue were discontinued). The cut-off for gene enrichment analysis was set to p.value < 0.05, Fisher Exact test < 0.05, number of affected genes ≥ 10, fold enrichment > 2. To generate **Figure 2A-C**, genes were annotated to compartments according to their GO:cellular component annotations (using Gene ontology annotation database available at geneontology.org). Genes could be associated with multiple compartments. Statistical divergence of Lysosome and Golgi-related genes from the general trend of the other regulated genes (**Figure 2 B**) was tested by chi-squared test analysis (with Bonferroni *post-hoc* correction for False Discovery Rate).

Microinjections, bacterial cultures and infection delivery – Where not differently specified, approximately 200 CFU of *Mycobacterium marinum* strain M (or where specified its isogenic mutant strains *Mm Δerp* or *Δrd1*) constitutively fluorescently labelled with eGFP, mCherry, mCrimson or Wasabi[22,48] were injected in a volume of 1-2 nl into the blood island/caudal vein of zebrafish embryos at 28-30 hpf. For the assessment of the microbicidal activity of macrophages against initial mycobacterial infection, a single-cell suspension of *MmΔerp*-Wasabi was injected from -80°C frozen single-use aliquots, using a protocol adapted from reference[22]. Briefly, bacteria from a 1-week-old plate were inoculated to an OD600 of 0.2 in 10 ml 7H9 medium supplemented with ADC enrichment. The culture was grown for 24 h to reach an OD of 1.0. Bacteria were washed 3 times in Phosphate Buffer Saline (PBS) and suspended in PBS supplemented with 10% glycerol to an OD600 of 5.0. 50 µl aliquots were frozen in liquid nitrogen and stored at -80°C. Upon thawing, the vital bacteria were quantified by plating as being approximately 100 CFU/nl. In all the other cases, bacteria were prepared from a fresh culture as described in reference[10]. For the acidification assay (**Figure 3A-D**) 1 ng *E. coli* pH-rodo bioparticles conjugate for phagocytosis (Invitrogen) were injected into the blood island/caudal vein at 32-37 hpf and imaged over the yolk at 30-45 mpi. Similarly, for the phagocytosis assay (**Figure 4E**) *Mm*M-mCrimson bacteria were injected in *mpeg1:mCherry-F* individuals at 33-34 hpf, fixed at 30-32 mpi and imaged over the yolk as fixed samples (see below).

LysoTracker staining – For visualisation of acidic compartments, 2 dpf embryos were stained for 1-2 hours with 10 µM LysoTracker green DND-26 (Invitrogen) in E2 medium via bath exposure. Before imaging, embryos were quickly rinsed 3 times with E2 medium supplemented with Tricaine.

Imaging and image quantification – For still image and time-lapse acquisition, fixed or live embryos/larvae were mounted in 1.5-2% low-melting-point agarose (SphaeroQ, Burgos, Spain) and imaged with a Zeiss Observer 6.5.32 laser-scanning confocal microscope (Carl Zeiss, Sliedrecht, The Netherlands). To quantify LysoTracker acidification of macrophages (**Figure 3A**), the mean intensity of LysoTracker staining overlapping with the *mpeg1:mCherry-F* transgene at 2dpf was measured using Fiji/Image J quantification tools. Similarly, to quantify *Mm* acidification *in vivo* (**Figure 4A**) the mean intensity of LysoTracker staining overlapping with *Mm*M-mCrimson signal (1 dpi/2 dpf) was measured. To evaluate acidification of *E. coli* bioparticles (**Figure 3B**), the intensity of bioparticles clusters was analysed from pictures. % of phagocytosis of *Mm*M at 30 mpi was quantified as % of *Mm*M-Wasabi signal overlapping with *mpeg1:mCherry-F* signal (over the yolk) from fixed (O/N in 4% paraformaldehyde in Phosphate Buffer Saline supplemented with 0.08% of Triton X100) embryos. All images used for quantification in **Figure 3-4** were acquired with Plan-Neofluar 40x/0.9 Imm corr objective (Carl Zeiss). Data are expressed as % relative to wt (set to 100%). To score the microbicidal activity of macrophages against mycobacteria (**Figure 4B-C**), *Tg(mpeg1:mCherry-F)* embryos injected with Wasabi-labelled *MmΔerp* were fixed at 44 hpi, according to reference[23] and intra-macrophage mycobacterial sites of growth were counted (blind) using a C-Apochromat 63x/1.20 W Korr UV-VIR-IR objective (Carl Zeiss). In **Figure 4C**, the level of infection per macrophage was classified into three classes based on the severity of bacterial content (1-5 bacteria, 6-10 bacteria or >10 bacteria). In **Figure 4B**, each larva was assigned to one of these three classes according to its predominant macrophage phenotype (most frequently observed class of macrophage phenotype per individual larva). In case multiple classes showed the same percentage of macrophage phenotype, larvae were assigned to the most severe class among those.

Time-lapse analysis – The average speed and tracks of macrophages (**Figure 1, Supplementary Figure 2**) were calculated as previously described in reference[10], from movies acquired with an EC Plan-Neofluar 10x/0.30 M27 objective (Carl Zeiss) for 1 hour and an acquisition frequency of 2 minutes. Localisation of lysosomes to the leading edge (**Figure 5**, **Supplementary Movie 1-2**) was quantified by time-lapse imaging of LysoTracker-positive moving macrophages using Plan-Neofluar 40x/0.9 Imm corr objective and at an acquisition rate of <1 photogram/30 sec. The position of LysoTracker was quantified at the maximum extension of the cell during the time-lapse acquisition, by determining the ratio between the level of cell LysoTracker staining in the anterior and in the posterior half of the cell in the direction of movement.

qRT-PCR – To address dependency of *cxcl11aa* on *myd88* signalling, and the effect of bacterial infection on *cxcl11aa* induction, RNA was isolated from *myd88*$^{-/-}$ and *myd88*$^{+/+}$ whole larvae (infected with *Mm*M, **Figure 6B**) and from *cxcr3.2*$^{-/-}$ and *cxcr3.2*$^{+/+}$ larvae (infected with *Mm*M or its isogenic attenuated strain *MmΔrd1,* **Supplementary Figure 1**) at 4 dpi according to reference[10]. To address the macrophage specificity of *cxcl11aa* induction during infection (**Figure 6A**), we sorted the macrophage population of *Tg(mpeg1:mCherry-F)* line (and the unlabelled population) from infected or uninfected (mock injected) larvae at 5 dpi and extracted RNA as described above. cDNA synthesis, qRT-PCR protocol and analysis were performed as previously described in reference[10]. Expression of *cxcl11aa* was compared to *ppiab* for whole-mount analyses and to *eif5* for FACS sorted cells. Primers for these genes were: *cxcl11aaFw*: ACTCAACATGGTGAAGCCAGTGCT; *cxcl11aaRv*:

CTTCAGCGTGGCTATGACTTCCAT; *ppiabFw*: ACACTGAAACACGGAGGCAAAG; *ppiabRv*: CATCCACAACCTTCCCGAACAC; *eif5Fw:* CAAGTTTGTGCTGTGTCCCG; *eif5Rv:* AGCCTTGCAGGAGTTTCCAA.

Statistical analysis – Statistical significance was analysed using GraphPad Prism 6 (GraphPad Software, La Jolla, CA, USA). RNA sequencing statistical analysis was performed as described above in the dedicated section. Data in **Figure 1**, **Figure 3**, **Figure 4A** and **Figure 5** were statistically analysed by two-tailed *t*-tests. Individual two-tailed *t*-tests were used also to analyse the difference in % of macrophage phenotypic class upon infection (**Figure 4C**). Chi-squared contingency was used to test different distribution of larva phenotypes upon infection (**Figure 4B**). No difference in number of infected macrophages in the counting area (**Figure 4D**) was assessed by Mann-Whitney test. Differences in infection burden in **Figure 6D** and in cell speed in **Supplementary Figure 2** were statistically tested by Kruskal-Wallis test followed by Šidák comparison test of selected pairs. For qRT-PCR, statistical significance was estimated by two-tailed *t*-tests on ln(n)-transformed relative induction folds. Significance (*P*-value) is indicated with: ns, non-significant; *$P<0.05$; **$P<0.01$; ***$P<0.001$; ****$P<0.0001$. Error bars: mean±s.e.m.

ACKNOWLEDGEMENTS

We acknowledge Julien Rougeot and Tomasz Prasjnar for suggestions and discussions, especially related to the RNAseq data presentation and analysis. We also acknowledge Frida Sommer for valuable help and support.

This work was supported by the Smart Mix Program of the Netherlands Ministry of Economic Affairs and the Ministry of Education, Culture and Science, the European Commission 7th framework project ZF-HEALTH (contract number HEALTH-F4-2010-242048), and the European Marie-Curie Initial Training Network FishForPharma (contract number PITN-GA-2011-289209).

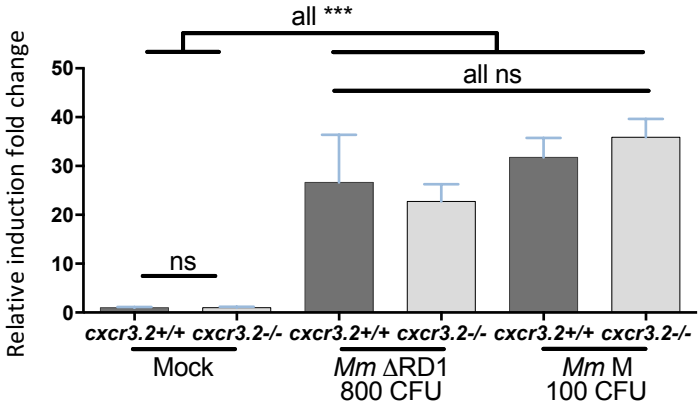

Supplementary Figure 1. cxcl11aa induction does not require the RD1 pathogenicity locus and *cxcr3.2* mutants are still able to upregulate *cxcl11aa* at comparable levels to wt.

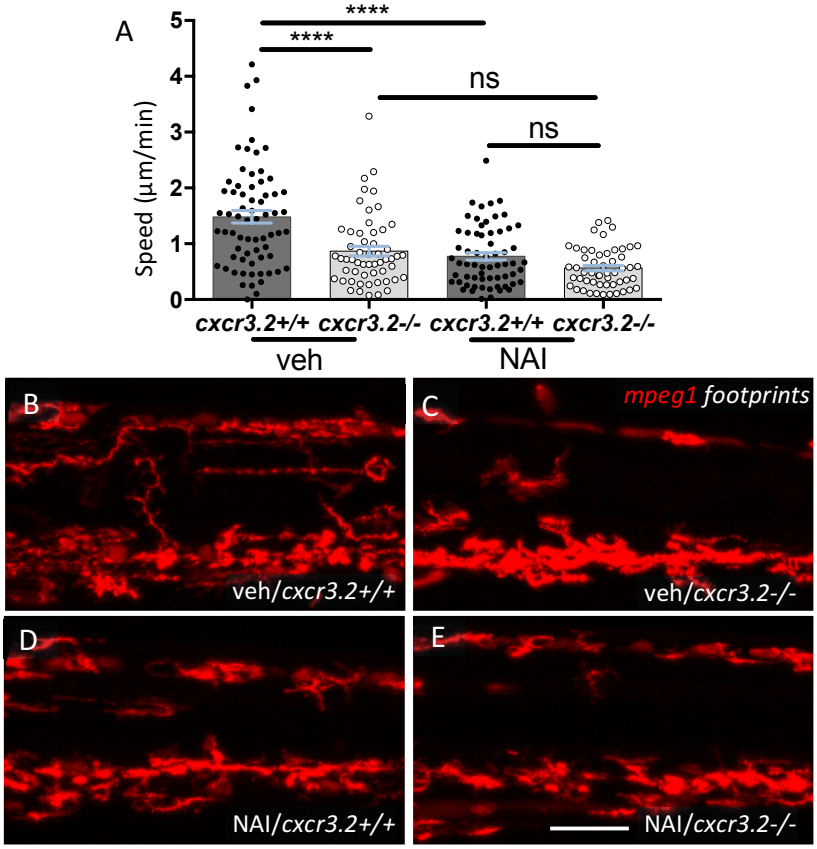

Supplementary Figure 2. Macrophage basal motility requires an active transduction of Nfκb signalling. A. Average speed of wt and mutant macrophage movement after 1 h treatment with 100 nM Nfκb activation inhibitor (NAI) or vehicle (veh); **B-E.** Representative macrophage footprints in wt and mutant embryos treated with Nfκb activation inhibitor or vehicle during the time of observations. Scale bar: 100 µm. Mutant and wt siblings expressing *Tg(mpeg1:mCherry-F)* were imaged at 3 dpf in the trunk area. Data derive from 2 cumulated experiments, run with 3 mutants and 3 wt each.

HYPERLINK TO SUPPLEMENTARY MOVIES

Supplementary Movies are available online at the following URL:
https://drive.google.com/open?id=0B_188Sfgn4xoUkRVNjNKdlNhSEE

REFERENCES

1 Griffith JW, Sokol CL, Luster AD. Chemokines and chemokine receptors: positioning cells for host defense and immunity. Annu Rev Immunol. 2014;32:659-702.
2 Stachowiak AN, Wang Y, Huang YC, Irvine DJ. Homeostatic lymphoid chemokines synergize with adhesion ligands to trigger T and B lymphocyte chemokinesis. J Immunol. 2006 Aug 15;177(4):2340-8.
3 del Pozo MA, Sánchez-Mateos P, Nieto M, Sánchez-Madrid F. Chemokines regulate cellular polarization and adhesion receptor redistribution during lymphocyte interaction with endothelium and extracellular matrix. Involvement of cAMP signaling pathway. J Cell Biol. 1995 Oct;131(2):495-508.
4 Campello S, Lacalle RA, Bettella M, Mañes S, Scorrano L, Viola A. Orchestration of lymphocyte chemotaxis by mitochondrial dynamics. J Exp Med. 2006 Dec 25;203(13):2879-86.

5 Colvin RA, Means TK, Diefenbach TJ, Moita LF, Friday RP, Sever S, Campanella GS, Abrazinski T, Manice LA, Moita C, Andrews NW, Wu D, Hacohen N, Luster AD. Synaptotagmin-mediated vesicle fusion regulates cell migration. Nat Immunol. 2010 Jun;11(6):495-502.
6 Xu Q, Li R, Monte MM, Jiang Y, Nie P, Holland JW, Secombes CJ, Wang T. Sequence and expression analysis of rainbow trout CXCR2, CXCR3a and CXCR3b aids interpretation of lineage-specific conversion, loss and expansion of these receptors during vertebrate evolution. Dev Comp Immunol. 2014 Aug;45(2):201-13.
7 Bajoghli B. Evolution and function of chemokine receptors in the immune system of lower vertebrates. Eur J Immunol. 2013 Jul;43(7):1686-92.
8 Kakuta Y, Okumi M, Miyagawa S, Tsutahara K, Abe T, Yazawa K, Matsunami K, Otsuka H, Takahara S, Nonomura N. Blocking of CCR5 and CXCR3 suppresses the infiltration of macrophages in acute renal allograft rejection. Transplantation. 2012 Jan 15;93(1):24-31.
9 Cuenca AG, Wynn JL, Kelly-Scumpia KM, Scumpia PO, Vila L, Delano MJ, Mathews CE, Wallet SM, Reeves WH, Behrns KE, Nacionales DC, Efron PA, Kunkel SL, Moldawer LL. Critical role for CXC ligand 10/CXC receptor 3 signaling in the murine neonatal response to sepsis. Infect Immun. 2011 Jul;79(7):2746-54.
10 Torraca V, Cui C, Boland R, Bebelman JP, van der Sar AM, Smit MJ, Siderius M, Spaink HP, Meijer AH. The CXCR3-CXCL11 signaling axis mediates macrophage recruitment and dissemination of mycobacterial infection. Dis Model Mech. 2015 Mar;8(3):253-69.
11 Chadzinska M, Golbach L, Pijanowski L, Scheer M, Verburg-van Kemenade BM. Characterization and expression analysis of an interferon-γ2 induced chemokine receptor CXCR3 in common carp (Cyprinus carpio L.). Dev Comp Immunol. 2014 Nov;47(1):68-76.
12 Zhou J, Tang PC, Qin L, Gayed PM, Li W, Skokos EA, Kyriakides TR, Pober JS, Tellides G. CXCR3-dependent accumulation and activation of perivascular macrophages is necessary for homeostatic arterial remodeling to hemodynamic stresses. J Exp Med. 2010 Aug 30;207(9):1951-66.
13 Oghumu S, Varikuti S, Terrazas C, Kotov D, Nasser MW, Powell CA, Ganju RK, Satoskar AR. CXCR3 deficiency enhances tumor progression by promoting macrophage M2 polarization in a murine breast cancer model. Immunology. 2014 Sep;143(1):109-19.
14 Krauthausen M, Kummer MP, Zimmermann J, Reyes-Irisarri E, Terwel D, Bulic B,Heneka MT, Müller M. CXCR3 promotes plaque formation and behavioral deficits in an Alzheimer's disease model. J Clin Invest. 2015 Jan;125(1):365-78.
15 Zhang X, Han J, Man K, Li X, Du J, Chu ES, Go MY, Sung JJ, Yu J. CXC chemokine, receptor 3 promotes steatohepatitis in mice through mediating inflammatory cytokines, macrophages and autophagy. J Hepatol. 2016 Jan;64(1):160-70.
16 Shen K, Sidik H, Talbot WS. The Rag-Ragulator Complex Regulates Lysosome Function and Phagocytic Flux in Microglia. Cell Rep. 2016 Jan 26;14(3):547-59.
17 Torraca V, Masud S, Spaink HP, Meijer AH. Macrophage-pathogen interactions in infectious diseases: new therapeutic insights from the zebrafish host model. Dis Model Mech. 2014 Jul;7(7):785-97.
18 Meijer AH. Protection and pathology in TB: learning from the zebrafish model. Semin Immunopathol. 2015 Sep 1.
19 Ramakrishnan L. The zebrafish guide to tuberculosis immunity and treatment. Cold Spring Harb Symp Quant Biol. 2013;78:179-92.
20 Cronan MR, Tobin DM. Fit for consumption: zebrafish as a model for tuberculosis. Dis Model Mech. 2014 Jul;7(7):777-84.
21 Cosma CL, Klein K, Kim R, Beery D, Ramakrishnan L. Mycobacterium marinum Erp is a virulence determinant required for cell wall integrity and intracellular survival. Infect Immun. 2006 Jun;74(6):3125-33.
22 Takaki K, Davis JM, Winglee K, Ramakrishnan L. Evaluation of the pathogenesis and treatment of Mycobacterium marinum infection in zebrafish. Nat Protoc. 2013 Jun;8(6):1114-24.
23 Roca FJ, Ramakrishnan L. TNF dually mediates resistance and susceptibility to mycobacteria via mitochondrial reactive oxygen species. Cell. 2013 Apr 25;153(3):521-34.
24 Majlessi L, Brodin P, Brosch R, Rojas MJ, Khun H, Huerre M, Cole ST, Leclerc C. Influence of ESAT-6 secretion system 1 (RD1) of Mycobacterium tuberculosis on the interaction between mycobacteria and the host immune system. J Immunol. 2005 Mar 15;174(6):3570-9.
25 van der Vaart M, Spaink HP, Meijer AH. Pathogen recognition and activation of the innate immune response in zebrafish. Adv Hematol. 2012;2012:159807.
26 Chen SC, de Groot M, Kinsley D, Laverty M, McClanahan T, Arreaza M, Gustafson EL, Teunissen MB, de Rie MA, Fine JS, Kraan M. Expression of chemokine receptor CXCR3 by lymphocytes and plasmacytoid dendritic cells in human psoriatic lesions. Arch Dermatol Res. 2010 Mar;302(2):113-23.
27 Kohrgruber N, Gröger M, Meraner P, Kriehuber E, Petzelbauer P, Brandt S, Stingl G, Rot A, Maurer D. Plasmacytoid dendritic cell recruitment by immobilized CXCR3 ligands. J Immunol. 2004 Dec 1;173(11):6592-602.

28 Wang T, Hanington PC, Belosevic M, Secombes CJ. Two macrophage colony-stimulating factor genes exist in fish that differ in gene organization and are differentially expressed. J Immunol. 2008 Sep 1;181(5):3310-22.
29 Wittamer V, Bertrand JY, Gutschow PW, Traver D. Characterization of the mononuclear phagocyte system in zebrafish. Blood. 2011 Jun 30;117(26):7126-35.
30 Zakrzewska A, Cui C, Stockhammer OW, Benard EL, Spaink HP, Meijer AH. Macrophage-specific gene functions in Spi1-directed innate immunity. Blood. 2010 Jul 22;116(3):e1-11.
31 Bergsbaken T, Fink SL, den Hartigh AB, Loomis WP, Cookson BT. Coordinated host responses during pyroptosis: caspase-1-dependent lysosome exocytosis and inflammatory cytokine maturation. J Immunol. 2011 Sep 1;187(5):2748-54.
32 Reddy A, Caler EV, Andrews NW. Plasma membrane repair is mediated by Ca(2+)-regulated exocytosis of lysosomes. Cell. 2001 Jul 27;106(2):157-69.
33 Koo IC, Wang C, Raghavan S, Morisaki JH, Cox JS, Brown EJ. ESX-1-dependent cytolysis in lysosome secretion and inflammasome activation during mycobacterial infection. Cell Microbiol. 2008 Sep;10(9):1866-78.
34 Settembre C, Fraldi A, Medina DL, Ballabio A. Signals from the lysosome: a control centre for cellular clearance and energy metabolism. Nat Rev Mol Cell Biol. 2013 May;14(5):283-96.
35 Sardiello M, Palmieri M, di Ronza A, Medina DL, Valenza M, Gennarino VA, Di Malta C, Donaudy F, Embrione V, Polishchuk RS, Banfi S, Parenti G, Cattaneo E, Ballabio A. A gene network regulating lysosomal biogenesis and function. Science. 2009 Jul 24;325(5939):473-7.
36 Medina DL, Fraldi A, Bouche V, Annunziata F, Mansueto G, Spampanato C, Puri C,Pignata A, Martina JA, Sardiello M, Palmieri M, Polishchuk R, Puertollano R, Ballabio A. Transcriptional activation of lysosomal exocytosis promotes cellular clearance. Dev Cell. 2011 Sep 13;21(3):421-30.
37 Palmieri M, Impey S, Kang H, di Ronza A, Pelz C, Sardiello M, Ballabio A. Characterization of the CLEAR network reveals an integrated control of cellular clearance pathways. Hum Mol Genet. 2011 Oct 1;20(19):3852-66.
38 Pan J, Sun ZY, Ji C, Ji YM, Yang Y, Yang HL. A case of unusual association of Gaucher's disease with spinal tuberculosis. Int J Rheum Dis. 2013 Jun;16(3):361-3.
39 Pérez-Calvo J, Bernal M, Giraldo P, Torralba MA, Civeira F, Giralt M, Pocovi M. Co-morbidity in Gaucher's disease results of a nationwide enquiry in Spain. Eur J Med Res. 2000 Jun 20;5(6):231-5.
40 Liel Y, Rudich A, Nagauker-Shriker O, Yermiyahu T, Levy R. Monocyte dysfunction in patients with Gaucher disease: evidence for interference of glucocerebroside with superoxide generation. Blood. 1994 May 1;83(9):2646-53.
41 Berg RD, Levitte S, O'Sullivan MP, O'Leary SM, Cambier CJ, Cameron J, Takaki KK, Moens CB, Tobin DM, Keane J, Ramakrishnan L. Lysosomal Disorders Drive Susceptibility to Tuberculosis by Compromising Macrophage Migration. Cell. 2016 Mar 24;165(1):139-52.
42 Shen K, Sidik H, Talbot WS. The Rag-Ragulator Complex Regulates Lysosome Function and Phagocytic Flux in Microglia. Cell Rep. 2016 Jan 26;14(3):547-59.
43 Bernut A, Herrmann JL, Kissa K, Dubremetz JF, Gaillard JL, Lutfalla G, Kremer L. Mycobacterium abscessus cording prevents phagocytosis and promotes abscess formation. Proc Natl Acad Sci U S A. 2014 Mar 11;111(10):E943-52.
44 Rougeot J, Zakrzewska A, Kanwal Z, Jansen HJ, Spaink HP, Meijer AH. RNA sequencing of FACS-sorted immune cell populations from zebrafish infection models to identify cell specific responses to intracellular pathogens. Methods Mol Biol. 2014;1197:261-74.
45 Love MI, Huber W, Anders S. Moderated estimation of fold change and dispersion for RNA-seq data with DESeq2. Genome Biol. 2014;15(12):550.
46 Huang da W, Sherman BT, Lempicki RA. Systematic and integrative analysis of large gene lists using DAVID bioinformatics resources. Nat Protoc. 2009;4(1):44-57.
47 Reimand J, Arak T, Vilo J. g:Profiler--a web server for functional interpretation of gene lists (2011 update). Nucleic Acids Res. 2011 Jul;39(Web Server issue):W307-15.
48 van der Sar AM, Abdallah AM, Sparrius M, Reinders E, Vandenbroucke-Grauls CM, Bitter W. Mycobacterium marinum strains can be divided into two distinct types based on genetic diversity and virulence. Infect Immun. 2004 Nov;72(11):6306-12.

Chapter 5

CRISPR/Cas9 mutagenesis of zebrafish Cxcr3.3 suggests opposing functions of atypical and canonical Cxcr3 paralogues on mycobacterial infection control

Vincenzo Torraca, Frida Sommer, Sarah Kamel, Natasja A. Otto and Annemarie H. Meijer

Institute of Biology, Leiden University, The Netherlands

Chapter 5

CRISPR/Cas9 mutagenesis of zebrafish Cxcr3.3 suggests opposing functions of atypical and canonical Cxcr3 paralogues on mycobacterial infection control

Vincenzo Torraca, Frida Sommer, Sarah Kamel, Natasja A. Otto and Annemarie H. Meijer

Institute of Biology, Leiden University, The Netherlands

Zebrafish immune cells express three homologues of the human chemokine receptor CXCR3. We have recently shown that one of these homologues, Cxcr3.2, plays an important role in macrophage migration and dissemination of mycobacterial infection, suggesting that inhibition of CXCR3 signalling could be used as a host-directed therapeutic strategy for treatment of tuberculosis. However, the functions of the other CXCR3 isoforms in zebrafish remain to be elucidated. Here, we successfully applied CRISPR/Cas9 genome editing tools to obtain non-sense mutants of the *cxcr3.3* gene. Additionally, we introduced several optimisations to the CRISPR/Cas9 editing system that facilitated an efficient application of the method in terms of time, costs and yield. As a result, *cxcr3.3* was efficiently mutated in 70% of injected embryos, leading to a similar yield of adult germ-line mosaic carriers. Initial characterisation of *cxcr3.3* mutants revealed that homozygote mutation is viable, does not provoke evident discomfort to the carriers and is maintained according to Mendelian proportions. When tested in the zebrafish tuberculosis model, *cxcr3.3* mutants displayed an increased burden of mycobacterial infection. Unexpectedly, this phenotype is opposite to that of *cxcr3.2* mutants that more efficiently counteract initial mycobacterial replication and mycobacterial dissemination in the granulomatous stage. Sequence analysis of CXCR3 from fish and other vertebrates revealed that Cxcr3.3 in zebrafish may function as an atypical chemokine receptor (ACKR), since it displays replacement of key amino acid residues essential to mediate the activation of heterotrimeric G-proteins. Notably, the presence of atypical Cxcr3 receptors appears conserved among fish species, although it was possibly lost at the radiation of tetrapods, since only classical CXCR3 receptors are present in amphibians, reptiles and mammals. This suggests that Cxcr3.3 may exert a regulatory function on Cxcr3.2 signalling by scavenging/competition for ligands. Further mechanistic studies should be performed to validate this hypothesis and to analyse the cross-talk between Cxcr3.2 and Cxcr3.3 receptors.

GRAPHICAL ABSTRACT

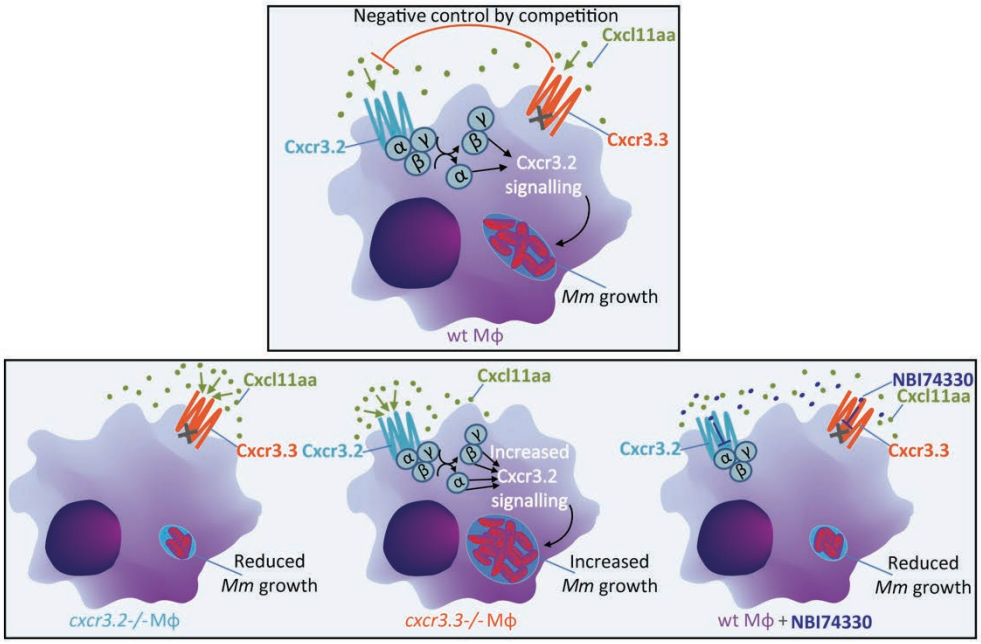

Zebrafish macrophages express both Cxcr3.2 and Cxcr3.3 receptors. Cxcr3.2 is able to evoke macrophage chemotaxis via its Cxcl11 cognate ligands and contains an intact DRY (Asp-Arg-Tyr) motif, which would permit its coupling with downstream G-protein signalling. Upon ligand binding to the receptor, heterotrimeric G-proteins would dissociate into Gα and Gβγ subunits and modulate the activity of their targets. We previously showed that Cxcr3.2-mediated signalling leads to increased susceptibility to mycobacterial infection and abolishment of this signalling benefits the host. We show here that unlike Cxcr3.2, Cxcr3.3 does not contain a DRY motif, suggesting that this receptor is unable to direct G-protein coupled receptor signalling, similarly to other atypical chemokine receptors. Additionally, *cxcr3.3* mutations increase susceptibility to infection. In our proposed model, wt Cxcr3.3 expression may exert a beneficial function by scavenging Cxcr3.2 ligands, therefore limiting activation of Cxcr3.2 pro-infection downstream signalling. That Cxcr3.3 requires simultaneous Cxcr3.2 expression to exert its function is also suggested by treatment with NBI74330, a CXCR3 antagonist that is thought to block both Cxcr3.2 and Cxcr3.3. In this situation, the susceptibility to infection is attenuated, phenocopying *cxcr3.2* mutation and not *cxcr3.3* mutation.

INTRODUCTION

Chemokines constitute a family of potent chemotactic molecules which play complex pleiotropic functions in the control of the immune response and of host-pathogen interactions[1]. The zebrafish (*Danio rerio*) is an attractive vertebrate model to study this complexity *in vivo,* as it provides both a genetically tractable system, to generate new genetically-encoded tools, and an optically-accessible platform to follow the dynamics of immune cells and processes intravitally[2]. The genetic tractability of zebrafish enabled generation of a multitude of transgenic and mutant lines of interest for the immune system and in particular to study chemokine receptors, a class of 7-loop transmembrane (7TM) and G-protein coupled receptors (GPCR) that signal via their cognate chemokine ligands. For example, wildtype (wt) and mutated versions of Cxcr4b have been fused with fluorescent proteins to study receptor expression/internalisation dynamics and its function in controlling cell migration and phagocyte mobilisation[3,4]. Random mutagenesis screening programmes[5] have provided widely used null chemokine ligand and receptor mutants, such as *cxcl12a*[6], *cxcr4b*[7], *cxcr7b*[8] (also known as atypical chemokine receptor 3b, *ackr3b*), and *cxcr3.2*[9]. These mutants, used in combination with transgenic reporters that allow differential labelling of immune cell types, have been critical for *in vivo* analysis of immune responses and cell motility.

Recent advances in genome editing strategies provided the possibility to specifically target genes of interest, including chemokine ligands and receptors[10,11]. As a consequence, these technologies are contributing to greatly expand the array of genetic tools available to the zebrafish field. State-of-the-art genome editing techniques include zinc finger nucleases (ZFN), transcription activator-like effector nucleases (TALEN), and clustered regularly interspaced short palindromic repeats-associated protein 9 (CRISPR/Cas9) technology[12,13,14]. All these techniques have been efficiently applied to zebrafish genome editing, for both insertion of transgenic constructs and generation of transmissible mutations[15,16,17,18]. However, CRISPR/Cas9 technology has several advantages when compared to ZFN and TALEN techniques and is, therefore, becoming the predominantly used method for genome manipulation[13]. In both ZFNs and TALENs, recognition of the DNA target site and the endonuclease activity are driven by specific protein domains. However, in CRISPR/Cas9 technology, recognition of the target depends on a short guide RNA (shgRNA) which pairs to the target site by nucleotide matches, while the actual endonuclease activity is catalysed by a universal Cas9 protein, driven to the target site by matching to a constant region of the shgRNA (**Figure 1**).

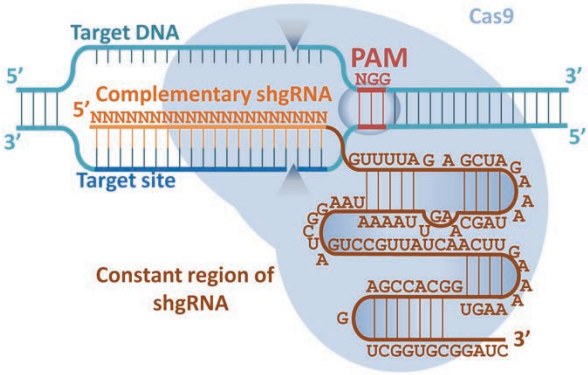

Figure 1. Schematic representation of the CRISPR/Cas9 system. The system uses a nuclease, CRISPR-associated 9 (Cas9), that complexes with short guide RNAs (shgRNAs) to cleave DNA in a sequence-specific manner upstream of the protospacer adjacent motif (PAM) in any genomic location. The endogenous CRISPR-Cas9 system is comprised of 2 separate guide RNAs known as the crRNA and tracrRNA. In the bioengineered version of the system, these two separate RNAs have been combined into a single guide RNA. Adapted from reference[14].

Because of this difference, the construction of ZFN and TALEN nucleases requires complex and laborious multistep cloning strategies or acquisition of costly synthetic constructs to build up the DNA templates encoding the target-specific ZFN/TALEN recognition protein domains. A major advantage of CRISPR/Cas9 technology is that it requires only simple molecular biology tools (primers/short oligo templates or simple cloning procedures) to engineer the shgRNA template responsible for the base-pairing-dependent target recognition.

In the CRISPR/Cas9 protocol used in this study, the shgRNA consists of 101 bases with a 20-nucleotide-long sequence complementary to the DNA target site (at its 5' extremity) (**Figure 1**)[12,13]. This sequence is fundamental for the target recognition via base-pairing. The remaining shgRNA sequence contains the RNA hairpins required to form a complex with the Cas9 endonuclease. Cas9 does not participate in the recognition of the 20-base target site; however, it requires that the target site is followed by a Protospacer Adjacent Motif (PAM) sequence (most commonly 5'-NGG-3')[12,13]. The PAM sequence provides an anchoring site, which is fundamental for efficient cleavage. Following recognition of the target site, a double strand break will be generated within the genomic target site, most likely three nucleotides upstream of the PAM sequence. The 8-12 bases immediately upstream of the PAM motif represent the "seeding sequence" and any mismatches in this region will abolish shgRNA/Cas9 activity. Mismatches beyond this nucleotide sequence are generally tolerable[12,13]. This has a direct impact on the specificity and on off-target effects that the CRISPR/Cas9 technique might have, compared with other gene editing techniques which generally require recognition of longer consensus sequences. However, a new variant of high fidelity Cas9, carrying sequence optimisations designed to reduce non-specific DNA contacts, is already available and appears to not provoke any detectable off-target effects[19]. Due to its simple approach, high efficiency and low costs, the CRISPR/Cas9 technique is becoming the elective technique for genome editing.

Like other teleosts, zebrafish have experienced three rounds of whole genome duplication (WGD) resulting in an increase of the copy number of several genes[20]. Moreover, some further zebrafish-specific chemokine gene cluster expansions have been observed. Comparative analysis of the zebrafish and human genomes revealed that whilst there are at least 36 putative chemokine receptors and 75 putative chemokine ligands in zebrafish, only 25 chemokine receptors and 45 chemokine ligands have been mapped to the human genome[20]. The CXC-motif subfamily of chemokine receptors and ligands (CXCRs/CXCLs) is involved in multiple processes, spanning from the trafficking of leukocytes to the regulation of angiogenesis. These CXCR/CXCL subfamilies are less divergent between lower vertebrates and mammals, compared with other chemokine ligand and receptor families. For example, at least 11 canonical CXCRs and 20 CXCLs have been identified in zebrafish, versus 7 canonical CXCRs and 17 CXCLs described in humans[20].

Several cases of functional and ligand/receptor partnership conservation have been described for the zebrafish and mammalian CXCR/CXCL counterparts. CXCR2/CXCL8 signalling leads to the chemoattraction of human neutrophils and their recruitment to inflamed sites[21,22]. Notably, an orthologous Cxcr2/Cxcl8a signalling axis exists in zebrafish[23], while this powerful neutrophil chemoattractant signal is not represented in rodents[24,25]. CXCR4/CXCL12 interaction is involved in haematopoietic stem cell (HSC) and leukocyte mobilisation/homoeostasis[26,27], in cancer and HIV pathogenesis[28,29]. Similarly, the Cxcr4b/Cxcl12a zebrafish axis recapitulates several conserved roles in innate

immunity, such as the retention of neutrophils and macrophages in haematopoietic tissues[4], recruitment of HSCs to the definitive sites of haematopoiesis[30] and in metastasis of cancer xenografts[31]. The CXCR4/CXCL12 axis is duplicated in zebrafish and a Cxcr4a/Cxcl12b axis also exists[32]. However, the two seemingly redundant systems experience sub-functionalisation and each control specific functions played by their mammalian CXCR4/CXCL12 counterpart. Notably, while disruption of this axis is embryonic lethal in mammals[33,34,35] the partial redundancy of the CXCR4/CXCL12 system permits the existence of viable knockouts, displaying attenuated and more specific phenotypes, which proved extremely useful to study particular aspects regulated by this axis *in vivo*.

CXCR3 is expressed by different types of leukocytes, including T lymphocytes, natural killer cells, macrophages and dendritic cells and plays an important part in trafficking and function of these cell types in inflammatory and autoimmune diseases[36,37,38,39]. The ligand of this receptor in mammals is represented by a triplet of inflammatory chemokines, namely CXCL9-10-11. In zebrafish, three copies of this gene are present, *cxcr3.1, cxcr3.2, cxcr3.3* (**Figure 2A**)[9]. Of these three isoforms, only *cxcr3.2* has been recently characterised, as being involved in controlling the microbicidal capability of macrophages[40], the migration of macrophages to infection foci, and macrophage-mediated dissemination of mycobacterial infection[9]. It is still unknown whether the other two isoforms have complementary/redundant functions. Likewise, the cluster of CXCL9-10-11 chemokines (which represent the class of interacting partners of CXCR3-like receptors) is also expanded in zebrafish and includes 7 ligands, namely Cxcl11aa-ac-ad-ae-af-ag-ah[9,20]. While the sole human CXCR3 responds to CXCL9-10-11, it seems that not all the zebrafish Cxcl11 ligands are able to elicit a Cxcr3.2-dependent response[9]. Cxcl11aa and Cxcl11af were shown to mobilise macrophages via Cxcr3.2, while Cxcl11ae was able to comparably recruit macrophages also in the *cxcr3.2* null mutants. This suggests that Cxcr3.1, Cxcr3.2 and Cxcr3.3 and their ligand partners are not completely redundant and interchangeable, similar to the Cxcr4a/b/Cxcl12a/b system[32]. RNA-sequencing and qRT-PCR data of Fluorescence-Activated Cell Sorting (FACS) of macrophages, neutrophils and immature T cells revealed that *cxcr3.1* was only detectable in immature T cells, while *cxcr3.2* and *cxcr3.3* were significantly expressed by both macrophages and neutrophils[9,41], suggesting cell-type functional specialisation.

Our previous analysis of a zebrafish *cxcr3.2* mutant in the zebrafish embryo model for tuberculosis suggested that inhibition of CXCR3 signalling could be used as a host-directed therapeutic strategy for treatment of the mycobacterial infection causing this disease[9]. As mentioned above, *cxcr3.2* and *cxcr3.3* display a similar macrophage and neutrophil-specific expression profile in the embryo model. Since a *cxcr3.3* mutant was not available and the function of this gene in recruitment, development and mobilisation of immune cells is unknown, we aimed here to apply CRISPR/Cas9 technology to disrupt *cxcr3.3*. We additionally present our own adaptations to the CRISPR/Cas9 method which allowed synthesis of shgRNAs from a PCR-based template and *in vivo* selection of target sites with high mutagenesis efficiency. Finally, we present a preliminary characterisation of the *cxcr3.3* mutants we obtained in the zebrafish tuberculosis model. Notably, *cxcr3.3* mutation revealed the opposite effect to that seen in the context of *cxcr3.2* mutation. Interestingly, *cxcr3.3* does not contain the DRY (Asp-Arg-Tyr) motif, which is fundamental to transduce GPCR signalling, which suggests that this receptor may act as an atypical chemokine receptor. These findings emphasise the need for an in-depth

characterisation of cross talk between Cxcr3.2 and Cxcr3.3 in controlling host-pathogen interactions.

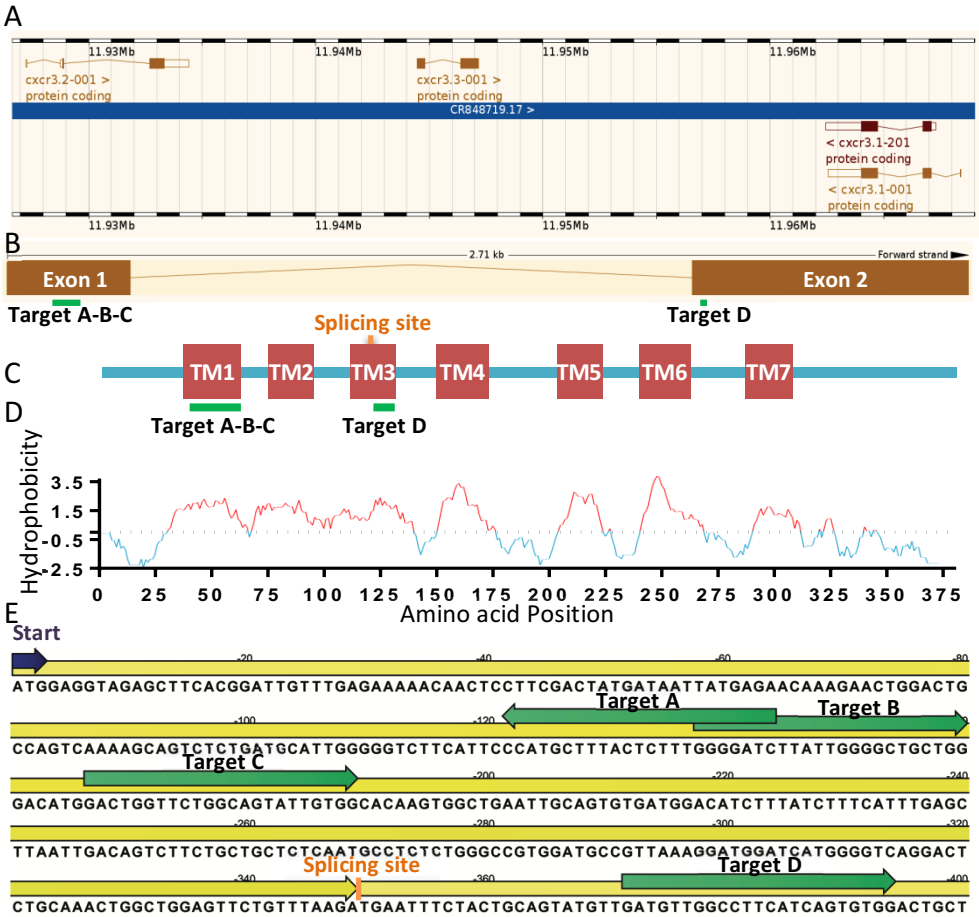

Figure 2. Design of CRISPR targets for *cxcr3.3*. A. Genomic locus of *cxcr3* zebrafish genes. The zebrafish genomic locus Chr16:11926632-11969001 (contig CR848719.17, zebrafish genome version GRCz10) contains three mammalian CXCR3 orthologues *cxcr3.1*, *cxcr3.2*, and *cxcr3.3*. **B-C.** Genomic and encoded protein architecture of the *cxcr3.3* locus. The *cxcr3.3* gene spans 2.71 kb and consists of two exons. Exon 1 encodes the N-terminal extracellular domain, the transmembrane domains TM1, TM2, and part of TM3; exon 2 codes for the remaining part of TM3, for TM4, TM5, TM6, TM7 and for the C-terminal intracellular domain. Lines in green depict the position of the CRISPR Targets A, B, C and D. **D.** Prediction of the TM domains was computed with an online transmembrane prediction tool (http://www.ch.embnet.org/cgi-bin/TMPRED_form_parser), based on the hydrophobicity plot and is consistent with the conventional structure of a seven loop transmembrane receptor. **E.** Nucleotide sequence of *cxcr3.3* in the region containing the targeting sites. Target sites are marked in green. The ATG codon in represented in violet and the splicing site is represented by a yellow bar.

RESULTS

CRISPR target design

There are several bioinformatic tools available to design CRISPR targets. Finding a putative target site is simple since virtually any genomic 5'-$(N)_{21}$GG-3' sequence is a possible site for CRISPR targeting (**Figure 1**). However, since the synthesis or shgRNA implies transcription from a T7 promoter and since T7 RNA-polymerase most preferably initiates transcription from a G, this forces the design of efficiently transcribed targets to respect the 5'-G$(N)_{20}$GG-3' sequence constraint. Notably, other transcription promoters may be used to drive expression of the shgRNA (e.g. U6, SP6), which would not require the presence of a G at the +1 position. Likewise, recently novel versions of Cas9 (derived from other bacteria and requiring alternative PAM sequences) are also available. Therefore, if necessary, alternative designs are possible. Apart from the transcription-related and Cas9-related constraints, many other filtering criteria apply when selecting a target site. These include the intronic-exonic architecture, the probability of epigenetic modification/accessibility of the target at the genomic site, the GC content, the specificity of the target site/probability of off-target effects, the existence of self-complementarities and secondary structures in the shgRNA. Therefore, different online tools provide a classification of the targets according to scoring criteria that take into account several variables.

To target *cxcr3.3*, we selected 4 candidate target sequences, respecting the 3'-G$(N)_{20}$GG-5' signature and falling into a relatively proximal region of the coding sequence of *cxcr3.3* (within 396 dNTPs/132 aa from the translation start) (**Figure 2B-E** and **Table 1**). The first 2 targets (Target A and B) were obtained using a CRISPR/Cas9-dedicated engine from ZiFiT Targeter Version 4.2 (http://zifit.partners.org/ZiFiT/CSquare9Nuclease.aspx). The other two targets (Targets C and D) were obtained as 2 top scoring hits by the CHOPCHOP web-tool (https://chopchop.rc.fas.harvard.edu/index.php)[42]. ZiFit does not provide any support in the selection of the targets, based on their properties. Therefore, the list of putative targets was screened manually, based on proximity of the target to the 5' end of *cxcr3.3* and on the presence of putative off-targets. Differently, the CHOPCHOP web-tool uses a specific algorithm that scores and ranks potential target sites[42]. A Bowtie-based alignment system (an ultrafast and efficient algorithm to align short sequences to full genomes[43]) allows the identification of the most specific target sites. Target sites are therefore ranked based on number of off-targets, number of mismatches (when searching for putative off-targets), proximity of the target site to the ATG of translation start (the more proximal, the better), GC content (best if 50-60%), and the presence of a G at position 20 (which appears to improve the cutting rate[44]). For comparison, we also used a published target for *eGFP*[15] (**Table 1**), aiming to assay by fluorescence the efficiency of the CRISPR knockout by mutation of an eGFP transgene from a zebrafish transgenic line (*Tg(fli1a:eGFP)*[45], see results sections for explanation and further details).

Preparation of shgRNA

Most of recent reports used a cloning-based strategy to obtain a DNA template for *in vitro* transcription of shgRNA[16,46,47.48,49,50,51]. However, few reports have indicated that short transcripts can be also transcribed with cloning-free systems based on synthetic DNA oligonucleotide templates[15,17,52,53]. This second option appears more desirable, since it would facilitate and accelerate the synthesis process, and is suited to set up a standardised

method that can be immediately adapted for targeting new genes of interest or to carry multiple targets at once. The downside of the oligonucleotide-based synthetic strategies versus the plasmid-based ones may be the limited yield of templates, the large costs of synthesis and the poor transcription efficiency to obtain the final RNA product. In order to identify the most efficient system to obtain shgRNA, we compared three different sources of DNA template (**Figure 3**): full-length (122-bases) synthetic single-stranded DNA (ssDNA) template (Method 1); dsDNA derived from a PCR-based complementation and amplification of full-length (122-bases) synthetic ssDNA oligonucleotide (Method 2); dsDNA template derived from PCR-based complementation and amplification of two 81-base-long semi-complementary oligonucleotides (Method 3). Although the T7 RNA polymerase does not require a dsDNA template, it requires the T7 promoter site to be double-stranded[54]. Therefore, for Method 1, RNA was transcribed upon annealing of an equimolar concentration of T7 primer, in order to complement the T7 promoter site (See Materials and Methods for more details). Comparing the yields of shgRNA product obtained with the 3 methods, we found that the Method 1 was extremely inefficient, yielding < 0.2 µg of total RNA. Method 2 and 3 had comparable efficiencies, yielding over 40 µg of total RNA product (**Table 2**). Between Method 2 and 3, we found Method 3 technically more convenient. Since the target site-specific sequence is localised at the 5' extremity of the DNA template, it could be confined entirely into the forward 81-mer oligonucleotide. This means that the reverse 81-mer oligonucleotide matches exclusively to the constant shgRNA region (common to any shgRNAs). Synthesis of >100 bp synthetic oligos (Method 1 and 2) is costly, takes longer delivery time, requires polyacrylamide gel electrophoresis (PAGE)-based purification, and is more prone to introduction of sequence errors. This is particularly true for a shgRNA template, that includes long stretches of repetitive nucleotides. By using Method 3, we could avoid ordering of a new 122-mer for each CRISPR and could minimise the order to 1 single 81-mer oligo for each new CRISPR.

	Target site, 5' to 3'	Orientation	Position
***cxcr3.3* Target A**	GATCCCCAAAGAGTAAAGCATGG	Reverse strand	122-144
***cxcr3.3* Target B**	GGGGATCTTATTGGGGCTGCTGG	Forward strand	138-160
***cxcr3.3* Target C**	GACTGGTTCTGGCAGTATTGTGG	Forward strand	167-189
***cxcr3.3* Target D**	GATGTTGGCCTTCATCAGTGTGG	Forward strand	372-394
***eGFP* Target**	GGGCACGGGCAGCTTGCCGGTGG	Reverse strand	149-171

Table 1. Target sites used in this study. Underlined NGG sequences represent the PAM consensus. Positions are relative to the translational Start and refer to the cDNA sequence.

	***eGFP* Target**	***cxcr3.3* Target A**	***cxcr3.3* Target B**	***cxcr3.3* Target C**	***cxcr3.3* Target D**
Method 1	<10	<10	<10	-	-
Method 2	1968.3	3023.0	1850.5	-	-
Method 3	-	-	-	1627.4	2514.5

Table 2. Yields (ng/µl) of the different methods used in this study. Concentration refers to 20 µl transcription reactions performed with 100 ng of ssDNA (Method 1) or 200 ng of dsDNA template (Methods 2-3). Upon column cleanup, RNA was eluted in 20 µl (2x10 µl) of RNAse-free water. 1 µl was used for nanodrop measurement.

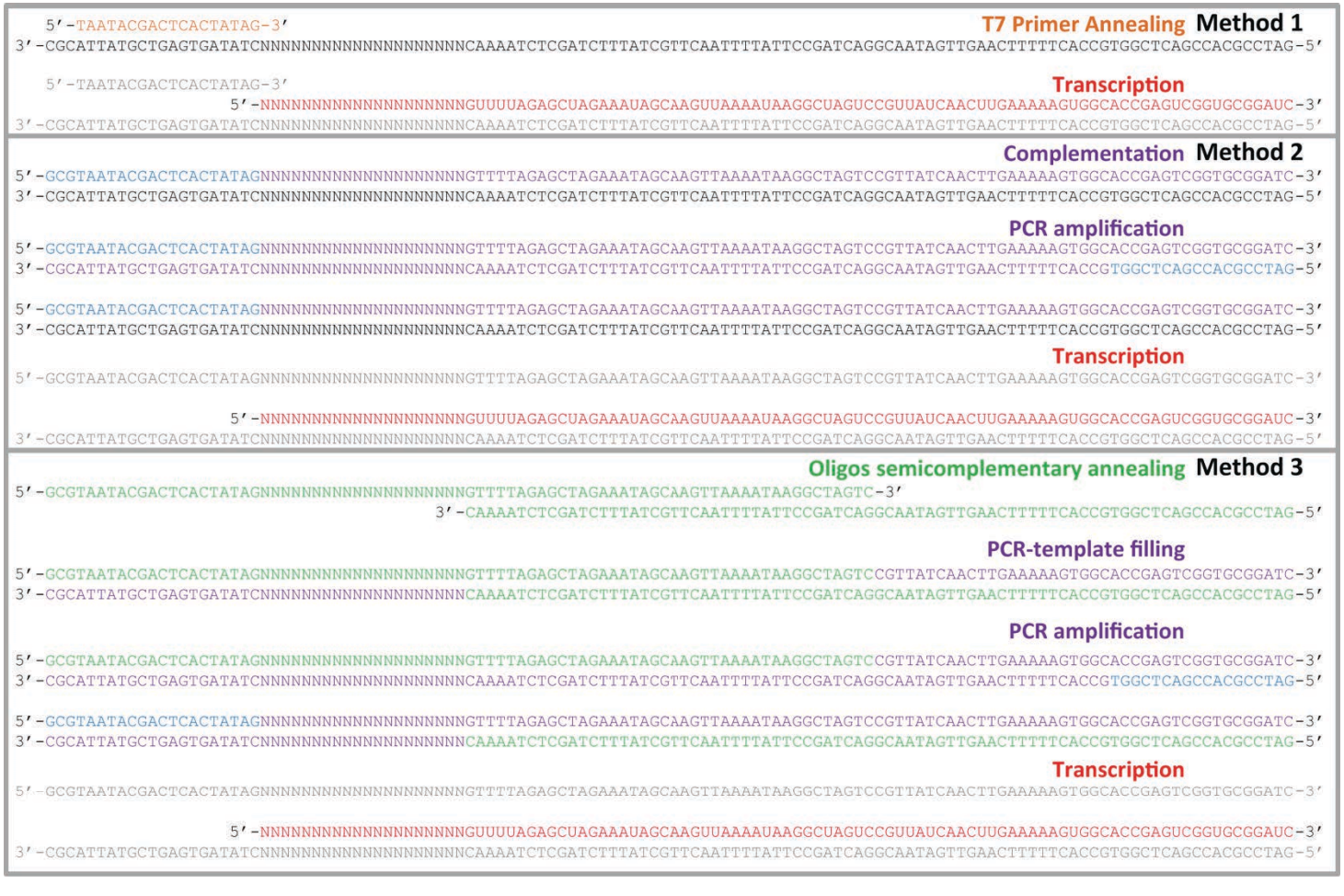

Figure 3. Methods for shgRNA transcription used in this study *(Legend on the next page).*

Figure 3. **Methods for shgRNA transcription used in this study** *(Figure on the previous page).* Method 1 uses a synthetic 122-bases ssDNA oligonucleotide (purified by PAGE, black), annealed to a T7 primer (orange) as a direct template for RNA transcription. Method 2 uses a dsDNA template derived from a PCR-based complementation and amplification (violet) of the 122-bases synthetic ssDNA oligonucleotide (as in Method 1). Method 3 uses a dsDNA template derived from PCR-based complementation and amplification (violet) of 2 half-length partially complementary oligonucleotides (81-bases each, purification by standard desalting method, green).

Of note, the 81-mer oligo can be synthesised and purified by standard methods used to synthesise custom-made primers. The use of a PCR-based shgRNA template described here eliminates completely laborious cloning steps and permits to obtain a working shgRNA within 7-9 hours from the receipt of the 81-mer primer, while a cloning-based method would require at least 5 working days, since several O/N steps are required (**Table 3**)[55].

	PCR-based shgRNA synthesis		Cloning-based shgRNA synthesis
	Ordering		
Day 1	1. Order 1 81-mer per shgRNA + a set of 3 constant primers (**1-2 days**)	**Day 1**	1. Order 2 primers per shgRNA + 1 constant receiving plasmid (**1-2 days**)
	Generation of shgRNA template		
Day 2	2. PCR reaction (**2 h**) 3. Gel electrophoresis (**0.5 h**) 4. Column PCR cleanup (**0.5 h**) 3. Validation by sequencing (**O/N**) **Note**: All the templates can be made using a universal synthetic strategy.	**Day 2-3-4-5**	2. Primer annealing (**1 h**) 3. Plasmid digestion (**2 h**) 4. Ligation (**> 4 h**) 5. Transformation (**3 h**) 6. Plating + colonies forming (**O/N**) 7. Liquid culture (**O/N**) 8 Plasmid isolation (**1 h**) 9. Gel electrophoresis (**0.5 h**) 9. Validation by sequencing (**O/N**) 10. Plasmid linearisation (**2 h**) 11. Linear plasmid cleanup (**1 h**) **Note**: Not all the templates can be cloned using a universal cloning strategy.
	shgRNA Transcription		
Day 3	4. *In vitro* transcription (**3-5 h**) 5. RNA cleanup (**1 h**) **Note**: PCR-based templates are transcribed with high efficiency (no risk of endotoxins, reduced amount of template, reduced likelihood of contamination with RNases).	**Day 6**	12. *In vitro* transcription (**3-5 h**) 13. RNA cleanup (**1 h**) **Note**: plasmid templates are transcribed with a reduced efficiency (chance of residual endotoxins, large amount of non-template DNA that can inhibit the reaction, more likely contamination with RNases).
Additional materials: DNA polymerase, PCR buffer + dNTPs.		**Additional materials:** Restriction enzyme, restriction buffer, ligase, ligation buffer + ATP, liquid and solid culturing media + antibiotics.	
Critical steps: RNA *in vitro* transcription.		**Critical steps:** primer annealing, ligation, transformation, clone selection and RNA *in vitro* transcription.	

Table 3. Comparison of the PCR-based shgRNA synthesis method used here with cloning strategies used elsewhere.

Method validation and RNA concentration titration for efficient targeting *in vivo*

To validate our method of shgRNA synthesis and to confirm the activity of the Cas9 mRNA, we co-injected the Cas9 mRNA with a shgRNA targeting eGFP in fertilised eggs of homozygote *Tg(fli1a-eGFP)*[45], a well-characterised zebrafish transgenic line where GFP is expressed by the endothelium of lymphatic and blood vessels[45]. We adapted to our synthetic strategy (Method 2) a published eGFP CRISPR target site which was already successfully used to suppress eGFP signal in a zebrafish transgenic line[15]. To assess the dependency of the targeting efficiency from the mRNA concentration and to assess general toxicity effects, a gradient of Cas9 mRNA and eGFP-shgRNA were injected ranging between 150 and 300 pg for the Cas9 mRNA and between 25 and 250 pg for the eGFP-shgRNA. Embryos were visualised under the fluorescent microscope at 30 and 48 hpf to screen for eGFP signal. Depending on the signal, the embryos were categorised into 3 groups: normal eGFP signal, mosaic eGFP expression or severe/complete abrogation of eGFP expression (**Figure 4A-D**). The combination of the highest doses (300 pg for Cas9 mRNA and 250 pg for eGFP-shgRNA) yielded the most effective targeting and resulted in the complete or almost complete loss of eGFP in about 20% of the *Tg(fli1a-eGFP)* and in a mosaic phenotype in 30% of embryos. The rest of the injected embryos maintained an apparent homogeneous eGFP expression, although the vast majority of them showed to some extent a reduced signal intensity when compared to the uninjected *Tg(fli1a-eGFP)* controls. It must be emphasised here that injections were performed in eggs which were homozygote for the *fli1a-eGFP* transgene, meaning that complete and mosaic loss of eGFP is derived from biallelic targeting in the whole organism or in a proportion of the cells. This experiment, therefore, demonstrates high efficiency of our PCR-based method for CRISPR-targeting.

Detection of CRISPR/Cas9 mutagenesis and efficiency

Next, we aimed to choose a screening methodology to validate active CRISPR targeting of genes such as *cxcr3.3* for which we did not expect a direct phenotypic targeting evidence. Several reports identify a T7 Endonuclease I (T7EI) assay as a screening methodology[15,16]. T7EI assay detects the presence of heteroduplex DNA (dsDNA carrying one or more mismatches), which is a result of the denaturation and renaturation of PCR amplicons derived from chimeric and/or heterozygote individuals. T7EI specifically digests heteroduplex DNA (e.g. derived from genome editing), by introducing double-strand breaks, whilst it does not digest homoduplex DNA (e.g. derived from uninjected controls). As a result, upon incubation with T7EI, the PCR product from individuals carrying mutations will be digested and will form multiple bands on agarose gels, whilst amplicons derived from wt embryos will appear unaffected and display a single band on gel. Detection of eGFP disruption could be achieved with this method (not shown); however, we have experienced poor robustness and reproducibility, since, in several cases, embryos with a complete loss of eGFP signal (and validated as disrupted eGFP individuals by Sanger sequencing) were indistinguishable from the uninjected embryos. At the end of a PCR reaction, all the DNA is in a homoduplex form. To permit formation of heteroduplex DNA, a specific protocol of denaturation-renaturation has to be performed (https://www.neb.com/protocols/2014/08/11/determining-genome-targeting-efficiency-using-t7-endonuclease-i). As a consequence, this method requires specific thermocycling conditions respecting precise timings and temperature gradients, which to some extent are also dependent on each specific PCR template (e.g. GC content, amplicon length etc.) and

should be fine-tuned empirically per each amplicon for optimal results. Therefore, we preferred screening of targeting by Sanger sequencing as a genotyping strategy.

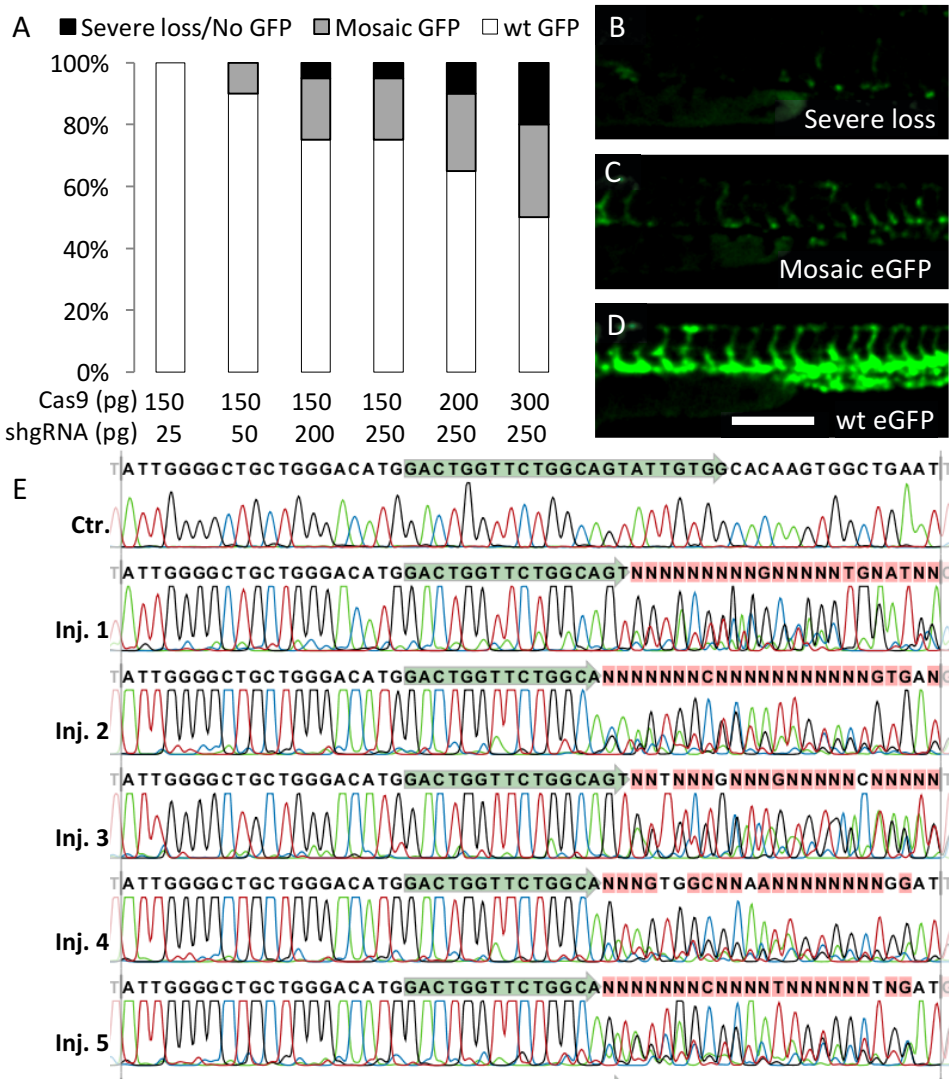

Figure 4. Efficiency of shgRNA/Cas9 mRNA injections. A-D. Effects of different concentrations of shgRNA/Cas9 RNA on the efficiency of eGFP CRISPR targeting. *Tg(Fli1a:eGFP)* embryos were injected with the indicated amounts of eGFP CRISPR shgRNA and Cas9 mRNA. In A, injected embryos were classified at 48 hpf based on the eGFP expression pattern. Increase of Cas9 and shgRNA correlated with increase of more severe phenotypes. B-D show representative images of eGFP-CRISPR injected fish, with different levels of GFP loss. **E.** Determination of *cxcr3.3* Target C sequence disruption by Sanger sequencing. CRISPR-injected fish exhibit sequence alterations (multiple peaks) downstream of the CRISPR target site (green label).

Comparing a wt and a mutated sequence by Sanger sequencing, one should observe a read composed of single peaks for the wt (indicating existence of only one base at each position in the amplicon), whilst a mutant sequence will be composed of single peaks upstream of the mutation point and by distorted multi-peaked reads from that point beyond, due to insertions and deletions of bases and to the simultaneous presence of wt and mutated reads (**Figure 4E**).

Of note, from our experience CRISPR mosaics display more than two alternative reads, indicating the concurrent occurrence of several mutations (**Figure 4-5**). Most likely this is due either to a) biallelic editing, leading to alternative mutations of the two genetic alleles, b) alternative repair mechanisms occurring in the forward and reverse strand of the genomic DNA, c) alternative mechanisms of repair taking place in daughter cells, or d) delayed CRISPR editing, occurring independently in individual daughter cells at more than 1-cell stage. Despite the fact that Sanger sequencing is required to confirm efficient targeting, we also found, in agreement with other laboratories, that long runs (>1h) on high percentage agarose gels (4%) permits detection of effective targeting in most of the samples where genome editing occurs. When compared to wt, amplifications derived from successful editing, do not appear as a sharp narrow band, but as a smeared band around the expected molecular weight (most commonly slightly higher). Of note, if electrophoresis is run for shorter times and/or on lower % agarose gels, mutant bands most commonly appear indistinguishable from wt.

Generation of a CRISPR/Cas9 mutant for *cxcr3.3*

ShgRNAs against the 4 target sites for *cxcr3.3* were injected at concentrations ranging between 30 and 150 pg along with 150 pg of Cas9mRNA. However, among the 4 selected targets, only one (Target C) displayed clear and efficient genome editing. When injected at the highest concentration, this shgRNA yielded an average efficiency per injection session of 70±17% as assessed via Sanger sequencing (**Figure 4E**). The other three targets consistently failed in generating mutations at the target site and were therefore discontinued. Over 200 eggs were injected with *cxcr3.3* Target C and raised to adulthood (F0). The offspring of 14 F0 adult fish (outcrossed to AB/TL) were genotyped. The results revealed that the final success rate of adult carriers was 71.4% (10/14). The tested carriers were able to transmit the mutated alleles with an efficiency of heterozygote F1 ranging between 17% and 100%, depending on the founder. The exact entity of the mutation carried by each heterozygote was determined by Sanger sequencing. By this method, heterozygotes display a double-peaked read from the mutated point onwards. By subtracting the wt sequence from the double-peaked read we could, therefore, obtain the read relative to the mutant allele (**Figure 5A**). This method proved very efficient for the selection of desirable mutations and of isogenic heterozygote carriers to generate full homozygote mutants by incross (**Figure 5B-E**). Our heterozygote sequence analysis also demonstrated that single F0 founders, when crossed to wt, could generate heterozygote offspring carrying different kinds of mutant alleles (**Figure 5E**). In particular, 4/10 founders generated offspring with more than 1 mutated allele and 3/10 transmitted more than 2 and up to 4 mutant alleles, indicating that the mechanisms of alternative repair and/or delayed targeting also contributed to the generation of alternative mutations, together with the biallelic targeting (**Figure 5E**).

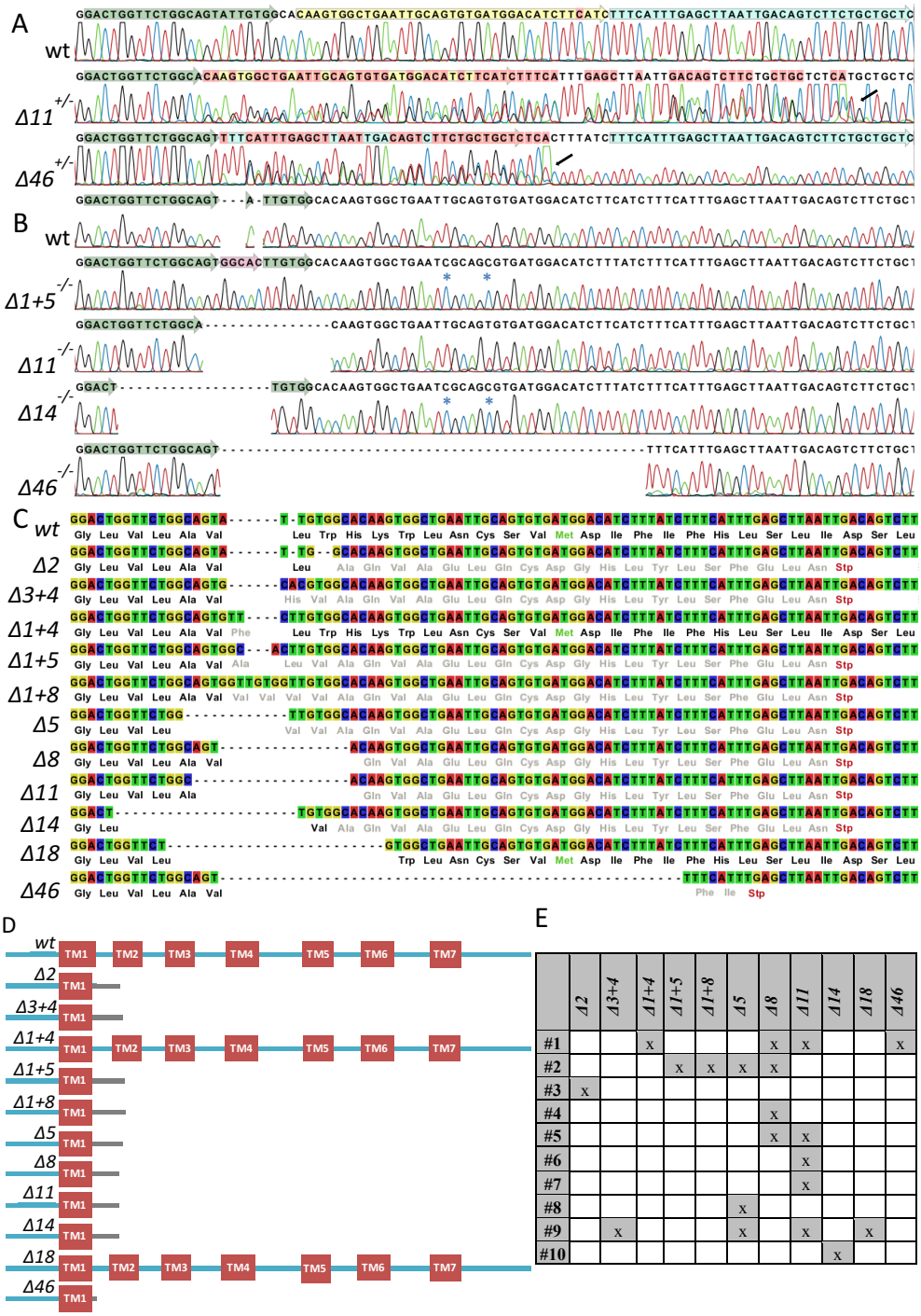

Figure 5. Identification and selection of *cxcr3.3* mutations *(Legend on the next page)*.

Figure 5. Identification and selection of *cxcr3.3* mutations *(Figure on the previous page)*. **A.** Double-peaked reads of heterozygote carriers. When compared to wt, heterozygote mutant carriers display double peaks from the start of the mutation sequence onwards. At each nucleotide position, the double read is due to the nucleotide read of the wt allele and the nucleotide read of the mutant allele, meaning that the mutation type can be identified by subtracting the wt sequence from the double-peaked read. Mutant *Δ11* displays a wt-subtracted read that matches the wt sequence 11 nucleotides downstream the start of the mutation (yellow label), indicating that the mutant carrying this alteration has a deletion of 11 nucleotides. Mutant *Δ46* displays a wt-subtracted read that matches the wt sequence 46 nucleotides downstream the start of the mutation (blue label), indicating that the mutant carrying this alteration has a deletion of 46 nucleotides. Black arrows at the end of the mutant sequences indicate where the shorter mutant allele sequence has terminated, due to the end of the amplicon. Upon this position only the longer wt sequence is read, therefore, the sequence appears again single-peaked. **B.** Sequence alignment of confirmed homozygote mutants, generated from incross of heterozygote carriers of the same mutation. Blue asterisks indicate nucleotides that are naturally polymorphic in the wt population. **C-D.** Alignment of all identified mutations and their consequence at protein level. In D, red boxes indicate the predicted transmembrane helices, regions in grey indicate sequences that diverge from the wt sequence (translation of inserted nucleotides and of frame-shifted coding sequences). Notably *Δ1+4* and *Δ18* mutations would lead to in-frame mutant variants, with 3 additional amino acids or 6 deleted amino acids at the end of the TM1 domain, respectively. All the other mutations would generate frameshifts and premature protein truncation. **E.** Analysis of the offspring of 10 *cxcr3.3* F0 founders (#1-#10). Several F0 can transfer multiple kinds of mutations to their offspring (crosses), indicating that biallelic targeting and alternative mechanisms of damage repair/delayed targeting contribute to the generation of alternative mutant alleles. Data also show that some individual founders carry identical mutations, suggesting that preferred types of mutations are mediated by CRISPR/Cas9 targeting.

The profile of the F1 generation from different founders also suggested that preferred mutations may occur. For example, specific mutations (*Δ5*, *Δ8* and *Δ11*) occurred in more independent founders (3/10, 4/10 and 5/10 respectively). Additionally, 6/10 independent founders carried at least one large (>10 dNTPs) mutation, which are particularly useful to permit a simple procedure for genotyping by PCR and gel electrophoresis.

Mutation of *cxcr3.3* does not alter development and survival of homozygote mutants, but affects *M. marinum* infection burden

Among the identified mutations we selected the non-sense *cxcr3.3Δ46* and the *cxcr3.3Δ11* alleles to further investigate the function of *cxcr3.3*. These mutations were chosen since they were transmitted with high frequency from the F0 founder to its heterozygote offspring, which enabled to timely obtain sufficiently-sized and properly mating isogenic families. Additionally, since these mutations consist of > 10 bp deletions, genotypes could be distinguished using PCR and gel electrophoresis. Heterozygote carriers of *cxcr3.3Δ46* and of *cxcr3.3Δ11* mutations were incrossed with isogenic mutation carriers to obtain homozygote mutant, heterozygote and homozygote wt offspring, which was raised to adulthood as mixed families. We found that in both families *cxcr3.3* mutants maintained Mendelian proportions with the other genotypes, therefore we concluded that *cxcr3.3* mutation is viable and does not confer a major disadvantage to the carriers (**Figure 6A-B**). Phenotypic inspection of embryos and larvae also did not reveal any significant developmental differences between mutant and wt siblings. Adult homozygote mutants were fertile and could produce viable offspring. To address whether *cxcr3.3* may have a function in controlling the immune response, we injected mutant and wt (either derived from heterozygote incross or from homozygote mutant and wt siblings incrosses) at 1 dpf with the fish pathogen *Mycobacterium marinum* (*Mm*). At 4 dpi both *cxcr3.3Δ46* and *cxcr3.3Δ11* mutant larvae displayed a significantly higher infection burden than their wt

counterparts, indicating that *cxcr3.3* mutation is detrimental to combat mycobacterial infection (**Figure 6C-F**). This phenotype is opposite to that previously described for a *cxcr3.2* mutant, which shows an attenuated formation of granulomatous lesions and increased resistance to *Mm* infection[9]. In view of the opposing infection phenotypes of these two receptor mutants, we analysed the infection burden evoked by *Mm* in larvae exposed to NBI74330, an antagonist of CXCR3 that, based on binding pocket similarity should inhibit both Cxcr3.2 and Cxcr3.3 in zebrafish (**Figure 6F-G**). Treatment with this compound revealed a *cxcr3.2* mutant-like phenotype and a reduction of mycobacterial infection burden (**Figure 6H**).

Cxcr3.3 in zebrafish and other teleosts displays sequence features common to atypical chemokine receptors

While further in-depth characterisation of *cxcr3.3* mutants is still necessary to fully understand the function of the Cxcr3.3 receptor and its crosstalk with Cxcr3.2, we used computational sequence analysis to examine whether the opposing functions of these receptors in controlling mycobacterial infection could have a structural basis. We found that, when compared to human CXCR3 and zebrafish Cxcr3.1 and Cxcr3.2, Cxcr3.3 displays specific amino acid substitutions. In particular, the DRY sequence (Asp-Arg-Tyr), an extremely conserved motif that permits coupling of the chemokine receptors to the heterotrimeric G-proteins, contains an R (Arg) to C (Cys) replacement (**Figure 7**, **Supplementary Figure 1**)[56].

The R of the DRY motif is the most conserved residue of functional G-coupling GPCRs and presents 100% conservation among typical human CXC receptors (CXCR1-2-3-4-5-6-8). Replacement of this residue is known to abolish transduction of heterotrimeric G-protein signalling in chemokine receptors[57], as this amino acid is believed to interact directly with the G subunits to catalyse GDP release and therefore serves as an effector for G-protein activation[58,59]. Alteration of the DRY consensus is recurrent in atypical chemokine receptors (ACKRs; > 71% of the cases in humans) and in related GPCRs, such as viral GPCR-like seven transmembrane proteins or atypical anaphylotoxin receptors. Examples in humans are DARC/ACKR1 (DRY to GHR), D6/ACKR2 (DRY to DKY), CCRL2/ACKR5 (DRY to QRY), PITPNM3/ACKR6 (DRY to SSR) and C5L2 (DRY to DLC, a decoy interceptor for the anaphylotoxin C5a). Exceptions are represented by CXCR7/ACKR3 and CCRL1/ACKR4, whose DRY sequences are not divergent, and in which failure of G-protein activation is most likely due to the replacement of other residues of the so-called micro-switch elements that permit transition of the GPCR from the inactive to the active form[60,61]. Notably, several replacements in the micro-switch elements are present also specifically in Cxcr3.3, when compared to its human and zebrafish orthologues (**Figure 7**).

To further dissect whether the existence of an atypical Cxcr3 is an exclusive prerogative of zebrafish, we analysed the sequence of the CXCR3 proteins derived from 19 vertebrate genomes (11 fish, 1 amphibian, 2 reptiles, and 5 mammals). We found that, while in tetrapods the R residue of CXCR3 is 100% conserved, in 82% of the fish species analysed here at least one Cxcr3 isoform displays an R residue substitution.

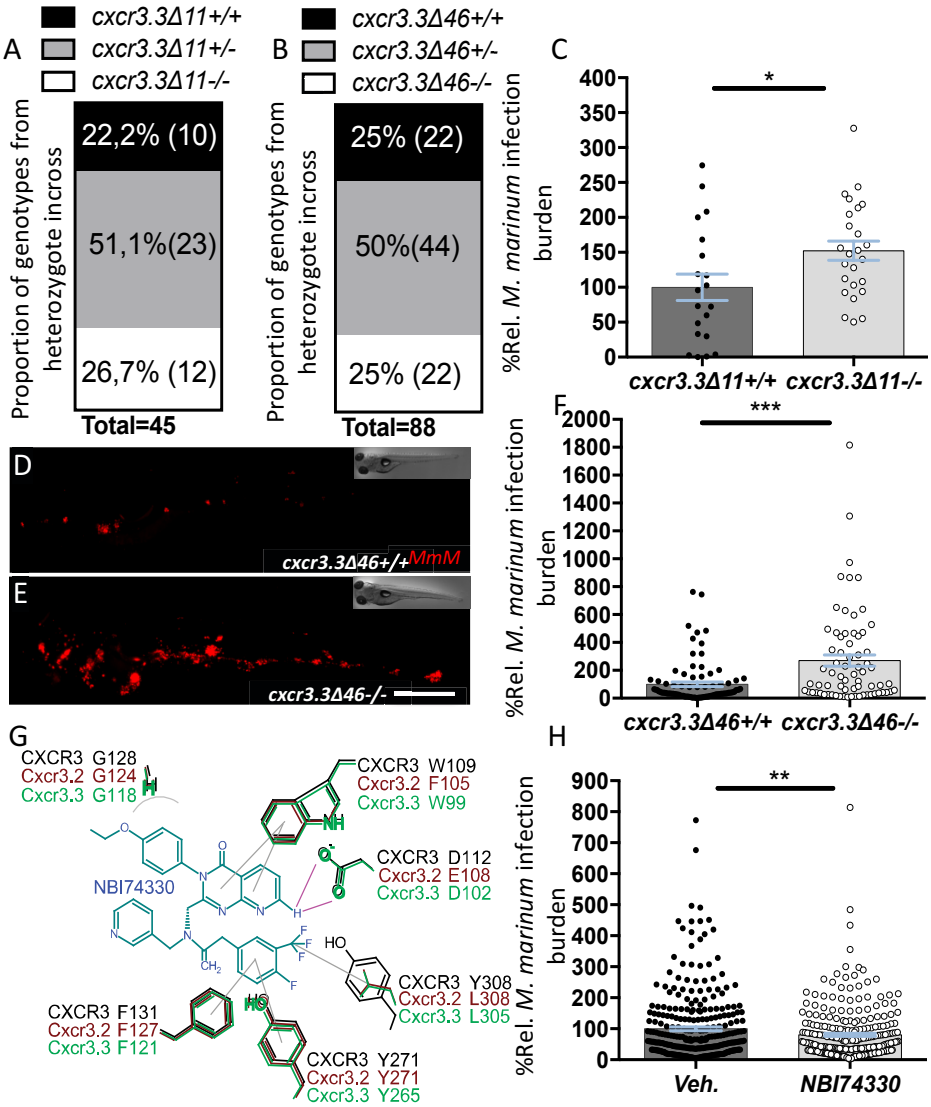

Figure 6. Characterisation of *cxcr3.3* mutants. A-B. Mendelian segregation of *cxcr3.3Δ46* and *cxcr3.3Δ11* mutant alleles. Families derived from incross of heterozygote carriers for one or the other mutation did not display deviation from Mendelian genotype ratios at the sexually mature age, indicating that *cxcr3.3* mutant alleles do not affect survival. **C-F.** Quantification (% relative to wt) of *Mm* infection burden at 4 dpi in *cxcr3.3Δ11* (C) and *cxcr3.3Δ46* (F) mutant and wt siblings. 28-30 hpf embryos were infected with 100-200 CFU of *Mm*. Representative pictures of infected wt and mutant larvae are shown in D-E**.** Data in C derive from 1 replicate. Data in F derive from three cumulated experiments. **G.** NBI74330 binding pocket of CXCR3, Cxcr3.2 and Cxcr3.3. Key amino acid residues are conserved, suggesting that this drug can antagonise both the human and the two zebrafish receptors. **H.** Quantification (% relative to vehicle DMSO, veh.) of *Mm* infection burden at 4 dpi in 25 µM NBI74330 and DMSO (Veh.)-treated group. 28-30 hpf embryos were infected with 200-250 CFU of *Mm*. Data are cumulative from three replicates. Treatment with NBI74330 mimics *cxcr3.2* phenotype and not *cxcr3.3* phenotype. Each data point in C, F, H represents a single individual. Error bars: mean±s.e.m. Scale bar: 500 µm.

Notably, as in the case of zebrafish Cxcr3.3, polymorphisms in the DRY sequence of Cxcr3 isoforms in other fish are also linked to the substitution of micro-switch elements (**Figure 8**). In one of the two fish species (Cod) where no DRY-altered isoforms are observed, several micro-switches are still present in one of the isoforms, which would, therefore, suggest that in this organism one of the Cxcr3 isoforms is also atypical (**Figure 8**). It must be noted that two tetrapod sequences also displayed alteration of the DRY sequence, although not of the R residue. (DRY to ERY and DRY to NRY). Synonymous D/E change (present in the anole lizard Cxcr3.2) is frequently observed in other GPCRs and is generally not thought to alter G-protein signal transduction[58].

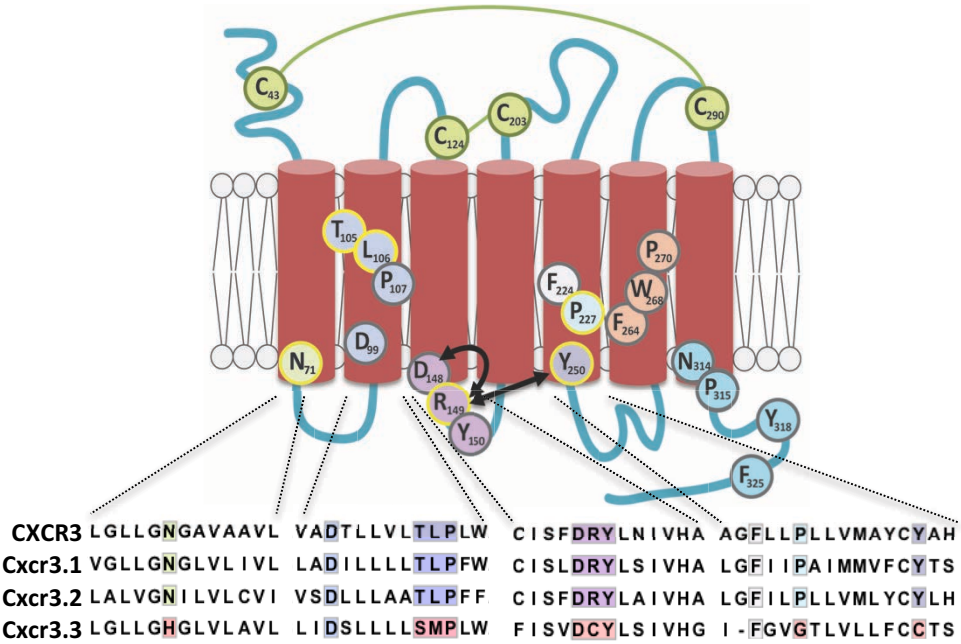

Figure 7. Cxcr3.3 displays replacement of several amino acids fundamental to G-protein-dependent signal transduction. Compared to its zebrafish homologues, Cxcr3.3 has several sequence alterations which suggest it might function as an atypical chemokine receptor. The TLP sequence (105-107) is known to be important for stabilisation of micro-conformational switches to transduce signalling upon binding to the chemokine ligand and is replaced with SMP in Cxcr3.3. The DRY (148-150) sequence and the Y_{250} are fundamental for the interaction and activation of the G-proteins. In the inactive state, R_{149} interacts with D_{148}, while in the active conformation R_{149} interacts with Y_{250} and G-proteins. R_{149} represents the most conserved residue among active chemokine receptor and is changed to C in Cxcr3.3. Similarly, Y_{250} is also highly conserved and substituted with a C in Cxcr3.3. Virus-encoded 7TM receptors and most of ACKRs, such as ACKR1-2-5, have altered DRY motifs, explaining their inability to mount classic chemotactic signals and their altered biological activities. Notably, Cxcr3.3 has also a replacement of N_{71} and P_{227} with H and G respectively. In chemokine receptors from different species these two residues represent the most conserved residues of TM1 and TM5, respectively, and they possibly also exert important functional roles in conformational changes and signal transduction. Amino acids circled in yellow are key residues that are specifically substituted in Cxcr3.3 when compared to its human and zebrafish homologues. Subscript positional numbers of the amino acid residues represent the progressive numeration of residues according to the human canonical CXCR3 isoform.

The non-conservative D/N replacement (present in xenopus Cxcr3.2) has been reported to abrogate chemokine signalling in some studies on other receptors[62]. However, no other micro-switch substitutions were associated with this Cxcr3 isoform, which therefore is most likely phylogenetically homologous to the typical Cxcr3 receptors. Overall, our study suggests that early in teleost evolution an alternative atypical *cxcr3* gene evolved, a feature that is currently maintained in a variety of modern fish species, but lost during the radiation of higher vertebrates.

Based on the fact that Cxcr3.3 receptors has an evolutionarily conserved alteration of the DRY motif and of regulative micro-switch elements, we propose that this receptor may antagonise the canonical Cxcr3 isoforms by competing for ligands. Changes in the DRY and in micro-switches do not generally alter the ligand binding domains and their capability to efficiently bind ligands. However, the expression of this atypical isoform may, in turn, reduce the possibility for Cxcl11 ligands to bind and signal via their classical receptors, therefore modulating the levels of signals evoked in the stimulated cells. In the context of mycobacterial infection, where depletion of canonical signalling via Cxcr3.2 is beneficial to the host, depletion of *cxcr3.3* could translate instead into an exuberant exploitation of Cxcr3.2 signalling with, in turn, detrimental effects on the host.

DISCUSSION

By using *cxcr3.3* targeting as a case study, we have set up a simple and fast protocol for efficient CRISPR/Cas9 mutagenesis in zebrafish (**Graphical protocol**). This method uses the synthesis of a dsDNA template by annealing, PCR filling and amplification of two semi-complementary 81-mer oligonucleotides. This DNA amplicon serves as a template for the shgRNA *in vitro* transcription. Upon transcription of the shgRNA and of a zebrafish-optimised NLS-Cas9-NLS mRNA, the two components can be coinjected into zebrafish embryos at the 1-cell stage. Target efficiency can be detected by Sanger sequencing of injected individuals, according to the emergence of secondary reads in the electropherogram within the target site. ShgRNAs that do not yield high targeting efficiency can be discontinued, while highly efficient targets can be injected in a larger egg batch for culturing. The selected target that we used to obtain *cxcr3.3* mutants, yielded over 70% efficiency in adult germ-line transmitted gene editing and required screening of as few as 10 F0 positive individuals to identify several large (> 10 dNTPs) mutations, which allowed easy detection of genotypes by PCR and gel electrophoresis. From the analysis of the F1 generations we found that our targeting method led to biallelic editing and that other mechanisms of independent attempts of repair/delayed targeting also contributed to the generation of alternative genome modifications. This translated into a high percentage (40%) of F0 founders carrying more than one mutation in their germ-line.

The high yield and the biallelic targeting of this strategy also imply that this approach might be explored as an alternative to morpholino-based transient knockdown, with the advantages that CRISPR/Cas9 constructs are more affordable in terms of costs, do not evoke morpholino-dependent toxicity phenotypes, and their targeting leads to stable gene mutations which denotes that their effect would not reduce in time by dilution and degradation.

Figure 8. Atypical Cxcr3 isoforms are recurrent in fish. Alignment of CXCR3 proteins in vertebrates. Most of the fish species analysed have at least 3 copies of CXCR3. With the exception of cod (gmo) and tetraodon (tni), the other species have at least one isoform where the DRY sequence has been modified in the conserved R_{149} residue. In most species, Cxcr3.3 presents also a replacement of the conserved Y_{250}, C_{290} and N_{314} residues. Y_{250} interacts with R_{149} during receptor coupling with the G-proteins. Therefore, it is likely that also in cod the Cxcr3.3 isoform, despite the DRY consensus, is unable to function due to Y_{250} replacement. In spotted gar (loc), only a DRY-disrupted Cxcr3.3 isoform is currently known. However, a functional Cxcr3 could exist in this species and might remain unidentified due to poor quality of the genome sequence in the *cxcr3* locus[63]. Amphibians and reptiles have one or two copies of CXCR3. In xenopus (xtr) and the anole lizard (aca), the DRY sequences of one of the two isoforms have been modified into NRY and ERY, respectively. These changes are predicted to impact less severely on the receptor coupling to G-proteins. Additionally Y_{250}, C_{290} and N_{314} remain conserved, suggesting that these isoforms may be functional and non-homologous to fish Cxcr3.3. In mammals, *CXCR3* is present as a single classical isoform. Legend: aca: *Anolis carolinensis* (anole lizard); ame: *Astyanax mexicanus (*cave fish); bta: *Bos taurus* (cow); dre: *Danio rerio* (zebrafish); gac: *Gasterosteus aculeatus* (stickleback); gmo: *Gadus morhua (*cod); hsa: *Homo sapiens* (human); laf: *Loxodonta africana* (elephant); loc: *Lepisosteus oculatus (*spotted gar); mus: *Mus musculus* (mouse); ola: *Oryzias latipes* (medaka); oni: *Oreochromis niloticus* (tilapia); psi: *Pelodiscus sinensis* (Chinese softshell turtle); pfo: *Poecilia formosa (*amazon molly); tni: *Tetraodon nigroviridis* (tetraodon); tru: *Takifugu rubripes* (fugu); xma: *Xiphophorus maculatus (*platyfish); sha: *Sarcophilus harrisii* (Tasmanian devil); xtr: *Xenopus tropicalis* (western clawed frog). Sequences were all obtained from Ensembl database.

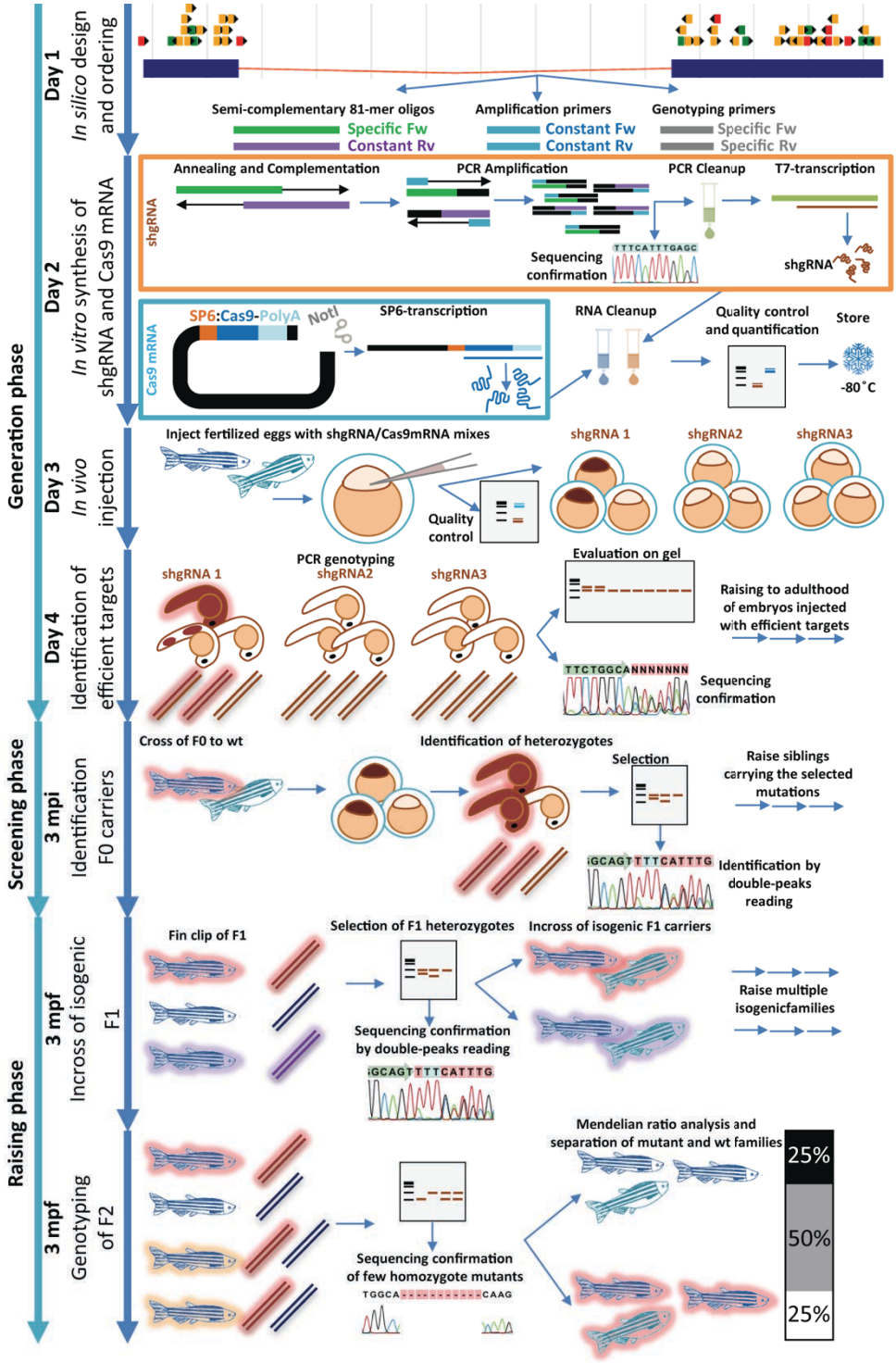

Graphical protocol *(Legend on the next page)*.

Graphical protocol *(Figure on the previous page)***.** The first phase to generate a CRISPR knockout zebrafish line consists in the *in silico* design and ordering of custom-made oligonucleotides, which will be used as a template to synthesise the shgRNA *in vitro* (81-mer semicomplementary oligomers and template amplification primers), or to genotype the animals via PCR and sequencing (genotyping primers). Different online tools are available to select suitable CRISPR targets and suitable genotyping primers. The left 81-mer oligonucleotide contains the T7 promoter sequence (necessary to initiate the RNA transcription once the template has been produced) followed by the CRISPR target sequence and part of the invariable sequence of the shgRNA. The right 81-mer oligonucleotide contains the complementary sequence to the terminal region of the left 81-mer and the remaining part that completes the invariable shgRNA sequence. The two oligos can anneal with each other and the shgRNA template can be filled by a few PCR cycles. To produce a quantitative amount of template, this product requires further PCR amplification using short constant primers that anneal to the termini of the product (T7 sequence and extremity of the invariable shgRNA sequence). Once the amplicon has been cleaned up and confirmed by sequencing, it can be used as a DNA template to produce the shgRNA. Simultaneously, also the Cas9 mRNA can be *in vitro* transcribed from a NotI-linearised plasmid template. The two mRNAs require column clean up, gel-electrophoresis and nanodrop quality control and quantification. Single-use aliquots of both RNAs can be stored for undefined time at -80°C. A mix of shgRNA and Cas9 mRNA can be injected into zebrafish fertilised eggs. Different shgRNA (shgRNA1, 2 and 3) may be injected side by side, to maximise the chance of identifying an efficient target site. From 24 hours post fertilisation, dechorionated embryos can be sacrificed for PCR genotyping, in order to verify successful genome editing and to estimate the targeting efficiency. The most efficient target can be injected on a larger scale to raise a family of potential founders (F0). F0 carriers can be screened as early as three months post injection (mpi), by single backcrosses to wt animals. The mutations will be transferred to part of the offspring in heterozygosis. Because the wt sequence is known, the exact mutations carried by each founder can be extrapolated from the double peak sequencing reads of their heterozygote offspring. The preferred mutations (e.g. large deletions generating a frameshift) can be selected for further characterisation. Since a single F0 founder has been shown to frequently transfer multiple mutated alleles to its offspring, it is likely that an F1 family will consist of a mixed population of animals carrying various mutations of the target gene. The different alleles can be distinguished by DNA extraction and genotyping from the fin clip. Isogenic founders can be pooled together to generate isogenic F1 families, carrying only one kind of mutation. Finally, at three months post fertilisation (mpf) these families (that consist exclusively of heterozygotes) can be incrossed to obtain homozygote mutants, wt and heterozygotes (F2). The ratio between the genotypes in F2 can be used to assess whether the mutation affects the survivability of the animals. Sibling families of homozygote mutants and wt can be kept as breeding colonies to collect embryos of known genotypes for experiments.

Using the CRISPR/Cas9 editing system we obtained several stable mutant lines of *cxcr3.3* and performed an initial characterisation of them. Under physiological conditions, we did not observe any advantage/disadvantage in carrying a *cxcr3.3* mutant allele, in either heterozygotes or homozygotes. However, we found that infected mutant individuals display an increased susceptibility to the pathogen *Mm*, which indicates an underlying function of Cxcr3.3 in the control of mycobacterial infection. We currently do not know the exact mechanisms by which Cxcr3.3 is required to respond to mycobacteria and further analysis is needed. Strikingly, the phenotype of this mutant in control of mycobacterial infection differs from that of the *cxcr3.2* mutants, which display a reduced susceptibility to the same pathogen[9]. A possible hypothesis, confirmed by structural predictions is that Cxcr3.2 and Cxcr3.3 antagonise each other by ligand competition and/or induction of alternative transduction signals. Several chemokine receptors have been shown to antagonise or synergise each other[64]. ACKRs, for example, are seven transmembrane receptors homologous to chemokine GPCRs that have a modified or missing canonical DRY motif within the second intracellular loop, which makes them unable to couple to G-proteins and induce the full spectrum of "classical" GPCR signalling and cellular

responses, including cell migration[65,66]. Several mechanisms by which ACKRs influence the responses to chemokines have been shown. D6/ACKR2, for example, is an ACKR for a wide array of CC chemokines. Upon binding to these ligands, the ligand-receptor complex is internalised and transferred to late endosomes. Here the ligands dissociate and are degraded by endolysosome maturation, while the receptor is recycled and re-expressed at the plasma membrane. This mechanism allows D6/ACKR2 to scavenge CC chemokines and reduce binding to their canonical G-protein coupled receptors[67].

CXCR7/ACKR3 is another member of the atypical chemokine receptor group, which cannot couple to G-proteins, despite still being able to bind β-arrestin and transmit MAPK-mediated signalling to some extent[60,64]. The zebrafish model has helped to elucidate the role of CXCR7 in the scavenging of CXCL12 ligand, thereby controlling the formation of a CXCL12 gradient which permits optimal migration. While binding of CXCL12 to CXCR4 transmits active chemokine signalling, binding of the same ligand to CXCR7 does not elicit G-coupled signal transduction. This translates into a reduced ligand binding to CXCR4 and therefore to an attenuated activation of the CXCR4-dependent cascade. This mechanism has been shown in zebrafish and mammals to finely control the direction of cell migration, as CXCR4 and CXCR7 are expressed with different expression dynamics and patterns (e.g. they mature and reside at the membrane with different timings)[6,68]. Additionally, similar to D6/ACKR2, CXCR7/ACKR3 sequesters CXCL12 and mediates its intracellular degradation[69].

Even "classical" chemokine receptors when simultaneously expressed may interfere with each other. Heterodimerisation of GPCRs is a well-known process. Several studies suggest that particular combinations may affect the receptor conformations and lead to dampened capability to bind ligands or to transduce signalling. Expression of chemokine receptors in absence of their ligands can also interfere with the signalling of other receptors whose ligands are present, when both are expressed by the same cell. Consuming/sequestering intracellular signalling molecules (e.g. β-arrestin or heterotrimeric G complexes, which are associated with resting receptors in unstimulated conditions) can in fact uncouple the antagonised receptor from its downstream signalling machinery[70].

Sequence alignment of zebrafish and human CXCR3 receptors indicates that the key DRY motif required to couple with heterotrimeric G-protein complexes is altered in Cxcr3.3, while Cxcr3.1 and Cxcr3.2 maintain an intact consensus sequence. Replacement of R with C in Cxcr3.3 suggests that this receptor belongs to the group of atypical chemokine receptors. In line with this theory it is possible that depletion of c*xcr3.3* would increase the availability of Cxcl11 ligands for Cxcr3.2, therefore inducing an enhanced (and detrimental for the host) Cxcr3.2-dependent signalling. Consistent with this hypothesis, the CXCR3 antagonist NBI74330, predicted to inhibit both Cxcr3.2 and Cxcr3.3, evokes an infection phenotype similar to that of *cxcr3.2* mutation, which means that Cxcr3.3 blockade cannot be detrimental if Cxcr3.2 signalling is also simultaneously depleted. That similar dynamics take place *in vivo* during mycobacterial infection is already indicated by a recent study on D6/ACKR2 knockout mice, which showed that these animals are more susceptible to mycobacterial infection, due to the increased number of monocyte/macrophages, DCs and T cells infiltrated in the lesioned tissues. Blockade of several chemokines with a combination of antibodies could rescue the phenotype of D6 deficiency, which suggests that the activity of D6/ACKR2 as a chemokine scavenger receptor is fundamental to maintain a balanced activation of leukocyte recruitment via the chemokine signalling[71].

Notably, interference with Cxcr3.2/Cxcr3.3 signalling might not act exclusively at the level of ligand-competition, since we also have previously found that *cxcr3.3* expression is controlled (at least in macrophages) by expression of *cxcr3.2*, as macrophages from *cxcr3.2*-deficienct larvae displayed a 1.5-fold decrease of *cxcr3.3* expression too[40]. This is particularly intriguing considering that not only did *cxcr3.2* control *cxcr3.3*, but also several genes for Cxcl11 ligands (Cxcl11aa-af-ag), whose expression in macrophages was 2-to-3-fold reduced in *cxcr3.2* mutants[40]. Functional signal transduction assays for Cxcr3.3 and analysis of *cxcr3.2-cxcr3.3* double mutant phenotypes will help to understand the exact interactions at play between these two paralogues.

It is noteworthy that, besides modifications in structural motifs required for G-protein activation, the preferential cellular expression and/or intracellular localisation may represent another aspect of Cxcr3.2/Cxcr3.3 biology contributing to their ability to activate G-protein-dependent signalling. Regarding cell specificity, both genes are expressed in macrophages and neutrophils. However, *cxcr3.2* is expressed more predominantly by macrophages, while *cxcr3.3* is more highly expressed by neutrophils[9]. This may result in a differential (cell-specific) ratio of receptor copies available for ligand binding in the two cell subsets. This may also explain why *cxcr3.2* mutation, despite the gene being expressed by both macrophages and neutrophils, displayed predominantly a macrophage phenotype rather than an effect on neutrophils. Injection of Cxcl11aa-af ligands, for example, could elicit significant macrophage recruitment, while neutrophil chemoattraction was comparable to mock-injected individuals[9]. This observation might indicate that the scavenging activity exerted by Cxcr3.3 in neutrophils reflects weak activation of G-protein signalling by Cxcl11 ligands in these cells, insufficient to support cell migration. In contrast, predominant expression of *cxcr3.2* over *cxcr3.3* in macrophages might permit sufficient active signal to sustain chemotaxis. Taken together, the generation and characterisation of the zebrafish *cxcr3.3* mutant line has provided more information on the translational utility of this model for biomedical research. Furthermore, it may also shed light on the evolution of typical and atypical chemokine receptors and on the selective forces acting on the immune system genes that, by duplication and functional specialisation, permitted the evolution of complex regulative mechanisms to tightly control biological processes.

MATERIAL AND METHODS

Synthesis of shgRNA – Primers and oligos up to 81 nucleotides were obtained from Sigma-Aldrich, using standard synthetic procedures (25 nmol synthesis scale, purification via desalting method). The 122-base template oligonucleotides were ordered from Integrated DNA Technologies (1 nmol synthesis scale, purification via PAGE Ultramer method), since the nucleotide length exceeds the maximum sequence length supported by Sigma-Aldrich and standard synthetic procedures. Sequences are reported in **Supplementary Table 1**. DNA template synthesis for the three methods described above was performed as follows.

In Method 1, the 122-mer oligos and the T7 promoter primer were suspended in TES buffer (10 mM Tris-HCl, pH=8, 1 mM EDTA, 0.1 M NaCl) to a 100 μM concentration. Before *in vitro* transcription, an equimolar amount (1:1 volumes, 50 μM each) of the 122-base oligo and of the T7 promoter primer were mixed. Annealing was obtained by

transferring the solution to a 95^{0}C water bath. After 1 min, the bath was switched off and let cool down to room temperature (about 30 minutes). The annealed mixture was then transferred to ice, diluted 10x with RNAse-free water and used as a template for *in vitro* transcription.

In Method 2, the 122-mer oligos were suspended as in Method 1 (100 µM in TES buffer) and 1 ng was used as a template in a PCR reaction (50 µl reaction, 200 µM dNTPs, 1 unit DreamTaq polymerase (Thermo Fisher Scientific), initial denaturation 95^{0}C/3 min 35 amplification cycles 95^{0}C/30 s, 55^{0}C/60 s, 72^{0}C/30 s, final extension step 72^{0}C/15 min), using template amplification primers as reported in **Supplementary Table 1** (0.5 µM each). The PCR product was column-purified using a PCR clean-up combo kit (Invitrogen), eluting the product in 20 µl of RNase-free water, and the expected size was checked by gel electrophoresis.

In Method 3, semi-complementary 81-mer oligo pairs (0.04 µM each) were annealed together and the product was completed by a short PCR program (50 µl reaction, 200 µM dNTPs, 1 unit DreamTaq polymerase, initial denaturation 95^{0}C/3 min, 5 amplification cycles 95^{0}C/30 s, 55^{0}C/60 s, 72^{0}C/60 s, final extension step 72^{0}C/15 min). The mix was removed from the thermocycler, maintained at room temperature, supplemented with template amplification primers as in Method 2 (0.5 µM each), and then returned to the thermocycler for further amplification (initial denaturation 95 ^{0}C/3 min, amplification 35 cycles 95^{0}C/30 s, 55^{0}C/60 s, 72^{0}C/30 s, final extension step 72^{0}C/15 min). The product was then purified by column clean-up as in Method 2. When running the PCR reaction using only one 81-mer oligo as a negative control we have frequently observed amplification at comparable size of the expected product of a complete reaction. This was most likely due to the existence of self-complementary stretches in the oligos. However, secondary reactions did not occur when both oligos were provided, as demonstrated by Sanger sequencing of the amplicons.

***In vitro* transcription of shgRNA** – For *in vitro* transcription of shgRNA, we used the MEGAshortscript T7 kit (Invitrogen) and 2530 fmols of template DNA (corresponding to 100 ng of ssDNA annealed to T7 primer for Method 1 and to 200 ng of PCR-derived dsDNA for Method 2 and 3). Purification of the shgRNA was achieved using the miRNeasy isolation kit (Qiagen) according to manufacturer's guidelines and eluting 2x10 µl in RNase-free water. Efficiencies for each method are reported in **Table 2**. Concentration was measured by nanodrop and integrity was checked by non-denaturing 2% gel electrophoresis and RNA-chip (RNA 6000 Pico kit, Agilent technologies) on 2100 Expert bioanalyzer (Agilent Technologies). The shgRNA may appear on the non-denaturing gel as a single or double band, depending on temperature and on how delayed the running of the gel is from the column elution. When maintained at room temperature the shgRNA formed two bands, with a more intense one at lower molecular weight. If the RNA was warmed to > 55^{0}C and immediately loaded, it appeared as a single band coinciding with the lowest molecular weight size. Most likely the secondary band, seen when shgRNA is maintained at RT, represents a dimeric form or an alternative conformational structure. For the purpose of storage, shgRNA was aliquoted and stored at -80^{0}C.

Preparation of Cas9 mRNA – Several versions of engineered Cas9 are currently available. For this study, we opted for a zebrafish-codon optimised Cas9 version derived

from *S. pyogenes*. The Cas9 we used was also engineered to contain (at both its amino and carboxyl termini) a Nuclear Localisation Signal (NLS) derived from the SV40 large T-antigen sequence, which would facilitate translocation of the protein to the cell nucleus. The plasmid used was previously described in reference[15]. In this plasmid, the Cas9 coding sequence is cloned downstream of the SP6 promoter and upstream of an SV40 polyadenylation site and a NotI unique restriction site, which is used for plasmid linearisation prior to *in vitro* transcription. The plasmid was purified using an EndoFree Plasmid Purification (Maxi prep) kit (Qiagen) from 100 ml of O/N culture, and according to manufacturer's guidelines. Total plasmid DNA was suspended in 700 µl and quantified as approximately 1 µg/µl concentration. 25 µg of DNA were linearised with 0.2 units/µl of NotI (New England BioLabs) in 1x NEB Buffer 3.1 for 2 h at 37^{0}C in a 200 µl reaction. Complete digestion was assessed by 1% agarose gel electrophoresis. The linearised plasmid was purified by precipitation by Sodium Acetate/EtOH method. The pellet was washed with 70% EtOH, air-dried and resuspended in 50 µl RNase-free water. The Cas9 mRNA was then synthesised using the mMESSAGE mMACHINE SP6 kit (Invitrogen), according to the manufacturer's guidelines and using 1 µg of purified linearised plasmid as a template for a 20 µl reaction. The mRNA was then column-purified using the RNeasy MiniElute Cleanup kit (Qiagen), eluted in 20 µl (2x10 µl) of RNase-free water and quantified by Nanodrop as approximately 1 µg/µl. The integrity of RNA was assessed by 2% non-denaturing agarose gel electrophoresis, on which Cas9 mRNA appeared with two discrete bands. Single use 2 µl aliquots of 1 µg/µl Cas9 mRNA were stored at -80 ^{0}C.

Zebrafish lines and maintenance – Zebrafish lines were handled in compliance with the local animal welfare regulations and maintained according to standard protocols (zfin.org). The breeding of adult fish was approved by the local animal welfare committee (DEC) of the University of Leiden (license number: 10612) and adhered to the international guidelines specified by the EU Animal Protection Directive 2010/63/EU. Adult zebrafish were not sacrificed for experiments. Fish lines used in this work were the following: wt strain AB/TL and *Tg(fli1a:eGFP^{y1})*[45]. Anaesthesia of embryos/larvae used for live imaging was achieved with 0.02% buffered Tricaine (3-aminobenzoic acid ethyl ester, Sigma-Aldrich) in egg water.

shgRNA/Cas9 microinjections – To assess efficiency and toxicity, eGFP-shgRNA and Cas9 mRNA were mixed and injected at different concentrations, as described in the results section and in **Figure 4**. For generation of the *cxcr3.3* mutant lines, 1 nl of 150 pg of Cas9 mRNA and 150 pg of *cxcr3.3*-shgRNA Target C was considered optimal as this did not lead to toxic/phenotypic effects or major lethality. Injections were performed in the cell of fertilised eggs at 5-10 minutes post fertilisation. Left over mix from the injection needle was run on 2% non-denaturing agarose gel to control integrity during the injection phase. The mix would segregate into 4 bands, 2 corresponding to the Cas9 mRNA and 2 corresponding to the shgRNA.

Genotyping – Genotypes were assessed by PCR using the primers reported in **Supplementary Table 1**, extracting genomic DNA from 1-2 dpf embryos or fin clips of > 6 week-old juveniles/adults. Successful injections were confirmed by Sanger sequencing (Baseclear or Macrogen, The Netherlands). Mutations were identified from heterozygote F1 fish by agarose gel electrophoresis (2-4%) and confirmed by Sanger sequencing from heterozygotes or F2 homozygotes.

Survival analysis – Heterozygotes carrying the same mutation were incrossed to generate homozygote mutants, wt and heterozygotes. The mixed family was cultured to sexual maturity and then genotyped by PCR/gel electrophoresis. No significant divergence from Mendelian proportions was observed in the genotype rates (assessed by chi-squared test).

Infection burden – Homozygote mutants and wt, derived either from heterozygote parents or from homozygote siblings incross, were injected via the blood island at 28-30 hpf with 100-250 CFU of mCherry-labelled *Mycobacterium marinum* M strain. Infection burden was quantified at 4 dpi by fluorescent pixel enumeration as previously described[9]. Significance was assessed by Mann-Whitney test (**Figure 6 C**) and with unpaired t-test with Welch's correction for data with different variances (**Figure 6F,H**). *P<0.05; **P<0.01; ***P<0.001. Error bars: mean±s.e.m.

ACKNOWLEDGEMENTS

We thank Anna-Pavlina Haramis and Rui Zhang for the discussions and the collaboration in setting up the CRISPR/Cas9 technology.

This work was supported by the Smart Mix Program of the Netherlands Ministry of Economic Affairs and the Ministry of Education, Culture and Science, the European Commission 7th framework project ZF-HEALTH (contract number HEALTH-F4-2010-242048), and the European Marie-Curie Initial Training Network FishForPharma (contract number PITN-GA-2011-289209).

Name	Target	Sequence (5'-3')	Method	Short description
eGFP 121-mer	eGFP	GATCCGCACCGACTCGGTGCCACTTTTTCAAGTTGATAACGGACTAGCCTTATTTTAACTTGCTATTTCTAGCTCTAAAACCCGGCAAGCTGCCCGTGCCCCTATAGTGAGTCGTATTACGC	1 and 2	Full length ssDNA oligos used for direct *in vitro* transcription (Method 1) or for generation of PCR templates for shgRNA transcription (Method 2)
cxcr3.3 Target A 122-mer	*cxcr3.3*	GATCCGCACCGACTCGGTGCCACTTTTTCAAGTTGATAACGGACTAGCCTTATTTTAACTTGCTATTTCTAGCTCTAAAACGCAGCCCCAATAAGATCCCCCTATAGTGAGTCGTATTACGC	1 and 2	
cxcr3.3 Target B 122-mer	*cxcr3.3*	GATCCGCACCGACTCGGTGCCACTTTTTCAAGTTGATAACGGACTAGCCTTATTTTAACTTGCTATTTCTAGCTCTAAAACTGCTTTACTCTTTGGGGATCCTATAGTGAGTCGTATTACGC	1 and 2	
T7 promoter primer	all 121-mers	TAATACGACTCACTATAG	1	Primer to complement T7 promoter by annealing to 121-mers
cxcr3.3 Target C 81-mer Fw	*cxcr3.3*	GCGTAATACGACTCACTATAGGACTGGTTCTGGCAGTATTGGTTTTAGAGCTAGAAATAGCAAGTTAAAATAAGGCTAGTC	3	Semi-complementary oligos used for generation of PCR templates for *in vitro* transcription of shgRNA
cxcr3.3 Target D 81-mer Fw	*cxcr3.3*	GCGTAATACGACTCACTATAGGATGTTGGCCTTCATCAGTGGTTTTAGAGCTAGAAATAGCAAGTTAAAATAAGGCTAGTC	3	
Constant 81-mer Rv	all Fw 81-mers	GATCCGCACCGACTCGGTGCCACTTTTTCAAGTTGATAACGGACTAGCCTTATTTTAACTTGCTATTTCTAGCTCTAAAAC	3	
Template amplif. Fw	all PCR templates	GATCCGCACCGACTCGGT	2 and 3	PCR primers to amplify the template for shgRNA transcription
Template amplif. Rv	all PCR templates	GCGTAATACGACTCACTATAG	2 and 3	
eGFP gFw	eGFP	AAACGGCCACAAGTTCAGCG	Genot.	Primers used for PCR genotyping of targeted genomic loci
eGFP gRv	eGFP	TCACCTTGATGCCGTTCTTCTG	Genot.	
cxcr3.3A-B gFw	*cxcr3.3*	ACATGGAGGTAGAGCTTCACGG	Genot.	
cxcr3.3A-B gRv	*cxcr3.3*	CTCACCTTAAACAGAACTCCAGCC	Genot.	
cxcr3.3C gFw	*cxcr3.3*	GAGGTAGAGCTTCACGGATTGT	Genot.	
cxcr3.3C gRv	*cxcr3.3*	GAGAGCAGCAGAAGACTGTCAA	Genot.	
cxcr3.3D gFw	*cxcr3.3*	TAAATTGATTTTAATCGACTTGACG	Genot.	
cxcr3.3D gRv	*cxcr3.3*	AAAGATCCATTCTGGGATGCTA	Genot.	

Supplementary Table 1. Primers and oligos used in this study. Sequences marked in blue correspond to the T7 promoter sequence. Sequences in green represent the target sites. Sequences in orange represent the semi-complementary stretches of the 81-mers used in Method 3.

```
hsaCXCR3   MVLEVSDHQVLND-AE-VAALLENFSSSYDYGENE-SDSCCTSPP-CPQDFSLNFDRAFL 56
dreCXCR3.1 ----------------MKDFS-DYTDLYNYSDYNDNESYGAGAV-CTQDSSMYFDSIFK 41
dreCXCR3.2 ----------MDN-ST-TAAEV-SAPTDYDYNSTSYDDDNPYAAP-CSLTETWNFLGRFA 46
dreCXCR3.3 -------------MAAPSNMEV-ELHGLFEKNNSFDYDNYENKELDCQSKAVSDALGVFI 46

hsaCXCR3   PALYSLLFLLGLLGNGAVAAVL--L--SRRTALS-S-TDTFLLHLAVADTLLVLTLPLWA 110
dreCXCR3.1 PILYSLAAVVGLLGNGLVLIVL--W--KKRAGLN-V-TDIFILHLSLADILLLLTLPFWA 95
dreCXCR3.2 PVAYILVFILALVGNILVLCVIRRYRQSRHSPCSFSLTDTFLLHLAVSDLLLAATLPFFA 106
dreCXCR3.3 PMLYSLGILLGLLGHGLVLAVL--W--HKWLNCS-V-MDIFIFHLSLIDSLLLLSMPLWA 100

hsaCXCR3   VDAAVQWVFGSGLCKVAGALFNINFYAGALLLACISFDRYLNIVHATQLYRRGPPARVTL 170
dreCXCR3.1 VEAVKEWIFGTPLCKLTGAMFRINFYCGIYMLSCISLDRYLSIVHAVQMYSRKKPMAVHC 155
dreCXCR3.2 VEWISEWVFGKVMCKITGALFSLNVYCGVLFLACISFDRYLAIVHAINISWRRKTCHAQL 166
dreCXCR3.3 VDAVKGWIMGSGLCKLAGVLFKMNFYCSMLMLAFISVDCYLSIVHGVQKLSRKKPMVVHG 160

hsaCXCR3   TCLAVWGLCLLFALPDFIFLSAHHDER-LNATHCQ--YN--FPQVGRTALRVLQLVAGFL 225
dreCXCR3.1 CCMIVWFFCFLLSIPDWILLGANKDSRRQDRTECV--NSEALSDFWVLVNRLIYHFLGFI 213
dreCXCR3.2 ACAFIWVICLGLSMVDMHFRDLVEIPG-MNRMVCQIVYSEQYSKQWQIGMQLVSMVLGFI 225
dreCXCR3.3 CCLIIWLVCLLLSIPEWIFLKSISDSTDQVKDECI--YFYP-DDSWHRSSRFPHHVI-FG 216

hsaCXCR3   LPLLVMAYCYAHI-LAVLLVSRGQRRL--RAMRLVVVVVVAFALCWTPYHLVVLVDI-LM 281
dreCXCR3.1 IPAIMMVFCYTSILLRLLLGSKCMQKK--RAIHVIVALVLAFFISWTPYNIALMADT-IH 270
dreCXCR3.2 LPLLVMLYCYLHI-FKALCHATRRQKR--RSLRLIISLVIVFVISWAPYNALRMTDS-LQ 281
dreCXCR3.3 VGTLVLLFCCTSIMLKLQRESMCQQKKMGRKTAIIAVLVLVFLICWTPYSIAFIVNTGAR 276

hsaCXCR3   -D-LGALARN--CGRESRVDVAKSVTSGLGYMHCCLNPLLYAFVGVKFRERM-WMLLLRL 336
dreCXCR3.1 TNRTDNNQTS--CETRTTLDVAITATSTFAYMHCCVNPILYAFVGVKFRQHL-LDMLRPL 327
dreCXCR3.2 -M-LGVIVKS--CALNNVLDVGILVTESLGLAHCALNPLLYGLVGVKFRRELAQMCKAAL 337
dreCXCR3.3 PVHIDPLTGESEC--EWRQWTATKITAIFGLLHCTINPVIYFCFSKEFRRRS-LAVIKFN 333

hsaCXCR3   GCPNQRGLQRQPSSSRRDSSWSETSEASYSG-L---------------------- 368
dreCXCR3.1 GFKLKGRAGLVSRKSSGWSESVDTSHTSAF------------------------- 357
dreCXCR3.2 G-P-QGCLGLVGWANGRGSS-TRRPTGSFSS-V-E------TE--NTSYFSVMA 378
dreCXCR3.3 ACESNNNDGSLWDSTAVNVNTTVQEEQGPLQQVNELKPKVQTQQQDT------- 380
```

Supplementary Figure 1. Full sequence alignment of human (hsa) CXCR3 with zebrafish (dre) Cxcr3.1, Cxcr3.2 and Cxcr3.3.

REFERENCES

1 Zlotnik A, Yoshie O. Chemokines: a new classification system and their role in immunity. Immunity. 2000 Feb;12(2):121-7.

2 Torraca V, Masud S, Spaink HP, Meijer AH. Macrophage-pathogen interactions in infectious diseases: new therapeutic insights from the zebrafish host model. Dis Model Mech. 2014 Jul;7(7):785-97.

3 Donà E, Barry JD, Valentin G, Quirin C, Khmelinskii A, Kunze A, Durdu S, Newton LR, Fernandez-Minan A, Huber W, Knop M, Gilmour D. Directional tissue migration through a self-generated chemokine gradient. Nature. 2013 Nov 14;503(7475):285-9.

4 Walters KB, Green JM, Surfus JC, Yoo SK, Huttenlocher A. Live imaging of neutrophil motility in a zebrafish model of WHIM syndrome. Blood. 2010 Oct 14;116(15):2803-11.

5 Busch-Nentwich E, Kettleborough R, Dooley CM, Scahill C, Sealy I, White R, Herd C, Mehroke S, Wali N, Carruthers S, Hall A, Collins J, Gibbons R, Pusztai Z, Clark R, Stemple DL. Sanger Institute Zebrafish Mutation Project mutant data submission. ZFIN Direct Data Submission. 2013.

6 Valentin G, Haas P, Gilmour D. The chemokine SDF1a coordinates tissue migration through the spatially restricted activation of Cxcr7 and Cxcr4b. Curr Biol. 2007 Jun 19;17(12):1026-31.

7 Knaut H, Werz C, Geisler R, Nüsslein-Volhard C; Tübingen 2000 Screen Consortium. A zebrafish homologue of the chemokine receptor Cxcr4 is a germ-cell guidance receptor. Nature. 2003 Jan 16;421(6920):279-82.

8 Lewellis SW, Nagelberg D, Subedi A, Staton A, LeBlanc M, Giraldez A, Knaut H. Precise SDF1-mediated cell guidance is achieved through ligand clearance and microRNA-mediated decay. J Cell Biol. 2013 Feb 4;200(3):337-55.

9 Torraca V, Cui C, Boland R, Bebelman JP, van der Sar AM, Smit MJ, Siderius M, Spaink HP, Meijer AH. The CXCR3-CXCL11 signaling axis mediates macrophage recruitment and dissemination of mycobacterial infection. Dis Model Mech. 2015 Mar;8(3):253-69.
10 Siekmann AF, Standley C, Fogarty KE, Wolfe SA, Lawson ND. Chemokine signaling guides regional patterning of the first embryonic artery. Genes Dev. 2009 Oct1;23(19):2272-7.
11 Bussmann J, Wolfe SA, Siekmann AF. Arterial-venous network formation during brain vascularization involves hemodynamic regulation of chemokine signaling. Development. 2011 May;138(9):1717-26.
12 Jinek M, Chylinski K, Fonfara I, Hauer M, Doudna JA, Charpentier E. A programmable dual-RNA-guided DNA endonuclease in adaptive bacterial immunity. Science. 2012 Aug 17;337(6096):816-21.
13 Mali P, Esvelt KM, Church GM. Cas9 as a versatile tool for engineering biology. Nat Methods. 2013 Oct;10(10):957-63.
14 Ran FA, Hsu PD, Wright J, Agarwala V, Scott DA, Zhang F. Genome engineering using the CRISPR-Cas9 system. Nat Protoc. 2013 Nov;8(11):2281-308.
15 Jao LE, Wente SR, Chen W. Efficient multiplex biallelic zebrafish genome editing using a CRISPR nuclease system. Proc Natl Acad Sci U S A. 2013 Aug 20;110(34):13904-9.
16 Hwang WY, Fu Y, Reyon D, Maeder ML, Tsai SQ, Sander JD, Peterson RT, Yeh JR,Joung JK. Efficient genome editing in zebrafish using a CRISPR-Cas system. Nat Biotechnol. 2013 Mar;31(3):227-9.
17 Hruscha A, Krawitz P, Rechenberg A, Heinrich V, Hecht J, Haass C, Schmid B. Efficient CRISPR/Cas9 genome editing with low off-target effects in zebrafish. Development. 2013 Dec;140(24):4982-7.
18 Auer TO, Del Bene F. CRISPR/Cas9 and TALEN-mediated knock-in approaches in zebrafish. Methods. 2014 Sep;69(2):142-50.
19 Kleinstiver BP, Pattanayak V, Prew MS, Tsai SQ, Nguyen NT, Zheng Z, Joung JK. High-fidelity CRISPR-Cas9 nucleases with no detectable genome-wide off-target effects. Nature. 2016 Jan 28;529(7587):490-5.
20 Nomiyama H, Osada N, Yoshie O. Systematic classification of vertebrate chemokines based on conserved synteny and evolutionary history. Genes Cells. 2013 Jan;18(1):1-16.
21 Lindley I, Aschauer H, Seifert JM, Lam C, Brunowsky W, Kownatzki E, Thelen M, Peveri P, Dewald B, von Tscharner V, et al. Synthesis and expression in Escherichia coli of the gene encoding monocyte-derived neutrophil-activating factor: biological equivalence between natural and recombinant neutrophil-activating factor. Proc Natl Acad Sci U S A. 1988 Dec;85(23):9199-203.
22 Hoffmann E, Dittrich-Breiholz O, Holtmann H, Kracht M. Multiple control of interleukin-8 gene expression. J Leukoc Biol. 2002 Nov;72(5):847-55.
23 de Oliveira S, Reyes-Aldasoro CC, Candel S, Renshaw SA, Mulero V, Calado A. Cxcl8 (IL-8) mediates neutrophil recruitment and behavior in the zebrafish inflammatory response. J Immunol. 2013 Apr 15;190(8):4349-59.
24 Tanino Y, Coombe DR, Gill SE, Kett WC, Kajikawa O, Proudfoot AE, Wells TN, Parks WC, Wight TN, Martin TR, Frevert CW. Kinetics of chemokine-glycosaminoglycan interactions control neutrophil migration into the airspaces of the lungs. J Immunol. 2010 Mar 1;184(5):2677-85.
25 Mukaida N. Pathophysiological roles of interleukin-8/CXCL8 in pulmonary diseases. Am J Physiol Lung Cell Mol Physiol. 2003 Apr;284(4):L566-77.
26 Nagasawa T, Hirota S, Tachibana K, Takakura N, Nishikawa S, Kitamura Y, Yoshida N, Kikutani H, Kishimoto T. Defects of B-cell lymphopoiesis and bone-marrow myelopoiesis in mice lacking the CXC chemokine PBSF/SDF-1. Nature. 1996 Aug 15;382(6592):635-8.
27 Sallusto F, Baggiolini M. Chemokines and leukocyte traffic. Nat Immunol. 2008 Sep;9(9):949-52.
28 Balkwill F. The significance of cancer cell expression of the chemokine receptor CXCR4. Semin Cancer Biol. 2004 Jun;14(3):171-9.
29 Feng Y, Broder CC, Kennedy PE, Berger EA. HIV-1 entry cofactor: functionalcDNA cloning of a seven-transmembrane, G protein-coupled receptor. Science. 1996 May 10;272(5263):872-7.
30 Tamplin OJ, Durand EM, Carr LA, Childs SJ, Hagedorn EJ, Li P, Yzaguirre AD, Speck NA, Zon LI. Hematopoietic stem cell arrival triggers dynamic remodeling of the perivascular niche. Cell. 2015 Jan 15;160(1-2):241-52.
31 Tulotta C, Stefanescu C, Beletkaia E, Bussmann J, Tarbashevich K, Schmidt T,Snaar-Jagalska BE. Inhibition of signaling between human CXCR4 and zebrafishligands by the small molecule IT1t impairs the formation of triple-negativebreast cancer early metastases in a zebrafish xenograft model. Dis Model Mech.2016 Feb 1;9(2):141-53.
32 Chong SW, Emelyanov A, Gong Z, Korzh V. Expression pattern of two zebrafish genes, cxcr4a and cxcr4b. Mech Dev. 2001 Dec;109(2):347-54.
33 Nagasawa T, Nakajima T, Tachibana K, Iizasa H, Bleul CC, Yoshie O, Matsushima K, Yoshida N, Springer TA, Kishimoto T. Molecular cloning and characterization of a murine pre-B-cell growth-stimulating

factor/stromal cell-derived factor 1 receptor, a murine homolog of the human immunodeficiency virus 1 entry coreceptor fusin. Proc Natl Acad Sci U S A. 1996 Dec 10;93(25):14726-9.
34 Tachibana K, Hirota S, Iizasa H, Yoshida H, Kawabata K, Kataoka Y, Kitamura Y,Matsushima K, Yoshida N, Nishikawa S, Kishimoto T, Nagasawa T. The chemokine receptor CXCR4 is essential for vascularization of the gastrointestinal tract. Nature. 1998 Jun 11;393(6685):591-4.
35 Zou YR, Kottmann AH, Kuroda M, Taniuchi I, Littman DR. Function of the chemokine receptor CXCR4 in haematopoiesis and in cerebellar development. Nature. 1998 Jun 11;393(6685):595-9.
36 Zhou J, Tang PC, Qin L, Gayed PM, Li W, Skokos EA, Kyriakides TR, Pober JS,Tellides G. CXCR3-dependent accumulation and activation of perivascular macrophages is necessary for homeostatic arterial remodeling to hemodynamic stresses. J Exp Med. 2010 Aug 30;207(9):1951-66.
37 Krauthausen M, Kummer MP, Zimmermann J, Reyes-Irisarri E, Terwel D, Bulic B, Heneka MT, Müller M. CXCR3 promotes plaque formation and behavioral deficits in an Alzheimer's disease model. J Clin Invest. 2015 Jan;125(1):365-78.
38 Oghumu S, Varikuti S, Terrazas C, Kotov D, Nasser MW, Powell CA, Ganju RK,Satoskar AR. CXCR3 deficiency enhances tumor progression by promoting macrophage M2 polarization in a murine breast cancer model. Immunology. 2014 Sep;143(1):109-19.
39 Cohen SB, Maurer KJ, Egan CE, Oghumu S, Satoskar AR, Denkers EY. CXCR3-dependent $CD4^+$ T cells are required to activate inflammatory monocytes for defense against intestinal infection. PLoS Pathog. 2013;9(10):e1003706.
40 Torraca V, in't Veld E, Meijer AH. Disruption of chemotactic signalling primes the lysosomal function of macrophages to counteract mycobacterial parasitism. *Chapter 4 of this thesis*.
41 Cui C. Chemokine signaling in innate immunity of zebrafish embryos. Doctoral Thesis, Leiden University. 2012 Dec 20.
42 Montague TG, Cruz JM, Gagnon JA, Church GM, Valen E. CHOPCHOP: a CRISPR/Cas9 and TALEN web tool for genome editing. Nucleic Acids Res. 2014 Jul;42(Web Server issue):W401-7.
43 Langmead B, Trapnell C, Pop M, Salzberg SL. Ultrafast and memory-efficient alignment of short DNA sequences to the human genome. Genome Biol. 2009;10(3):R25.
44 Wang T, Wei JJ, Sabatini DM, Lander ES. Genetic screens in human cells using the CRISPR-Cas9 system. Science. 2014 Jan 3;343(6166):80-4.
45 Lawson ND, Weinstein BM. In vivo imaging of embryonic vascular developmentusing transgenic zebrafish. Dev Biol. 2002 Aug 15;248(2):307-18.
46 Grone BP, Marchese M, Hamling KR, Kumar MG, Krasniak CS, Sicca F, Santorelli FM, Patel M, Baraban SC. Epilepsy, Behavioral Abnormalities, and Physiological Comorbidities in Syntaxin-Binding Protein 1 (STXBP1) Mutant Zebrafish. PLoS One. 2016 Mar 10;11(3):e0151148.
47 D'Agostino Y, Locascio A, Ristoratore F, Sordino P, Spagnuolo A, Borra M, D'Aniello S. A Rapid and Cheap Methodology for CRISPR/Cas9 Zebrafish Mutant Screening. Mol Biotechnol. 2016 Jan;58(1):73-8.
48 Taylor SM, Alvarez-Delfin K, Saade CJ, Thomas JL, Thummel R, Fadool JM, Hitchcock PF. The bHLH Transcription Factor NeuroD Governs Photoreceptor Genesis and Regeneration Through Delta-Notch Signaling. Invest Ophthalmol Vis Sci. 2015 Nov;56(12):7496-515.
49 Chang N, Sun C, Gao L, Zhu D, Xu X, Zhu X, Xiong JW, Xi JJ. Genome editing with RNA-guided Cas9 nuclease in zebrafish embryos. Cell Res. 2013 Apr;23(4):465-72.
50 Yu C, Zhang Y, Yao S, Wei Y. A PCR based protocol for detecting indel mutations induced by TALENs and CRISPR/Cas9 in zebrafish. PLoS One. 2014 Jun 5;9(6):e98282.
51 Irion U, Krauss J, Nüsslein-Volhard C. Precise and efficient genome editing in zebrafish using the CRISPR/Cas9 system. Development. 2014 Dec;141(24):4827-30.
52 Varshney GK, Pei W, LaFave MC, Idol J, Xu L, Gallardo V, Carrington B, Bishop K, Jones M, Li M, Harper U, Huang SC, Prakash A, Chen W, Sood R, Ledin J, Burgess SM. High-throughput gene targeting and phenotyping in zebrafish using CRISPR/Cas9. Genome Res. 2015 Jul;25(7):1030-42.
53 Brocal I, White RJ, Dooley CM, Carruthers SN, Clark R, Hall A, Busch-Nentwich EM, Stemple DL, Kettleborough RN. Efficient identification of CRISPR/Cas9-induced insertions/deletions by direct germline screening in zebrafish. BMC Genomics. 2016 Mar 24;17(1):259.
54 Arnaud-Barbe N, Cheynet-Sauvion V, Oriol G, Mandrand B, Mallet F. Transcription of RNA templates by T7 RNA polymerase. Nucleic Acids Res. 1998 Aug 1;26(15):3550-4.
55 Ran FA, Hsu PD, Wright J, Agarwala V, Scott DA, Zhang F. Genome engineering using the CRISPR-Cas9 system. Nat Protoc. 2013 Nov;8(11):2281-308.
56 Nomiyama H, Yoshie O. Functional roles of evolutionary conserved motifs and residues in vertebrate chemokine receptors. J Leukoc Biol. 2015 Jan;97(1):39-47

57 Lagane B, Ballet S, Planchenault T, Balabanian K, Le Poul E, Blanpain C, Percherancier Y, Staropoli I, Vassart G, Oppermann M, Parmentier M, Bachelerie F. Mutation of the DRY motif reveals different structural requirements for the CC chemokine receptor 5-mediated signaling and receptor endocytosis. Mol Pharmacol. 2005 Jun;67(6):1966-76.
58 Rovati GE, Capra V, Neubig RR. The highly conserved DRY motif of class A G protein-coupled receptors: beyond the ground state. Mol Pharmacol. 2007 Apr;71(4):959-64.
59 Acharya S, Karnik SS. Modulation of GDP release from transducin by the conserved Glu134-Arg135 sequence in rhodopsin. J Biol Chem. 1996 Oct 11;271(41):25406-11.
60 Cancellieri C, Vacchini A, Locati M, Bonecchi R, Borroni EM. Atypical chemokine receptors: from silence to sound. Biochem Soc Trans. 2013 Feb 1;41(1):231-6.
61 Nygaard R, Frimurer TM, Holst B, Rosenkilde MM, Schwartz TW. Ligand binding and micro-switches in 7TM receptor structures. Trends Pharmacol Sci. 2009 May;30(5):249-59.
62 Auger GA, Pease JE, Shen X, Xanthou G, Barker MD. Alanine scanning mutagenesis of CCR3 reveals that the three intracellular loops are essential for functional receptor expression. Eur J Immunol. 2002 Apr;32(4):1052-8.
63 Zou J, Redmond AK, Qi Z, Dooley H, Secombes CJ. The CXC chemokine receptors of fish: Insights into CXCR evolution in the vertebrates. Gen Comp Endocrinol. 2015 May 1;215:117-31.
64 Ulvmar MH, Hub E, Rot A. Atypical chemokine receptors. Exp Cell Res. 2011 Mar 10;317(5):556-68.
65 Nibbs R, Graham G, Rot A. Chemokines on the move: control by the chemokine "interceptors" Duffy blood group antigen and D6. Semin Immunol. 2003 Oct;15(5):287-94.
66 Mantovani A, Bonecchi R, Locati M. Tuning inflammation and immunity by chemokine sequestration: decoys and more. Nat Rev Immunol. 2006 Dec;6(12):907-18.
67 Fra AM, Locati M, Otero K, Sironi M, Signorelli P, Massardi ML, Gobbi M, Vecchi A, Sozzani S, Mantovani A. Cutting edge: scavenging of inflammatory CC chemokines by the promiscuous putatively silent chemokine receptor D6. J Immunol. 2003 Mar 1;170(5):2279-82.
68 Dambly-Chaudière C, Cubedo N, Ghysen A. Control of cell migration in the development of the posterior lateral line: antagonistic interactions between the chemokine receptors CXCR4 and CXCR7/RDC1. BMC Dev Biol. 2007 Mar 29;7:23.
69 Naumann U, Cameroni E, Pruenster M, Mahabaleshwar H, Raz E, Zerwes HG, Rot A, Thelen M. CXCR7 functions as a scavenger for CXCL12 and CXCL11. PLoS One. 2010 Feb 11;5(2):e9175.
70 Bamberg CE, Mackay CR, Lee H, Zahra D, Jackson J, Lim YS, Whitfeld PL, Craig S, Corsini E, Lu B, Gerard C, Gerard NP. The C5a receptor (C5aR) C5L2 is a modulator of C5aR-mediated signal transduction. J Biol Chem. 2010 Mar 5;285(10):7633-44.
71 Di Liberto D, Locati M, Caccamo N, Vecchi A, Meraviglia S, Salerno A, Sireci G, Nebuloni M, Caceres N, Cardona PJ, Dieli F, Mantovani A. Role of the chemokine decoy receptor D6 in balancing inflammation, immune activation, and antimicrobial resistance in Mycobacterium tuberculosis infection. J Exp Med. 2008 Sep 1;205(9):2075-84.

Chapter 6

The chemokine receptor CXCR4 promotes granuloma formation by sustaining a mycobacteria-induced angiogenesis programme

Vincenzo Torraca, Claudia Tulotta, B. Ewa Snaar-Jagalska and Annemarie H. Meijer

Institute of Biology, Leiden University, The Netherlands

Manuscript in preparation

Chapter 6

The chemokine receptor CXCR4 promotes granuloma formation by sustaining a mycobacteria-induced angiogenesis programme

Vincenzo Torraca, Claudia Tulotta, B. Ewa Snaar-Jagalska and Annemarie H. Meijer

Institute of Biology, Leiden University, The Netherlands

CXC chemokine receptor 4 (CXCR4) plays a critical role in chemotaxis and leukocyte differentiation. Furthermore, there is increasing evidence that links this receptor to angiogenesis. Using the well-established zebrafish-*Mycobacterium marinum* model for tuberculosis, angiogenesis was recently found to be essential to promote the development of cellular aggregates called granulomas that contain the mycobacterial infection and are the hallmark of tuberculosis disease. Here, we found that initiation of the infection-dependent pro-angiogenic programme in mycobacterial disease is dependent on CXCR4 signalling. The nascent granulomas in *cxcr4b*-deficient zebrafish embryos were poorly vascularised, which in turn also delayed bacterial growth in these mutants. Suppressed infection expansion in *cxcr4b* mutants could not be attributed to an overall deficient recruitment of leukocytes or to different intramacrophage bacterial growth rate, as *cxcr4b* mutants displayed similar microbicidal capabilities against initial mycobacterial infection and the cellular composition of granulomatous lesions was similar to wildtype siblings. Expression of *vegfaa* was upregulated to a similar extent in *cxcr4b* mutants and wildtypes, suggesting that the granuloma vascularisation phenotype of *cxcr4b* mutants is independent of vascular endothelial growth factor. However, transcriptional analysis of pro-inflammatory markers (*il1b*, *cxcl18b*) showed that poor vascularisation of the infected tissues in *cxcr4b* mutants is associated with an attenuated inflammatory response. In summary, our study demonstrates that CXCR4-mediated signalling is necessary to induce granuloma-associated angiogenesis and suggests that targeting CXCR4 could provide a potential new anti-angiogenic therapy to suppress the formation of granulomas in TB patients.

GRAPHICAL ABSTRACT

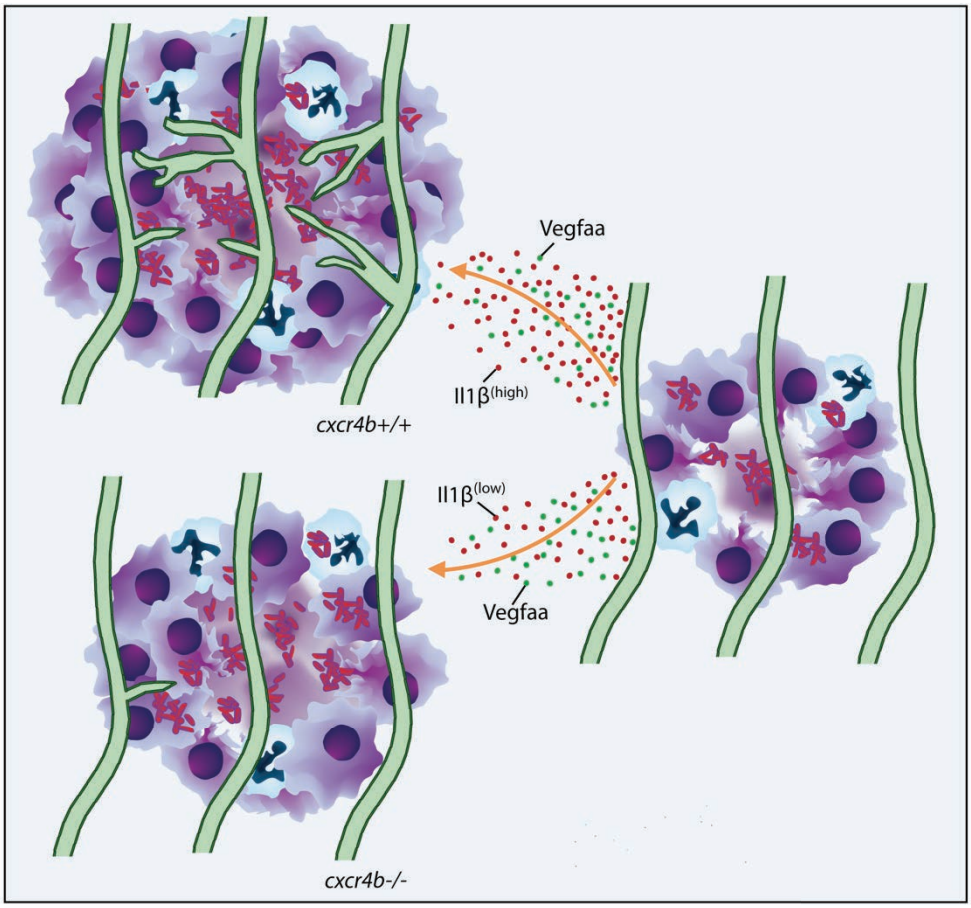

In poorly vascularised tissues, granuloma expansion depends on initiation of an angiogenic programme. Mutation of the chemokine receptor *cxcr4b* can limit the induction of granuloma vascularisation and, in turn, leads to a better containment of bacterial burden. Transcriptional analysis of *cxcr4b* mutants indicates that, while transcription of the main endothelium proliferating factor *vegfaa* remains globally similar in mutants versus wildtypes, *cxcr4b* mutants show reduced induction of the inflammatory mediator *il1b*, which in mammalian systems is known to synergise with VEGF signalling in promoting angiogenesis. Taken together, we propose a model in which blockade of Cxcr4b signalling, via curtailing induction of inflammation limits the initiation of the granuloma vascularisation and therefore the bacterial growth.

INTRODUCTION

CXCR4 is a critical chemokine receptor that controls migration and differentiation of a variety of cell types. In the bone marrow, interaction of CXCR4 with its ligand CXCL12 (SDF1) is required for retention of haematopoietic stem/progenitor cells and their complete differentiation before release into circulation[1,2]. During inflammatory responses, CXCR4 also sustains the trafficking of mature myeloid and lymphoid cells to sites of inflammation. Additionally, CXCR4 signalling on other cells is involved in key migratory mechanisms during development/embryogenesis and CXCR4 has been linked to the metastatic behaviour of cancer cells[3,4,5,6,7,8]. CXCR4 is also well known to play a critical function in HIV pathogenesis, since this factor represents an important HIV co-receptor, mediating viral entry into the host cells[9].

The zebrafish model system has been widely used to study the implication of CXCR4 signalling in different processes. The zebrafish Cxcr4b/Cxcl12a signalling system is implicated in the migration of the primordial germ cells, the lateral line primordium, the migration of haematopoietic stem cells, the recruitment of leukocytes to infectious foci and sites of injury and the invasive movement of cancer cells in tumour metastasis[2,7,10,11,12,13,14]. In other model systems, CXCR4 signalling has also been connected to tumour-sustained angiogenesis[15,16,17]. In particular, CXCR4 stimulation was found to induce expression of vascular endothelial growth factor (VEGF) in human breast carcinoma cells and conversely blockade of CXCR4/CXCL12 signalling was able to suppress tumour angiogenesis and tumour growth *in vivo* in a murine model[15].

Tuberculosis (TB) is caused by *Mycobacterium tuberculosis* (*Mtb*) infection and this disease typically manifests by the formation of aggregates of infected and non-infected immune cells that are known as granulomas. Several studies reported that human tuberculous granulomas are extensively vascularised[18,19,20]. However, very little is understood about the actual relevance of angiogenesis for granuloma formation in TB patients. Additionally, the mechanism by which the vascularisation programme is initiated by the pathogen remains elusive[21,22]. In zebrafish larvae, *Mycobacterium marinum* (*Mm*), a close relative of *Mtb*, causes a disease that recapitulates significant aspects of human TB, which include the formation of necrotising granulomas and the initiation of specific transcriptional and morphological changes in *Mycobacterium*-infected macrophages[23,24]. Using the zebrafish model, it was recently found that *Mm* can also induce granuloma-associated angiogenesis and that initiation of this programme coincides with local induction of hypoxia and of the pro-angiogenic factor *vegfaa*[22]. Notably, the presence of macrophages was strictly necessary for mycobacterial-induced *vegfaa* expression and initiation of granuloma vascularisation. In tumours, activation of CXCR4/CXCL12 signalling is tightly linked to both the development of hypoxia and to the activation of angiogenesis[15,16,17]. Therefore, we hypothesised that this signalling might also affect granuloma vascularisation.

Here we show that Cxcr4b-deficient zebrafish larvae display an attenuated induction of the angiogenic programme at the nascent granulomas. This phenotype was not due to different cellular composition of granulomas, to different chemotaxis of immune cells to the infected areas or to a direct transcriptional control on *vegfaa*, which was still produced in the *cxcr4b* deficient fish, despite the lack of granuloma vascularisation. Our data suggest that *cxcr4b* might be alternatively implicated in pathogenic angiogenesis by controlling the release of

inflammatory pro-angiogenic mediators which maintain a permissive microenvironment that sustains vascularisation. Taken together, our study indicates that Cxcr4b-mediated signalling is required to mediate the full angiogenesis response to mycobacterial infections, and that suppression of pathological angiogenesis with CXCR4 blockers could be explored as an adjuvant treatment of TB patients.

RESULTS

Cxcr4b signalling controls granuloma-induced angiogenesis

To study granuloma-associated angiogenesis, a trunk infection model was recently established in zebrafish embryos (**Figure 1A-B**). In this model a transgenic *Tg(kdrl:eGFP)* background (labelling arterial and venous endothelium) was used to monitor host vascularisation in the environment of the nascent granulomatous lesions (**Figure 1C-E**) [22,25]. To study whether *cxcr4b* has a function in granuloma vascularisation, we injected mCherry-fluorescent *Mm* in *cxcr4b* mutant and wildtype (wt) siblings at 2 days post fertilisation (dpf) and measured bacterial expansion and vascularisation of the infected area at 5 days post infection (dpi) (**Figure 1F-K**).

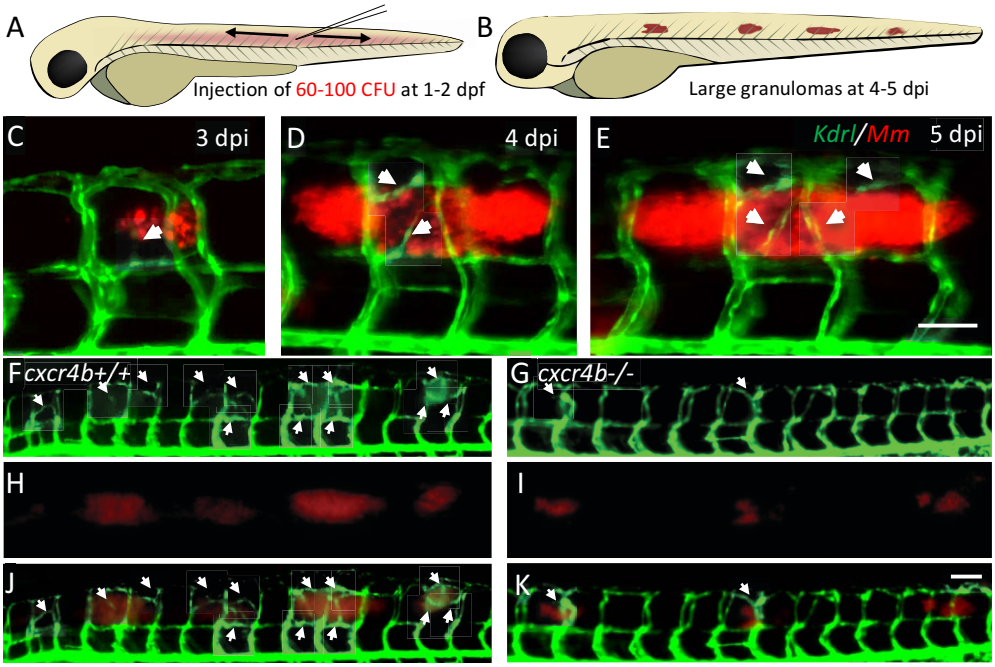

Figure 1. Trunk granuloma formation and induction of angiogenesis by *M. marinum*. A-B. Schematic representation of injection location and of granuloma expansion in zebrafish embryos/larvae upon injection of *Mm* into the trunk. **C-E.** Longitudinal imaging of vascular and bacterial growth during development of a trunk granuloma in the *Tg(kdrl:eGFP)* line at 3, 4 and 5 dpi. **F-K.** Formation of trunk granulomas and their vascularisation in a *cxcr4b*$^{+/+}$ and *cxcr4b*$^{-/-}$ larva at 5 dpi. White arrows indicate sites of abnormal vascularisation associated to bacterial growth, notably largely initiated in the wt but rare in the mutant. Scale bars: 100 µm.

In *cxcr4b*$^{-/-}$ larvae, the expansion of the infection progressed at a significantly lower rate as compared to the lesions in wt (**Figure 1F-K**). Simultaneously, the association of vascularisation with the granulomas was impaired in these mutants and, differently from wt, *cxcr4b* mutants did not have a significant positive correlation between granuloma size and length of associated abnormal vasculature (**Figure 2A-C**). Corroborating these results, even large granulomas failed vascularisation in *cxcr4b*$^{-/-}$ (**Figure 2D-I**).

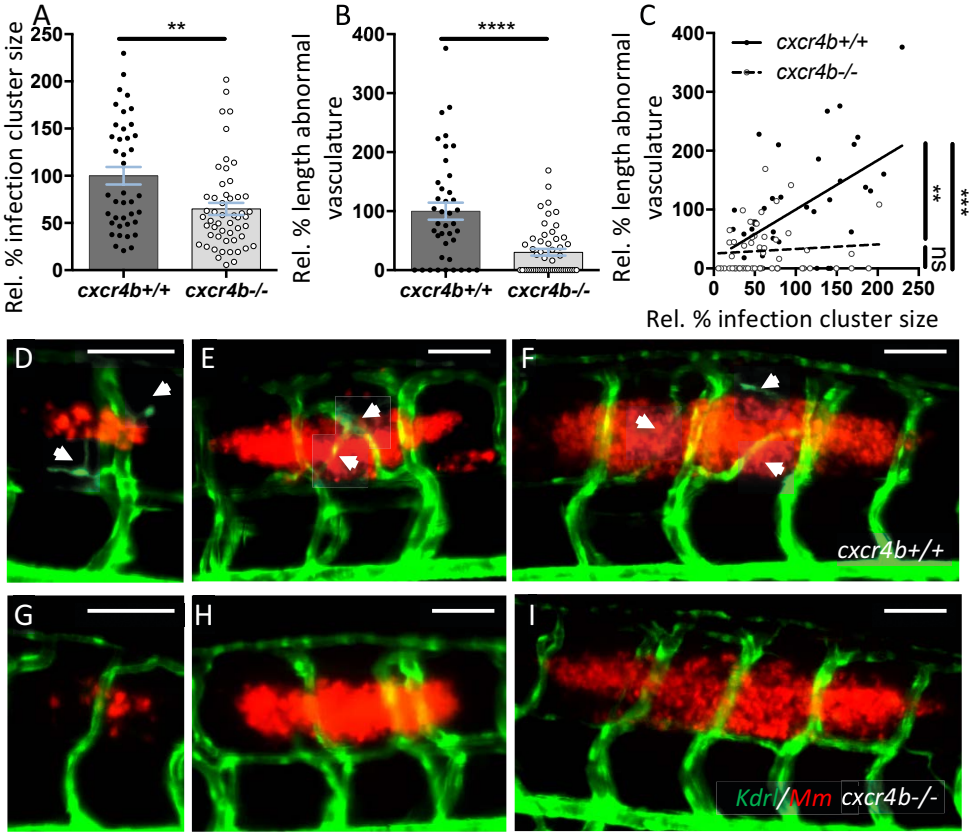

Figure 2. Cxcr4b mutation impairs granuloma-induced angiogenesis. A-B. *cxcr4b* mutants display a reduced expansion rate of local granulomatous lesions (A), which coincided with the incapability to induce an angiogenic programme (B). **C**. Vascularisation/granuloma expansion correlation analysis. In wt, the expansion of the granulomas depends on the activation of the angiogenetic programme at the infection focus. Differently, in *cxcr4b* mutants, no significant correlation between granuloma size and vessel length could be observed and even large granulomas failed to initiate angiogenesis, suggesting that the differential activation of the angiogenic programme is not the effect, rather the cause, of reduced burden in mutants. Data points refer to individual trunk granulomas at 5 dpi (3 replicates cumulated). Values are expressed in % relative to average wt (set to 100%). Significance in C indicates that the slopes of *cxcr4b*$^{-/-}$ and *cxcr4b*$^{+/+}$ trend lines are different and that in wt (but not in mutants) this slope is different from 0 (*x* axis). **D-I.** Representative images of comparably-sized 5 dpi trunk granulomas in *cxcr4b*$^{-/-}$ and *cxcr4b*$^{+/+}$, notably *cxcr4b*$^{-/-}$ granulomas display a defect in local vascularisation, which is independent of the granuloma size. Scale bars: 100 µm.

The interdependence between granuloma expansion and angiogenesis had been previously described[22] and mechanistically resembles closely the angiogenic switch in tumorigenesis, in which tumour size is directly related to the local induction of pathogenic vascularisation[26]. Altogether, our findings suggest that *cxcr4b* mutation affects granuloma expansion by primarily affecting the initiation of the angiogenesis programme, and the difference in infection burden appears to be the consequence, rather than the cause, of impaired angiogenetic support of granuloma formation.

cxcr4b mutation does not alter the migratory and microbicidal capabilities of macrophages or the cellular composition of the granulomatous lesions

Since others had previously found that intramacrophage residence of mycobacteria is indispensable for initiation of angiogenesis[22], we investigated whether the difference in promotion of angiogenesis in *cxcr4b* mutants could be explained by aberrant macrophage recruitment (and therefore different intracellular/extracellular ratios), differential microbicidal capability of macrophages, or alteration in the macrophage composition of granulomatous lesions. When mycobacteria were injected locally into the hindbrain ventricle, a comparable number of leukocytes were promptly recruited (3 hpi) to the infected site in mutants and wt (**Figure 3A-B**). To assess the possibility of an altered microbicidal capability, we injected the *Mm* mutant strain *Δerp*, which is highly susceptible to macrophage clearance and replicates intracellularly at a low rate, thereby permitting quantification of mycobacterial growth in individual macrophages by live microscopy. At 44 hpi the percentage of macrophages displaying low (1-5 bacteria), moderate (6-10 bacteria) or high (>10 bacteria) infection load was quantified and *cxcr4b* mutants showed similar distribution of the infection phenotypes as wt siblings, indicating that depletion of *cxcr4b* does not alter the macrophages capability to counteract intracellular infection (**Figure 3C-D**). That *cxcr4b* mutation might affect the content of macrophages in the mature granulomas was also excluded, as the percentage of mycobacteria co-localising with macrophages was similar in mutant and wt siblings (**Figure 3E-G**). In zebrafish larvae, *cxcr4b* is expressed both by the macrophage lineage (marked by *mpeg1*) and by the neutrophil lineage (marked by *mpx*) (**Figure 3H**). However, it is unlikely that the angiogenesis deficiency in *cxcr4b* mutants depended on *cxcr4b* expression by neutrophils, as suggested by *irf8* morpholino knockdown, which skews myelopoiesis towards neutropoiesis at the expense of primitive macrophage development (**Figure 3I-J**)[27]. In this situation the initial deficiency in macrophages was already sufficient to abrogate the angiogenetic response, indicating that neutrophils alone cannot support angiogenesis and therefore that the *cxcr4b* mutation phenotype implicates a macrophage-related function. However, since recruitment of macrophages, cellular composition of lesions and intramacrophage killing of bacteria were comparable between mutants and wt (**Figure 3**), we hypothesised that *cxcr4b* mainly affects the interaction of the macrophages with the surrounding tissue.

The granuloma vascularisation defect in *cxcr4b* mutants associated with reduced inflammatory gene expression

Since CXCR4 was previously linked to tumour angiogenesis via a transcriptional control on VEGF signalling[15], we addressed whether *cxcr4b* mutation controlled granuloma angiogenesis by affecting Vegf signalling.

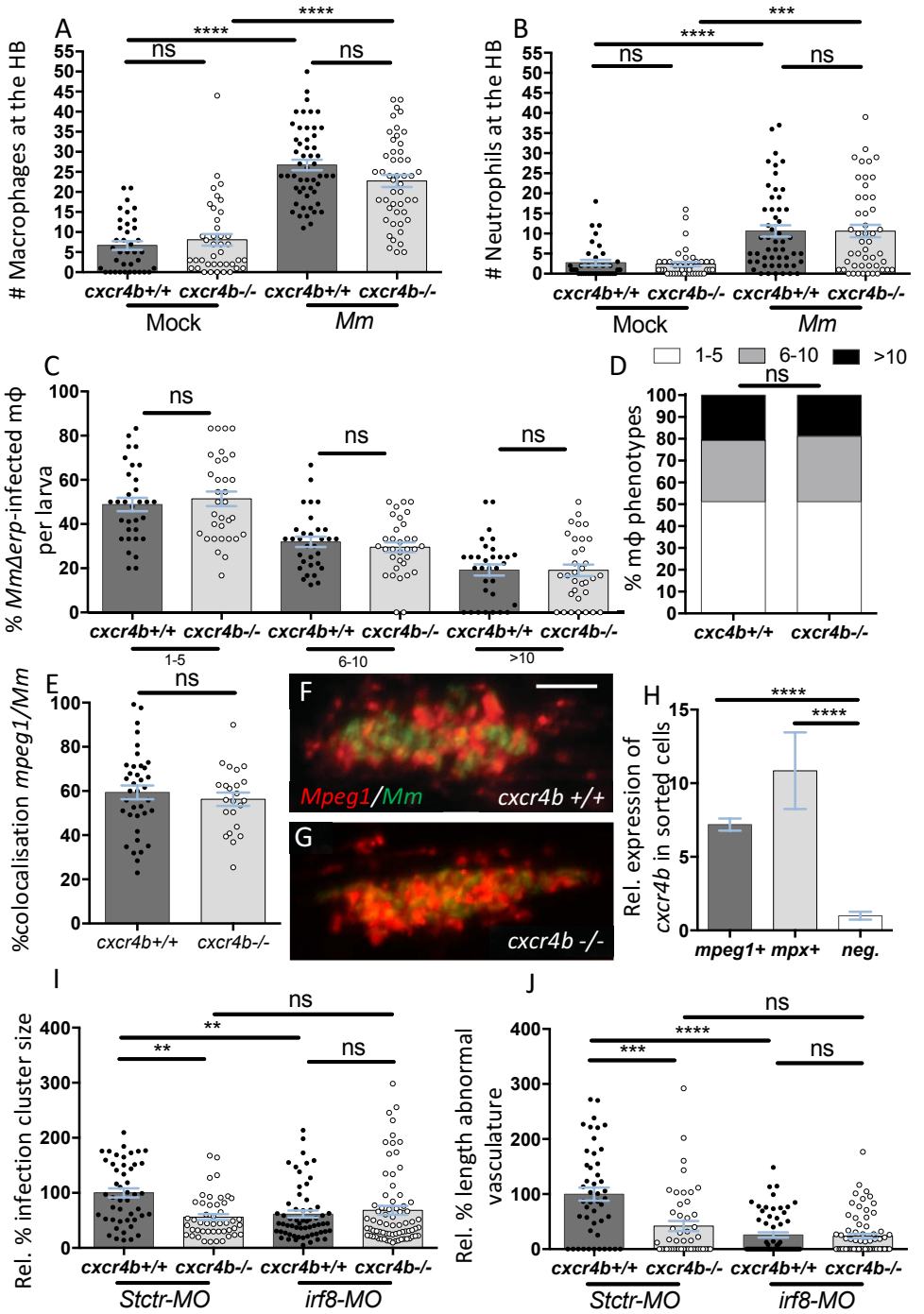

Figure 3. *cxcr4b* is not required for the establishment of macrophage parasitism, but macrophages are necessary to mediate *cxcr4b*-dependent angiogenesis *(Legend on the next page)*.

Figure 3. *cxcr4b* is not required for the establishment of macrophage parasitism, but macrophages are necessary to mediate *cxcr4b*-dependent angiogenesis *(Figure on the previous page).* **A-B.** Recruitment of macrophages (A) and neutrophils (B) 3 hours post local hindbrain (HB) infection at 2 dpf with *Mm* was unaffected by *cxcr4b* mutation. Each value represents the recruitment measured in 1 embryo (2 replicates, cumulated). **C-D.** *cxcr4b* is dispensable for the capability of macrophages to counteract intracellular replication of *Mm Δerp.* Infected macrophages (*mpeg1:mCherry-F*$^{+}$) were classified into three phenotypic classes, according to the severity of intracellular infection (1-5, 6-10, or >10 bacteria). C represents the % of macrophages per larva that populates each class. D represents the overall distribution of macrophage phenotypes (macrophages from all larvae cumulated). Graphs are cumulated from 2 independent replicates. **E-G.** % of *mpeg1:mCherry-F* signal overlapping with *Mm-GFP* signal in *cxcr4b*$^{-/-}$ and *cxcr4b*$^{+/+}$. No significant deviation in macrophage composition of the trunk granuloma lesions was detected. Each data point represents 1 lesion (1 replicate). Representative example images are shown in F and G. **H.** Expression of *cxcr4b* in macrophages (*mpeg1*$^{+}$) and neutrophils (*mpx*$^{+}$). Both cell subsets express *cxcr4b* at significantly higher levels than the negative (non-fluorescent) cell population. Data represent fold changes relative to the negative cell fraction. Cells were sorted at 2 dpf (3 replicates). **I-J.** Macrophages are indispensable to mediate granuloma vascularisation (I) and an increased number of neutrophils (by *irf8* morpholino knockdown) cannot compensate for macrophage deficiency, neither in *cxcr4b*$^{-/-}$ nor in *cxcr4b*$^{+/+}$. Deficient bacterial expansion in *irf8* knockdown condition (*irf8-MO*) compared to standard control morpholino treatment (*Stctr-MO*) can be attributed to the lack of vascularisation as suggested by non-significant differences in burden between the knockdowns and control *cxcr4b*$^{-/-}$ (J). Data are analysed as in Figure 2A-B, but infections were performed at 33 hpf, instead of 2 dpf (1 replicate).

Treatment with Sunitinib (a Vegf receptors inhibitor)[28] or *cxcr4b* mutation reduced trunk granuloma size to the same level (**Figure 4A**), although Vegf receptor inhibition could still synergise with *cxcr4b* mutation and could more severely suppress granuloma vascularisation (**Figure 4B**). However, it should be noted that treatment with Sunitinib (but not *cxcr4b* mutation) also affected to some extent physiological angiogenesis, as the frequency of physiological sprouting from intersegmental vessels and their lateral fusion was also reduced by this treatment (not shown). Since the angiogenesis response to mycobacterial infection was found to coincide with local induction of *vegfaa*[22] and since mammalian CXCR4 has been linked to a transcriptional regulation of *VEGFA*[15], we addressed whether *cxcr4b* affected angiogenesis by exerting a similar transcriptional control on *vegfaa* expression in our model. Whole mount qRT-PCR analysis revealed that both mutants and wt upregulated *vegfaa* to a comparable level (**Figure 4C**). We also found that the levels of *vegfaa* induction, although significant, were limited (1.5-fold) when compared to the induction of other infection-inducible genes, which could be seen highly upregulated in the same conditions (**Figure 4C**). Likewise, expression of *cxcl12a* (encoding the ligand of Cxcr4b) showed limited but comparable induction in mutants and wt (**Figure 4C)**. Expression of *Cxcr4b* mRNA was not relevantly altered by the infection and remained comparable between *wt* and mutants (the *cxcr4b* mutant mRNA differs from the wt only because of a point mutation and can, therefore, be normally tested by qRT-PCR). Signalling via CXCR4 has been linked to the induction of inflammatory genes during the response to infections[29,30] and the local chronic induction of inflammation mediators is known to play a critical role to sustain vascularisation of damaged/inflamed tissues[31,32]. Several inflammatory molecules (mainly interleukins IL1β-6-8 and TNFα) have been largely connected to the sustenance of pathological vascularisation in inflammatory diseases[32,33].

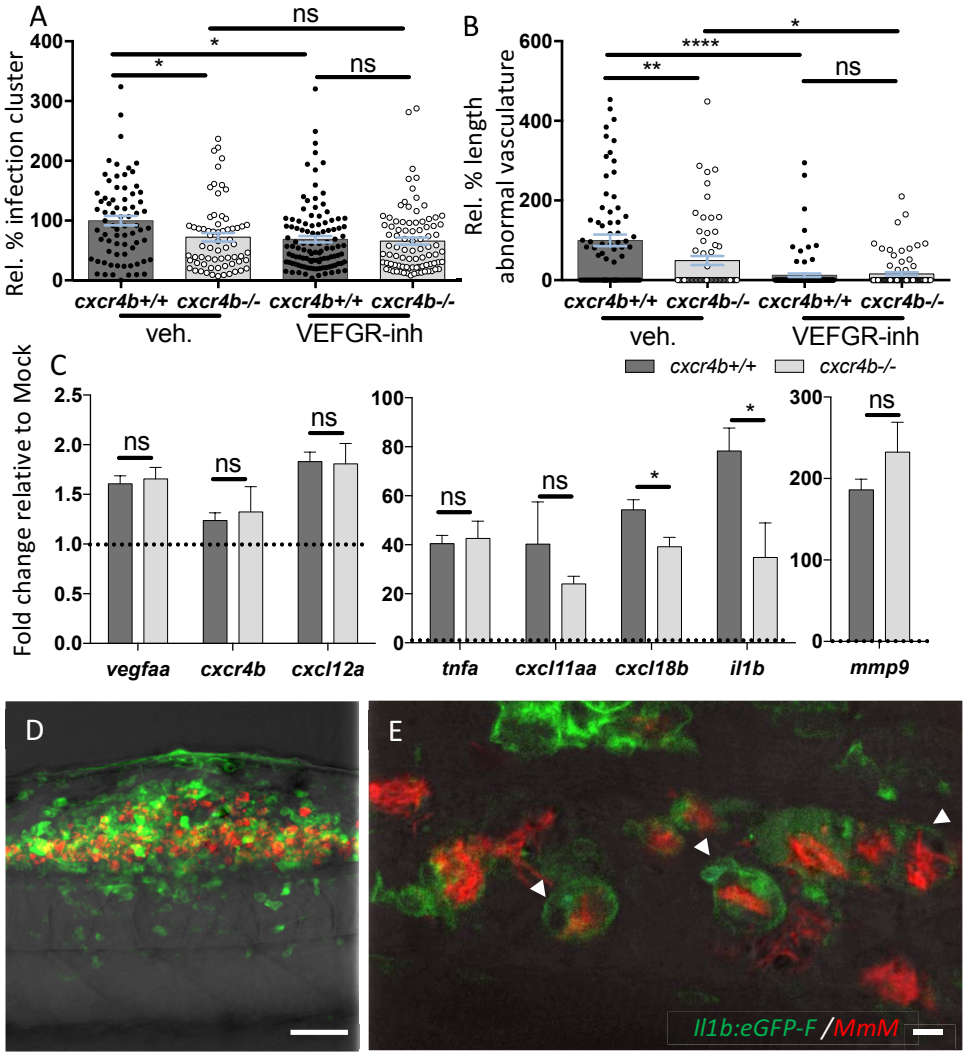

Figure 4. *cxcr4b* mutation does not affect *vegfaa* expression but attenuates expression of inflammatory genes. **A-B.** Cxcr4b deficiency reduced granuloma expansion to a similar extent as blockade of Vegf signalling (VEGFR-inh, treatment with Sunitinib) (A), although Vegf inhibition can more severely affect angiogenesis. (B). Data are analysed as in Figure 2A-B (2 replicates, cumulated). **C**. At 5 dpi, Cxcr4b does not exert a transcriptional control on *vegfaa* expression, but affects the inflammatory response to mycobacterial infection. qRT-PCR were performed whole mount from pools of at least 10 embryos (4 replicates). Data represent fold changes of *Mm* infection groups relative to their mock injection (2% PVP in PBS) control group (set to 1, dotted line). No significant differences in basal expression levels were found between mutants and wt for the analysed genes. **D-E.** Induction of the pro-angiogenetic inflammatory mediator *il1b* at the trunk granuloma. The large granuloma forming in the trunk contains a high number of *il1b*-expressing cells, predominantly consisting of infected cells. Confocal images were acquired at 5 dpi from infected *Tg(il1b:eGFP-F)* larvae. Scale bars: D: 50 µm; E: 5 µm.

In agreement, the use of the transgenic reporter *Tg(il1b:eGFP-F)*[34] revealed high expression of *il1b* by *Mm*-infected cells composing the granulomatous lesions in zebrafish larvae (**Figure 4D-E**). Therefore, we analysed the expression profile of *il1b* and several other *Mm*-inducible inflammatory genes (*tnfa*, *cxcl11aa*, *cxcl18b* and *mmp9*). All these genes could be still induced in *cxcr4b* mutants. However, two of the analysed genes, namely *cxcl18b* and *il1b* were significantly less induced in the mutants, when compared to wt (**Figure 4C**). Taken together, this suggests that a differential inflammatory response can be elicited in *cxcr4b* mutants and wt during the infection progression.

DISCUSSION

Using intravital imaging in the zebrafish–*Mm* infection model, we have investigated the function of the homoeostatic chemokine receptor Cxcr4 in the development of mycobacterial infection and granuloma formation. We found that zebrafish embryos/larvae carrying a homozygote mutation of *cxcr4b* developed an attenuated disease which could be associated with the inability of these mutants to induce local angiogenesis. Supporting that Cxcr4b promotes granuloma formation by sustaining a mycobacteria-induced angiogenesis programme, the positive correlation between granuloma growth and vascularisation that is normally observed in wt larvae, was lost in *cxcr4b* mutants. Furthermore, pharmacological blockade of the angiogenesis programme by Vegfr inhibitor could fully abolish the differences between mutants and wt in the exacerbation of mycobacterial infection. The use of angiogenesis inhibitors has previously been proposed as a host-targeted therapy to suppress the formation of granulomas in TB patients[22]. Based on our results, the CXCR4 receptor could be explored as a novel target for anti-angiogenic tuberculosis therapy.

It is unlikely that the granuloma vascularisation phenotype requires expression of *cxcr4b* by the endothelial cells *per se*, since several studies have identified that venous/arterial endothelium (*kdrl*$^{+}$) does not express high levels of *cxcr4b* and that this gene can be found expressed only in sporadic sprouting lymphatic vessels (*kdrl*$^{-}$)[12,35]. Although our own transcriptional analysis of FACS-sorted *kdrl*$^{+}$ cells at 5 dpi revealed that transcript of *cxcr4b* can be detected in these cells, this gene is more abundantly expressed by the macrophage (*mpeg1*$^{+}$) fraction (**Supplementary Figure 1**). Our study suggests that *cxcr4b* function in evoking angiogenesis requires the presence of macrophages, since skewing haematopoiesis towards neutrophils at the expenses of macrophages severely affected the induction of the angiogenesis. This conclusion is in line with previous data showing that macrophage depletion by transcription factor *spi1/pu.1* knockdown reduced the recruitment of new vessels to the *Mm* infection foci[22]. Together, these results support that *cxcr4b* exerts its function on macrophages in a cell-autonomous fashion, and affects their capability to promote angiogenesis.

Macrophages of *cxcr4b* mutants were normally capable of migrating to initial mycobacterial infection foci and were equally suited to contain initial intramacrophage bacterial replication, therefore excluding significant effects of *cxcr4b* on the establishment of mycobacteria/macrophage parasitism. Apart from the deficiency in the expansion rate and the absence of associated vascularisation, infectious lesions of *cxcr4b*$^{-/-}$ were structurally undistinguishable from those of wt when granulomas of similar sizes were compared. Since previous studies reported that *vegfaa* expression pattern coincided with the local promotion of granuloma angiogenesis[22], we hypothesised that Cxcr4b might support angiogenesis via promotion of *vegfaa* expression. The induction levels of *vegfaa* in

Mm infected larvae were low and we could not detect a significant difference between infected *cxcr4b* mutants and wt. Several studies have shown that VEGF induction in inflammatory processes can be transient and largely variable[36,37,38]. Therefore, a direct function of *cxcr4b* in the regulation of Vegf/Vegfr signalling cannot be completely excluded by our study. Interestingly, we observed a more pronounced effect of *cxcr4b* mutation on the induction of inflammatory mediators, especially *ilb* and *cxcl18b.* Several reports showed that CXCR4 signalling can support inflammation. In particular, elegant studies revealed that CXCR4 can cross-talk with the plasma membrane Toll-like receptor TLR4 and act as a potent co-stimulatory mediator[29,30]. This leads us to hypothesise that *cxcr4b* may contribute to the maintenance of a favourable pro-angiogenesis microenvironment, by sustaining the production of inflammatory factors.

There is growing evidence of a tight link between the angiogenesis process and inflammation[31,32]. Many factors that are produced to promote the inflammatory response can also promote angiogenesis. Inflammatory cells, especially macrophages, are exceptional producers of these pro-angiogenic mediators, which include prostaglandins, TNFα, interleukins (especially IL1β-6-8)[31,32,33]. IL8/CXCL8 is both chemotactic and mitogenic for endothelial cells[39,40]. Similarly, IL1β has been reported to be a potent inducer of endothelial cell migration and proliferation, which induces profound morphological transformations of these cells and changes in the expression profile, including induction of genes that are intimately involved in the regulation of blood vessel formation[33,41,42]. A transcriptional analysis of endothelial cells upon stimulation with either VEGF or IL1 reported about 80% overlap of their transcriptional signature, which coincided with a cluster of core pro-angiogenetic genes involved in cell proliferation, chemotaxis and blood vessel differentiation[43]. In a matrigel model for angiogenesis, both IL1β and VEGF signalling were indispensable and neutralisation of either one of these factors was sufficient to fully abolish the angiogenic response[33,42].

In our study Il1β, which was significantly suppressed at transcriptional levels in infected *cxcr4b* mutants compared to infected wt larvae, may represent a key impaired pro-angiogenetic mediator. Additionally, Cxcl18b, a fish specific chemokine, appeared also significantly downregulated in these mutants. Despite that the role of this chemokine has not been fully elucidated, our own studies indicate that this chemokine shares high functional similarities with IL8/CXCL8[44], indicating that, similarly to IL8/CXCL8, Cxcl18b might also be important for chemotaxis and cell division of the endothelial cells. The importance of inflammation for granuloma vascularisation in the zebrafish trunk-granuloma model is also suggested by previous studies, where attenuated (ESX1-deficient) *Mm* could not induce angiogenesis even when larvae were injected with larger inoculums to compensate for the infection burden difference[22]. Similarly, also non-chronic infections (*E. coli*) did not evoke the angiogenetic programme[22]. Whether *cxcr4b* sustains activation of the angiogenic programme by supporting the release of inflammatory mediators that are chemotactic/mitogenic for the endothelial cells will require additional characterisation and the zebrafish model may represent an elective surrogate system to further address the angiogenesis/inflammation co-dependency *in vivo*.

Concluding, the angiogenesis programme mounted at the granuloma is important to sustain the further expansion of the lesion and is a complex multifaceted process that involves pathogen virulence factors, macrophage response to intracellular infection and granuloma aggregation, induction of local hypoxia and *vegfaa* signalling[22]. Our addition to this

scenario is that the homoeostatic chemokine receptor CXCR4 is critical to permit the induction of the angiogenetic programme, a mechanism that could be exerted by modulation of the inflammatory pro-angiogenetic mediators released in the granuloma microenvironment, such as IL1β. Manipulation of the inflammation/angiogenesis interface triggers significant consequences to the pathology of the mycobacterial infection and interfering with this programme via host-directed therapies can be useful to limit mycobacterial disease. This and previous studies have shown that similar suppression of mycobacterial growth can be obtained by directly blocking VEGF/VEGFR signalling or by limiting the inflammatory response[22,23,45,46,47]. However, blockade of CXCR4 may provide a preferential treatment, for example in HIV-positive TB patients, where CXCR4 plays also a relevant function in viral entry, therefore, its suppression would simultaneously counteract both mycobacterial and viral infection.

MATERIALS AND METHODS

Zebrafish lines and maintenance – Zebrafish lines were handled in compliance with the local animal welfare regulations and maintained according to standard protocols (zfin.org). The study was approved by the local animal welfare committee (DEC) of the University of Leiden (licence number: 10612). Fish lines used in this work were the following: wildtype strain AB/TL, *Tg(il1b:eGFP-F^{cf550})*[34] the double transgenic line *Tg(mpeg1:mCherry-F^{ump2}/mpx:eGFP^{i114})*[48,49], *cxcr4b* homozygote mutant (*cxcr4b$^{-/-}$*) and wildtype (*cxcr4b$^{+/+}$*) siblings of *(cxcr4b^{t26035})*[8,14] crossed into the transgenic backgrounds of *Tg(kdrl:eGFP^{s843})*[25] or *Tg(mpeg1:mCherry-F^{ump2})*. Embryos were grown at 28.5°C in egg water (60 µg/ml sea salt, Sera Marin, Heinsberg, Germany). Larvae destined to image acquisition were maintained in egg water supplemented with 0.003% PTU (1-phenyl-2-thiourea, Sigma-Aldrich, St Louis, MO, USA) from 8-12 hpf to prevent melanisation. Anaesthesia of embryos/larvae used for live imaging was achieved with 0.02% buffered Tricaine (3-aminobenzoic acid ethyl ester, Sigma-Aldrich) in egg water.

Bacterial cultures and infection delivery – Approximately 60-100 CFU suspended in a volume of 10 nl of *M. marinum* strain M (or where specified its isogenic mutant strain *Δerp*) constitutively expressing mCherry, eGFP or Wasabi[50,51] were injected into the trunk at 2 dpf[22], while approximately 50 CFU in a volume of 1 nl were injected into the hindbrain (HB, 2 dpf). For recruitment assays and qRT-PCR experiments, the same volume of mock [2% polyvinylpyrrolidone-40 (Sigma-Aldrich) in phosphate buffer saline (PBS)] was injected in control embryos, as a reference control. Bacteria were grown and harvested from an O/N culture as described previously[52,53]. For morpholino experiments (*irf8* knockdown) and collection of samples for qRT-PCR, trunk infections were performed at 33 hpf (instead of 2 dpf). For the assessment of the microbicidal activity of macrophages against initial mycobacterial infection, single cell suspensions of *Mm Δerp*-mWasabi were injected into the caudal vein at 33 hpf from -80ºC frozen single-use aliquots, using a protocol adapted from reference[51]. Briefly, bacteria from a 1-week-old plate were inoculated to an OD600 of 0.2 in 10 ml 7H9 medium supplemented with ADC enrichment. The culture was grown for 24 h to reach an OD of approximately 1.0. Bacteria were washed 3 times with PBS and suspended in PBS supplemented with 10% glycerol to an OD600 of 5.0. To generate a single cell suspension, bacteria were passed 10 times through a syringe. 50 µl aliquots were frozen in liquid nitrogen and stored at -80ºC. Upon thawing, the vital bacteria were quantified by plating as being approximately 100 CFU/nl. For quantification of macrophage and neutrophils recruitment to mycobacteria, 2 dpf embryos

were infected in the hindbrain, fixed at 3 hpi in 4% paraformaldehyde in PBS supplemented with 0.08% Triton X-100 and prepared for combined L-plastin (Lp) immunostaining and myeloperoxidase (Mpx) enzymatic activity staining as in reference[54]. Leukocytes accumulated at the injected cavity (macrophages: Lp-positive and Mpx-negative; neutrophils: Mpx-positive) were counted using a Leica MZ16FA fluorescence stereomicroscope (Leica Microsystems, Rijswijk, The Netherlands).

RNA isolation, FACS and qRT-PCR – To evaluate the induction of genes upon infections (**Figure 4C**), whole-embryo RNA extraction, cDNA synthesis and qRT-PCR were performed at 5 dpi from a pool of embryos injected at 33 hpi (4 replicates), according to the procedure described in reference[52]. To demonstrate expression by phagocytes (**Figure 3H**), RNA was isolated from *mpx*$^{+}$ and *mpeg1*$^{+}$ cells sorted at 2 dpf from the double transgenic line *Tg(mpeg1:mCherry-F*^{ump2}*/mpx:eGFP*^{i114}*),* according to previous reports[55,52]. Similarly, to evaluate expression of *cxcr4b* by endothelial cells (**Supplementary Figure 1**), RNA was isolated from *kdrl*$^{+}$ or *mpeg*1^{+} cells of *cxcr4b*$^{+/+}$ and *cxcr4b*$^{-/-}$ larvae (5 dpi/6 dpf) derived from paired crosses of *Tg(mpeg1:mCherry-F/cxcr4b*$^{+/+}$*)* x *Tg(kdrl:eGFP/cxcr4b*$^{+/+}$*)* and *Tg(mpeg1:mCherry-F/cxcr4b*$^{-/-}$*)* x *Tg(kdrl:eGFP/cxcr4b*$^{-/-}$*).*

Reference housekeeping genes were *ppia1b* for whole-mount samples and *eif4a1b* for FACS-sorted samples. qRT-PCR primers are reported in **Supplementary Table S1**.

Pharmacological inhibition of VEGF signalling – For pharmacological inhibition of VEGF signalling, the VEGFR tyrosine kinase inhibitor Sunitinib (1 µM, Sigma-Aldrich) or vehicle treatment (0.1% DMSO, Sigma-Aldrich), were applied directly to the egg water and refreshed every 2 days according to reference[28].

***Irf8* knockdown** – 1 nl of 1 mM *irf8* splicing morpholino (5′-AATGTTTCGCTTACTTTGAAAATGG-3′, Gene tools)[27] or the same concentration of a standard control morpholino (5′-CCTCTTACCTCAGTTACAATTTATA-3′, Gene tools) were injected in one-cell stage zebrafish fertilised eggs according to reference[27].

Imaging and image quantification – Fixed or live embryos and larvae were imaged using a Leica MZ16FA fluorescence stereomicroscope. The size of individual granulomas was quantified at 5 dpi (at 4 dpi in case of *irf8* morpholino knockdown) by pixel count, using Fiji/ImageJ software (NIH, Bethesda, MD, USA) according to reference[52]. The length of abnormal vasculature at the granulomas was quantified at the same stage from images according to reference[22]. To score the microbicidal activity of macrophages against mycobacteria, *MmΔerp*-Wasabi bacteria prepared as described above were injected into the caudal vein of *Tg(mpeg1:mCherry-F)/cxcr4b*$^{-/-}$ and *Tg(mpeg1:mCherry-F)/cxcr4b*$^{+/+}$ embryos. Intramacrophage mycobacterial sites of growth were counted (blind) from fixed embryos at 44 hpi according to reference[47] , using Zeiss Observer 6.5.32 confocal microscope and a C-Apochromat 63x/1.20 W Korr UV-VIR-IR M27 objective (Carl Zeiss, Sliedrecht, The Netherlands). The level of infection per macrophage was classified into three groups based on bacterial content (1-5 bacteria, 6-10 bacteria or >10 bacteria). To estimate similar macrophage content of granulomas, the percentage of colocalisation of *Tg(mpeg1:mCherry-F)* and *Mm* M-eGFP was quantified ad 5 dpi using Fiji/ImageJ dedicated colocalisation plugin. Confocal images in **Figure 4** were taken from trunk granulomas at 5 dpi/6 dpf, using Zeiss Observer 6.5.32 confocal microscope and an EC

Plan-Neofluar 20x/0.50 M27 (**Figure 4D**) or C-Apochromat 63x/1.20 W Korr UV-VIR-IR M27 objective (**Figure 4E**).

Statistical analysis – Statistical significance was analysed using GraphPad Prism 6 (GraphPad Software, La Jolla, CA, USA). Differences in granuloma sizes, angiogenesis, recruitment and bacteria/macrophage co-localisation were statistically tested by Mann-Whitney test (comparison between 2 groups) or Kruskal-Wallis test followed by Šidák comparison test (multiple group comparisons) (**Figure 2A-B**, **Figure 3A-B-E**, **Figure 4A-B**). Bacterial cluster size/angiogenesis correlation (**Figure 2C**) was analysed by Pearson correlation test and the difference between mutant and wt regressions was computed by GraphPad Prism 6 dedicated linear regression analysis tool. No differences in bacterial replication and in the distribution of macrophages in the three phenotypic classes (as defined above) were analysed by two-tailed *t*-tests per each phenotypic class (**Figure 3C**) and by chi-square contingency test (**Figure 3D**) respectively. For qRT-PCR (**Figure 4C**), statistical significance was estimated by two-tailed *t*-tests on ln(n)-transformed relative induction folds. Significance (*P*-value) is indicated with: ns, non-significant; **P*<0.05; ***P*<0.01; ****P*<0.001, *****P*<0.0001. Error bars: mean±s.e.m.

ACKNOWLEDGEMENTS

We thank Georges Lutfalla for having provided the *Tg(il1b:eGFP-F)* transgenic line.

This work was supported by the European Marie-Curie Initial Training Network FishForPharma (contract number PITN-GA-2011-289209) and by the Netherlands Organisation for Scientific Research (TOP GO Grant: 854.10.012).

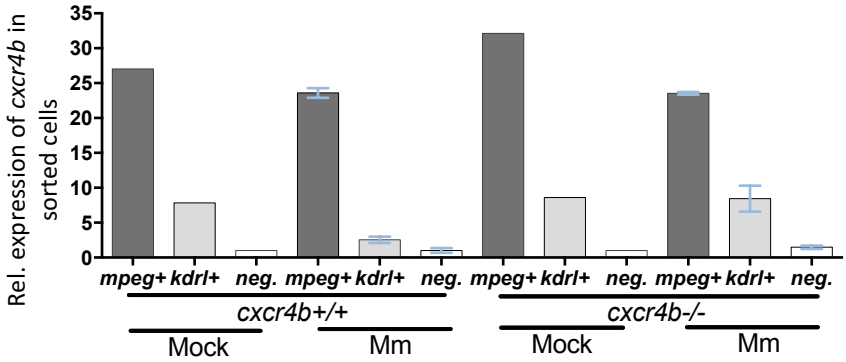

Supplementary Figure 1. Expression levels of *cxcr4b* in FACS-sorted macrophages and endothelial cells during mycobacterial infection. Data represent fold changes relative to the negative cell population. Cells were sorted at 5 dpi (2 replicates for *Mm* infected groups and 1 replicate for mock control) from pools of embryos injected at 33 hpf.

Gene	Transcript reference	qRT-PCR Fw (5'-3')	qRT-PCR Rv (5'-3')	Ref.
vegfaa	ENSDART00000167719	TGCTCCTGCAAATTCACACAA	ATCTTGGCTTTTCACATCTGCAA	Li *et al.* 2012
cxcr4b	ENSDART00000061499	GCGACCTCTCAGTCAGCAAT	TCACAAGCACCACAAGTCCA	-
cxcl12a	ENSDART00000053946	GCTGGTGCCGTTCCACAGTCA	GGGGCAGTTGGGTGTGTGGAG	-
tnfa	ENSDART00000025847	AGACCTTAGACTGGAGAGATGAC	CAAAGACACCTGGCTGTAGAC	Stockhammer *et al.* 2009
cxcl11aa	ENSDART00000169606	ACTCAACATGGTGAAGCCAGTGCT	CTTCAGCGTGGCTATGACTTCCAT	Torraca *et al.* 2015
cxcl18b	ENSDART00000111598	TCTTCTGCTGCTGCTTGCGGT	GGTGTCCCTGCGAGCACGAT	Van der Vaart *et al.* 2013
il1b	ENSDART00000169225	GAACAGAATGAAGCACATCAAACC	ACGGCACTGAATCCACCAC	Stockhammer *et al.* 2009
mmp9	ENSDART00000062845	CATTAAAGATGCCCTGATGTATCCC	AGTGGTGGTCCGTGGTTGAG	Stockhammer *et al.* 2009
ppiab	ENSDART00000166085	ACACTGAAACACGGAGGCAAAG	CATCCACAACCTTCCCGAACAC	Stockhammer *et al.* 2009
eif4a1b	ENSDART00000140602 ENSDART00000011878	TTCAGAAACTCAGTACTAGCATACA	GTGACATCCAACACCTCTGC	Benard *et al.* 2015

Supplementary Table 1. Primers used for qRT-PCR in this study.

REFERENCES

1 Furze RC, Rankin SM. Neutrophil mobilization and clearance in the bone marrow. Immunology. 2008 Nov;125(3):281-8.

2 Walters KB, Green JM, Surfus JC, Yoo SK, Huttenlocher A. Live imaging of neutrophil motility in a zebrafish model of WHIM syndrome. Blood. 2010 Oct 14;116(15):2803-11.

3 Fricker SP. A novel CXCR4 antagonist for hematopoietic stem cell mobilization. Expert Opin Investig Drugs. 2008 Nov;17(11):1749-60.

4 Uy GL, Rettig MP, Cashen AF. Plerixafor, a CXCR4 antagonist for the mobilization of hematopoietic stem cells. Expert Opin Biol Ther. 2008 Nov;8(11):1797-804.

5 Doitsidou M, Reichman-Fried M, Stebler J, Köprunner M, Dörries J, Meyer D, Esguerra CV, Leung T, Raz E. Guidance of primordial germ cell migration by the chemokine SDF-1. Cell. 2002 Nov 27;111(5):647-59.

6 Gelmini S, Mangoni M, Serio M, Romagnani P, Lazzeri E. The critical role of SDF-1/CXCR4 axis in cancer and cancer stem cells metastasis. J Endocrinol Invest. 2008 Sep;31(9):809-19.

7 Mukherjee S, Manna A, Bhattacharjee P, Mazumdar M, Saha S, Chakraborty S, Guha D, Adhikary A, Jana D, Gorain M, Mukherjee SA, Kundu GC, Sarkar DK, Das T. Non-migratory tumorigenic intrinsic cancer stem cells ensure breast cancer metastasis by generation of CXCR4(+) migrating cancer stem cells. Oncogene. 2016 Feb 29.

8 Tulotta C, Stefanescu C, Beletkaia E, Bussmann J, Tarbashevich K, Schmidt T, Snaar-Jagalska BE. Inhibition of signaling between human CXCR4 and zebrafish ligands by the small molecule IT1t impairs the formation of triple-negative breast cancer early metastases in a zebrafish xenograft model. Dis Model Mech. 2016 Feb 1;9(2):141-53.

9 Alkhatib G, Berger EA. HIV coreceptors: from discovery and designation to new paradigms and promise. Eur J Med Res. 2007 Oct 15;12(9):375-84.

10 Donà E, Barry JD, Valentin G, Quirin C, Khmelinskii A, Kunze A, Durdu S, Newton LR, Fernandez-Minan A, Huber W, Knop M, Gilmour D. Directional tissue migration through a self-generated chemokine gradient. Nature. 2013 Nov 14;503(7475):285-9.

11 Haas P, Gilmour D. Chemokine signaling mediates self-organizing tissue migration in the zebrafish lateral line. Dev Cell. 2006 May;10(5):673-80.

12 Tamplin OJ, Durand EM, Carr LA, Childs SJ, Hagedorn EJ, Li P, Yzaguirre AD, Speck NA, Zon LI. Hematopoietic stem cell arrival triggers dynamic remodeling of the perivascular niche. Cell. 2015 Jan 15;160(1-2):241-52.

13 Raz E, Mahabaleshwar H. Chemokine signaling in embryonic cell migration: a fisheye view. Development. 2009 Apr;136(8):1223-9.
14 Knaut H, Werz C, Geisler R, Nüsslein-Volhard C; Tübingen 2000 Screen Consortium. A zebrafish homologue of the chemokine receptor Cxcr4 is a germ-cell guidance receptor. Nature. 2003 Jan 16;421(6920):279-82.
15 Liang Z, Brooks J, Willard M, Liang K, Yoon Y, Kang S, Shim H. CXCR4/CXCL12 axis promotes VEGF-mediated tumor angiogenesis through Akt signaling pathway. Biochem Biophys Res Commun. 2007 Aug 3;359(3):716-22.
16 Massena S, Christoffersson G, Vågesjö E, Seignez C, Gustafsson K, Binet F, Herrera Hidalgo C, Giraud A, Lomei J, Weström S, Shibuya M, Claesson-Welsh L, Gerwins P, Welsh M, Kreuger J, Phillipson M. Identification and characterization of VEGF-A-responsive neutrophils expressing CD49d, VEGFR1, and CXCR4 in mice and humans. Blood. 2015 Oct 22;126(17):2016-26.
17 Katkoori VR, Basson MD, Bond VC, Manne U, Bumpers HL. Nef-M1, a peptide antagonist of CXCR4, inhibits tumor angiogenesis and epithelial‐to‐mesenchymal transition in colon and breast cancers. Oncotarget. 2015 Sep 29;6(29):27763-77.
18 Alatas F, Alatas O, Metintas M, Ozarslan A, Erginel S, Yildirim H. Vascular endothelial growth factor levels in active pulmonary tuberculosis. Chest. 2004 Jun;125(6):2156-9.
19 Tsai MC, Chakravarty S, Zhu G, Xu J, Tanaka K, Koch C, Tufariello J, Flynn J, Chan J. Characterization of the tuberculous granuloma in murine and human lungs: cellular composition and relative tissue oxygen tension. Cell Microbiol. 2006 Feb;8(2):218-32.
20 Matsuyama W, Hashiguchi T, Matsumuro K, Iwami F, Hirotsu Y, Kawabata M, Arimura K, Osame M. Increased serum level of vascular endothelial growth factor in pulmonary tuberculosis. Am J Respir Crit Care Med. 2000 Sep;162(3 Pt1):1120-2.
21 Saita N, Fujiwara N, Yano I, Soejima K, Kobayashi K. Trehalose 6,6'-dimycolate (cord factor) of Mycobacterium tuberculosis induces corneal angiogenesis in rats. Infect Immun. 2000 Oct;68(10):5991-7.
22 Oehlers SH, Cronan MR, Scott NR, Thomas MI, Okuda KS, Walton EM, Beerman RW, Crosier PS, Tobin DM. Interception of host angiogenic signalling limits mycobacterial growth. Nature. 2015 Jan 29;517(7536):612-5.
23 Ramakrishnan L. Revisiting the role of the granuloma in tuberculosis. Nat Rev Immunol. 2012 Apr 20;12(5):352-66.
24 Meijer AH. Protection and pathology in TB: learning from the zebrafish model. Semin Immunopathol. 2016 Mar;38(2):261-73.
25 Jin SW, Beis D, Mitchell T, Chen JN, Stainier DY. Cellular and molecular analyses of vascular tube and lumen formation in zebrafish. Development. 2005 Dec;132(23):5199-209.
26 Folkman J. Role of angiogenesis in tumor growth and metastasis. Semin Oncol. 2002 Dec;29(6 Suppl 16):15-8.
27 Li L, Jin H, Xu J, Shi Y, Wen Z. Irf8 regulates macrophage versus neutrophil fate during zebrafish primitive myelopoiesis. Blood. 2011 Jan 27;117(4):1359-69.
28 He S, Lamers GE, Beenakker JW, Cui C, Ghotra VP, Danen EH, Meijer AH, Spaink HP, Snaar-Jagalska BE. Neutrophil-mediated experimental metastasis is enhanced by VEGFR inhibition in a zebrafish xenograft model. J Pathol. 2012 Aug;227(4):431-45.
29 Triantafilou M, Lepper PM, Briault CD, Ahmed MA, Dmochowski JM, Schumann C, Triantafilou K. Chemokine receptor 4 (CXCR4) is part of the lipopolysaccharide "sensing apparatus". Eur J Immunol. 2008 Jan;38(1):192-203.
30 Kishore SP, Bungum MK, Platt JL, Brunn GJ. Selective suppression of Toll-like receptor 4 activation by chemokine receptor 4. FEBS Lett. 2005 Jan31;579(3):699-704.
31 Naldini A, Carraro F. Role of inflammatory mediators in angiogenesis. Curr Drug Targets Inflamm Allergy. 2005 Feb;4(1):3-8.
32 Jackson JR, Seed MP, Kircher CH, Willoughby DA, Winkler JD. The codependence of angiogenesis and chronic inflammation. FASEB J. 1997 May;11(6):457-65.
33 Carmi Y, Dotan S, Rider P, Kaplanov I, White MR, Baron R, Abutbul S, Huszar M, Dinarello CA, Apte RN, Voronov E. The role of IL-1β in the early tumor cell-induced angiogenic response. J Immunol. 2013 Apr 1;190(7):3500-9.
34 Nguyen-Chi M, Phan QT, Gonzalez C, Dubremetz JF, Levraud JP, Lutfalla G. Transient infection of the zebrafish notochord with E. coli induces chronic inflammation. Dis Model Mech. 2014 Jul;7(7):871-82.
35 Cha YR, Fujita M, Butler M, Isogai S, Kochhan E, Siekmann AF, Weinstein BM. Chemokine signaling directs trunk lymphatic network formation along the preexisting blood vasculature. Dev Cell. 2012 Apr 17;22(4):824-36.
36 Hudlicka O, Milkiewicz M, Cotter MA, Brown MD. Hypoxia and expression of VEGF-A protein in relation to capillary growth in electrically stimulated rat and rabbit skeletal muscles. Exp Physiol. 2002 May;87(3):373-81.

37 Stone J, Itin A, Alon T, Pe'er J, Gnessin H, Chan-Ling T, Keshet E. Development of retinal vasculature is mediated by hypoxia-induced vascular endothelial growth factor (VEGF) expression by neuroglia. J Neurosci. 1995 Jul;15(7 Pt 1):4738-47.
38 Datta M, Via LE, Kamoun WS, Liu C, Chen W, Seano G, Weiner DM, Schimel D, England K, Martin JD, Gao X, Xu L, Barry CE 3rd, Jain RK. Anti-vascular endothelial growth factor treatment normalizes tuberculosis granuloma vasculature and improves small molecule delivery. Proc Natl Acad Sci U S A. 2015 Feb 10;112(6):1827-32.
39 Azenshtein E, Meshel T, Shina S, Barak N, Keydar I, Ben-Baruch A. The angiogenic factors CXCL8 and VEGF in breast cancer: regulation by an array of pro-malignancy factors. Cancer Lett. 2005 Jan 10;217(1):73-86.
40 Heidemann J, Ogawa H, Dwinell MB, Rafiee P, Maaser C, Gockel HR, Otterson MF, Ota DM, Lugering N, Domschke W, Binion DG. Angiogenic effects of interleukin 8 (CXCL8) in human intestinal microvascular endothelial cells are mediated by CXCR2. J Biol Chem. 2003 Mar 7;278(10):8508-15.
41 Voronov E, Shouval DS, Krelin Y, Cagnano E, Benharroch D, Iwakura Y, Dinarello CA, Apte RN. IL-1 is required for tumor invasiveness and angiogenesis. Proc Natl Acad Sci U S A. 2003 Mar 4;100(5):2645-50.
42 Voronov E, Carmi Y, Apte RN. The role IL-1 in tumor-mediated angiogenesis. Front Physiol. 2014 Mar 28;5:114.
43 Schweighofer B, Testori J, Sturtzel C, Sattler S, Mayer H, Wagner O, Bilban M, Hofer E. The VEGF-induced transcriptional response comprises gene clusters at the crossroad of angiogenesis and inflammation. Thromb Haemost. 2009 Sep;102(3):544-54.
44 Torraca V, Otto NA, Tavakoli-Tameh A, Meijer AH, The inflammatory chemokine Cxcl18b exerts neutrophil-specific chemotaxis via the promiscuous chemokine receptor Cxcr2 in zebrafish. *Chapter 7 of this thesis.*
45 Tobin DM, Vary JC Jr, Ray JP, Walsh GS, Dunstan SJ, Bang ND, Hagge DA, Khadge S, King MC, Hawn TR, Moens CB, Ramakrishnan L. The lta4h locus modulates susceptibility to mycobacterial infection in zebrafish and humans. Cell. 2010 Mar 5;140(5):717-30.
46 Tobin DM, Roca FJ, Oh SF, McFarland R, Vickery TW, Ray JP, Ko DC, Zou Y, Bang ND, Chau TT, Vary JC, Hawn TR, Dunstan SJ, Farrar JJ, Thwaites GE, King MC, Serhan CN, Ramakrishnan L. Host genotype-specific therapies can optimize the inflammatory response to mycobacterial infections. Cell. 2012 Feb 3;148(3):434-46.
47 Roca FJ, Ramakrishnan L. TNF dually mediates resistance and susceptibility to mycobacteria via mitochondrial reactive oxygen species. Cell. 2013 Apr 25;153(3):521-34.
48 Bernut A, Herrmann JL, Kissa K, Dubremetz JF, Gaillard JL, Lutfalla G, Kremer L. Mycobacterium abscessus cording prevents phagocytosis and promotes abscess formation. Proc Natl Acad Sci U S A. 2014 Mar 11;111(10):E943-52.
49 Renshaw SA, Loynes CA, Trushell DM, Elworthy S, Ingham PW, Whyte MK. A transgenic zebrafish model of neutrophilic inflammation. Blood. 2006 Dec 15;108(13):3976-8.
50 van der Sar AM, Abdallah AM, Sparrius M, Reinders E, Vandenbroucke-Grauls CM, Bitter W. Mycobacterium marinum strains can be divided into two distinct types based on genetic diversity and virulence. Infect Immun. 2004 Nov;72(11):6306-12.
51 Takaki K, Davis JM, Winglee K, Ramakrishnan L. Evaluation of the pathogenesis and treatment of Mycobacterium marinum infection in zebrafish. Nat Protoc. 2013 Jun;8(6):1114-24.
52 Torraca V, Cui C, Boland R, Bebelman JP, van der Sar AM, Smit MJ, Siderius M, Spaink HP, Meijer AH. The CXCR3-CXCL11 signaling axis mediates macrophage recruitment and dissemination of mycobacterial infection. Dis Model Mech. 2015 Mar;8(3):253-69.
53 Benard EL, van der Sar AM, Ellett F, Lieschke GJ, Spaink HP, Meijer AH. Infection of zebrafish embryos with intracellular bacterial pathogens. J Vis Exp. 2012 Mar 15;(61).
54 Cui C, Benard EL, Kanwal Z, Stockhammer OW, van der Vaart M, Zakrzewska A, Spaink HP, Meijer AH. Infectious disease modeling and innate immune function in zebrafish embryos. Methods Cell Biol. 2011;105:273-308.
55 Rougeot J, Zakrzewska A, Kanwal Z, Jansen HJ, Spaink HP, Meijer AH. RNA sequencing of FACS-sorted immune cell populations from zebrafish infection models to identify cell specific responses to intracellular pathogens. Methods Mol Biol.2014;1197:261-74.

Chapter 7

The inflammatory chemokine Cxcl18b exerts neutrophil-specific chemotaxis via the promiscuous chemokine receptor Cxcr2 in zebrafish

Vincenzo Torraca, Natasja A. Otto, Aidin Tavakoli-Tameh and Annemarie H. Meijer

Institute of Biology, Leiden University, The Netherlands

Manuscript in preparation

Chapter 7

The inflammatory chemokine Cxcl18b exerts neutrophil-specific chemotaxis via the promiscuous chemokine receptor Cxcr2 in zebrafish

Vincenzo Torraca, Natasja A. Otto, Aidin Tavakoli-Tameh and Annemarie H. Meijer

Institute of Biology, Leiden University, The Netherlands

The zebrafish (*Danio rerio*) model has proven successful in many infection/inflammation-related studies. To ensure the translational impact of the zebrafish model in this field, it is important to clarify the homologies between the zebrafish and the human immune systems. Cxcl18b is a chemokine found in zebrafish and conserved in several piscine and amphibian species, although this lineage has not been maintained in the divergence of amniotes. The function of Cxcl18b is yet to be elucidated. However, this ligand represents a valid inflammatory marker in fish, found recurrently upregulated during infection/inflammation. In this study, we produced recombinant zebrafish Cxcl18b and, by local injections *in vivo,* we found that this ligand exhibits specific chemotactic properties towards neutrophils, comparable to those exerted by Cxcl8a, also known as Il8, the best characterised neutrophil chemotactic factor in both humans and teleosts. By pharmacological manipulations, we found that, like Cxcl8a, Cxcl18b requires the chemokine receptor Cxcr2 for optimal chemotaxis, although Cxcl18b, differently from Cxcl8a, could still mediate residual recruitment of neutrophils under conditions of Cxcr2 inhibition. However, the remaining recruitment of Cxcl18b did not rely on expression of *cxcr1* or *cxcr4b,* two other known neutrophil receptors. To visualise the *cxcl18b* expression pattern we generated a *Tg(cxcl18b:eGFP)* reporter line and found that this transgene is induced upon bacterial infection with *Mycobacterium marinum*, in agreement with previous mRNA expression data. The *cxcl18b* reporter expression coincides with the areas of bacterial growth but seems not directly induced in infected cells. Instead, it is predominantly expressed by non-infected cells participating in the initial formation of inflammatory granulomatous lesions that are critical to the pathogenesis of mycobacterial infection. Together, these results suggest that Cxcl18b could be an important contributor to neutrophil chemotaxis in the granuloma microenvironment in the zebrafish model and emphasise the need for a better understanding of how this inflammatory chemokine relates to the better-characterised class of Cxcl8 neutrophil chemotactic factors.

GRAPHICAL ABSTRACT

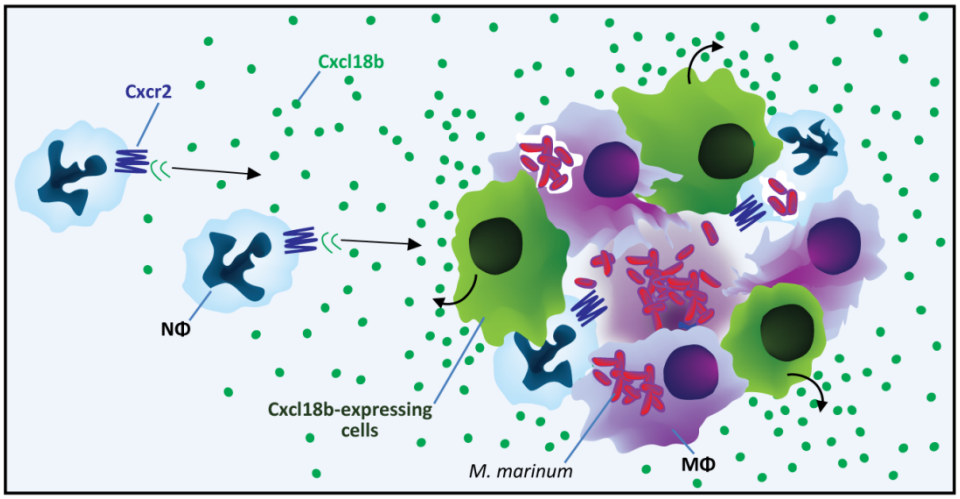

The chemokine Cxcl18b is able to specifically promote neutrophil chemotaxis. This is at least partly evoked by signalling via the neutrophil chemokine receptor CXCR2. During infection with *M. marinum*, several cells that participate in the formation of the granulomas produce the chemokine ligand Cxcl18b. Generally, these cells are not intracellularly infected and do not express the neutrophil and macorphage markers *lyz* and *mpeg1,* suggesting that they do not represent phagocytic cells, but stromal cells that contribute to the granuloma structure.

INTRODUCTION

The constant interplay between microbes and their hosts is the driving force for the evolution of pathogens and of the host immune system. Complex systems of pathogen virulence and corresponding control mechanisms in their hosts have originated from their co-evolution. Studying infectious diseases in the context of a whole living organism provides the possibility to better understand these mechanisms and to translate them into novel therapeutic strategies. Both the innate and the adaptive immune systems are well conserved among vertebrates and the zebrafish (*Danio rerio*) is an excellent model organism to study the biology of infectious and inflammatory diseases, especially because of the optical accessibility of its early embryonic and larval stages[1,2]. The transparency of the zebrafish allows direct visualisation of cellular migration processes in response to chemotactic cues and infections. To facilitate *in vivo* analysis, many fluorescent reporter lines have been developed that label different immune cell types, including macrophages and neutrophils[3,4]. Additionally, the use of the zebrafish has been extended by combining the optical properties of this model with pharmacological and genetic tools that well apply to this species, due to high permeability to compounds by submersion and to the ease of application of gene editing techniques[5,6].

Chemokines are a family of small cell-signalling proteins that direct the migration of cells expressing the corresponding receptors towards a ligand concentration gradient. The CXC subgroup of chemokines (containing the Cysteine-X-Cysteine motif) is well conserved between mammalian and teleost species. In mammals, this family can be further divided into ELR+ and ELR− chemokines, based on the presence or absence of the Glutamic acid-Leucine-Arginine motif preceding the CXC sequence. ELR+ chemokines include CXCL1-2-3 (GROα-β-γ), CXCL5 (ENA78), CXCL6 (GCP2), CXCL7 (NAP2) and CXCL8 (IL8). These are potent chemoattractants of neutrophils[7,8,9,10,11,12], while ELR− chemokines, such as CXCL9 (MIG), CXCL10 (IP-10) and CXCL11 (I-TAC), are best known for the attraction of lymphocytes and monocyte/macrophages and possess poor chemotactic ability towards neutrophils. In fish, the ELR sequence is not conserved in chemokines that exert neutrophil chemotactic properties[13]. However, it has been demonstrated that the zebrafish Cxcl8/Il8 (Interleukin 8) paralogues, despite being ELR-deficient, are still potent attractors of neutrophils[5,14,15].

CXCL8 is the best-studied neutrophil chemoattractant in humans[11,12] and is conserved in zebrafish[5,14,15], while absent in rodents[16,17]. In both zebrafish and mammals, Cxcl8/CXCL8 signals via the receptor Cxcr2/CXCR2[5,12,14]. In mice this receptor still exerts a chemotactic activity towards neutrophils, but this is evoked by binding to other ELR+ chemokines CXCL1-2-3-5-7[12], to the non-chemokine tripeptide PGP (Pro-Gly-Pro, a molecule that derives from extracellular matrix breakdown)[18] and to MIF (macrophage migration inhibitory factor, a non-chemokine component which inhibits macrophage migration but sustains neutrophil recruitment)[19]. The CXCR2 receptor is promiscuous in humans too and can respond to CXCL1-2-3-5-6-7-8[7,8,12], PGP[18,20] and MIF[19]. Finally, in humans, the activity of CXCL8 is non-specific for CXCR2, since this ligand, together with CXCL6-7, can also induce neutrophil chemotaxis via CXCR1, another chemokine receptor, closely related to CXCR2[21]. We currently know that two zebrafish Cxcl8 chemokines, Cxcl8a and Cxcl8bb, require the chemokine receptor Cxcr2 to promote neutrophil chemotaxis[5,14,15]. It is also known that Cxcl8a, differently from its human counterpart, does not require the zebrafish Cxcr1 receptor and chemoattracts neutrophils essentially via Cxcr2[14]. Whether

other lineages of chemokine and non-chemokine ligands are chemotactic towards Cxcr1-2 in zebrafish is not currently known.

A cluster of genes that conserves high sequence homology and synteny with the human CXCL9-10-11 gene cluster also exists in zebrafish[22,23]. Two of these (Cxcl11aa and Cxcl11af) are infection-inducible and require the chemokine receptor Cxcr3.2, an orthologue of mammalian CXCR3. Similarly to the mammalian axis, the Cxcr3.2 receptor induces macrophage recruitment[23]. In addition, macrophages and neutrophils in zebrafish express and are mobilised via Cxcr4b[24] and this receptor has been shown to cross communicate with the human CXCL12, the ligand of human CXCR4[25].

Together with the conservation of the CXCR2, CXCR3, and CXCR4 signalling axes, zebrafish also has a series of other CXC motif chemokines that cannot be unambiguously classified with respect to the mammalian counterparts, due to the short sequence and the fast evolution and divergence of chemokine genes[22]. The absence of the ELR motif in neutrophil-competent teleost chemokines additionally complicates phylogenetic reconstructions and functional classification. Cxcl18b (formerly named Cxcl-c1c) is highly induced in zebrafish upon infection with different pathogens and shares sequence similarities and expression patterns with the zebrafish orthologues of both Cxcl8 and Cxcl11 chemokines (48-53% amino acid similarities to Cxcl8a, Cxcl8bb, Cxcl11aa and Cxcl11af)[22,26,27,28]. Blasting Cxcl18b to the murine and human protein databases reveals instead that murine CXCL3 and human CXCL11 are its two most closely related mammalian chemokines (48% and 47% amino acid similarity, respectively).

Like other inflammatory chemokines, c*xcl18b* transcription was found to rely on the activation of the Myd88-dependent innate immunity signalling pathway during the response to *Edwardsiella tarda*, *Mycobacterium marinum (Mm)* and *Salmonella enterica* serovar Typhimurium[26,27]. Recently, it was also demonstrated that Cxcl18b is upregulated in response to treatment with toxic and pro-apoptotic compounds, which indicates this gene as a marker of inflammation in general[28,29]. However, the function of Cxcl18b has yet to be elucidated and clarification of its role has an important translational significance, since the zebrafish model is being increasingly used to study chemokine axes, leukocyte biology, and inflammatory processes[30]. This study demonstrates that Cxcl18b is an additional neutrophil chemotactic factor. We show that the function of Cxcl18b relies, at least partly on chemokine receptor Cxcr2, and not on Cxcr1 and Cxcr4b. Finally, using a novel reporter line, we show the expression of this chemokine during the pathological inflammation occurring upon mycobacterial infection.

RESULTS

Production and quality confirmation of recombinant Cxcl18b

In order to study the chemotactic properties of Cxcl18b, we set out to produce recombinant protein using a yeast (*Pichia pastoris*) expression system. The coding sequence for Cxcl18b was synthetically generated according to the Ensembl database accession (ENSDARG00000075045/ENSDART00000111598). The sequence was codon optimised for expression in yeast and supplemented with an HA (human influenza haemagglutinin)-tag at the C-terminus, to permit identification with an anti-HA-antibody. Additionally, to facilitate secretion by *Pichia pastoris*, the predicted zebrafish signal peptide of Cxcl18b was replaced with the yeast alpha-factor secretion signal, as a result of cloning of the

Cxcl18b sequence into the pPICZα expression vector. Expression of the construct in successful (Zeocine-resistant) transformants was induced by culturing several isolates in buffered minimal medium supplemented with 0.5% methanol that is used as an inducer of gene expression in this system.

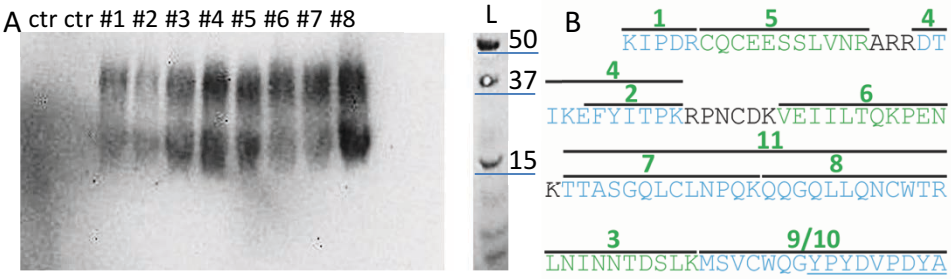

C

CXCLc1c_HA Mass: 11828 Score: 1704 Queries matched: 90 emPAI: 11.70

Query	Observed	Mr(expt)	Mr(calc)	ppm	Miss	Score	Expect	Rank	Peptide	
17	314.6928	627.3710	627.3704	0.90	1	30	0.019	1	**-.KIPDR.C**	1
244	449.2398	896.4650	896.4644	0.75	0	43	0.0012	1	**K.EFYITPK.R**	2
565	566.3031	1130.5916	1130.5931	-1.36	0	35	0.015	1	**R.LNINNTDSLK.M**	3
1118	677.8694	1353.7242	1353.7180	4.55	1	64	1.3e-05	1	**R.DTIKEFYITPK.R**	4
1222	691.2958	1380.5771	1380.5762	0.66	0	69	1e-06	1	**R.CQCEESSLVNR.A**	5
1333	706.4123	1410.8101	1410.8082	1.36	0	74	8.5e-07	1	**K.VEIILTQKPENK.T**	6
1353	709.3580	1416.7014	1416.7031	-1.23	0	87	8.3e-08	1	**K.TTASGQLCLNPQK.Q**	7
1784	766.3750	1530.7355	1530.7361	-0.43	0	66	9.5e-06	1	**K.QQGQLLQNCWTR.L**	8
2938	975.9084	1949.8022	1949.7964	2.95	0	38	0.00064	1	**K.MSVCWQGYPYDVPDYA.-**	9
2988	983.9038	1965.7930	1965.7914	0.84	0	(30)	0.0039	1	**K.MSVCWQGYPYDVPDYA.-**	10
4249	977.4811	2929.4215	2929.4287	-2.47	1	72	1.9e-06	1	**K.TTASGQLCLNPQKQQGQLLQNCWTR.L**	11

Figure 1. Cxcl18b recombinant protein production. A. Western blot analysis of the supernatant derived from eight (#1-#8) isolates of *Pichia pastoris* transformed with Cxcl18b-HA expression vector. The protein was visualised by a HRP-conjugated anti-HA antibody. Lanes marked as ctr refer to the supernatant of two non-transformed isolates. The expected molecular weight of Cxcl18b-HA is 11.5 kDa. However, in the western blot analysis Cxcl18b displayed two bands, one at about 20 kDa and one at about 40 kDa. The 40 kDa band represents most likely a dimer of the 20 kDa product. Increased molecular weight of Cxcl18b as compared to expectation can be explained by glycosylation, difference in salinity/ionic force between the *Pichia pastoris* culture supernatants and the reference protein ladder (L), and high protein concentration in the samples that may delay electrophoretic run. Isolate #8, which appeared to produce the highest levels of recombinant protein, was selected for purification and confirmation by mass spectrometry. **B-C**. Electrospray mass spectrometry analysis of trypsinised Cxcl18b-HA. Virtually all the peptides derived from trypsinisation of Cxcl18b (peptides 1-11) could be detected. Short stretches of the protein could not be identified with statistical significance, because of the high frequency of trypsin digestion sites (.K or .R) on those protein parts (predicted peptides ARR, A, R, PNCD consist of ≤4 residues and are too short for univocal identification). No other zebrafish or *Pichia pastoris* proteins were significantly indicated by the mass spectrometry analysis of purified Cxcl18b. Bars in black in B show the sequence covered by mass spectrometry analysis. The sequence underlined in blue indicates the C-terminal HA tag, used for western blot readout in A. Table of peptide statistics in C was elaborated via Mascott analysis of the Cxcl18b-HA spectrum.

Eight colonies were tested for optimal expression and secretion, by western blot analysis against the HA-sequence on the supernatant of induced cultures (**Figure 1A**). In western blot analysis Cxcl18b displayed two bands (~20 kDa and ~40 kDa), of which the one with the higher molecular weight most likely represents a dimer, as chemokine ligands are known to form very stable dimers[31,32,33,34]. Deviation of molecular weight of the monomer from expectation (11.5 kDa), is most likely due to extensive glycosylation, as multiple glycosylation sites were predicted and chemokines are known to be highly glycosylated[15]. The Cxcl18b-positive clone that appeared to produce the highest levels of chemokine was used for macroscale preparation of Cxcl18b. The supernatant of an induced culture, containing Cxcl18b was concentrated and purified in PBS (phosphate buffer saline) by column filtration. Identity and purity of Cxcl18b in the sample was determined by trypsinisation and electrospray mass spectrometry analysis, which revealed high purity of the protein and undetectable protein contaminations of the recombinant Cxcl18b with *Pichia pastoris* proteins (**Figure 1B-C**).

Cxcl18b induces chemotaxis of neutrophils, but not macrophages

To study the function of Cxcl18b, the isolated chemokine was injected into the hindbrain ventricle of embryos at 2 dpf (days post fertilisation), in neutrophil-specific (*mpx:eGFP*-positive cells[4]) or macrophage-specific (*mpeg1:Gal4/UAS:Kaede*-positive cells[3]) transgenic reporter backgrounds. Embryos were fixed 3 hours post injection (hpi). As a negative control for injections (mock), the supernatant of a non-transformed *Pichia pastoris* culture was processed with the same purification procedure. Injection of either 0.2 or 2 ng of purified recombinant Cxcl18b elicited significantly higher mobilisation of neutrophils when compared to mock, while it did not impact on macrophage recruitment (**Figure 2**), indicating that Cxcl18b has chemotactic specificity toward neutrophils. Injection of either 0.2 or 2 ng of Cxcl18b did not affect the overall level of recruitment in a dose-dependent manner, suggesting that receptor saturation may have occurred.

Cxcl18b requires Cxcr2 receptor, but not Cxcr1 and Cxcr4b, for efficient recruitment of neutrophils

The chemokine receptor Cxcr2/CXCR2 is a key controller of neutrophil chemotaxis in both teleosts and mammalian species[5,12,14]. In mammals, activation of neutrophil migration via CXCR2 can be obtained by stimulation with a wide spectrum of inflammatory CXC chemokines, including CXCL1-2-3-5-6-7-8[7,8,9]. Hence, CXCR2 represents a ligand-promiscuous, but neutrophil-specific, receptor. In zebrafish, 2 functional Cxcl8 ligands (Cxcl8a and Cxcl8bb) of Cxcr2 have been identified[5,14,22]. However, considering the capability of the mammalian CXCR2 to accommodate a multiplicity of chemokines of different lineages, it is very likely that also in zebrafish other CXC chemokines are redundant with Cxcl8 ligands. Therefore, we hypothesised that the neutrophil chemotactic properties of Cxcl18b might also be exerted by activation of Cxcr2. To test this hypothesis we pharmacologically inhibited Cxcr2 with SB225002, a non-peptide inhibitor that can suppress both mammalian and zebrafish CXCR2 activity against its ligands, such as CXCL1 and CXCL8[5,35]. As a positive control, zebrafish Cxcl8a (ENSDARG00000104795/ENSDART00000161996), isolated with a comparable method[23], was used, since it was previously demonstrated that blockade of Cxcr2 with SB225002 can affect Cxcl8-dependent chemotaxis in zebrafish[5]. Cxcl8a and Cxcl18b elicited increased recruitment of neutrophils in control (DMSO vehicle-treated) groups and a significantly diminished chemotactic potency in SB225002-treated groups, which indicated that both

Cxcl8a and Cxcl18b require Cxcr2 to mediate optimal neutrophil chemotaxis (**Figure 3A**). However, the chemotactic capability of Cxcl8a was more severely suppressed by the drug treatment, as compared to the effect exerted by the same treatment on Cxcl18b chemotaxis, since this could still recruit more neutrophils than mock in Cxcr2-depleted condition. We also tested the activity of Cxcl18b under condition of *cxcr1* morpholino knockdown and in a *cxcr4b* mutant line, since these other two receptors are also expressed by zebrafish neutrophils[14,24]. However, Cxcl18b did not display significantly diminished chemoattractant power in *cxcr1* or *cxcr4b* depleted conditions, indicating that these receptors are dispensable for Cxcl18b sensing (**Figure 3B-C**).

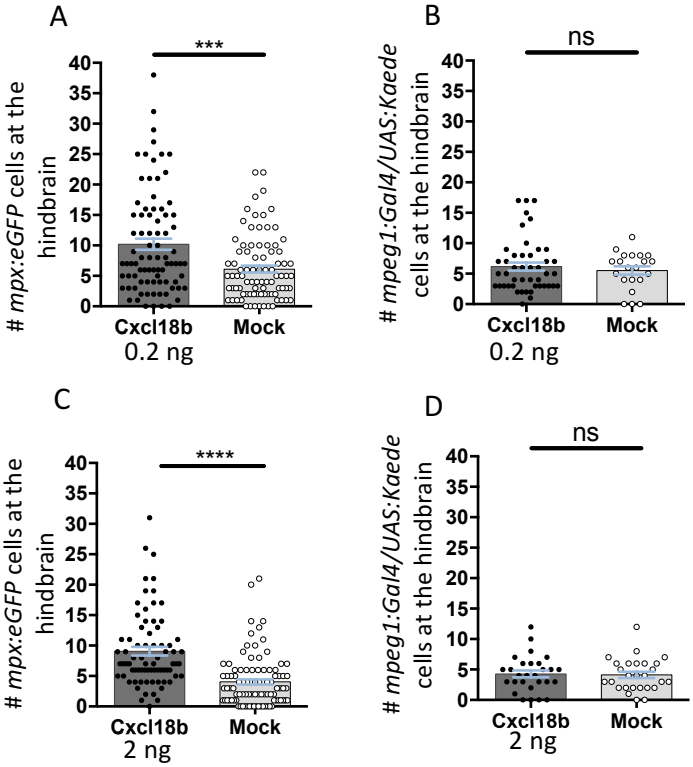

Figure 2. Cxcl18b exerts a neutrophil-specific chemoattraction *(Figure on the previous page)***.** Purified Cxcl18b-HA (0.2 or 2 ng) or mock (isovolumetric) were injected in the hindbrain of 2 dpf zebrafish embryos from *Tg(mpx:eGFP)* or *Tg(mpeg1:Gal4/UAS:Kaede)* lines. Samples were collected at 3 hpi. While Cxcl18b did not significantly chemoattract macrophages more than mock at both concentrations (B,D), Cxcl18b injection induced an increased infiltration of neutrophils to the hindbrain (A,C), indicating the chemotactic capability of this ligand towards neutrophils. Each data point represents an individual embryo. Data are cumulated from 4 (A), 2 (B-C) or 1 (D) replicates.

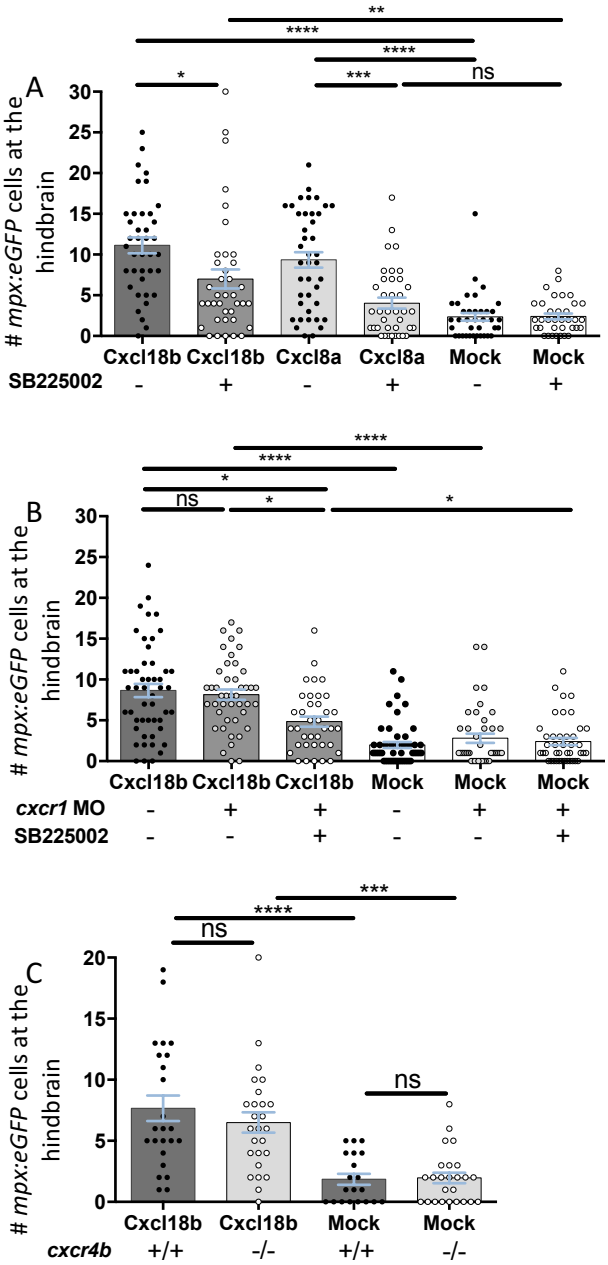

Figure 3. Pharmacological inhibition of CXCR2, but not *cxcr1* knockdown or homozygote mutation of *cxcr4b*, attenuates neutrophil recruitment to Cxcl18b local injections. A. Injections in the hindbrain of Cxcl18b (2 ng) or Cxcl8a (0.5 ng) were performed as in Figure 2. Pharmacological inhibition of Cxcr2 by bath exposure to 5 µM SB225002 affected the chemoattraction of neutrophils to both Cxcl8a and Cxcl18b but did not entirely suppress the chemotactic response to Cxcl18b, suggesting that Cxcl18b could be sensed by an additional receptor. **B.** Morpholino knockdown of *cxcr1* did not affect neutrophil migration to Cxcl18b and did not synergise with Cxcr2 inhibition, as Cxcr1/2 deficient embryos still displayed residual recruitment when compared to mock-injected controls. **C.** *cxcr4b* null mutant embryos did not display impaired neutrophil recruitment to Cxcl18b, indicating that this receptor is not required for the Cxcl18b-dependent chemotaxis of neutrophils. Data are cumulated from 2 (A-B) or 1 (C) replicates.

To address whether redundant function between Cxcr1 and Cxcr2 might explain that *cxcr1* morpholino injection did not impair neutrophil recruitment, we blocked Cxcr1/2 signalling by *cxcr1* knockdown and simultaneous Cxcr2 pharmacological inhibition. Similar as in the case of Cxcr2 inhibition (**Figure 3A**), simultaneous blockade of Cxcr1 and Cxcr2 significantly reduced neutrophil recruitment, but some residual chemotactic activity was observed (**Figure 3B**).

A *Tg(cxcl18b:eGFP)* reporter lines labels mycobacterial-induced inflammation

Since previous expression studies indicated that Cxcl18b is induced in response to several bacterial infections[26,27], we constructed a *Tg(cxcl18b:eGFP)* reporter line to visualise and longitudinally follow the expression pattern of *cxcl18b in vivo*. To validate inflammation-dependent induction of the reporter line, we injected embryos with *Mycobacterium marinum* (*Mm*), a fish pathogen which leads to the formation of granulomatous lesions in the zebrafish species and is widely used as a surrogate model for tuberculosis[36]. These inflammatory lesions consist of immune cell aggregates that have migrated and collected bacteria at the infection focus.

The initial stages of granuloma formation mostly consist of macrophages, while neutrophils are mostly recruited at a more advanced stage. Granulomas in the zebrafish embryonic/larval model form without requiring the presence of adaptive immune cells, as these lesions can be generated at developmental stages that anticipate ontogenesis of lymphocytes[36]. When *Tg(cxcl18b:eGFP)* embryos were challenged with *Mm*, the *cxcl18b*-driven eGFP accumulated in the areas where initial aggregates were forming (**Figure 4**), consistent with previous evidence reported by transcriptomic and *in situ* gene expression studies[26,27]. At 36 hpi, cells residing in the caudal haematopoietic tissue and endothelial cells appeared to upregulate the transgene. (**Figure 4E-F**). As the infection progressed, the expression of the reporter continued to accumulate at the nascent granulomas in the cells surrounding the lesion. However, confocal imaging of the infected larvae indicates that the infected cells are not the main producers of *cxcl18b*, rather this is produced by non-infected cells in the immediate surrounding tissue (**Figure 5A-F**). However, these *cxcl18b*-expressing cells localised in tight proximity to the cells where most of the infection was residing, participating in the formation of the nascent granulomatous aggregates. At 3-4 dpi (days post infection), highly *cxcl18b*-expressing cells could be found within the granuloma lesion. Considering the capability of some of the Cxcl18b^{+} cells to emit long dendrites (**Figure 5C-F**), we investigated whether these cells could represent uninfected phagocytes (macrophages and neutrophils). Therefore, we crossed the *Tg(cxcl18b:eGFP)* transgenic line with *Tg(lyz:DsRed)* or *Tg(mpeg1:mCherry-F)* lines and infected the offspring with *Mm*-mCrimson to induce Cxcl18b expression. As expected, the infection resided essentially in c*xcl18b*-negative cells, although the nascent granuloma aggregates contained several c*xcl18b*-positive cells. Strikingly, the c*xcl18b* transgene expression did not overlap with *lyz* and *mpeg1* transgenes, indicating that Cxcl18b is expressed by non-phagocytic cells that participate in the granuloma aggregate. Since we identified Cxcl18b as a potent neutrophil chemoattractant and neutrophils are known to be attracted to the granulomatous aggregates[37,38], we propose that Cxcl18b-producing non-phagocytic cells that compose the granuloma stroma might be important to drive neutrophil recruitment to the mycobacterial infection foci.

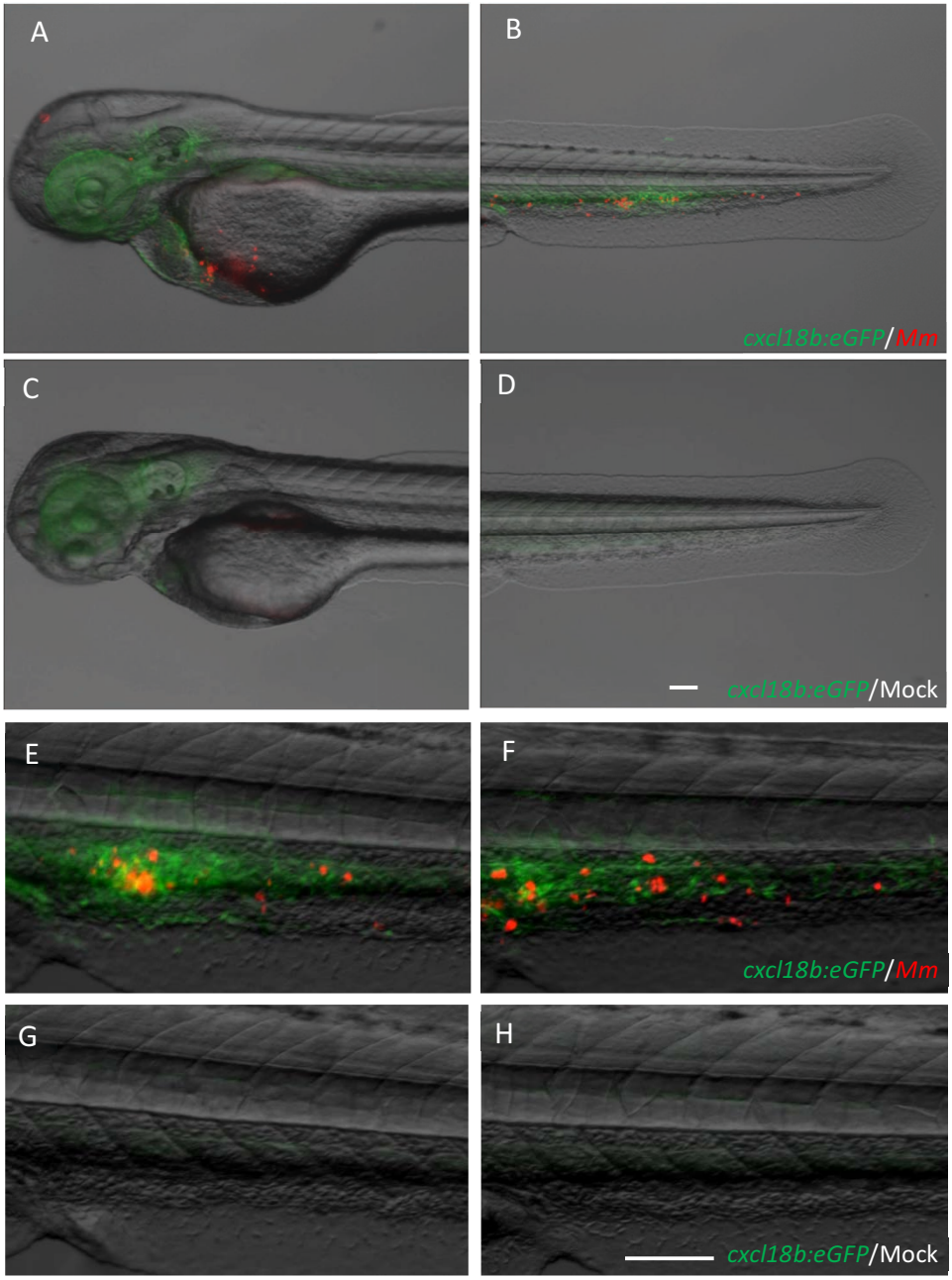

Figure 4. *cxcl18b:eGFP* is expressed by the tissue surrounding *M. marinum* infection sites. Injections of approximately 200 CFU of *M. marinum* M-mCrimson (*Mm*) via the caudal vein (A-B and E-F), but not mock injection (2% PVP in PBS, C-D and G-H) induced expression of the *cxcl18b:eGFP* transgene in the infected areas, especially localised around the sites of bacterial growth. Images were taken at 36 hpi. Scale bars: 100 µm.

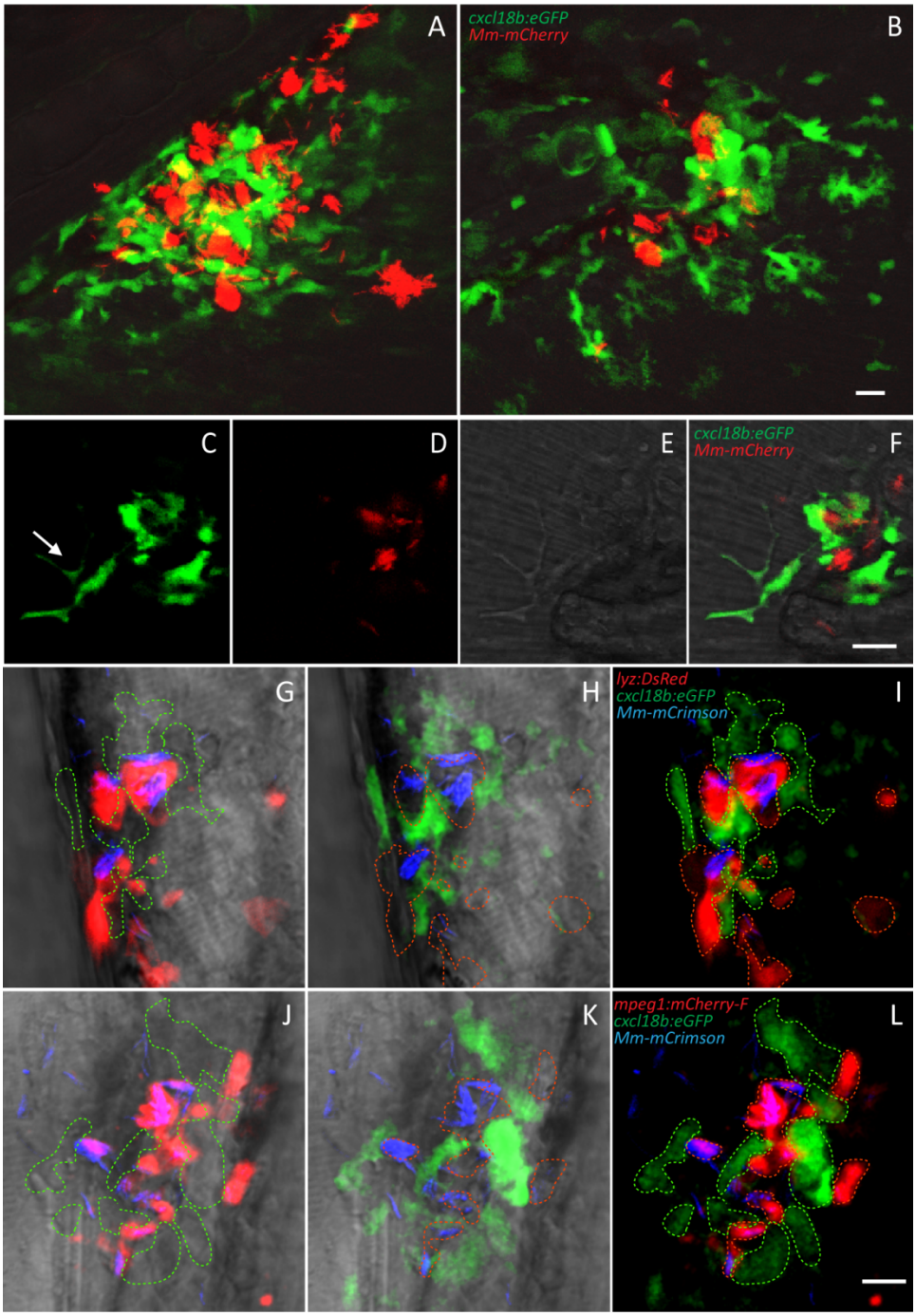

Figure 5. *cxcl18b:eGFP* is mostly expressed by non-infected cells accumulated at the nascent granuloma *(Legend on the next page)*.

Figure 5. *cxcl18b:eGFP* is expressed by non-infected cells accumulated at the nascent granuloma *(Figure on the previous page)*. **A-F.** During the formation of granulomas, the cells that express high levels of *cxcl18b:eGFP* consist predominantly of uninfected cells that participate in the cell aggregates initiating the granuloma. Phenotypic inspection shows that some of these cells can emit long protrusions (arrow in C). **G-L.** Cxcl18b-expressing cells do not represent phagocytic cells since this marker does not overlap with established neutrophil and macrophage markers l*yz* (G-I) and *mpeg1* (J-L). Images are representative of granulomas forming at 3 dpi (A-F) or 4 dpi (G-L). A-B are multiple z-stack maximum projections, C-L are split channels and overlay of an individual optical layer. In G-L outlines of green and red cells are marked with dashed lines of the corresponding colour. Scale bars: 10 µm.

DISCUSSION

Our study reports that the inflammatory chemokine Cxcl18b, a reliable marker of inflammation in zebrafish, displays expression patterns and chemotactic properties towards neutrophils, similar to those of the zebrafish Cxcl8 paralogues. Both Cxcl8 chemokines and Cxcl18b require the chemokine receptor/neutrophil marker Cxcr2 to mediate an optimal neutrophil emigration[5].

Our study therefore indicates that, like in mammalian species, the zebrafish Cxcr2 is a promiscuous receptor, able to respond to a variety of CXC ligands[12]. However, while Cxcl8a heavily relies on Cxcr2 activity to induce chemotaxis, Cxcl18b can still elicit significant (although diminished) neutrophil recruitment in Cxcr2-depleted conditions, indicating that another neutrophil receptor can mediate residual Cxcl18b chemotaxis in Cxcr2-blocked conditions. We excluded the possibility that this receptor may be Cxcr4b or Cxcr1, other two chemokine receptors expressed by the neutrophil lineage which can affect neutrophil chemotaxis in zebrafish and/or mammals[21,24], since Cxcl18b could still elicit normal recruitment of neutrophil in a *cxcr4b* mutant line or in *cxcr1* knockdown conditions. These data are in line with previous studies in zebrafish that demonstrated that Cxcr1 is also not required to sense the zebrafish Cxcl8a and Cxcl8bb chemokines that essentially recruit via Cxcr2[5,14], and with the fact that Cxcr4b mostly elicits cell recruitment via the Cxcl12a ligand[39]. The residual recruitment of neutrophils upon Cxcl18b injection can be explained either with the existence of another neutrophil receptor that contributes to Cxcl18b-mediated recruitment, or with the possibility that the Cxcr2 inhibitor may not have completely suppressed Cxcr2 function, which could lead to some residual neutrophil recruitment when saturating doses of chemokine ligands are provided.

In this study, we have also constructed a *cxcl18b* reporter line that can be used to further investigate what cell types are involved in the production of the Cxcl18b neutrophil-chemotactic cue. Our analysis of the Cxcl18b transgene expression indicates that non-phagocytic cells at the infection site are responsible for *cxcl18b* expression in response to *Mm* bacterial challenge. This observation suggests an important contribution of stromal cells in the granuloma microenvironment to the development of inflammation. A better understanding of responses in the granuloma microenvironment is particularly relevant in view of the emerging role of inflammation in the pathogenesis of tuberculosis, with several recent studies emphasising the need for a well-balanced inflammatory response in order to provide protective functions yet prevent pathological consequences[40,41]. Additional combination of *Tg(cxcl18b:eGFP)* with other reporter lines for inflammatory phagocytes or inflamed tissues (e.g. *tnfa*[42] and *il1b*[43] reporters) and transcriptional profiling of *cxcl18b*-expressing cells may further help to elucidate the nature and the importance of the *cxcl18b*

positive cells in the promotion of inflammation and in driving neutrophilic infiltration in mycobacterial granulomas.

In a recent study, Cxcl18b was the most upregulated chemoattractant detected at 4 hours post tail fin amputations[44], indicating that Cxcl18b is also induced upon sterile acute inflammation. Notably, in this study the expression of Cxcl18b was fully suppressed by treatment with the glucocorticoid beclomethasone. Treatment with this anti-inflammatory drug coincided with the abolishment of neutrophil recruitment to the wound, while it did not affect macrophage recruitment[44]. Given our evidence that Cxcl18b is a powerful and neutrophil-specific chemotactic cue, it is very likely that neutrophil chemotaxis was impaired by beclomethasone treatment owing at least partly to suppression of *cxcl18b* induction. Previous studies performed in a similar model showed that, at 1 hour post wounding (hpw), the two zebrafish Cxcl8a and Cxcl8bb genes were also significantly induced. While induction of Cxcl18b was not addressed at 1 hpw, induction of Cxcl8a and Cxcl8bb was found to be very transient and significantly dropped down at 4 hpw[5]. Taken together, these studies suggest that Cxcl8a-bb and Cxcl18b might represent differently timed chemotactic cues which may be responsible for the recruitment of different waves of neutrophils during acute and chronic inflammatory responses. The recombinant Cxcl8a and Cxcl18b proteins and the c*xcl18b* reporter line presented here will possibly aid in studying the dynamics of *cxcl18b* expression and permit to clarify shared and distinct functions of Cxcl8 isoforms and Cxcl18b in orchestrating neutrophil function. Understanding to what extent Cxcl18b is redundant with Cxcl8 isoforms and whether the two clades of chemokines also display specific functions in the regulation of the inflammatory response could also shed light on the divergences and/or convergences existing between fish and mammalian chemokine axes and on the evolutionary diversification of chemokine ligands.

MATERIALS AND METHODS

Zebrafish lines and embryo/larvae handling – Zebrafish were handled in compliance with the local (Leiden University) animal welfare policies and were maintained according to standard protocols (zfin.org). All experiments in this study were performed on 2 dpf embryos, therefore prior the free feeding stage and did not fall under animal experimentation law according to the EU Animal Protection Directive 2010/63/EU. Embryos were kept in egg water (60 µg/ml sea salt; Sera Marin) at 28.5°C. To prevent pigmentation, embryos were maintained in water supplemented with 0.003% PTU (1-phenyl-2-thiourea, Sigma-Aldrich). For the recruitment assays, neutrophils and macrophages were labelled with the transgenes *Tg(mpx:eGFP^{i114})*[4] or *Tg(mpeg1:Gal4-VP16^{gl24}/UAS-E1b:Kaede^{s1999t})*[3] [in short referred to as *Tg(mpeg1:Gal4/UAS:Kaede)*], respectively. For confocal microscopy (**Figure 5**), neutrophil and macrophage lines *Tg(lyz:DsRed^{nz50})*[45] and *Tg(mpeg1:mCherry-F^{ump2})*[46] were single crossed to the *cxcl18b:eGFP* line (see below). To address chemotactic properties of Cxcl18b via Cxcr4b, mutants (*cxcr4b$^{-/-}$*) and wildtype siblings (*cxcr4b$^{+/+}$*) of *(cxcr4b^{t26035})*[47], crossed into the *Tg(mpx:eGFP^{i114})* background were used.

Production and verification of recombinant Cxcl18b – The coding sequence for Cxcl18b (ENSDARG00000075045/ENSDART00000111598) was optimised for expression in yeast, supplemented with an HA (human influenza haemagglutinin)-tag at the C-terminus and cloned into pPICZα expression vector (Invitrogen, Life Technologies). The expression plasmid was linearised with SacI and transformed into *Pichia pastoris* strain X-

33 as described previously[23,48]. Successful transformants were selected on YPD-agar (1% yeast extract 2% peptone 2% dextrose 2% agar, Sigma-Aldrich) by resistance to 100 µg/ml Zeocine and reselected on 1000 µg/ml Zeocine plates. Highly resistant clones were selected for expression efficiency by liquid culturing the isolates in 10 ml YPD medium (30ºC, 180 rpm, O/N), transfer to 2.5 ml buffered minimal methanol medium (100 mM potassium phosphate buffer pH 6, 1.34% yeast nitrogen base, $4 \cdot 10^{-5}$% biotin, 0.5% methanol, Sigma-Aldrich), and cultured (30ºC, 180 rpm) for five days (with additional 0.5% methanol supplemented daily). The supernatant of the cultures was probed for anti-HA reactivity on western blot, using a custom-made horseradish peroxidase-directly conjugated antibody. One clone was selected for large-scale culture (250 ml). Cxcl18b-HA accumulated in the supernatant was concentrated and purified in PBS by filtration between columns with a cut-off of 50 kDa and 3 kDa (Amicon Ultra Centrifugal filters, Merck KGaA). Identity and purity of Cxcl18b in the sample was determined by trypsinisation and electrospray mass spectrometry analysis, which revealed high quality of the protein and undetectable protein contaminations of the recombinant Cxcl18b with *Pichia pastoris* proteins (Figure 1B-C). To obtain a mock control for injections, isolation was performed from the supernatant of non-transformed isogenic *P. pastoris*, cultured in identical condition (with the exception of Zeocine 100 µg/ml present in the starter plate and pre-culture for the transformed isolate). We confirmed chemokine purity and identity by in-solution trypsinisation and electrospray mass spectrometry. Quantification was obtained by BCA-assay (Micro BCATM Protein Assay Kit, Thermo Fisher Scientific, Life Technologies), the protein concentration assessed by the assay in the mock is subtracted from the total Cxcl18b protein concentration.

Recruitment assays – Cxcl18b, Cxcl8a or mock (produced as described above), were diluted in PBS to the desired concentration (0.2 ng/nl and 2 ng/nl) and injected (1 nl) into the hindbrain ventricle of 2 dpf embryos. Prior and during injections, embryos were anaesthetised in egg water medium containing 0.02% buffered Tricaine (3-aminobenzoic acid ethyl ester; Sigma-Aldrich). The embryos were fixed (O/N) at 3 hours post injection (hpi) in PBSTx (1× PBS supplemented with 0.8% Triton X-100, Sigma-Aldrich) containing 4% paraformaldehyde. Subsequently, the embryos were washed in PBS and the fluorescently labelled cells within the hindbrain perimeter were counted (blinded) using a Leica MZ16FA fluorescence stereomicroscope.

Pharmacological inhibition of Cxcr2 – For the Cxcr2 inhibition assays, we followed and adapted the protocol used in reference[5]. Briefly, 2 dpf larvae were preincubated for 1 hour at 28.5°C in presence or absence of the selective nonpeptide inhibitor SB225002 (Sigma-Aldrich) at a concentration of 5 µM in egg water. Since the compound is initially suspended in DMSO, the control group was exposed to the same concentration of DMSO (Sigma-Aldrich) alone (0.05%) as in the SB225002 group. Upon injection, embryos were returned and maintained in SB225002 or vehicle treatment until they were fixed (3 hpi) in 4% paraformaldehyde in PBSTx O/N.

Knockdown of Cxcr1 – 3 nl of 75 µM *cxcr1* morpholino (5′-TGTCAGGATACTAAACTTACCAGTC-3′, targeting exon1-intron 1 splicing site, Gene tools) or the same volume and concentration of a standard control morpholino (5′-CCTCTTACCTCAGTTACAATTTATA-3′, Gene tools) were injected at 1 cell stage in zebrafish fertilised eggs, according to previous reports[14].

Cloning of *cxcl18b* promoter and construction of *Tg(cxcl18b:eGFP)* reporter line – 3.04 kb of *cxcl18b* promoter immediately proximal to the transcriptional start were amplified from genomic DNA derived from a pool of AB/TL embryos, using the following amplification primers: *XhoI-Cxcl18bFw:* 5′-GGGCCCCTCGAGGTCTCCTCATGCATTGACTAC-3′ and *BamHI-Cxcl18bRv:* 5′-GGGCCCGGATCCAATTGCTGCAAACTATATGTAGG-3′. The PCR resulted in a single band on gel electrophoresis at the expected molecular weight. The primers supplemented the sequence with a unique XhoI site at the 5' end, a unique BamHI site at the 3' end and with exceeding 5′-GGGCCC-3′ extremities preceding both restriction sites to facilitate digestion. XhoI and BamHI extremities were activated by double enzymatic digestion to permit cloning into a custom-adapted pTol2^{+} destination vector, upstream of the eGFP coding sequence. Briefly, the destination vector was derived from *pTol2^{+}/coro-1a:eGFP-SV40pA* vector, previously described and kindly provided by the Wen lab[49]. The *7.03* kb *coro-1a* promoter sequence was fully removed by double restriction and gel extraction and replaced by a multiple cloning site, containing a BamHI proximal to the eGFP transcription start and an XhoI site more distally. Both vector and *XhoI-cxcl18b-BamHI* constructs where BamHI/XhoI digested and ligated together to obtain *pTol2^{+}/cxcl18b:eGFP-SV40pA*. The plasmid was purified and injected into zebrafish fertilised eggs together with the Tol2-transposase mRNA, according to previous reports[3]. Several founders were identified and appeared very similar in basal eGFP expression. One eGFP-positive founder was selected, outcrossed to AB/TL and the positive F1 offspring was raised to adulthood. Further single crosses of the F1 founders to AB/TL produced significantly >25% positive animals, suggesting the presence of multiple integrations.

Mycobacterial infection and image acquisition – *Tg(cxcl18b:eGFP)* embryos were injected with 200 CFU of mCrimson-labeled *M. marinum* strain M by the caudal vein injection route (**Figure 4**) or with 50 CFU via the trunk injection route (**Figure 5**). Bacteria were handled, prepared and injected as previously described[23,50]. Stereo-fluorescence images in **Figure 4** were taken with a Leica MZ16FA fluorescence stereomicroscope connected to a Leica DFC420C camera (Leica Microsystems). Confocal images were acquired with a Leica TCS SPE microscope equipped with a HCX APO L U-V-I 40x/WATER objective (Leica Microsystems).

Statistical analysis – All data were analysed using GraphPad Prism 5 (GraphPad Software). For comparison between two groups (**Figure 2**), a Mann-Whitney test was used. For comparisons between more than two groups (**Figure 3**) a Kruskal-Wallis test was used, followed by Sidak's multiple comparisons post-hoc test for selected groups. Significance (P-value) is indicated as: ns (non-significant); * (P<0.05); ** (P<0.01); *** (P<0.001); **** (P<0.0001). Error bars in all the graphs are mean±s.e.m.

ACKNOWLEDGEMENTS

We thank Bobby Florea for the help with mass spectrometry validation of recombinant Cxcl18b and Julien Rougeot for providing the custom-adapted pTol2^{+} destination vector. We also acknowledge Monica Álvarez-Varela for valuable suggestions and for critically reading the manuscript.

This work was supported by the European Marie-Curie Initial Training Network FishForPharma (contract number PITN-GA-2011-289209).

REFERENCES

1 Torraca V, Masud S, Spaink HP, Meijer AH. Macrophage-pathogen interactions in infectious diseases: new therapeutic insights from the zebrafish host model. Dis Model Mech. 2014 Jul;7(7):785-97.
2 Meijer AH, Spaink HP. Host-pathogen interactions made transparent with the zebrafish model. Curr Drug Targets. 2011 Jun;12(7):1000-17.
3 Ellett F, Pase L, Hayman JW, Andrianopoulos A, Lieschke GJ. mpeg1 promoter transgenes direct macrophage-lineage expression in zebrafish. Blood. 2011 Jan 27;117(4):e49-56.
4 Renshaw SA, Loynes CA, Trushell DM, Elworthy S, Ingham PW, Whyte MK. A transgenic zebrafish model of neutrophilic inflammation. Blood. 2006 Dec 15;108(13):3976-8.
5 de Oliveira S, Reyes-Aldasoro CC, Candel S, Renshaw SA, Mulero V, Calado A. Cxcl8 (IL-8) mediates neutrophil recruitment and behavior in the zebrafish inflammatory response. J Immunol. 2013 Apr 15;190(8):4349-59.
6 Hruscha A, Schmid B. Generation of zebrafish models by CRISPR /Cas9 genome editing. Methods Mol Biol. 2015;1254:341-50.
7 Ahuja SK, Murphy PM. The CXC chemokines growth-regulated oncogene (GRO) alpha, GRObeta, GROgamma, neutrophil-activating peptide-2, and epithelial cell-derived neutrophil-activating peptide-78 are potent agonists for the type B, but not the type A, human interleukin-8 receptor. J Biol Chem. 1996 Aug 23;271(34):20545-50.
8 Wolf M, Delgado MB, Jones SA, Dewald B, Clark-Lewis I, Baggiolini M. Granulocyte chemotactic protein 2 acts via both IL-8 receptors, CXCR1 and CXCR2. Eur J Immunol. 1998 Jan;28(1):164-70.
9 Pelus LM, Horowitz D, Cooper SC, King AG. Peripheral blood stem cell mobilization. A role for CXC chemokines. Crit Rev Oncol Hematol. 2002 Sep;43(3):257-75.
10 Clark-Lewis I, Dewald B, Geiser T, Moser B, Baggiolini M. Platelet factor 4 binds to interleukin 8 receptors and activates neutrophils when its N terminus is modified with Glu-Leu-Arg. Proc Natl Acad Sci U S A. 1993 Apr 15;90(8):3574-7.
11 Van Damme J, Decock B, Conings R, Lenaerts JP, Opdenakker G, Billiau A. The chemotactic activity for granulocytes produced by virally infected fibroblasts is identical to monocyte-derived interleukin 8. Eur J Immunol. 1989 Jul;19(7):1189-94.
12 Russo RC, Garcia CC, Teixeira MM, Amaral FA. The CXCL8/IL-8 chemokine family and its receptors in inflammatory diseases. Expert Rev Clin Immunol. 2014 May;10(5):593-619.
13 Cai Z, Gao C, Zhang Y, Xing K. Functional characterization of the ELR motif in piscine ELR+ CXC-like chemokine. Mar Biotechnol (NY). 2009 Jul-Aug;11(4):505-12.
14 Deng Q, Sarris M, Bennin DA, Green JM, Herbomel P, Huttenlocher A. Localized bacterial infection induces systemic activation of neutrophils through Cxcr2 signaling in zebrafish. J Leukoc Biol. 2013 May;93(5):761-9.
15 Sarris M, Masson JB, Maurin D, Van der Aa LM, Boudinot P, Lortat-Jacob H, Herbomel P. Inflammatory chemokines direct and restrict leukocyte migration within live tissues as glycan-bound gradients. Curr Biol. 2012 Dec 18;22(24):2375-82.
16 Tanino Y, Coombe DR, Gill SE, Kett WC, Kajikawa O, Proudfoot AE, Wells TN, Parks WC, Wight TN, Martin TR, Frevert CW. Kinetics of chemokine-glycosaminoglycan interactions control neutrophil migration into the airspaces of the lungs. J Immunol. 2010 Mar 1;184(5):2677-85.
17 Mukaida N. Pathophysiological roles of interleukin-8/CXCL8 in pulmonary diseases. Am J Physiol Lung Cell Mol Physiol. 2003 Apr;284(4):L566-77.
18 Weathington NM, van Houwelingen AH, Noerager BD, Jackson PL, Kraneveld AD, Galin FS, Folkerts G, Nijkamp FP, Blalock JE. A novel peptide CXCR ligand derived from extracellular matrix degradation during airway inflammation. Nat Med. 2006 Mar;12(3):317-23.
19 Bernhagen J, Krohn R, Lue H, Gregory JL, Zernecke A, Koenen RR, Dewor M, Georgiev I, Schober A, Leng L, Kooistra T, Fingerle-Rowson G, Ghezzi P, Kleemann R, McColl SR, Bucala R, Hickey MJ, Weber C. MIF is a noncognate ligand of CXC chemokine receptors in inflammatory and atherogenic cell recruitment. Nat Med. 2007 May;13(5):587-96.
20 Gaggar A, Jackson PL, Noerager BD, O'Reilly PJ, McQuaid DB, Rowe SM, Clancy JP, Blalock JE. A novel proteolytic cascade generates an extracellular matrix-derived chemoattractant in chronic neutrophilic inflammation. J Immunol.2008 Apr 15;180(8):5662-9.
21 Stillie R, Farooq SM, Gordon JR, Stadnyk AW. The functional significance behind expressing two IL-8 receptor types on PMN. J Leukoc Biol. 2009 Sep;86(3):529-43.
22 Nomiyama H, Osada N, Yoshie O. Systematic classification of vertebrate chemokines based on conserved synteny and evolutionary history. Genes Cells. 2013 Jan;18(1):1-16.

23 Torraca V, Cui C, Boland R, Bebelman JP, van der Sar AM, Smit MJ, Siderius M, Spaink HP, Meijer AH. The CXCR3-CXCL11 signaling axis mediates macrophage recruitment and dissemination of mycobacterial infection. Dis Model Mech. 2015 Mar;8(3):253-69.
24 Walters KB, Green JM, Surfus JC, Yoo SK, Huttenlocher A. Live imaging of neutrophil motility in a zebrafish model of WHIM syndrome. Blood. 2010 Oct 14;116(15):2803-11.
25 Tulotta C, Stefanescu C, Beletkaia E, Bussmann J, Tarbashevich K, Schmidt T, Snaar-Jagalska BE. Inhibition of signaling between human CXCR4 and zebrafish ligands by the small molecule IT1t impairs the formation of triple-negative breast cancer early metastases in a zebrafish xenograft model. Dis Model Mech. 2016 Feb 1;9(2):141-53.
26 Stockhammer OW, Zakrzewska A, Hegedûs Z, Spaink HP, Meijer AH. Transcriptome profiling and functional analyses of the zebrafish embryonic innate immune response to Salmonella infection. J Immunol. 2009 May 1;182(9):5641-53.
27 van der Vaart M, van Soest JJ, Spaink HP, Meijer AH. Functional analysis of a zebrafish myd88 mutant identifies key transcriptional components of the innate immune system. Dis Model Mech. 2013 May;6(3):841-54.
28 Jiang J, Wu S, Wang Y, An X, Cai L, Zhao X, Wu C. Carbendazim has the potential to induce oxidative stress, apoptosis, immunotoxicity and endocrine disruption during zebrafish larvae development. Toxicol In Vitro. 2015 Oct;29(7):1473-81.
29 Jiang J, Wu S, Wu C, An X, Cai L, Zhao X. Embryonic exposure to carbendazim induces the transcription of genes related to apoptosis, immunotoxicity and endocrine disruption in zebrafish (Danio rerio). Fish Shellfish Immunol. 2014 Dec;41(2):493-500.
30 Bird S, Tafalla C. Teleost Chemokines and Their Receptors. Biology (Basel). 2015 Nov 11;4(4):756-84.
31 Clore GM, Appella E, Yamada M, Matsushima K, Gronenborn AM. Three-dimensional structure of interleukin 8 in solution. Biochemistry. 1990 Feb 20;29(7):1689-96.
32 Gangavarapu P, Rajagopalan L, Kolli D, Guerrero-Plata A, Garofalo RP, Rajarathnam K. The monomer-dimer equilibrium and glycosaminoglycan interactions of chemokine CXCL8 regulate tissue-specific neutrophil recruitment. J Leukoc Biol. 2012 Feb;91(2):259-65.
33 Swaminathan GJ, Holloway DE, Colvin RA, Campanella GK, Papageorgiou AC, Luster AD, Acharya KR. Crystal structures of oligomeric forms of the IP-10/CXCL10 chemokine. Structure. 2003 May;11(5):521-32.
34 Ray P, Lewin SA, Mihalko LA, Lesher-Perez SC, Takayama S, Luker KE, Luker GD. Secreted CXCL12 (SDF-1) forms dimers under physiological conditions. Biochem J. 2012 Mar 1;442(2):433-42.
35 White JR, Lee JM, Young PR, Hertzberg RP, Jurewicz AJ, Chaikin MA, Widdowson K, Foley JJ, Martin LD, Griswold DE, Sarau HM. Identification of a potent, selective non-peptide CXCR2 antagonist that inhibits interleukin-8-induced neutrophil migration. J Biol Chem. 1998 Apr 24;273(17):10095-8.
36 Davis JM, Clay H, Lewis JL, Ghori N, Herbomel P, Ramakrishnan L. Real-time visualization of mycobacterium-macrophage interactions leading to initiation of granuloma formation in zebrafish embryos. Immunity. 2002 Dec;17(6):693-702.
37 Yang CT, Cambier CJ, Davis JM, Hall CJ, Crosier PS, Ramakrishnan L. Neutrophils exert protection in the early tuberculous granuloma by oxidative killing of mycobacteria phagocytosed from infected macrophages. Cell Host Microbe. 2012 Sep 13;12(3):301-12.
38 Elks PM, Brizee S, van der Vaart M, Walmsley SR, van Eeden FJ, Renshaw SA, Meijer AH. Hypoxia inducible factor signaling modulates susceptibility to mycobacterial infection via a nitric oxide dependent mechanism. PLoS Pathog. 2013;9(12):e1003789.
39 Valentin G, Haas P, Gilmour D. The chemokine SDF1a coordinates tissue migration through the spatially restricted activation of Cxcr7 and Cxcr4b. Curr Biol. 2007 Jun 19;17(12):1026-31.
40 Matty MA, Roca FJ, Cronan MR, Tobin DM. Adventures within the speckled band:heterogeneity, angiogenesis, and balanced inflammation in the tuberculous granuloma. Immunol Rev. 2015 Mar;264(1):276-87.
41 Dorhoi A, Kaufmann SH. Perspectives on host adaptation in response to Mycobacterium tuberculosis: modulation of inflammation. Semin Immunol. 2014 Dec;26(6):533-42.
42 Nguyen-Chi M, Laplace-Builhe B, Travnickova J, Luz-Crawford P, Tejedor G, Phan QT, Duroux-Richard I, Levraud JP, Kissa K, Lutfalla G, Jorgensen C, Djouad F. Identification of polarized macrophage subsets in zebrafish. Elife. 2015 Jul 8;4:e07288.
43 Nguyen-Chi M, Phan QT, Gonzalez C, Dubremetz JF, Levraud JP, Lutfalla G. Transient infection of the zebrafish notochord with E. coli induces chronic inflammation. Dis Model Mech. 2014 Jul;7(7):871-82.
44 Chatzopoulou A, Heijmans JP, Burgerhout E, Oskam N, Spaink HP, Meijer AH, Schaaf MJ. Glucocorticoid-induced attenuation of the inflammatory response in zebrafish. Endocrinology. 2016 May 24:en20152050.
45 Hall C, Flores MV, Storm T, Crosier K, Crosier P. The zebrafish lysozyme C promoter drives myeloid-specific expression in transgenic fish. BMC Dev Biol. 2007 May 4;7:42.
46 Bernut A, Herrmann JL, Kissa K, Dubremetz JF, Gaillard JL, Lutfalla G, Kremer L. Mycobacterium abscessus cording prevents phagocytosis and promotes abscess formation. Proc Natl Acad Sci U S A. 2014 Mar 11;111(10):E943-52.

47 Knaut H, Werz C, Geisler R, Nüsslein-Volhard C; Tübingen 2000 Screen Consortium. A zebrafish homologue of the chemokine receptor Cxcr4 is a germ-cell guidance receptor. Nature. 2003 Jan 16;421(6920):279-82.
48 Wu S, Letchworth GJ. High efficiency transformation by electroporation of Pichia pastoris pretreated with lithium acetate and dithiothreitol. Biotechniques. 2004 Jan;36(1):152-4.
49 Li L, Yan B, Shi YQ, Zhang WQ, Wen ZL. Live imaging reveals differing roles of macrophages and neutrophils during zebrafish tail fin regeneration. J Biol Chem. 2012 Jul 20;287(30):25353-60.
50 Benard EL, van der Sar AM, Ellett F, Lieschke GJ, Spaink HP, Meijer AH. Infection of zebrafish embryos with intracellular bacterial pathogens. J Vis Exp. 2012 Mar 15;(61).

Chapter 8

General discussion and final conclusions

Chapter 8

General discussion and final conclusions

Rationale of using a non-mammalian host to model mycobacterial diseases

In this thesis we applied the *Danio rerio* (zebrafish)-*Mycobacterium marinum* (*Mm*) infection model to obtain novel insights into how chemokines orchestrate the response of immune cells to mycobacterial infection. *Mm* is a natural pathogen of zebrafish and is phylogenetically very close to *Mycobacterium tuberculosis* (*Mtb*)[1], the causative agent of human tuberculosis (TB). The *Mtb* bacillus is carried by one third of the world population and remains the most severe global health problem of bacterial entity since its emergency and adaptation to humans in prehistorical eras, before the out-of-Africa emigration of the *Homo sapiens* species (~70.000 years ago)[2,3,4]. *Mtb* mainly provokes a lung disease[5], although it is able to colonise extrapulmonary tissues of the host (including the central nervous system and meninges[6,7], the eye[8], the breast[9], the liver[10], the kidney[11], the gastrointestinal tract[12], the genitourinary tract[13], the skin[14], the bones[15] and the lymph nodes[16]). In all these tissues *Mtb* infection can lead to the formation of granulomas, a hallmark of local inflammation. Granuloma formation is initiated by infected macrophages that subsequently attract new macrophages and other immune cells that confine the pathogen and the necrotising tissue[17]. Since *Mtb* can persist in granulomas for many years, the host-pathogen interplay that drives granuloma formation is key for our understanding of TB pathogenesis.

In comparison to *Mtb*, *Mm* represents a less host-specialised pathogen that can infect an expanded niche of ectothermic species, including fresh- and salt-water fish, amphibians, but also invertebrates and protists[18,19,20,21,22,23,24,25,26]. Furthermore, in sporadic cases, *Mm* can infect endothermic animals, including humans, where it is generally restricted to the dermis, since it grows very poorly at human internal body temperature[27,28]. *Mm*, in its multicellular hosts can induce formation of granulomatous aggregates, similar to human-*Mtb* granulomas[27,28]. Almost two decades of use of the zebrafish model have proven that the two pathogens in their respective natural hosts rely on the activation of specific and evolutionary conserved disease-causing programmes, in order to induce granuloma aggregation[20,29,30,31,32]. This is also illustrated by the fact that in the rare cases of *Mm* infection in humans, this pathogen can still induce formation of dermal granulomas, that are phenotypically indistinguishable from those that *Mtb* would form in the same tissue[27,33].

The ability to grow within host macrophages is the key virulence attribute of pathogenic mycobacteria. This is well exemplified by studies in macrophage-like models, such *Dictyostelium discoideum* amoebas, where *Mm* can establish lasting intracellular parasitosis, similarly to those evoked *in vivo* in vertebrates and in macrophage cell cultures[25,34,35]. Interestingly, the pathogenesis in the monocellular models (including macrophage cultures) substantially relies on the capability to escape to the cytosol and on non-lytic ejection, which are important virulence traits that pathogenic mycobacteria

maintain also when infecting vertebrate host macrophages *in vivo*[25,36,37,38,39,40]. Despite this, in complex animal models, additional mechanisms of pathogenesis add to these core mechanisms of disease. These include, for example, the formation of distinct cell aggregates (the granulomas)[17], the manipulation of host angiogenesis[41] (**Chapter 6**) and the control of the inflammatory process via intricate cross talks that can solely occur in multicellular hosts[42]. Notably both aspects of mycobacterial pathogenesis that act at cellular and multicellular level are largely driven by virulence factors encoded by the RD1 (Region of Difference 1) locus, a genomic region conserved among tubercular bacilli (including *Mm*) and remarkably absent in environmental mycobacteria (e.g. *M. smegmatis*) and in the non-pathogenic BCG (bacillus of Calmette–Guérin) *M. bovis* strain, used to provide immunisation against *Mtb*.

Rodents and lagomorphs have been largely applied as *in vivo* models to study the histological aspects of mycobacterial disease. However, mice granulomas generally do not caseate[43] (necrotising granulomas, a typical characteristic of tuberculosis granulomas in humans) and the limited genetic tools available for the other rodents and lagomorphs that do form caseating granulomas (e.g. guinea pigs and rabbits[44]) make these models less attractive, due to restricted research opportunities. To date, the animal model that most closely resembles human tuberculosis is the macaque-*Mtb* model, that in terms of histopathology, physiopathology and disease progression/manifestation (including the existence of active and latent forms of TB) is near-identical to the human disease[45,46]. However, for obvious ethical, economical and practical restrictions, the use of this model is very limited. In contrast to the mice-*Mtb* model, caseating granulomas, wasting syndrome effects (another common symptom of TB displayed in primates) and latency have been observed when fish are infected with *Mm*[19,20,21,47].

Evolutionary, *Mtb* and *Mm* are very close and share about 85% of genome identity[1]. The genome of *Mm* is ~1.5 fold larger than the *Mtb* genome, which is likely related with the ubiquitous distribution of *Mm* in waters of different ecological niches and to the capability of *Mm* to infect a larger spectrum of hosts[1,28,48]. However, there is also a 14% of *Mtb*-specific genome sequence, which does not have orthologues in *Mm*, and which has likely arisen after their evolutionary divergence. About 8% of this *Mtb*-specific genetic material was estimated to have derived from horizontal gene transfer from other microbes that share a similar niche (e.g. respiratory microflora)[1,49,50,51,52] and is essentially related to niche adaptation (differences in temperature, organ-specificity, host-to-host transmission mechanisms), rather than to the central mechanisms of virulence.

Taken together, the *Mm* and *Mtb* species have most likely diverged from an *Mm*-like common ancestor, which was already adapted to the intra-macrophage life in vertebrate animals, was able to induce granuloma aggregation with a wide tissue tropism, and was able to alternate phases of life inside the host with phases of environmental life. This hypothesis is also justified by the fact that intramacrophage-specific and granuloma-specific genes exist in both *Mm* and *Mtb*, which are activated when the pathogens resides in phagocytic cells and when the granuloma aggregation is initiated[53,54].

Leprosy, the disease caused by *Mycobacterium leprae,* represents a severe cause of deformity and life-long disability in developing countries[55]. Unfortunately, the pathology of leprosy remains still poorly characterised, partly because culturing this pathogen axenically is near-impossible[56,57,58], and partly because there is a limited availability of

animal models[59,60,61]. The main experimental model for leprosy consists of the murine footpad infection[59] where the temperature of approximately 30°C mirrors the cooler tissues (skin and peripheral nerves) preferentially infected in humans. However, immunologically competent mice develop a poor infection with *M. leprae* and, apart from humans, armadillos are the only other known hosts of *M. leprae*, which represents the sole animal model to study the pathology of *M. leprae* infection in a natural host[60].

The evidence that leprosy predominantly affects peripheral tissues reflects the fact that, similarly to *Mycobacterium marinum*, the optimal growth temperature of this pathogen is lower than the human body temperature. Noteworthy, it has been described that *M. leprae* can infect and replicate in a variety of cold-blooded experimentally-injected species, including several fish, such as goldfish (*Carassius auratus*), spots (*Leiostomus xanthurus*), spotted sea-trout (*Cynoscion nebulosus*) and croakers (*Micropogon undulates*)[62,63]. Not only could *M. leprae* persist and replicate in these heterologous hosts, but the bacilli could also establish a distinctive type of intracellular parasitism of *M. leprae* infections, referred to as "lepra cells", large foamy macrophages containing numerous intracellular bacilli. These evidences suggest that the zebrafish model might be explored also as an experimental model to study *M. leprae* infection and, in particular, its use might help to elucidate the function of the innate immune cells and of immune signalling pathways in the onset of different manifestations of leprosy.

Function of chemotactic cues in driving granuloma aggregation

Mtb strongly induces chemokine expression and both TB patients and cell/animal models infected with *Mtb* exhibit a rapid induction of many of these chemotactic peptides[64]. We and others have found that also zebrafish infected with *Mm* displays large induction of chemokines, which include the mammalian counterparts of CXCL9-10-11 (CXCL11aa-ae-af-ag, **Chapter 3-4**), CXCL1-2-3-5-6-7-8 (Cxcl8a-8bb-18b[65,66,67] **Chapter 7**) and CCL2[68] (**Figure 1**). Since mycobacteria mostly reside in macrophages, these cells experience profound transcriptomic changes and represent a primary source of chemokine ligands[69,70,71,72,73,74,75,76] (**Chapter 1**). In agreement with this, we have found here that infected macrophages inside the zebrafish host largely upregulate *cxcl11aa*, the ligand of Cxcr3.2 (**Chapters 3-4**). However, also non-infected cells participate in the production of chemokines. Our studies, for example, show that Cxcl18b, a neutrophil-specific zebrafish chemokine, functionally similar to the ELR+ chemokines of mammals (**Chapters 1,7**), does not derive from infected or uninfected phagocytic cells (macrophages and neutrophils), but from stromal cells that reside within the granuloma microenvironment (**Figure 1D**). Similarly, it was suggested that one of the putative zebrafish orthologues of CCL2, which is able to induce macrophage chemotaxis, is mostly expressed by epithelial cells (**Figure 1A**)[68].

The initial stages of granulomas are characterised by a continuous, bidirectional trafficking of innate immune cells[22,41] (**Figure 1**, **Chapter 2**). We and others have shown that, since most macrophages are unable to readily eradicate the intracellular mycobacterial infection, the pathogen can take advantage of this in/out trafficking that guarantees a continuous supply of the mycobacterial infection niche (**Figure 1B**) and generates a mechanism for secondary dissemination[41,77] (**Figure 1B,E**, **Chapters 2-3**).

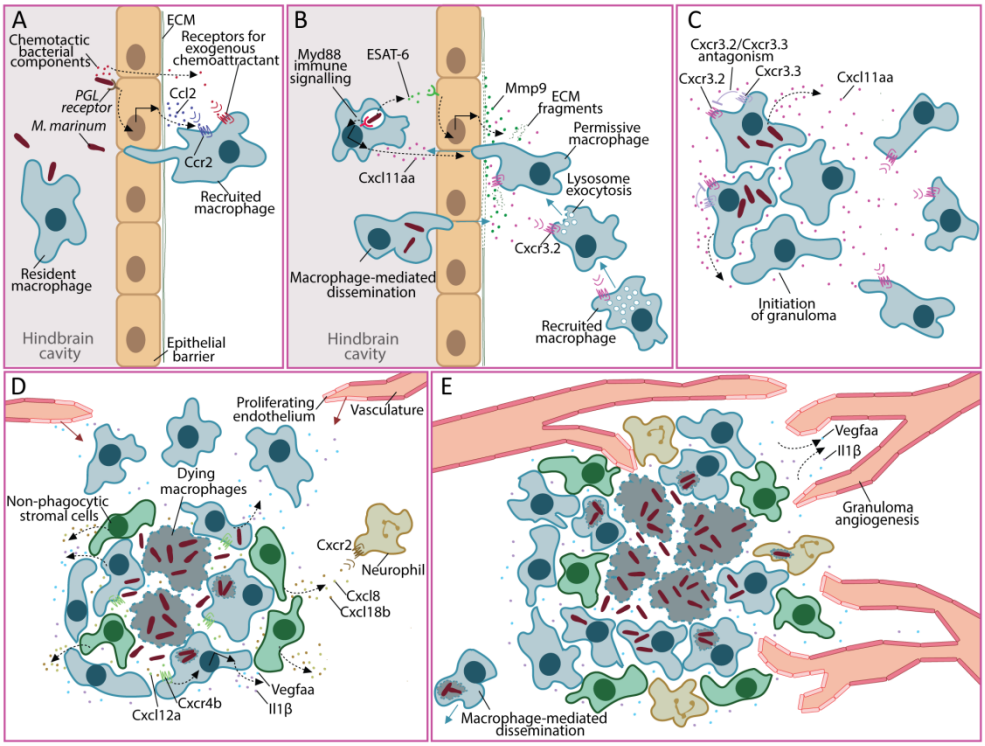

Figure 1. Host and pathogen signalling mechanisms that drive granuloma formation. A. Recruitment of macrophages to invading mycobacteria (e.g. injected in the hindbrain cavity) can be guided by several bacterial molecules. Additionally, it has been proposed that recognition of phenolic glycolipids (PGL) by the epithelium mediates induction of the macrophage chemokine CCL2. However, mycobacteria are also phagocytosed by tissue-resident macrophages and active chemotaxis may not be essential to establish the initial intracellular parasitosis. **B.** When resident in macrophages, mycobacteria produce ESAT-6, which induces expression of Mmp9 by the epithelium. By digesting the extracellular matrix (ECM), Mmp9 facilitates macrophage infiltration into the infected focus. Once the intramacrophage infection is established, this triggers expression of chemokines in the host macrophages. In particular, the macrophage chemokine Cxcl11aa is highly induced in infected macrophages, with a mechanism that requires Myd88-dependent pathogen sensing. Signalling of Cxcl11aa via its receptor Cxcr3.2 can control lysosomal function, for example via induction of exocytosis, therefore, this signalling not only controls macrophage recruitment, it might also contribute to generate and maintain an infection-permissive phenotype. Already from these very initial stages, some infected macrophages are seen to mediate mycobacterial dissemination to other tissues. **C.** The Mmp9 and Cxcl11aa signalling mechanisms continue to sustain macrophage recruitment and the aggregation of macrophages indicates the initiation of granulomas. Although mechanistically still unclear, the atypical Cxcr3.3 receptor exerts a host protective function and limits infection, most likely by antagonising Cxcr3.2. **D.** Macrophages that do not contain infection die releasing the bacteria, most of which will be re-phagocytosed when still encapsulated in cell debris. The inflammatory properties of the granuloma progressively increase. Neutrophil chemokines, including Cxcl8a and Cxcl18b, are also locally released. Induction of local hypoxia determines the production of Vegf and primes neutrophil protective functions. Cxcr4b, which can control the level of inflammation by modulating production of Il1β, cooperates with the Vegfaa signalling to support inflammation-associated angiogenesis. **E.** The vascularisation of the granuloma further supports its expansion and departure of infected cells from the lesion can seed new granulomas.

Despite their capability to persist in macrophages, pathogenic mycobacteria grow very slowly in their host, when compared to non-pathogenic environmental mycobacterial strains, such as *M. smegmatis*[78,79]. These two opposing forces, together with the capability of macrophages to contain the infection to a certain extent in healthy situations, generate a balanced dynamic equilibrium. This equilibrium is characterised by granuloma lesions that expand slowly or do not expand at all, and by a disease that develops into its active form only in about 10% of cases[80,81]. This balance of host and pathogen responses probably emerged from host-pathogen reciprocal adaptations and likely represents an important aspect of evolutionary fitness, as both the host and the pathogen survive when the infection is contained by granulomas[80,81,82]. The zebrafish model has been used to show that bacterial persistence in granulomas is accomplished by the spread of bacteria from dying macrophages to newly arriving ones[22]. When a macrophage can no more contain the intracellular bacterial replication, it undergoes cell death and leaves viable bacteria still encapsulated within the cell debris. Simultaneously, new uninfected macrophages are recruited to the granuloma, which engulf the bacteria and the remains of dead macrophages (**Figure 1D**).

The concomitant activity and the integration of host and pathogen factors plays an important role in the process of granuloma formation. Previous studies implicated the ESX-1 secretion system (one of the virulence determinants encoded by the RD1 locus) into driving macrophage aggregation during the initial stages of granuloma formation, most likely via the release of the virulence factor ESAT-6 (**Figure 1B**)[83]. However, the ESAT-6 virulence factor requires the response of the host to mediate this mechanism. A study in zebrafish showed that ESAT-6 induces the production of the matrix metalloproteinase 9 (Mmp9) in epithelial cells surrounding the nascent infectious lesion, which in turn facilitates macrophage infiltration and formation of granulomatous cell aggregates (**Figure 1B**)[83].

Here we have found that the induction of the macrophage chemokine Cxcl11aa is also important to sustain the granuloma aggregation and to maintain a proper macrophage trafficking via its receptor Cxcr3.2 (**Figure 1B**, **Chapters 3-4**). In fact, *cxcr3.2* mutant macrophages were recruited to a reduced extent to the infectious foci, which resulted in delayed granuloma expansion and reduced bacterial dissemination (**Chapter 3**). Sorting of macrophages from infected larvae followed by transcriptional quantification, showed that macrophages themselves are the main responsible cell type for the production of Cxcl11aa. These findings suggest a macrophage-autonomous mechanism by which mycobacterial infection induces production of the macrophage chemoattractant Cxcl11aa, to support further macrophage aggregation (**Figure 1B**, **Chapters 3-4**). Notably, Cxcl11aa induction does not require the presence of the RD1 locus while it requires active Myd88 (Myeloid differentiation factor 88)-dependent immune signalling (**Chapter 4**). Myd88 is a central adaptor that links innate pathogen recognition via most of the Toll-like receptors (Tlr) to a downstream machinery that modulates transcription of immune and inflammatory genes. Signalling via Tlr/Myd88 has been shown to be fundamental for the induction of inflammatory genes in the zebrafish-*Mm* model and to drive host protection, for example by activating bacterial clearance via autophagy[84]. Notably, Myd88-deficient larvae develop a more severe mycobacterial infection, but strikingly fail to upregulate Cxcl11aa (**Chapter 4**).

The studies presented above indicate that the ESX-1/ESAT-6/Mmp9 and the Myd88/Cxcl11aa/Cxcr3.2 mechanisms of recruitment represent two distinct, but synergistic, systems (**Figure 1B**). However, differently from the Myd88/Cxcl11aa/Cxcr3.2 axis, the ESX-1/ESAT-6/Mmp9 pathway is not likely to induce active recruitment, rather it would facilitate macrophage infiltration by generating local inflammation and by loosening the matrix resistance (**Figure 1B**). It is however also possible that local activity of Mmp9 might facilitate recruitment directly by mediating release of matrix-derived chemotactic peptides or by processing chemotactic mediators[85]. On the other hand, it must be noted that in mammals, MMP9 processing has been shown to exclusively activate neutrophil chemokines (and not macrophage chemokines) and to produce matrix debris that are solely able to activate neutrophil recruitment[85]. Therefore, the indirect macrophage recruitment model is the most likely mechanism of action of Mmp9. In contrast to the passive Mmp9-mediated recruitment, the Myd88/Cxcl11aa/Cxcr3.2 signalling can induce direct macrophage recruitment to the infection focus, since the Cxcl11aa/Cxcr3.2 signalling can mediate directional cell migration, sustain cell anteroposterior polarisation and increase basal motility (**Figure 1B**, **Chapters 3-4**).

The zebrafish model has helped to clarify that granuloma aggregation, which was historically regarded as a host-protective mechanism, can benefit the bacteria in many different ways: recruitment and coalescence of macrophages fuel the infectious focus with novel cells to be infected and to replace the dying ones, which is an advantage for a pathogen that essentially is adapted for an intracellular life (**Figure 1**)[22]. Additionally, by curtailing tissue necrosis with efferocytosis (collection and clearance of cell debris), newly recruited macrophages also moderate tissue inflammation to a level that is suitable to maintain the parasitic relationship (**Figure 1D**)[42,86]. Furthermore, departure of infected macrophages from a mature granuloma can seed new granulomas in healthy tissues of the host (**Figure 1E**, **Chapters 2-3**)[41,77]. Finally, establishment of an intra-macrophage niche permits host signalling subversion and the initiation of specific pathogen-beneficial programmes, which include the induction of angiogenesis (**Figure 1D-E**, **Chapter 5**) [41]. Taken together, it is not surprising that attenuation of macrophage trafficking can benefit the host and, in agreement with this, the knockdown of *mmp9* and the null mutation *cxcr3.2* confer resistance to the host, reducing infection burden and granuloma formation (**Chapter 3**)[83]. Host-beneficial effects from disrupting CXCL9-10-11/CXCR3 signalling and Mmp9 function have also been observed in murine animal models for TB and have been suggested by human clinical and genetic association studies. CXCR3 knockout BALB/c mice developed a limited disease upon exposure to *Mtb*[87] and a study performed on the Chinese population revealed a host-beneficial association between TB and a -135G>A proximal promoter polymorphism of CXCL10. This replacement, which is in the proximity of a putative NFκB binding site, was suggested to impair the infection-dependent inducibility of this gene[88]. Similarly, increased MMP9 secretion is associated with increased severity and mortality in TB meningitis[89,90] and increased expression of all CXCR3 ligands (CXCL9-10-11) is correlated with active TB[91].

Initial macrophage recruitment to mycobacteria: insights into a "chicken and egg"-like paradox

Intriguingly, both the Cxcl11aa/Cxcr3.2 and the ESAT-6/Mmp9 pathways that drive macrophage recruitment to mycobacterial infectious foci substantially require a pre-existing intramacrophage infection (**Figure 1B**). Infection-dependent induction of *cxcl11aa*

occurs in macrophages and requires Myd88-signalling and active pathogen recognition (**Chapter 4**). Similarly, the ESAT-6 secretion by mycobacteria requires pathogen adaptation to the intramacrophage life style[83]. Therefore, these two recruitment axes seem to be predominantly exploited to maintain an appropriate macrophage supply once the lesion has been established, rather than mediate its very initial onset (**Figure 1A-B**). Another zebrafish study has suggested that an additional chemokine axis, an orthologue of the mammalian CCL2/CCR2, might be important for the initial recruitment of macrophages to the invading bacteria, via a mechanism that does not require Myd88 signalling and intramacrophage infection (**Figure 1A**)[68]. This axis was shown to rely on recognition of extracellular mycobacteria via specific mycobacterial wall lipids by the neighbouring epithelial cells. This recognition would, in turn, activate production of the macrophage chemokine Ccl2 and therefore macrophage recruitment. However, evidence from the murine model and from human disease-polymorphism association studies are contradictory on the function of CCL2/CCR2. In mice, this axis seemed to permit better containment of high doses of bacteria but did not abolish granuloma aggregation neither reduced infection susceptibility to low doses[92,93], which is in contrast with the hypothesis that the Ccl2/Ccr2 pathway would not require Myd88 signalling and classical Tlr-mediated pathogen recognition. On the contrary, these data suggest that CCL2/CCR2 may not be crucial to establish the initial parasitism (considering that CCR2-deficient mice have the same susceptibility to low-dose infection as wt), rather to contain the effects provoked by a larger and more inflammatory inoculum. Human polymorphism studies also fuel the debate on the real significance of CCL2, since some studies indicate that higher expression levels of CCL2 increase susceptibility to infection in some populations, although the same correlation could not be replicated in other populations[94,95]. A similar indication in this direction also comes from the fact that PGL (the mycobacterial lipid that has been proposed to mediate CCL2 release in Myd88-independent conditions[68]) is not essential for the virulence of *Mtb* strains and many clinical *Mtb* isolates exist that do not express PGL[96]. An alternative to the CCL2-mediated mechanism could be that the initial establishment of intramacrophage parasitosis may depend on direct chemotaxis to bacterial components or may simply not require active recruitment, since the tissues, including the human alveoli, contain resident macrophages that can readily engulf invading pathogens when these are presented in a limited number (**Figure 1A**).

Function of chemokines and cell motility in controlling macrophage intrinsic immune competence

We have found that in uninfected conditions, macrophages express basal levels of *cxcl11aa* and that the Cxcr3.2-dependent signalling can facilitate macrophage basal patrolling under physiological conditions, presumably by activating an autocrine loop (**Chapters 3-4**). This mechanism possibly generates continuous adjustments of macrophage anteroposterior polarity that leads to random walks. The capability to random patrol might be intrinsic to macrophages and might influence the ability of these cells to exert a sentinel function into tissues. In this perspective, the establishment of initial parasitism could be impacted by Cxcl11aa/Cxcr3.2 signalling, with mechanisms that not necessarily require Myd88-dependent upregulation of *cxcl11aa*. Our own evidence is that macrophages use the Cxcl11aa/Cxcr3.2 signalling pathway to maintain their capability to random patrol and that in the absence of this signalling axis, macrophages upregulate lysosomal genes and become more microbicidal (**Chapters 3-4**). Thus, our data indicate that Cxcl11aa/Cxcr3.2 signalling directly correlates chemotaxis/motility to intrinsic immune competence,

although the molecular mechanism that triggers this phenotype still remains to be elucidated. A known connection between motility and lysosome function is that chemokine signals lead to the fusion of lysosomes to the plasma membrane to sustain cell movement[97]. Therefore, one hypothesis to explain why lysosomal genes are upregulated in a situation of deficient motility is that the cell is alerted and promotes lysosomal biogenesis, in the attempt to restore normal motility dynamics. There is evidence that, if the flux of lysosomes to the plasma membrane is compromised, this leads to the CLEAR (Coordinated Lysosomal Expression and Regulation) response and production of more lysosomes[98,99,100]. In addition, macrophage motility seems to be severely affected by excessive phagocytosis and by the inability to digest phagocytosed debris[101]. In lysosomal storage disorders (LSD), macrophages are amply vacuolated and the presence of these large intracellular compartments severely perturbs their motility[101]. Activation of the lysosome pathway can rescue the LSD disease by facilitating elimination of the undigested inclusions[98,99,102], which in turn would restore motility too. Therefore, the reduction of motility below certain levels might function as an alarm signal that suggests a post-phagocytosis phenotype and therefore increased need of digestive lysosomal contents.

Several genetic diseases associated with LSD are associated with impaired lysosomal function and increased susceptibility to infections[103,104,105]. Also in zebrafish the knockdown of the orthologues of three genes linked with LSD in human (*glucocerebrosidase 1*, *hexosaminidase A*, and *arylsulfatase A*) resulted in LSD and hypersusceptibility to *Mm* infection[101]. In this respect, our study indicates an important complementary aspect: if the content of functional lysosomes is increased without leading to the LSD phenotype, this benefits the host, by boosting the intrinsic capability of macrophages to counteract infection, with beneficial rather than detrimental effects. This hypothesis is in line with the proposed idea that genetic conditions that in homozygosis associate with LSD and increased susceptibility to TB, might provide resistance to TB when carried in heterozygosis.

To discuss the hypothetical links between LSD-associated genetic conditions and susceptibility to TB, the Ashkenazi Jewish (AJ) population (and their descendants) represents an interesting case, since 6 independent mutated alleles for four LSD diseases (2 mutations leading to Tay-Sachs disease, 2 mutations leading to Gaucher disease, 1 mutation leading to Niemann-Pick disease and 1 mutation leading to mucolipidosis type IV) are fixed in this population with anomalously increased frequencies[106,107]. The selection of these four genetic disorders is unlikely derived from stochastic genetic drifting events and might be explained if these disorders provide a selective advantage to the heterozygote carriers. Notably, among the AJ population, the frequency of TB-associated deaths is reduced, when compared to ethnically-separated populations residing in similar areas[108,109.110,111]. Additionally, dividing the AJ population based on their geographical origin, it was shown that the AJ groups with ancestry in areas of higher incidence of TB have also increased prevalence of the Tay-Sachs allele, compared with the AJ groups that were originally from areas with reduced TB prevalence[112,110,111].

The heterozygote advantage hypothesis for the Tay-Sachs mutations in TB has been debated[106,113,114], since the proportion of the LSD-allele carriers does not occur at such high frequency (3 to 6% of AJ population[107,112]) to provide a substantial population protection, differently, for example, from the well-known associations of sickle-cell anaemia and other haemoglobinopathies with malarial endemic areas (3 to 40% of endemic populations[115]).

However, recent studies have elucidated how the Tay-Sachs allele could provide carrier advantage against TB. The Tay-Sachs alleles consist of genetic mutations of the gene coding for the alpha subunit of hexosaminidase A (HEXA), an important enzyme that mediates lipid degradation (especially neuronal gangliosides). Hexosaminidase A is a two-subunit enzyme and its beta-subunit is encoded by a different gene (HEXB). A second functional isoenzyme, hexosaminidase B, exists which is instead composed of two beta-subunits. In Tay-Sachs patients, the disease is caused by the homozygote mutation of the HEXA gene (and concomitant complete absence of functional hexosaminidase A isoform). Mutations of HEXB gene are very rare (Sandhoff disease), and lead to more severe dysfunctions and LSD. The main consequence of the Tay-Sachs disease is a deficient digestion of gangliosides, which accumulate into cells and provoke vacuolation. Interestingly, it has been found that Tay-Sachs heterozygotes express higher levels of hexosaminidase genes and have increased enzymatic activity of the hexosaminidase B isoenzyme than healthy individuals[109,116,117], which permits normal processing of accumulating lipids and, prevents the onset of Tay-Sachs disease. Of note, hexosaminidases are target of the CLEAR response and can be induced in lysosomal stress conditions via the CLEAR transcriptional programme[99,102]. Therefore, a possible explanation of why Tay-Sachs carriers are less susceptible to TB might be that this deficiency in heterozygosis induces lysosomal stress and the CLEAR response, in the attempt to restore normal hexosaminidase activity. However, if lysosomal stress and the CLEAR response are activated, this will lead to increased expression, not only of hexosaminidases, but also of many other lysosomal genes, and therefore to a better intrinsic microbicidal function. That dysfunction of one lysosomal component is accompanied by upregulation of many other lysosomal-related genes is a recurrent observation in LSD patients and in LSD *in vitro* models[99,102,118]. Additionally, most of LSD syndromes can be, at least partly, restored by transcriptional stimulation of CLEAR *in vitro*[99,102,119]. Therefore, these observations suggest that genetic manipulation of the lysosomal function at transcriptional level might be explored for therapeutic purposes also against bacterial infections.

It is well known that mycobacteria can counteract phagosome maturation and can mount countermeasures to persist in acidified compartments. On the other hand, it has been shown that they are susceptible to anti-bacterial autophagy and degradation via autophagolysosomes[84]. Intriguingly, among the mechanisms by which mycobacteria hijack the host macrophage, there is the promotion of lipid inclusions formation, which results in the "foamy cell" macrophage phenotype. It has been hypothesised that the fatty acids derived from lipid bodies might be an important energy source for the pathogen, or that they provide to the mycobacteria a mechanism to interfere with the eicosanoid biosynthesis and therefore with the production of pro- or anti-inflammatory components[120]. Given the fact that lipid bodies can be counteracted via induction of CLEAR activation, triggering lysosomal stress might contribute to fight this peculiar mechanism of virulence.

In mammals, the CLEAR pathway is controlled by a group of factors, including MITF (microphthalmia-associated transcription factor), TFEB, TFEC and TFE3 (transcription factor EB, EC, E3). These genes are conserved in zebrafish (**Figure 2A**), which has a single orthologue for TFEB and TFEC (Tfeb, Tfec) and 2 orthologues for MITF and TFE3 (Mitfa, Mitfb, Tfe3a, Tfe3b)[121]. Additionally, there is evidence that the genetic control of the CLEAR response is similar in humans and in zebrafish[122]. Our transcriptome data suggest that the increased lysosomal function of *cxcr3.2* mutant macrophages derives from

activation of the CLEAR response. While expression of Mitf, Tfeb and Tfe3 genes did not significantly differ between *cxcr3.2* mutants and wt, Tfec was approximately 1.8 fold downregulated in *cxcr3.2* mutants (**Chapter 4**).

TFEB is currently the most studied inducer of the lysosomal stress response[123]. However, while TFEB and TFE3 are ubiquitously expressed[123], TFEC expression is restricted to myeloid cells[124], indicating a specific function of this gene in innate immune cells. TFEC function has not been characterised to the same extent as that of the other members of this transcription factor family and its function needs further elucidation. It is known that in physiological conditions TFEC mutation does not generate any apparent phenotype in mice[125]. Interestingly, TFEC could be induced in macrophages by stimulation with T-helper 2 cytokines (IL4 and IL13) or lipopolysaccharide treatment[125]. However, even after its upregulation, TFEC did not evoke major transcriptional changes in murine macrophages. It should be noted that TFEC diverges significantly, in terms of structure, from the other TFEs (**Figure 2**). In the study that initially identified TFEC, it was found that this factor can act a negative regulator of the other members of the TFE family, by formation of non-functional heterodimers and by DNA binding competition[126]. Both TFEB and TFE3 possess an important MITF/TFEB N-terminal homology domain and a conserved bridging sequence between the N-terminal domain and the basic helix-loop-helix (bHLH) DNA-binding domain (**Figure 2B**). This linking sequence was shown to be important to activate transcription of the canonical TFE target genes, although not required for the DNA binding *per se*[126,127]. Notably, the MITF/TFEB N-terminal homology domain of TFEC is truncated when compared to those of TFEB and TFE3 (**Figure 2B**), and the region immediately upstream of the bHLH domain is also specifically divergent in TFEC. On the other hand, TFEC maintains highly conserved bHLH and basic Leucine zipper (bZip) domains, which are required to bind the DNA and to form homo/heterodimers within the TFE family members. The alterations in the N-terminal and in the bridging region involved in transcription regulation justify why induction of TFEC alone or its knockout, did not provoke large transcriptional consequences, as this factor, that antagonises TFEB and TFE3, would display transcriptional effects only in situations where TFEB and TFE3 are activated, such as during the CLEAR response. Structurally, zebrafish Tfec resembles closely the human TFEC and displays similar aberration in the MITF/TFEB N-terminal homology domain and in the region that supports target transcription in TFEB and TFE3 (**Figure 2B**). Therefore, this suggests a conserved function of Tfec and indicates that the zebrafish model could contribute substantially to understand the importance of this factor.

Reduced expression of *tfec* in *cxcr3.2* mutant macrophages indicates that *cxcr3.2* mutation might lead to the CLEAR response by suppressing a negative regulator of Tfeb/Tfe3. In future work, this hypothesis could be tested by overexpressing *tfec* in the *cxcr3.2* mutant background, which is predicted to prevent the induction of the CLEAR programme and thereby revert the increased microbicidal capacity of *cxcr3.2* mutant macrophages.

Concluding, our results indicate that the CXCR3-CXCL11 axis exerts different functions on macrophages, and that disruption of this axis reduces macrophage recruitment to infection, while enhancing the macrophage intrinsic microbicidal capability via induction of a lysosomal stress response (**Chapters 3-4**). In response to these functions, mycobacteria seem to have evolved several mechanisms for manipulating this axis to regulate macrophage trafficking during granuloma aggregation, drive macrophage-

mediated dissemination and suppress the basal bactericidal property of the host cell. Therefore, use of CXCR3 antagonists may represent a therapeutic regime that, by acting on a single target, could counteract mycobacterial infection at multiple levels. Additionally, considering the work performed in the murine model, CXCR3 blockade might be beneficial also to prime a more efficient anti-mycobacterial T-cell mediated adaptive immunity[87].

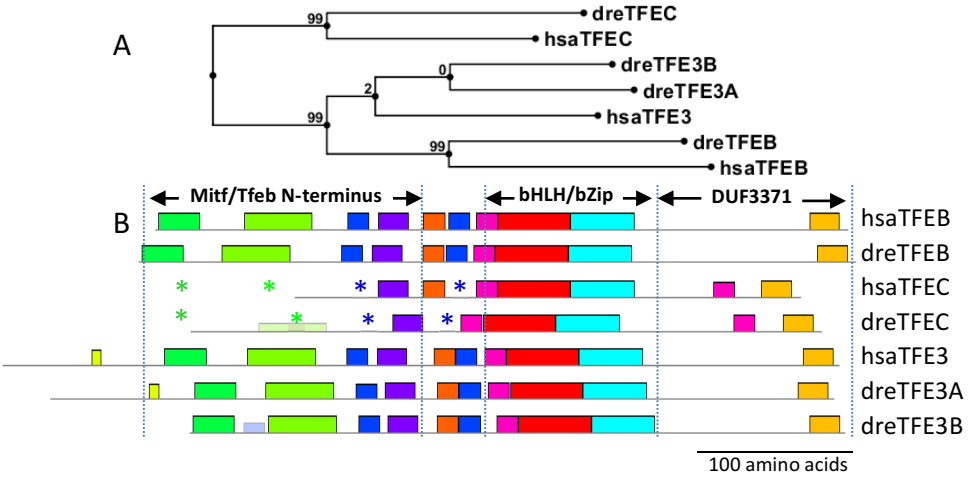

Figure 2. Conservation of Transcription factor E family members between human and zebrafish. A. Sequence alignment tree, showing that in zebrafish (dre) there are direct homologues of the three human (hsa) transcription factor E family members. There is only one homologue of TFEB and TFEC while there are two homologues of TFE3. The tree also shows that the TFEC cluster diverges from the TFEB/TFE3 cluster. **B.** Conservation of protein domains and amino acid motifs in TFE sequences. TFE proteins have essentially three domains: a conserved Mitf/Tfeb domain, a DNA binding/protein dimerisation domain composed by a basic helix-loop-helix (bHLH) followed by a basic Leucine zipper (bZip) consensus and finally a variable C-terminal domain named DUF3371 (domain of unknown function 3371). These domains encompass conserved sequence motifs, visualised here with boxes of identical colour and size. Notably, the N-terminal region of both human and zebrafish TFEC are characterised by absence (or poor amino acid conservation indicated by fainter boxes) for several motifs otherwise maintained in TFEB and TFE3 (asterisks). Like the other TFE members, TFEC proteins highly conserve instead the domain that serves to bind the DNA and to form homo- or hetero- dimers (bHLH/bZip). The N-terminal region and the area immediately upstream the bHLH/bZip are important to modulate the efficiency of transcription of target genes, which is the reason why TFEC is unable to efficiently drive gene expression and essentially is believed to act as a regulator of the other TFE members. The fact that the zebrafish Tfec has similar sequence alterations and truncation of the N-terminal as the human TFEC indicates that zebrafish Tfec may recapitulate the function of the human counterpart. The TFE tree was generated by CLC Bio workbench, from full-length protein sequence alignment. The identification of conserved sequence motifs was obtained by MEME motif discovery suite (http://meme-suite.org/).

Atypical CXCR3 receptors and emerging functions of ACKRs in inflammatory diseases

Atypical chemokine receptors (ACKRs) are 7-loop transmembrane proteins, evolutionary close to the classical chemokine receptors. However, because of a modified or missing canonical E/DRY motif and altered micro-switch elements, ACKRs are unable to interact with G-proteins and are therefore unable to induce G-protein coupled receptor (GPCR) signalling (**Chapters 1,5**)[128].

The most obvious consequence of the altered sequence in ACKRs is that these molecules are unable to directly mediate cell migration[128]. However, ACKRs are not silent molecules and can activate GPCR-independent signalling and exert important regulatory functions[129]. An important feature of the ACKR class is for example the capability to efficiently mediate ligand internalisation[130]. Because ACKRs are generally not very specific in terms of ligand binding, these receptors can intercept a wide range of chemokine ligands and mediate their transport to the lysosomes for degradation[128,130]. In some circumstances the ACKR/ligand recycling has also been seen to mediate the transcytosis of chemokines and therefore their transport across biological barriers[131]. Several ACKRs have shown to play an important function to control speed and directionality of chemotactic movements, by tightly titrating the chemokine ligand concentration and by shaping the chemokine gradients[132]. Since binding of excessive amounts of chemokine ligands to their classical receptors can induce desensitisation via receptor internalisation, the expression of ACKRs can also help to maintain appropriate signalling by avoiding complete downregulation of classical chemokine receptors[133].

There is increasing evidence that ACKRs also control the overall inflammatory response, by preventing exceeding chemokine-derived inflammatory signals. This condition has been recently demonstrated by using a murine knockout for the wide spectrum chemokine scavenger D6/ACKR2. The mutant animals are basically indistinguishable from wt littermates in physiological conditions. However, when challenged by wounding, chemicals, cancer or infections, these animals develop a higher inflammatory status[134,135,136,137138]. In infections with *Mtb,* the uncontrolled inflammation occurring in D6/ACKR2 knockouts is lethal and D6/ACKR2 expression is essential to prevent the inflammatory storm and to attenuate excessive infiltration of leukocytes into the lungs[137]. Similar anti-inflammatory functions have been demonstrated also for other ACKRs that scavenge inflammatory chemokines, for example DARC/ACKR1[139,140], which can sequester large amounts of circulating chemokines and dampen leukocyte activity. However, the function of DARC/ACKR1 is multifaceted, given the fact that this receptor can also sustain the transport of chemokines through physical barriers and function as a chemokine reservoir which can in some circumstances generate opposing pro-inflammatory phenotypes[141,142,143]. In fact, during inflammatory disorders of the brain, binding of chemokines to DARC can facilitate their shuttling through the blood brain barrier via transcytosis. Additionally, binding of chemokines to DARC expressed by erythrocytes can reduce exaggerated levels of freely circulating chemokines during acute inflammatory responses but also help to maintain a steadier concentration of them in the longer term, since chemokines can continue to dissociate from the receptor and become again available.

In **Chapter 5** we have identified and characterised a novel chemokine receptor, Cxcr3.3, which, based on its altered E/DRY motif (Glu/Asp-Arg-Tyr) and on altered micro-switch elements, likely represents an ACKR. Similarly to the results found in D6/ACKR2 mutants, *cxcr3.3* mutants displayed an increased infection burden, and intriguingly an opposing phenotype as mutants for the canonical chemokine receptor *cxcr3.2* (Chapter 3-5). This phenotype suggests that *cxcr3.3* may antagonise *cxcr3.2* function, for example by attenuating the inflammatory response or moderating leukocyte infiltration to the infected tissues (**Figure 1C**)[138]. Based on sequence and synteny reconstruction, we have found that atypical Cxcr3-like receptors exist in a large number of fish species, although not in tetrapods (**Chapter 5**). Due to high sequence similarity with classical Cxcr3 genes and due to its close synteny to the other *cxcr3* genes throughout fish species, it is likely that the atypical *cxcr3* products have originated from an ancestral *cxcr3* gene which encoded a functional chemokine receptor, able to bind CXCL9-10-11-like ligands. To our knowledge, in sharks (*Callorhinchus milii*) there is also only one copy of Cxcr3, which contains a normal E/DRY sequence, while in ray-fish that have diverged before the teleost-specific whole genome duplication such as the spotted gar (*Lepisosteus oculatus*), there is already existence of E/DRY-depleted Cxcr3 genes (**Figure 1**, **Chapter 5**). Therefore, the origin of atypical *cxcr3* genes may have occurred before the teleosts whole genome duplication, but after the divergence of bony fishes from cartilaginous fishes.

We currently do not know whether Cxcr3.3 acts as a scavenger of Cxcl11-like chemokines, the classical ligands of the Cxcr3.2 receptor (**Chapter 3-4**). However, since Cxcr3.3 forms a homophyletic group and is in a synteny cluster with Cxcr3.1 and Cxcr3.2 throughout fish species (**Figure 3**, **Chapter 5**), this is a plausible hypothesis. In this case, the *cxcr3.3* genes may have differentiated in the attempt to more strictly regulate the activity of the CXCR3 axis and its central role in adaptive and innate immunity. We also currently do not know whether this CXCR3 atypical axis, that appears a fish-specific system, has parallels in mammals. Intriguingly, despite the lack of atypical CXCR3 receptors, mammalian CXCL9-10-11 ligands can be still scavenged by two other ACKRs, CXCR7/ACKR3, and DARC/ACKR1[130,144,145] (**Chapter 1**).

In Actinopterygii, which includes the zebrafish, an orthologue for every human ACKR can be found, with the exception of DARC/ACKR1, which can be first found in coelacanths (*Latimeria chalumnae*), a rare group of fish regarded as living fossils that are directly related to the last fully-aquatic ancestor of tetrapods (**Figure 3**). The coelacanth does not possess an atypical Cxcr3, as its three copies of the Cxcr3 gene all contain intact E/DRY motifs. This suggests that the evolution of ACKR1 has occurred during speciation of Sarcopterygii (lobe-finned fish and tetrapods) and coincided with the loss of atypical CXCR3 isoforms. It is possible that the emergence of a novel wide spectrum chemokine scavenger (DARC/ACKR1) determined the loss of the atypical CXCR3, due to redundant function. It should also be mentioned that ACKR3/CXCR7, which is also able to scavenge CXCL11, is not redundant with DARC/ACKR1, since it is best known for its scavenging activity against CXCL12[132,144]. This receptor is the sole ACKR able to bind CXCL12 and, similarly to the classical receptor of CXCL12 (CXCR4), exerts a unique function in mammals, as demonstrated by the fact that CXCR7 mice homozygote mutants are lethal *in utero*.

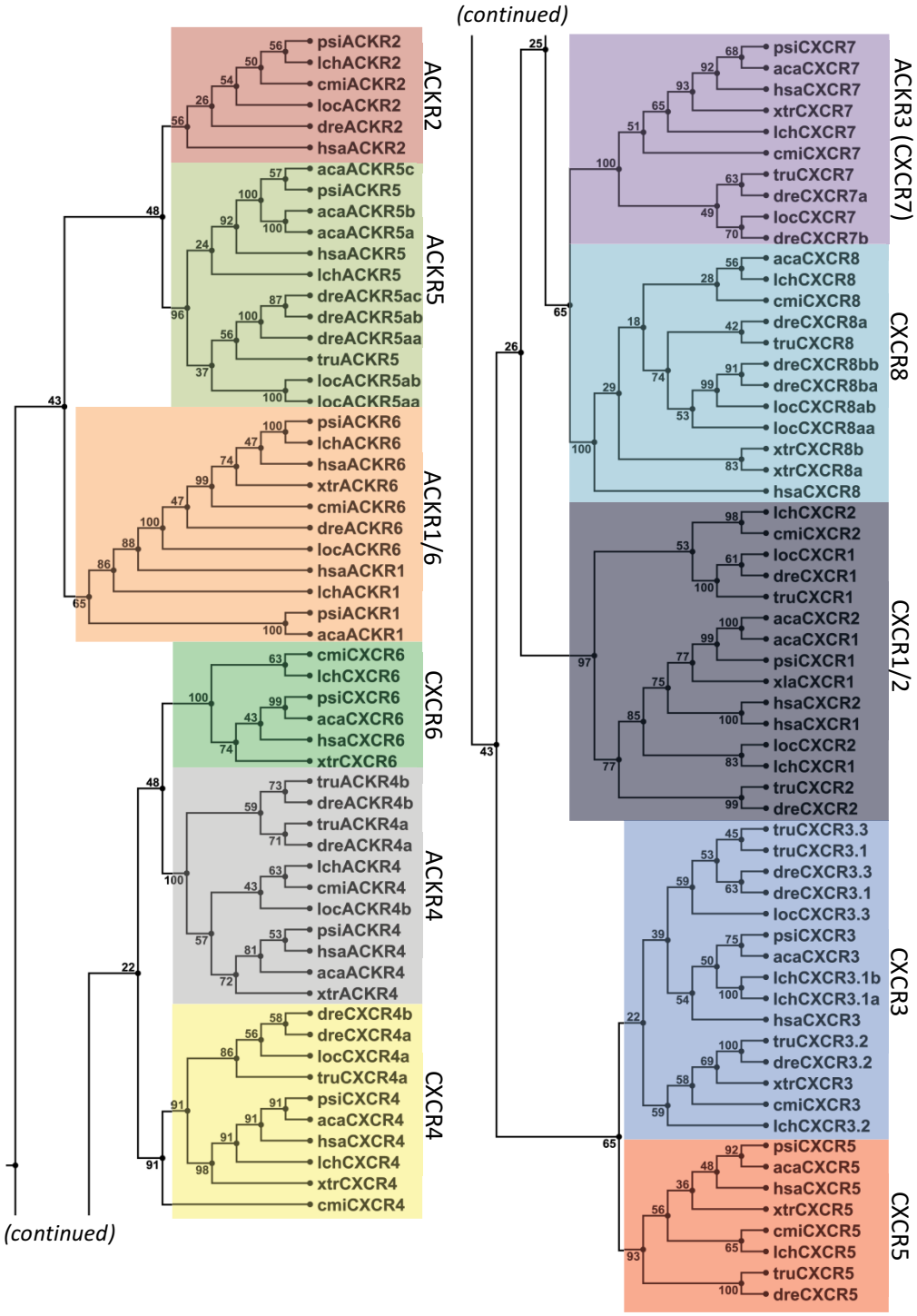

Figure 3. CXCR and ACKR phylogenetic tree *(Legend on the next page)*.

Figure 3. CXCR and ACKR phylogenetic tree *(Figure on the previous page)***.** Sequences were obtained from Ensembl, ncbi or uniprot databases. The tree was constructed from full-length sequence alignments, using CLC bio workbench. Legend: aca: *Anolis carolinensis* (anole lizard); cmi: *Callorhinchus milii* (elephant shark); dre: *Danio rerio* (zebrafish); hsa: *Homo sapiens* (human); lch: *Latimeria chalumnae* (coelacanth); loc: *Lepisosteus oculatus* (spotted gar); psi: *Pelodiscus sinensis* (Chinese softshell turtle); tru: *Takifugu rubripes* (fugu); xtr: *Xenopus tropicalis* (western clawed frog). Note: since Cxcr1/2 receptors have not been identified in *Xenopus tropicalis*, we included the CXCR1 sequence of the close species xla: *Xenopus laevis* (African clawed frog) to provide the tree with an amphibian sequence for this class of receptors.

According to alignment-based phylogenetic reconstruction, it is unlikely that ACKR1 had radiated directly from a CXCR3-like ancestor, due to large sequence differences. However, by blasting the lchDARC/ACKR1 protein to the coelacanth protein database, its closest intraspecific orthologue is in fact the lchCxcr3.1. Unfortunately, the coelacanth genome has not been assembled, which makes it impossible to support phylogenetic reconstructions with synteny studies. However, a hypothesis that could explain the large divergence of ACKR1 from the other chemokine receptors (including CXCR3) could be that stringent selective pressures have acted on this atypical receptor and mediated its diversification. This idea is supported by that fact that we have examples of large diversification of DARC/ACKR1 sequences in primates, due to selective advantages provided by DARC/ACKR1 variants against *Plasmodium* infections[146,147,148]. DARC/ACKR1 can in fact also act as a parasite receptor and facilitate entry of certain *Plasmodium* species into the erythrocytes.

Concluding, *in vivo* studies during the course of inflammatory processes have been crucial to demonstrate that ACKRs play a fundamental role, not only in the trafficking of the immune cells, but also in the regulation of the inflammatory process itself. The use of zebrafish Cxcr7/Ackr3 mutants (and the remarkable conservation of specificity for Cxcl12) has already provided fundamental insight into the function of ACKRs in homoeostatic contexts[149,150,151]. With the exception of DARC/ACKR1, all the other mammalian atypical chemokine receptors are present in zebrafish too, which is both striking and valuable in scientific terms, as it suggests high functional conservation throughout vertebrates and the possibility to use zebrafish to obtain a better understanding of the origin of ACKRs and their function in inflammatory diseases.

Function of chemokine signals as modulators of inflammation and angiogenesis in mature granulomas

As illustrated by studies in cancer treatment, targeting pathological angiogenesis has potential therapeutic applications. Inhibition of tumour-associated vessel formation has long been known to have anti-neoplastic properties, as the microvasculature contributes to the growth and dissemination of cancer cells. However, *in vivo* results suggest that, depending on the stage and nature of the tumour, in some circumstances a pro-angiogenetic therapy, rather than an anti-angiogenic one, may benefit the patient. It has been proven, for example, that improving the angiogenetic response can lead to a better delivery of chemotherapeutics and promote healing and inflammation resolution by preventing hypoxia[152]. Reasoning on TB, similar conclusions can be drawn. An anti-angiogenic treatment might help restrict bacterial dissemination and granuloma formation, while a pro-angiogenic treatment might be beneficial as adjuvant therapy to a better delivery of first line antibiotics, by promoting tissue repair, remodelling, resolution of inflammation, and by preventing granuloma caseation[153].

Studies on TB patients corroborate the hypotheses that the function of angiogenesis in either limiting or sustaining development of the disease is not univocal and that in different situations, an anti- or pro-angiogenetic therapy might be advisable to counteract the diseases. In general, vascular endothelial growth factor (VEGF), an important angiogenesis promoter, has been shown to increase in the circulation of individuals with active TB at a greater extent, compared to both uninfected subjects and infected patients that do not display active TB[154,155]. A study also correlated increased levels of VEGF with the lack of lung cavitation in TB patients, suggesting that high levels of VEGF are at least protective against induction of central necrotisation of the granuloma and the formation of caseating lesions. This seems to indicate that, in an active TB state, a pro-angiogenic host-targeted therapy might be beneficial[156]. On the other hand, there is also evidence that in TB patients treated with anti-VEGF compounds, the vascular integrity was normalised, which led to beneficial effects by promoting small molecule delivery[157]. Evidence for a host beneficial effect of anti-VEGF treatment also comes from the *Mm* zebrafish infection model, where it was shown that innate immune cells, most likely macrophages, were required for the induction of granuloma angiogenesis (**Figure 1D-E**)[41]. In this model, inhibiting VEGF proved to be beneficial by reducing vascular leakage, and by reducing the oxygen availability for mycobacteria. A VEGF receptor inhibitor, Pazopanib, which is currently in clinical trials, was tested in the zebrafish-*Mm* model where it reduced bacterial burden, vascular leakiness and bacterial dissemination[41]. Additionally, this treatment increased also the effectiveness of rifampicin, a first line anti-tubercular antibiotic[41].

In **Chapter 6** we found that under knockout condition of the chemokine receptor Cxcr4b, the induction of angiogenesis to the granuloma aggregates was largely suppressed, which also reduced bacterial burden (**Chapter 6**). However, macrophage and neutrophil recruitment to mycobacteria and macrophage basal motility are unaffected in *cxcr4b* mutants (**Chapter 6**)[158], suggesting that no major mechanistic alterations are evoked in the initiation of granuloma formation. There are several hypotheses that could explain the *cxcr4b* phenotype in the regulation of angiogenesis. One possibility is that *cxcr4b* is important to complete myeloid differentiation in the haematopoietic tissues, since the Cxcr4b/Cxcl12a signalling axis is important to establish the definitive haematopoietic niches[159]. However, the number of macrophages was not largely altered in *cxcr4b* mutants in the developmental window used in our study and these cells did not display difference in basal microbicidal capability (**Chapter 6**), which indicates both quantitative and qualitative normal macrophage competence. Another hypothesis relates to the fact that Cxcr4b, like CXCR4 in mammals, is an M2-type macrophage marker that is upregulated in macrophages engaged in inflammation resolution[160]. It is possible that absence of *cxcr4b* may lead to incomplete polarisation, since M2 macrophages are also the cells that in cancer promote angiogenesis via induction of VEGF[161]. However, our study seems to indicate that *vegfaa* is induced at comparable levels in *cxcr4b* mutants and wt (**Chapter 6**), suggesting that aberration of Vegfaa signalling is not the main phenotype cause.

A more mechanistic explanation of the *cxcr4b* mutant phenotype in granuloma-angiogenesis could be that macrophages are also required to promote infiltration of endothelial cells and vessels sprouting[162] and that this mechanism would require a Cxcr4b/Cxcl12a crosstalk between the endothelium and the macrophages. Finally, although more highly expressed by macrophages, *cxcr4b* is expressed to some extent by endothelial cells too (**Chapter 6**), which would suggest that this signalling may be required for the directed recruitment of the endothelium, with a mechanism that not necessarily requires a

macrophage function[163]. Despite these considerations, our study seems to indicate that *cxcr4b* deficiency in granuloma-associated angiogenesis is related to the modulatory function that *cxcr4b* exerts on the inflammatory mediators (**Figure 1D-E**, **Chapter 6**). In TB patients and in other inflammatory disorders, the presence of inflammatory mediators such as CXCL8/IL8, IL1β and TNFα has also been correlated with the level of angiogenic activity, suggesting that, synergistically to VEGF, these mediators play a role in inflammation-associated angiogenesis[164,165,166,167,168]. Notably, the level of *il1b*, a key factor to propagate inflammation that also promotes proliferation and migration of endothelial cells[165,166,169,170], was induced to a lower extent in *cxcr4b* mutants (**Chapter 6**), which suggests that Cxcr4b can control the induction of the local inflammation. Since *il1b* is largely induced in infected cells (**Chapter 6**), it is likely that this mechanism is macrophage dependent (**Figure 1D-E**). Studies *in vitro* have shown that mammalian CXCR4 is an important co-receptor to mediate activation of Tlr signalling, for example by contributing to Lipopolysaccharide recognition[171,172]. Therefore, deficiency of *cxcr4b* might reduce the capability of immune cells to upregulate inflammatory genes via Tlr/My88/Nfκb pathway. Therefore, we propose a model where Cxcr4b deficiency, by limiting the induction of inflammation, especially via suppression of *il1b*, can reduce the levels of pro-angiogenetic signals and restrict vascularisation and bacterial growth (**Figure 1D-E**).

Overall, angiogenesis represents a promising target for granuloma-suppressive therapy, although more research is needed to determine under which circumstances its inhibition or promotion is more desirable in TB patients. In cases when anti-angiogenesis therapy can be applied, it should be considered that its direct blockade via VEGF-signalling inhibitors could have several contraindications, since this leads to risks of vascular disruption also in healthy tissues[173]. Therefore, in this respect an indirect antagonism via curtailing inflammation or CXCR4 signalling (which seems only implicated into inflammation-dependent vascularisation) might represent a better alternative. Additionally, since CXCR4 represents an important co-receptor for HIV entry into macrophages, use of CXCR4 antagonists might benefit especially patients that are both TB and HIV positive[174].

Chemotaxis of neutrophils to the granulomas and its protective function

Neutrophils can be recruited to mycobacterial infection and play an important protective role. However, when bacteria are systemically injected, macrophages are the main cell type that phagocytoses *Mm* and neutrophils are not actively engaged with mycobacteria[175]. It might be pointed that systemic injections in zebrafish are mostly started at 1 day post fertilisation, when neutrophils are not fully functional. However, the predominant macrophage phagocytosis can be reproduced also when bacteria are injected at later times, such as at 2 or 5 dpf[175]. In part, the poor phagocytosis of *Mm* by neutrophils could be explained by the fact that zebrafish neutrophils do not phagocytose well bacteria dispersed in solution and scavenge efficiently only pathogens that are associated to surfaces[176] (**Chapter 2**). In agreement with this hypothesis, *Mm* can be readily phagocytosed by both neutrophils and macrophages when infections are performed in the fin tissue[177]. It is likely that increased phagocytosis of bacteria by neutrophils in this tissue can be due to the fact that in the thin tissue, most bacteria are presented in association to surfaces[176].

When injections are performed locally in the hindbrain (at developmental stages where fully-competent neutrophils are already present), not only does *Mm* appear to essentially

reside into macrophages, it also seems to not induce neutrophil recruitment. Injection of other pathogens in this ventricle (such as *Pseudomonas aeruginosa*[175]) is able to induce comparable macrophage and neutrophil recruitment. In contrast with this phenotype, injections of *Mm* in the fin tissue seem to initially induce a comparable level of both macrophages and neutrophils[177]. It is, however, possible that injection of the pathogen in this tissue inevitably induces a significant wound response and that neutrophils may be recruited via wound-induced signals (e.g. H_2O_2)[178]. Furthermore, in the hindbrain it is possible to induce recruitment of neutrophils to *Mm* by providing additional signals, such as co-injection with *P. aeruginosa*[175]. In this case, the level of neutrophil infiltration is comparable to that of *P. aeruginosa* injection alone, which indicates that *Mm* does not chemoattract, but also does not chemorepel neutrophils[175]. Despite this scarce recruitment of neutrophils in the hindbrain model, *in vitro* mammalian cell models and *in vivo* zebrafish studies have demonstrated that neutrophil-chemotactic chemokines are induced as early as a few hours post-infection[67] (**Chapter 1**). In zebrafish systemic injections, a first wave of the neutrophil chemoattractants *cxcl8a* and *cxcl18b* is induced in the acute phase response and peaks at 4 hpi[67] (**Chapter 7**). *In situ* detection of *cxcl18b* also showed local induction to *Mm* at the injection point, as early as 3 hpi[66]. Additionally, our transgenic reporter *Tg(cxcl18b:eGFP)* is similarly upregulated in the tissue surrounding the infection, and notably not in infected or uninfected phagocytes (**Chapter 7**). However, systemic injection studies suggest that induction of neutrophil chemoattractants is transient and drops between 8 and 24 hours[67]. From 24 hpi, a second induction wave starts, which is characterised by a continuous increase of *cxcl8a* and *cxcl18b* mediators. In agreement with this, while neutrophils associate poorly to the initial mycobacterial infection, their presence in the granuloma increases over time (**Figure 1D-E**)[175]. Importantly, neutrophils that have engulfed mycobacteria can be more recurrently seen in mature granulomas, although it seems that the increased predisposition of neutrophils to get infected in mature granulomas is due to their "accidental" ingestion via efferocytosis of cell debris, which mostly derives from dying macrophages and can contain viable bacteria (**Figure 1E**)[175,177]. Engulfment of mycobacteria by neutrophils at this stage also leads to a better bacterial containment, since neutrophils can counteract the infection by induction of respiratory stress[175]. A recent study also showed that early after *Mm* infection, when the pathogen essentially resides in macrophages, uninfected neutrophils appear responsive to mycobacterial infection and increase their immune competence by activating a nitrosative stress response. This indicates that neutrophils do not exert exclusively a passive scavenging function within the granuloma, but that they possess (direct or indirect) mechanisms of mycobacterial sensing that contribute to their priming against the infection[179].

Concluding, the involvement of neutrophils increases (both quantitatively and qualitatively) with the increase of the inflammatory nature of the granulomatous lesion. Interestingly, the augmented competence and presence of neutrophils in the granuloma recapitulates the progressively increased expression of the neutrophil chemoattractant *cxcl18b* and c*xcl8a* (**Figure 1D-E**). It is possible that these molecules not only participate in the neutrophil recruitment to the granuloma, but they might be important also to activate specific antibacterial neutrophil responses. CXCL8 and other mammalian neutrophil chemokines are able to induce neutrophil degranulation[180,181], netosis[182] (a particular kind of neutrophil death that leads to release of traps composed of decondensed chromatine) and participate in the activation of the neutrophil respiratory burst[183,184] (production of reactive oxygen and nitrogen species) *in vitro*. The zebrafish model has already contributed relevantly to elucidate all these aspects of neutrophil biology upon bacterial and

inflammatory insults[175,178,179,185,186]. Therefore, further use of the zebrafish model may help to elucidate the mechanistic implication of chemokines into orchestrating not only neutrophil motility, but also their microbicidal/inflammatory function in TB and other inflammatory/infectious diseases[187].

Summarising conclusions

In summary, the work discussed in this thesis has contributed to elucidate novel mechanisms by which mycobacterial infection can benefit from chemotactic cues to initiate bacterial-beneficial programmes and to facilitate persistence of the infection. We have shown that Cxcr3.2 signalling is involved in the granuloma formation and can additionally support infection dissemination and dampen the basal microbicidal capability of immune cells. In contrast, the atypical Cxcr3.3 receptor seems to antagonise the pro-granuloma programme and exerts therefore a host protective function. We have additionally found that Cxcr4b-dependent signalling can affect the activation of the pro-granuloma angiogenesis, leading to a better infection control. Finally, we have characterised Cxcl18b and show that this novel neutrophilic cue is locally induced during the formation of granulomas.

We believe that our work has helped to shed light on the fact that chemokine signals occupy a very central position in the control of immunity. These signals, which are mostly regarded as a class of cytokines dedicated to cell migration, exert in fact extremely diversified functions, which include control of gene transcription, cell-autonomous immune functions and inflammation. The chemokine network displays an intricate texture, composed of receptors, their ligand partners and receptors that have evolved to act as ligand scavengers. Despite responding to general rules of signalling architecture, the affinity of some receptors to one specific ligand or more ligands is strikingly diversified. Additionally, the preferential activation of specific pathways of the downstream machinery can be also a prerogative of each chemokine receptor. Therefore, the application of the zebrafish model, which can be used for intravital imaging, has been crucial to obtain new insight on these highly dynamic signalling mediators and to comprehend new functions that the chemokine axes play in immunity.

REFERENCES

1 Stinear TP, Seemann T, Harrison PF, Jenkin GA, Davies JK, Johnson PD, Abdellah Z, Arrowsmith C, Chillingworth T, Churcher C, Clarke K, Cronin A, Davis P, Goodhead I, Holroyd N, Jagels K, Lord A, Moule S, Mungall K, Norbertczak H, Quail MA, Rabbinowitsch E, Walker D, White B, Whitehead S, Small PL, Brosch R, Ramakrishnan L, Fischbach MA, Parkhill J, Cole ST. Insights from the complete genome sequence of Mycobacterium marinum on the evolution of Mycobacterium tuberculosis. Genome Res. 2008 May;18(5):729-41.
2 Gagneux S. Host-pathogen coevolution in human tuberculosis. Philos Trans R Soc Lond B Biol Sci. 2012 Mar 19;367(1590):850-9.
3 Wirth T, Hildebrand F, Allix-Béguec C, Wölbeling F, Kubica T, Kremer K, van Soolingen D, Rüsch-Gerdes S, Locht C, Brisse S, Meyer A, Supply P, Niemann S. Origin, spread and demography of the Mycobacterium tuberculosis complex. PLoS Pathog. 2008 Sep 19;4(9):e1000160.
4 Comas I, Coscolla M, Luo T, Borrell S, Holt KE, Kato-Maeda M, Parkhill J, Malla B, Berg S, Thwaites G, Yeboah-Manu D, Bothamley G, Mei J, Wei L, Bentley S, Harris SR, Niemann S, Diel R, Aseffa A, Gao Q, Young D, Gagneux S. Out-of-Africa migration and Neolithic coexpansion of Mycobacterium tuberculosis with modern humans. Nat Genet. 2013 Oct;45(10):1176-82.
5 Byrne AL, Marais BJ, Mitnick CD, Lecca L, Marks GB. Tuberculosis and chronic respiratory disease: a systematic review. Int J Infect Dis. 2015 Mar;32:138-46.
6 Bartzatt R. Tuberculosis infections of the central nervous system. Cent Nerv Syst Agents Med Chem. 2011 Dec 1;11(4):321-7.

7 Schoeman JF, Donald PR. Tuberculous meningitis. Handb Clin Neurol. 2013;112:1135-8.
8 Shakarchi FI. Ocular tuberculosis: current perspectives. Clin Ophthalmol. 2015 Nov 26;9:2223-7.
9 Thimmappa D, Mallikarjuna MN, Vijayakumar A. Breast Tuberculosis. Indian J Surg. 2015 Dec;77(Suppl 3):1378-84
10 Hickey AJ, Gounder L, Moosa MY, Drain PK. A systematic review of hepatic tuberculosis with considerations in human immunodeficiency virus co-infection. BMC Infect Dis. 2015 May 6;15:209.
11 Daher Ede F, da Silva GB Jr, Barros EJ. Renal tuberculosis in the modern era. Am J Trop Med Hyg. 2013 Jan;88(1):54-64.
12 Debi U, Ravisankar V, Prasad KK, Sinha SK, Sharma AK. Abdominal tuberculosis of the gastrointestinal tract: revisited. World J Gastroenterol. 2014 Oct 28;20(40):14831-40.
13 Zajaczkowski T. Genitourinary tuberculosis: historical and basic science review: past and present. Cent European J Urol. 2012;65(4):182-7.
14 Singal A, Sonthalia S. Cutaneous tuberculosis in children: the Indian perspective. Indian J Dermatol Venereol Leprol. 2010 Sep-Oct;76(5):494-503.
15 Murray MR, Schroeder GD, Hsu WK. Granulomatous Vertebral Osteomyelitis: An Update. J Am Acad Orthop Surg. 2015 Sep;23(9):529-38.
16 Handa U, Mundi I, Mohan S. Nodal tuberculosis revisited: a review. J Infect Dev Ctries. 2012 Jan 12;6(1):6-12.
17 Guirado E, Schlesinger LS. Modeling the Mycobacterium tuberculosis Granuloma - the Critical Battlefield in Host Immunity and Disease. Front Immunol. 2013 Apr 22;4:98.
18 Bercovier H, Vincent V. Mycobacterial infections in domestic and wild animals due to Mycobacterium marinum, M. fortuitum, M. chelonae, M. porcinum, M. farcinogenes, M. smegmatis, M. scrofulaceum, M. xenopi, M. kansasii, M. simiae and M. genavense. Rev Sci Tech. 2001 Apr;20(1):265-90.
19 Talaat AM, Reimschuessel R, Wasserman SS, Trucksis M. Goldfish, Carassius auratus, a novel animal model for the study of Mycobacterium marinum pathogenesis. Infect Immun. 1998 Jun;66(6):2938-42.
20 Swaim LE, Connolly LE, Volkman HE, Humbert O, Born DE, Ramakrishnan L. Mycobacterium marinum infection of adult zebrafish causes caseating granulomatous tuberculosis and is moderated by adaptive immunity. Infect Immun. 2006 Nov;74(11):6108-17.
21 Broussard GW, Ennis DG. Mycobacterium marinum produces long-term chronic infections in medaka: a new animal model for studying human tuberculosis. Comp Biochem Physiol C Toxicol Pharmacol. 2007 Feb;145(1):45-54.
22 Davis JM, Clay H, Lewis JL, Ghori N, Herbomel P, Ramakrishnan L. Real-time visualization of mycobacterium-macrophage interactions leading to initiation of granuloma formation in zebrafish embryos. Immunity. 2002 Dec;17(6):693-702.
23 Haridy M, Tachikawa Y, Yoshida S, Tsuyuguchi K, Tomita M, Maeda S, Wada T, Ibi K, Sakai H, Yanai T. Mycobacterium marinum infection in Japanese forest green tree frogs (Rhacophorus arboreus). J Comp Pathol. 2014 Aug-Oct;151(2-3):277-89.
24 Ramakrishnan L, Valdivia RH, McKerrow JH, Falkow S. Mycobacterium marinum causes both long-term subclinical infection and acute disease in the leopard frog (Rana pipiens). Infect Immun. 1997 Feb;65(2):767-73.
25 Kennedy GM, Morisaki JH, Champion PA. Conserved mechanisms of Mycobacterium marinum pathogenesis within the environmental amoeba Acanthamoeba castellanii. Appl Environ Microbiol. 2012 Mar;78(6):2049-52.
26 Bouley DM, Ghori N, Mercer KL, Falkow S, Ramakrishnan L. Dynamic nature of host-pathogen interactions in Mycobacterium marinum granulomas. Infect Immun. 2001 Dec;69(12):7820-31.
27 McLain EH. Case study: mariner's TB. AAOHN J. 1989 Aug;37(8):329-32.
28 Haenen OL, Evans JJ, Berthe F. Bacterial infections from aquatic species: potential for and prevention of contact zoonoses. Rev Sci Tech. 2013 Aug;32(2):497-507.
29 Meijer AH. Protection and pathology in TB: learning from the zebrafish model. Semin Immunopathol. 2016 Mar;38(2):261-73.
30 van Leeuwen LM, van der Sar AM, Bitter W. Animal models of tuberculosis: zebrafish. Cold Spring Harb Perspect Med. 2014 Nov 20;5(3):a018580.
31 Pagán AJ, Ramakrishnan L. Immunity and Immunopathology in the Tuberculous Granuloma. Cold Spring Harb Perspect Med. 2014 Nov 6;5(9).
32 Cronan MR, Tobin DM. Fit for consumption: zebrafish as a model for tuberculosis. Dis Model Mech. 2014 Jul;7(7):777-84.
33 Travis WD, Travis LB, Roberts GD, Su DW, Weiland LW. The histopathologic spectrum in Mycobacterium marinum infection. Arch Pathol Lab Med. 1985 Dec;109(12):1109-13.
34 Solomon JM, Leung GS, Isberg RR. Intracellular replication of Mycobacterium marinum within Dictyostelium discoideum: efficient replication in the absence of host coronin. Infect Immun. 2003 Jun;71(6):3578-86.
35 Hagedorn M, Rohde KH, Russell DG, Soldati T. Infection by tubercular mycobacteria is spread by nonlytic ejection from their amoeba hosts. Science. 2009 Mar 27;323(5922):1729-33.

36 Stamm LM, Morisaki JH, Gao LY, Jeng RL, McDonald KL, Roth R, Takeshita S,Heuser J, Welch MD, Brown EJ. Mycobacterium marinum escapes from phagosomes and is propelled by actin-based motility. J Exp Med. 2003 Nov 3;198(9):1361-8.
37 McDonough KA, Kress Y, Bloom BR. Pathogenesis of tuberculosis: interaction of Mycobacterium tuberculosis with macrophages. Infect Immun. 1993 Jul;61(7):2763-73.
38 Myrvik QN, Leake ES, Wright MJ. Disruption of phagosomal membranes of normal alveolar macrophages by the H37Rv strain of Mycobacterium tuberculosis. A correlate of virulence. Am Rev Respir Dis. 1984 Feb;129(2):322-8.
39 van der Wel N, Hava D, Houben D, Fluitsma D, van Zon M, Pierson J, Brenner M, Peters PJ. M. tuberculosis and M. leprae translocate from the phagolysosome to the cytosol in myeloid cells. Cell. 2007 Jun 29;129(7):1287-98.
40 Stamm LM, Pak MA, Morisaki JH, Snapper SB, Rottner K, Lommel S, Brown EJ. Role of the WASP family proteins for Mycobacterium marinum actin tail formation. Proc Natl Acad Sci U S A. 2005 Oct 11;102(41):14837-42.
41 Oehlers SH, Cronan MR, Scott NR, Thomas MI, Okuda KS, Walton EM, Beerman RW, Crosier PS, Tobin DM. Interception of host angiogenic signalling limits mycobacterial growth. Nature. 2015 Jan 29;517(7536):612-5.
42 Tobin DM, Roca FJ, Oh SF, McFarland R, Vickery TW, Ray JP, Ko DC, Zou Y, Bang ND, Chau TT, Vary JC, Hawn TR, Dunstan SJ, Farrar JJ, Thwaites GE, King MC, Serhan CN, Ramakrishnan L. Host genotype-specific therapies can optimize the inflammatory response to mycobacterial infections. Cell. 2012 Feb 3;148(3):434-46.
43 Tsai MC, Chakravarty S, Zhu G, Xu J, Tanaka K, Koch C, Tufariello J, Flynn J, Chan J. Characterization of the tuberculous granuloma in murine and human lungs: cellular composition and relative tissue oxygen tension. Cell Microbiol. 2006 Feb;8(2):218-32.
44 Via LE, Lin PL, Ray SM, Carrillo J, Allen SS, Eum SY, Taylor K, Klein E, Manjunatha U, Gonzales J, Lee EG, Park SK, Raleigh JA, Cho SN, McMurray DN, Flynn JL, Barry CE 3rd. Tuberculous granulomas are hypoxic in guinea pigs, rabbits, and nonhuman primates. Infect Immun. 2008 Jun;76(6):2333-40.
45 Flynn JL, Gideon HP, Mattila JT, Lin PL. Immunology studies in non-human primate models of tuberculosis. Immunol Rev. 2015 Mar;264(1):60-73.
46 Scanga CA, Flynn JL. Modeling tuberculosis in nonhuman primates. Cold Spring Harb Perspect Med. 2014 Sep 11;4(12):a018564.
47 Parikka M, Hammarén MM, Harjula SK, Halfpenny NJ, Oksanen KE, Lahtinen MJ, Pajula ET, Iivanainen A, Pesu M, Rämet M. Mycobacterium marinum causes a latent infection that can be reactivated by gamma irradiation in adult zebrafish. PLoS Pathog. 2012 Sep;8(9):e1002944.
48 Stamm LM, Brown EJ. Mycobacterium marinum: the generalization and specialization of a pathogenic mycobacterium. Microbes Infect. 2004 Dec;6(15):1418-28.
49 Gutierrez MC, Brisse S, Brosch R, Fabre M, Omaïs B, Marmiesse M, Supply P, Vincent V. Ancient origin and gene mosaicism of the progenitor of Mycobacterium tuberculosis. PLoS Pathog. 2005 Sep;1(1):e5.
50 Kinsella RJ, Fitzpatrick DA, Creevey CJ, McInerney JO. Fatty acid biosynthesis in Mycobacterium tuberculosis: lateral gene transfer, adaptive evolution, and gene duplication. Proc Natl Acad Sci U S A. 2003 Sep 2;100(18):10320-5.
51 Rosas-Magallanes V, Deschavanne P, Quintana-Murci L, Brosch R, Gicquel B, Neyrolles O. Horizontal transfer of a virulence operon to the ancestor of Mycobacterium tuberculosis. Mol Biol Evol. 2006 Jun;23(6):1129-35.
52 Becq J, Gutierrez MC, Rosas-Magallanes V, Rauzier J, Gicquel B, Neyrolles O, Deschavanne P. Contribution of horizontally acquired genomic islands to the evolution of the tubercle bacilli. Mol Biol Evol. 2007 Aug;24(8):1861-71.
53 Ramakrishnan L, Federspiel NA, Falkow S. Granuloma-specific expression of Mycobacterium virulence proteins from the glycine-rich PE-PGRS family. Science. 2000 May 26;288(5470):1436-9.
54 Tobin DM, Ramakrishnan L. Comparative pathogenesis of Mycobacterium marinum and Mycobacterium tuberculosis. Cell Microbiol. 2008 May;10(5):1027-39.
55 Chaptini C, Marshman G. Leprosy: a review on elimination, reducing the disease burden, and future research. Lepr Rev. 2015 Dec;86(4):307-15.
56 Biswas SK. Cultivation of Mycobacterium leprae in artificial culture medium. Indian J Med Sci. 1989 Jan;43(1):5-10.
57 Levy L, Ji B. The mouse foot-pad technique for cultivation of Mycobacterium leprae. Lepr Rev. 2006 Mar;77(1):5-24. Review. Erratum in: Lepr Rev. 2006 Jun;77(2):170
58 Singh S, Eldin C, Kowalczewska M, Raoult D. Axenic culture of fastidious and intracellular bacteria. Trends Microbiol. 2013 Feb;21(2):92-9.
59 Avci P, Sadasivam M, Gupta A, De Melo WC, Huang YY, Yin R, Chandran R, Kumar R, Otufowora A, Nyame T, Hamblin MR. Animal models of skin disease for drug discovery. Expert Opin Drug Discov. 2013

Mar;8(3):331-55.
60 Balamayooran G, Pena M, Sharma R, Truman RW. The armadillo as an animal model and reservoir host for Mycobacterium leprae. Clin Dermatol. 2015 Jan-Feb;33(1):108-15.
61 Adams LB, Pena MT, Sharma R, Hagge DA, Schurr E, Truman RW. Insights from animal models on the immunogenetics of leprosy: a review. Mem Inst Oswaldo Cruz. 2012 Dec;107 Suppl 1:197-208.
62 Truman R, Fine PE. 'Environmental' sources of Mycobacterium leprae: issues and evidence. Lepr Rev. 2010 Jun;81(2):89-95.
63 Couret M. The behavior of *Bacillus leprae* in cold-blooded animals. J Exp Med. 1911 May 1;13(5):576-89.
64 Rhoades ER, Cooper AM, Orme IM. Chemokine response in mice infected with Mycobacterium tuberculosis. Infect Immun. 1995 Oct;63(10):3871-7.
65 van der Vaart M, van Soest JJ, Spaink HP, Meijer AH. Functional analysis of a zebrafish myd88 mutant identifies key transcriptional components of the innate immune system. Dis Model Mech. 2013 May;6(3):841-54.
66 Cui C. Chemokine signaling in innate immunity of zebrafish embryos. Doctoral Thesis, Leiden University. 2012 Dec 20.
67 Benard EA. Key innate immune components controlling intracellular infection. Doctoral Thesis, Leiden University. 2014 Sep 25.
68 Cambier CJ, Takaki KK, Larson RP, Hernandez RE, Tobin DM, Urdahl KB, Cosma CL, Ramakrishnan L. Mycobacteria manipulate macrophage recruitment through coordinated use of membrane lipids. Nature. 2014 Jan 9;505(7482):218-22.
69 Sadek MI, Sada E, Toossi Z, Schwander SK, Rich EA. Chemokines induced by infection of mononuclear phagocytes with mycobacteria and present in lung alveoli during active pulmonary tuberculosis. Am J Respir Cell Mol Biol. 1998 Sep;19(3):513-21.
70 Saukkonen JJ, Bazydlo B, Thomas M, Strieter RM, Keane J, Kornfeld H. Beta-chemokines are induced by Mycobacterium tuberculosis and inhibit its growth. Infect Immun. 2002 Apr;70(4):1684-93.
71 Peters W, Scott HM, Chambers HF, Flynn JL, Charo IF, Ernst JD. Chemokine receptor 2 serves an early and essential role in resistance to Mycobacterium tuberculosis. Proc Natl Acad Sci U S A. 2001 Jul 3;98(14):7958-63.
72 Lin Y, Gong J, Zhang M, Xue W, Barnes PF. Production of monocyte chemoattractant protein 1 in tuberculosis patients. Infect Immun. 1998 May;66(5):2319-22.
73 Scott HM, Flynn JL. Mycobacterium tuberculosis in chemokine receptor 2-deficient mice: influence of dose on disease progression. Infect Immun. 2002 Nov;70(11):5946-54.
74Hingley-Wilson SM, Connell D, Pollock K, Hsu T, Tchilian E, Sykes A, Grass L, Potiphar L, Bremang S, Kon OM, Jacobs WR Jr, Lalvani A. ESX1-dependent fractalkine mediates chemotaxis and Mycobacterium tuberculosis infection in humans. Tuberculosis (Edinb). 2014 May;94(3):262-70.
75 Guirado E, Schlesinger LS, Kaplan G. Macrophages in tuberculosis: friend or foe. Semin Immunopathol. 2013 Sep;35(5):563-83.
76 Indrigo J, Hunter RL Jr, Actor JK. Influence of trehalose 6,6'-dimycolate (TDM) during mycobacterial infection of bone marrow macrophages. Microbiology. 2002 Jul;148(Pt 7):1991-8.
77 Clay H, Davis JM, Beery D, Huttenlocher A, Lyons SE, Ramakrishnan L. Dichotomous role of the macrophage in early Mycobacterium marinum infection of the zebrafish. Cell Host Microbe. 2007 Jul 12;2(1):29-39.
78 Gordon RE, Smith MM. Rapidly growing, acid fast bacteria. I. Species'descriptions of Mycobacterium phlei Lehmann and Neumann and Mycobacterium smegmatis (Trevisan) Lehmann and Neumann. J Bacteriol. 1953 Jul;66(1):41-8.
79 Reyrat JM, Kahn D. Mycobacterium smegmatis: an absurd model for tuberculosis? Trends Microbiol. 2001 Oct;9(10):472-4.
80 Gagneux S. Host-pathogen coevolution in human tuberculosis. Philos Trans R Soc Lond B Biol Sci. 2012 Mar 19;367(1590):850-9.
81 Brites D, Gagneux S. Co-evolution of Mycobacterium tuberculosis and Homo sapiens. Immunol Rev. 2015 Mar;264(1):6-24.
82 Bañuls AL, Sanou A, Anh NT, Godreuil S. Mycobacterium tuberculosis: ecology and evolution of a human bacterium. J Med Microbiol. 2015 Nov;64(11):1261-9.
83 Volkman HE, Pozos TC, Zheng J, Davis JM, Rawls JF, Ramakrishnan L. Tuberculous granuloma induction via interaction of a bacterial secreted protein with host epithelium. Science. 2010 Jan 22;327(5964):466-9.
84 van der Vaart M, Korbee CJ, Lamers GE, Tengeler AC, Hosseini R, Haks MC, Ottenhoff TH, Spaink HP, Meijer AH. The DNA damage-regulated autophagy modulator DRAM1 links mycobacterial recognition via TLR-MYD88 to autophagic defense. Cell Host Microbe. 2014 Jun 11;15(6):753-67.
85 Van Lint P, Libert C. Chemokine and cytokine processing by matrix metalloproteinases and its effect on leukocyte migration and inflammation. J Leukoc Biol. 2007 Dec;82(6):1375-81.
86 Roca FJ, Ramakrishnan L. TNF dually mediates resistance and susceptibility to mycobacteria via mitochondrial reactive oxygen species. Cell. 2013 Apr 25;153(3):521-34.

87 Chakravarty SD, Xu J, Lu B, Gerard C, Flynn J, Chan J. The chemokine receptor CXCR3 attenuates the control of chronic Mycobacterium tuberculosis infection in BALB/c mice. J Immunol. 2007 Feb 1;178(3):1723-35.
88 Tang NL, Fan HP, Chang KC, Ching JK, Kong KP, Yew WW, Kam KM, Leung CC, Tam CM, Blackwell J, Chan CY. Genetic association between a chemokine gene CXCL-10 (IP-10, interferon gamma inducible protein 10) and susceptibility to tuberculosis. Clin Chim Acta. 2009 Aug;406(1-2):98-102.
89 Elkington PT, Green JA, Emerson JE, Lopez-Pascua LD, Boyle JJ, O'Kane CM, Friedland JS. Synergistic up-regulation of epithelial cell matrix metalloproteinase-9 secretion in tuberculosis. Am J Respir Cell Mol Biol. 2007 Oct;37(4):431-7.
90 Price NM, Farrar J, Tran TT, Nguyen TH, Tran TH, Friedland JS. Identification of a matrix-degrading phenotype in human tuberculosis in vitro and in vivo. J Immunol. 2001 Mar 15;166(6):4223-30.
91 Lee K, Chung W, Jung Y, Kim Y, Park J, Sheen S, Park K. CXCR3 ligands as clinical markers for pulmonary tuberculosis. Int J Tuberc Lung Dis. 2015 Feb;19(2):191-9.
92 Lu B, Rutledge BJ, Gu L, Fiorillo J, Lukacs NW, Kunkel SL, North R, Gerard C, Rollins BJ. Abnormalities in monocyte recruitment and cytokine expression in monocyte chemoattractant protein 1-deficient mice. J Exp Med. 1998 Feb 16;187(4):601-8.
93 Kipnis A, Basaraba RJ, Orme IM, Cooper AM. Role of chemokine ligand 2 in the protective response to early murine pulmonary tuberculosis. Immunology. 2003 Aug;109(4):547-51.
94 Flores-Villanueva PO, Ruiz-Morales JA, Song CH, Flores LM, Jo EK, Montaño M, Barnes PF, Selman M, Granados J. A functional promoter polymorphism in monocyte chemoattractant protein-1 is associated with increased susceptibility to pulmonary tuberculosis. J Exp Med. 2005 Dec 19;202(12):1649-58.
95 Jamieson, S.E., E.N. Miller, G.F. Black, C.S. Peacock, H.J. Cordell, J.M.M. Howson, M.-A. Shaw, D. Burgner, W. Xu, Z. Lins-Lainson, et al. 2004. Evidence for a cluster of genes on chromosome 17q11-q21 controlling susceptibility to tuberculosis and leprosy in Brazilians. *Genes Immun.* 5:46–57.
96 Reed MB, Domenech P, Manca C, Su H, Barczak AK, Kreiswirth BN, Kaplan G, Barry CE 3rd. A glycolipid of hypervirulent tuberculosis strains that inhibits the innate immune response. Nature. 2004 Sep 2;431(7004):84-7.
97Colvin RA, Means TK, Diefenbach TJ, Moita LF, Friday RP, Sever S, Campanella GS, Abrazinski T, Manice LA, Moita C, Andrews NW, Wu D, Hacohen N, Luster AD. Synaptotagmin-mediated vesicle fusion regulates cell migration. Nat Immunol. 2010 Jun;11(6):495-502.
98 Settembre C, Fraldi A, Medina DL, Ballabio A. Signals from the lysosome: a control centre for cellular clearance and energy metabolism. Nat Rev Mol Cell Biol. 2013 May;14(5):283-96.
99 Sardiello M, Palmieri M, di Ronza A, Medina DL, Valenza M, Gennarino VA, Di Malta C, Donaudy F, Embrione V, Polishchuk RS, Banfi S, Parenti G, Cattaneo E, Ballabio A. A gene network regulating lysosomal biogenesis and function. Science. 2009 Jul 24;325(5939):473-7.
100 Medina DL, Fraldi A, Bouche V, Annunziata F, Mansueto G, Spampanato C, Puri C,Pignata A, Martina JA, Sardiello M, Palmieri M, Polishchuk R, Puertollano R, Ballabio A. Transcriptional activation of lysosomal exocytosis promotes cellular clearance. Dev Cell. 2011 Sep 13;21(3):421-30.
101 Berg RD, Levitte S, O'Sullivan MP, O'Leary SM, Cambier CJ, Cameron J, Takaki KK, Moens CB, Tobin DM, Keane J, Ramakrishnan L. Lysosomal Disorders Drive Susceptibility to Tuberculosis by Compromising Macrophage Migration. Cell. 2016 Mar 24;165(1):139-52.
102 Song W, Wang F, Savini M, Ake A, di Ronza A, Sardiello M, Segatori L. TFEB regulates lysosomal proteostasis. Hum Mol Genet. 2013 May 15;22(10):1994-2009.
103 Pan J, Sun ZY, Ji C, Ji YM, Yang Y, Yang HL. A case of unusual association of Gaucher's disease with spinal tuberculosis. Int J Rheum Dis. 2013 Jun;16(3):361-3.
104 Pérez-Calvo J, Bernal M, Giraldo P, Torralba MA, Civeira F, Giralt M, Pocovi M. Co-morbidity in Gaucher's disease results of a nationwide enquiry in Spain. Eur J Med Res. 2000 Jun 20;5(6):231-5.
105 Liel Y, Rudich A, Nagauker-Shriker O, Yermiyahu T, Levy R. Monocyte dysfunction in patients with Gaucher disease: evidence for interference of glucocerebroside with superoxide generation. Blood. 1994 May 1;83(9):2646-53.
106 Risch N, Tang H, Katzenstein H, Ekstein J. Geographic distribution of disease mutations in the Ashkenazi Jewish population supports genetic drift over selection. Am J Hum Genet. 2003 Apr;72(4):812-22.
107 Goodman RM, Motulsky AG. Genetic diseases among Ashkenazi Jews. Raven Press, New York. 1979.
108 Rotter JI, Diamond JM. What maintains the frequencies of human genetic diseases? Nature. 1987 Sep 24-30;329(6137):289-90.
109 Withrock IC, Anderson SJ, Jefferson MA, McCormack GR, Mlynarczyka GSA, Nakama A, Lange JK, Berg CA, f, Acharya S, Stock ML, Lind MS, Luna KC, Kondru NC, Manne S, Patel BB, de la Rosa BM, Huang KP, Sharma S, Hu HZ, Kanuri SH, Carlson SA. Genetic diseases conferring resistance to infectious diseases. Genes Ds. 2015 Sep;2(3):247-54.
110 Myrianthopoulos NC, Aronson SM. Population dynamics of Tay-Sachs disease. I. Reproductive fitness and selection. Am J Hum Genet. 1966 Jul;18(4):313-27.

111 Myrianthopoulos NC, Melnick M. Tay-Sachs disease: a genetic-historical view of selective advantage. Prog Clin Biol Res. 1977;18:95-106.
112 Petersen GM, Rotter JI, Cantor RM, Field LL, Greenwald S, Lim JS, Roy C, Schoenfeld V, Lowden JA, Kaback MM. The Tay-Sachs disease gene in North American Jewish populations: geographic variations and origin. Am J Hum Genet. 1983 Nov;35(6):1258-69.
113 Spyropoulos B, Moens PB, Davidson J, Lowden JA. Heterozygote advantage in Tay-Sachs carriers? Am J Hum Genet. 1981 May;33(3):375-80.
114 Fraikor AL. Tay-Sachs disease: genetic drift among the Ashkenazim Jews. Soc Biol. 1977 Summer;24(2):117-34.
115 Angastiniotis M, Modell B, Englezos P, Boulyjenkov V. Prevention and control of haemoglobinopathies. Bull World Health Organ. 1995;73(3):375-86.
116 Kaback MM, Desnick RJ. Hexosaminidase A Deficiency. GeneReviews. 1999 Mar 11.
117 Fernandes Filho JA, Shapiro BE. Tay-Sachs disease. Arch Neurol. 2004 Sep;61(9):1466-8.
118 Schultz ML, Tecedor L, Chang M, Davidson BL. Clarifying lysosomal storage diseases. Trends Neurosci. 2011 Aug;34(8):401-10.
119 Fraldi A, Klein AD, Medina DL, Settembre C. Brain Disorders Due to Lysomal Dysfunction. Annu Rev Neurosci. 2016 Apr 18.
120 Hawn TR, Matheson AI, Maley SN, Vandal O. Host-directed therapeutics for tuberculosis: can we harness the host? Microbiol Mol Biol Rev. 2013 Dec;77(4):608-27.
121 Lister JA, Lane BM, Nguyen A, Lunney K. Embryonic expression of zebrafish MiT family genes tfe3b, tfeb, and tfec. Dev Dyn. 2011 Nov;240(11):2529-38.
122 Shen K, Sidik H, Talbot WS. The Rag-Ragulator Complex Regulates Lysosome Function and Phagocytic Flux in Microglia. Cell Rep. 2016 Jan 26;14(3):547-59.
123 Martina JA, Diab HI, Li H, Puertollano R. Novel roles for the MiTF/TFE family of transcription factors in organelle biogenesis, nutrient sensing, and energy homeostasis. Cell Mol Life Sci. 2014 Jul;71(13):2483-97.
124 Rehli M, Lichanska A, Cassady AI, Ostrowski MC, Hume DA. TFEC is a macrophage-restricted member of the microphthalmia-TFE subfamily of basic helix-loop-helix leucine zipper transcription factors. J Immunol. 1999 Feb 1;162(3):1559-65.
125 Rehli M, Sulzbacher S, Pape S, Ravasi T, Wells CA, Heinz S, Söllner L, El Chartouni C, Krause SW, Steingrimsson E, Hume DA, Andreesen R. Transcription factor Tfec contributes to the IL-4-inducible expression of a small group of genes in mouse macrophages including the granulocyte colony-stimulating factor receptor. J Immunol. 2005 Jun 1;174(11):7111-22.
126 Zhao GQ, Zhao Q, Zhou X, Mattei MG, de Crombrugghe B. TFEC, a basic helix-loop-helix protein, forms heterodimers with TFE3 and inhibits TFE3-dependent transcription activation. Mol Cell Biol. 1993 Aug;13(8):4505-12.
127 Beckmann H, Su LK, Kadesch T. TFE3: a helix-loop-helix protein that activates transcription through the immunoglobulin enhancer muE3 motif. Genes Dev. 1990 Feb;4(2):167-79.
128 Mantovani A, Bonecchi R, Locati M. Tuning inflammation and immunity by chemokine sequestration: decoys and more. Nat Rev Immunol. 2006 Dec;6(12):907-18.
129 Fra AM, Locati M, Otero K, Sironi M, Signorelli P, Massardi ML, Gobbi M, Vecchi A, Sozzani S, Mantovani A. Cutting edge: scavenging of inflammatory CC chemokines by the promiscuous putatively silent chemokine receptor D6. J Immunol.2003 Mar 1;170(5):2279-82.
130 Nibbs R, Graham G, Rot A. Chemokines on the move: control by the chemokine "interceptors" Duffy blood group antigen and D6. Semin Immunol. 2003 Oct;15(5):287-94.
131 Pruenster M, Mudde L, Bombosi P, Dimitrova S, Zsak M, Middleton J, Richmond A, Graham GJ, Segerer S, Nibbs RJ, Rot A. The Duffy antigen receptor for chemokines transports chemokines and supports their promigratory activity. Nat Immunol. 2009 Jan;10(1):101-8.
132 Sánchez-Martín L, Sánchez-Mateos P, Cabañas C. CXCR7 impact on CXCL12 biology and disease. Trends Mol Med. 2013 Jan;19(1):12-22.
133 Abe P, Mueller W, Schütz D, MacKay F, Thelen M, Zhang P, Stumm R. CXCR7 prevents excessive CXCL12-mediated downregulation of CXCR4 in migrating cortical interneurons. Development. 2014 May;141(9):1857-63.
134 Jamieson T, Cook DN, Nibbs RJ, Rot A, Nixon C, McLean P, Alcami A, Lira SA,Wiekowski M, Graham GJ. The chemokine receptor D6 limits the inflammatory response in vivo. Nat Immunol. 2005 Apr;6(4):403-11.
135 Martinez de la Torre Y, Locati M, Buracchi C, Dupor J, Cook DN, Bonecchi R, Nebuloni M, Rukavina D, Vago L, Vecchi A, Lira SA, Mantovani A. Increased inflammation in mice deficient for the chemokine decoy receptor D6. Eur J Immunol. 2005 May;35(5):1342-6.
136 Nibbs RJ, Gilchrist DS, King V, Ferra A, Forrow S, Hunter KD, Graham GJ. The atypical chemokine receptor D6 suppresses the development of chemically induced skin tumors. J Clin Invest. 2007 Jul;117(7):1884-92.

137 Berres ML, Trautwein C, Zaldivar MM, Schmitz P, Pauels K, Lira SA, Tacke F, Wasmuth HE. The chemokine scavenging receptor D6 limits acute toxic liver injury in vivo. Biol Chem. 2009 Oct;390(10):1039-45.
138 Di Liberto D, Locati M, Caccamo N, Vecchi A, Meraviglia S, Salerno A, Sireci G, Nebuloni M, Caceres N, Cardona PJ, Dieli F, Mantovani A. Role of the chemokine decoy receptor D6 in balancing inflammation, immune activation, and antimicrobial resistance in Mycobacterium tuberculosis infection. J Exp Med. 2008 Sep 1;205(9):2075-84.
139 Dawson TC, Lentsch AB, Wang Z, Cowhig JE, Rot A, Maeda N, Peiper SC. Exaggerated response to endotoxin in mice lacking the Duffy antigen/receptor for chemokines (DARC). Blood. 2000 Sep 1;96(5):1681-4.
140 Reutershan J, Harry B, Chang D, Bagby GJ, Ley K. DARC on RBC limits lung injury by balancing compartmental distribution of CXC chemokines. Eur J Immunol. 2009 Jun;39(6):1597-607.
141 Wan W, Liu Q, Lionakis MS, Marino AP, Anderson SA, Swamydas M, Murphy PM. Atypical chemokine receptor 1 deficiency reduces atherogenesis in ApoE-knockout mice. Cardiovasc Res. 2015 Jun 1;106(3):478-87.
142 Minten C, Alt C, Gentner M, Frei E, Deutsch U, Lyck R, Schaeren-Wiemers N, Rot A, Engelhardt B. DARC shuttles inflammatory chemokines across the blood-brain barrier during autoimmune central nervous system inflammation. Brain. 2014 May;137(Pt 5):1454-69.
143 Novitzky-Basso I, Rot A. Duffy antigen receptor for chemokines and its involvement in patterning and control of inflammatory chemokines. Front Immunol. 2012 Aug 17;3:266.
144 Ulvmar MH, Hub E, Rot A. Atypical chemokine receptors. Exp Cell Res. 2011 Mar 10;317(5):556-68.
145 Naumann U, Cameroni E, Pruenster M, Mahabaleshwar H, Raz E, Zerwes HG, Rot A, Thelen M. CXCR7 functions as a scavenger for CXCL12 and CXCL11. PLoS One. 2010 Feb 11;5(2):e9175.
146 Camargos Costa D, Pereira de Assis GM, de Souza Silva FA, Araújo FC, de Souza Junior JC, Braga Hirano ZM, Satiko Kano F, Nóbrega de Sousa T, Carvalho LH, Ferreira Alves de Brito C. Plasmodium simium, a Plasmodium vivax-related malaria parasite: genetic variability of Duffy binding protein II and the Duffy antigen/receptor for chemokines. PLoS One. 2015 Jun 24;10(6):e0131339.
147 Huang BH, Liao PC. Tracing evolutionary relicts of positive selection on eight malaria-related immune genes in mammals. Innate Immun. 2015 Jul;21(5):463-76.
148 Hodgson JA, Pickrell JK, Pearson LN, Quillen EE, Prista A, Rocha J, Soodyall H, Shriver MD, Perry GH. Natural selection for the Duffy-null allele in the recently admixed people of Madagascar. Proc Biol Sci. 2014 Aug 22;281(1789):20140930.
149 Dalle Nogare D, Somers K, Rao S, Matsuda M, Reichman-Fried M, Raz E, Chitnis AB. Leading and trailing cells cooperate in collective migration of the zebrafish posterior lateral line primordium. Development. 2014 Aug;141(16):3188-96.
150 Venkiteswaran G, Lewellis SW, Wang J, Reynolds E, Nicholson C, Knaut H. Generation and dynamics of an endogenous, self-generated signaling gradient across a migrating tissue. Cell. 2013 Oct 24;155(3):674-87.
151 Donà E, Barry JD, Valentin G, Quirin C, Khmelinskii A, Kunze A, Durdu S, Newton LR, Fernandez-Minan A, Huber W, Knop M, Gilmour D. Directional tissue migration through a self-generated chemokine gradient. Nature. 2013 Nov 14;503(7475):285-9.
152 Folkman J. Role of angiogenesis in tumor growth and metastasis. Semin Oncol. 2002 Dec;29(6 Suppl 16):15-8.
153 Dartois V. The path of anti-tuberculosis drugs: from blood to lesions to mycobacterial cells. Nat Rev Microbiol. 2014 Mar;12(3):159-67.
154 Alatas F, Alatas O, Metintas M, Ozarslan A, Erginel S, Yildirim H. Vascular endothelial growth factor levels in active pulmonary tuberculosis. Chest. 2004 Jun;125(6):2156-9.
155 Matsuyama W, Hashiguchi T, Matsumuro K, Iwami F, Hirotsu Y, Kawabata M, Arimura K, Osame M. Increased serum level of vascular endothelial growth factor in pulmonary tuberculosis. Am J Respir Crit Care Med. 2000 Sep;162(3 Pt 1):1120-2.
156 Abe Y, Nakamura M, Oshika Y, Hatanaka H, Tokunaga T, Ohkubo Y, Hashizume T, Suzuki K, Fujino T. Serum levels of vascular endothelial growth factor and cavity formation in active pulmonary tuberculosis. Respiration. 2001;68(5):496-500.
157 Datta M, Via LE, Kamoun WS, Liu C, Chen W, Seano G, Weiner DM, Schimel D, England K, Martin JD, Gao X, Xu L, Barry CE 3rd, Jain RK. Anti-vascular endothelial growth factor treatment normalizes tuberculosis granuloma vasculature and improves small molecule delivery. Proc Natl Acad Sci U S A. 2015 Feb 10;112(6):1827-32.
158 Tulotta C, Stefanescu C, Beletkaia E, Bussmann J, Tarbashevich K, Schmidt T, Snaar-Jagalska BE. Inhibition of signaling between human CXCR4 and zebrafish ligands by the small molecule IT1t impairs the formation of triple-negative breast cancer early metastases in a zebrafish xenograft model. Dis Model Mech. 2016 Feb 1;9(2):141-53.
159 Tamplin OJ, Durand EM, Carr LA, Childs SJ, Hagedorn EJ, Li P, Yzaguirre AD, Speck NA, Zon LI. Hematopoietic stem cell arrival triggers dynamic remodeling of the perivascular niche. Cell. 2015 Jan 15;160(1-2):241-52.

160 Nguyen-Chi M, Laplace-Builhe B, Travnickova J, Luz-Crawford P, Tejedor G, Phan QT, Duroux-Richard I, Levraud JP, Kissa K, Lutfalla G, Jorgensen C, Djouad F. Identification of polarized macrophage subsets in zebrafish. Elife. 2015 Jul 8;4:e07288.
161 Liang Z, Brooks J, Willard M, Liang K, Yoon Y, Kang S, Shim H. CXCR4/CXCL12 axis promotes VEGF-mediated tumor angiogenesis through Akt signaling pathway. Biochem Biophys Res Commun. 2007 Aug 3;359(3):716-22.
162 Fantin A, Vieira JM, Gestri G, Denti L, Schwarz Q, Prykhozhij S, Peri F, Wilson SW, Ruhrberg C. Tissue macrophages act as cellular chaperones for vascular anastomosis downstream of VEGF-mediated endothelial tip cell induction. Blood. 2010 Aug 5;116(5):829-40.
163 Xu C, Hasan SS, Schmidt I, Rocha SF, Pitulescu ME, Bussmann J, Meyen D, Raz E,Adams RH, Siekmann AF. Arteries are formed by vein-derived endothelial tip cells. Nat Commun. 2014 Dec 15;5:5758.
164 Zielonka TM, Demkow U, Michalowska-Mitczuk D, Filewska M, Bialas B, Zycinska K, Obrowski MH, Kus J, Skopinska-Rozewska E. Angiogenic activity of sera from pulmonary tuberculosis patients in relation to IL-12p40 and TNFα serum levels. Lung. 2011 Aug;189(4):351-7.
165 Jackson JR, Seed MP, Kircher CH, Willoughby DA, Winkler JD. The codependence of angiogenesis and chronic inflammation. FASEB J. 1997 May;11(6):457-65.
166 Voronov E, Shouval DS, Krelin Y, Cagnano E, Benharroch D, Iwakura Y, Dinarello CA, Apte RN. IL-1 is required for tumor invasiveness and angiogenesis. Proc Natl Acad Sci U S A. 2003 Mar 4;100(5):2645-50
167 Koch AE, Polverini PJ, Kunkel SL, Harlow LA, DiPietro LA, Elner VM, Elner SG, Strieter RM. Interleukin-8 as a macrophage-derived mediator of angiogenesis. Science. 1992 Dec 11;258(5089):1798-801.
168 Krupa A, Fol M, Dziadek BR, Kepka E, Wojciechowska D, Brzostek A, Torzewska A, Dziadek J, Baughman RP, Griffith D, Kurdowska AK. Binding of CXCL8/IL-8 to Mycobacterium tuberculosis Modulates the Innate Immune Response. Mediators Inflamm. 2015;2015:124762.
169 Voronov E, Carmi Y, Apte RN. The role IL-1 in tumor-mediated angiogenesis. Front Physiol. 2014 Mar 28;5:114.
170 Schweighofer B, Testori J, Sturtzel C, Sattler S, Mayer H, Wagner O, Bilban M, Hofer E. The VEGF-induced transcriptional response comprises gene clusters at the crossroad of angiogenesis and inflammation. Thromb Haemost. 2009 Sep;102(3):544-54.
171 Triantafilou M, Lepper PM, Briault CD, Ahmed MA, Dmochowski JM, Schumann C, Triantafilou K. Chemokine receptor 4 (CXCR4) is part of the lipopolysaccharide "sensing apparatus". Eur J Immunol. 2008 Jan;38(1):192-203.
172 Kishore SP, Bungum MK, Platt JL, Brunn GJ. Selective suppression of Toll-like receptor 4 activation by chemokine receptor 4. FEBS Lett. 2005 Jan31;579(3):699-704.
173 Kamba T, McDonald DM. Mechanisms of adverse effects of anti-VEGF therapy for cancer. Br J Cancer. 2007 Jun 18;96(12):1788-95.
174 Alkhatib G, Berger EA. HIV coreceptors: from discovery and designation to new paradigms and promise. Eur J Med Res. 2007 Oct 15;12(9):375-84.
175 Yang CT, Cambier CJ, Davis JM, Hall CJ, Crosier PS, Ramakrishnan L. Neutrophils exert protection in the early tuberculous granuloma by oxidative killing of mycobacteria phagocytosed from infected macrophages. Cell Host Microbe. 2012 Sep 13;12(3):301-12.
176 Colucci-Guyon E, Tinevez JY, Renshaw SA, Herbomel P. Strategies of professional phagocytes in vivo: unlike macrophages, neutrophils engulf only surface-associated microbes. J Cell Sci. 2011 Sep 15;124(Pt 18):3053-9.
177 Hosseini R. The innate immune response against mycobacterial infection: analysis by a combination of light and electron microscopy. Doctoral Thesis, Leiden University. 2015 Oct 10.
178 Deng Q, Harvie EA, Huttenlocher A. Distinct signalling mechanisms mediate neutrophil attraction to bacterial infection and tissue injury. Cell Microbiol. 2012 Apr;14(4):517-28.
179 Elks PM, Brizee S, van der Vaart M, Walmsley SR, van Eeden FJ, Renshaw SA, Meijer AH. Hypoxia inducible factor signaling modulates susceptibility to mycobacterial infection via a nitric oxide dependent mechanism. PLoS Pathog. 2013;9(12):e1003789.
180 Hayashi S, Kurdowska A, Miller EJ, Albright ME, Girten BE, Cohen AB. Synthetic hexa- and heptapeptides that inhibit IL-8 from binding to and activating human blood neutrophils. J Immunol. 1995 Jan 15;154(2):814-24.
181 Barlic J, Andrews JD, Kelvin AA, Bosinger SE, DeVries ME, Xu L, Dobransky T, Feldman RD, Ferguson SS, Kelvin DJ. Regulation of tyrosine kinase activation and granule release through beta-arrestin by CXCRI. Nat Immunol. 2000 Sep;1(3):227-33.
182 Gupta AK, Giaglis S, Hasler P, Hahn S. Efficient neutrophil extracellular trap induction requires mobilization of both intracellular and extracellular calcium pools and is modulated by cyclosporine A. PLoS One. 2014 May 12;9(5):e97088.

183 Jones SA, Wolf M, Qin S, Mackay CR, Baggiolini M. Different functions for the interleukin 8 receptors (IL-8R) of human neutrophil leukocytes: NADPH oxidase and phospholipase D are activated through IL-8R1 but not IL-8R2. Proc Natl Acad Sci U S A. 1996 Jun 25;93(13):6682-6.
184 Stillie R, Farooq SM, Gordon JR, Stadnyk AW. The functional significance behind expressing two IL-8 receptor types on PMN. J Leukoc Biol. 2009 Sep;86(3):529-43.
185 Nguyen-Chi M, Phan QT, Gonzalez C, Dubremetz JF, Levraud JP, Lutfalla G.Transient infection of the zebrafish notochord with E. coli induces chronic inflammation. Dis Model Mech. 2014 Jul;7(7):871-82.
186 Palić D, Andreasen CB, Ostojić J, Tell RM, Roth JA. Zebrafish (Danio rerio) whole kidney assays to measure neutrophil extracellular trap release and degranulation of primary granules. J Immunol Methods. 2007 Jan 30;319(1-2):87-97.
187 Henry KM, Loynes CA, Whyte MK, Renshaw SA. Zebrafish as a model for the study of neutrophil biology. J Leukoc Biol. 2013 Oct;94(4):633-42.

Summary

The main objective of the work enclosed in this thesis has been to analyse the functions exerted by chemokines in shaping the host-pathogen interface at play between the cells of the innate immune system and mycobacterial pathogens. Chemokines are small chemotactic cytokines, which are host signalling molecules that occupy a central position in immunity and inflammation. There is a large body of evidence that several chemokine mediators are activated in response to mycobacterial infections. These chemokines can have host protective functions, but may also contribute to disease pathology, as exemplified by the work in this thesis.

Human tuberculosis (TB) is a global health concern caused by *Mycobacterium tuberculosis*. This human-adapted mycobacterial pathogen has been parasitising the mankind since prehistorical eras, provoking debilitation, illness and death worldwide. In the 21st century and more than 130 years after the discovery of its infectious agent, we are still far from eradicating TB, since it is estimated that about one third of the global population is chronically infected by *M. tuberculosis* and may therefore develop an active disease. A major complication of modern days' TB control is the emergency of drug-resistant strains that do not respond to the conventional therapeutic regimen, which consists of prolonged treatment with a cocktail of antibiotics disrupting different processes essential for bacterial growth, such as cell wall synthesis or DNA and protein synthesis. The problem of multi-drug resistances emphasises the need of novel strategies to counteract the disease. Establishment of *M. tuberculosis* infections is intimately connected with the capability of the pathogen to manipulate the host signalling machinery. Therefore, it is an attractive hypothesis that drugs for TB treatment might be identified that act on the host rather than on the pathogen itself. Identifying the host targets for development of such drugs would not only largely expand the therapeutic opportunities, but also provide a more difficult system for the pathogen to develop new drug resistances.

The chemokine signalling system, by exerting a crucial function in immunity, may be involved in relevant aspects of TB. On one hand this signalling might function in host defence; on the other hand it might also be exploited by mycobacteria, similarly to other immune-related pathways that are subverted by these pathogens. Chemokines act via a class of G-protein coupled receptors, which are currently the most successful drug targets in practice for a number of diseases. Therefore, the chemokine axes may represent easily druggable therapeutic targets that could be used to develop novel host-directed therapies to combat TB.

As we further elaborate on in **Chapter 1** and **Chapter 2**, the zebrafish (*Danio rerio*) has proved to be an excellent animal model to study both the biology of innate immune cells (macrophages and neutrophils) and the molecular and cellular basis of infectious diseases. This is especially true for the embryonic and larval stages of zebrafish, which are optically transparent as well as chemically and genetically tractable. The zebrafish is naturally susceptible to *Mycobacterium marinum*, a bacterium that is closely related to *M. tuberculosis*. The zebrafish-*M. marinum* model is characterised by a disease that faithfully recapitulates the main molecular, cellular and histopathological aspects of human TB. The

striking similarity of fish TB with the human disease is not only interesting from an evolutionary point of view, but also scientifically attractive for the study of TB. This is particularly significant if we consider that *M. tuberculosis* does not fully reproduce the human disease in the murine model and there are severe restrictions to work with this human pathogen. In recent years, it additionally became clear that several human chemotactic signalling axes maintain remarkable molecular and functional conservation in zebrafish, suggesting that their role in limiting or driving susceptibility to mycobacterial infection might have homologies in the two infectious systems. Therefore, the embryonic/larval zebrafish platform represented for us an insightful system to model and challenge mycobacterial disease, and led to the discovery of new virulence mechanisms that involve chemokine signalling.

In **Chapter 3** we found that zebrafish conserves a Cxcr3.2/Cxcl11aa-11af signalling axis that exerts important functions in macrophages, as its orthologous CXCR3/CXCL9-10-11 axis does in mammals. Homozygote *cxcr3.2* mutants displayed deficiency in macrophage recruitment to recombinant Cxcl11aa-11af and to bacterial infections (including *M. marinum),* which promptly induce the Cxcr3.2 ligands. Strikingly, *cxcr3.2* mutation conferred resistance against mycobacterial infection, since this mutation, by attenuating macrophage trafficking, reduced mycobacterial dissemination and delayed the expansion of the so-called granulomas. Granulomas are infectious and inflammatory lesions consisting of immune cells (especially macrophages) that collect the pathogen and the necrotising tissue debris. Tuberculous granulomas are the disease-causing hallmark of mycobacterial infection and represent the natural niche of pathogenic mycobacteria. Within the granuloma, mycobacteria essentially persist intracellularly in the macrophages and extracellularly in the necrotic centre that results from the death of infected macrophages. Therefore, the Cxcr3.2 receptor, by increasing the engagement of macrophages with mycobacteria, represents a pro-granuloma determinant. The small CXCR3 inhibitor NBI74330 could phenocopy the deficient macrophage mobilisation to mycobacteria in zebrafish, therefore suggesting that CXCR3 antagonistic therapy might be used to curtail TB infection.

In **Chapter 4** we further analysed the downstream signalling dependent on Cxcr3.2. Therefore, we sorted macrophages from *cxcr3.2* mutants and we profiled their transcriptome by RNA-sequencing. Intriguingly, we discovered that *cxcr3.2* mutation leads to a lysosome stress signature and to a coordinated upregulation of several lysosomal genes, including acid hydrolases and lysosomal proton pump subunits. To corroborate these results, we demonstrated that this macrophage signature goes together with an increased acidification of bacteria-containing compartments and increased microbicidal activity against mycobacteria *in vivo*. To obtain more mechanistic insight on how lysosome stress is evoked in macrophages by deficient sensing of chemotactic cues, we tracked macrophages with stained lysosomes. Surprisingly, we found that *cxcr3.2* mutation attenuated the recruitment of lysosomes to the leading edge in moving cells. The accumulation of lysosomes at the leading edge of wildtype macrophages is possibly indicating local lysosome exocytosis, which can be triggered by chemokines and is important to provide new membrane to the protruding lamellipodia. Remarkably, we show that macrophages themselves upregulate Cxcl11aa during mycobacterial parasitosis and that active Myd88-mediated immune recognition of the pathogen is essential to Cxcl11aa synthesis. We therefore hypothesise that the existence of this immune recognition/chemokine signalling/lysosome function circuit might benefit the pathogen in

two ways: induction of Cxcr3.2-dependent signalling not only would fuel the granuloma with new macrophages to be infected, it would also generate a more permissive intra-macrophage phenotype by hijacking lysosome function.

In **Chapter 5** we preliminarily characterised the function of Cxcr3.3, another zebrafish orthologue of CXCR3, and we describe the CRISPR/Cas9 genome editing pipeline that we optimised to obtain a *cxcr3.3* mutant. Besides the technical improvements of the CRISPR/Cas9 mutagenesis method in zebrafish that we propose (as further detailed in the chapter), we found that the *cxcr3.3* mutants are more susceptible to mycobacterial infection, which is diametrically opposite to the *cxcr3.2* mutant phenotype. A *cxcr3.2/cxcr3.3* double mutant line will be necessary to shed light on this controversy. However, we found that treatment with the NBI74330 inhibitor, which is predicted to equally antagonise Cxcr3.3 and Cxcr3.2, still attenuated susceptibility to infection and evoked a more *cxcr3.2*-like phenotype. This suggested that Cxcr3.3 requires Cxcr3.2 to exert its function. In support of this hypothesis we discovered that Cxcr3.3 displays significant sequence modification, the most remarkable of which is the replacement of an Arginine residue within the Aspartic acid-Arginine-Tyrosine (DRY) motif, the most conserved motif within functional G-protein coupled receptors. The Arginine residue in the DRY motif is 100% conserved in fully functional human CXCR receptors, as it serves to interact with the heterotrimeric G-proteins and activate the downstream signalling. The DRY motif is instead recurrently modified (or absent) in atypical chemokine receptors that essentially function as ligand scavengers and tight regulators of chemokine concentrations and gradients. Notably, the existence of one atypical CXCR3 isoform is recurrent in bony fish, although lost in tetrapods and tetrapodomorph lobe-finned fish (fully aquatic species directly related to tetrapods). Therefore, atypical Cxcr3.3 receptors do not exclusively exist in zebrafish and might have important conserved function in fish immunology and could additionally help to reconstruct the evolutionary history of chemokine receptors.

In **Chapter 6** we have analysed the function of the chemokine receptor Cxcr4b and observed that Cxcr4b mutation can limit expansion of granulomas forming in the poorly vascularised tissues of the trunk. This phenotype correlated with a concomitant deficiency in triggering angiogenesis, a process that promotes the growth of granulomas in the wildtype situation. In the attempt to elucidate the mechanistic pathway that leads to granuloma vascularisation via Cxcr4b, we found that *cxcr4b* mutants had a limited induction of inflammatory mediators, especially the master regulator of inflammation, *il1b*. This pleiotropic molecule, which is also well known to exert proliferative and pro-angiogenic functions on endothelial cells, is largely expressed by infected cells in the granulomas and might represent the main connector between Cxcr4b and the induction of granuloma-associated inflammation.

In **Chapter 7** we characterised the function of the fish-specific chemokine Cxcl18b and by injection of recombinant chemokine we demonstrate that this molecule serves as a potent chemoattractant of neutrophils, while it does not affect macrophage recruitment. We additionally show that, at least partly, Cxcl18b exerts its function via the chemokine receptor Cxcr2, which was previously described as being the receptor partner of other two CXCL8/IL8-like chemokines in zebrafish, Cxcl8a and Cxcl8bb. Similarly to these CXCL8/IL8-like chemokines, Cxcl18b did not require the chemokine receptor Cxcr1, the zebrafish counterpart of mammalian CXCR1 that is redundant with CXCR2. Expression of *cxcl18b* is significantly and reliably induced by mycobacterial infection and by other

inflammatory conditions. Therefore *cxcl18b* expression may represent an important marker to longitudinally track the development of inflammation. We constructed a *cxcl18b* reporter and show that, in this line, the reporter reproduces the endogenous induction of *cxcl18b* during mycobacterial infection. Intriguingly, it seems that within the granuloma aggregate, the infected cells are not the main source of Cxcl18b. Instead, uninfected cells, that participated in the lesion but did not represent phagocytes, highly expressed the transgene. This observation suggests that further use of this reporter could permit to distinguish responses that are activated in defined subsets of non-phagocytic cells in the granuloma microenvironment, which might be important for the recruitment of neutrophils. This transgenic line could therefore be useful to study the function exerted by neutrophils in mycobacterial diseases, which remains poorly understood.

This dissertation is concluded by a general discussion in **Chapter 8**, which relates our findings with recently emerged concepts in innate immunity and mycobacterial disease. We discuss the dual function of macrophages in restricting and sustaining mycobacterial disease and the effects of macrophage-recruitment axes to establish, maintain and disseminate the infection. We elaborate on how the lysosome stress response and lysosomal storage diseases are emerging as opposing forces driving resistance or susceptibility to TB and discuss how this knowledge could be translated into novel therapeutic strategies. We try to explain our results on the atypical Cxcr3.3 receptor, of which mutation causes increased infection susceptibility, by comparing our findings to a study carried in a mice mutant of another atypical chemokine receptor, which essentially led to a comparable phenotype when infected with *M. tuberculosis*. We corroborate our findings on Cxcr4b/inflammation/angiogenesis with the complementary literature, which confirms a function of CXCR4 in induction of pathological angiogenesis and in modulating inflammation. We continue with a section discussing how the zebrafish model might help to clarify the function of chemokines in controlling neutrophilic involvement in mycobacterial diseases. Finally, we conclude with some general reflections on the pleiotropic functions and complexity behind the chemokine signalling network and on how the zebrafish model is contributing to our understanding of this and other multidimensional biological processes.

Concluding, the work described here has contributed to clarify how the chemokine network is implicated into different aspects of mycobacterial disease. We have emphasised how this intricate network can drive pathogen or host beneficial responses and we have shown that chemokine signalling not only controls recruitment of immune cells, but also their expression profile and their immune competence against the invading bacteria. More importantly, using the zebrafish model, we were able to follow longitudinally both the cellular dynamics and the molecular pathways that activate (or are activated by) the chemokine signalling *in vivo*. Finally the use of intravital imaging in this genetically tractable host model permitted to directly relate these new findings to pathological consequences at the level of the entire host during the course of the mycobacterial disease. This approach has helped us to comprehend to a deeper level the complexity behind the mycobacterial disease and how different cell types (e.g. neutrophils, macrophages, endothelium) and different host factors (e.g. chemokines, inflammatory mediators, angiogenesis factors) interact with each other and ultimately work together as a whole, in a system that eventually leads to the establishment of the disease.

Dutch summary / Samenvatting

Het belangrijkste doel van het werk beschreven in dit proefschrift was om de functie van chemokinen bij de interactie tussen het aangeboren immuunsysteem en mycobacteriële pathogenen te onderzoeken. Chemokinen (chemotactische cytokinen) zijn kleine signaaleiwitten die een centrale rol spelen bij immuniteit en ontstekingsreacties. De verschillende chemokinen die door een gastheer geproduceerd worden als reactie op een mycobacteriële infectie kunnen beschermende functies hebben, maar kunnen ook bijdragen aan de pathologie van de ziekte, zoals geïllustreerd wordt door het werk in dit proefschrift.

Tuberculose (TBC) vormt een wereldwijd gezondheidsprobleem. Deze ziekte wordt veroorzaakt door infectie met *Mycobacterium tuberculosis*, een bacterie die zich al sinds prehistorische tijden aan de mens heeft aangepast en door de eeuwen heen veel dodelijke slachtoffers heeft gemaakt. In de 21^{e} eeuw, meer dan 130 jaar na de ontdekking van deze besmettelijke ziekteverwekker, zijn we nog ver verwijderd van het uitbannen van TBC. Er wordt geschat dat ongeveer een derde van de wereldbevolking chronisch is geïnfecteerd met *M. tuberculosis* en daarom de kans heeft om TBC te ontwikkelen. TBC kan genezen worden door langdurige behandeling met een cocktail van antibiotica die verschillende essentiële processen van de bacteriegroei verstoren, zoals celwandsynthese of DNA- en eiwitsynthese. Een belangrijke complicatie bij de hedendaagse TBC-bestrijding is de opkomst van resistente stammen die niet meer reageren op de conventionele antibioticatherapie. Het probleem van multiresistentie benadrukt de noodzaak tot het ontwikkelen van nieuwe strategieën om de ziekte tegen te gaan. *M. tuberculosis* heeft het vermogen om immuuncellen van de gastheer te parasiteren. Om dat te bewerkstelligen manipuleert de bacterie verschillende signaleringssystemen van de gastheercellen. Het is daarom een aantrekkelijke hypothese dat TBC mogelijk behandeld zou kunnen worden met geneesmiddelen die op de gastheer werken in plaats van op de ziekteverwekker zelf. Met de ontwikkeling van geneesmiddelen voor zulke gastheerdoelwitten zouden niet alleen de behandelingsmogelijkheden voor TBC uitgebreid kunnen worden, maar zou ook de kans dat de bacteriën resistenties ontwikkelen verkleind kunnen worden.

Omdat het chemokinennetwerk cruciaal is voor de communicatie tussen cellen van het immuunsysteem, kan dit netwerk betrokken zijn bij verschillende aspecten van TBC. Enerzijds kunnen chemokinen de afweer van de gastheer stimuleren, maar anderzijds kunnen de processen die door chemokinen worden aangestuurd ook omzeild of zelfs benut worden door mycobacteriën. Chemokinen werken via de klasse van zogenoemde G-eiwit-gekoppelde receptoren. Deze receptoren zijn in de praktijk zeer succesvolle doelwitten gebleken voor de ontwikkeling van geneesmiddelen tegen verschillende ziekten. Daarom zijn de chemokinereceptoren mogelijk ook geschikte therapeutische doelwitten voor nieuwe gastheer-gerichte therapieën tegen TBC.

Zoals wordt uitgewerkt in **Hoofdstuk 1** en **Hoofdstuk 2** is de zebravis (*Danio rerio*) een uitstekend diermodel voor het bestuderen van de biologie van aangeboren immuuncellen (macrofagen en neutrofielen) en de moleculaire en cellulaire basis van infectieziekten. Dit geldt vooral voor de embryonale en larvale stadia, die behalve optisch transparant, ook chemisch en genetisch traceerbaar zijn. De zebravis is een natuurlijke gastheer voor

Mycobacterium marinum, een bacterie die nauw verwant is aan *M. tuberculosis*. Het zebravis-*M. marinum*-model recapituleert de belangrijkste moleculaire, cellulaire en histopathologische aspecten van humane TBC. De treffende gelijkenis tussen vissen-TBC en de humane ziekte is niet alleen interessant vanuit een evolutionair oogpunt, maar ook wetenschappelijk aantrekkelijk voor onderzoek naar TBC. Dit is niet alleen vanwege de strenge restricties om te werken met de humane pathogeen, maar ook omdat *M. tuberculosis* in muizen de humane ziekte niet volledig kan reproduceren. De laatste jaren is bovendien gebleken dat verscheidene humane chemotactische signalen moleculair en functioneel geconserveerd zijn in de zebravis, wat suggereert dat deze signalen mogelijk ook een overeenkomstige rol bij mycobacteriële infecties zouden kunnen spelen. Daarom biedt het embryonale/larvale zebravisplatform een inzichtelijk systeem om mycobacteriële infecties te modelleren. De toepassing van dit model heeft geleid tot de ontdekking van nieuwe virulentiemechanismen waarbij chemokinensignalering een rol speelt.

In **Hoofdstuk 3** hebben wij gevonden dat de zebravis een geconserveerde Cxcr3.2/Cxcl11aa-11af-signalering heeft met een belangrijke functie in macrofagen, net zoals de homologe CXCR3/CXCL9-10-11-signalering in zoogdieren. Homozygote *cxcr3.2*-mutanten lieten een deficiëntie zien in het rekruteren van macrofagen naar recombinante Cxcl11aa-11af-eiwitten en naar infecties met bacteriën (waaronder *M. marinum*) die de productie van Cxcr3.2-liganden opwekken. Opvallend was dat de *cxcr3.2*-mutatie tot resistentie tegen mycobacteriële infectie leidt, doordat deze mutatie de verspreiding van de bacteriën vermindert en de ontwikkeling van de zogenoemde granulomen vertraagt. Granulomen zijn besmettelijke ontstekingshaarden die bestaan uit geïnfecteerde immuuncellen (vooral macrofagen) die worden ingesloten door andere ongeïnfecteerde immuuncellen. Het ontstaan van tuberculeuze granulomen is een belangrijk kenmerk van de mycobacteriële infectie en deze structuren vormen de natuurlijke niche van mycobacteriën. Binnen het granuloom verblijven de mycobacteriën voornamelijk intracellulair in de macrofagen en extracellulair in het necrotisch centrum dat ontstaat door de dood van geïnfecteerde macrofagen. De Cxcr3.2-receptor bevordert de migratie van macrofagen en is daarom een belangrijke factor in de granuloomvorming. De migratie van macrofagen naar mycobacteriën in de zebravis kon behalve door mutatie van *cxcr3.2* ook geremd worden met behulp van een CXCR3-antagonist (NBI74330). Deze resultaten suggereren dat behandeling met CXCR3-remmers mogelijk zou kunnen worden toegepast om TBC-infectie te beperken.

In **Hoofdstuk 4** hebben wij verder onderzoek gedaan naar de signaleringsprocessen die afhankelijk zijn van Cxcr3.2. Hiertoe hebben we macrofagen gesorteerd uit *cxcr3.2*-mutanten en hun transcriptoom geprofileerd met RNA-sequentieanalyse. Verrassend genoeg ontdekten we dat de *cxcr3.2*-mutatie tot kenmerken van lysosomale stress leidt en zorgt voor een gecoördineerde inductie van verschillende lysosomale genen, waaronder genen die coderen voor hydrolytische enzymen en onderdelen van de lysosomale protonpompen. Om deze resultaten te bevestigen hebben we aangetoond dat deze kenmerken samengaan met een verhoogde verzuring van de bacterie-bevattende compartimenten en met een versterkte microbicide activiteit. Om meer inzicht te krijgen in hoe lysosomale stress in macrofagen wordt opgewekt door een tekort aan chemotactische signalen, hebben we de migratie van macrofagen gevolgd na toepassing van een lysosoomkleuring. Opvallend was dat de lysosomen zich tijdens het migratieproces verplaatsen naar de voorkant van de bewegende cel en dat *cxcr3.2*-mutatie hier een remmend effect op heeft. De ophoping van lysosomen aan de voorkant van migrerende

cellen is mogelijk een teken van de exocytose van lysosomen, een proces dat kan worden geïnduceerd door chemokinen en belangrijk is voor membraanvoorziening aan de uitgestrekte lamellipodia. Een interessante waarneming was dat macrofagen zelf de expressie van *cxcl11aa* induceren tijdens de mycobacteriële infectie. De Myd88-signaalroute, die betrokken is bij de herkenning van pathogenen door het immuunsysteem, bleek essentieel te zijn voor de expressie van *cxcl11aa*. Daarom veronderstellen we dat het circuit van immuunherkenning, chemokinesignalering en lysosoomfunctie mogelijk de pathogeen op twee manieren kan bevoordelen. Ten eerste kan de inductie van Cxcr3.2-afhankelijke signalering het granuloom voeden met nieuwe macrofagen die vervolgens besmet kunnen worden en ten tweede kan deze signalering voor een meer toegankelijke intracellulaire niche zorgen, omdat de lysosomale functies onderdrukt worden.

Hoofdstuk 5 rapporteert over een voorlopige karakterisering van de functie van Cxcr3.3, een andere homoloog van de humane CXCR3-receptor in de zebravis. In dit hoofdstuk wordt allereerst beschreven hoe we de CRISPR/Cas9-methode hebben toegepast om een *cxcr3.3*-mutant te verkrijgen, waarbij we een aantal verbeteringen in het protocol hebben ingevoerd om de mutagenese te optimaliseren. De analyse van *cxcr3.3*-mutanten liet vervolgens zien dat deze gevoeliger zijn voor mycobacteriële infecties, wat tegenovergesteld is aan het fenotype van de *cxcr3.2*-mutant. Een dubbelmutant van *cxcr3.2* en *cxcr3.3* zal nodig zijn om deze tegenstelling verder te onderzoeken, maar als alternatief hebben we gekeken naar het effect van behandeling met de NBI74330-remmer, die even goed tegen Cxcr3.2 als tegen Cxcr3.3 zou moeten werken vanwege de overeenkomstige structuur van de receptoren. Deze receptorantagonist had een positief effect op de resistentie van zebravisembryo's tegen mycobacteriële infectie, overeenkomstig met het fenotype van de enkele *cxcr3.2*-mutant. Dit resultaat suggereert dat de functie van de Cxcr3.3-receptor afhankelijk is van die van de Cxcr3.2-receptor. Ter ondersteuning van deze hypothese ontdekten wij dat de sequentie van Cxcr3.3 een aantal belangrijke verschillen vertoont in vergelijking met andere G-eiwit-gekoppelde chemokinereceptoren. Het meest opmerkelijke verschil is de vervanging van een Arginine-residu in het Asparaginezuur-Arginine-Tyrosine-motief (DRY-motief), het meest geconserveerde motief van de functionele G-eiwit-gekoppelde receptoren. Het Arginine-residu is 100% geconserveerd in de functionele humane CXCR-receptoren en is noodzakelijk voor de interactie met heterotrimere G-eiwitten en voor de activering van de onderliggende signaalroute. Het DRY-motief is daarentegen vaak afwijkend (of geheel afwezig) in atypische chemokinereceptoren. Deze atypische receptoren competeren met de functionele receptoren voor de binding van chemokinen en kunnen op die manier chemokine-concentratiegradiënten reguleren. Het voorkomen van atypische CXCR3-isovormen is een terugkerend fenomeen in beenvissen, terwijl het verloren lijkt te zijn gegaan tijdens de evolutie van tetrapoden en kwastvinnige vissen, die nauw verwant zijn aan tetrapoden. Atypische Cxcr3.3-receptoren zijn daarom niet uniek voor de zebravis en hebben mogelijk een belangrijke geconserveerde functie in het immuunsysteem van vissen. Verder onderzoek hiernaar kan helpen om de evolutionaire geschiedenis van chemokinereceptoren te reconstrueren.

In **Hoofdstuk 6** hebben wij de functie van de chemokinereceptor Cxcr4b geanalyseerd en geconstateerd dat mutatie van deze receptor de groei van granulomen in de weefsels van de romp van zebravisembryo's beperkt. Een kenmerk van de weefsels in de romp is dat hier weinig bloedvaten doorheen lopen. Om in grootte te kunnen toenemen, moeten de granulomen in deze weefsels daarom nieuwe bloedvaten aantrekken (angiogenese). De

beperkte groei van granulomen in *cxcr4b*-mutanten bleek een correlatie te vertonen met verminderde angiogenese. In een poging om te ontrafelen hoe Cxcr4b de bloedvatvoorziening van granulomen bevordert, vonden we dat *cxcr4b*-mutanten een verminderde inductie vertonen van genen betrokken bij ontstekingsreacties, in het bijzonder het gen dat codeert voor het ontstekingsbevorderende cytokine Il1b. Dit cytokine is een pleiotroop molecuul dat ook bekend staat om zijn proliferatieve en pro-angiogene effecten op de cellen van de wand van bloedvaten (endotheelcellen). Het *il1b*-gen komt grotendeels tot expressie in de geïnfecteerde cellen in de granulomen en vormt mogelijk een belangrijke verbinding tussen Cxcr4b en de activering van de ontstekingsreactie in deze structuren.

In **Hoofdstuk 7** karakteriseren wij de functie van Cxcl18b, een chemokine dat specifiek is voor de zebravis. Door middel van injectie van recombinant Cxcl18b-eiwit laten we zien dat dit chemokine een krachtige chemoattractant van neutrofielen is, terwijl het geen invloed heeft op het aantrekken van macrofagen. We hebben bovendien aangetoond dat Cxcl18b zijn functie in ieder geval gedeeltelijk uitoefent via de chemokinereceptor Cxcr2, die eerder werd beschreven als de receptor voor twee CXCL8/IL8-achtige chemokinen. De expressie van *cxcl18b* is sterk induceerbaar door mycobacteriële infecties en andere ontstekingscondities. Daarom kan *cxcl18b* een bruikbare marker zijn om de ontwikkeling van ontstekingsreacties te volgen. We hebben een *cxcl18b*-reporter geconstrueerd en zagen dat deze reporter de endogene inductie van *cxcl18b* reproduceert tijdens mycobacteriële infectie. Interessant genoeg bleek dat de geïnfecteerde cellen niet de belangrijkste bron van expressie van de *cxcl18b*-reporter zijn, maar dat ongeïnfecteerde cellen in de granulomen het transgen sterk tot expressie brengen. Deze observatie suggereert dat de reporter kan worden gebruikt om reacties te onderscheiden die worden geactiveerd in specifieke subpopulaties van cellen waaruit granulomen bestaan en die belangrijk zouden kunnen zijn voor de rekrutering van neutrofielen. Deze transgene lijn lijkt daarom nuttig voor toekomstig onderzoek naar de functie van neutrofielen in mycobacteriële ziekten, waarover nu nog weinig bekend is.

Dit proefschrift wordt afgesloten met een algemene discussie in **Hoofdstuk 8**, waarin onze resultaten worden besproken in relatie tot recente inzichten in aangeboren immuniteit en mycobacteriële ziekten. We bediscussiëren de dubbele functie van macrofagen, die aan de ene kant noodzakelijk zijn om een mycobacteriële infectie in te perken, maar aan de andere kant juist kunnen bijdragen aan de verspreiding van de bacteriën in de weefsels van de gastheer. Tevens gaan we erop in op hoe de lysosomale stressreactie bij kan dragen aan resistentie tegen infecties, terwijl lysosomale stapelingsziekten juist geassocieerd zijn met een grotere vatbaarheid voor infecties. Hierbij bespreken we hoe deze kennis benut zou kunnen worden voor nieuwe therapeutische strategieën. Daarnaast hebben we getracht om een verklaring te vinden voor onze resultaten met betrekking tot de atypische Cxcr3.3-receptor, waarvan mutatie tot verhoogde vatbaarheid voor infectie leidt. Hiertoe hebben we onze bevindingen vergeleken met een studie in muizen die een mutatie hebben in een andere atypische chemokinereceptor en die een vergelijkbaar fenotype vertonen na infectie met *M. tuberculosis.* Voorts plaatsen we onze resultaten over het effect van Cxcr4b op angiogenese en de ontstekingsreactie in granulomen in de context van literatuur waarmee de functie van CXCR4 bij inductie van pathologische angiogenese en modulatie van ontstekingsreacties wordt ondersteund. Vervolgens wordt besproken hoe het zebravismodel kan helpen om meer inzicht te verkrijgen in de functie van chemokinen bij het reguleren van de betrokkenheid van neutrofielen in mycobacteriële ziekten. Het hoofdstuk wordt

besloten met enkele algemene reflecties over de pleiotropische functies en complexiteit achter het chemokine-signaleringsnetwerk en over hoe het zebravismodel kan bijdragen aan ons begrip van deze en andere multidimensionale biologische processen.

Concluderend, het onderzoek dat in dit proefschrift wordt beschreven heeft bijgedragen aan het verduidelijken van de betrokkenheid van het chemokinennetwerk bij verschillende aspecten van mycobacteriële infectie. Onze resultaten benadrukken hoe dit intrigerende netwerk kan leiden tot verschillende uitkomsten die gunstig kunnen zijn voor de gastheer of juist voor de pathogeen. Daarnaast hebben we laten zien dat signalering door chemokinen niet alleen de rekrutering van immuuncellen reguleert, maar ook het expressieprofiel van deze cellen en hun immuuncompetentie tegen de binnendringende bacteriën. Bovendien heeft het zebravismodel longitudinaal *in vivo* onderzoek mogelijk gemaakt om de cellulaire dynamica en moleculaire routes te volgen die de chemokinensignalering activeren (of hierdoor worden geactiveerd). Ten slotte heeft het gebruik van dit gastheermodel het mogelijk gemaakt om deze nieuwe bevindingen over chemokinensignalering rechtstreeks te relateren aan pathologische consequenties op het niveau van de gastheer tijdens de mycobacteriële ziekte. Deze aanpak heeft ons geholpen om op een dieper niveau inzicht te krijgen in de complexiteit achter de mycobacteriële ziekte en om te begrijpen hoe verschillende celtypen (zoals neutrofielen, macrofagen, en endotheelcellen) en verschillende gastheerfactoren (zoals chemokinen, ontstekingsmoleculen en angiogenesefactoren) een interactie met elkaar aan gaan en als geheel in een systeem samenwerken, wat uiteindelijk leidt tot de ontwikkeling van de ziekte.

List of abbreviations

AB/TL	AB/Tupfel long fin
AC	Adenylyl cyclase
Ackr	Atypical chemokine receptor
AGM	Aorta, gonads and mesonephros
AJ	Ashkenazi Jewish
ASMase	Acid sphingomyelinase
BALB/c	Bagg Albino/c
BCA	Bicinchoninic acid
Bcc	*Burkholderia cenocepacia*
BCG	Bacillus of Calmette–Guérin
bHLH	Basic helix-loop-helix
BLT1	Leukotriene B4 receptor 1
bZip	Basic Leucine zipper
C/ebpβ	CCAAT enhancer-binding protein β
cAMP	Cyclic adenosine monophosphate
Cas9	CRISPR-associated protein 9
Ccl1	Cys-Cys motif chemokine ligand
Ccr1	Cys-Cys motif chemokine receptor
Cdc42	Cell division control protein 42 homologue
CFU	Colony forming unit
CHT	Caudal haematopoietic tissue
CLEAR	Coordinated lysosomal expression and regulation
Coro-1a	Coronin 1a
COX	Cycloxygenase
CRISPR	Clustered regularly interspaced short palindromic repeats
CV	Caudal vein
Cx3cl	Cys-X3-Cys motif chemokine ligand
Cx3cr	Cys-X3-Cys motif chemokine receptor
Cxcl	Cys-X-Cys motif chemokine ligand
Cxcr	Cys-X-Cys motif chemokine receptor
Cxl	Cys-X motif chemokine ligand
Cxr	Cys-X motif chemokine receptor
CYPD	Cyclophilin D
DAG	Diacylglycerol
DARC	Duffy antigen chemokine receptor
DC	Denditic cell
DMSO	Dimethyl sulfoxide
Dpf	Days post fertilisation
Dpi	Days post infection\injection
DRY	Asp-Arg-Tyr
dsDNA	Double-stranded DNA
DUOX	Dual oxidase
Ec	*Escherichia coli*
ECM	Extracellular matrix
eGFP	Enhanced Green fluorescent protein
Eif	Eukariotic initiation factor
ELR	Glu-Leu-Arg
ENA78	Epithelial-derived neutrophil-activating peptide 78
ER	Endoplasmic reticulum
ERP	Exported repeated protein
ESAT-6	Early secretory antigenic target 6 kDa
ESX-1	ESAT-6 secretion system 1
FACS	Fluorescence-activated cell sorting
Fli1a	Friend leukemia integration 1a
GCP2	Granulocyte chemotactic protein 2
Gcsf	Granulocyte colony stimulating factor
GDP, GTP	Guanosine 5'-diphosphate, triphosphate
GEF	Guanine nucleotide exchange factor
GPCR	G-protein-coupled receptor
GPR35	G-protein-coupled receptor 35
GR	Glucocorticoid receptor
Grb2	Growth factor receptor-bound protein 2
GROα, GROβ, GROγ	Growth-regulated protein alpha, beta, gamma
HA	Human influenza haemagglutinin
HB	Hindbrain
HEXA, HEXB	Hexosaminidase A, B
Hif-1α, Hif-2α	Hypoxia-inducible factor 1 alpha, 2 alpha
Hpf	Hours post fertilisation
Hpi	Hours post infection/injection
Hpw	Hours post wounding
HSPC	Haematopoietic stem and progenitor cell
I-TAC	Interferon-inducible T-cell alpha chemoattractant
Ifnγ	Interferon gamma
Il1β, Il8, Il13	Interleukin 1 beta, 8, 13
iNOS	Inducible nitric oxide synthase
IP-10	Interferon gamma-inducible protein 10
IP3	inositol 1,4,5-trisphosphate
Irf8	Interferon regulatory factor 8
Irg1	Immunoresponsive gene 1
JAK	Janus kinase
kDa	kilo Dalton
Kdrl	Kinase insert domain receptor-like
KO	Knockout
Lamp3	Lysosomal associated membrane protein 3
Lc3	Microtubule-associated protein 1A/1B-light chain 3
Lck	Lymphocyte cell-specific protein-tyrosine kinase
Lp/Lcp1	Leukocyte plastin/ Lymphocyte

	cytosolic protein 1
LSD	Lysosomal storage disorder
Lta4h	Leukotriene A4 hydrolase
LTB4	Leukotriene B4
Lyz	Lysozyme
M(Φ)	Monocyte/macrophage
MAPK	Mitogen-activated protein kinases
MIF	Macrophage migration inhibitory factor
MIG	monokine induced by interferon γ
miRNA	Micro RNA
Mitf	Microphthalmia-associated transcription factor
MLCK	Myosin light-chain kinase
Mm	*Mycobacterium marinum*
Mmp 9	Matrix metalloproteinase 9
Mpeg1	Macrophage expressed gene 1
mPTPC	Mitochondrial permeability transition pore complex
Mpx	Myeloperoxidase
Mtb	*Mycobacterium tuberculosis*
Myd88	Myeloid differentiation primary response gene 88
MΦ	Macrophage
NADPH	Nicotinamide adenine dinucleotide phosphate
NAI	Nfκb activation inhibitor
NAP2	Neutrophil-activating peptide 2
Nfκb	Nuclear factor kappa-light-chain-enhancer of activated B cells
NK	Natural killer cell
Nlr	Nod-like receptor
NSAID	Non-steroid antinflammatory drug
NΦ	Neutrophil
P/DAMP	Pathogen and Damage-associated molecular pattern
PAM	Protospacer adjacent motif
PBS, PBSTx	Phosphate buffer saline, triton x
pC3	Previously chromosome 3
PCR	Polymerase chain reaction
PDIM	Phthiocerol dimycocerosate
PGL	Phenolic glycolipid
PGP	Pro-Gly-Pro
PH	Plekstrin homology
PHOX	Phagocytic oxidase
PI3K	Phosphatidylinositol-4,5-bisphosphate 3-kinase
PIP2	Phosphatidylinositol 4,5-bisphosphate
PIP3	Phosphatidylinositol (3,4,5)-trisphosphate
PITPNM3	Phosphatidylinositol transfer protein, membrane-associated 3
PKC	Protein kinase C
PLA, PLC	Phospholipase A, C
Ppiab	Peptidylprolyl isomerase ab
PRR	Pattern recognition receptor
PTK	Protein tyrosine kinase
Ptpn6/Shp1	Protein tyrosine phosphatase, non-receptor type 6/ Src homology region 2 domain-containing phosphatase 1
Ptprc/Cd45	Protein tyrosine phosphatase receptor type C/Cd45
PTU	Phenylthiourea
PVP	Polyvinylpyrrolidone
qRT-PCR	Quantitative real time polymerase chain reaction
Rac1	Ras-related C3 botulinum toxin substrate
RD1	Region of difference 1
RhoA	Ras homologue gene family member A
RNS	Reactive nitrogen species
ROCK	Rho-associated protein kinase
ROS	Reactive oxygen species
shgRNA	Short guide RNA
SNARE	Soluble NSF attachment protein receptor
Spi1/Pu.1	Spleen Focus Forming Virus (SFFV) Proviral Integration Oncogene 1/Pu.1
Sqstm1/p62	Sequestosome 1/Ubiquitin-binding protein of 62 kDa
ssDNA	Single-stranded DNA
St	*Salmonella enterica* Serovar Typhimurium
STAT	Signal transducer and activator of transcription
SV40pA	Simian virus 40 polyadenylation signal
T3SS	Type III secretion system
T7SS	Type VII secretion system
TALEN	Transcription activator-like effector nuclease
TB	Tuberculosis
Tfeb, Tfec, Tfe3	Transcription factor E, C, 3
Tg	Transgenic
Tiam1	T-lymphoma invasion and metastasis-inducing protein 1
Tlr	Toll-like receptor
TM	Transmembrane
TMT	Trasmembrane transporter
Tnfα	Tumour necrosis factor alpha
Traf6	TNF receptor-associated factor 6
UAS	Upstream activating sequence
Vegf	Vascular endothelial growth factor
Vegfr	Vascular endothelial growth factor receptor
WGD	Whole genome duplication
WHO	World health organisation
Wt	Wildtype
Xcl	X- Cysteine motif chemokine ligand
Xcr	X- Cysteine motif chemokine receptor
YPD	Yeast extract peptone dextrose
ZFN	Zinc finger nuclease

Nomenclature of zebrafish chemokine ligands

Name in this thesis	Ensembl gene name	zfin gene name	Ensembl gene ID/Alignment position	Ensembl protein ID	Previous /synonymous names and notes
ccl18ab	CR762483.1	-	ENSDARG00000074487	ENSDARP00000101228	-
ccl19aa	ccl19a.1	ccl19a.1	ENSDARG00000058389	ENSDARP00000090385	ccl-c5a, dr-scNA10579-CCL19-34.3%-DN, si:ch211-89f7.4
ccl19ab	ccl19a.2	ccl19a.2	ENSDARG00000035632	ENSDARP00000051667	ccl-c5b, DrUn_WGA13047_1_39000, WGA710_1_710182, zgc:194112, zgc:194121
ccl19b	ccl19b	ccl19b	ENSDARG00000039351	ENSDARP00000114954	ccl19, ccl-c10a, Dr10_WGA780_1_413112, si:dkey-200l5.2
ccl20aa	-	-	unmappable	no protein assigned	-
ccl20ab	ENSDARG00000100432	-	ENSDARG00000100432	ENSDARP00000138620	-
ccl20ac	ccl20a.3	ccl20a.3	ENSDARG00000101040	ENSDARP00000138701	chemokine-1, CH73-320I17.1, LOC100004509GN, zgc:195209, zgc:195195
ccl20ad	-	-	2:45319950-45317434 (-)	no protein assigned	Incomplete sequence/pseudogene
ccl20b	ccl20b	ccl20b	ENSDARG00000094511	ENSDARP00000122800 ENSDARP00000122912	ccl20, ccl-c24a, Dr24_WGA1806_1_416955, dr-chr24-CCL20-34.6%-DN, si:dkey-150o13.1
ccl25a	CU693369.1	-	ENSDARG00000089534	ENSDARP00000111107	-
ccl25b	ccl25b	ccl25b	ENSDARG00000070873	ENSDARP00000095178	ccl21, ccl-c11a, Dr11_WGA839_1_159228, dr-chr11-CCL21-36.7%-DN
ccl27a	ccl27a	ccl27a	ENSDARG00000058570	ENSDARP00000075898 ENSDARP00000137864	ccl1, Dr8_WGA606_1_66363, wu:fa96a04
ccl27b	ccl27b	ccl27b	ENSDARG00000079713	ENSDARP00000104032	ccl-c10b, Dr9_WGA697_1_854420, dr-chr9-CCL13-28.2%-DN, dr-chr9-CCL17-22.3%-DN
ccl32ab	ccl32a.2	ccl32a.2	ENSDARG00000095049	ENSDARP00000122846 ENSDARP00000141410	ccl-c2c, Dr7_WGA489_1_245599, si:ch211-122l24.2
ccl32ac	-	-	2:40365520-40370475 (+)	no protein assigned	-
ccl32ad	-	-	2:40387422-40388412 (+)	no protein assigned	-
ccl32ae	-	-	unmappable	no protein assigned	-
ccl32bc	CT574575.1	-	ENSDARG00000098656	ENSDARP00000137910 ENSDARP00000140796	-
ccl32ca	-	-	KN149905:570-1 (-)	no protein assigned	-
ccl32cb	-	-	KN149905:2766-1821 (-)	no protein assigned	-
ccl32d	-	-	KN150005:21462-23168 (+)	no protein assigned	-
ccl33aa	-	-	25:25106427-25106501 (+)	no protein assigned	Incomplete sequence/pseudogene
ccl33ab	ccl33.2	ccl33.2	ENSDARG00000102519	ENSDARP00000130735 ENSDARP00000138153 ENSDARP00000138433	ccl-c25h, dr-chr25-CCL8-35.6%-EP41974b, si:ch211-149o7.6
ccl33ac	ccl33.3	ccl33.3	ENSDARG00000099401	no protein assigned	ccl-c25a, ccl-c25g, Dr25_WGA1873_1_709505, Dr25_WGA1872_1_17999, dr-chr25-CCL8-30.8-EP41974a, chr25-CCL24-35.6-DN, si:ch211-149o7.4
ccl34aa	-	-	unmappable	no protein assigned	-
ccl34ab	-	-	unmappable	no protein assigned	-
ccl34ac	ccl34a.3	ccl34a.3	ENSDARG00000094983	no protein assigned	ccl-c2e, Dr11_WGA879_1_762108, Dr11_WGA879_1_759152, Dr11_WGA879_1_755946, si:ch211-122l24.5
ccl34ad	ccl34a.4	ccl34a.4	ENSDARG00000090873	no protein assigned	ccl-c2d, CC-Chemokine, dr-chr11-CCL19-33.7%-DN, dr-chr11-CCL19-32.7%-DN, si:ch211-122l24.4
ccl34ba	ccl34b.1	ccl34b.1	ENSDARG00000093608	ENSDARP00000116086 ENSDARP00000136441	ccl-c24m, Dr22_WGA1631_1_283786, dr-chr22-CCL19-30.3%-DN, si:dkey-25o1.6
ccl34bb	-	-	24:27327959-27327535 (-)	no protein assigned	-
ccl34bb	-	-	unmappable	no protein assigned	-

Name in this thesis	Ensembl gene name	zfin gene name	Ensembl gene ID/Alignment position	Ensembl protein ID	Previous /synonymous names and notes
ccl34bc	ccl34b.3	ccl34b.3	ENSDARG00000032993	ENSDARP00000041769	ccl-c24k, DrUn_WGA7827_1_9830, dr-scNA5340-CCL19-30.5%-DN, si:dkey-25o1.9
ccl34bd	ccl34b.4	ccl34b.4	ENSDARG00000094002	ENSDARP00000117348 ENSDARP00000136530	ccl-c24j, DrUn_WGA7827_1_17321, si:dkey-25o1.5
ccl34be	CR383669.1	-	ENSDARG00000099782	ENSDARP00000137755	-
ccl34bf	CR383669.2	-	ENSDARG00000100520	ENSDARP00000137901	-
ccl34bg	-	-	KN150005:21462-21536 (+)	no protein assigned	-
ccl34bh	ccl34b.8	ccl34b.8	ENSDARG00000093098	ENSDARP00000121266	ccl-c24c, si:dkey-25o1.4
ccl34bi	ccl34b.9	ccl34b.9	ENSDARG00000078205	ENSDARP00000098604	ccl-c24b, si:dkey-25o1.3
ccl34bl	-	-	24:27403153-27402859 (-)	no protein assigned	Incomplete sequence/pseudogene
ccl34bm	-	-	24:27411537-27411245 (-)	no protein assigned	Incomplete sequence/pseudogene
ccl34bn*	si:dkey-25o1.7	si:dkey-25o1.7	ENSDARG00000093570	ENSDARP00000121438 ENSDARP00000130107 ENSDARP00000135013	-
ccl34ea	CABZ01001434.1	-	ENSDARG00000098602	ENSDARP00000133785 ENSDARP00000133418	-
ccl34eb	-	-	unmappable	no protein assigned	-
ccl35aa	ccl35.1	ccl35.1	ENSDARG00000103466	ENSDARP00000132604	ccl-c25y, Dr1_WGA6_1_97332, dr-chr1-CCL26-33.3%-EP26489, zgc:193743, zgc:193706
ccl35ab	ccl35.2	ccl35.2	ENSDARG00000070378	ENSDARP00000093979	ccl-c25ab, DrUn_WGA2406_1_18581, Dr25_WGA1872_1_197377, zgc:193706
ccl36aa	-	-	7:39442461-39442771 (+)	no protein assigned	Incomplete sequence/pseudogene
ccl36ab	BX908792.2	-	ENSDARG00000105263	ENSDARP00000138949	-
ccl38aa	ccl38.1	ccl38.1	ENSDARG00000041919	ENSDARP00000061433 ENSDARP00000113398 ENSDARP00000128783	ccl-c20g, Dr20_WGA1544_1_1446828, dr-chr20-CCL7-40.0%-DN, si:dkey-217m5.3
ccl38ac	-	ccl38a.3	unmappable	no protein assigned	ccl-c20e, Dr20_WGA1544_1_375272, Dr20_WGA1544_1_390316, dr-chr20-CCL14-32.9%-DN, si:dkeyp-59a8.5
ccl38ad	ccl38a.4	ccl38a.4	ENSDARG00000041917	ENSDARP00000061431	ccl-c20d, Dr20_WGA1544_1_386533, zgc:171266, si:dkeyp-59a8.3
ccl2 (ccl38ae)	ccl38a.5	ccl38a.5	ENSDARG00000041835	ENSDARP00000061310	ccl-c20c, Dr20_WGA1544_1_382837, si:dkeyp-59a8.2
ccl38af	ccl38.6	ccl38.6	ENSDARG00000041923	ENSDARP00000061436 ENSDARP00000120680 ENSDARP00000123921	ccl-c20b, Dr20_WGA1544_1_380308, Dr20_WGA1544_1_390316, dr-chr20-CCL7-35.6-DN, wu:fj16d01, si:dkeyp-59a8.1
ccl39aa	ccl39.1	ccl39.1	ENSDARG00000101041	ENSDARP00000130968	ccl-c25q, dr-chr25-CCL13-38.9%-DN, si:dkeyp-55h4.5
ccl39ab	ccl39.2	ccl39.2	ENSDARG00000102945	ENSDARP00000138051 ENSDARP00000141835	ccl-c25p, dr-chr25-CCL2-37.5%-DN, si:ch211-149o7.5
ccl39ac	ccl39.3 (ch. 25)	ccl39.3	ENSDARG00000100295	ENSDARP00000141922 ENSDARP00000138620	ccl-c25o, dr-chr25-CCL13-35.9%-DN, si:dkeyp-55h4.6
ccl39ad	ccl39.4	ccl39.4	ENSDARG00000104002	ENSDARP00000130829 ENSDARP00000138036	ccl-c25n, Dr25_WGA1872_1_141073, dr-chr25-CCL11-31.2%-DN, si:dkeyp-55h4.7
ccl39ae	ccl39.5	ccl39.5	ENSDARG00000098460	ENSDARP00000141305	ccl-c25m, dr-chr25-CCL2-35.0%-DN, dr-chr25-CCL2-36.4%-DN, si:dkeyp-55h4.8
ccl39af	ccl39.6	ccl39.6	ENSDARG00000105089	ENSDARP00000132580	ccl-c25l, si:dkeyp-55h4.9
ccl39ag	ccl39.7	ccl39.7	ENSDARG00000099982	ENSDARP00000133318 ENSDARP00000138980	ccl-c25k, Dr25_WGA1873_1_857912, si:dkeyp-55h4.10
ccl39ah	CR450808.1	-	ENSDARG00000100484	ENSDARP00000135517	-
ccl39ai	-	-	25:12816818-12816285 (-)	no protein assigned	Incomplete sequence/pseudogene
ccl39aj*	ccl39a.10	ccl39a.10	ENSDARG00000096060	ENSDARP00000125562	ccl-c25z, si:ch211-202c4.2 Incomplete sequence/pseudogene
ccl39ba*	ccl39.3 (ch. 6)	-	ENSDARG00000101499	ENSDARP00000130440	-
ccl44	ccl44	ccl44	ENSDARG00000074772	ENSDARP00000101027	ccl-c11b, Dr11_WGA839_1_233313
cxcl8a	CT826376.2	cxcl8a	ENSDARG00000104795	ENSDARP00000137520	cxcl8, il8, cxcl-c1a, CXCL8_L1_chr1, dr-chr1-CXCL8, si:dkey-151b16.2
cxcl8ba	-	-	7:7671156-7665921 (-)	no protein assigned	-

Name in this thesis	Ensembl gene name	zfin gene name	Ensembl gene ID/Alignment position	Ensembl protein ID	Previous /synonymous names and notes
cxcl8bb	cxcl8b.1	cxcl8b.1	ENSDARG00000102299	ENSDARP00000131403 ENSDARP00000136965	il8l2, cxcl8_l2_chr17
cxcl8bc	cxcl8b.3	cxcl8b.3	ENSDARG00000099169	ENSDARP00000136707	cxcl-c13d, CXCL8_L2_chr7, dr-scNA16716-CXCL8
cxcl11aa	CXCL11 (1 of many)	cxcl11.1	ENSDARG00000100662	ENSDARP00000135444	cxcl11l, cxcl-c5d, dr-chr5-CXCL11, vig7, SCYB9B, b-R1, IP-9, H174, SCYB11, I-TAC
cxcl11ab	-	cxcl11.2	5:42290344-42290046 (-)	no protein assigned	dr-chr5-CXCL11-27.4-DN Incomplete sequence/pseudogene
cxcl11ac	ENSDARG00000102514	cxcl11.3	ENSDARG00000102514	ENSDARP00000136965	cxc-66, cxcl-c5e, dr-chr5-CXCL11-37.2-EK12810
cxcl11ad	CXCL11 (1 of many)	cxcl11.4	ENSDARG00000101138	ENSDARP00000133434	cxcl11l2, cxc-56, cxcl-c5f, dr-chr5-CXCL9-35.1-EK43819, SCYB9B, b-R1, IP-9, H174, SCYB11, I-TAC
cxcl11ae	cxcl11.5	cxcl11.5	ENSDARG00000092423	ENSDARP00000115162 ENSDARP00000136838	cxcl-c5g, dr-chr1-CXCL11-37.1-DN, si:ch211-202a12.7
cxcl11af	cxcl11.6	cxcl11.6	ENSDARG00000094706	ENSDARP00000112794	cxcl-c5h, si:ch211-202a12.8
cxcl11ag	cxcl11.7	cxcl11.7	ENSDARG00000093779	ENSDARP00000116772	cxcl-c5i, dr-chr1-CXCL9-37.2-EK42273, si:ch211-202a12.9,
cxcl11ah	cxcl11.8	cxcl11.8	ENSDARG00000095747	ENSDARP00000123477	cxc-64, cxcl-c5b, dr-chr5-CXCL11-25.2-EP22087, si:dkey-58f10.5
cxcl12a	cxcl12a	cxcl12a	ENSDARG00000037116	ENSDARP00000053945	cxcl12, sdf1, sdf1a, unm t30516, unm_t30516, wu:fa55e10, wu:fc16h12, wu:fj84c02
cxcl12b	cxcl12b	cxcl12b	ENSDARG00000055100	ENSDARP00000071878	sdf1b, zgc:136720
cxcl13	si:dkey-58f10.3	-	ENSDARG00000095112	no protein assigned	-
cxcl14	cxcl14	cxcl14	ENSDARG00000056627	ENSDARP00000109550	scyba, fb67g04, wu:fb67g04
cxcl18aa	-	-	13:30566063-30568522 (+)	no protein assigned	Incomplete sequence/pseudogene
cxcl18b	cxcl18b	cxcl18b	ENSDARG00000075045	ENSDARP00000102296	cxcl-c1c, dr-chr25-CXCL11-28.0-EP27297, si:ch73-6k14.1GN
cxcl19	cxcl19	cxcl19	ENSDARG00000102776	ENSDARP00000135787	cxcl-c13d, dr-scNA11550-CXCL2-36.0%-DN
cxcl20b	cxcl20	cxcl20	ENSDARG00000075163	ENSDARP00000102486	cxcl-c5c, dareCXCc, dr-chr5-CXCL10-28.6%-DN
cxcl32ba	cxcl32b.1	cxcl32b.1	ENSDARG00000071499	ENSDARP00000096549	cxcl-c24e, si:ch211-260d11.1, scNA16670-CCL8-33.3-DN
cxcl32bb	CT574575.2	-	ENSDARG00000099822	ENSDARP00000131333	-
cxl34bj	-	-	24:27385246-27384292 (-)	no protein assigned	
cxl34bk	cxl34b.11	cxl34b.11	ENSDARG00000092283	ENSDARP00000115786	cxl-c24a, cxl1, si:dkey-25o1.2
cxl34c	cxl34c	cxl34c	ENSDARG00000096664	ENSDARP00000126667	cxl-c12a, wu:fb09d09, si:ch211-125g7.3
cxl34d	-	-	7:57100469-57102607 (+)	no protein assigned	-
xcl32aa	xcl32a.1	xcl32a.1	ENSDARG00000093906	ENSDARP00000118951	cxl-c2a, si:ch211-122l24.3

Notes: Comparison of the nomenclature applied in this work (column 1) with the nomenclature used in Ensembl and zfin databases or elsewhere in literature (columns 2-6). The nomenclature adopted here essentially reflects the systematic classification suggested by Nomiyama *et al.*, *Genes Cells*. 2013. Exceptions are made for genes where other names are largely in use (for these cases the name according to Nomiyama *et al.,* 2013 is reported in brackets in column 1). Names followed by asterisks (*) indicate sequences which were not annotated in Nomiyama *et al.,* 2013. Rows highlighted in grey represent either incomplete sequences or previously reported genes that cannot be mapped on the current version of the zebrafish genome (Ensembl, GRCz10, September 2016).

Nomenclature of zebrafish chemokine receptors

Name in this thesis	Ensembl gene name	zfin gene name	Ensembl gene ID/Alignment position	Ensembl protein ID	Previous /synonymous names and notes
ackr2/d6*	CU633991.1	-	ENSDARG00000086314	ENSDARP00000108059	-
ackr3a/cxcr7a	ackr3 (1 of many)	ackr3a	ENSDARG00000062478	ENSDARP00000084847	drRDC1a, si:dkey-191g15.12, si:dkeyp-74a11.11
ackr3b/cxcr7b	ackr3b	ackr3b	ENSDARG00000058179	ENSDARP00000063664	drRDC1b, sb:cb900, si:dkey-96h14.2
ackr4a/ccrl1a	ackr4a	ackr4a	ENSDARG00000078729	ENSDARP00000116973	zfCCRL1-1
ackr4b/ccrl1b	ackr4b	ackr4b	ENSDARG00000040133	ENSDARP00000058702	drCCRL1b, zfCCRL1-2, sb:eu250
ackr6/pitpnm3*	pitpnm3	pitpnm3	ENSDARG00000055255	ENSDARP00000072049	wu:fk08b02, fk08b02
ccr4laa	ccr8.1	ccr8.1	ENSDARG00000095789	ENSDARP00000125541	ccr4l1, dr-chr16-CCR4-43.1-EK47490, zfCCR8-1
ccr4lab	CABZ01093075.1	CABZ01093075.1	ENSDARG00000086616	ENSDARP00000105159	zfCCR8-2
ccr4lac	ccr8	si:cabz01093077.1	ENSDARG00000105467	ENSDARP00000142256	GPR-CY6, CMKBR8, TER1, CY6, CKR-L1, CDw198, CMKBRL2
ccr6a	ccr6a	ccr6a	ENSDARG00000087474	ENSDARP00000106824	zfCCR6-2, si:bx813304.1, zgc:86782, si:dkey-47g2.1
ccr6b	ccr6b	ccr6b	ENSDARG00000038968	ENSDARP00000128924 ENSDARP00000056883	zfCCR6-1, wu:fk31f08
ccr7	ccr7	ccr7	ENSDARG00000044561	ENSDARP00000118528	zfCCR7, zgc:165629
ccr9a	ccr9a	ccr9a	ENSDARG00000055186	ENSDARP00000071978	ccr9, zfCCR9-1, dr-chr2-CCR9-44.2-EK8447, sb:eu630
ccr9b	ccr9b	ccr9b	ENSDARG00000099738	ENSDARP00000134711 ENSDARP00000137365	ccr9l, dr-chr9-CCR9-39.2-EK48843, zfCCR9-2, LOC100006078
ccr10	ccr10	ccr10	ENSDARG00000040643	ENSDARP00000099267	zgc:91924
ccr11aa	ccr11.1	ccr11.1	ENSDARG00000070755	ENSDARP00000094951 ENSDARP00000142387	cx3cr1l, zfCCR2-1, dr-chr21-CX3CR1-40.7%-EK41814,
ccr2 (ccr11ab)	si:ch211-207g17.2	si:ch211-207g17.2	ENSDARG00000079829	ENSDARP00000142081 ENSDARP00000094958	-
ccr11ac	si:ch211-207g17.3	si:ch211-207g17.3	ENSDARG00000105363	ENSDARP00000142057	-
ccr12a	ccr12a	ccr12a	ENSDARG00000038541	ENSDARP00000122747	ccr12.3, zfCCR3-3, si:ch211-106n13.2
ccr12ba	ccr12b.1	ccr12b.1	ENSDARG00000059410	ENSDARP00000126464	ccr12.1, zfCCR3-1, si:dkey-225n22.5
ccr12bb	ccr12b.2	ccr12b.2	ENSDARG00000026417	ENSDARP00000066871	ccr5.2, ccr12.2, CCR12bb, CCR5-35.0%-EK36093, zfCCR3-2
cxcr1 (cxcr1ba)	si:ch73-54b5.2	si:ch73-54b5.2	ENSDARG00000052088	ENSDARP00000068360	zmp:0000001086
cxcr2 (cxcr1bb)	cxcr2	cxcr2	ENSDARG00000054975	ENSDARP00000071727	si:ch73-54b5.1
cxcr3.1 (cxcr3ab)	cxcr3.1	cxcr3.1	ENSDARG00000007358	ENSDARP00000137552	dr-chr16-CXCR3-41.8-EK27498, sb:eu378
cxcr3.2 (cxcr3l)	cxcr3.2	cxcr3.2	ENSDARG00000041041	ENSDARP00000122984	dr-chr16-CXCR3-37.5-EK27053, zgc:92301
cxcr3.3 (cxcr3aa)	cxcr3.3	cxcr3.3	ENSDARG00000070669	ENSDARP00000119122	si:dkey-269d20.3
cxcr4a	cxcr4a	cxcr4a	ENSDARG00000057633	ENSDARP00000074800 ENSDARP00000123851	cb824
cxcr4b	cxcr4b	cxcr4b	ENSDARG00000041959	ENSDARP00000061498	cxcr4, odysseus, ody, cb403, drCXCR4b1, zgc:109863
cxcr5	cxcr5	cxcr5	ENSDARG00000010514	ENSDARP00000010091	MDR15, BLR1, CD185
cxcr8a/gpr35a*	ENSDARG00000075877	-	ENSDARG00000075877	ENSDARP00000103013	-
cxcr8ba/gpr35ba*	gpr35.1	gpr35.1	ENSDARG00000074633	ENSDARP00000133176 ENSDARP00000103106	zgc:171586
cxcr8bb/gpr35bb*	ENSDARG00000086776	gpr35.2	ENSDARG00000086776	ENSDARP00000111768	zmp:0000001226
xcr1aa	xcr1a.1	xcr1a.1	ENSDARG00000054847	ENSDARP00000071590 ENSDARP00000103498	xcr1, xcr1a
xcr1ab	si:ch73-217b7.4	xcr1a.2	ENSDARG00000054846	no protein assigned	Incomplete sequence/pseudogene

Name in this thesis	Ensembl gene name	zfin gene name	Ensembl gene ID/Alignment position	Ensembl protein ID	Previous /synonymous names and notes
xcr1ac	si:ch73-217b7.3	xcr1a.3	ENSDARG00000087978	no protein assigned	Incomplete sequence/pseudogene
xcr1ba	CABZ01053221.1	xcr1b.2	ENSDARG00000058774	ENSDARP00000076150	drXCR1b
xcr1bc	XCR1 (1 of many)	xcr1b.1	ENSDARG00000052988	ENSDARP00000069429	xcr1b, GPR5, CCXCR1, zmp:0000001090
xcr1bd	CABZ01053219.1	xcr1b.3	ENSDARG00000089840	ENSDARP00000110709	ccr8.3, zfCCR8-3

Notes: Comparison of the nomenclature applied in this work (column 1) with the nomenclature used in Ensembl and zfin databases or elsewhere in literature (columns 2-6). The nomenclature adopted here essentially reflects the systematic classification suggested by Nomiyama *et al.*, *Genes Cells*. 2013. Exceptions are made for genes where other names are largely in use (for these cases the name according to Nomiyama *et al.,* 2013 is reported in brackets in column 1). Names followed by asterisks (*) indicate sequences which were not annotated in Nomiyama *et al.,* 2013. Rows highlighted in grey represent either incomplete sequences or previously reported genes that cannot be mapped on the current version of the zebrafish genome (Ensembl, GRCz10, September 2016).

Curriculum vitae

Vincenzo Torraca was born on September 6th, 1987 in Salerno, Italy. He obtained his high school diploma and professional certificate in Industrial and Food Chemistry in 2006, at the Technical and Industrial Institute B. Focaccia, in Salerno. At Salerno University, he obtained his bachelor degree in 2009 (*summa cum laude*) in computational and molecular biology, after completing an internship on the molecular characterisation of different natural and commercial accessions of *Origanum vulgare* (CRA-ORT, research centre for the horticulture, Battipaglia, Italy, under supervision of dr. F. Campanile and dr. M. Zaccardelli) and on the catalytic activity of genomic DNA for the Michael reaction (Salerno University, under supervision of dr. M. De Rosa and prof. dr. A. Soriente). In 2010, he was selected for the European Erasmus summer school "multidisciplinary approaches to microarray data analysis", Ascea Italy. In 2011, he obtained his master degree (*summa cum laude*) in Biology by Salerno University, after having carried a research internship at Leiden University (the Netherlands), through the European LLP-Erasmus exchange program. Under the supervision of dr. A. Chatzopoulou, dr. M.J. Schaaf (Leiden University) and prof. dr. E.A. Illingworth (Salerno University), he investigated the function of an alternative splicing isoform of the glucocorticoid receptor, using the zebrafish (*Danio rerio*) model. In 2011, he obtained the national qualification as professional senior biologist, by the University of Sannio (Benevento, Italy). In 2012, he joined the group of prof. dr. A.H. Meijer (Institute of Biology, Leiden University) as a PhD candidate, funded by the Marie Skłodowska-Curie Initial Training Network FishForPharma. During his PhD he obtained extensive training on the zebrafish *in vivo* model for infectious diseases and specifically analysed in-depth the function of host chemokine signalling during infection with *Mycobacterium marinum*. In 2016, he was awarded with an individual Marie Skłodowska-Curie postdoctoral fellowship to join the group of dr. S. Mostowy (Imperial College London, UK), where he will continue his research on the zebrafish-*M. marinum* host-pathogen model and study the function of cytoskeleton dynamics during mycobacterial infections.

List of publications

Torraca V, in't Veld E, Meijer AH. **Disruption of chemotactic signaling primes the lysosomal function of macrophages to counteract mycobacterial parasitism.** *Manuscript in preparation*.

Tulotta C, Stefanescu C, **Torraca V**, Meijer AH, Snaar-Jagalska BE. **CXCR4 signaling in the tumor microenvironment orchestrates experimental metastasis formation by controlling myeloid cell motility and response to malignant cells.** *Manuscript in preparation*.

Torraca V, Otto NA, Tavakoli-Tameh A, Meijer AH. **The inflammatory chemokine Cxcl18b exerts neutrophil-specific chemotaxis via the promiscuous chemokine receptor Cxcr2 in zebrafish.** *Submitted manuscript*.

Torraca V, Tulotta C, Snaar-Jagalska BE, Meijer AH. **The chemokine receptor CXCR4 promotes granuloma formation by sustaining a mycobacteria-induced angiogenesis program.** *Submitted manuscript*.

Torraca V and Mostowy S. **Septins and Bacterial Infection.** *Front Cell Dev Biol. In press.*

Masud S, **Torraca V**, Meijer AH. **Modeling infectious diseases in the context of a developing immune system.** *Curr Top Dev Biol. In press.*

Torraca V, Cui C, Boland R, Bebelman JP, van der Sar AM, Smit MJ, Siderius M, Spaink HP, Meijer AH. **The CXCR3/CXCL11 signaling axis mediates macrophage recruitment and dissemination of mycobacterial infection**. *Dis Model Mech.* 2015, 8:253-69.

Torraca V, Masud S, Spaink HP, Meijer AH. **Macrophage-pathogen interactions in infectious diseases: new therapeutic insights from the zebrafish host model**. *Dis Model Mech.* 2014 7:785-97.

Spaink HP, Cui C, Wiweger MI, Jansen HJ, Veneman WJ, Marín-Juez R, de Sonneville J, Ordas A, **Torraca V**, van der Ent W, Leenders WP, Meijer AH, Snaar-Jagalska BE, Dirks RP. **Robotic injection of zebrafish embryos for high-throughput screening in disease models**. *Methods.* 2013, 62:246-54.

Zhou X, Laroche F, Lamers GEM, **Torraca V**, Voskamp P, Lu T, Chu F, Spaink HP, Abrahams JP, Liu Z. **Ultra-small graphene oxide functionalized with polyethylenimine (PEI) for very efficient gene delivery in cell and zebrafish embryos**. *Nano Res.* 2012, 5:703–709.